



## 2017 Coastal Master Plan

---

# Chapter 4 – Model Outcomes and Interpretations



Report: Version II

Date: November 2016

Prepared By: Vadim Alymov (Coastal Engineering Consultants, Inc.), Zach Cobell (Arcadis); Kim de Mutsert (George Mason University), Zhifei Dong (Chicago Bridge & Iron Company), Scott Duke-Sylvester (University of Louisiana at Lafayette), Jordan Fischbach (RAND), Kevin Hanegan (Moffatt & Nichol), Kristy Lewis (George Mason University), David Lindquist (Coastal Protection and Restoration Authority of Louisiana), Alex McCorquodale (University of New Orleans), Michael Poff (Coastal Engineering Consultants, Inc.), Hugh Roberts (Arcadis), Jenni Schindler (Fenstermaker), Jenneke Visser (University of Louisiana at Lafayette), Yushi Wang (The Water Institute of the Gulf), Zhanxian 'Jonathan' Wang (Moffatt & Nichol), and Eric White (The Water Institute of the Gulf)

## Coastal Protection and Restoration Authority

This document was prepared in support of the 2017 Coastal Master Plan being prepared by the Coastal Protection and Restoration Authority (CPRA). CPRA was established by the Louisiana Legislature in response to Hurricanes Katrina and Rita through Act 8 of the First Extraordinary Session of 2005. Act 8 of the First Extraordinary Session of 2005 expanded the membership, duties, and responsibilities of CPRA and charged the new authority to develop and implement a comprehensive coastal protection plan, consisting of a master plan (revised every five years) and annual plans. CPRA's mandate is to develop, implement, and enforce a comprehensive coastal protection and restoration master plan.

### Suggested Citation:

Alymov, V., Cobell, Z., de Mutsert, K., Dong, Z., Duke-Sylvester, S., Fischbach, J., Hanegan, K., Lewis, K., Lindquist, D., McCorquodale, J. A., Poff, M., Roberts, H., Schindler, J., Visser, J. M., Wang, Z., Wang, Y., & White, E. (2016). *2017 Coastal Master Plan: Appendix C: Chapter 4 – Model Outcomes and Interpretations*. Version II. (pp. 1-246). Baton Rouge, Louisiana: Coastal Protection and Restoration Authority.

## Acknowledgements

This document was developed as part of a broader Model Improvement Plan in support of the 2017 Coastal Master Plan under the guidance of the Modeling Decision Team (MDT):

- The Water Institute of the Gulf - Ehab Meselhe, Alaina Grace, and Denise Reed
- Coastal Protection and Restoration Authority (CPRA) of Louisiana - Mandy Green, Angelina Freeman, and David Lindquist
- This effort was funded by the Coastal Protection and Restoration Authority (CPRA) of Louisiana under Cooperative Endeavor Agreement Number 2503-12-58, Task Order No. 03.

DRAFT

## Executive Summary

This chapter focuses on how the models described in previous chapters were used to predict future changes to the landscape, ecosystem, and risk characteristics of the Louisiana coast. Example outputs are provided from the models for the 50-year simulations for various environmental and risk scenarios. For landscape and ecosystem modeling, the Integrated Compartment Model (ICM) and the Ecopath with Ecosim (EwE) models were used. The ICM is made up of the following subroutines: hydrology, morphology, barrier islands, vegetation, and habitat suitability indices. The EwE model predicts fish and shellfish biomass. In terms of storm surge and risk, the Advanced CIRCulation (ADCIRC) model was used to predict storm surge, the Simulating Waves Nearshore (SWAN) model was used to predict waves, and the Coastal Louisiana Risk Assessment (CLARA) model was used to predict risk/damage.

The models were used to assess change over 50 years without the implementation of additional restoration or risk reduction projects (Future Without Action – FWOA). Then, additional model runs were conducted to compare the effects of individual projects and groups of projects (alternatives) against the FWOA. How the project attributes were reflected in the models and how adjustments in inputs or model dynamics were adjusted are described in Section 1. The second section outlines the initial conditions for the landscape and ecosystem, which were primarily defined by existing data as described below and in previous chapters. Section 2 also describes how the effects of storms and waves on flood depths and damages for the initial conditions were derived using modeling. FWOA output is described in Section 3 of this chapter. Project-level outputs and interpretations are provided in Section 4, and project-interactions will be discussed in Section 5. Lastly, outcomes and interpretations of the draft and final 2017 Coastal Master Plan model outputs will be included in Section 6.

## Table of Contents

Coastal Protection and Restoration Authority .....	ii
Acknowledgements .....	iii
Executive Summary .....	iv
List of Tables .....	vii
List of Figures .....	vii
List of Abbreviations .....	xix
1.0 Project Implementation .....	1
1.1 Hydrologic Restoration .....	1
1.2 Shoreline Protection .....	2
1.3 Bank Stabilization .....	3
1.4 Ridge Restoration .....	3
1.5 Levees .....	3
1.6 Oyster Reefs .....	4
1.7 Marsh Creation .....	4
1.8 Diversions .....	4
1.9 Barrier Islands .....	6
1.10 Surge and Wave Modeling of Restoration Projects .....	6
1.11 Structural Protection .....	7
1.11.1 ADCIRC / SWAN .....	7
1.11.2 CLARA .....	8
1.12 Nonstructural .....	9
2.0 Initial Conditions .....	11
2.1 Landscape and Ecosystem .....	11
2.2 Flood Depth .....	15
2.3 Damage .....	22
3.0 Future Without Action .....	23
3.1 Stage .....	23
3.2 Salinity .....	44
3.3 Land Change .....	58
3.4 Vegetation .....	74
3.5 Barrier Islands .....	81
3.5.1 Annual Processes and Forcing Functions .....	81
3.5.2 Episodic Processes and Forcing Functions .....	84
3.5.3 Regional Results .....	87
3.5.4 Land Area Analysis .....	90
3.6 Habitat Suitability Indices (HSIs) .....	98
3.6.1 Eastern Oyster .....	98
3.6.2 Small Juvenile Brown Shrimp .....	98
3.6.3 Adult Spotted Seatrout .....	99
3.6.4 Largemouth Bass .....	99
3.6.5 Green-Winged Teal .....	99
3.6.6 American Alligator .....	100
3.7 Ecopath with Ecosim Fish and Shellfish Model .....	118
3.8 Storm Surge and Waves .....	135
3.8.1 Low Scenario .....	135
3.8.2 Medium Scenario .....	141
3.8.3 High Scenario .....	145

3.8.4 Cross-Scenario Comparisons.....150

3.9 Flood Depths and Damage.....155

4.0 Project Outputs and Interpretations .....164

4.1 Mid-Breton Sound Diversion (001.DI.23).....164

4.1.1 Landscape .....164

4.2 Fish, Shellfish, and Wildlife .....173

4.3 South Terrebonne Marsh Creation project (03a.MC.100).....179

4.3.1 Landscape .....179

4.3.2 Fish, Shellfish, and Wildlife .....182

4.4 Calcasieu Ship Channel Salinity Control Measures (004.HR.06) .....185

4.4.1 Landscape .....185

4.4.2 Fish, Shellfish, and Wildlife .....194

4.5 Lake Hermitage Shoreline Protection (002.SP.100) .....197

4.6 Grand Lake Bank Stabilization (004.BS.01) .....198

4.7 Bayou Decade Ridge Restoration (03a.RC.01) .....201

4.8 Barataria Pass to Sandy Point Barrier Island Restoration (002.BH.04).....204

4.9 Biloxi Marsh Oyster Reef (001.OR.01a) .....210

4.9.1 Landscape .....210

4.9.2 Oyster Habitat Suitability .....212

4.10 Upper Barataria Risk Reduction (002.HP.06) .....214

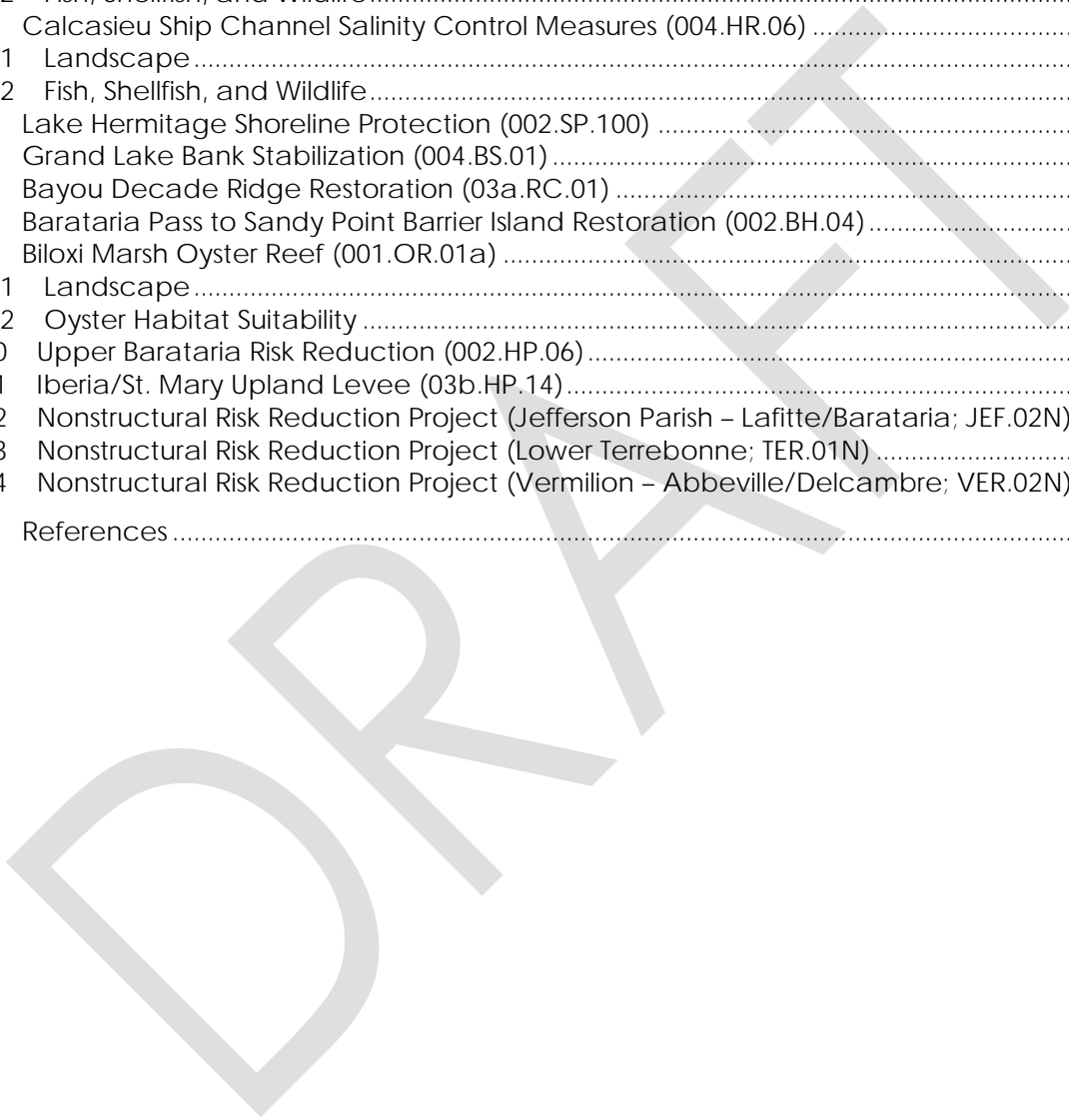
4.11 Iberia/St. Mary Upland Levee (03b.HP.14).....218

4.12 Nonstructural Risk Reduction Project (Jefferson Parish – Lafitte/Barataria; JEF.02N).....221

4.13 Nonstructural Risk Reduction Project (Lower Terrebonne; TER.01N) .....222

4.14 Nonstructural Risk Reduction Project (Vermilion – Abbeville/Delcambre; VER.02N) .....223

5.0 References .....225



## List of Tables

---

Table 1: Selected Nonstructural Project Variants.....	10
Table 2: Nonstructural Project Duration Assumptions.....	11
Table 3: Compartments of Interest within Each Region. ....	23
Table 4: Mechanisms within ICM Driving Land Gain and Marsh Collapse. ....	67
Table 5: List of Vegetation Species Included in Each Habitat Type.....	75
Table 6: Land Area Changes for Low Scenario. ....	97
Table 7: Land Area Changes for Medium Scenario.....	97
Table 8: Land Area Changes for High Scenario.....	97
Table 9: Initial Water Levels and Sea Level Rise Values for the Low Scenario. ....	135
Table 10: Initial Water Levels and Sea Level Rise Values for the Medium Scenario.....	141
Table 11: Initial Water Levels and Sea Level Rise Values for the High Scenario.....	146

## List of Figures

---

Figure 1: (a) Project is Able to be Projected to the Compartment Boundary; (b) Project Cannot be Projected to the Compartment Boundary Due to Other Flow Considerations or Placement Within the Interior of a Compartment.....	2
Figure 2: Example Hurricane Protection Project Grouping for the Project Implementation phase. ....	7
Figure 3: Initial Topography and Bathymetry for the 2017 Coastal Master Plan Modeling Effort....	12
Figure 4: Initial Land/Water for the 2017 Coastal Master Plan Modeling Effort.....	13
Figure 5: Initial Vegetation Cover for the 2017 Coastal Master Plan Modeling Effort. ....	14
Figure 6: Topography and Bathymetry (meters, NAVD88 2009.55) Used for Simulation of the Initial Conditions.....	15
Figure 7: Manning's n Values Used for Simulation of the Initial Conditions. ....	16
Figure 8: Directional Roughness Length Used for Simulation of the Initial Conditions. Values shown are for wind blowing from south to north. ....	17
Figure 9: Maximum Surge Elevations (meters, NAVD88 2009.55) During the Initial Conditions Simulation of Storm 014. ....	17
Figure 10: Maximum Surge Elevations (meters, NAVD88 2009.55) During the Initial Conditions Simulation of Storm 014. ....	18
Figure 11: Maximum Significant Wave Heights (meters) and Associated Directions During the Initial Conditions Simulation of Storm 014. ....	19
Figure 12: Peak Wave Periods (seconds) and Associated Directions During the Initial Conditions Simulation of Storm 014. ....	19
Figure 13: Maximum Surge Elevations (meters, NAVD88 2009.55) During the Initial Conditions Simulation of Storm 218. ....	20

Figure 14: Maximum Surge Elevations (meters, NAVD88 2009.55) During the Initial Conditions Simulation of Storm 218. .... 20

Figure 15: Maximum Significant Wave Heights (meters) and Associated Directions During the Initial Conditions Simulation of Storm 218. .... 21

Figure 16: Peak Wave Periods (seconds) and Associated Directions During the Initial Conditions Simulation of Storm 218. .... 21

Figure 17: Initial Conditions 100-Year Coast Wide Flood Depths – IPET Fragility Scenario..... 22

Figure 18: Initial Conditions Expected Annual Damage by Risk Region – IPET Fragility Scenario. .... 23

Figure 19: Mean Daily Stage in Compartment 248 - East Lake Salvador in PB for the Low Scenario (Representative of Inland Compartment Results). .... 24

Figure 20: Mean Daily Stage in Compartment 278 - Mud Lake/Upper Barataria Bay in PB for the Low Scenario (Representative of Intermediate Compartment Results). .... 25

Figure 21: Mean Daily Stage in Compartment 284 - Northeast of Grand Isle in PB for the Low Scenario (Representative of Near Coast Compartment Results). .... 25

Figure 22: Mean Daily Stage in Compartment 248 - East Lake Salvador in PB for the High Scenario (Representative of Inland Compartment Results). .... 26

Figure 23: Mean Daily Stage in Compartment 278 - Mud Lake/Upper Barataria Bay in PB for the High Scenario (Representative of Intermediate Compartment Results). .... 27

Figure 24: Mean Daily Stage in Compartment 284 - Northeast of Grand Isle in PB for the High Scenario (Representative of Near Coast Compartment Results). .... 27

Figure 25: Mean Daily Stage in Compartment 482 – Lake Palourde in AA for the Low Scenario (Representative of Inland Compartment Results). .... 28

Figure 26: Mean Daily Stage in Compartment 512 – Lake de Cade in AA for the Low Scenario (Representative of Intermediate Compartment Results). .... 29

Figure 27: Mean Daily Stage in Compartment 585 – Caillou Bay in AA for the Low Scenario (Representative of Near Coast Compartment Results)..... 29

Figure 28: Mean Daily Stage in Compartment 482 – Lake Palourde in AA for the High Scenario (Representative of Inland Compartment Results). .... 30

Figure 29: Mean Daily Stage in Compartment 512 – Lake de Cade in AA for the High Scenario (Representative of Intermediate Compartment Results)..... 30

Figure 30: Mean Daily Stage in Compartment 585 – Caillou Bay in AA for the High Scenario (Representative of Near Coast Compartment Results)..... 31

Figure 31: Mean Daily Stage in Compartment 796 – Northwest Grand Lake in CP for the Low Scenario (Representative of Inland Compartment Results). .... 32

Figure 32: Mean Daily Stage in Compartment 844 – East Calcasieu Lake in CP for the Low Scenario (Representative of Intermediate Compartment Results)..... 32

Figure 33: Mean Daily Stage in Compartment 893 – Holly Beach in CP for the Low Scenario (Representative of Near Coast Compartment Results)..... 33

Figure 34: Mean Daily Stage in Compartment 796 – Northwest Grand Lake in CP for the High Scenario (Representative of Inland Compartment Results). .... 34

Figure 35: Mean Daily Stage in Compartment 844 – East Calcasieu Lake in CP for the High Scenario (Representative of Intermediate Compartment Results)..... 34

Figure 36: Mean Daily Stage in Compartment 893 – Holly Beach in CP for the High Scenario (Representative of Near Coast Compartment Results)..... 35

Figure 37: Temporal Changes in the Stage Profiles for the Pontchartrain Estuary for the Low Scenario (1 = Inland; 2 = Intermediate; 3 = Near Coast; and 4 = Off-Shore). ..... 36

Figure 38: Temporal Changes in the Stage Profiles for the Barataria Estuary for the Low Scenario (1= Inland; 2 = Intermediate; and 3 = Coastal)..... 36

Figure 39: Temporal Changes in the Stage Profiles for the Pontchartrain Estuary for the Medium Scenario (1 = Inland; 2 = Intermediate; 3 = Near Coast; and 4 = Off-Shore). ..... 37

Figure 40: Temporal Changes in the Stage Profiles for the Barataria Estuary for the Medium Scenario (1= Inland; 2 = Intermediate; and 3 = Coastal)..... 37

Figure 41: Temporal Changes in the Stage Profiles for the Pontchartrain Estuary for the High Scenario (1 = Inland; 2 = Intermediate; 3 = Near Coast; and 4 = Off-Shore). ..... 38

Figure 42: Temporal Changes in the Stage Profiles for the Barataria Estuary for the High Scenario (1= Inland; 2 = Intermediate; and 3 = Coastal)..... 38

Figure 43: Mean Tidal Range as a Function of Location and Time for the Pontchartrain Estuary for the Low Scenario (1 = Inland; 2 = Intermediate; 3 = Near Coast; and 4 = Off-Shore)..... 39

Figure 44: Mean Tidal Range as a Function of Location and Time for the Barataria Estuary for the Low Scenario (1= Inland; 2 = Intermediate; and 3 = Coastal). ..... 39

Figure 45: Mean Tidal Range as a Function of Location and Time for the Pontchartrain Estuary for the High Scenario (1 = Inland; 2 = Intermediate; 3 = Near Coast; and 4 = Off-Shore)..... 40

Figure 46: Mean Tidal Range as a Function of Location and Time for the Barataria Estuary for the High Scenario (1= Inland; 2 = Intermediate; and 3 = Coastal). ..... 40

Figure 47: Temporal Changes in the Tidal Range Profile for AA for the Low Scenario (1= Inland; 2 = Intermediate; and 3 = Coastal)..... 41

Figure 48: Temporal Changes in the Tidal Range Profile for AA for the High Scenario (1= Inland; 2 = Intermediate; and 3 = Coastal). ..... 41

Figure 49: Temporal Changes in the Stage Profiles for AA for the Low Scenario (1= Inland; 2 = Intermediate; and 3 = Coastal)..... 42

Figure 50: Temporal Changes in the Stage Profiles for AA for the Medium Scenario (1= Inland; 2 = Intermediate; and 3 = Coastal)..... 42

Figure 51: Temporal Changes in the Stage Profiles for AA for the High Scenario (1= Inland; 2 = Intermediate; and 3 = Coastal)..... 43

Figure 52: Temporal Changes in the Tidal Range Profile for CP for the High Scenario (1= Inland; 2 = Intermediate; and 3 = Coastal). ..... 43

Figure 53: Temporal Changes in the Stage Profiles for CP for the High Scenario (1= Inland; 2 = Intermediate; and 3 = Coastal)..... 44

Figure 54: Mean Salinities (ppt) by Compartment for Year 50 for the Medium Scenario FWOA (G001)..... 45

Figure 55: Mean Monthly Salinity in Compartment 248 - East Lake Salvador in PB for the Low Scenario (Representative of Inland Compartment Results). ..... 46

Figure 56: Mean Monthly Salinity in Compartment 278 - Mud Lake/Upper Barataria Bay in PB for the Low Scenario (Representative of Intermediate Compartment Results). ..... 46

Figure 57: Mean Monthly Salinity in Compartment 284 - Northeast of Grand Isle in PB for the Low Scenario (Representative of Near Coast Compartment Results). ..... 47

Figure 58: Mean Monthly Salinity in Compartment 248 - East Lake Salvador in PB for the High Scenario (Representative of Inland Compartment Results). ..... 48

Figure 59: Mean Monthly Salinity in Compartment 278 - Mud Lake/Upper Barataria Bay in PB for the High Scenario (Representative of Intermediate Compartment Results). ..... 48

Figure 60: Mean Monthly Salinity in Compartment 284 - Northeast of Grand Isle in PB for the High Scenario (Representative of Near Coast Compartment Results). ..... 49

Figure 61: Mean Monthly Salinity in Compartment 482 – Lake Palourde in AA for the Low Scenario (Representative of Inland Compartment Results). ..... 50

Figure 62: Mean Monthly Salinity in Compartment 512 – Lake de Cade in AA for the Low Scenario (Representative of Intermediate Compartment Results). ..... 50

Figure 63: Mean Monthly Salinity in Compartment 585 – Caillou Bay in AA for the Low Scenario (Representative of Near Coast Compartment Results). ..... 51

Figure 64: Mean Monthly Salinity in Compartment 482 – Lake Palourde in AA for the High Scenario (Representative of Inland Compartment Results). ..... 52

Figure 65: Mean Monthly Salinity in Compartment 512 – Lake de Cade in AA for the High Scenario (Representative of Intermediate Compartment Results). ..... 52

Figure 66: Mean Monthly Salinity in Compartment 585 – Caillou Bay in AA for the High Scenario (Representative of Near Coast Compartment Results). ..... 53

Figure 67: Mean Monthly Salinity in Compartment 796 – Northwest Grand Lake in CP for the Low Scenario (Representative of Inland Compartment Results). ..... 54

Figure 68: Mean Monthly Salinity in Compartment 844 – East Calcasieu Lake in CP for the Low Scenario (Representative of Intermediate Compartment Results). ..... 54

Figure 69: Mean Monthly Salinity in Compartment 893 – Holly Beach in CP for the Low Scenario (Representative of Near Coast Compartment Results). ..... 55

Figure 70: Mean Monthly Salinity in Compartment 796 – Northwest Grand Lake in CP for the High Scenario (Representative of Inland Compartment Results). ..... 56

Figure 71: Mean monthly Salinity in Compartment 844 – East Calcasieu Lake in CP for the High Scenario (Representative of Intermediate Compartment Results). ..... 56

Figure 72: Mean Monthly Salinity in Compartment 893 – Holly Beach in CP for the High Scenario (Representative of Near Coast Compartment Results). ..... 57

Figure 73: Response of Coast Wide Mean Year 50 Salinity (Averaged Over Inland, Intermediate, and Near Coast Locations) to the Mean Year 50 Stage (Averaged Over Inland, Intermediate, and Near Coast Locations) for All Three Scenarios (Low, Medium, and High). ..... 58

Figure 74: 2017 Coastal Master Plan Ecoregions. .... 60

Figure 75: Land Area through Time within the Upper Pontchartrain Ecoregion. .... 61

Figure 76: Land Area through Time within the Lower Pontchartrain Ecoregion. .... 61

Figure 77: Land Area through Time within the Bird’s Foot Delta Ecoregion. .... 62

Figure 78: Land Area through Time within the Breton Ecoregion. .... 62

Figure 79: Land Area through Time within the Upper Barataria Ecoregion. .... 63

Figure 80: Land Area through Time within the Lower Barataria Ecoregion. .... 63

Figure 81: Land Area through Time within the Lower Terrebonne Ecoregion. .... 64

Figure 82: Land Area through Time within the Atchafalaya/Vermilion/Teche Ecoregion. .... 64

Figure 83: Land Area through Time within the Mermentau/Lakes Ecoregion. .... 65

Figure 84: Land Area through Time within the Calcasieu/Sabine Ecoregion. .... 65

Figure 85: Land Area through Time within the Eastern Chenier Ridge Ecoregion..... 66

Figure 86: Land Area through Time within the Western Chenier Ridge Ecoregion. .... 66

Figure 87: Land Change from Initial Conditions after 25 Years of Low Scenario – FWOA. Net Land Change (Land Gain-Land Loss) at Year 25 is -1,170 km<sup>2</sup> for the Low Scenario. .... 68

Figure 88: Land Change from Initial Conditions after 50 Years of Low Scenario – FWOA. Net Land Change (Land Gain-Land Loss) at Year 50 is -4,610 km<sup>2</sup> for the Low Scenario. .... 69

Figure 89: Land Change from Initial Conditions after 25 Years of Medium Scenario – FWOA. Net Land Change (Land Gain-Land Loss) at Year 25 is -1,590 km<sup>2</sup> for the Medium Scenario. .... 70

Figure 90: Land Change from Initial Conditions after 50 years of Medium scenario – FWOA. Net Land Change (Land Gain-Land Loss) at Year 50 is -7,320 km<sup>2</sup> for the Medium Scenario. .... 71

Figure 91: Land Change from Initial Conditions after 25 Years of High Scenario – FWOA. Net Land Change (Land Gain-Land Loss) at Year 25 is -3,340 km<sup>2</sup> for the High Scenario. .... 72

Figure 92: Land Change from Initial Conditions after 50 Years of High Scenario – FWOA. Net Land Change (Land Gain-Land Loss) at Year 50 is -10,990 km<sup>2</sup> for the High Scenario. .... 73

Figure 93: Coast Wide Change in Habitats Over the 50 Year Forecast Using the Low Scenario.... 76

Figure 94: Change in Habitats Forecasted Using the Low Scenario: Coast Wide and Three Regions of the Coast. .... 77

Figure 95: Coast Wide Change in Habitats Over the 50 Year Forecast Using the Medium Scenario.78

Figure 96: Change in Habitats Forecasted Using the Medium Scenario: Coast Wide and Three Regions of the Coast. .... 79

Figure 97: Coast Wide Change in Habitats Over the 50-Year Forecast Using the High Scenario... 80

Figure 98: Change in Habitats Forecasted Using the High Scenario: Coast Wide and Three Regions of the Coast. .... 81

Figure 99: Plan View of East-Trinity Island Shoreline Changes through Year 20. .... 82

Figure 100: Representative Cross Sectional Comparison of East-Trinity Island through Year 20. .... 83

Figure 101: Plan View of Grand Terre Gulf-Side and Bayside Shorelines through Year 30..... 84

Figure 102: Representative Cross Sectional Comparison of East-Trinity Island through Year 20. .... 85

Figure 103: Plan View of Pre and Post-Storm Shorelines for Chaland Headland at Years 34-35. .... 86

Figure 104: Pre and Post-Storm Cross Sectional Comparison for Chaland Headland at Years 34-35. .... 87

Figure 105: Plan View of East-Trinity Island Gulf-Side and Bayside Shorelines through Year 50 for Low Scenario..... 88

Figure 106: Cross Sections of Caminada Headland through Year 50 for Low, Medium, and High Scenarios..... 89

Figure 107: Land Area Changes Over Time for Isle Dernieres Barrier Shorelines. .... 91

Figure 108: Land Area Changes Over Time for Timbalier Barrier Shorelines. .... 92

Figure 109: Land Area Changes Over Time for Caminada Barrier Shorelines..... 93

Figure 110: Land Area Changes Over Time for Barataria Barrier Shorelines..... 94

Figure 111: Land Area Changes Over Time for Breton Barrier Shorelines..... 95

Figure 112: Land Area Changes Over Time for Chandeleur Barrier Shorelines..... 96

Figure 113: Coast Wide Habitat Suitability for Eastern Oyster at Years 25 and 50 of the Low FWOA Scenario..... 101

Figure 114: Coast Wide Habitat Suitability for Eastern Oyster at Years 25 and 50 of the Medium FWOA Scenario.. .... 102

Figure 115: Coast Wide Habitat Suitability for Eastern Oyster at Years 25 and 50 of the High FWOA Scenario. .... 103

Figure 116: Coast Wide Habitat Suitability for Small Juvenile Brown Shrimp at Years 25 and 50 of the Low FWOA Scenario..... 104

Figure 117: Coast Wide Habitat Suitability for Small Juvenile Brown Shrimp at Years 25 and 50 of the Medium FWOA Scenario..... 105

Figure 118: Coast Wide Habitat Suitability for Small Juvenile Brown Shrimp at Years 25 and 50 of the High FWOA Scenario..... 106

Figure 119: Coast Wide Habitat Suitability for Adult Spotted Seatrout at Years 25 and 50 of the Low FWOA Scenario..... 107

Figure 120: Coast Wide Habitat Suitability for Adult Spotted Seatrout at Years 25 and 50 of the Medium FWOA Scenario..... 108

Figure 121: Coast Wide Habitat Suitability for Adult Spotted Seatrout at Years 25 and 50 of the High FWOA Scenario ..... 109

Figure 122: Coast Wide Habitat Suitability for Largemouth Bass at Years 25 and 50 of the Low FWOA Scenario..... 110

Figure 123: Coast Wide Habitat Suitability for Largemouth Bass at Years 25 and 50 of the Medium FWOA Scenario..... 111

Figure 124: Coast Wide Habitat Suitability for Largemouth Bass at Years 25 and 50 of the High FWOA Scenario..... 112

Figure 125: Coast Wide Habitat Suitability for Green-Winged Teal at Years 25 and 50 of the Low FWOA Scenario..... 113

Figure 126: Coast Wide Habitat Suitability for Green-Winged Teal at Years 25 and 50 of the Medium FWOA Scenario..... 114

Figure 127: Coast Wide Habitat Suitability for Green-Winged Teal at Years 25 and 50 of the High FWOA Scenario..... 115

Figure 128: Coast Wide Habitat Suitability for American Alligator at Years 25 and 50 of the Low FWOA Scenario..... 116

Figure 129: Coast Wide Habitat Suitability for American Alligator at Years 25 and 50 of the Medium FWOA Scenario..... 117

Figure 130: Coast Wide Habitat Suitability for American Alligator at Years 25 and 50 of the High FWOA Scenario.. ..... 118

Figure 131: Distribution of TKN: Year 25 of the Low Scenario. .... 120

Figure 132: Biomass Distribution of Adult Spotted Seatrout in Year 25 (top) and Year 50 (Bottom) of the Low Scenario. .... 121

Figure 133: Biomass Distribution of Juvenile Brown Shrimp in Year 25 (top) and Year 50 (Bottom) of the Low Scenario. .... 122

Figure 134: Mean Monthly Salinity in April of Year 25 and Year 50 in the Low Scenario Compared. 123

Figure 135: Biomass Distribution of Eastern Oyster (Sack) in Year 25 (Top) and Year 50 (Bottom) of the Low Scenario. .... 124

Figure 136: Biomass Distribution of Juvenile Largemouth Bass in Year 25 (Top) and Year 50 (Bottom) of the Low Scenario. .... 125

Figure 137: Biomass Distribution of Adult Spotted Seatrout in Year 25 (Top) and Year 50 (Bottom) of the Medium Scenario. .... 126

Figure 138: Biomass Distribution of Juvenile Brown Shrimp in Year 25 (Top) and Year 50 (Bottom) of the Medium Scenario. .... 127

Figure 139: Biomass Distribution of Eastern Oyster (Sack) in Year 25 (Top) and Year 50 (Bottom) of the Medium Scenario. .... 128

Figure 140: Biomass Distribution of Juvenile Largemouth Bass in Year 25 (Top) and Year 50 (Bottom) of the Medium Scenario. .... 129

Figure 141: Biomass Distribution of Adult Spotted Seatrout in Year 25 (Top) and Year 50 (Bottom) of the High Scenario. .... 130

Figure 142: Biomass Distribution of Juvenile Brown Shrimp in Year 25 (Top) and Year 50 (Bottom) of the High Scenario. .... 131

Figure 143: Percent Wetland in Year 25 of the Low Scenario (Top) and Year 50 of the High Scenario (Bottom), Showing the Differences in Projected Wetland Loss Depending on Time and Scenario. .... 132

Figure 144: Biomass Distribution of Eastern Oyster (Sack) in Year 25 (Top) and Year 50 (Bottom) of the High Scenario. .... 133

Figure 145: Biomass Distribution of Juvenile Largemouth Bass in Year 25 (Top) and Year 50 (Bottom) of the High Scenario. .... 134

Figure 146: Differences Between Maximum Surge Elevations (meters) in Southeastern Louisiana for FWOA and Initial Conditions for Storm 014 in Year 10 of the Low Scenario. .... 137

Figure 147: Differences Between Maximum Wave Height (meters) in Southeastern Louisiana for FWOA and Initial Conditions for Storm 014 in Year 10 of the Low Scenario. .... 137

Figure 148: Differences Between Maximum Surge Elevations (meters) in Southeastern Louisiana for FWOA and Initial Conditions for Storm 014 in Year 25 of the Low Scenario. .... 138

Figure 149: Differences Between Maximum Wave Height (meters) in Southeastern Louisiana for FWOA and Initial Conditions for Storm 014 in Year 25 of the Low Scenario. .... 138

Figure 150: Differences Between Maximum Surge Elevations (meters) in Southeastern Louisiana for FWOA and Initial Conditions for Storm 014 in Year 50 of the Low Scenario. .... 139

Figure 151: Differences Between Maximum Wave Height (meters) in Southeastern Louisiana for FWOA and Initial Conditions for Storm 014 in Year 50 of the Low Scenario. .... 139

Figure 152: Surge Elevation (meters, NAVD88 2009.55) Time Series for Storm 014 in Lake Borgne for the Low Scenario..... 140

Figure 153: Surge Elevation (meters, NAVD88 2009.55) Time Series for Storm 014 in the Barataria Bay for the Low Scenario..... 141

Figure 154: Differences Between Maximum Surge Elevations (meters) in Southeastern Louisiana for FWOA and Initial Conditions for Storm 014 in Year 10 of the Medium Scenario..... 142

Figure 155: Differences Between Maximum Wave Height (meters) in Southeastern Louisiana for FWOA and Initial Conditions for Storm 014 in Year 10 of the Medium Scenario..... 142

Figure 156: Differences Between Maximum Surge Elevations (meters) in Southeastern Louisiana for FWOA and Initial Conditions for Storm 014 in Year 25 of the Medium Scenario..... 143

Figure 157: Differences Between Maximum Wave Height (meters) in Southeastern Louisiana for FWOA and Initial Conditions for Storm 014 in Year 25 of the Medium Scenario..... 143

Figure 158: Differences Between Maximum Surge Elevations (meters) in Southeastern Louisiana for FWOA and Initial Conditions for Storm 014 in Year 50 of the Medium Scenario..... 144

Figure 159: Differences Between Maximum Wave Height (meters) in Southeastern Louisiana for FWOA and Initial Conditions for Storm 014 in Year 50 of the Medium Scenario..... 144

Figure 160: Surge Elevation (meters, NAVD88 2009.55) Time Series for Storm 014 in Lake Borgne for the Medium Scenario..... 145

Figure 161: Surge Elevation (meters, NAVD88 2009.55) Time Series for Storm 014 in Barataria Bay for the Medium Scenario..... 145

Figure 162: Differences Between Maximum Surge Elevations (meters) in Southeastern Louisiana for FWOA and Initial Conditions for Storm 014 in Year 10 of the High Scenario..... 146

Figure 163: Differences Between Maximum Wave Height (meters) in Southeastern Louisiana for FWOA and Initial Conditions for Storm 014 in Year 10 of the High Scenario..... 147

Figure 164: Differences Between Maximum Surge Elevations (meters) in Southeastern Louisiana for FWOA and Initial Conditions for Storm 014 in Year 25 of the High Scenario..... 147

Figure 165: Differences Between Maximum Wave Height (meters) in Southeastern Louisiana for FWOA and Initial Conditions for Storm 014 in Year 25 of the High Scenario..... 148

Figure 166: Differences Between Maximum Surge Elevations (meters) in Southeastern Louisiana for FWOA and Initial Conditions for Storm 014 in Year 50 of the High Scenario..... 148

Figure 167: Differences Between Maximum Surge Elevations (meters) in Southwestern Louisiana for FWOA and Initial Conditions for Storm 014 in Year 50 of the High Scenario..... 149

Figure 168: Surge Elevation (meters, NAVD88 2009.55) Time Series for Storm 014 in Lake Borgne for the High Scenario..... 149

Figure 169: Surge Elevation (meters, NAVD88 2009.55) Time Series for Storm 014 in Barataria Bay for the High Scenario..... 150

Figure 170: Differences Between Maximum Surge Elevations (meters) in Southwestern Louisiana for FWOA and Initial Conditions for Storm 218 of the Low Scenario. .... 150

Figure 171: Differences Between Maximum Surge Elevations (meters) in Southwestern Louisiana for FWOA and Initial Conditions for Storm 218 of the Medium Scenario..... 151

Figure 172: Differences Between Maximum Surge Elevations (meters) in Southwestern Louisiana for FWOA and Initial Conditions for Storm 218 of the High Scenario. .... 151

Figure 173: Surge Elevation (meters, NAVD88 2009.55) Time Series for Storm 014 near Lake Maurepas during Year 50 for All Scenarios. .... 153

Figure 174: Differences Between Maximum Surge Elevations (meters) near Lake Maurepas for FWOA and Initial Conditions for Storm 014 during Year 50 for All Scenarios. .... 153

Figure 175: Change in Manning's n Roughness between the Initial Conditions and the High Scenario in Year 50. .... 154

Figure 176: Change in Directional Roughness Length for an East to West Wind between the Initial Conditions and the High Scenario Year 50. .... 155

Figure 177: FWOA Low Scenario 100-Year Coast Wide Flood Depths – IPET Fragility Scenario. .... 158

Figure 178: FWOA High Scenario 100-Year Coast Wide Flood Depths – IPET Fragility Scenario. .... 159

Figure 179: Change in 100-Year Coast Wide Flood Depths by Environmental Scenario and Year – IPET Fragility Scenario. .... 160

Figure 180: FWOA 500-Year Flood Depths, High Scenario - Greater New Orleans. .... 161

Figure 181: FWOA Coast Wide EAD Over Time by Environmental and Population Growth Scenario. .... 161

Figure 182: FWOA Coast Wide EAD Bar plot Summary by Year, Environmental, and Fragility Scenario. .... 162

Figure 183: FWOA Coast Wide EAD Map by Year and Environmental Scenario. .... 163

Figure 184: Change in Land Area within the Breton Sound Ecoregion and in the Eastern Coast in Response to the Mid-Breton Sound Diversion (relative to FWOA, high scenario). .... 165

Figure 185: Land Change from the Mid-Breton Sound Diversion Relative to FWOA (year 10; high scenario). .... 166

Figure 186: Change in Mean Annual Water Level Resulting from the Mid-Breton Sound Diversion Relative to FWOA (year 10; high scenario). .... 166

Figure 187: Change in Mean Annual Salinity Resulting from the Mid-Breton Sound Diversion Relative to FWOA (year 10; high scenario). .... 167

Figure 188: Change in Wetland Habitat Over Time within the Breton Sound Ecoregion under FWOA and with Mid-Breton Sound Diversion (high scenario). .... 168

Figure 189: Land Change from the Mid-Breton Sound Diversion Relative to FWOA (year 30; high scenario). Inset focusses on immediate outfall area of the diversion. .... 170

Figure 190: Change in Mean Annual Water Level from the Mid-Breton Sound Diversion Relative to FWOA (year 30; high scenario). .... 170

Figure 191: Change in Mean Annual Salinity from the Mid-Breton Sound Diversion Relative to FWOA (year 30; high scenario). .... 170

Figure 192: Land Change from the Mid-Breton Sound Diversion Relative to FWOA (year 50; high scenario). .... 171

Figure 193: Change in Wetland Habitat over Time within the Breton Sound Basin under FWOA and with the Mid-Breton Sound Diversion (medium scenario). .... 172

Figure 194: Change in Land Area within the Breton Sound Ecoregion and in the Eastern Coast in Response to the Mid-Breton Sound Diversion (relative to FWOA; medium scenario). .... 173

Figure 195: Difference in Small Juvenile Brown Shrimp Habitat Suitability for the Mid-Breton Diversion Relative to FWOA (years 10, 30, and 50; high scenario)..... 174

Figure 196: Difference in American Alligator Habitat Suitability for the Mid-Breton Diversion Relative to FWOA (years 10, 30, and 50; high scenario). .... 176

Figure 197: Difference in Juvenile Largemouth Bass Biomass for the Mid-Breton Diversion Relative to FWOA (years 10, 30, and 50; high scenario).. .... 177

Figure 198: Difference in Juvenile Brown Shrimp Biomass for the Mid-Breton Diversion Relative to FWOA (years 10, 30, and 50; high scenario)..... 178

Figure 199: Land Change from the South Terrebonne Marsh Creation Relative to FWOA (year 20; high scenario). .... 179

Figure 200: Land Change from the South Terrebonne Marsh Creation Relative to FWOA (year 30; high scenario). .... 180

Figure 201: Monthly Salinity (ppt) for the ICM Hydrology Compartment North of the South Terrebonne Marsh Creation Area between Years 19 and 30 of the Simulation..... 181

Figure 202: Land Change from the South Terrebonne Marsh Creation Relative to FWOA (year 50; high scenario). .... 181

Figure 203: Difference in Small Juvenile Brown Shrimp Habitat Suitability Associated with the South Terrebonne Marsh Creation Relative to FWOA (years 20, 30, and 50; high scenario).. .... 183

Figure 204: Difference in Largemouth Bass Habitat Suitability Associated with the South Terrebonne Marsh Creation Relative to FWOA (years 20, 30, and 50; high scenario).. .... 184

Figure 205: Change in Salinity from the Calcasieu Ship Channel Salinity Control Measures Project Relative to FWOA (year 10; high scenario). .... 186

Figure 206: Land Change from the Calcasieu Ship Channel Salinity Control Measures Project Relative to FWOA (year 10; high scenario). .... 186

Figure 207: Change in Wetland Habitat over Time within the Calcasieu/Sabine Ecoregion in FWOA and with the Calcasieu Ship Channel Salinity Control Measures Project (high scenario). 187

Figure 208: Change in Land Area within the Calcasieu/Sabine Ecoregion and in the Western Coast in Response to the Calcasieu Ship Channel Salinity Control Measures Project (relative to FWOA; high scenario)..... 188

Figure 209: Land Change from the Calcasieu Ship Channel Salinity Control Measures Project Relative to FWOA (year 30; high scenario). .... 189

Figure 210: Change in Salinity Resulting from the Calcasieu Ship Channel Salinity Control Measures Project Relative to FWOA (year 30; high scenario). .... 189

Figure 211: Wetland Habitat Distribution Associated with the Calcasieu Ship Channel Salinity Control Measures Project (year 30; high scenario). .... 190

Figure 212: Land Change from the Calcasieu Ship Channel Salinity Control Measures Project Relative to FWOA (year 50; high scenario). .... 191

Figure 213: Change in Wetland Habitat over Time within the Calcasieu/Sabine Ecoregion in FWOA and with the Calcasieu Ship Channel Salinity Control Measures Project (medium scenario). .... 192

Figure 214: Change in Land Area within the Calcasieu/Sabine Ecoregion and in the Western Coast in Response to the Calcasieu Ship Channel Salinity Control Measures Project (relative to FWOA; medium scenario). .... 193

Figure 215: Change in Salinity from the Calcasieu Ship Channel Salinity Control Measures Project Relative to FWOA (year 30; medium scenario)..... 193

Figure 216: Difference in Eastern Oyster Habitat Suitability Associated with the Calcasieu Ship Channel Salinity Control Measures Project Relative to FWOA (years 20, 30, and 50; high scenario)..... 195

Figure 217: Difference in Largemouth Bass Habitat Suitability Associated with the Calcasieu Ship Channel Salinity Control Measures Project Relative to FWOA (years 20, 30, and 50; high scenario)..... 196

Figure 218: Land Change from Lake Hermitage Shoreline Protection Relative to FWOA (year 10; high scenario)..... 197

Figure 219: Land Change from Grand Lake Bank Stabilization Relative to FWOA (year 20; high scenario)..... 199

Figure 220: Land Change from Grand Lake Bank Stabilization Relative to FWOA (year 40; high scenario)..... 200

Figure 221: Land Change from Bayou Decade Ridge Restoration Relative to FWOA (year 20; high scenario)..... 202

Figure 222: Land change from Bayou Decade Ridge Restoration relative to FWOA (year 40; high scenario)..... 203

Figure 223: Plan View of Chaland Headland Shoreline Changes through Year 20 with Project Implementation..... 205

Figure 224: Representative Cross Sectional Comparison of Eastern Chaland Headland through Year 20 for FWOA and with the Project (FWA); Year 1 FWOA and with the Project are the Same Profile..... 206

Figure 225: Plan View of Pre- and Post-Storm Shorelines for Chaland Headland at Years 34-35 with Project Implementation..... 207

Figure 226: Pre- and Post-Storm Cross Sectional Comparison for Chaland Headland at Years 34-35 for FWOA and with the Project (FWA). ..... 207

Figure 227: Plan View of Central Chaland Headland Shoreline Changes through Year 20 for FWOA and with the Project (FWA). ..... 208

Figure 228: Representative Cross Sectional Comparison of Central Chaland Headland through Year 20 for FWOA and with the Project (FWA)..... 209

Figure 229: Net Change in Land Area over Time for the Barataria Pass to Sandy Point Barrier Island Restoration Project. .... 210

Figure 230: Land Change from Biloxi Marsh Oyster Reef Relative to FWOA (year 10; high scenario)..... 211

Figure 231: Land Change from Biloxi Marsh Oyster Reef Relative to FWOA (year 50; high scenario)..... 212

Figure 232: Difference in Eastern Oyster Habitat Suitability Associated with the Biloxi Marsh Oyster Reef Relative to FWOA (years 20, 30, and 50; high scenario)..... 213

Figure 233: Upper Barataria Risk Reduction Alignment, as Indicated by the Pink Line..... 214

Figure 234: Differences in Maximum Water Surface Elevation (m) due to Implementation of the Upper Barataria Risk Reduction Project (year 50; high scenario) during Storm 012.. ..... 215

Figure 235: Differences in Maximum Water Surface Elevation (m) due to Implementation of the Upper Barataria Risk Reduction Project (year 50; high scenario) during Storm 018. ....215

Figure 236: Difference in Median 100-Year Flood Depths due to Implementation of the Upper Barataria Risk Reduction Project (FWP) compared to FWOA (year 50; high scenario). ....216

Figure 237: Change in EAD from Implementation of the Upper Barataria Risk Reduction Project (year 50; high scenario; historical growth; IPET fragility scenarios).....217

Figure 238: Iberia/St. Mary Upland Levee Alignment, as Indicated by the Pink Line. ....218

Figure 239: Differences in Maximum Water Surface Elevation (m) due to Implementation of Iberia/St. Mary Upland Levee Alignment (year 50; high scenario) during Storm 223.....219

Figure 240: (A) Maximum Water Surface Elevation (m, NAVD88) and (B) Differences in Maximum Water Surface Elevation (m) due to Implementation of Iberia/St. Mary Upland Levee Alignment (year 50; high scenario) during Storm 232.....219

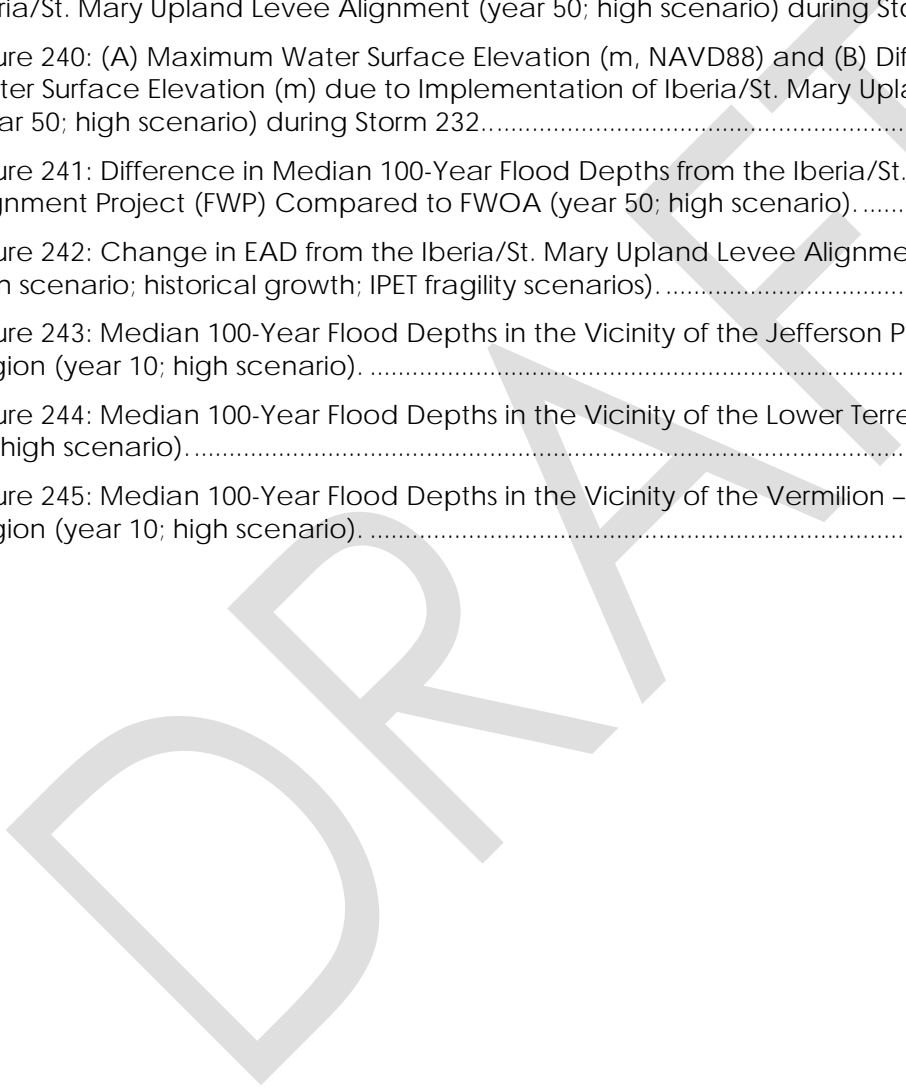
Figure 241: Difference in Median 100-Year Flood Depths from the Iberia/St. Mary Upland Levee Alignment Project (FWP) Compared to FWOA (year 50; high scenario).....220

Figure 242: Change in EAD from the Iberia/St. Mary Upland Levee Alignment Project (year 50; high scenario; historical growth; IPET fragility scenarios). ....221

Figure 243: Median 100-Year Flood Depths in the Vicinity of the Jefferson Parish - Lafitte/Barataria Region (year 10; high scenario). ....222

Figure 244: Median 100-Year Flood Depths in the Vicinity of the Lower Terrebonne Region (year 10; high scenario). ....223

Figure 245: Median 100-Year Flood Depths in the Vicinity of the Vermilion – Abbeville/Delcambre Region (year 10; high scenario). ....224



## List of Abbreviations

---

AA	Atchafalaya/Terrebonne
ADCIRC	Advanced Circulation (model)
AEP	Annual Exceedance Probability
BIMODE	Barrier Island Model
CLARA	Coastal Louisiana Risk Assessment (model)
CP	Chenier Plain
CPRA	Coastal Protection and Restoration Authority
DEM	Digital Elevation Model
EAD	Expected Annual Damage
ESLR	eustatic sea level rise
EWE	Ecopath with Ecosim (model)
FEMA	Federal Emergency Management Agency
FWOA	Future Without Action
FWP	Future With Project
GOHSEP	Governor's Office of Homeland Security and Emergency Preparedness
HSDRRS	Hurricane and Storm Damage Risk Reduction System
HSI	Habitat Suitability Index
HUD	Department of Housing and Urban Development
ICM	Integrated Compartment Model
IPET	Interagency Performance Evaluation Taskforce

JPM-OS	Joint-Probability Method—Optimal Sampling
KMZ	Keyhole Markup Language
LaVegMod v2	Louisiana Vegetation Model (version 2)
LMI	low to moderate income
MTTG	Morganza to the Gulf
NAVD88	North American Vertical Datum of 1988
PB	Pontchartrain/Barataria
RL	Repetitive Loss
RSLR	Relative Sea Level Rise
SRL	Severe Repetitive Loss
SWAN	Simulating Waves Nearshore
TKN	Total Kjeldahl Nitrogen
TRG	Tidal Ranges



## 1.0 Project Implementation

The initial conditions for the 2017 Coastal Master Plan analysis were derived from existing data for topography, bathymetry, and vegetation cover (see Attachment C3 -27), with projects added to the landscape that were not represented in the initial data sets but are assumed to be in existence for the 2017 Coastal Master Plan FWOA condition. The FWOA landscape included all projects, even if they were very small features (i.e., smaller than project selected for consideration in the 2017 Coastal Master Plan). This was considered important to ensure that the performance of candidate projects was based on as realistic a landscape as possible. Refer to Appendix A – Project Definitions for a list of projects included in the FWOA landscape. The modeling of individual candidate projects was based on a 50-year simulation.

This section describes how the candidate projects were added to the ICM, ADCIRC, and/or CLARA models, either through direct modification of topography/bathymetry (e.g., marsh creation), changes in how the model modifies land-water character (e.g., buffer behind a shoreline protection project to reduce marsh edge erosion), or through changes in model links that determine hydrologic exchanges (e.g., structure used for hydrologic restoration). Projects were incorporated as part of the model run “set-up” phase and were put into the landscape based on the specific attributes, including the implementation year, provided by CPRA. For project-level analysis, some model runs contained more than one project, yet care was taken to assure these were sufficiently separated in the model domain to avoid project interactions. The set-up for each type of project is described below. Appendix A – Project Definitions provides more information on the project types and assumptions used to develop the project attributes provided to the modeling teams.

### 1.1 Hydrologic Restoration

Hydrologic restoration projects include the introduction of culverts, tide gates, locks, plugs, weirs, siphons, and pump stations into the model domain. These projects are primarily used to convey fresh water to proposed outfall areas or to improve water circulation and reduce saltwater intrusion within a hydrologic system. In most cases, the implementation of a hydrologic restoration project required the adjustment of existing model links or the addition of new links. The link type added or modified (channel, weir, lock, tide gate, orifice, culvert, or pump station) depends on the project specifics stated in the project attributes. In some cases, a project will include a plug, which requires blocking an existing channel link. To implement these projects, the modeler determines if a channel link is entirely blocked due to the plug, or if the channel link (whether representative of a single channel or composite channel) has a reduction in width due to the plug. For pump stations, tide gates, and other link types which feature control operations, it should be noted that the operation rules remain the same overall years of implementation within the model (i.e., the structure operation rules remain static over time even though actual operation can vary in response to conditions). For instance, it is not possible to implement a project in the ICM at year five with a prescribed operational trigger of 2.2 m stage in year 10 and switch to a trigger of 3 m stage in year 22. In cases with complex operational rules (such as operation at specific stage *and* salinity criteria), the hydrology code used in that model run was specifically modified to ensure correct operation of the project. However, this was only necessary for a few projects.

If at all possible, subdividing model compartments was avoided during project implementation. In some cases, this meant “projecting” the structure location near the boundary of the compartment for the establishment of link attributes. However, this procedure was only used if

the hydraulic conveyance between the compartments was identical at the project location and at the compartment face. Effects of projects located within the interior of a compartment that do not affect exchange between two compartments were not captured within the ICM. Examples are provided in Figure 1a and 1b.

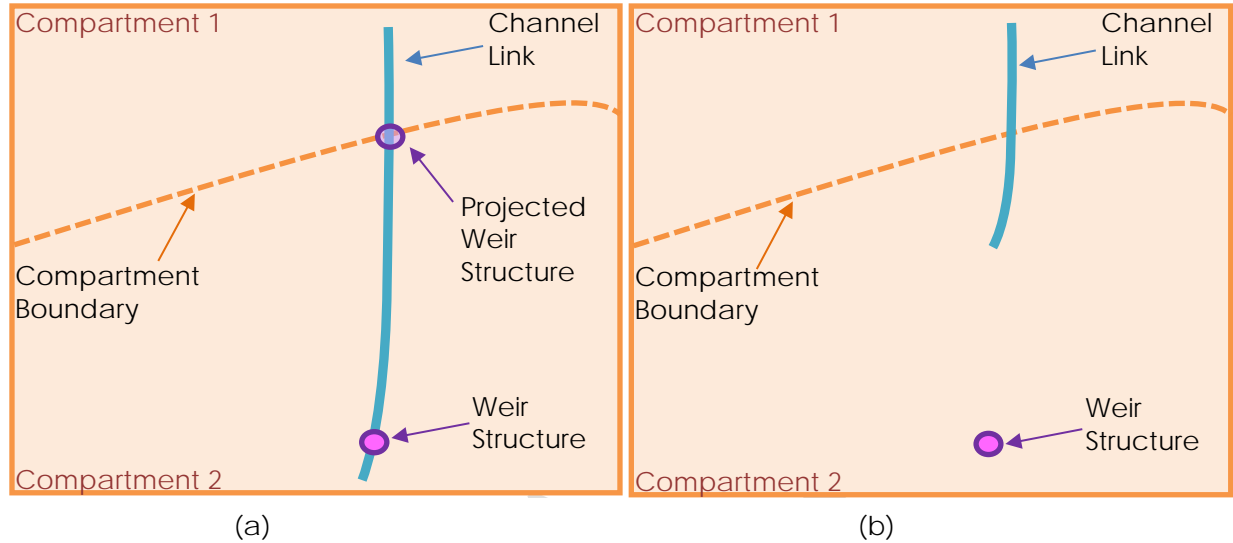


**Figure 1: (a) Project is Able to be Projected to the Compartment Boundary; (b) Project Cannot be Projected to the Compartment Boundary Due to Other Flow Considerations or Placement Within the Interior of a Compartment.**

## 1.2 Shoreline Protection

Shoreline protection projects are defined as near shore segmented rock breakwaters and are primarily used to reduce wave energies on shorelines in open bays, lakes, and natural and manmade channels. The project footprints were not included in the landscape (Digital Elevation Model, DEM) or incorporated into the hydrology subroutine. These projects were implemented by adjusting the marsh edge erosion rate for any part of the compartment within the influence area behind the structure. This influence area was defined by a 200 m buffer on the landward side of the structure. The project effect on marsh edge erosion rate was applied at the 30 m grid level in the morphology subroutine. The amount of eroded sediment to be added to the compartment sediment pool was also proportionally reduced to account for the length of marsh edge within a compartment that would be protected by the project.

The marsh edge retreat rate was reduced for compartments impacted by the 200 m buffer. Equation 1 was used to determine the revised marsh edge erosion rate for each compartment containing the shoreline protection project:

$$MEE_{new} = \left( (MEE_{original}) \left( \frac{A_{project}}{A_{total}} \right) (F_r) \right) + \left( 1 - \left( \frac{A_{project}}{A_{total}} \right) (MEE_{original}) \right) \quad (1)$$

where

- $MEE_{new}$  = the compartment's marsh edge erosion rate, as reduced by the project
- $A_{project}$  = project edge area = shoreline protection project length \* assumed marsh edge width of one 30 meter land/water pixel in morphology subroutine
- $A_{total}$  = total marsh edge area

$F_r$  = project reduction factor = wave (erosion) attenuation rate/100%

The project attributes included the designated wave (erosion) attenuation rate, which (as shown in Equation 1) was used as the percent reduction in the historic marsh edge erosion rate for each compartment containing the project. The new marsh edge erosion rate was then included in the revised compartment attribute input file.

### 1.3 Bank Stabilization

Bank stabilization projects are defined as the on shore placement of earthen fill and vegetative plantings and are primarily used to maintain shorelines in open bays, lakes, and natural and manmade channels. The procedure for modeling bank stabilization projects followed the guidelines outlined above for shoreline protection projects. The project footprints were not included in the landscape (DEM) or incorporated into the hydrology subroutine, but a 200 m buffer was used to determine the influence area of the project. Wave attenuation rates, as specified in the project attributes, were used to determine the new marsh edge erosion rate to be used in the compartment attribute input file.

### 1.4 Ridge Restoration

Ridge restoration projects are intended to re-establish historical ridges through sediment placement and vegetative plantings to provide additional storm surge attenuation and to restore forested maritime habitats. Ridge restoration projects were implemented in the ICM using the same procedure and approach used for levee projects. Ridge restoration projects were modeled via implementation in the landscape by adjusting the Digital Elevation Model (DEM) as well as through modification/addition of hydrology links. The project was incorporated into the DEM based on the footprint shapefile provided by CPRA and the project elevation specified in the project attributes. If a ridge was added to the landscape, existing links were inspected, additional links were added (if needed), and the existing marsh or channel links were adjusted to reflect the dimensions after the ridge project was in place. Attributes such as ridge crest elevation and base width (per the project attributes) were carried over into the link attributes specified in the links input file. These links allowed for overtopping of the ridge in the ICM. They blocked the flow between compartments where a ridge was present if the stage was less than the ridge crest elevation. If the stage was greater than the ridge crest elevation, the ridge link allowed conveyance as a channel link would, until the stage dropped below that of the ridge crest elevation.

### 1.5 Levees

When levee features were implemented in the ICM as a component of structural protection projects, the approach described above for ridge restoration projects was used. In addition to the link deactivation as described in Section 1.4, a large number of hydraulic control structures were included with the structural protection projects. These newly activated control structures were implemented in the ICM in the same manner that was used for activating new control structures in the hydrologic restoration projects (Section 1.1)

## 1.6 Oyster Reefs

Oyster reef restoration projects construct bioengineered reefs with shell cultch or engineered/artificial substrate that promotes oyster colonization. Continued oyster recruitment and growth is expected to augment the constructed reef to enhance protection and coastal restoration benefits, including protecting shorelines from erosive forces, reducing saline intrusion, and reducing open water fetches. The oyster reef candidate projects for the 2017 Coastal Master Plan are landscape-scale projects with features and effects large enough to be resolved by the ICM.

Within the model, an oyster restoration project affected the landscape evolution with a reduction in the marsh edge erosion rate. The project footprints were not included in the landscape (DEM) or incorporated into the hydrology subroutine. Instead, a polygon shapefile bounded by the oyster reef crest and a 1 km inland buffer delineated the affected shoreline areas. The marsh edge erosion rates and the eroded sediment within the compartment were then updated in a manner identical to the implementation of shoreline protection projects.

Oyster reef restoration projects also directly impacted the Attachment C3 -12 Oyster Habitat Suitability Index Model (HSI), where the HSI is a function of the computed salinity and the percent of the water bottom covered in oyster cultch. For model runs that incorporated oyster reef projects, separate HSI initial condition rasters were developed that increased the cultch bottom cover percentage within the oyster reef project footprint.

## 1.7 Marsh Creation

Marsh creation projects created wetlands in open water areas and re-graded existing marsh land through placement of dredged material and vegetative plantings. Marsh creation projects were incorporated into the ICM via the DEM and hydrology links. The footprint shapefile of the marsh creation project was used to insert the project into the DEM, using the attributes (such as marsh elevation) specified. It was specified in the code that marsh creation projects were not implemented in locations where the water depth was greater than 0.76 m North American Vertical Datum of 1988 (NAVD88) at the year the project was implemented. This was done to avoid inadvertent filling of channels on the landscape. As the implementation year varied per project, the fill volume was calculated at the time of implementation to more accurately determine the fill volume required to reach the desired marsh elevation.

The hydrology links in the ICM were also adjusted to implement the marsh creation projects. Marsh links were added at compartment faces as needed and existing were modified or removed due to the placement of the project. All channel links within the marsh creation polygons were converted to "maintained channel" links with a constant bottom elevation if they were intended to remain channel links following project implementation. Channel links were converted to "composite channel" links if they represented non-channelized flow in marsh areas. The cross-sectional area of these composite channel links was updated via the marsh creation project implementation code to adjust exchange as the composite link fills in with sediment.

## 1.8 Diversions

Diversion projects create new conveyance channels to divert fresh water and sediment from coastal Louisiana's rivers into adjacent basins. Diversion projects were modeled within the ICM in

multiple ways, depending upon the upstream source of water to be diverted. Many of the modeled diversions involved diverting flow from the Mississippi River into the wetland areas adjacent to the river. The Mississippi River is not included within the ICM model domain, though its influence on the estuarine basins is modeled as a series of flow distributaries; a fixed amount of the Mississippi River flow is modeled as direct flow input into specific model compartments adjacent to the channel. For example, the model compartment representing West Bay in the Bird's Foot Delta received an influx of flow (with suspended sediment and water quality constituents) that is equal to a defined portion of the river flow. This same approach was used to implement all of the diversion projects that propose to divert the Mississippi River water into the adjacent wetland areas.

Some diversion projects were modeled at a relatively small but constant design flowrate, such as the 5,000 cubic foot per second (cfs) Central Wetlands diversion (001.DI.18). For these projects, the design flowrate was added as a direct, constant flowrate input into the receiving model compartment. However, the majority of the diversion projects were modeled with an assumed operation regime dependent upon the flowrate within the river. The flowrate of diverted waters were calculated from linear rating curves based upon the design flowrate defined by CPRA. Many diversions were operated such that during low river flow periods, the diversion was inactive. Once the Mississippi River was flowing at a rate greater than the low flow threshold, the diversion flowrate would increase linearly based upon the rating curve assigned. The design capacity of each diversion project, as well as the river flowrates used to define the design flowrate, and the low flow thresholds are provided in Appendix A – Project Definitions.

For all Mississippi River diversion projects, the flowrate within the river immediately downstream of the diversion intake was updated to account for the diverted flow. This residual flow was then used for the next diversion point downstream (either proposed or an existing distributary). While the Mississippi River was not included within the hydrodynamic subroutine, a mass/flow balance was conducted on the inflow boundary conditions, a priori, in order to accurately calculate the river flow available to be diverted at each location.

The above procedure was used for modeling diversion projects along the Mississippi River. There were three other diversion projects that were implemented using a different methodology. One of these was the Manchac Landbridge Diversion (001.DI.100), a proposed diversion connecting the Bonnet Carre Spillway to the adjacent swamp forest area. This hydraulic connection was modeled by simply adding a new open channel link within the hydrology subroutine, connecting the model compartment representing the Spillway to the model compartment representing the adjacent swamp area. When water levels within the Spillway were high enough to enter this channel (either during Bonnet Carre gate openings or high water periods in Lake Pontchartrain), the model would divert flow into the swamp area as a function of the differential water elevations represented in the model.

The other projects that utilized a different approach were the two diversion projects diverting water from the Atchafalaya River: Atchafalaya River Diversion (03a.DI.05) and Increase Atchafalaya Flow to Terrebonne (03b.DI.04). Unlike the Mississippi River, the Atchafalaya River is within the ICM domain; the model compartments and links automatically update the river flowrate downstream of the diversion locations based upon the hydrodynamics of the modeled system. To implement these two projects, a new open channel link was added to the model domain representing each diversion location. The flow within these diversion links was then assigned as directly proportional to the flow within the main stem of the Atchafalaya River immediately upstream of the diversion location. The portion of flow diverted for 03b.DI.04 was 11% of the Atchafalaya River flow, and 03a.DI.05 diverted 26%. If a simulation was required with both of these diversions active at the same time, the diverted flow reduced to 8% and 17% of

the Atchafalaya River flow for 03b.DI.04 and 03a.DI.05, respectively. The proportion of river flow diverted was determined from a study of these two proposed projects (Moffatt & Nichol, 2016).

## 1.9 Barrier Islands

Barrier island restoration projects were implemented in the ICM by incorporating a project design template into the DEM that represents the cross-shore profiles (spaced at 100 m in the long-shore direction) within the Barrier Island Model (BIMODE) subroutine. The project design template specified a project footprint area and a cross-shore profile with defined elevations for beach, dune, and back barrier marsh zones. When implemented within the model, the pre-project elevation data were updated to meet the elevations prescribed in the design template. The amount of fill required to build to the design elevation varied based upon implementation year and scenario; therefore, the required fill volume was calculated to accurately determine the variation in project costs.

The design elevation and areal extent of the barrier island restoration projects were prescribed prior to model implementation. However, the exact location of the project was not predetermined due to different rates of island migration over time. The project location was determined by matching the template shoreline location with the FWOA shoreline location at the beginning of the implementation year. This was required because the fill volume calculation was performed by comparing the pre- and post-project elevations. If a static template location was used, fill volumes (and subsequent project costs) would be inaccurate due to the migration of barrier island shorelines over time.

The BIMODE subroutine has a model structure defined by cross-shore profiles; the spatial resolution is 2 m in the cross-shore direction with 100 m spacing of profiles in the long-shore direction. This resolution was sufficient to accurately represent the project design template, but the resolution was adjusted when BIMODE output was passed to the wetland morphology subroutine. The BIMODE cross-shore profiles are interpolated into a 30 x 30 m DEM that is stitched into the coast wide DEM used by the wetland morphology subroutine. This 30 m DEM is the elevation dataset that was provided to the ADCIRC+SWAN model; however, the barrier island portion of the ADCIRC+SWAN domain utilized the high resolution cross-shore profile data directly from the post-project BIMODE output.

## 1.10 Surge and Wave Modeling of Restoration Projects

The ADCIRC+SWAN model implemented restoration projects using the project properties as they were described by the ICM model outputs. The projects were applied to the ADCIRC+SWAN model in the form of changes to topographic/bathymetric elevation and changes to land use characteristics which were converted into frictional parameters. The same control volume averaging method used to implement future environmental scenarios was also applied here (Attachment C3-25.1; Appendix 3, Figure 53).

The exceptions to the control volume averaging method were for the treatment of ridge restoration and barrier island projects. Like other raised features, such as roadways and coastal ridges, which are not modeled as weirs but are still important for flood routing, ridge restoration projects and barrier islands had explicitly defined crown elevations. This approach avoided artificially lowering crown elevations due to smoothing associated with the control volume averaging technique. Ridge crown elevations were applied using the DEM processed from ICM model outputs. Barrier island crown elevations were similarly mapped from BIMODE outputs.

## 1.11 Structural Protection

### 1.11.1 ADCIRC / SWAN

Structural hurricane protection projects evaluated in the 2017 Coastal Master Plan include one or more of the following basic components: earthen levee, concrete T-wall, and floodgates. Floodgates are typically constructed at road, railroad, and water body crossings. Additionally, pump stations are included in the interior of ring levees. The ADCIRC+SWAN model was used to evaluate how structural protection projects affected water surface elevation (surge) and wave response throughout coastal Louisiana.

To maximize computational efficiency, structural protection projects were divided into six model mesh groupings. An example grouping is shown on Figure 2 and contains four projects. Groupings were chosen such that projects would not interact and, therefore, could be studied in isolation though they were simulated in the same model mesh.



Figure 2: Example Hurricane Protection Project Grouping for the Project Implementation phase.

Project features (i.e., earthen levee, concrete T-wall, and floodgates) were implemented using ADCIRC’s weir boundary condition. The ADCIRC weir boundary condition defines a feature that is too small to be captured accurately solely using finite elements in a particular model region. Overtopping volumes were computed using the formula for a broad crested weir when the computed stillwater elevation on either side of the boundary exceeds the specified crest elevation. Crest elevations are defined by the design elevations for each project feature. If the crest elevation is not exceeded, the feature appears numerically as a vertical wall.

The SWAN model also implements these features as vertical walls; however, wave heights are assumed to be reduced to zero when crossing the feature before being allowed to redevelop on the opposite side of the boundary. Overtopping volumes due to waves were not computed within ADCIRC+SWAN.

Many other such features are implemented in ADCIRC this way, including significant local levees and federal levees such as the Mississippi River levees, Greater New Orleans levees, and the levees encompassing Larose to Golden Meadow. For the purposes of this modeling effort, all structures were assumed to be in their closed position, and pumps were not operated.

### 1.11.2 CLARA

Structural risk reduction projects, including new or upgraded earthen levees, concrete T-walls, floodgates, and pumps were evaluated using the CLARA model to estimate their potential for flood depth and damage reduction. The structural features evaluated in the 2017 analysis are described in Appendix A of the 2017 Coastal Master Plan (McMann et al., 2016).

Structural projects are represented as elevated weir features in surge and wave hydrodynamic modeling. These projects are each incorporated into one of six coast wide groups that include sets of projects expected to provide independent utility and benefits, so that the effects of one project in a group do not interact or conflict with another. In the case of unenclosed protection projects (i.e., fronting barriers), storm surge and wave results from a sample of 60 simulated storms are used directly for statistical flood depth calculations in the CLARA model pre-processing module at each CLARA grid point (Fischbach et al., 2016).

For upgraded or newly enclosed protected systems, alternately, storm surge and wave results are provided with the project in place for a series of “surge and wave points” (SWPs) surrounding the protection system. In these cases, information about the new or upgraded system within the CLARA model flood depth module is also utilized to estimate flood depths in enclosed areas. The additional information includes structure heights, fill or armoring characteristics, geospatial alignment, and the location of transition features such as pumps or gates (see Appendix A). Enclosed protected systems are then evaluated using the CLARA model flood depth module using the same approach described in Fischbach et al. (2012 & 2016).

The CLARA model generates statistical estimates of flood depth annual exceedance probabilities at every CLARA grid point with both unenclosed and enclosed projects in place for each group to produce a final set of future with project (FWP) flood depths. This exercise is repeated for every combination of project group, environmental scenario, and fragility scenario in the 2017 analysis. All scenarios are evaluated in year 25 and year 50 future conditions. Note, however, that only the low environmental scenario is evaluated in year 10; CPRA assumes that these results can be used as a reasonable proxy for the year 10 medium and high scenario conditions to better conserve supercomputer resources for hydrodynamic modeling.

Next, a series of geospatial polygons are generated which indicate the zone of influence for each structural project within a group. These polygons are developed based on a combination of storm surge and wave results and expert judgment. These polygons are used to estimate the effects of the individual structural projects within each group, with the assumption that only grid points within the polygon for a given project will change from the FWOA to FWP. Flood depth changes outside of the project influence zone are disregarded. In this way, a coast wide project group can be divided into a series of individual, regionally focused project effects. Furthermore, when evaluating enclosed protected systems, only changes to SWPs within the project influence zones are considered in the flood depth module; if a portion of the system lies outside of any

project influence zone, the FWOA surge and wave values are used instead. This is done to reduce the potential impact of noise in the ADCIRC and SWAN models.

Finally, the CLARA model damage module is used to estimate direct damage from flooding with the project in place and summarized using the expected annual damage (EAD) metric at each CLARA model grid point. Influence zone polygons are again used to assign FWP damage to individual projects. Results from the FWP and FWOA analysis are then summed and aggregated using the methods described in Fischbach et al. (2016), Sec. 5.3.4, to estimate the mean and standard deviation of the change in EAD (risk reduction project benefit) for each of the 54 summary risk regions across the Louisiana coast. Except for year 10, for reasons noted above, this process is repeated for every project group, environmental scenario, and fragility scenario evaluated in the CLARA model. The damage estimates also include three distinct population and asset growth scenarios (Fischbach et al., 2016), adding an additional layer of scenario uncertainty on the flood depth results using full factorial combination.

## 1.12 Nonstructural

Nonstructural projects are evaluated directly in the CLARA damage module according to the methods described in Fischbach et al. (2012 & 2016).<sup>1</sup> For the 2017 analysis, these projects consider different levels of investment in flood hazard mitigation in different coastal communities, all compared to the FWOA flood damage level as a baseline. The CLARA model uses a set of decision rules to determine where and how much investment would be made. Specifically, “project variants” describe how decisions are made regarding which 1) locations and 2) structures are eligible for elevation, floodproofing, or acquisition.

Project variants are defined by the standards for mitigation heights used to determine which structures should be elevated, floodproofed, or acquired. The standards are determined by median estimates of the 100-year flood depths at each CLARA model grid point under a specified landscape scenario and year, plus two feet of “freeboard” above the median 100-year depth. Project variants differ in which landscape scenario and year these depths are drawn from; grid point locations with no 100-year flood depths are not considered for investment in a given variant. More detail on the iterative process used to identify project variants can be found in Groves et al. (2016).

The CLARA team developed and provided an initial set of analysis results to the Planning Tool Team to support CPRA’s identification of nonstructural project variants. These data were provided for each proposed variant and CLARA model grid point under each of the future scenarios under consideration. Specific data provided include:

- Counts of the structures elevated, floodproofed, and acquired;
- Costs of elevations, floodproofing, and acquisitions; and
- Benefits of nonstructural risk reduction (reduction in EAD compared to FWOA).

The CLARA team also provided data summarizing other relevant characteristics of areas considered for nonstructural risk reduction investment to help support the identification of project variants. These include the percentage of households categorized as low to moderate income (LMI), the number of properties that have suffered repetitive loss (RL) or severe repetitive loss (SRL) from flood events in the past, and estimates of median 100-year flood depths under

---

<sup>1</sup> Note that a version of this discussion also appears in Fischbach et al. (2016), Sec. 8.4.

initial conditions and in selected future scenarios. Estimates of the percentage of LMI households and the number of RL and SRL properties by grid point were derived from the Department of Housing and Urban Development (HUD) FY 2014 low to moderate income summary data (HUD, 2015), as well as data provided by CPRA originally provided by the Federal Emergency Management Agency (FEMA) and the Louisiana Governor’s Office of Homeland Security and Emergency Preparedness (GOHSEP), respectively.

Key assumptions related to nonstructural project implementation in the CLARA model include:

- Following the 2012 analysis, this analysis assumes 70% participation when voluntary nonstructural mitigation incentives are offered. This means that 70% of eligible structures are mitigated in targeted CLARA model grid points.
- Residential structures can be elevated up to a maximum of 4.3 m above existing adjacent grade. If the standard exceeds this level, the structure is acquired instead.
- Commercial, industrial, and public buildings can receive dry floodproofing if the foundation is three feet or less below the reference standard. Residential dry floodproofing is not considered in this analysis.

The parameter values for the seven project variants chosen for evaluation by CPRA are summarized in Table 1. The mitigation standards determined by each variant were run through the CLARA economic module for every combination of flood depth and economic scenario. Separate decisions are made in the Planning Tool for each of 54 “nonstructural project areas,” which correspond directly to the CLARA model risk regions but only include geographic regions that have assets identified as eligible for nonstructural investment (see Fischbach et al., 2016). The seven variants were run through each of the 54 nonstructural project areas, yielding a total of  $7 \times 54 = 378$  separate nonstructural projects for consideration in the 2017 Coastal Master Plan analysis.

**Table 1: Selected Nonstructural Project Variants.**

Project variant	Landscape scenario	Year	Additional filters
1	-	1 (initial conditions)	-
2	Low	10	-
3	Medium	10	-
4	High	10	-
5	Medium	10	Only grid points where LMI > 30%
6	Medium	25	-
7	High	25	-

Using the final set of nonstructural project variants identified, the CLARA team provides data to the Planning Tool Team describing results from the analysis for each variant in each future year and scenario condition. One data set describes the characteristics of the project variants, including their construction costs, the numbers of structures mitigated by structure type, and nonstructural project duration. Duration is calculated as a function of the total number of structures mitigated in each risk region using a crosswalk provided by CPRA (Table 2).

**Table 2: Nonstructural Project Duration Assumptions.**

Structures mitigated (risk region)	Assumed duration (years)
0-30	1
31-200	2
201-500	3
501-1000	4
1,001-2,000	5
2,001+	7

Another dataset describes the summary characteristics of the areas where nonstructural mitigation is implemented, including percent LMI, count of RL and SRL properties, and number of structures eligible for mitigation. As with the structural projects, all of these results are summarized by risk region. Finally, a third set details the estimated EAD reduction benefits from each nonstructural project, comparing the with-project and FWOA damage values using the same methods described above for structural projects. The final results are summarized by nonstructural project variant, risk region, scenario, and year.

## 2.0 Initial Conditions

### 2.1 Landscape and Ecosystem

The initial characteristics of landscape and ecosystem are, for the most part, derived from existing data sources. Information about these initial conditions datasets, data sources, and data preparation is provided in Attachment C3-27 – Landscape Data. Some adjustments were made to account for projects recently constructed or that are expected to be constructed in the near future (Appendix A). The graphics below show the initial conditions for the 2017 Coastal Master Plan modeling effort. Figure 3 shows starting elevations across the coast, Figure 4 shows coast wide land-water configuration, and Figure 5 shows initial vegetation cover.

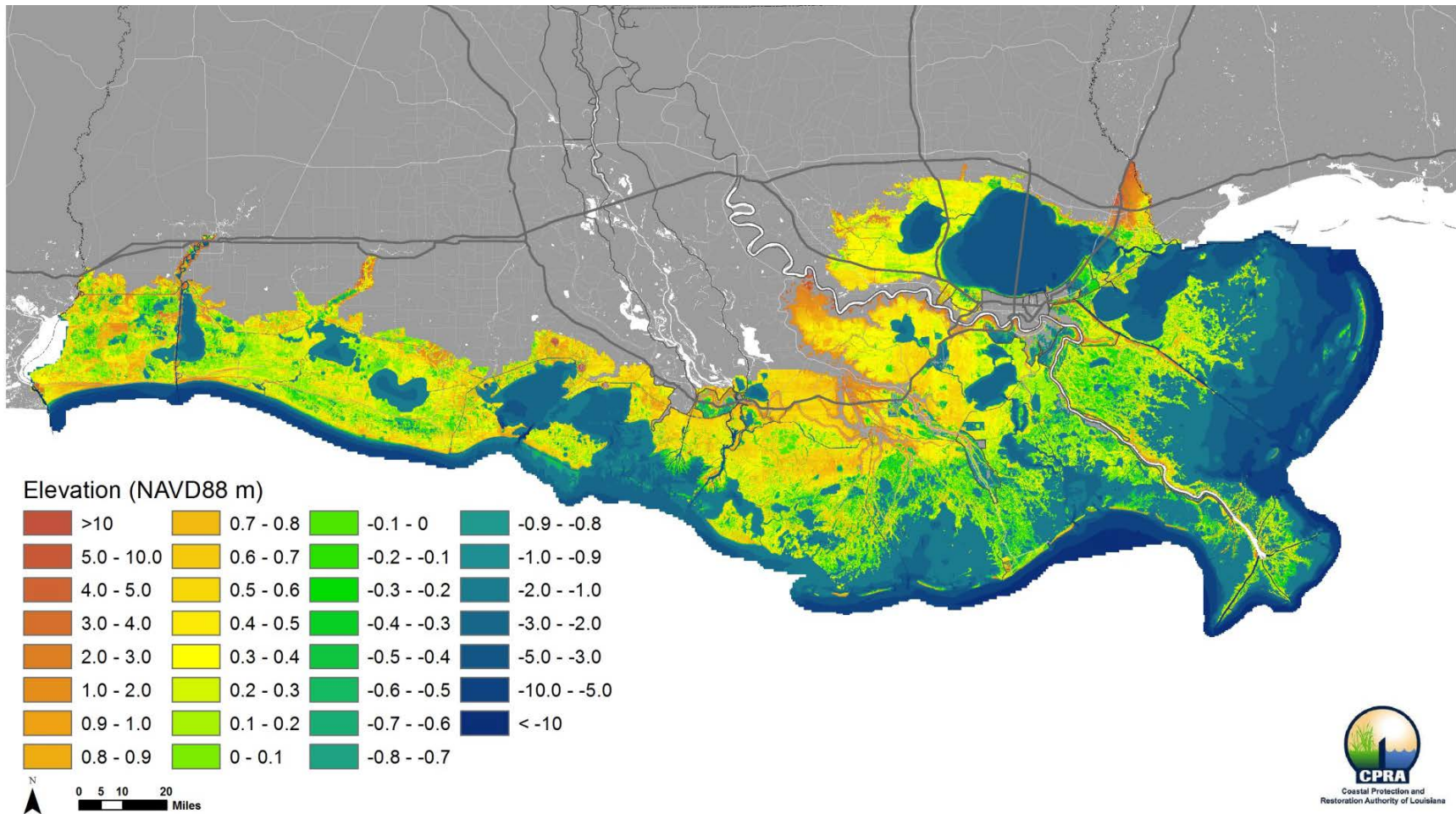


Figure 3: Initial Topography and Bathymetry for the 2017 Coastal Master Plan Modeling Effort.

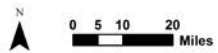
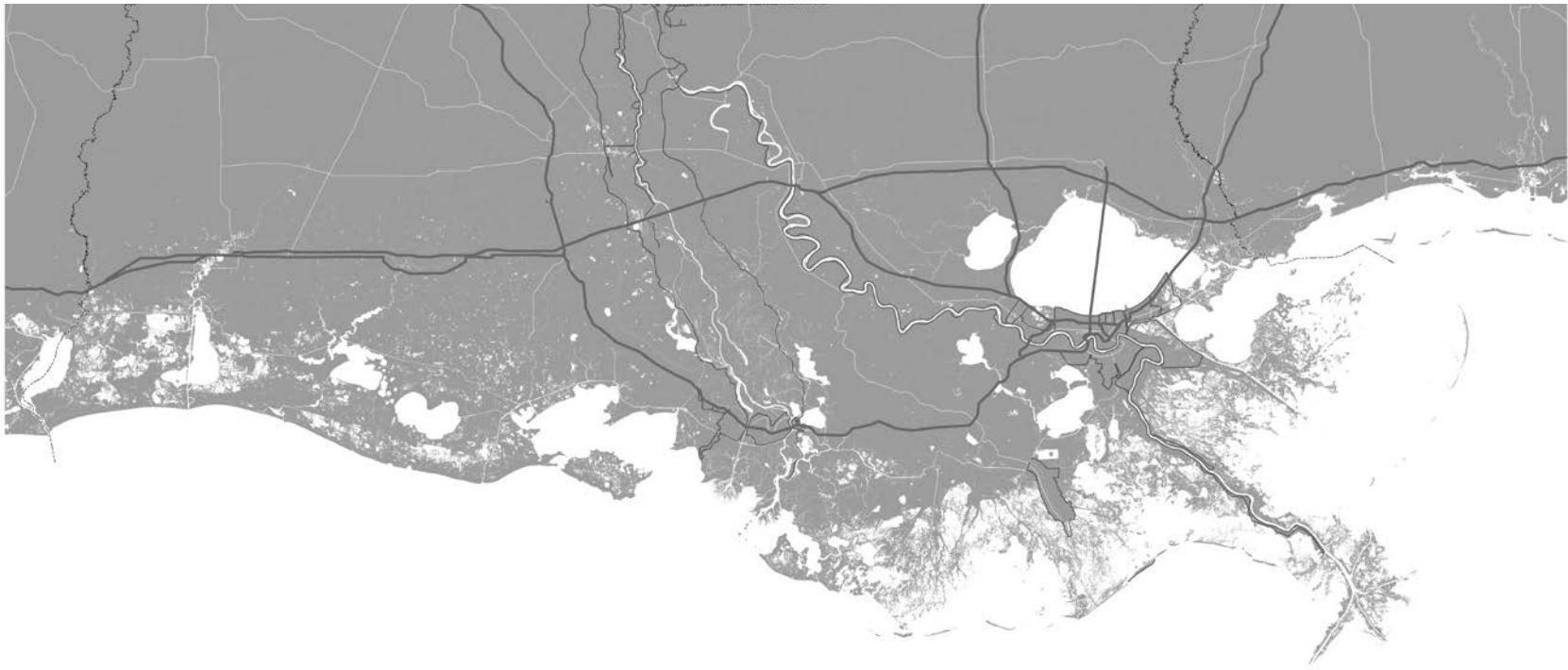


Figure 4: Initial Land/Water for the 2017 Coastal Master Plan Modeling Effort.

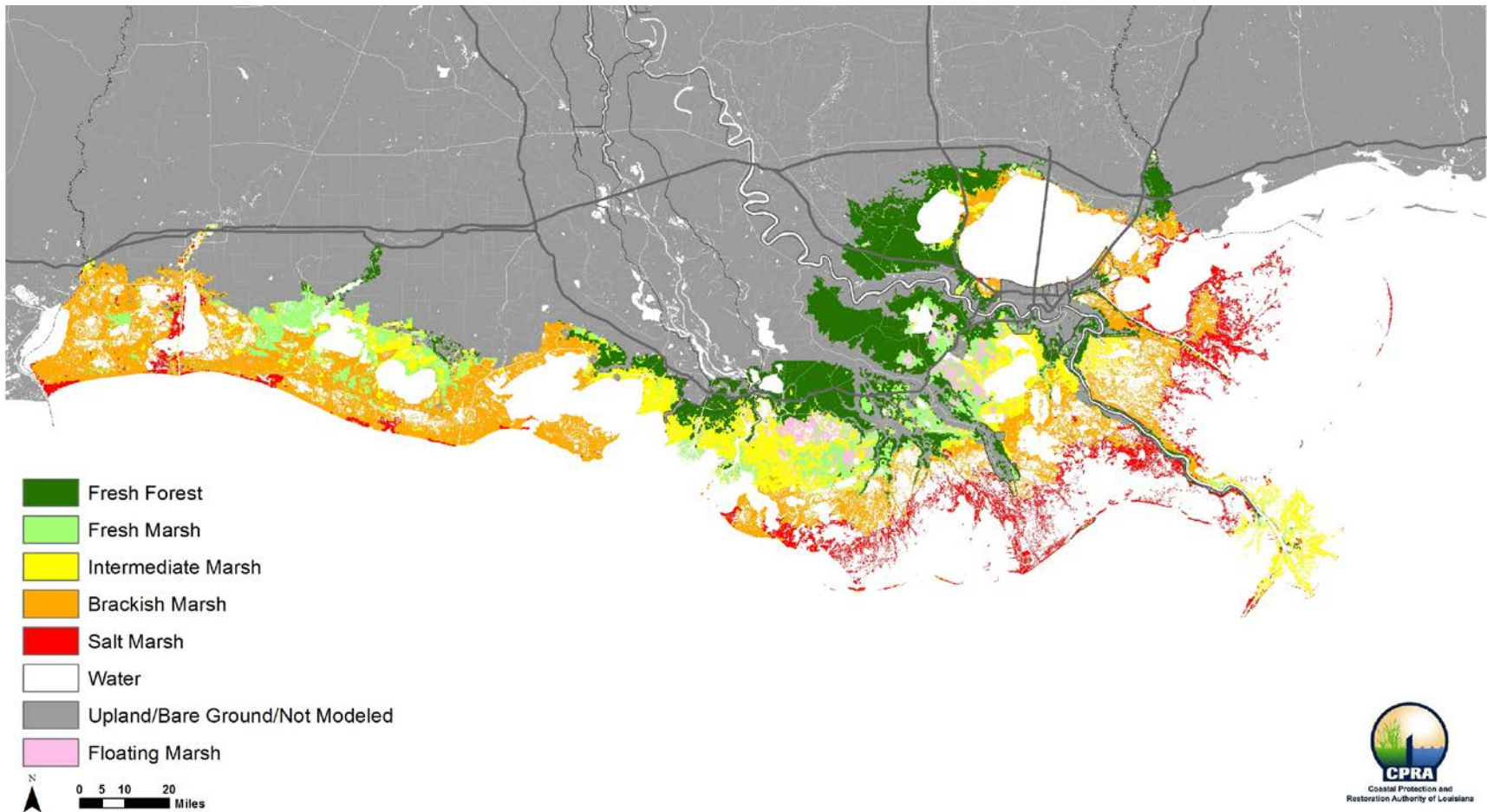


Figure 5: Initial Vegetation Cover for the 2017 Coastal Master Plan Modeling Effort.

## 2.2 Flood Depth

ADCIRC and SWAN simulations were conducted on the initial conditions model geometry to ensure model stability and performance, validate the model, and establish surge and wave responses for comparison to future scenarios. The mesh was created using the best available data sources for present-day bathymetry, topography, levee crest elevations, and other raised-feature elevations (e.g., roadways and coastal ridges) (CPRA, 2015). In addition to the landscape information described above, land cover data that included the distribution of vegetation species was also used (see Attachment C3-27 – Landscape Data). Model parameters, including Manning’s  $n$  (frictional resistance to flow) and directional roughness length (applied as a wind velocity reduction factor), were assigned using the initial conditions land cover. Figure 6 through Figure 8 show the elevation, Manning’s  $n$ , and directional roughness length model inputs used for the initial conditions simulations for surge and waves.

Maximum surge, maximum significant wave height, peak wave period and wave direction were examined for initial conditions simulations. For the purposes of illustration, images of maximum surge, maximum wave height, wave period, and time series surges are shown for two storms. The wave period and directions shown are those that occurred at the same time as the maximum wave height. Figure 9 through Figure 12 show storm 014, which makes landfall in the eastern side of the state. Figure 13 through Figure 16 show storm 218, which makes landfall in the western side of the state.

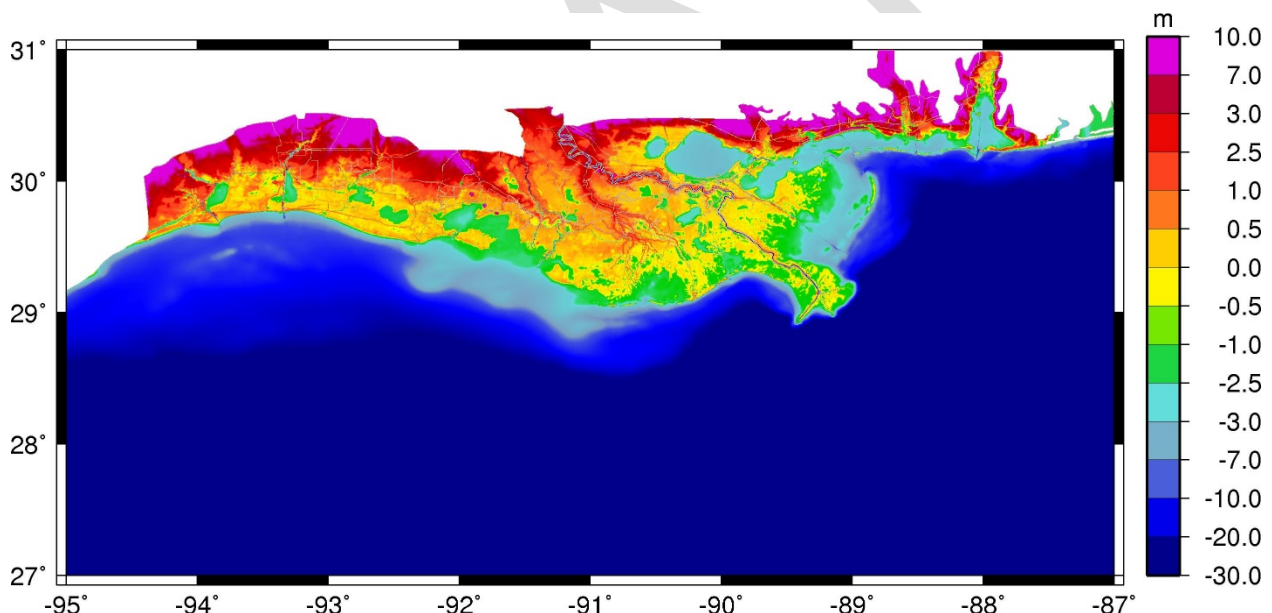


Figure 6: Topography and Bathymetry (meters, NAVD88 2009.55) Used for Simulation of the Initial Conditions.

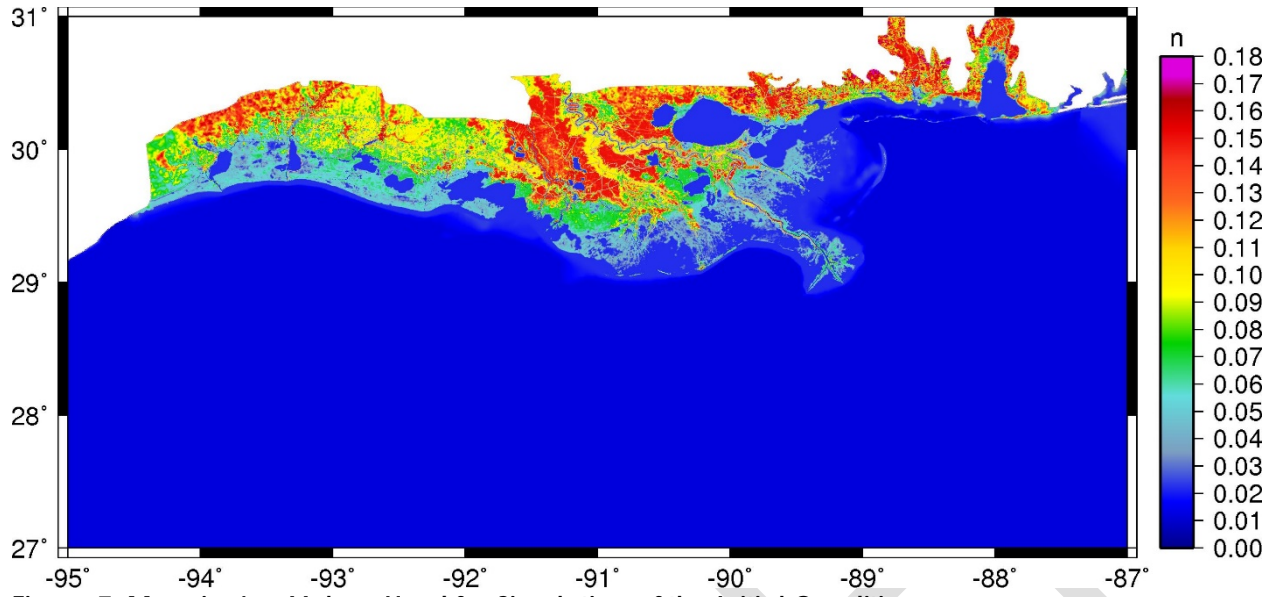


Figure 7: Manning's n Values Used for Simulation of the Initial Conditions.

DRAFT

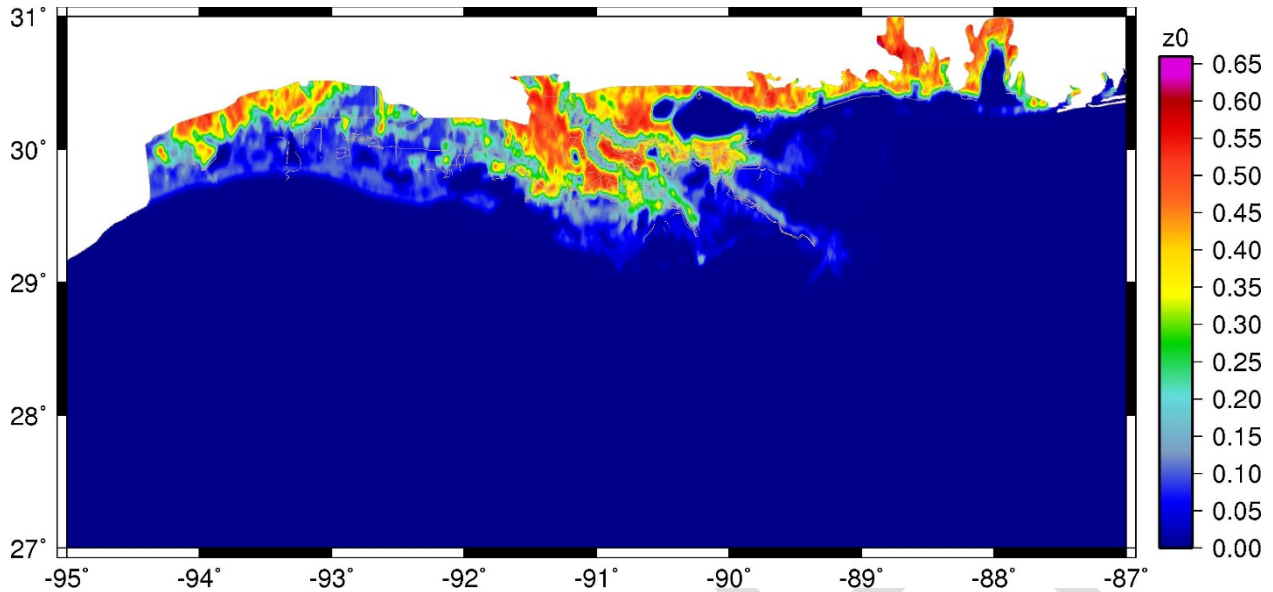


Figure 8: Directional Roughness Length Used for Simulation of the Initial Conditions. Values shown are for wind blowing from south to north.

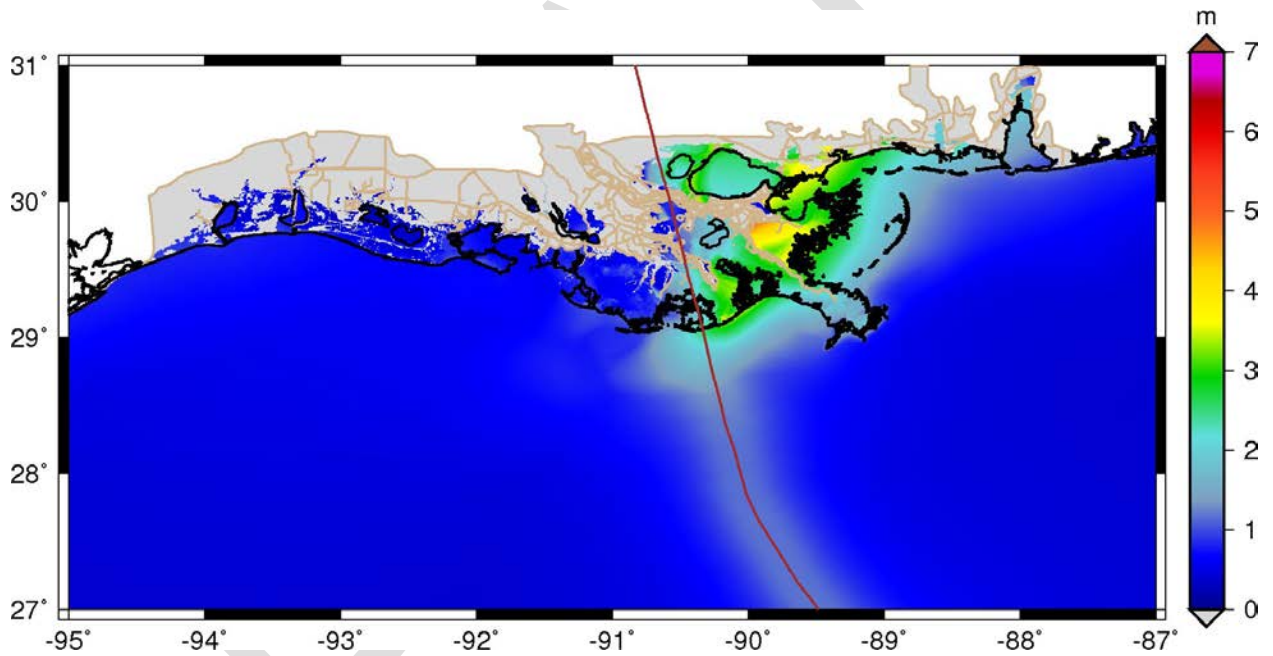


Figure 9: Maximum Surge Elevations (meters, NAVD88 2009.55) During the Initial Conditions Simulation of Storm 014.

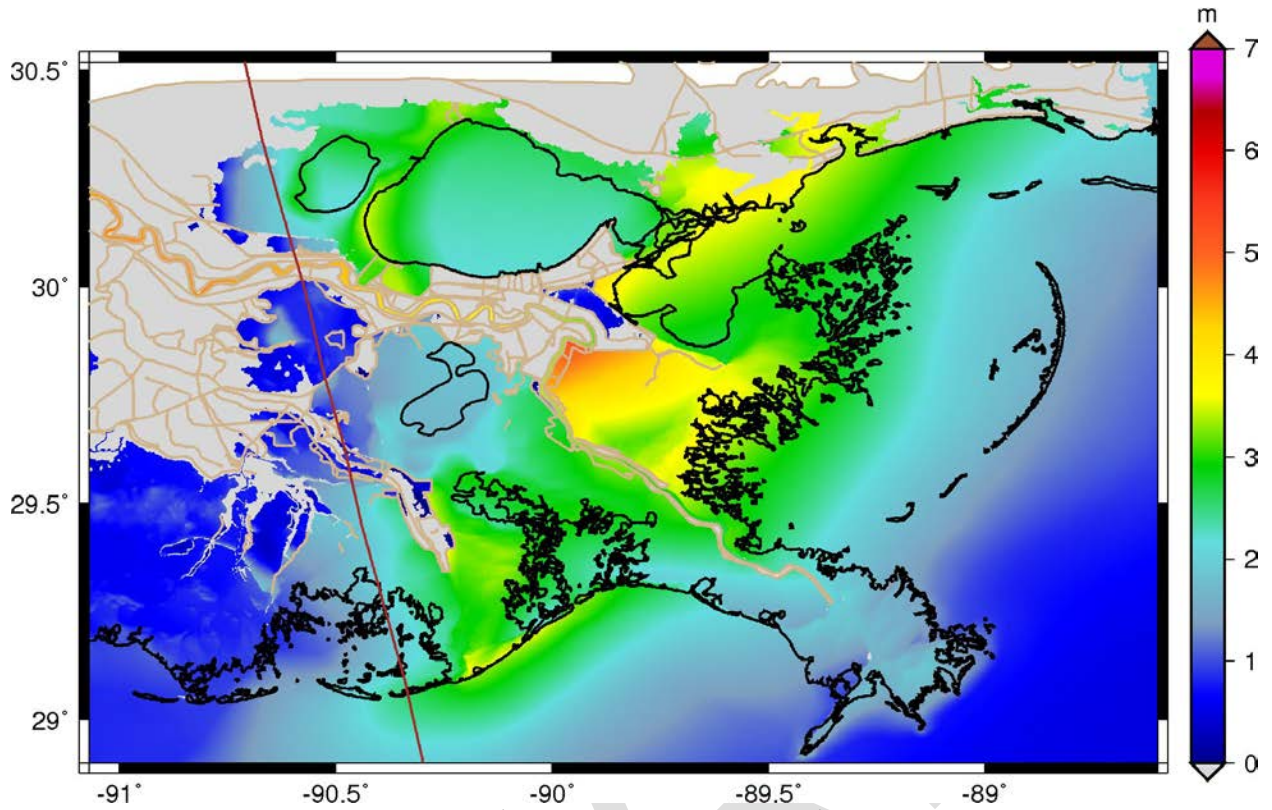


Figure 10: Maximum Surge Elevations (meters, NAVD88 2009.55) During the Initial Conditions Simulation of Storm 014.

DRAFT

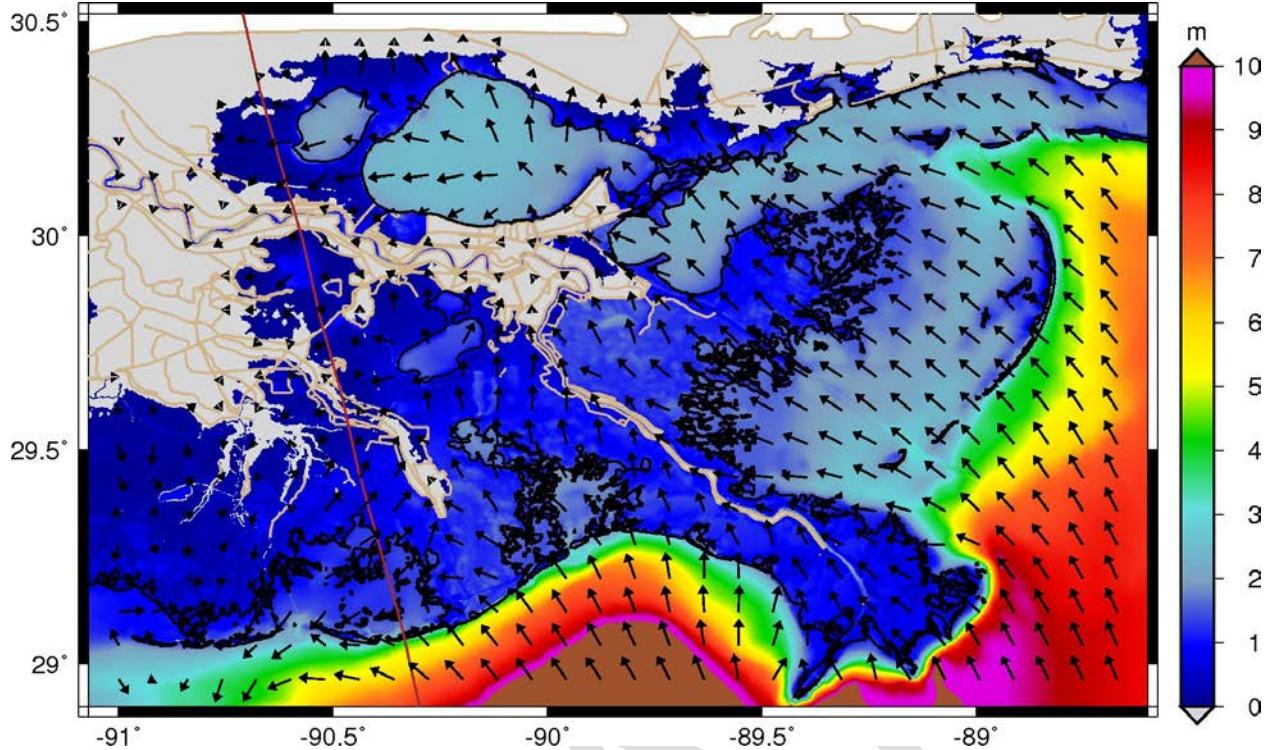


Figure 11: Maximum Significant Wave Heights (meters) and Associated Directions During the Initial Conditions Simulation of Storm 014.

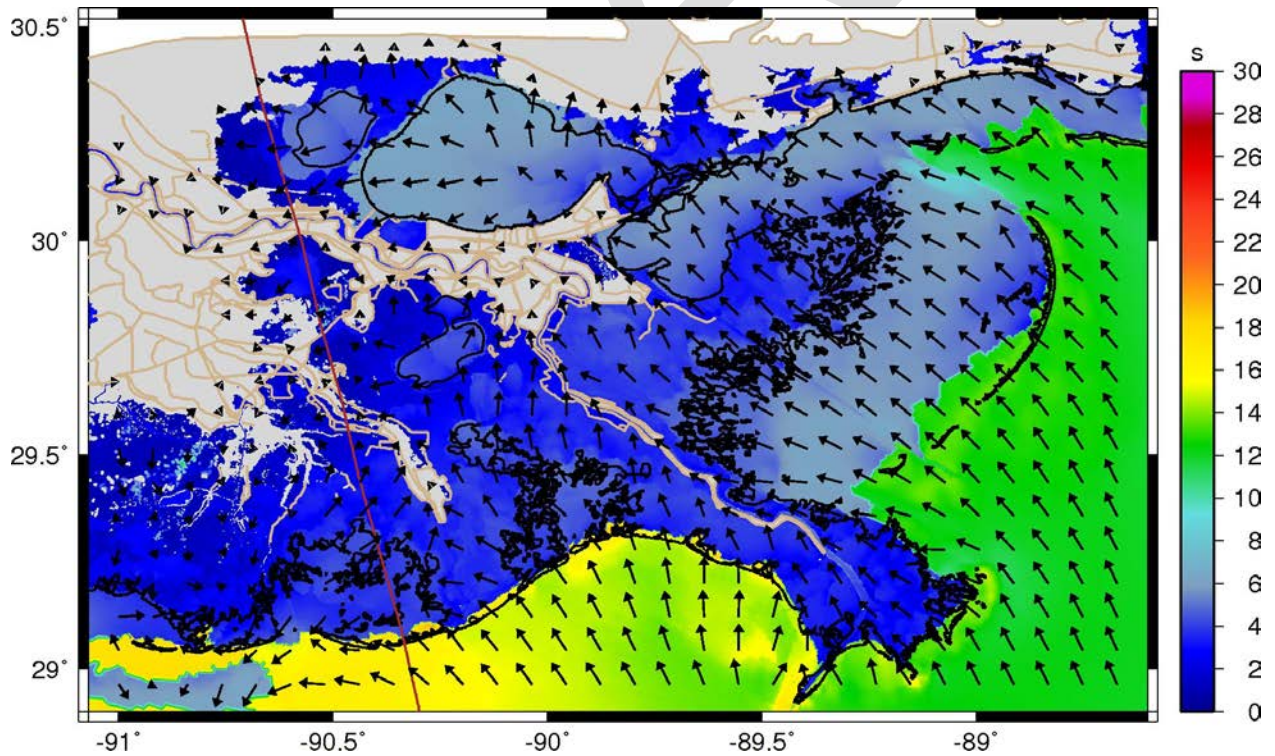


Figure 12: Peak Wave Periods (seconds) and Associated Directions During the Initial Conditions Simulation of Storm 014.

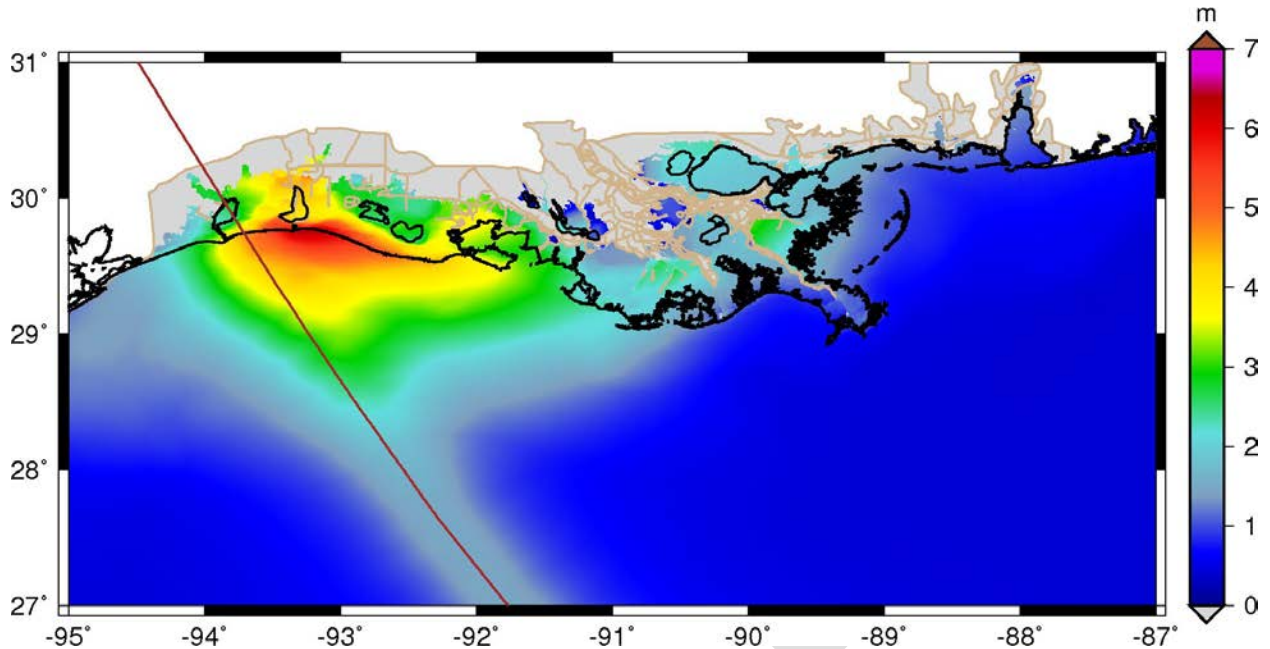


Figure 13: Maximum Surge Elevations (meters, NAVD88 2009.55) During the Initial Conditions Simulation of Storm 218.

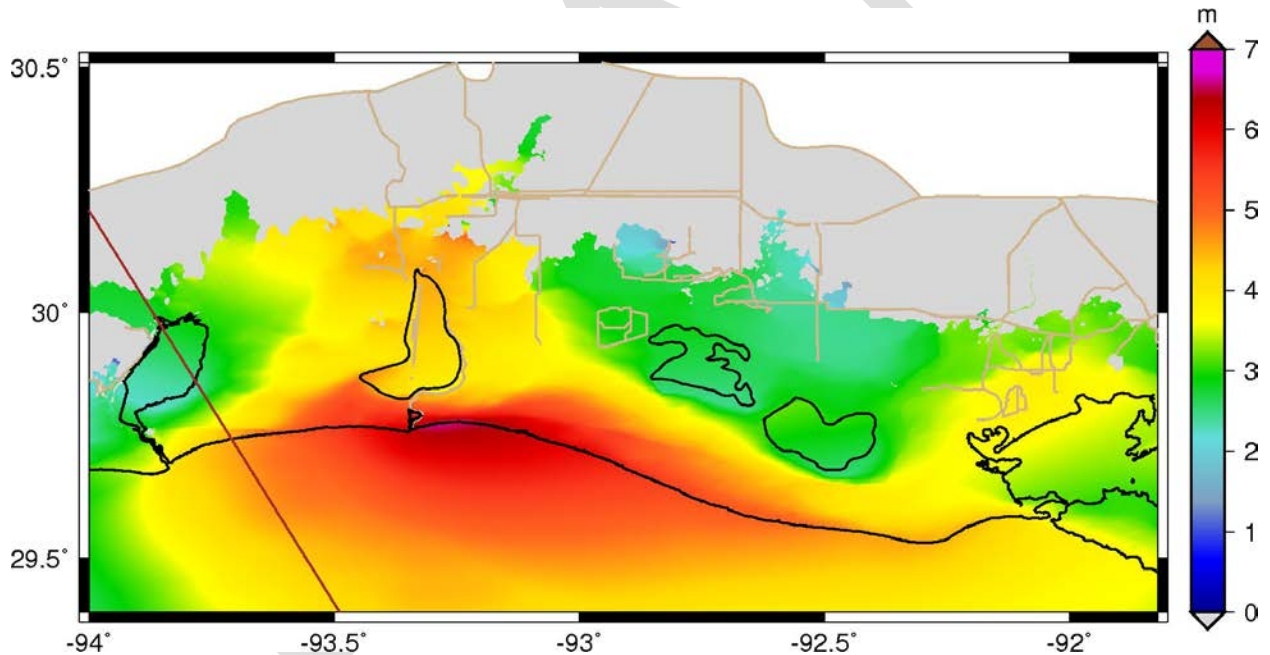


Figure 14: Maximum Surge Elevations (meters, NAVD88 2009.55) During the Initial Conditions Simulation of Storm 218.

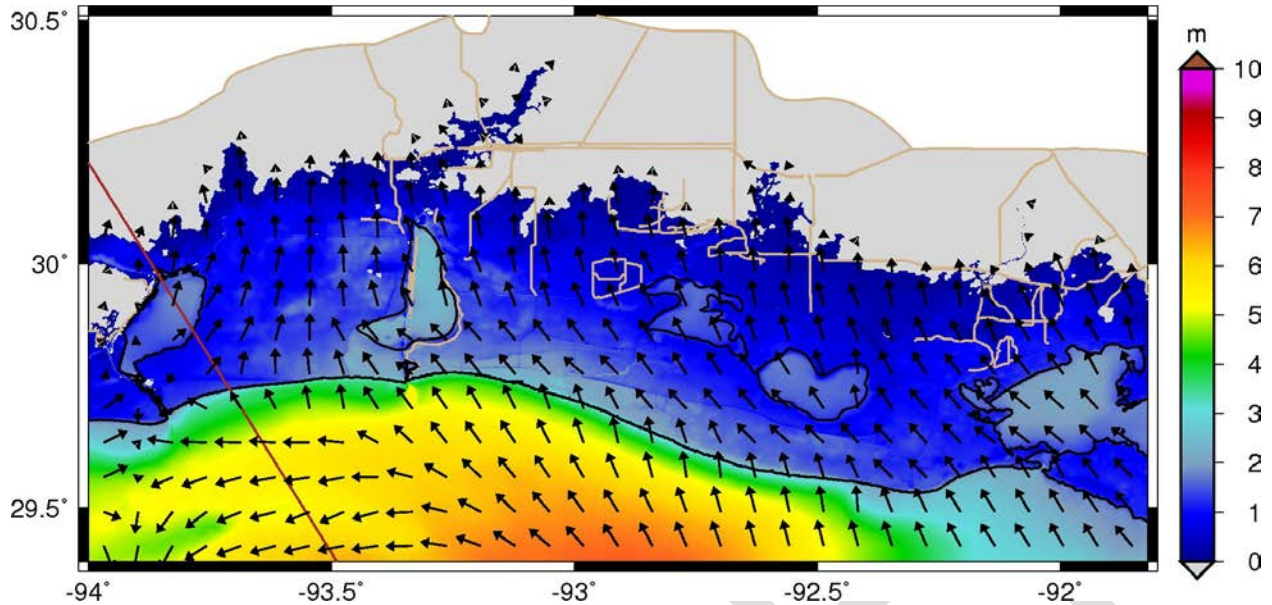


Figure 15: Maximum Significant Wave Heights (meters) and Associated Directions During the Initial Conditions Simulation of Storm 218.

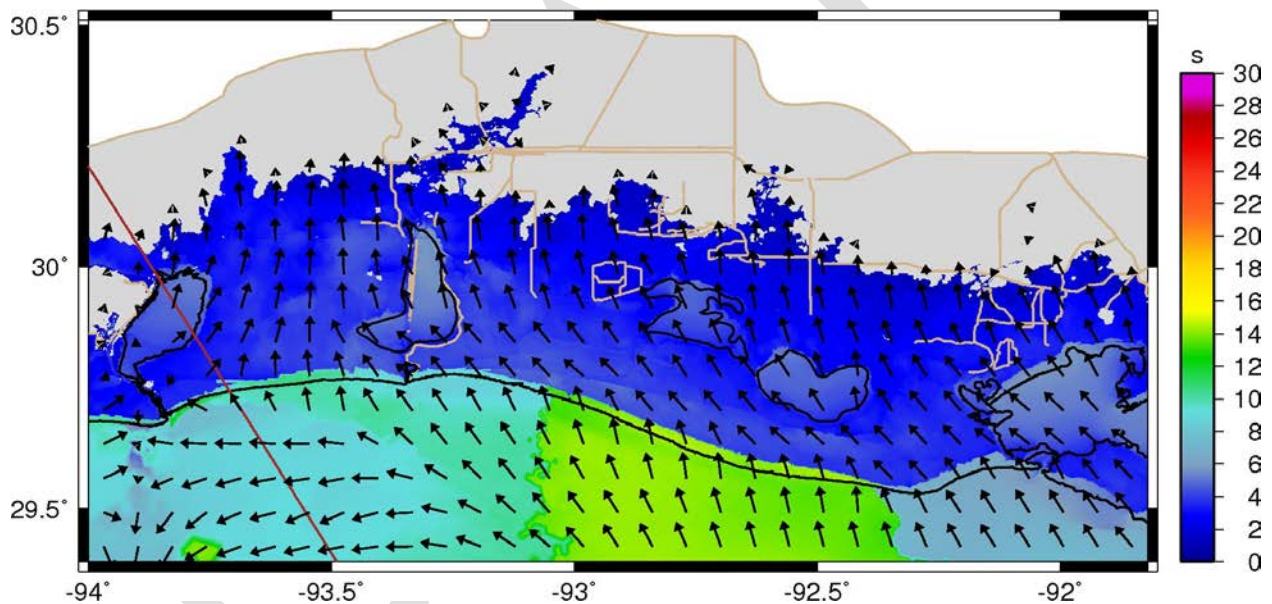


Figure 16: Peak Wave Periods (seconds) and Associated Directions During the Initial Conditions Simulation of Storm 218.

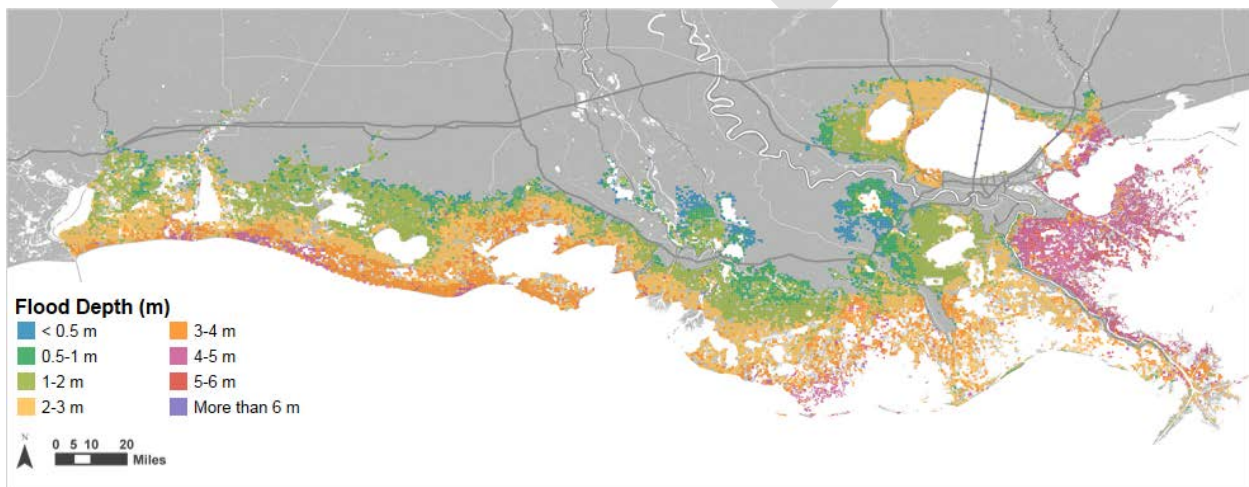
Statistical results for initial conditions were generated using an adapted Joint-Probability Method-Optimal Sampling (JPM-OS) approach from a set of 92 hypothetical storms simulated using the ADCIRC and SWAN storm surge and wave models (see Attachment C3-25, Sec. 6.5). Flood depth recurrence was estimated for unenclosed areas and enclosed areas, respectively, from the 10-year (10% chance) to the 2,000-year (0.005% chance) annual exceedance probability (AEP) interval.

For enclosed protected areas, three scenarios were included to represent alternative assumptions about the fragility of protection structures when overtopped:

- **No Fragility:** Storm surge and wave overtopping can occur, but no structure failure or breach flows occur;
- **IPET:** Fragility assumptions adapted from the Interagency Performance Evaluation Taskforce (IPET) Risk and Reliability Model (IPET, 2009); and
- **MTTG:** Fragility assumptions adapted from the U.S. Army Corps of Engineers Morganza to the Gulf (MTTG) Reformulation Study (USACE, 2013).

The possibility of levee failure was considered for all coastal levee, floodwall, and gate structures surrounding enclosed protected systems in the study region. Protection structures along the Mississippi River (Mississippi River and tributaries projects), by contrast, were assumed to have no probability of failure even when overtopped. For more information on the fragility scenarios and key related assumptions, see Attachment C3-25, Sec. 4.

Results for the 100-year AEP interval flood depths in the IPET fragility scenario are shown in Figure 17 for unenclosed areas of the coast. Many areas of the coast face more than 2 m of flooding at the 100-year interval in the initial conditions, while areas further upland show 1-2 m of depth for much of the remaining study area domain. Portions of the southeastern coast, including Lake Borgne and the east bank of Plaquemines Parish, face 100-year depths of 4-6 m in this analysis.



Note: 50th percentile 100-year flood depths of at least 0.2 m shown.

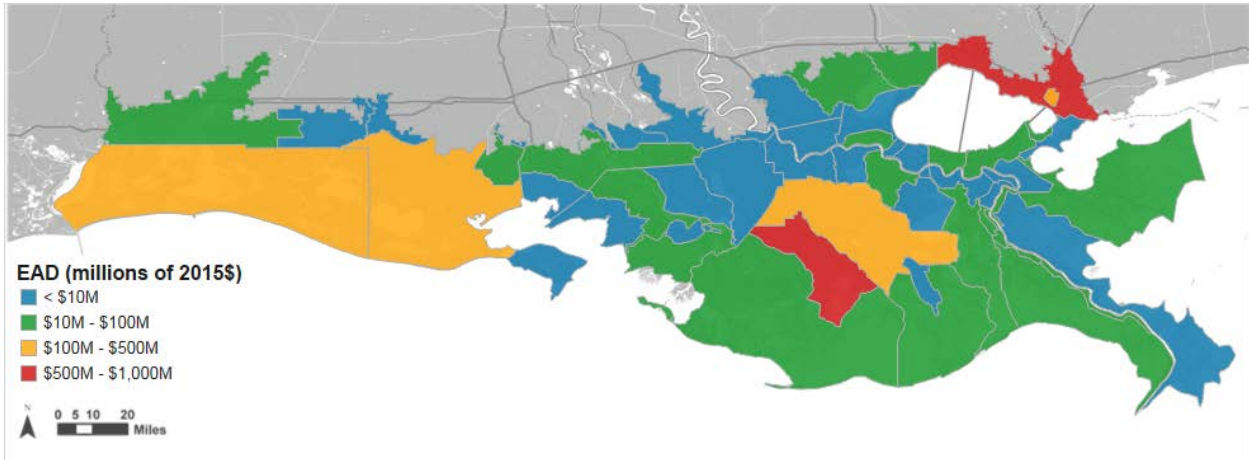
Figure 17: Initial Conditions 100-Year Coast Wide Flood Depths – IPET Fragility Scenario.

## 2.3 Damage

Direct damage from coastal flooding was also estimated with the CLARA model for initial conditions. Damage is summarized coast wide using the EAD metric, which represents an average of annual damage or loss for coastal Louisiana from Atlantic storms attaining a minimum central pressure deficit of 985 millibars (mb) or lower. Results are summed for each of 54 unique “risk regions” identified across the study area to support the 2017 Coastal Master Plan analysis (see Attachment C3-25, Sec. 8.3).

Overall, coast wide EAD in the initial conditions is estimated at \$2.7 billion (2015 constant dollars) in the IPET fragility scenario, with similar results observed in the No Fragility and MTTG scenarios (not shown). Levels of EAD in initial conditions vary by risk region (Figure 18). Regions with the highest initial EAD, exceeding \$100 million, include Cameron and Vermilion parishes, developed

areas in and around Houma (Terrebonne Parish) and Raceland (Lafourche Parish), and Slidell and other developed areas of St. Tammany Parish.



Note: Map shows mean expected annual damage for each risk region in the IPET fragility scenario.

**Figure 18: Initial Conditions Expected Annual Damage by Risk Region – IPET Fragility Scenario.**

### 3.0 Future Without Action

This section presents example outputs from the models for the 50-year FWOA simulations. Example outputs are included for key outputs for each of the models for each scenario. For the landscape and ecosystem outputs, the ICM was run for 50 years for each environmental scenario (Appendix C – Chapter 2). Storm surge, wave and risk models were run across landscape/land cover conditions generated by the ICM for year 10, year 25 and year 50.

#### 3.1 Stage

Stage is generated for over 900 different locations across the coast. To reflect aspects of the variation, the coast was divided into three hydrologic regions: PB: Pontchartrain/Barataria (including Bird’s Foot Delta), AA: Atchafalaya/Terrebonne, and CP: Chenier Plain. To assess the coast-landward gradients in each region, inland, intermediate, and coastal compartments were selected as shown in Table 3.

**Table 3: Compartments of Interest within Each Region.**

Region	Compartment of interest	Descriptive location	Location relative to the Gulf of Mexico coast
PB	248	East Lake Salvador	Inland
PB	278	Mud Lake/North Barataria Bay	Intermediate
PB	284	Northeast of Grand Isle	Near coast

Region	Compartment of interest	Descriptive location	Location relative to the Gulf of Mexico coast
AA	481	Lake Palourde	Inland
AA	512	Lake de Cade	Intermediate
AA	649	Caillou Bay	Near coast
CP	796	Northwest Grand Lake	Inland
CP	844	East Calcasieu Lake	Intermediate
CP	893	Holly Beach	Near coast

Figure 19 through Figure 21 show the 50-year time series for mean daily stage for PB (Barataria) for the low scenario for the inland, intermediate, and near coast compartments, respectively. Averaging has filtered the diurnal tides; the resulting stage record reflects the seasonal changes in the Gulf stage and the effect of wind. Sea level rise is evident in all these time series. The spikes in the record are due to storm surge events that are averaged in the daily stage and consequently, the spikes are much lower than the maximum surge level.

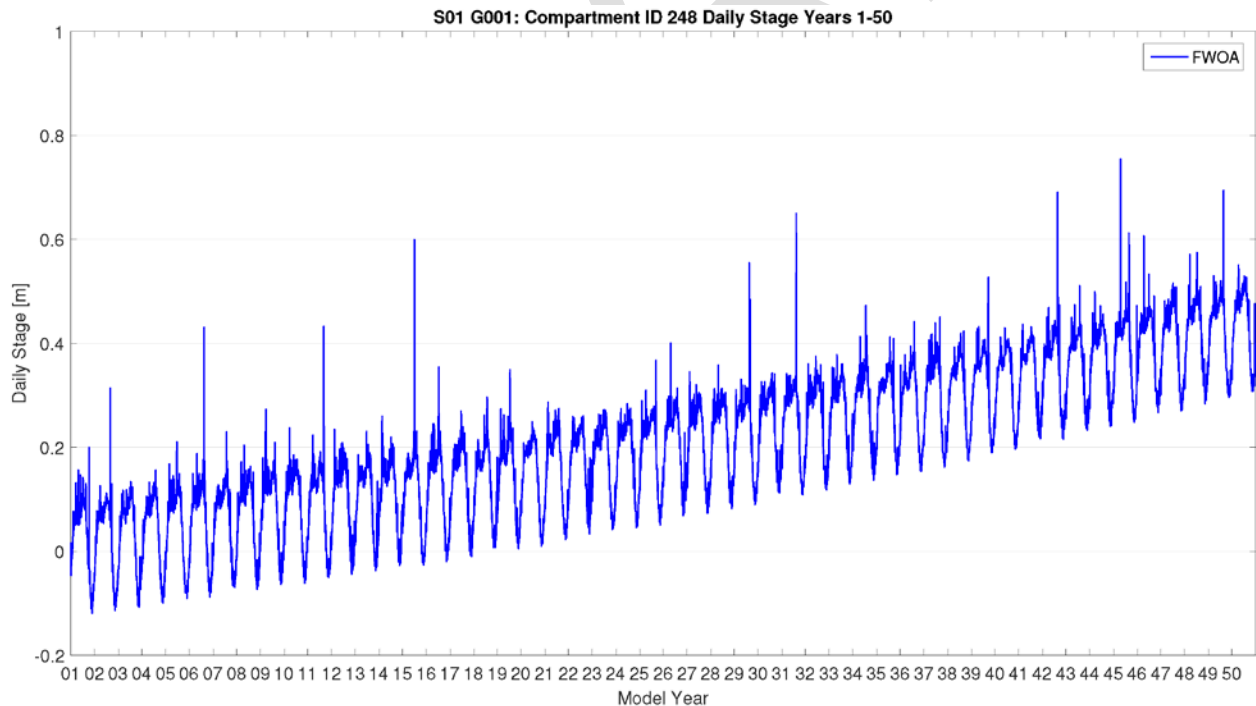


Figure 19: Mean Daily Stage in Compartment 248 - East Lake Salvador in PB for the Low Scenario (Representative of Inland Compartment Results).

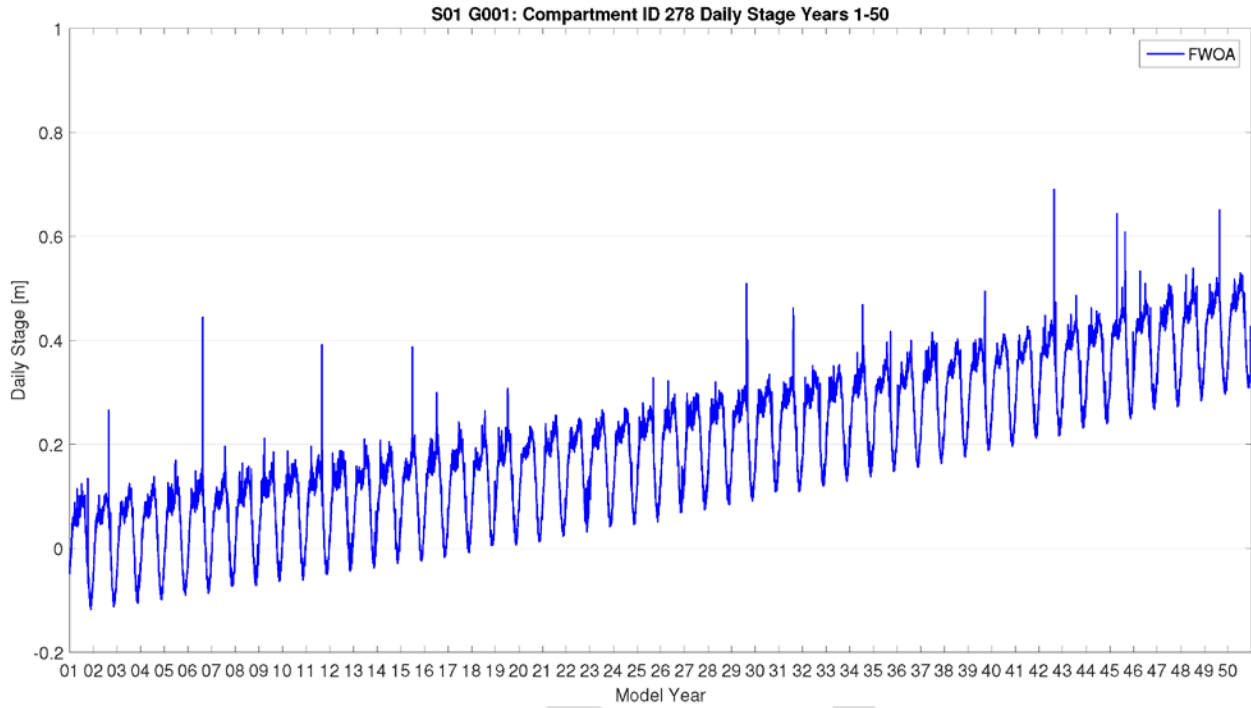


Figure 20: Mean Daily Stage in Compartment 278 - Mud Lake/Upper Barataria Bay in PB for the Low Scenario (Representative of Intermediate Compartment Results).

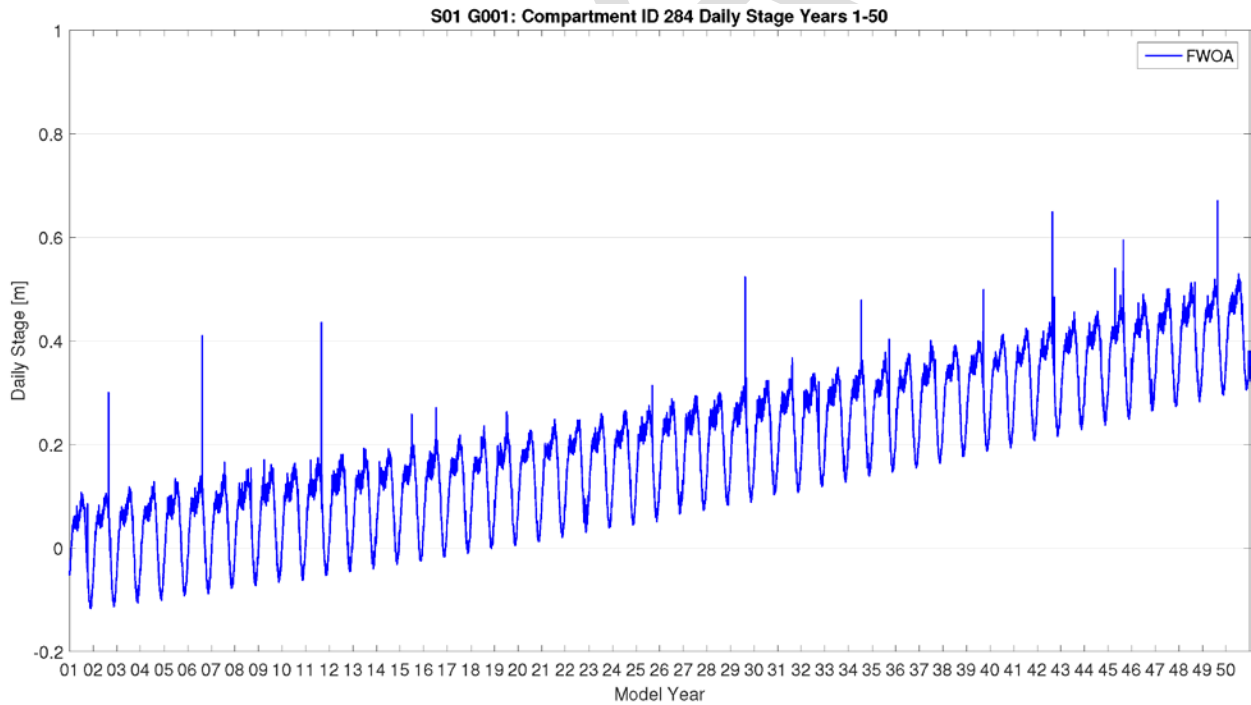


Figure 21: Mean Daily Stage in Compartment 284 - Northeast of Grand Isle in PB for the Low Scenario (Representative of Near Coast Compartment Results).

Figure 22 through Figure 24 show the 50-year time series for mean daily stage for PB (Barataria) for the high scenario for the inland, intermediate, and near coast compartments, respectively.

The format of the data is the same as for the figures above. Excluding hurricanes, the mean daily stage for the high scenario is approximately 0.4 m higher than for the low and 0.2 m higher than the medium scenario.

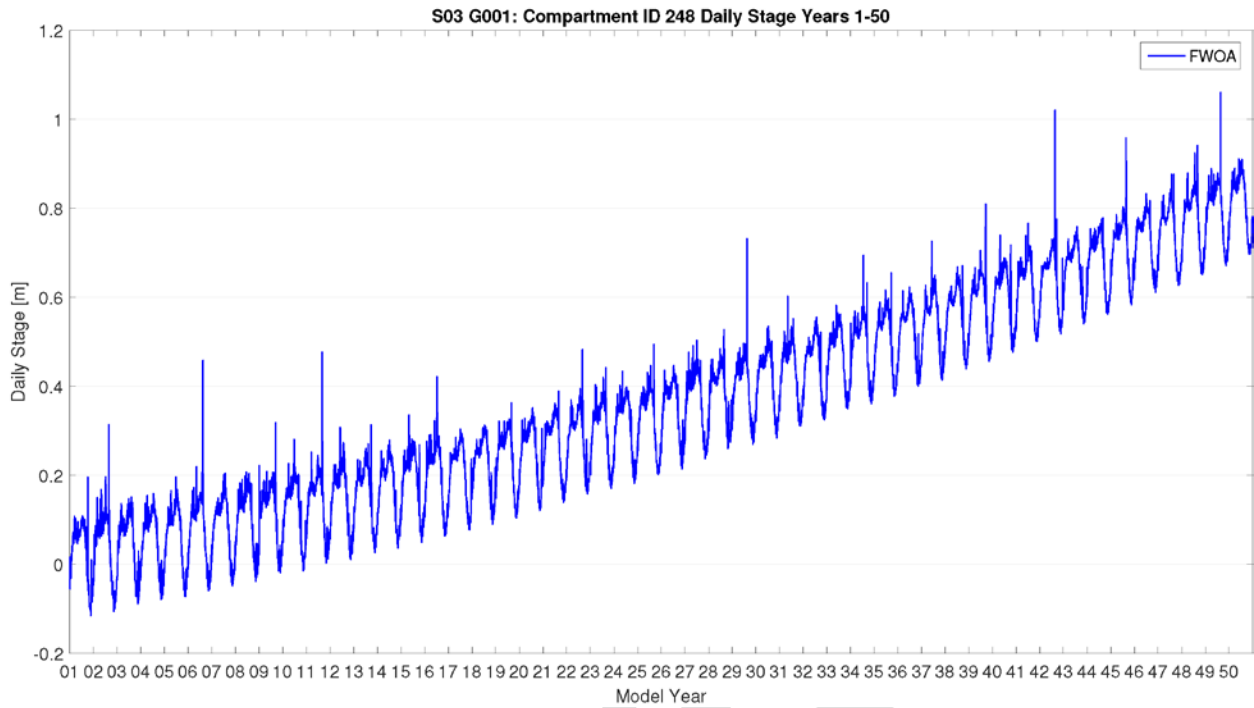


Figure 22: Mean Daily Stage in Compartment 248 - East Lake Salvador in PB for the High Scenario (Representative of Inland Compartment Results).

DRAFT

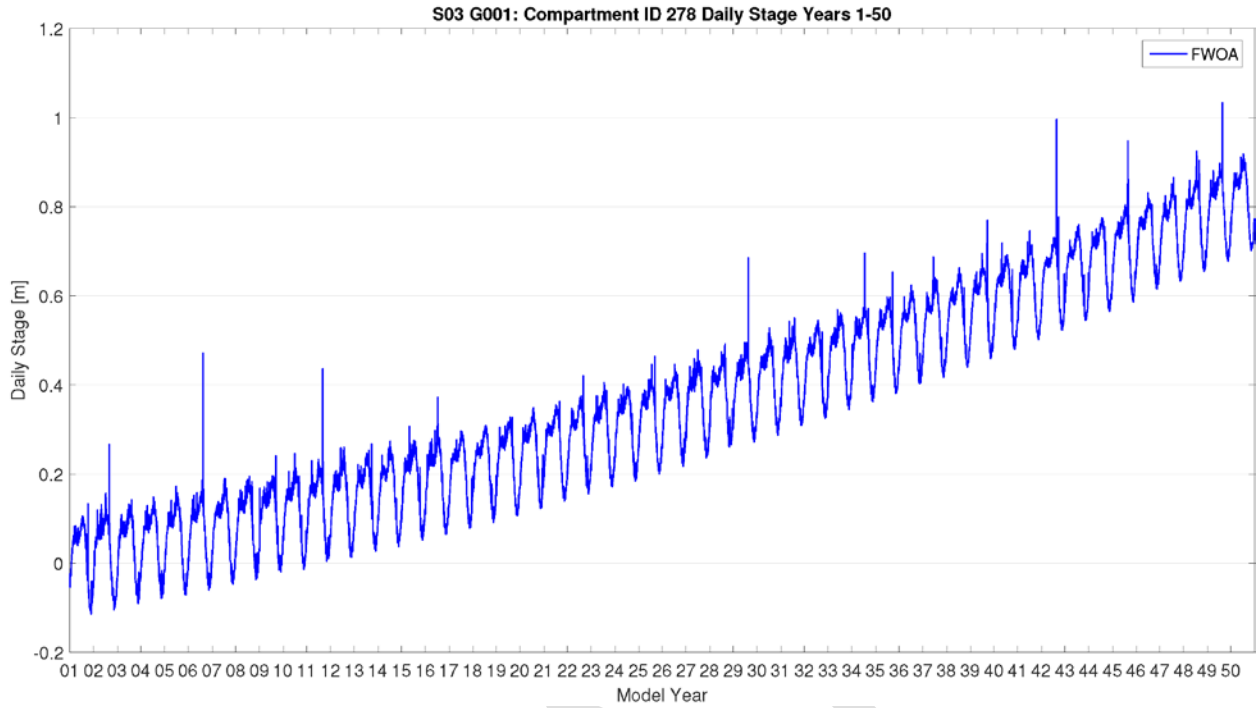


Figure 23: Mean Daily Stage in Compartment 278 - Mud Lake/Upper Barataria Bay in PB for the High Scenario (Representative of Intermediate Compartment Results).

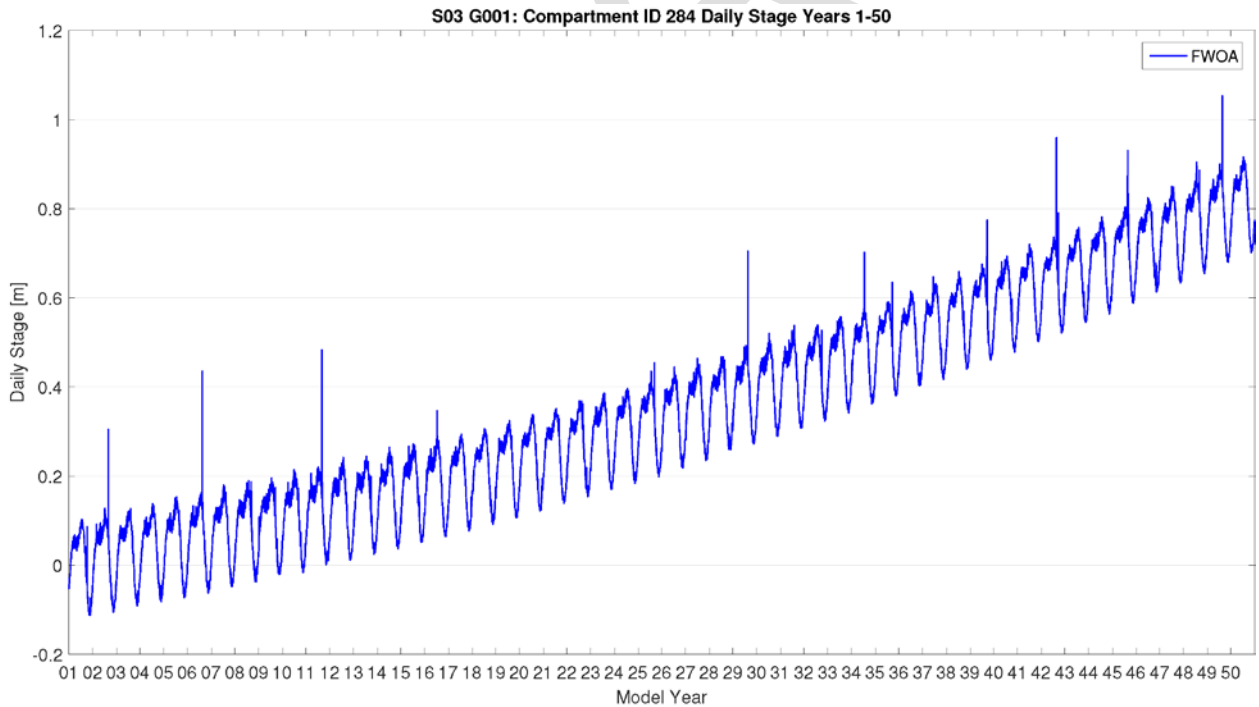


Figure 24: Mean Daily Stage in Compartment 284 - Northeast of Grand Isle in PB for the High Scenario (Representative of Near Coast Compartment Results).

Figure 25 through Figure 27 show the 50-year time series for mean daily stage for the AA (Atchafalaya/Terrebonne) region for the low scenario for the inland, intermediate, and near coast compartments, respectively.

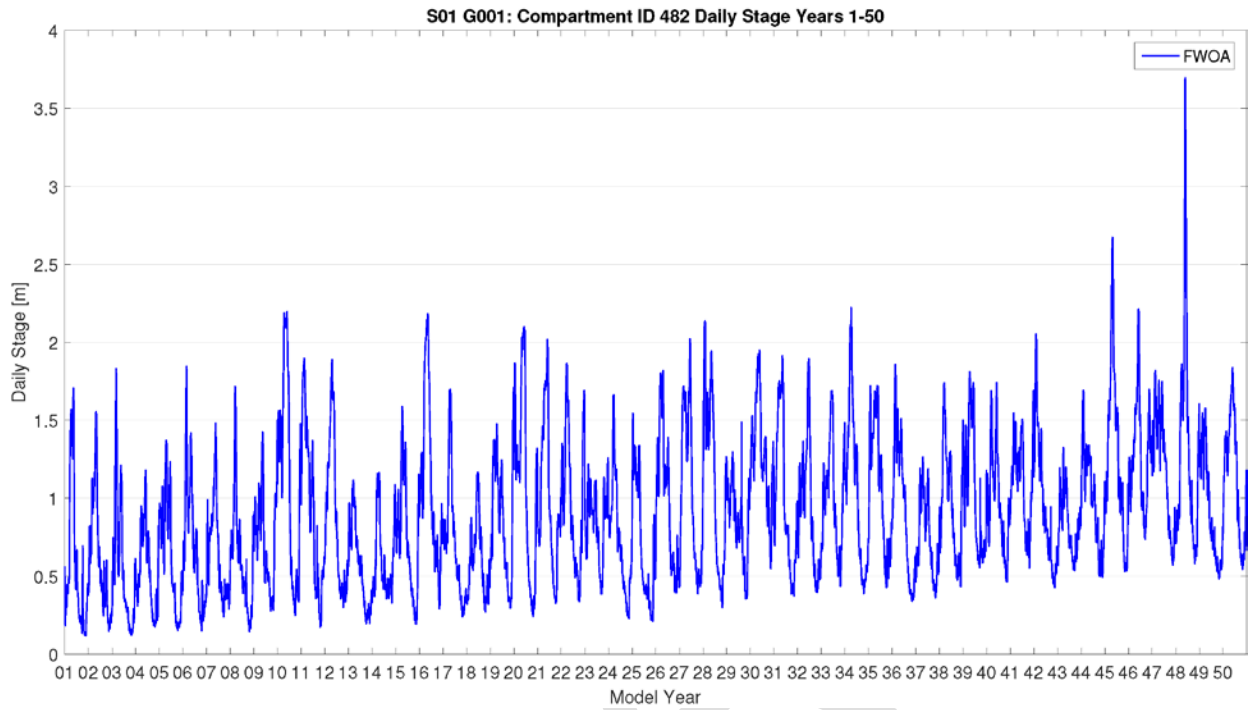
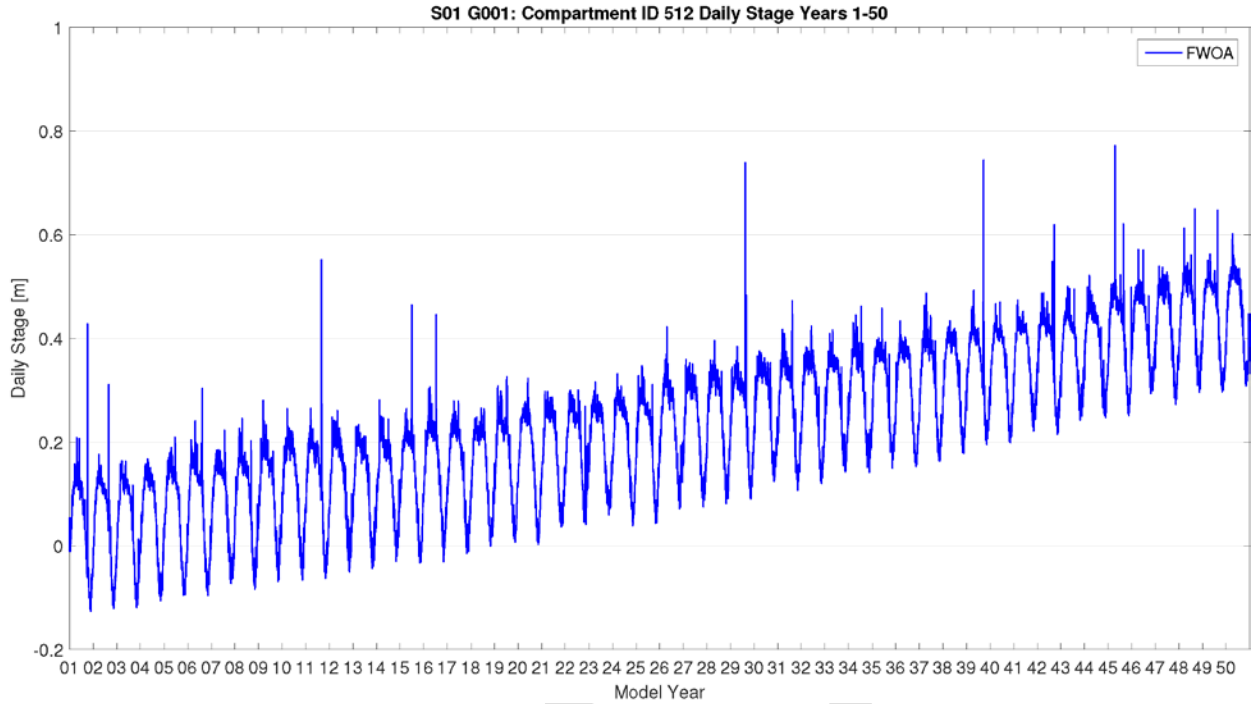
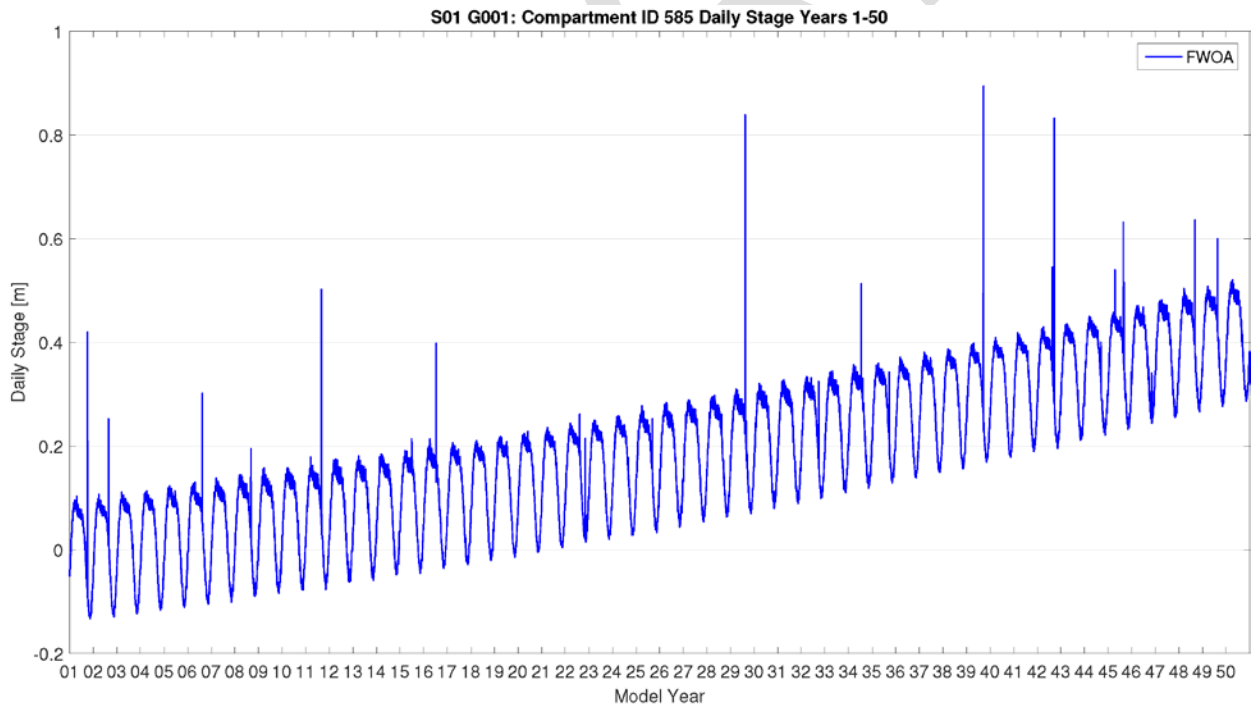


Figure 25: Mean Daily Stage in Compartment 482 – Lake Palourde in AA for the Low Scenario (Representative of Inland Compartment Results).

DRY



**Figure 26: Mean Daily Stage in Compartment 512 – Lake de Cade in AA for the Low Scenario (Representative of Intermediate Compartment Results).**



**Figure 27: Mean Daily Stage in Compartment 585 – Caillou Bay in AA for the Low Scenario (Representative of Near Coast Compartment Results).**

Figure 28 through Figure 30 show the 50-year time series for mean daily stage for the AA (Atchafalaya/Terrebonne) region for the high scenario for the inland, intermediate, and near coast compartments, respectively.

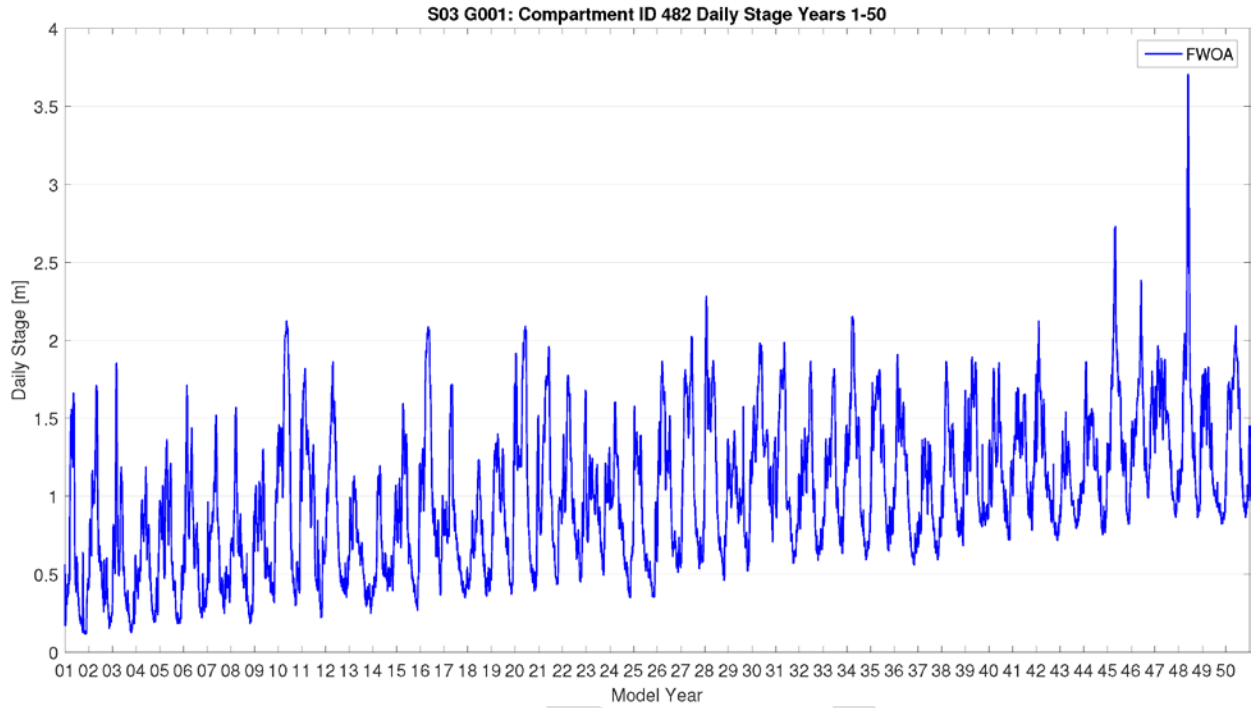


Figure 28: Mean Daily Stage in Compartment 482 – Lake Palourde in AA for the High Scenario (Representative of Inland Compartment Results).

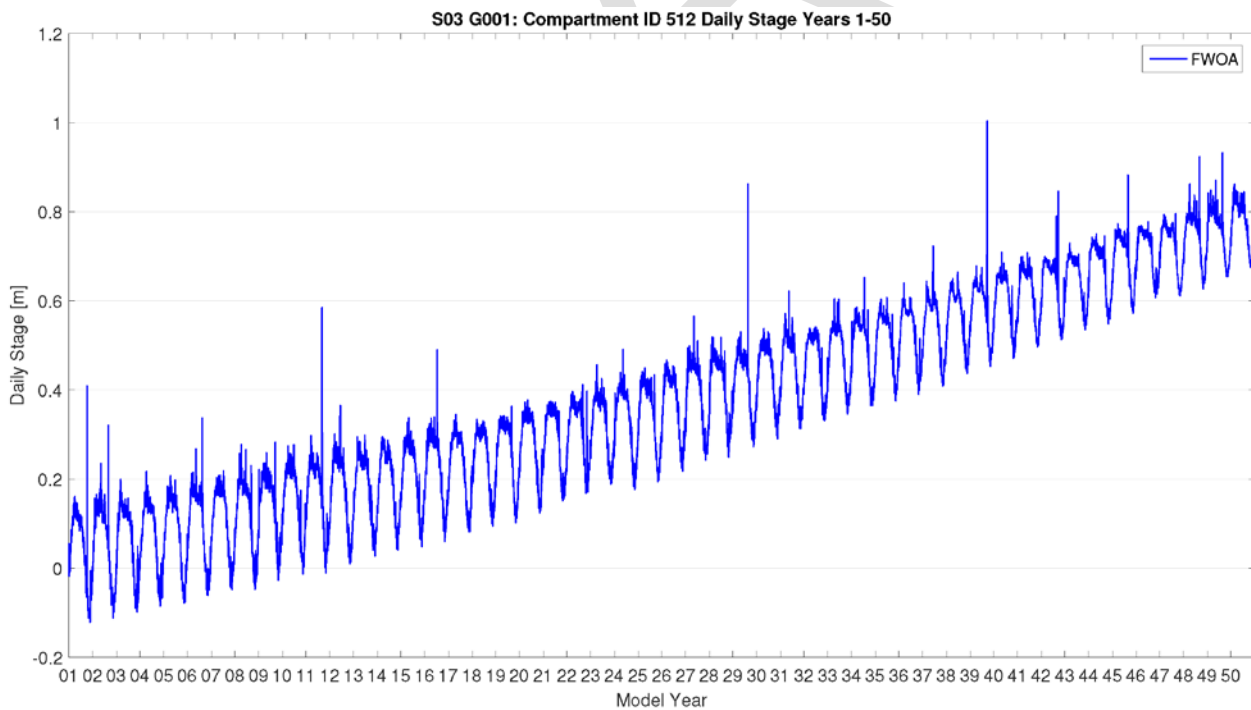
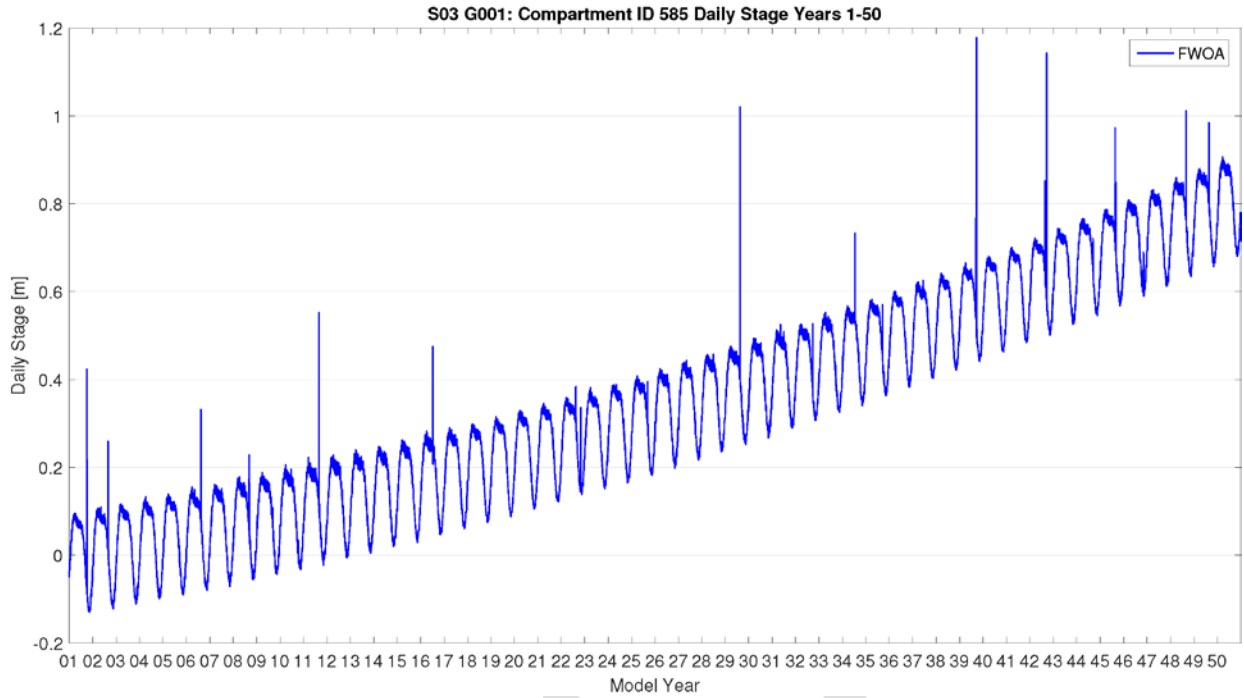
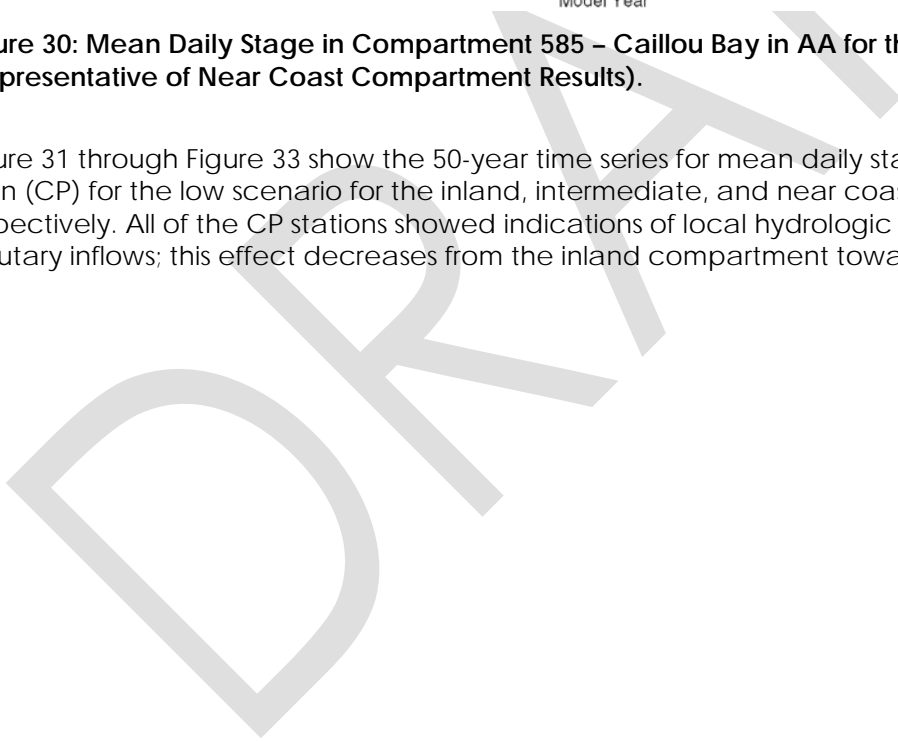


Figure 29: Mean Daily Stage in Compartment 512 – Lake de Cade in AA for the High Scenario (Representative of Intermediate Compartment Results).



**Figure 30: Mean Daily Stage in Compartment 585 – Caillou Bay in AA for the High Scenario (Representative of Near Coast Compartment Results).**

Figure 31 through Figure 33 show the 50-year time series for mean daily stage for the Chenier Plain (CP) for the low scenario for the inland, intermediate, and near coast compartments, respectively. All of the CP stations showed indications of local hydrologic inputs due to rainfall or tributary inflows; this effect decreases from the inland compartment towards the coast.



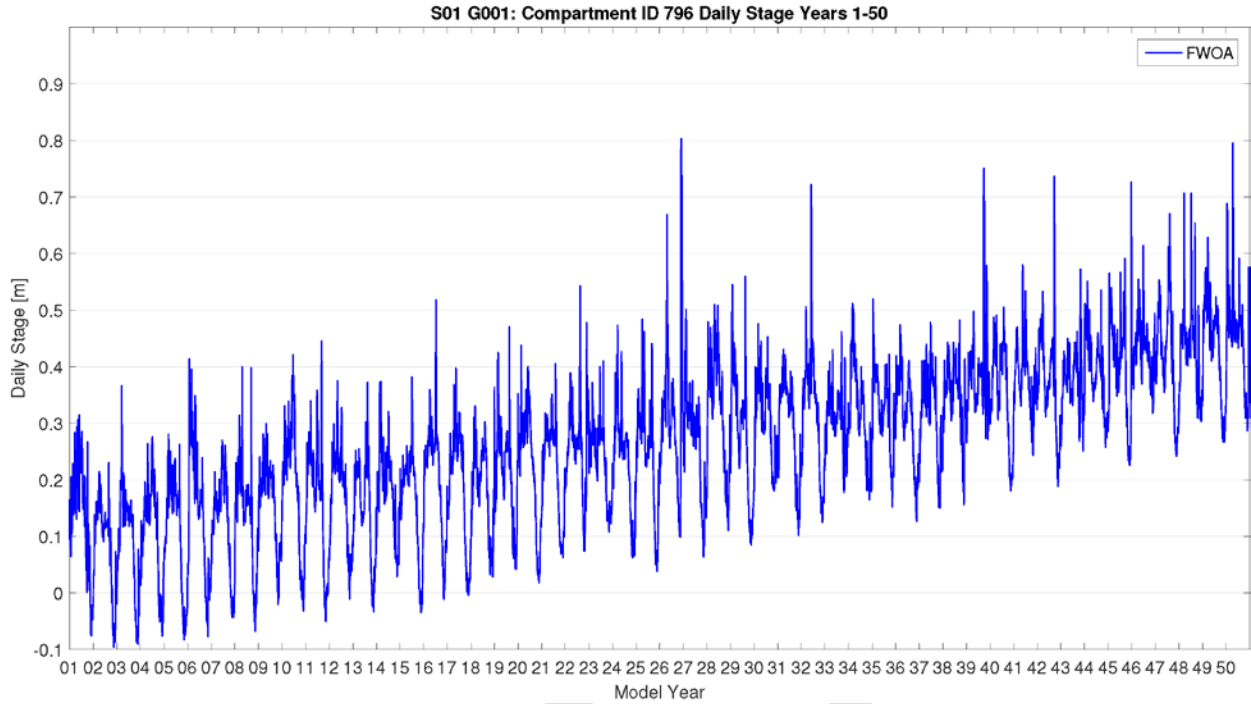


Figure 31: Mean Daily Stage in Compartment 796 – Northwest Grand Lake in CP for the Low Scenario (Representative of Inland Compartment Results).

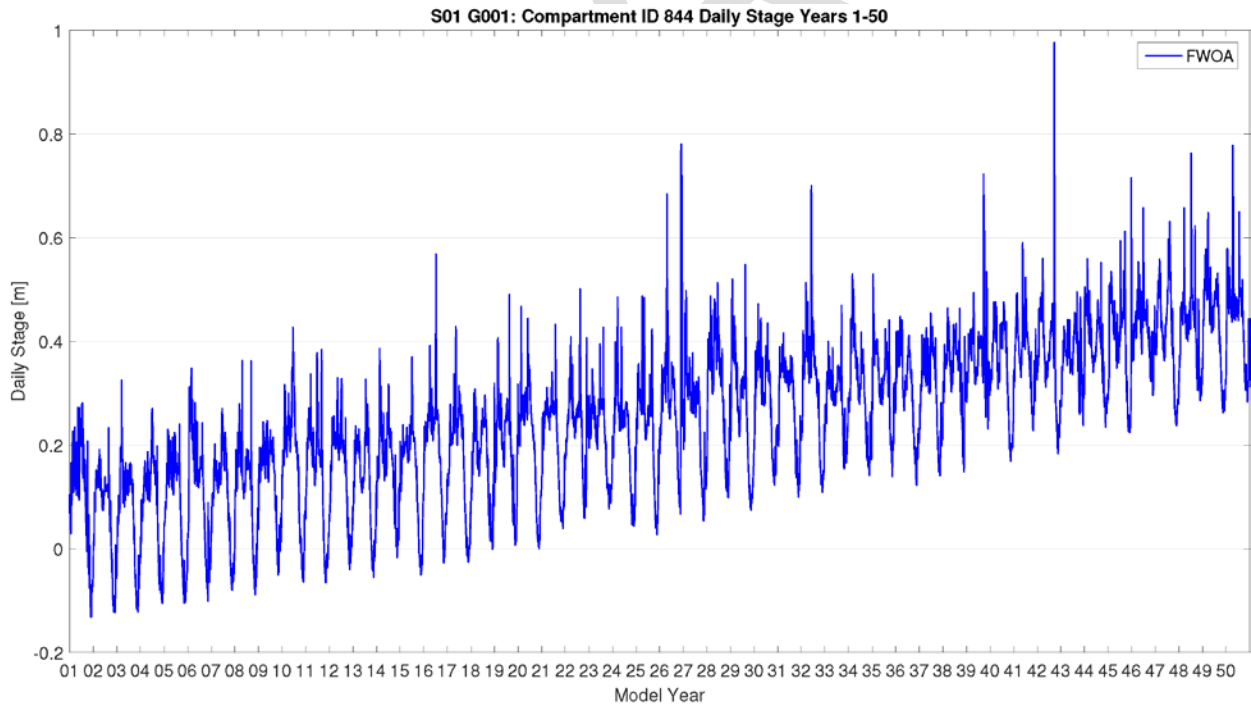
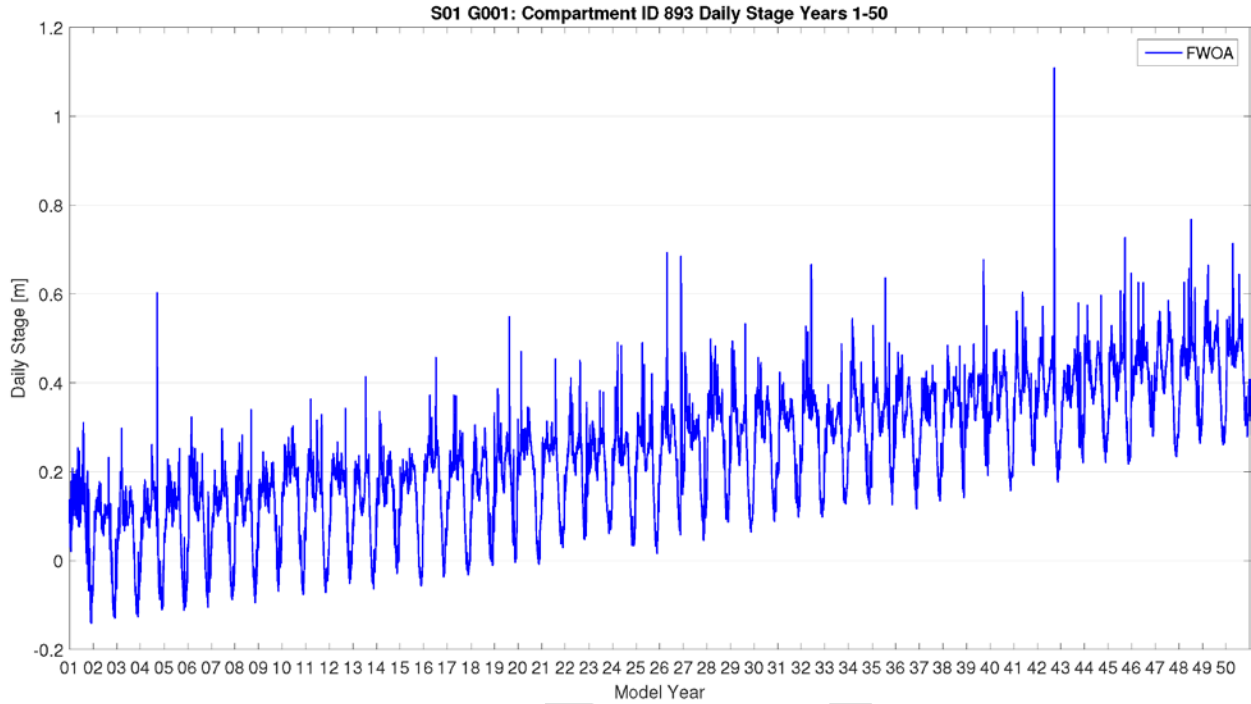


Figure 32: Mean Daily Stage in Compartment 844 – East Calcasieu Lake in CP for the Low Scenario (Representative of Intermediate Compartment Results).



**Figure 33: Mean Daily Stage in Compartment 893 – Holly Beach in CP for the Low Scenario (Representative of Near Coast Compartment Results).**

Figure 34 through Figure 36 show the 50-year time series for mean daily stage for the Chenier Plain (CP) for high scenario for the inland, intermediate, and near coast compartments, respectively. The hydrologic signal noted in the low scenario is also present in the high scenario, but it is more subdued possibly because of the higher stage and increased tidal prism.

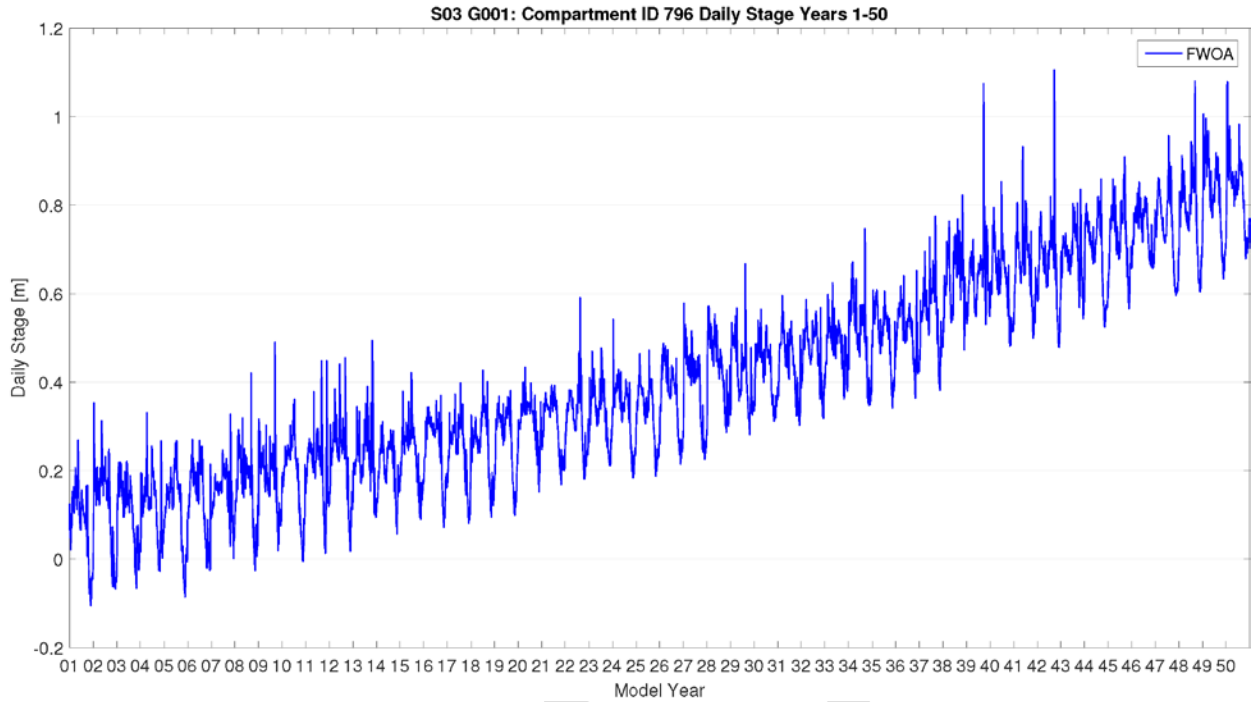


Figure 34: Mean Daily Stage in Compartment 796 – Northwest Grand Lake in CP for the High Scenario (Representative of Inland Compartment Results).

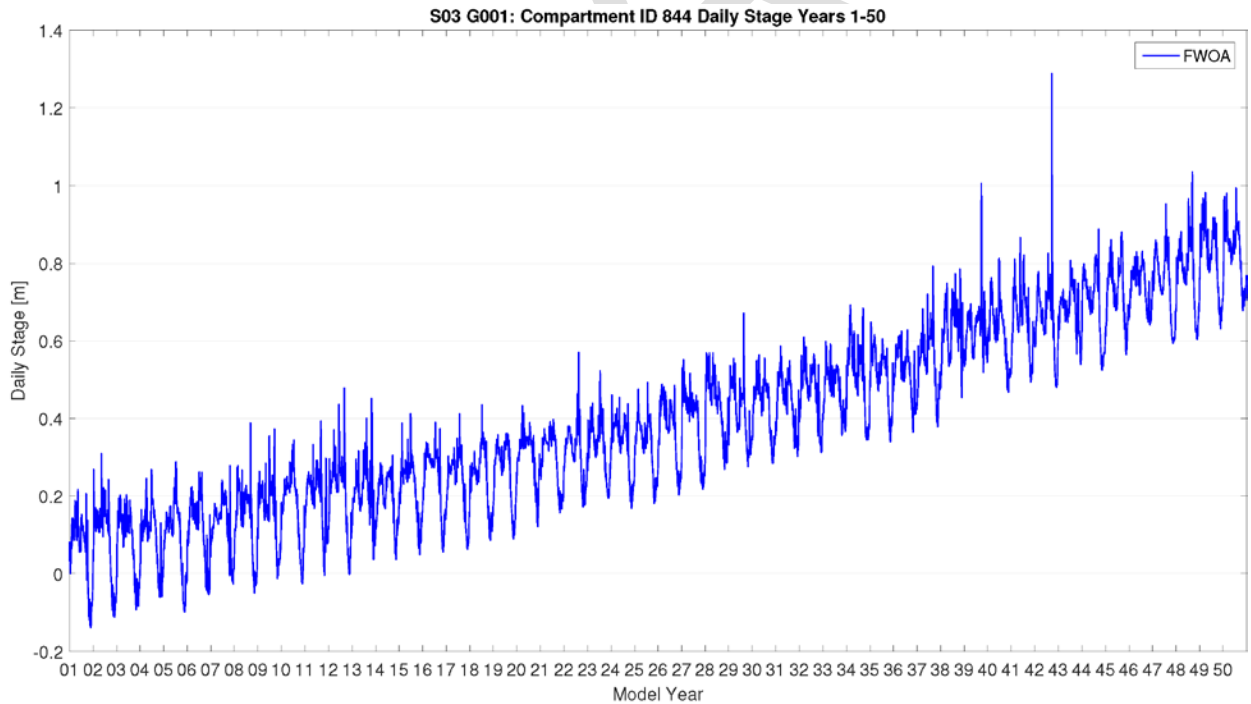
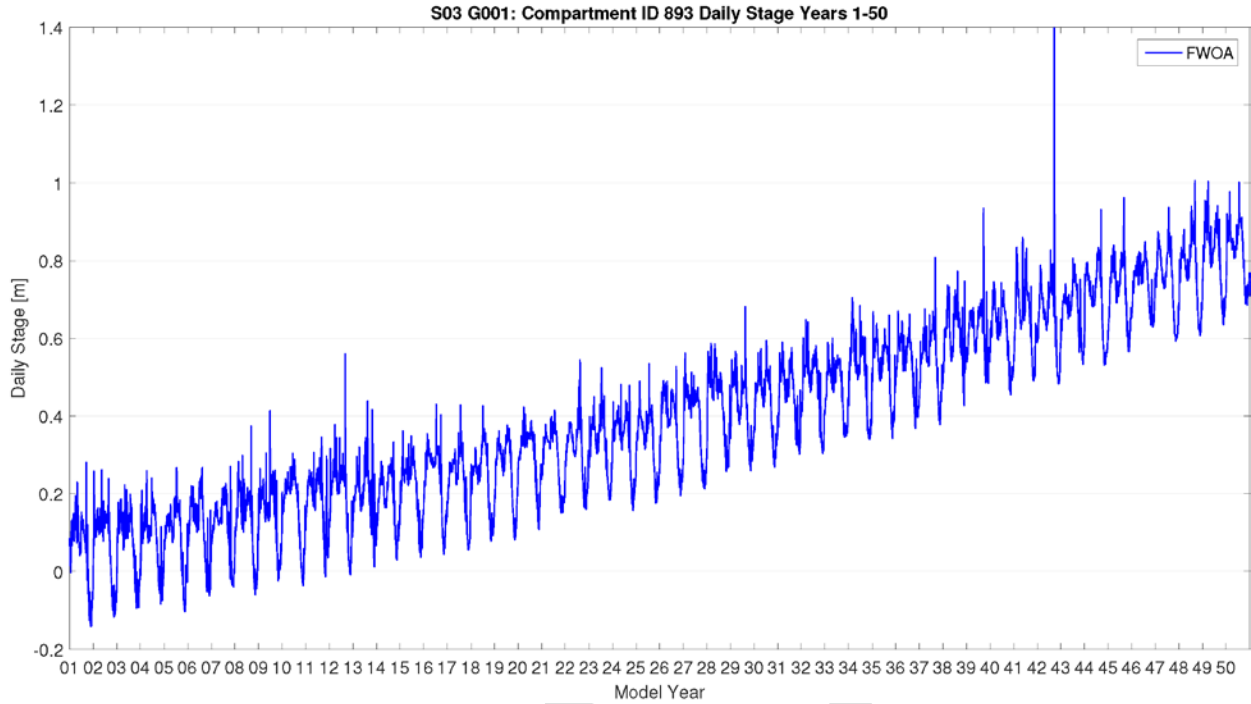


Figure 35: Mean Daily Stage in Compartment 844 – East Calcasieu Lake in CP for the High Scenario (Representative of Intermediate Compartment Results).



**Figure 36: Mean Daily Stage in Compartment 893 – Holly Beach in CP for the High Scenario (Representative of Near Coast Compartment Results).**

Figure 37 through Figure 42 present the temporal changes in the stage profile for the low, medium, and high scenarios for Pontchartrain Estuary and Barataria Estuary, respectively. Here, the stage profile references the stage versus position inland from the coast. These profiles show how the stage is very similar between the two estuaries for each scenario. Based on these relationships, the proximity to the Gulf is not a large driver in the stage values.

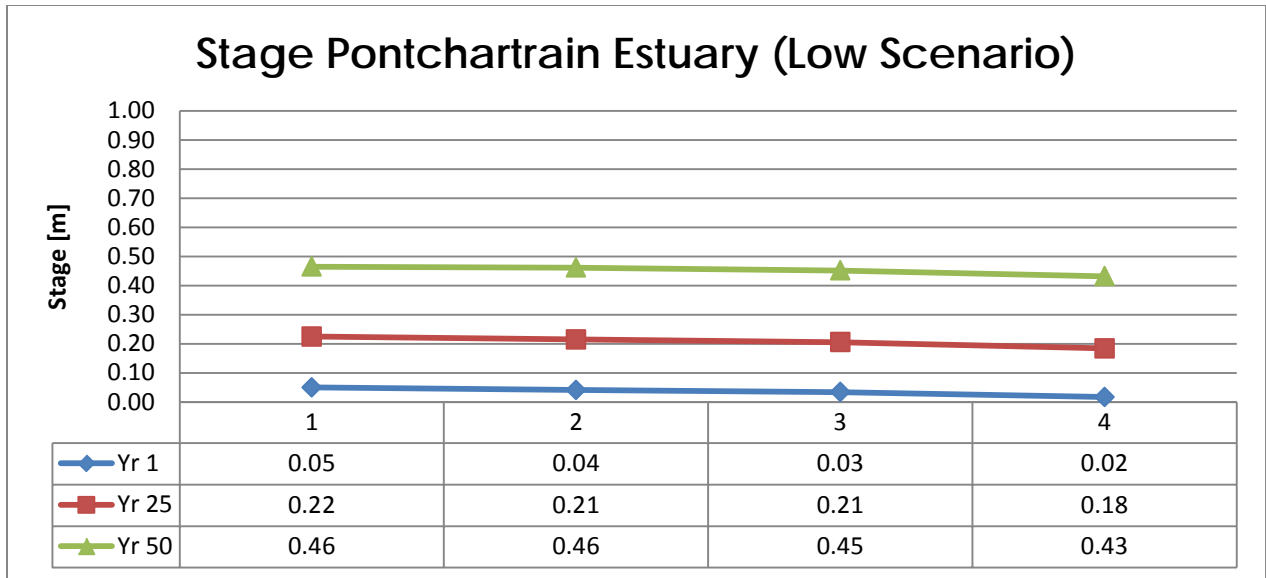


Figure 37: Temporal Changes in the Stage Profiles for the Pontchartrain Estuary for the Low Scenario (1 = Inland; 2 = Intermediate; 3 = Near Coast; and 4 = Off-Shore).

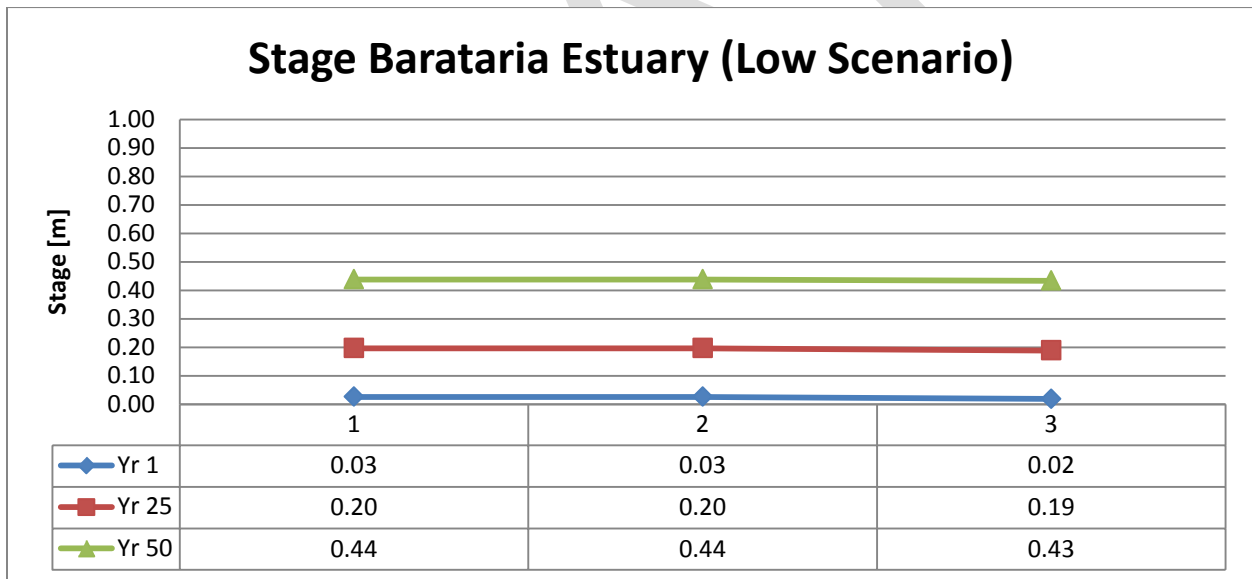


Figure 38: Temporal Changes in the Stage Profiles for the Barataria Estuary for the Low Scenario (1= Inland; 2 = Intermediate; and 3 = Coastal).

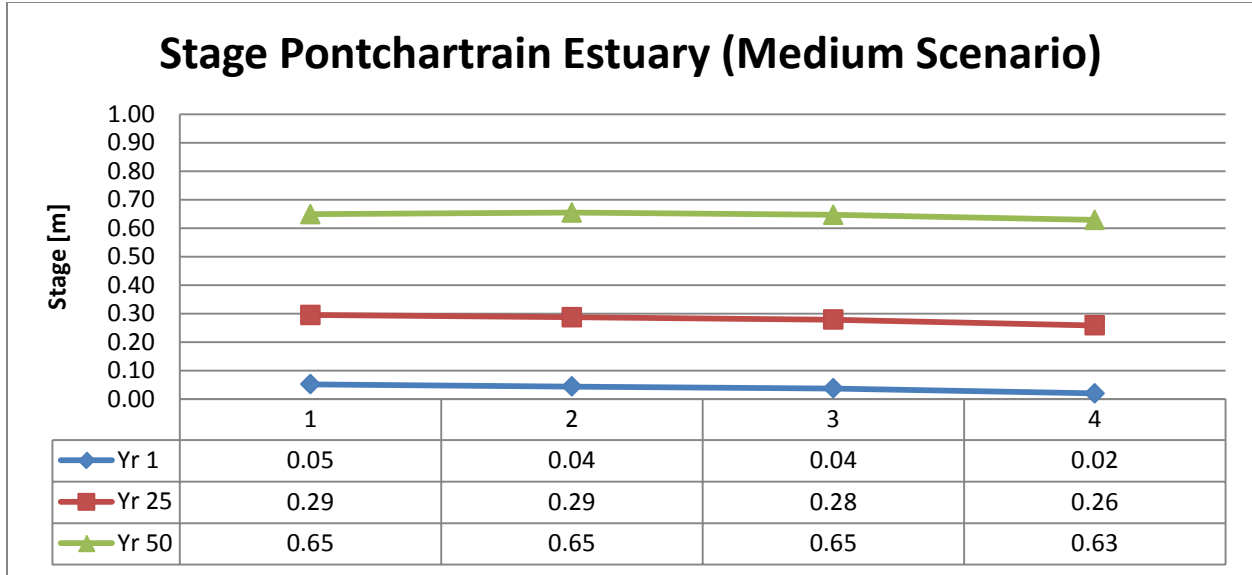


Figure 39: Temporal Changes in the Stage Profiles for the Pontchartrain Estuary for the Medium Scenario (1 = Inland; 2 = Intermediate; 3 = Near Coast; and 4 = Off-Shore).

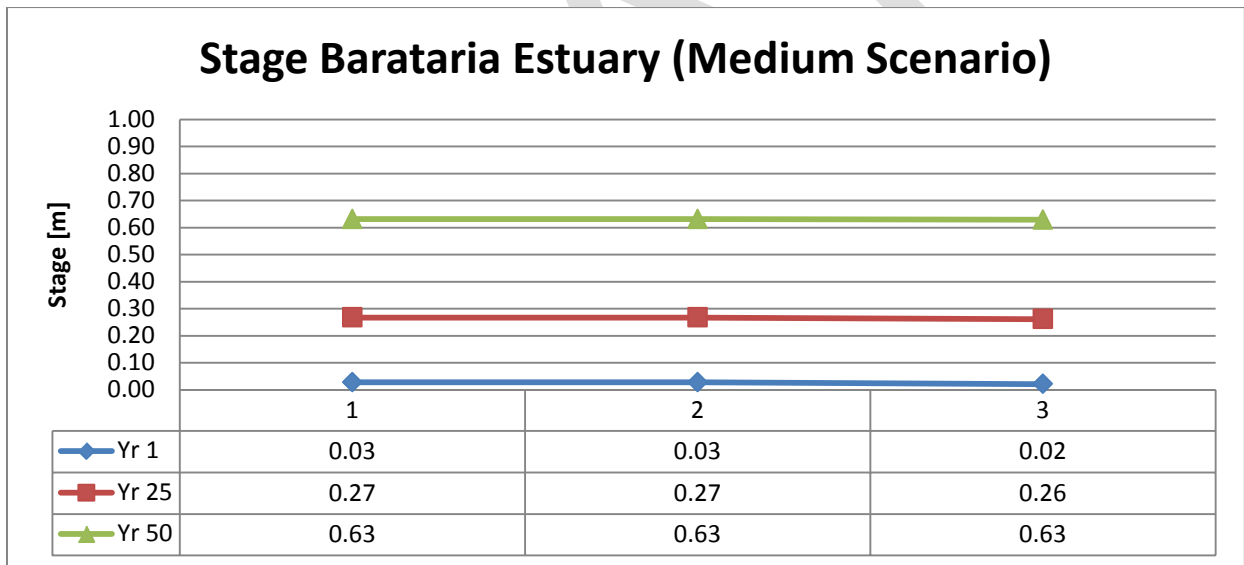


Figure 40: Temporal Changes in the Stage Profiles for the Barataria Estuary for the Medium Scenario (1= Inland; 2 = Intermediate; and 3 = Coastal).

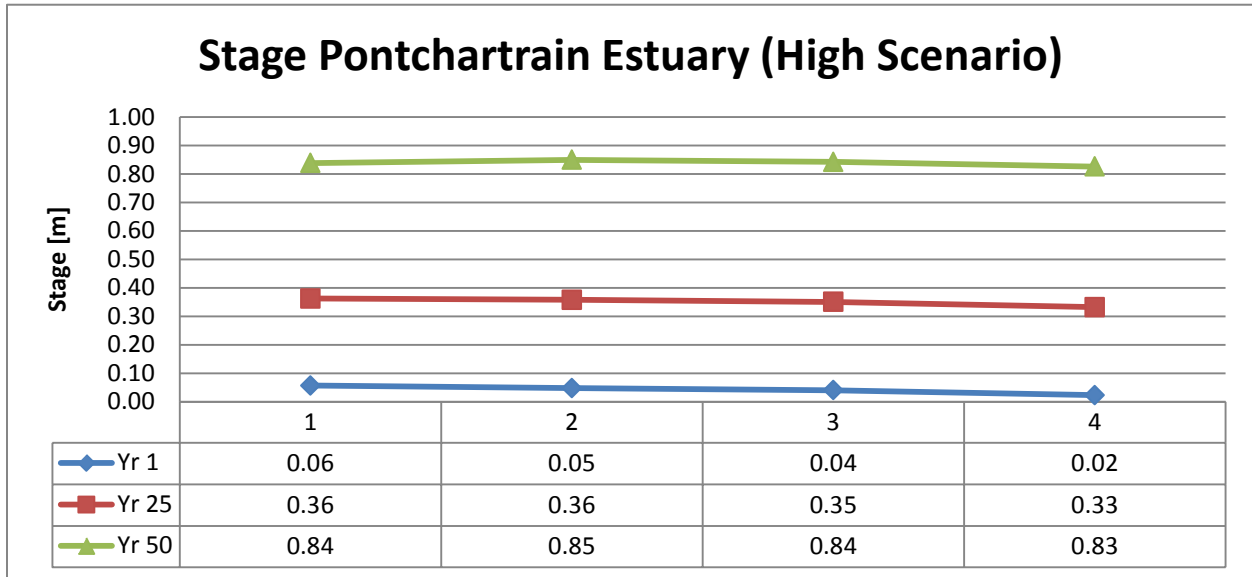


Figure 41: Temporal Changes in the Stage Profiles for the Pontchartrain Estuary for the High Scenario (1 = Inland; 2 = Intermediate; 3 = Near Coast; and 4 = Off-Shore).

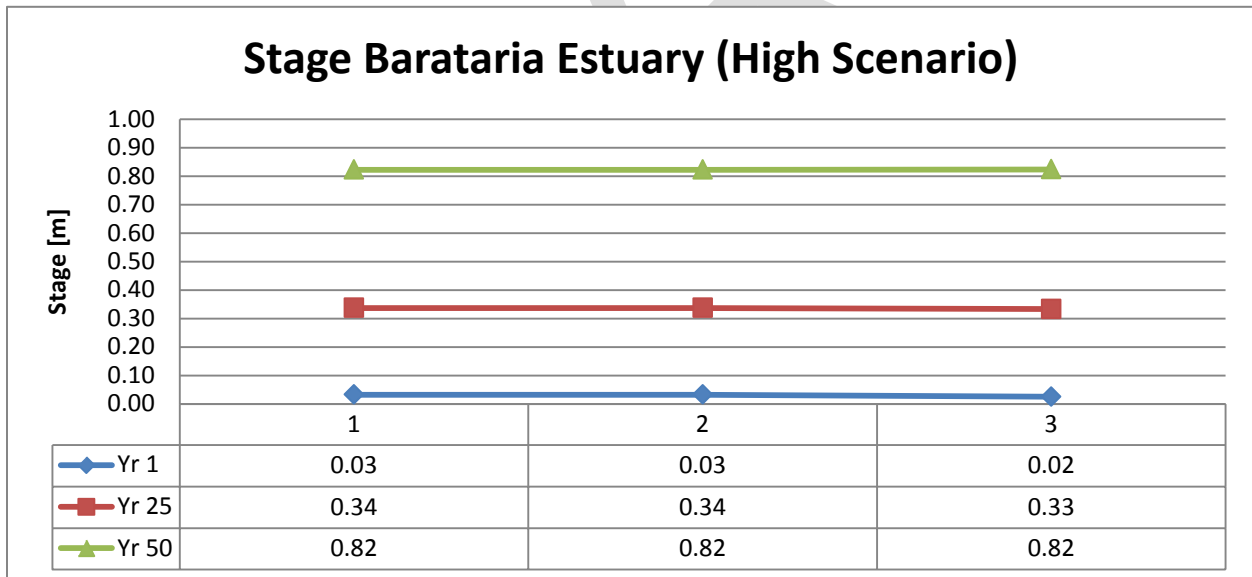


Figure 42: Temporal Changes in the Stage Profiles for the Barataria Estuary for the High Scenario (1= Inland; 2 = Intermediate; and 3 = Coastal).

In addition to the mean daily stage, the tidal range (TRG) was considered. Figure 43 and Figure 44 show the tidal range for the low scenario for Pontchartrain and Barataria (1 denotes the inland compartment; 2 refers to an intermediate compartment while 3 and 4 are the coastal areas). The TRG have been averaged for year 1, year 25 and year 50. In the Pontchartrain Estuary, there is a gradual attenuation of the tide going from the coast towards Lake Maurepas for all years. After 50 years, there is approximately 10% increase in the TRG. The coastal

compartment in Barataria shows a similar increase in the TRG; however, the two inland locations experience slightly less increase. This is consistent with the progressive land loss within the basin and the associated deepening of the hydraulic conveyance links. The tidal prism is increased due to this increased TRG and the increased open water area.

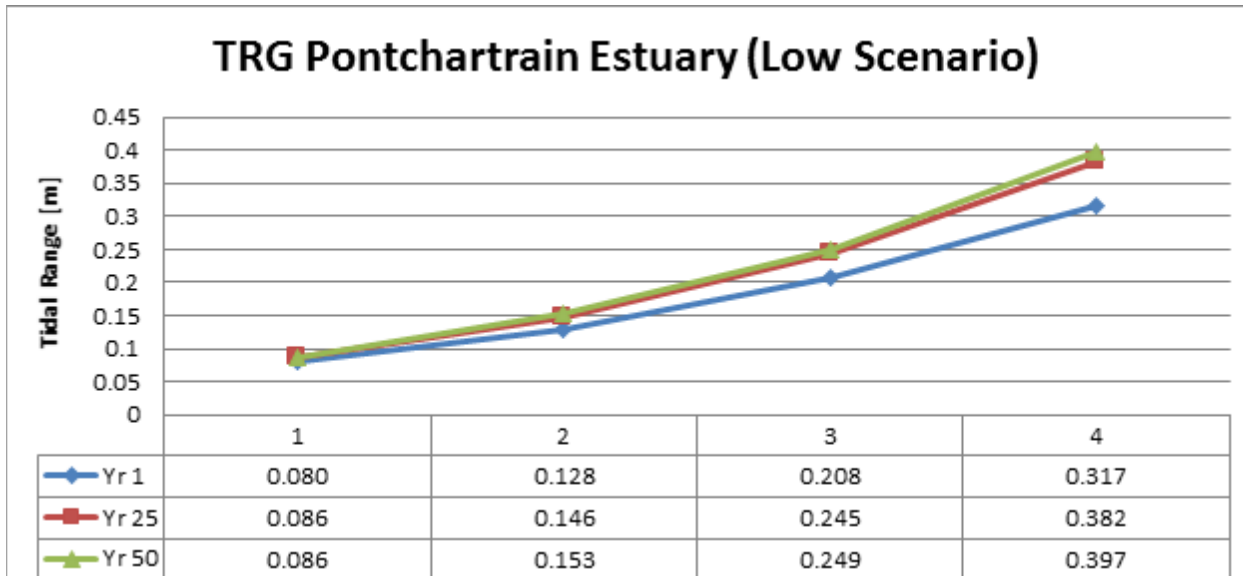


Figure 43: Mean Tidal Range as a Function of Location and Time for the Pontchartrain Estuary for the Low Scenario (1 = Inland; 2 = Intermediate; 3 = Near Coast; and 4 = Off-Shore).

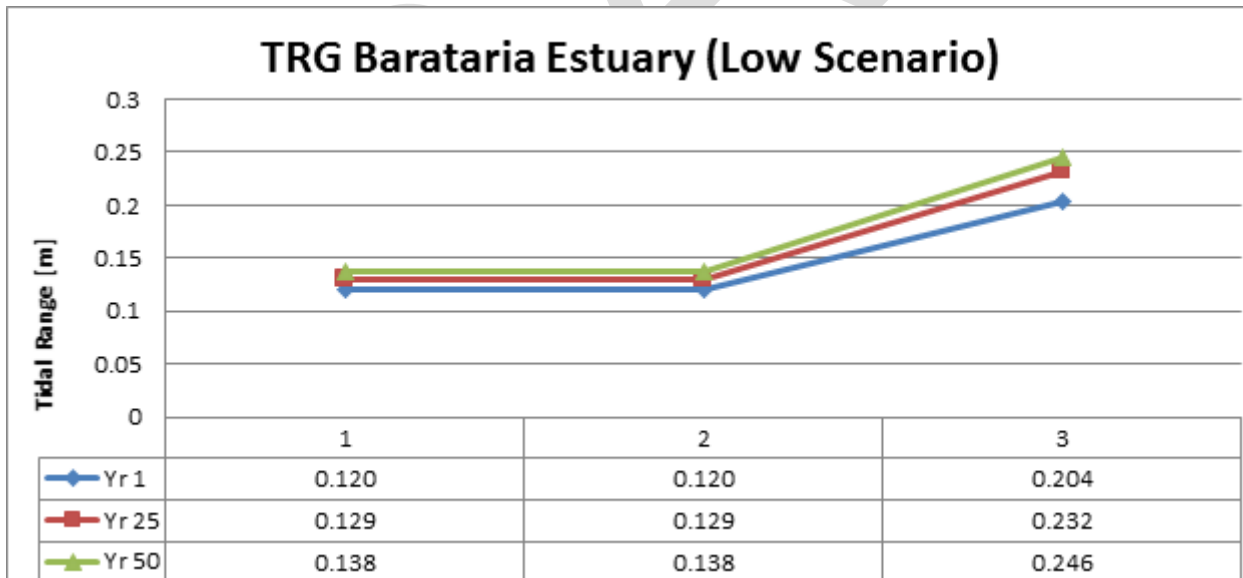


Figure 44: Mean Tidal Range as a Function of Location and Time for the Barataria Estuary for the Low Scenario (1= Inland; 2 = Intermediate; and 3 = Coastal).

Similarly, Figure 45 and Figure 46 show the TRG for the high scenario for PB (1 denotes the inland compartment; 2 refers to an intermediate compartment while 3 and 4 are the coastal areas). The TRG have been averaged for year 1, year 25 and year 50. In the Pontchartrain Estuary, there is a gradual attenuation of the tide going from the coast towards Lake Maurepas for all years. After 50 years, there is approximately 10% increase in the TRG. The coastal compartment in

Barataria shows a similar increase in the TRG; however, the two inland locations experience slightly less increase. This is consistent with the progressive land loss within the basin and the associated deepening of the hydraulic conveyance links. The tidal prism is increased due to this increased TRG and the increased open water area. The difference between the low and high scenario is approximately 10%, which can be attributed to the increased sea level rise in the high scenario.

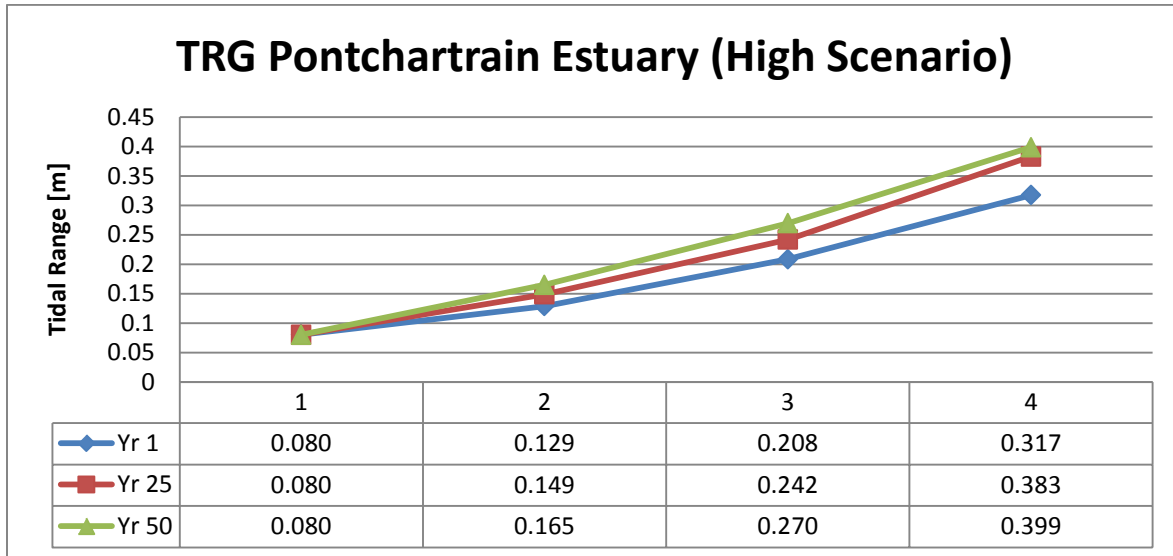


Figure 45: Mean Tidal Range as a Function of Location and Time for the Pontchartrain Estuary for the High Scenario (1 = Inland; 2 = Intermediate; 3 = Near Coast; and 4 = Off-Shore).

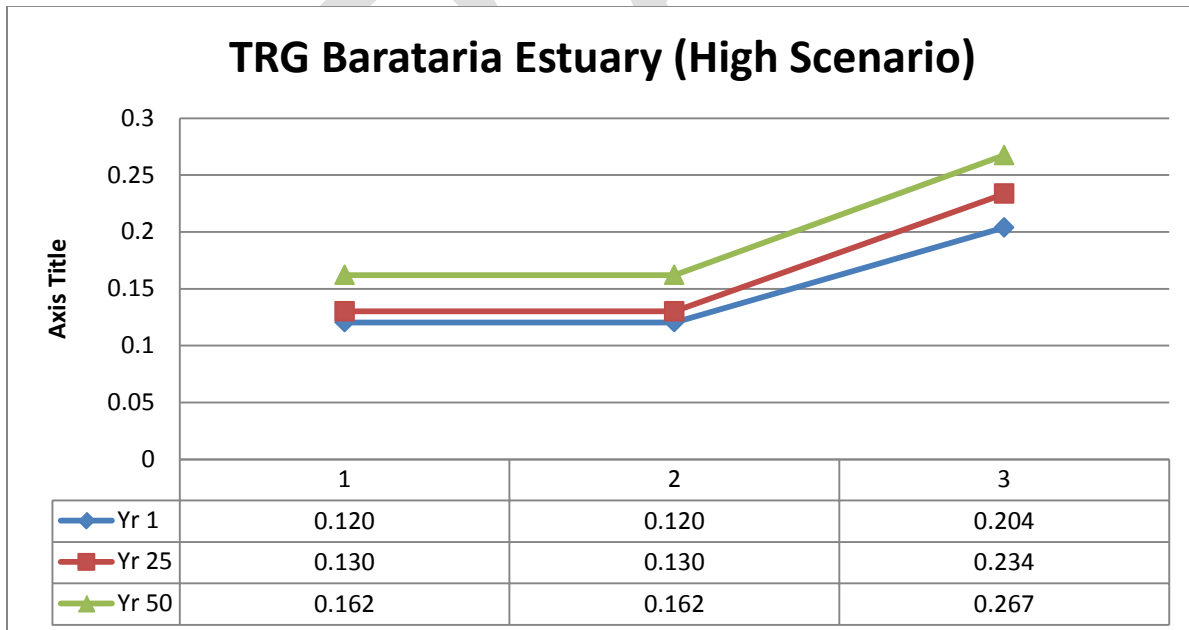


Figure 46: Mean Tidal Range as a Function of Location and Time for the Barataria Estuary for the High Scenario (1= Inland; 2 = Intermediate; and 3 = Coastal).

In the AA region, TRG is overwhelmed by the influence of the Atchafalaya River. Figure 47 and Figure 48 show the large riverine related tidal attenuation at the interior cells for the low scenario and high scenario. Similar results occurred for the medium scenario, indicating that (regardless of scenario) there is a strong riverine influence in the AA region.

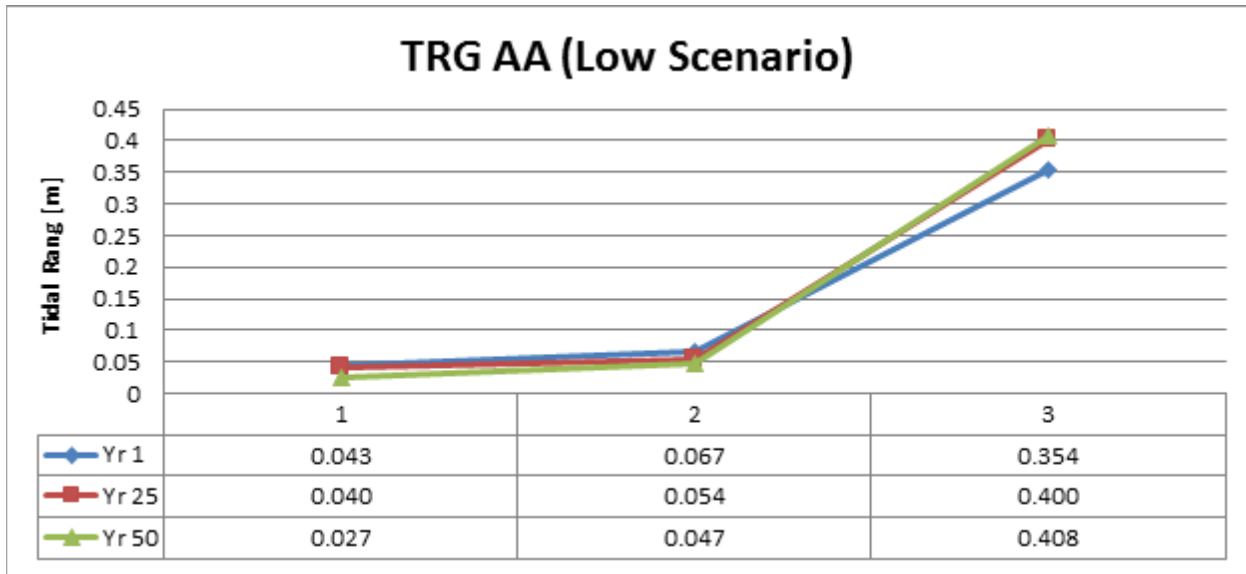


Figure 47: Temporal Changes in the Tidal Range Profile for AA for the Low Scenario (1= Inland; 2 = Intermediate; and 3 = Coastal).

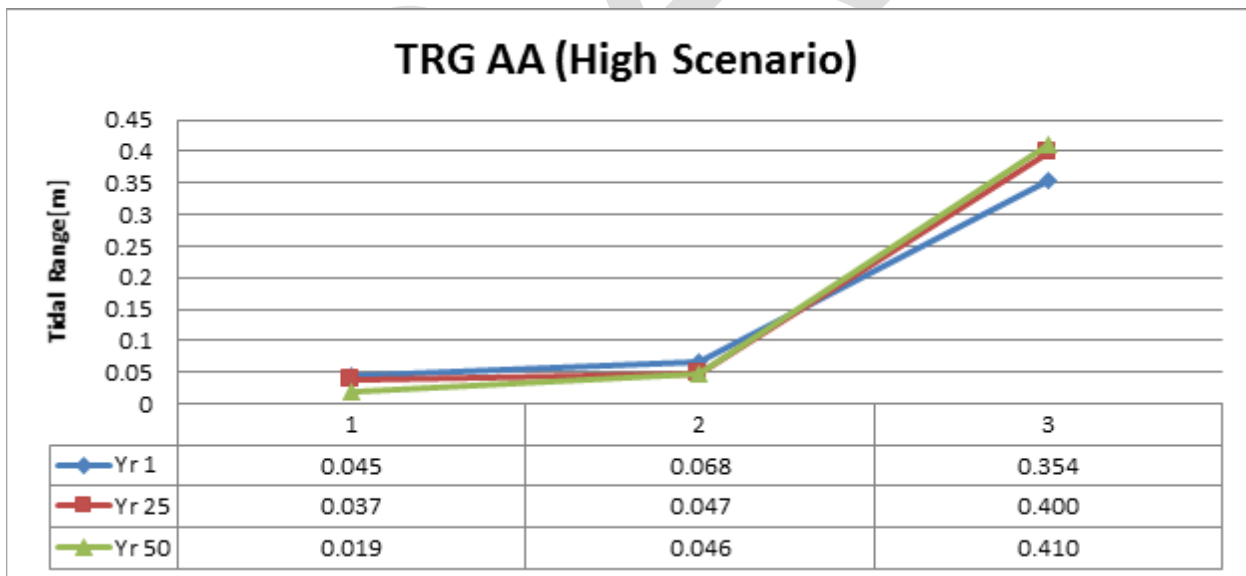


Figure 48: Temporal Changes in the Tidal Range Profile for AA for the High Scenario (1= Inland; 2 = Intermediate; and 3 = Coastal).

Figure 49 through Figure 51 present the temporal changes in the stage profile for the low, medium, and high scenarios, respectively. Here, the stage profile references the stage versus position inland from the coast. These profiles show how the backwater from the Gulf affects the river stages.

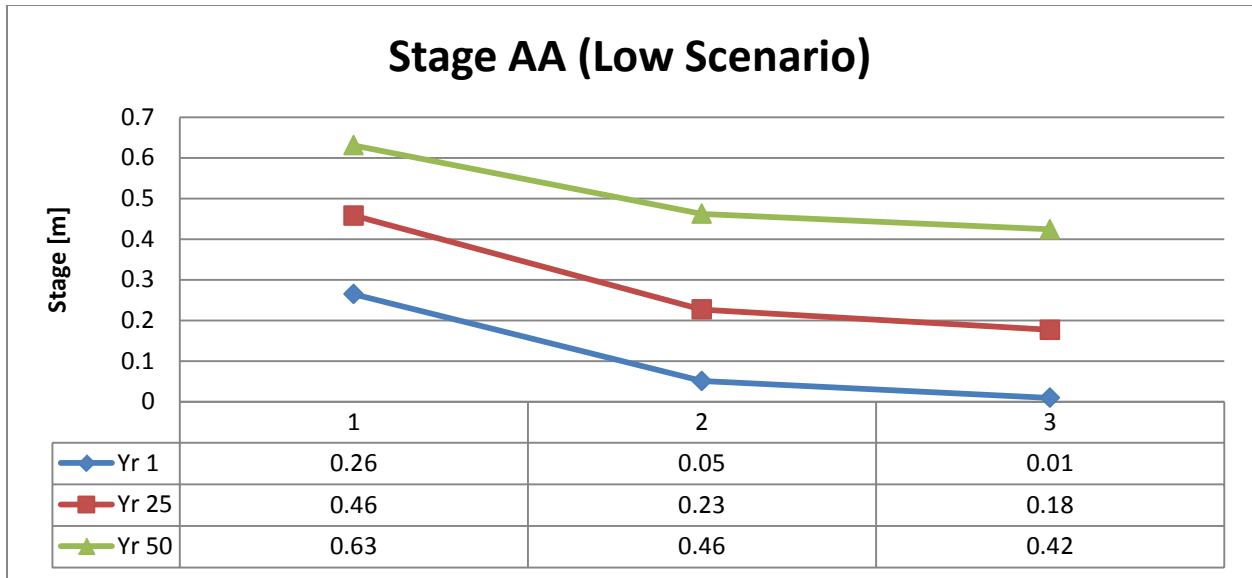


Figure 49: Temporal Changes in the Stage Profiles for AA for the Low Scenario (1= Inland; 2 = Intermediate; and 3 = Coastal).

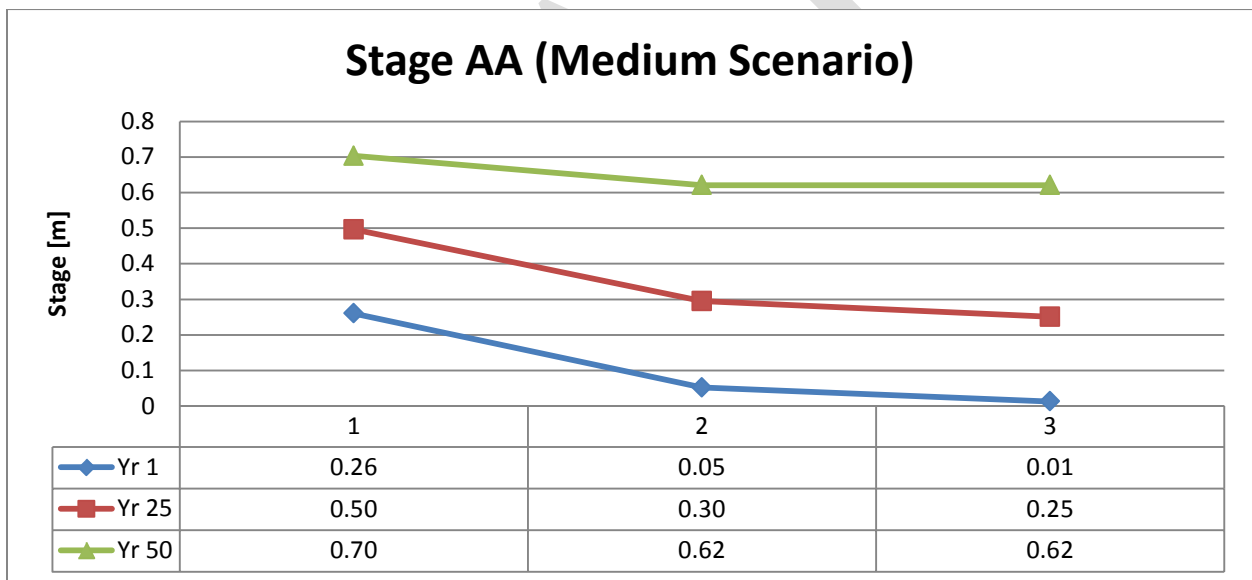


Figure 50: Temporal Changes in the Stage Profiles for AA for the Medium Scenario (1= Inland; 2 = Intermediate; and 3 = Coastal).

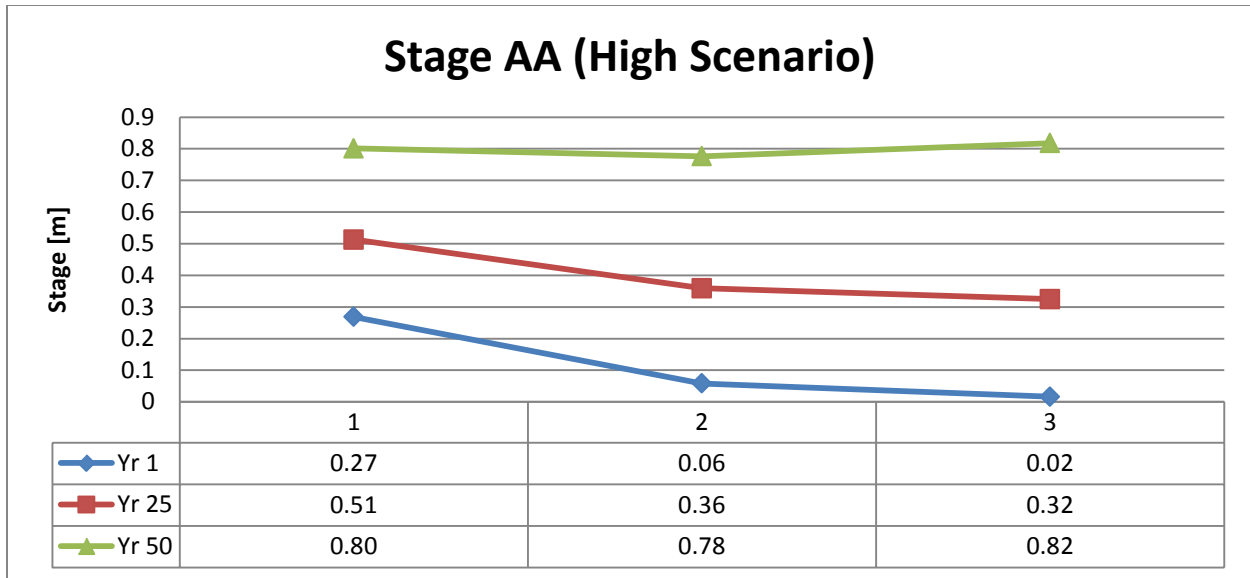


Figure 51: Temporal Changes in the Stage Profiles for AA for the High Scenario (1= Inland; 2 = Interstal; and 3 = Coastal).

The mean TRG in CP at all three selected compartments is very small for the low and medium scenarios, and it remains low for 50 years. The higher relative sea level rise rate in the high scenario resulted in an increase in the mean TRG at the coastal compartment; however, it still remains quite small (Figure 52). The corresponding high scenario stage profiles essentially follow the Gulf stage as illustrated in Figure 53. The difference in mean stage between the coastal compartment and the inland compartment is about 8 cm in year 1 and 1 cm in year 50. It appears as though, in year 50 in the coastal compartment, the compartment is receiving more tidal influence, which may correspond with sea level rise and a subsequent increase overland flow.

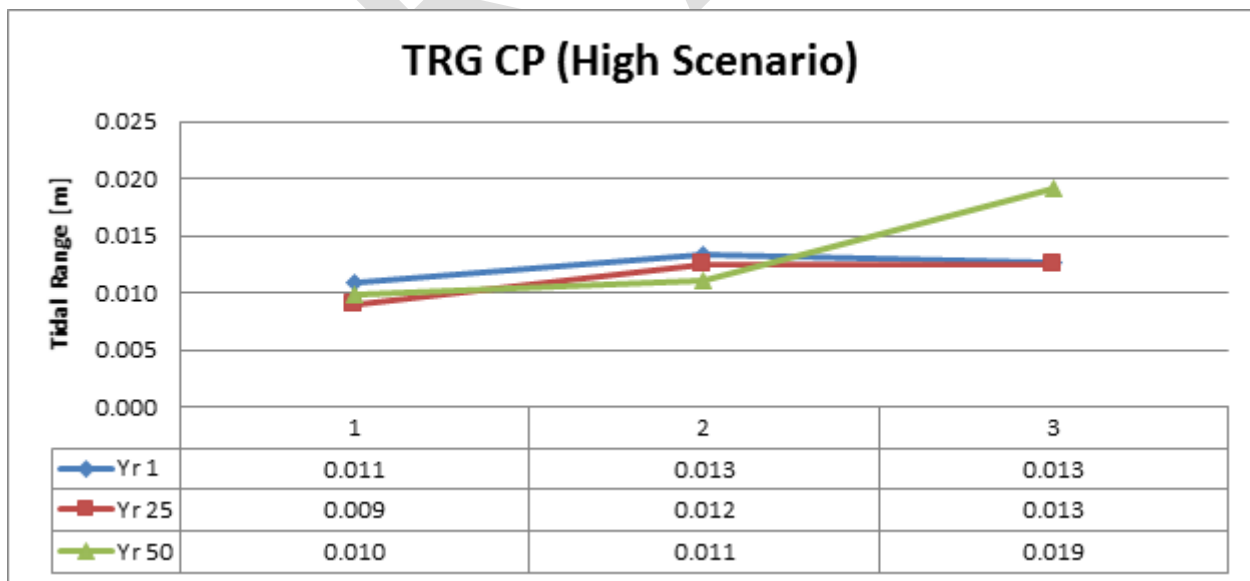


Figure 52: Temporal Changes in the Tidal Range Profile for CP for the High Scenario (1= Inland; 2 = Intermediate; and 3 = Coastal).

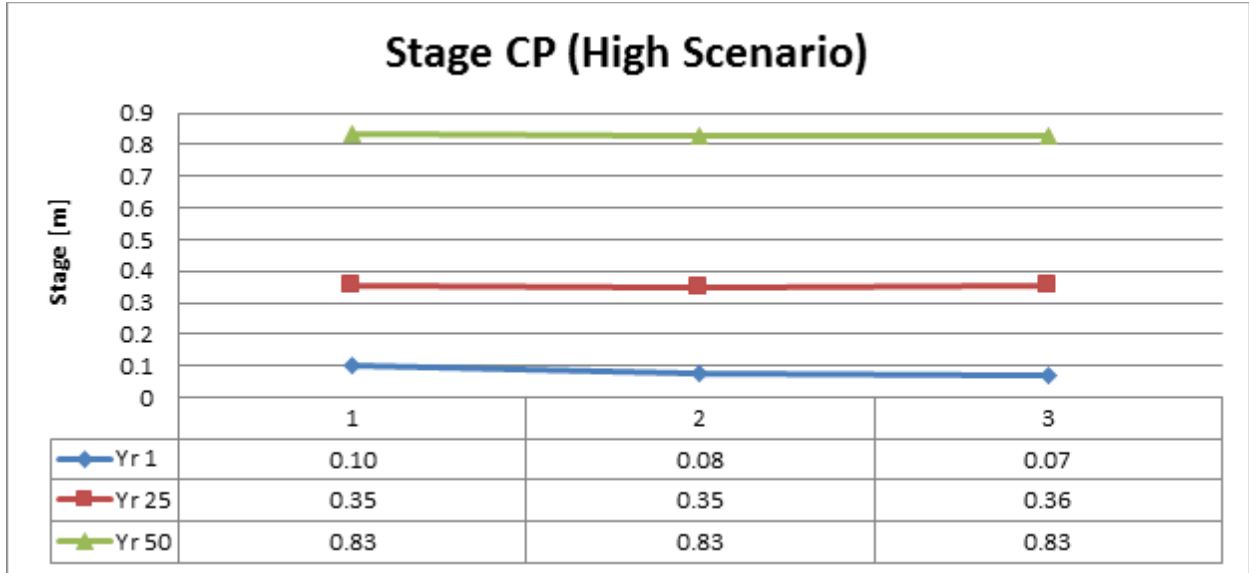


Figure 53: Temporal Changes in the Stage Profiles for CP for the High Scenario (1= Inland; 2 = Intermediate; and 3 = Coastal).

### 3.2 Salinity

The temporal response of the cross-coast salinity gradient varies greatly from one region to another under all scenarios. Figure 54 shows the coast wide mean salinities for year 50 for the medium scenario. The mean annual system salinity for all of the compartments is 7.1 ppt in year 1. After 50 years, the mean system salinity increased to 10.7 ppt for the low scenario, 13.4 ppt for the medium scenario, and 15 ppt for the high scenario. This indicates a strong saltwater intrusion for all scenarios presumably with relative sea level rise as a major driver. There are a few anomalous compartments in each region that are possibly due to instabilities related to low hydraulic conveyance in the connecting links coupled with low open water areas; this can lead to intermittent activation of the marsh links as the sea level rises. This intermittent activation leads to false projections of flushing or stagnation of singular compartments. The issue was addressed in ICM model - version 3 (refer to Attachment C3-22 ICM Development).

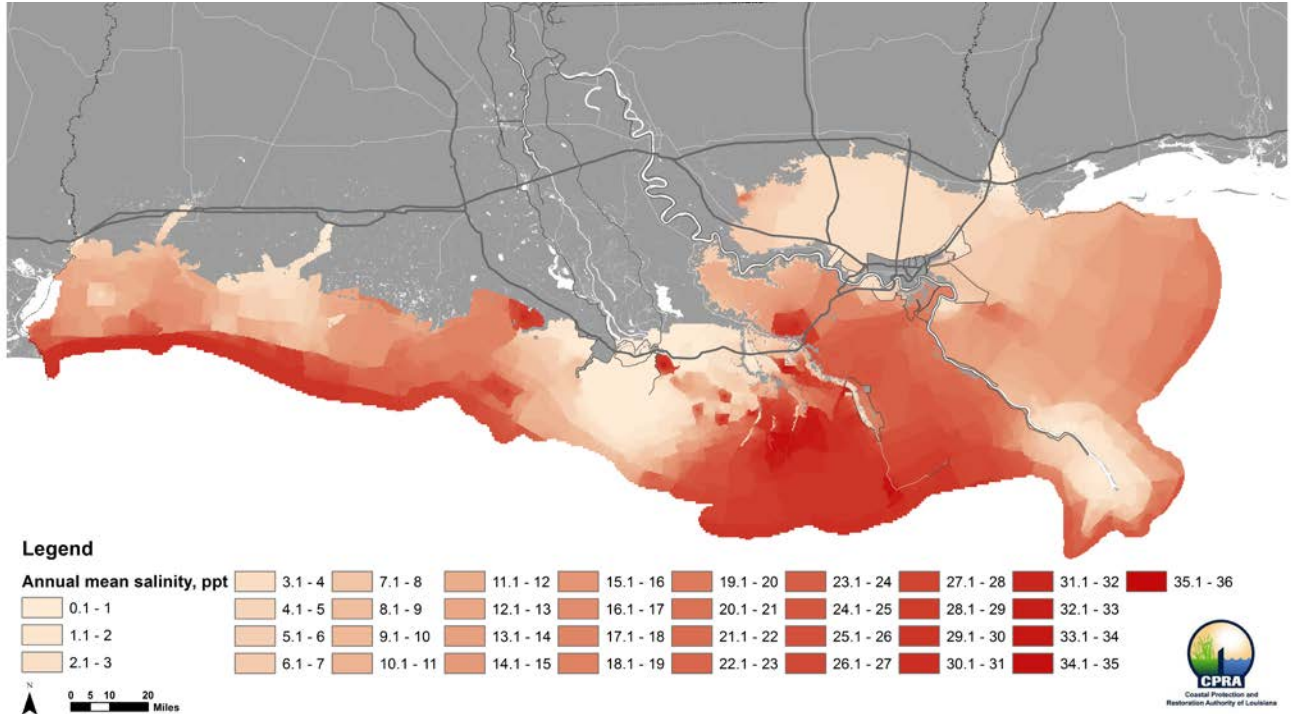


Figure 54: Mean Salinities (ppt) by Compartment for Year 50 for the Medium Scenario FWOA (G001).

Figure 55 through Figure 57 show the 50-year time series for mean monthly salinity for PB (Barataria Basin) for the low scenario for the inland, intermediate, and near coast compartments, respectively. The averaging has filtered the diurnal tide effects and most wind effects. Increasing salinity reaches the inland compartment at about year 33. An increase in salinity is noted in the intermediate compartment starting in year 30.

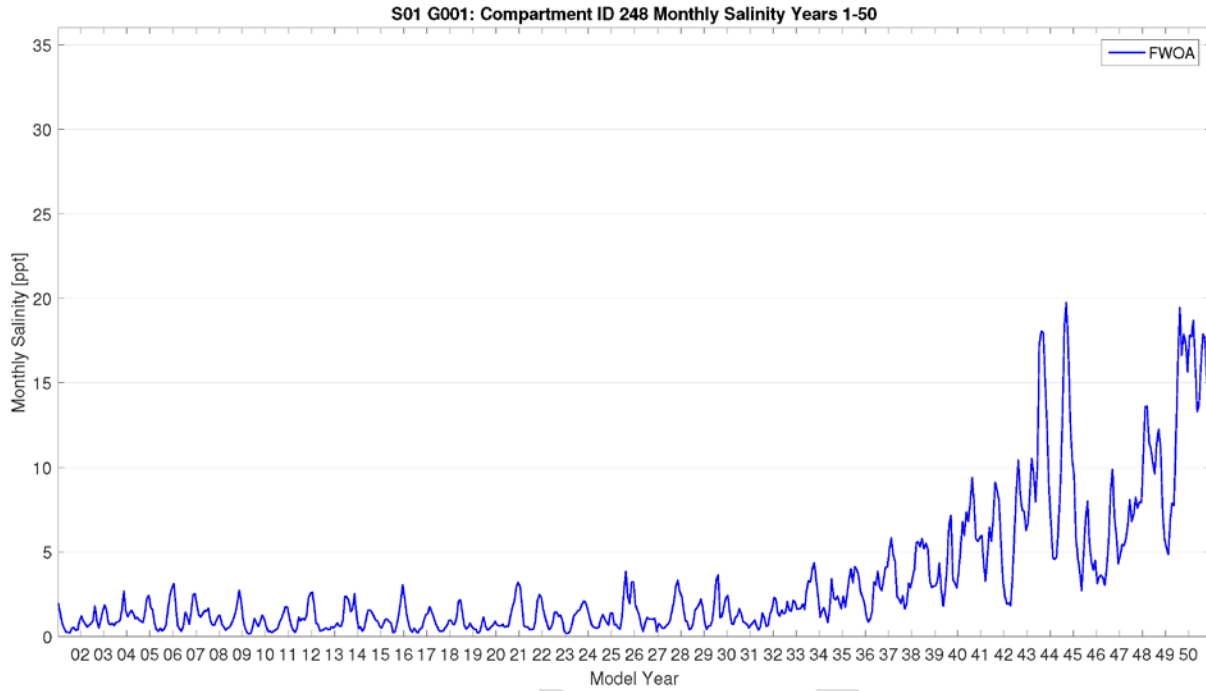


Figure 55: Mean Monthly Salinity in Compartment 248 - East Lake Salvador in PB for the Low Scenario (Representative of Inland Compartment Results).

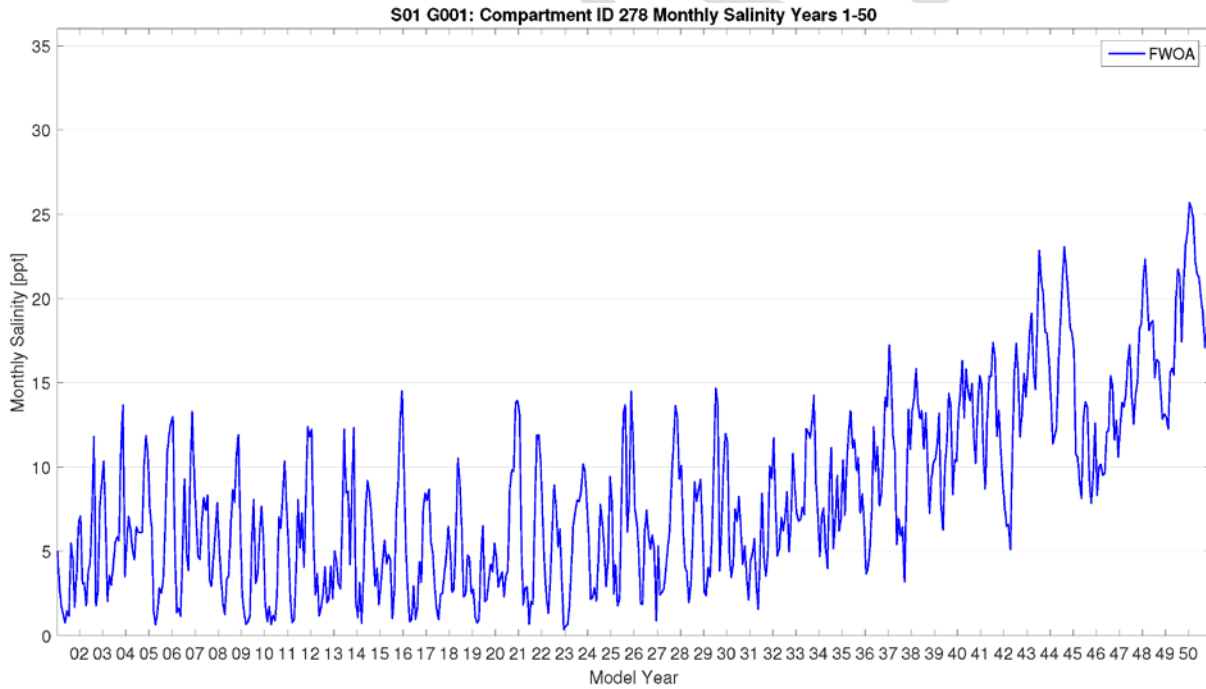
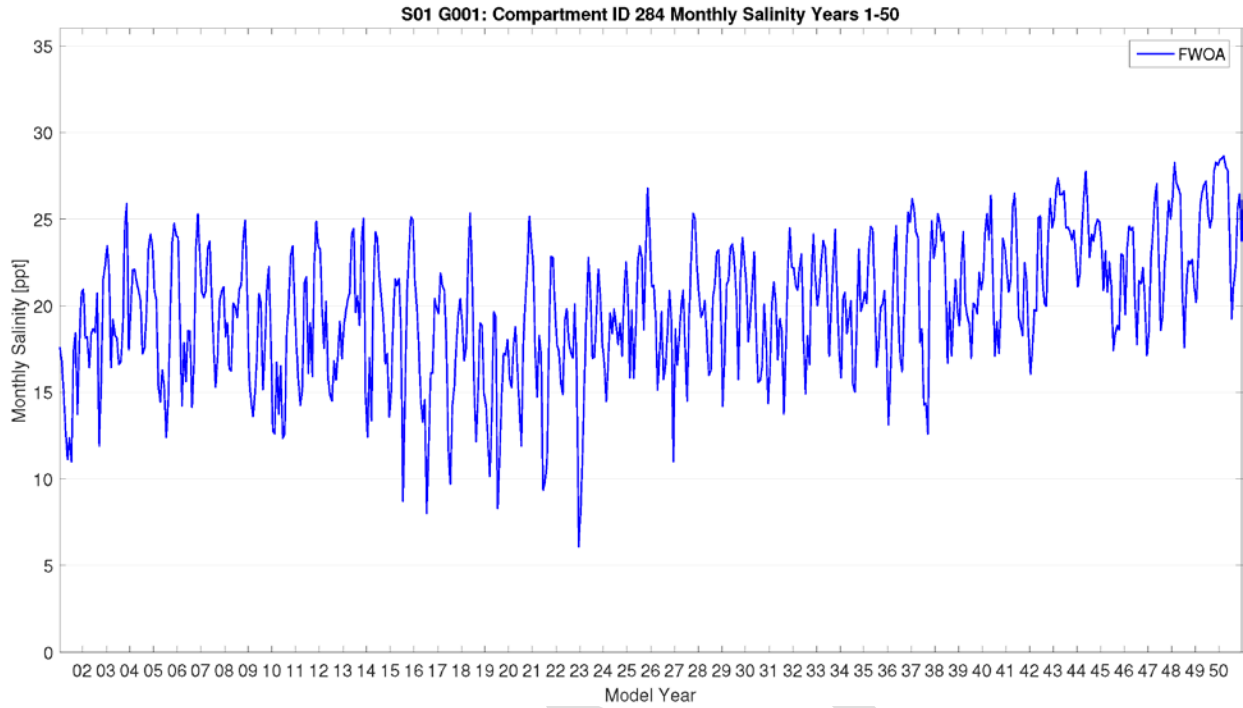


Figure 56: Mean Monthly Salinity in Compartment 278 - Mud Lake/Upper Barataria Bay in PB for the Low Scenario (Representative of Intermediate Compartment Results).



**Figure 57: Mean Monthly Salinity in Compartment 284 -Northeast of Grand Isle in PB for the Low Scenario (Representative of Near Coast Compartment Results).**

Figure 58 through Figure 60 show the 50-year time series for mean monthly salinity for PB (Barataria Basin) for the high scenario for the inland, intermediate, and near coast compartments, respectively. Salinity increases in the inland compartment in about year 18. An increase in salinity is noted in the intermediate compartment starting in year 10. After 50 years, the mean daily salinity for the high scenario is approximately 10 ppt higher than for the low scenario and 3 ppt higher than the medium scenario.

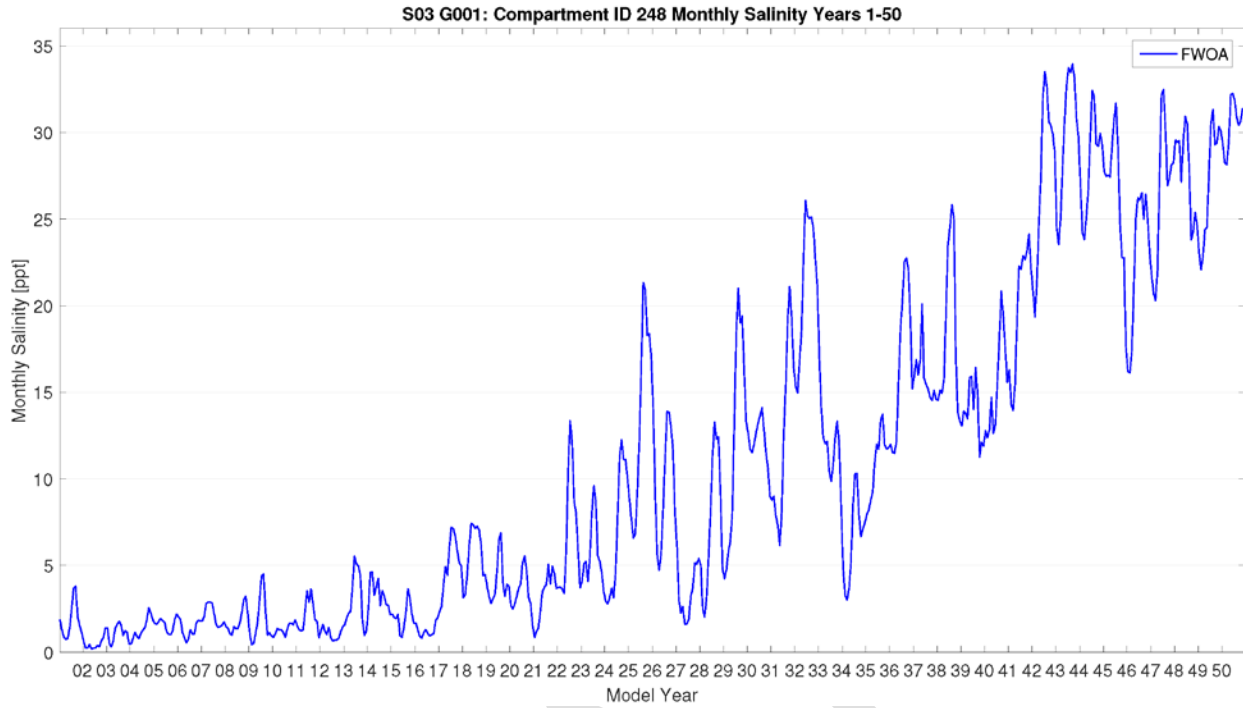


Figure 58: Mean Monthly Salinity in Compartment 248 - East Lake Salvador in PB for the High Scenario (Representative of Inland Compartment Results).

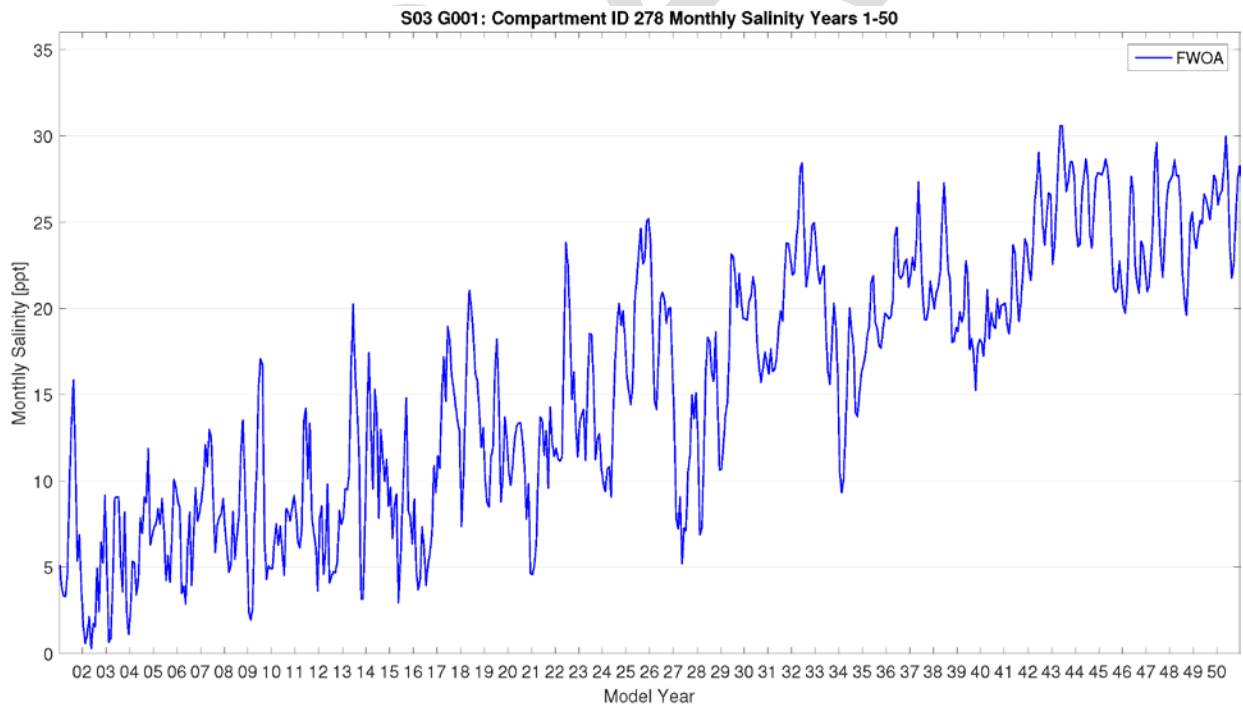
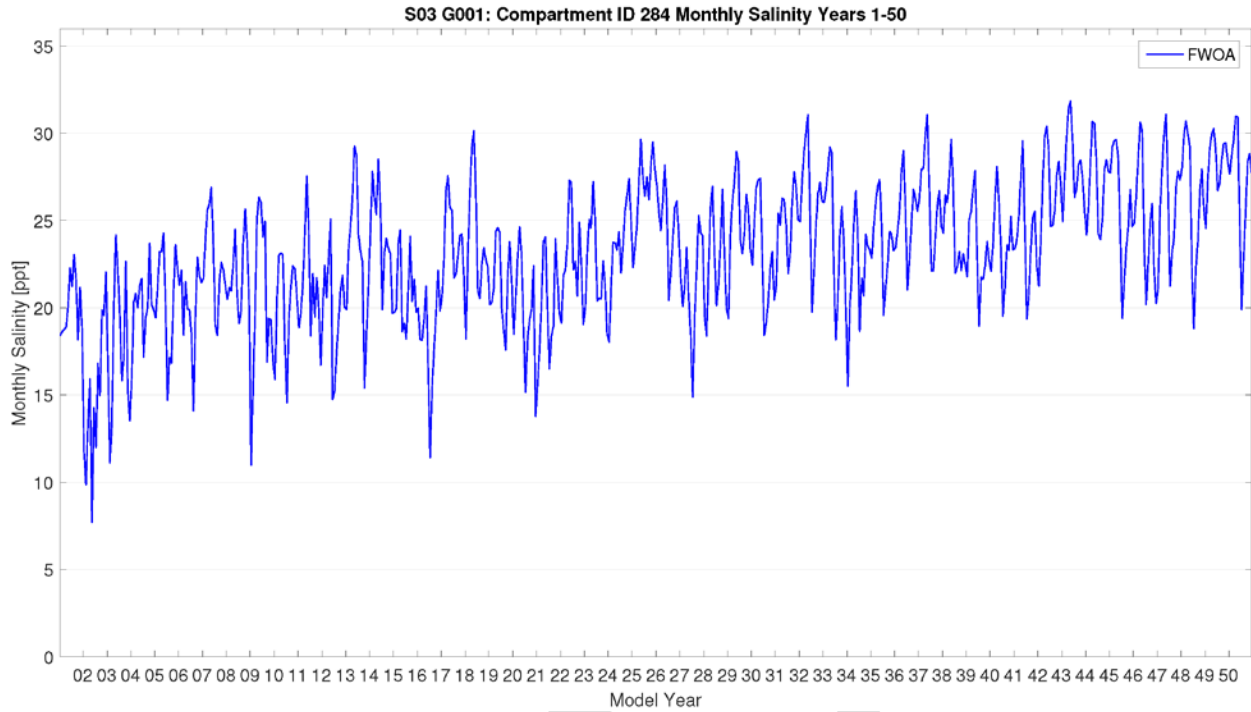


Figure 59: Mean Monthly Salinity in Compartment 278 - Mud Lake/Upper Barataria Bay in PB for the High Scenario (Representative of Intermediate Compartment Results).



**Figure 60: Mean Monthly Salinity in Compartment 284 - Northeast of Grand Isle in PB for the High Scenario (Representative of Near Coast Compartment Results).**

Figure 61 through Figure 63 show the 50-year time series for mean monthly salinity for the AA region for the low scenario for the inland, intermediate, and near coast compartments, respectively. In this scenario, the inland compartment remains fresh water; this is reasonable since it is fed by river water. In the intermediate compartment, the salinity increase starts around year 40 and reaches approximately 10 ppt. The coastal compartment starts with a salinity of about 15 ppt and increases to around 22 ppt over 50 years.

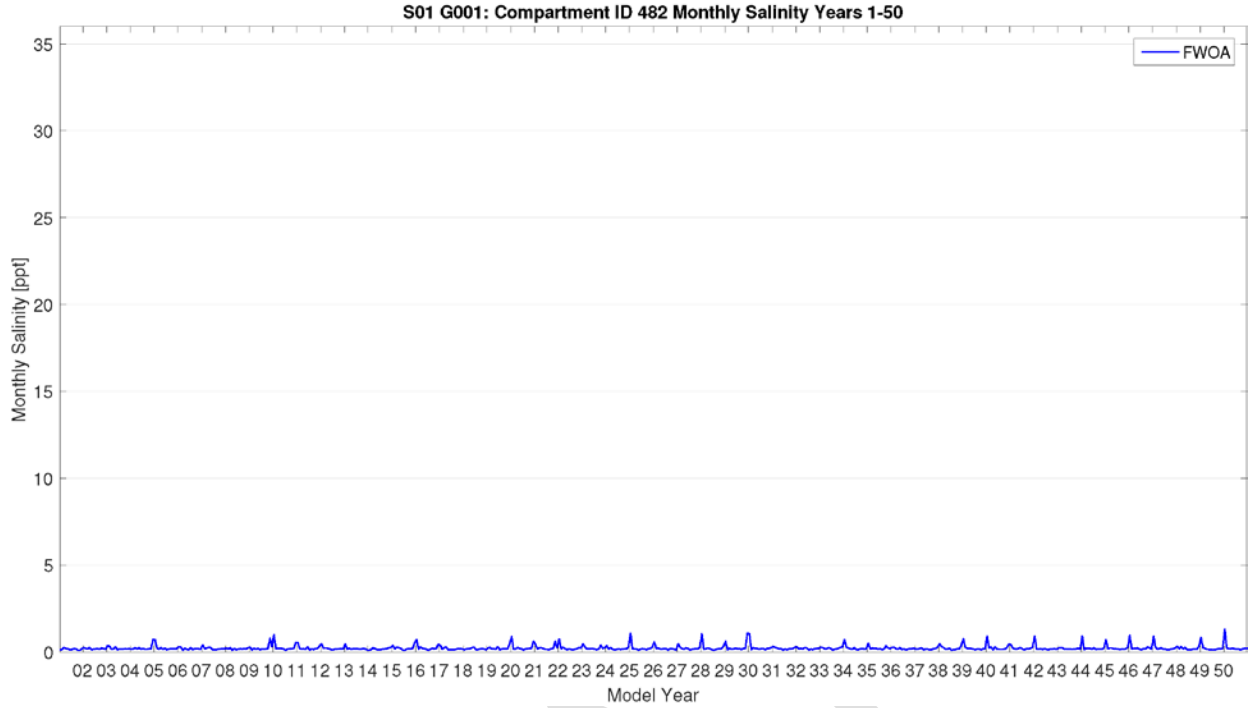


Figure 61: Mean Monthly Salinity in Compartment 482 – Lake Palourde in AA for the Low Scenario (Representative of Inland Compartment Results).

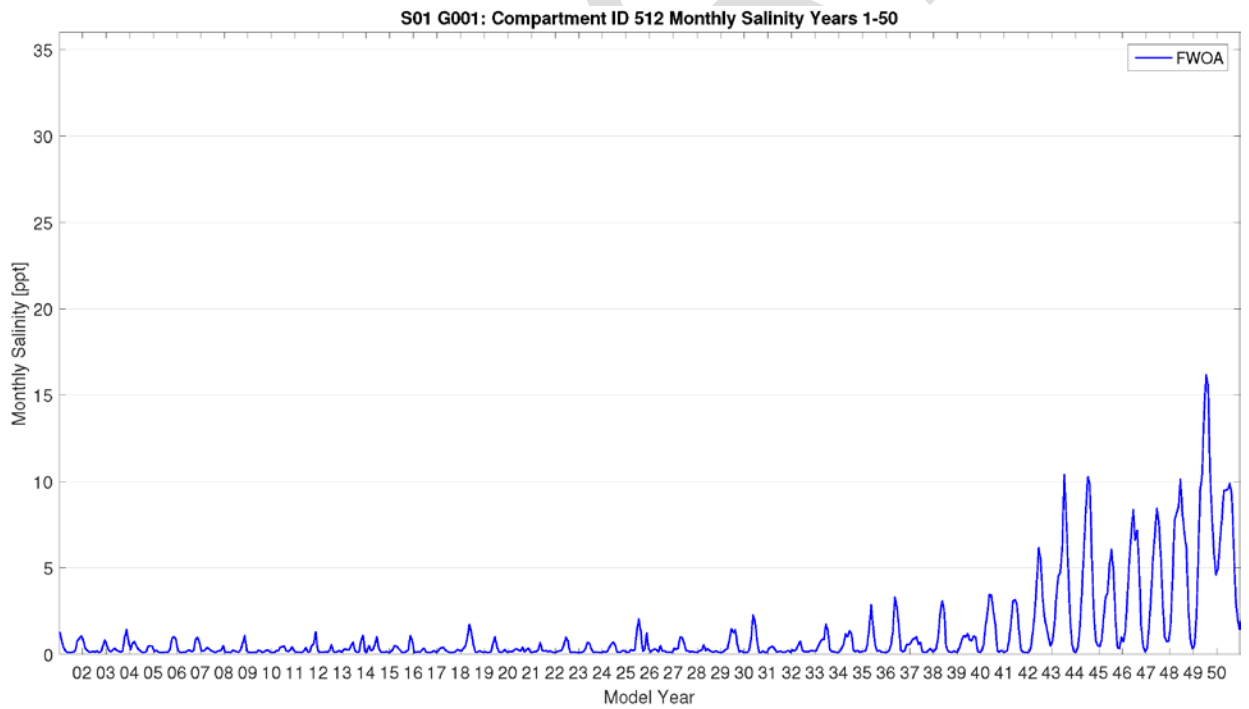
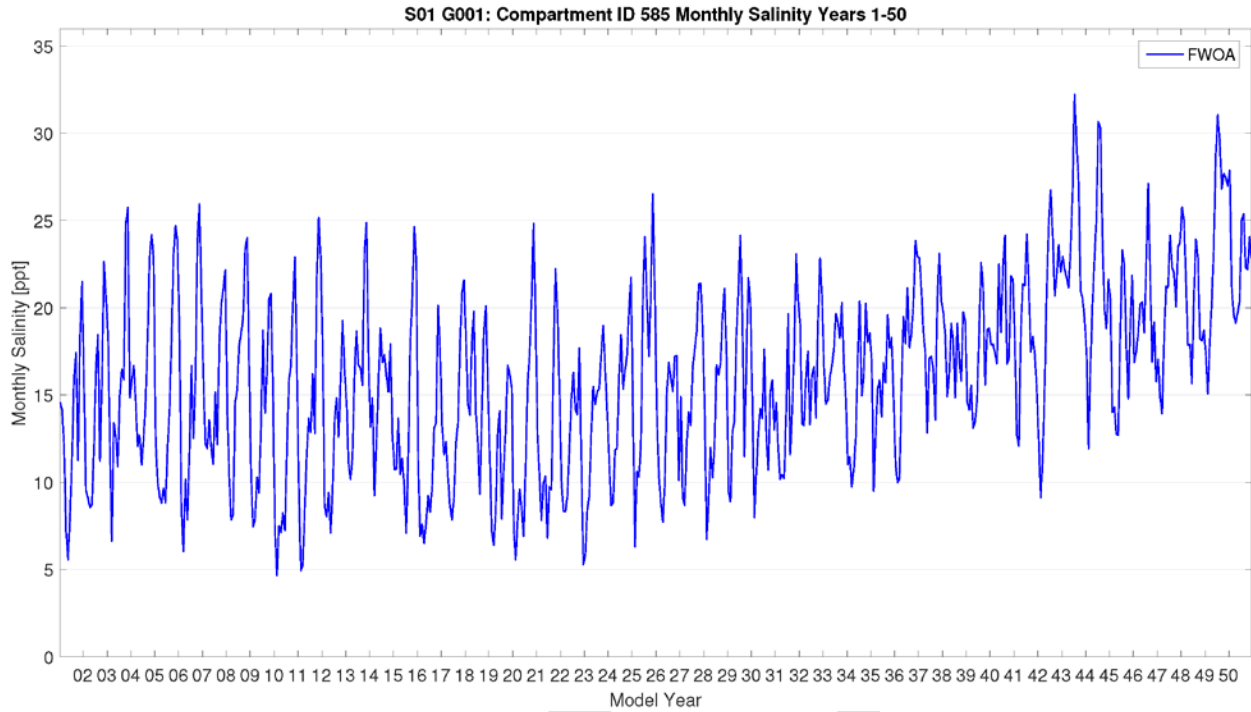


Figure 62: Mean Monthly Salinity in Compartment 512 – Lake de Cade in AA for the Low Scenario (Representative of Intermediate Compartment Results).



**Figure 63: Mean Monthly Salinity in Compartment 585 – Caillou Bay in AA for the Low Scenario (Representative of Near Coast Compartment Results).**

Figure 64 through Figure 66 show the 50-year time series for mean monthly salinity for the AA region for the high scenario for the inland, intermediate, and near coast compartments, respectively. In this scenario, the inland compartment remains fresh water; this is reasonable since it is fed by river water. In the intermediate compartment, salinity increase starts around year 12 and reaches approximately 22 ppt in 50 years. The coastal compartment starts with a salinity of about 15 ppt and increases to around 25 ppt over 50 years.

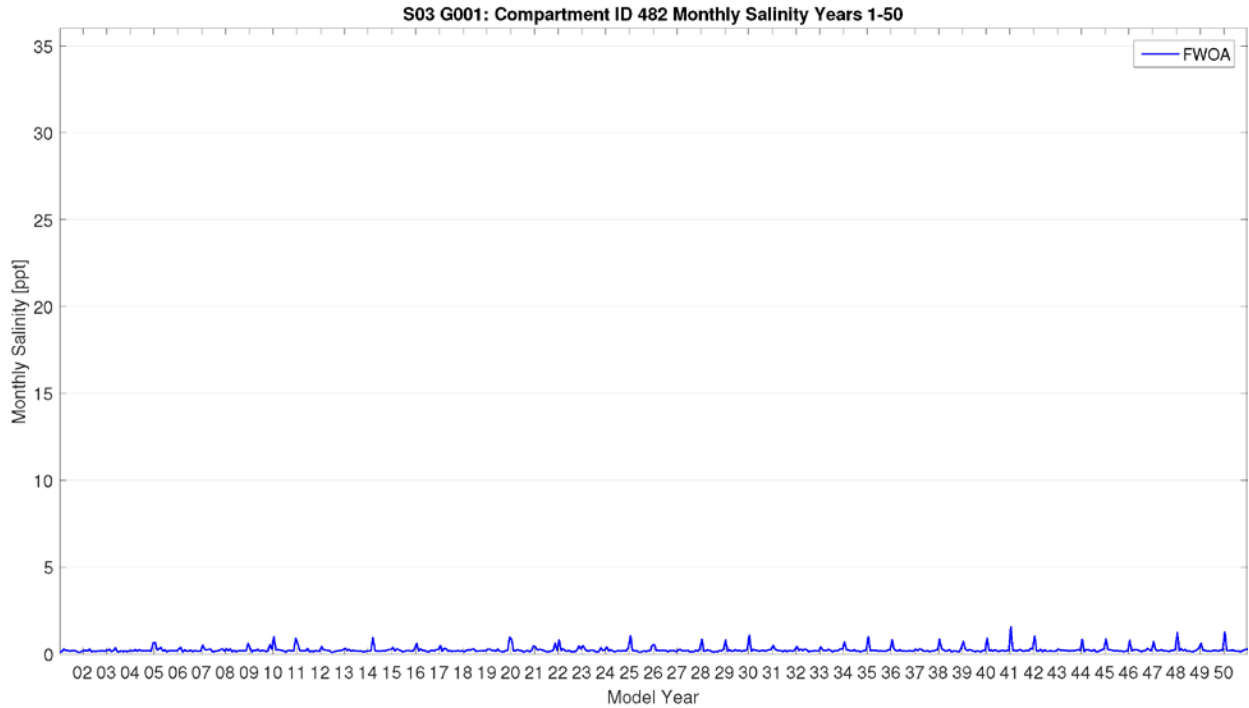


Figure 64: Mean Monthly Salinity in Compartment 482 – Lake Palourde in AA for the High Scenario (Representative of Inland Compartment Results).

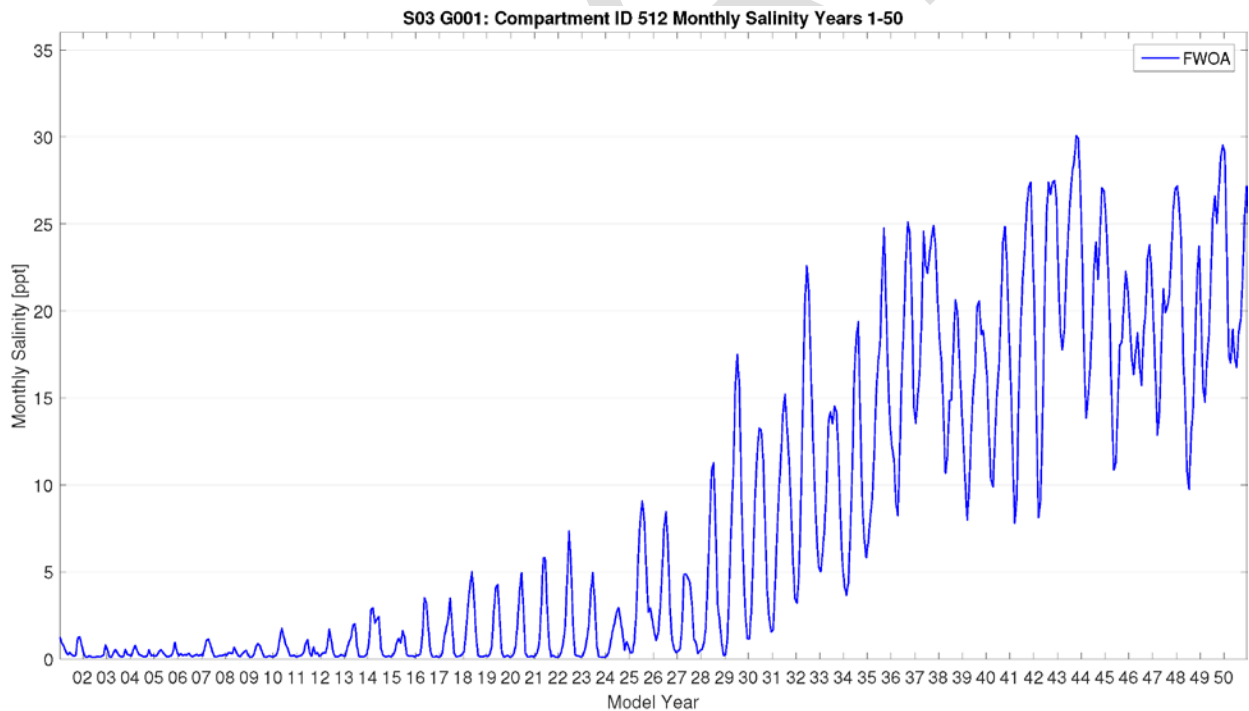
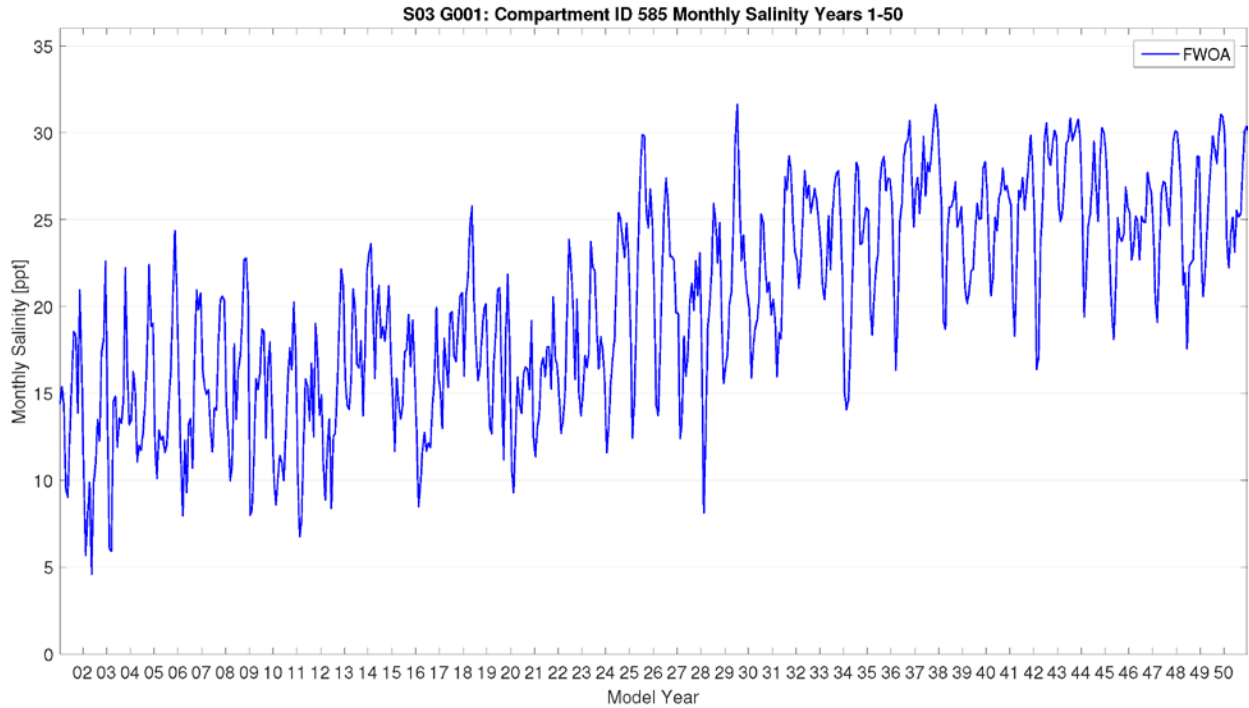


Figure 65: Mean Monthly Salinity in Compartment 512 – Lake de Cade in AA for the High Scenario (Representative of Intermediate Compartment Results).



**Figure 66: Mean Monthly Salinity in Compartment 585 – Caillou Bay in AA for the High Scenario (Representative of Near Coast Compartment Results).**

Figure 67 through Figure 69 show the 50-year time series for mean monthly salinity for the Chenier Plain (CP) for the low scenario for the inland, intermediate, and near coast compartments, respectively. All of the CP stations showed indications of local hydrologic inputs due to rainfall or tributary inflows; this effect decreases from the inland compartment towards the coast. Salinity increase reaches the inland compartment around year 33 with salinities in the range of 2 -12 ppt. In the intermediate compartment, the salinity increase starts around year 37 and reaches approximately 17 ppt. The coastal compartment starts with a salinity of about 7 ppt and increases to around 17 ppt over 50 years.

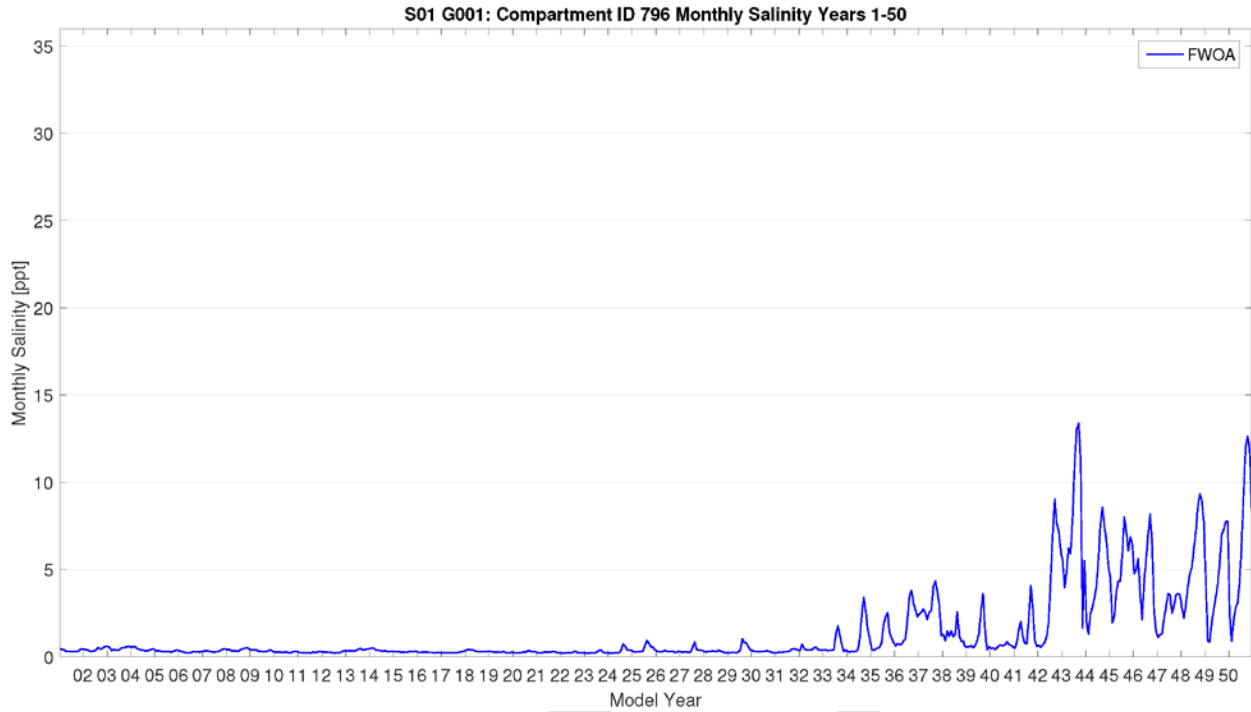


Figure 67: Mean Monthly Salinity in Compartment 796 – Northwest Grand Lake in CP for the Low Scenario (Representative of Inland Compartment Results).

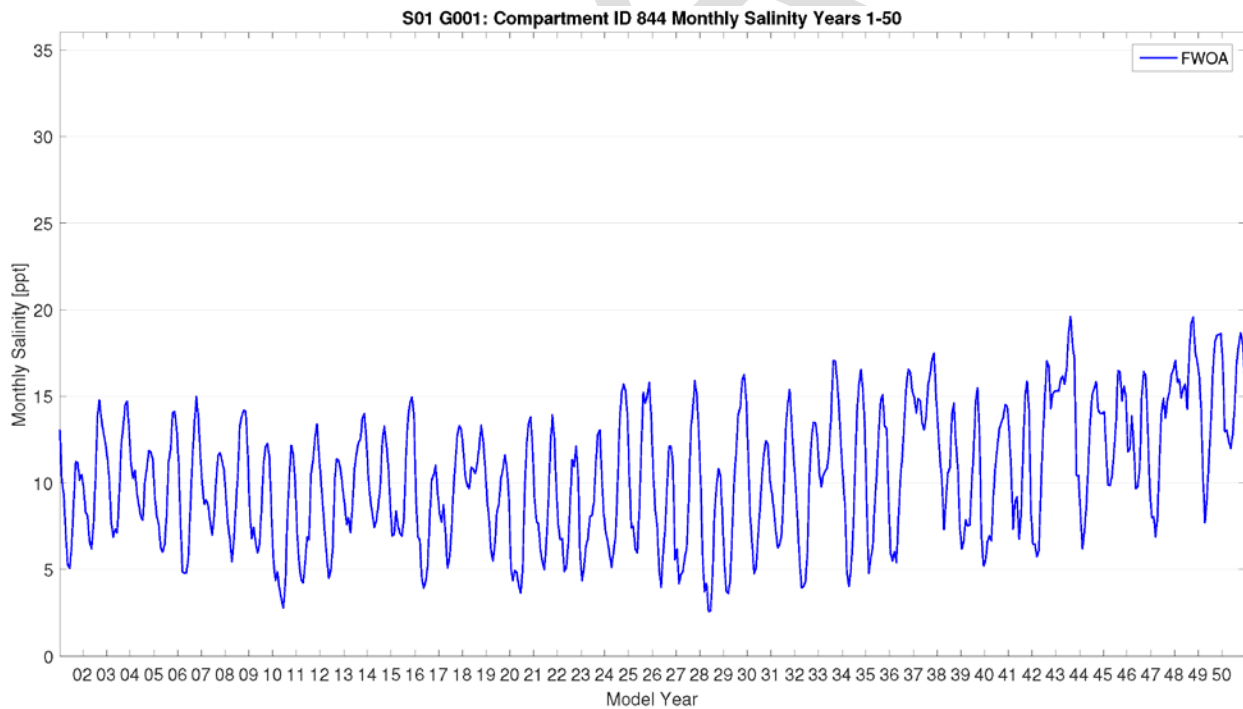
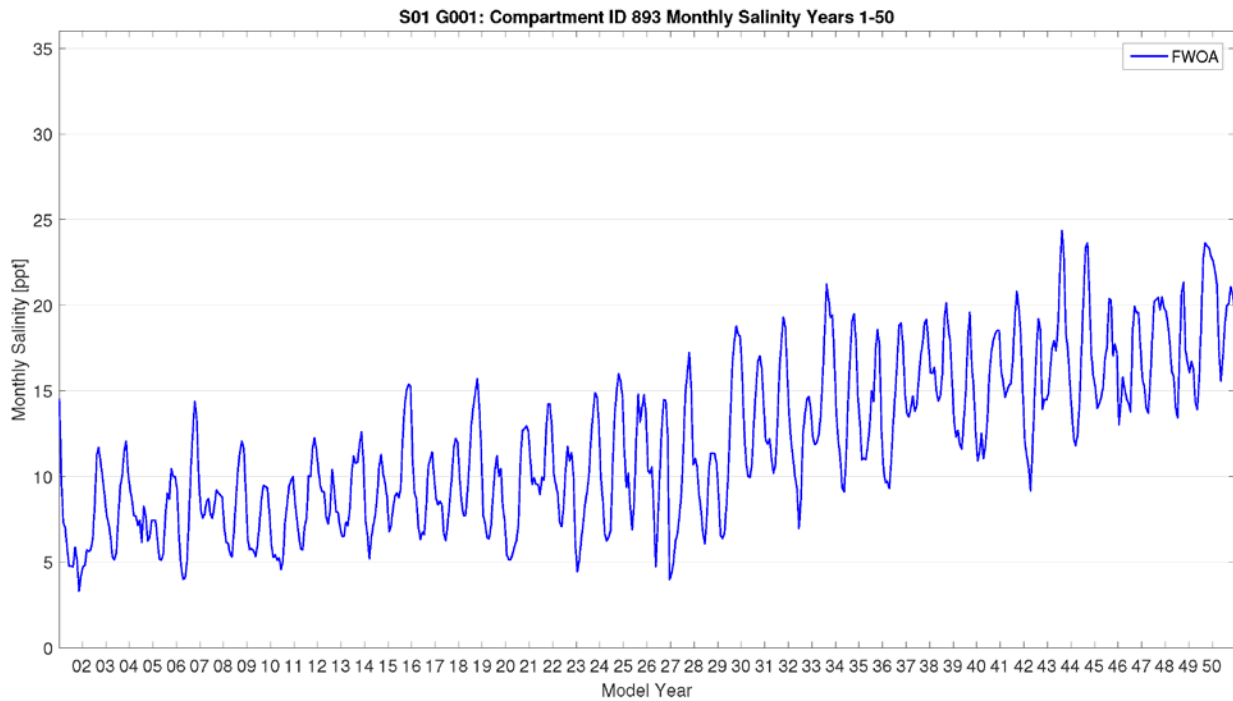


Figure 68: Mean Monthly Salinity in Compartment 844 – East Calcasieu Lake in CP for the Low Scenario (Representative of Intermediate Compartment Results).



**Figure 69: Mean Monthly Salinity in Compartment 893 – Holly Beach in CP for the Low Scenario (Representative of Near Coast Compartment Results).**

Figure 70 through 72 show the 50-year time series for mean monthly salinity for the CP for the high scenario for the inland, intermediate, and near coast compartments, respectively. Salinity increase reaches the inland compartment around year 22 with salinities in the range of 2-20 ppt. The coastal cell increased from about 10 ppt to 20 ppt in 50 years. The spike in salinity at approximately year 37 (and subsequent drop in salinity) is due to an unstable interaction between the marsh links and the Kadlec Knight marsh exchange equations. These issues are generally a result of the assumption that the salinity in the marsh is equal to the salinity in the open water areas – which was complicated by the marsh link network. In essence, this assumption was no longer valid in later simulation years when there were large masses of water being routed through the marsh link network (whether from accelerated sea level rise or some other mechanism) as well as via the Kadlec Knight marsh exchange equation. This assumption effectively routed water from marsh links to the marsh surface but did not bring the salinity with it. Instead, it was routed to the open water area, resulting in these instability spikes. This only shows up in later years when marsh links that were not subjected to such large flows/salinities during the calibration period were ‘activated’. This issue was corrected in a subsequent version of the model (used for simulation of alternatives).

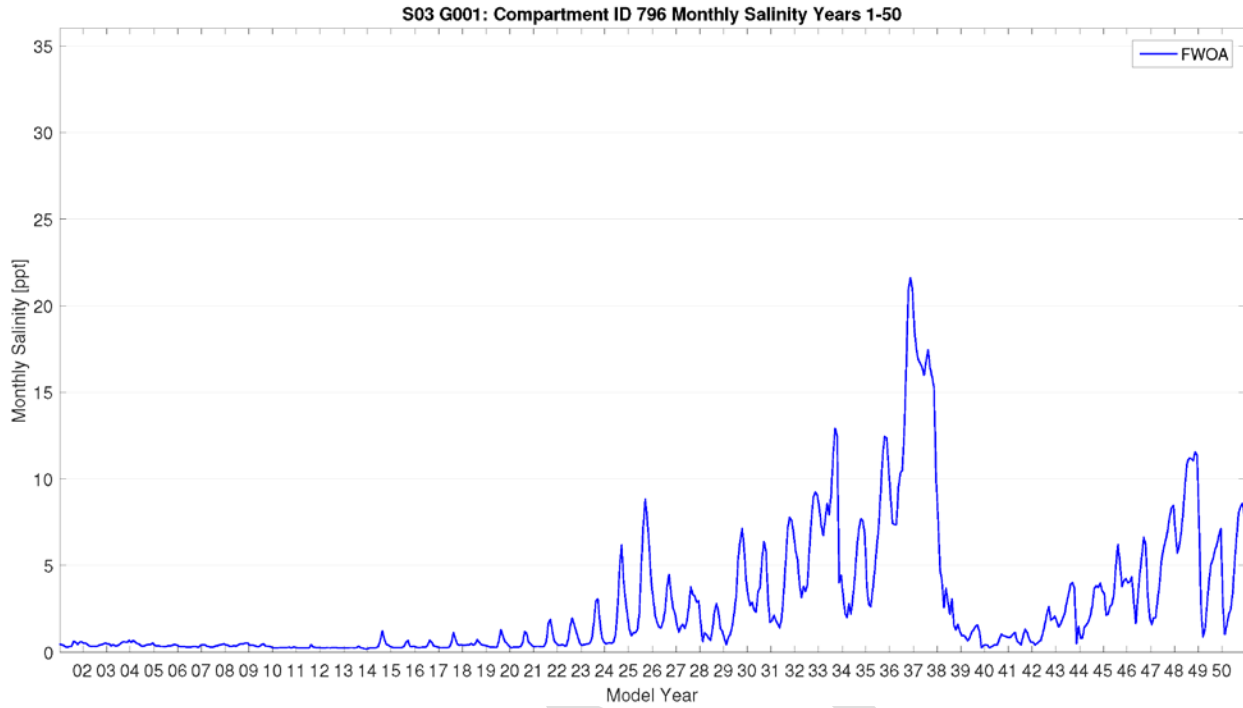


Figure 70: Mean Monthly Salinity in Compartment 796 – Northwest Grand Lake in CP for the High Scenario (Representative of Inland Compartment Results).

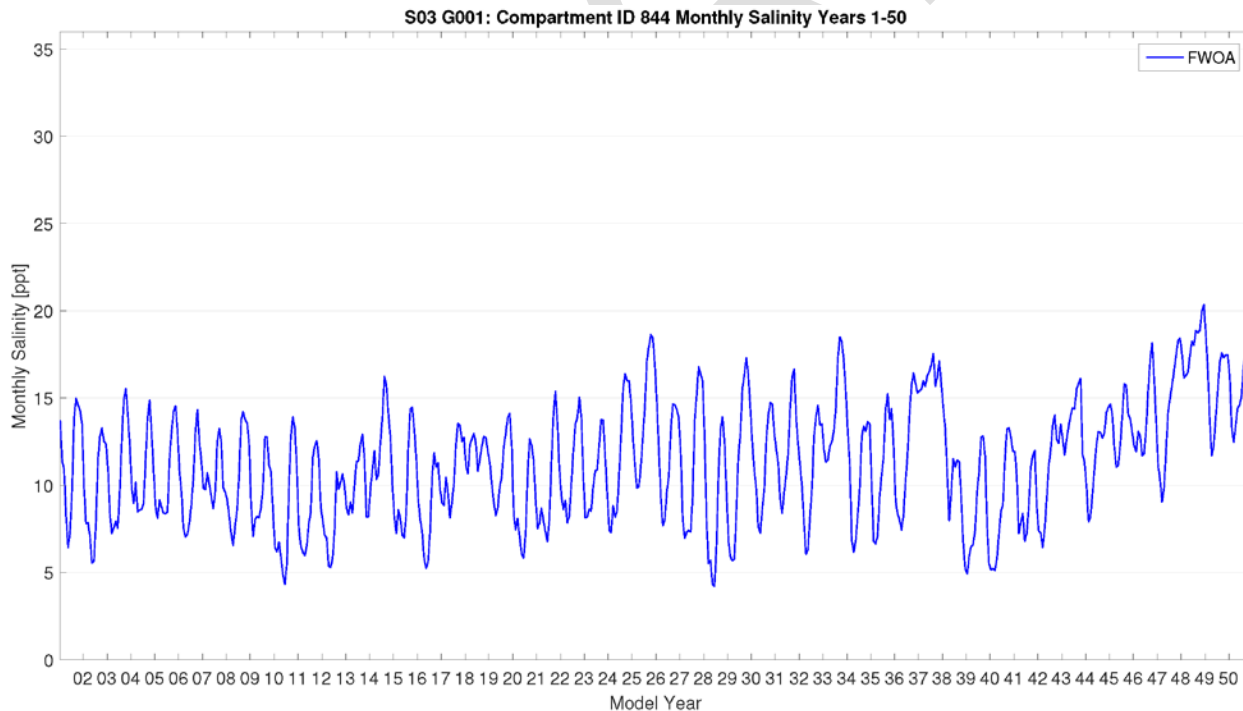


Figure 71: Mean monthly Salinity in Compartment 844 – East Calcasieu Lake in CP for the High Scenario (Representative of Intermediate Compartment Results).

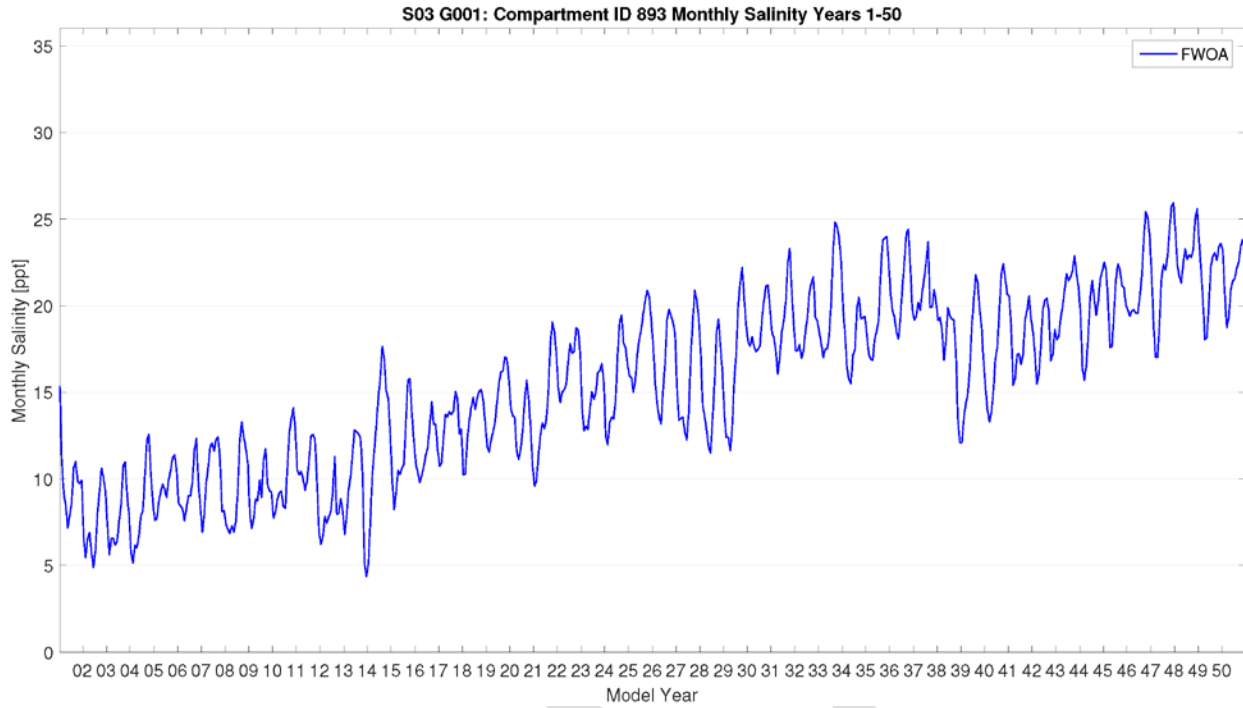
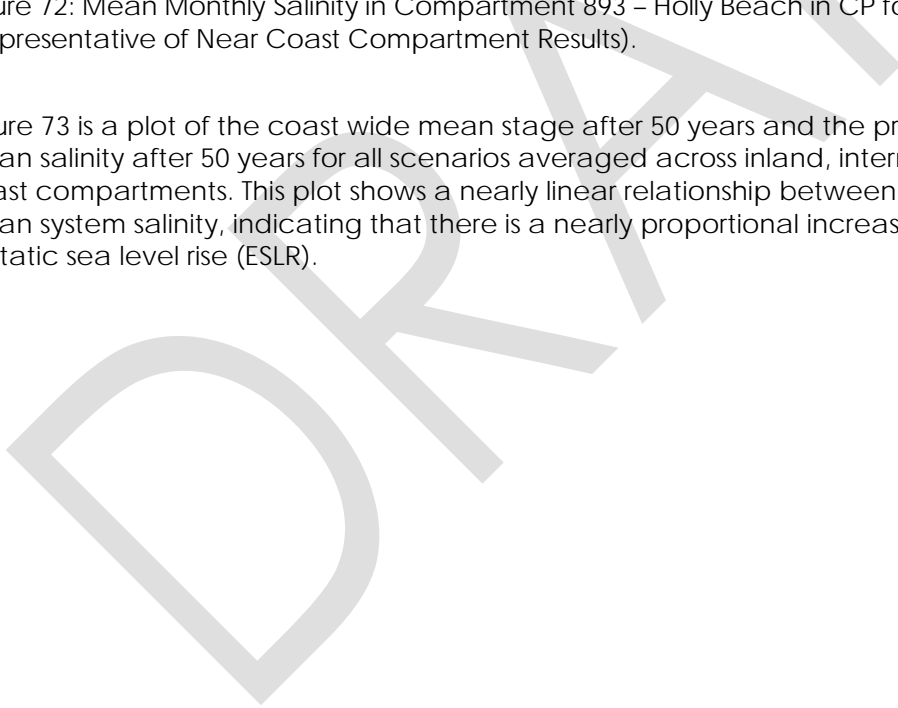


Figure 72: Mean Monthly Salinity in Compartment 893 – Holly Beach in CP for the High Scenario (Representative of Near Coast Compartment Results).

Figure 73 is a plot of the coast wide mean stage after 50 years and the predicted coast wide mean salinity after 50 years for all scenarios averaged across inland, intermediate, and near coast compartments. This plot shows a nearly linear relationship between mean stage and the mean system salinity, indicating that there is a nearly proportional increase of salinity with eustatic sea level rise (ESLR).



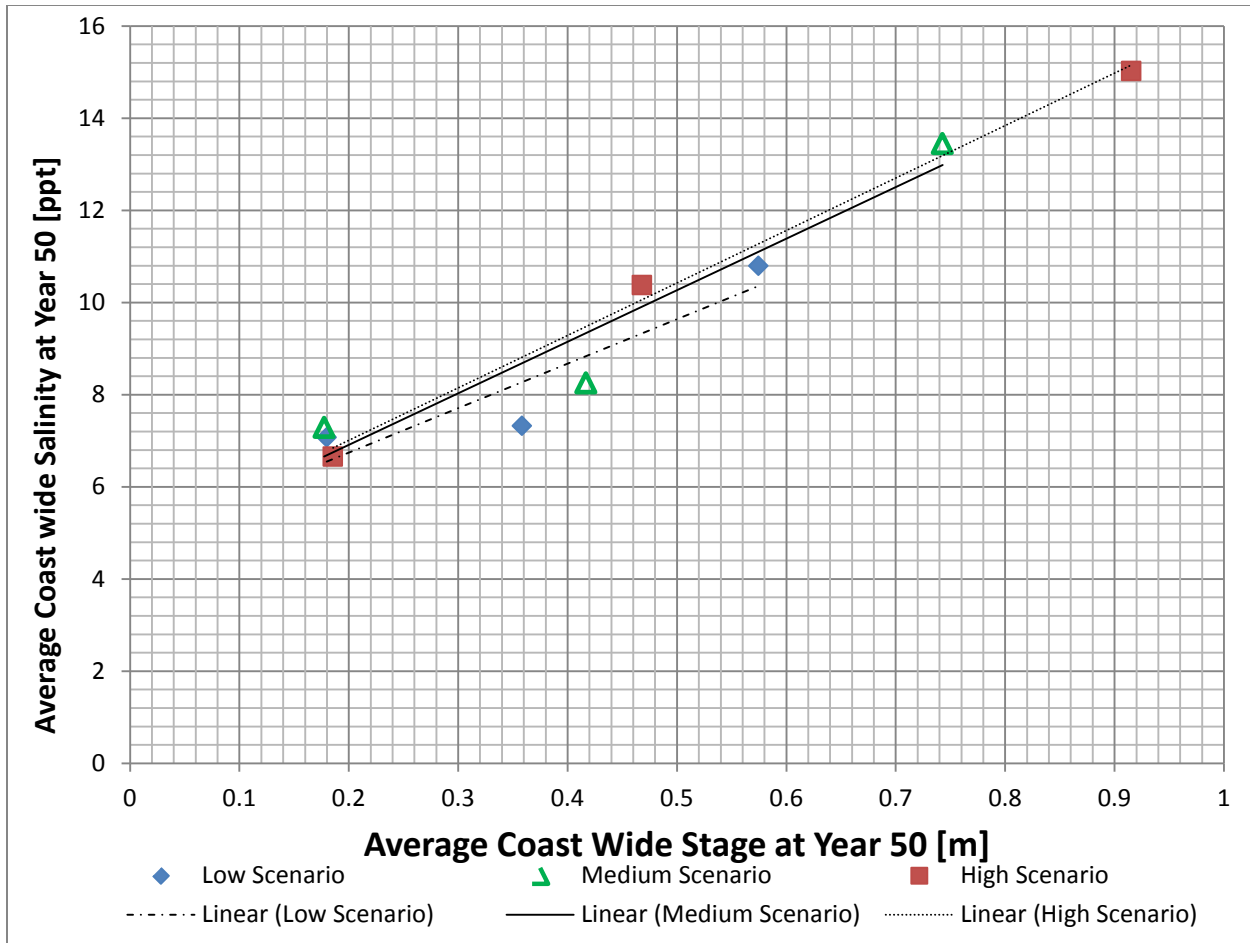


Figure 73: Response of Coast Wide Mean Year 50 Salinity (Averaged Over Inland, Intermediate, and Near Coast Locations) to the Mean Year 50 Stage (Averaged Over Inland, Intermediate, and Near Coast Locations) for All Three Scenarios (Low, Medium, and High).

### 3.3 Land Change

To facilitate the description of land change over time, ecoregions were used to define specific coastal areas (Figure 74). The curves of land area over time show trends that vary depending upon the collapse mechanism that triggers specific episodes of land loss (Figure 75-Figure 86). When large, abrupt shifts in land area appear in the land area time series, it is generally indicative of a salinity collapse threshold (see Table 4) being met during a specific model year. For example, the Bird's Foot Delta (BFD) (Figure 77) and Upper Pontchartrain (UPO) (Figure 75) ecoregions have very clear periods of abrupt land loss where substantial areas of coastal wetlands collapse during a single model year. Inspection of the vegetation maps indicate that the Bird's Foot Delta ecoregion experiences repeated periods of substantial fresh marsh collapse during years 24 and 25 under all three scenarios. This loss corresponds to low river years in the 50-year historic Mississippi River hydrograph (which is unchanged across all three scenarios). Under the high scenario, the Bird's Foot Delta ecoregion also experienced an episode of fresh marsh collapse during yet another low river year, year 43. The salinity stress collapse mechanism will only collapse fresh marsh areas that are inundated by the annual mean water level. Therefore, while the low river years are constant across scenarios, the amount of land inundated will

change, particularly in the later years of scenarios with higher rates of sea level rise. These abrupt episodes of collapse due to salinity thresholds being met are evident primarily only in the eastern portion of the model domain where the influence of the Mississippi River fresh water supply is important to both vegetation cover (e.g., fresh marsh near the river) and the short-term salinity patterns that will impact collapse thresholds being met or not. However, areas remote from direct riverine influence in both the Atchafalaya/Vermillion/Teche (AVT) (Figure 82) and Mermentau/Lakes (MEL) (Figure 83) ecoregions have some areas of fresh wetland areas that collapse due to short-term periods of high salinity which may be caused by annual variation in precipitation and evapotranspiration.

The second trend visible in the land area over time curves is the continuous (e.g., non-piecewise) loss of coastal land area throughout all of the ecoregions. This non-abrupt, continuous loss of land is a function of the combined effects of subsidence and ESLR, both of which vary by scenario, on non-fresh wetlands; hence, the varying slopes and the modeled accretion of marsh elevation (a function of inorganic sediment deposition and organic loading) is unable to keep up with the relative sea level rise in each scenario, and as the rates of ESLR accelerate in later years, the rate of land loss increases as well. If only subsidence were resulting in land change through time, the coastal land area susceptible to inundation-derived collapse would be decreasing at a directly proportional rate with a constant slope, since modeled subsidence rates do not change through time. The addition of a non-constant rate of change in the eustatic sea level, however, results in an increasing negative slope over time. This increasingly negative slope is most evident in the high scenario than in the medium and low scenarios, a function of the fact that the high scenario has the largest acceleration of the three ESLR scenarios, followed by the medium scenario, and at last the low (see Appendix C - Chapter 2 and Attachment C2-1).

The exact depth of inundation resulting in collapse varies by vegetation type (see Table 4), and subsequently varies spatially across the coast; however, there are no clear spatial or temporal patterns evident that indicate a strong sensitivity to these different inundation depth thresholds. While no strong sensitivity to inundation depth threshold is evident, a sharp differentiation can be seen (both spatially and temporally) between collapse mechanisms. In other words, the loss pattern is driven by whether salinity is the driving force in collapse (e.g., fresh forested and fresh marsh areas) or whether inundation, regardless of threshold depth, will result in marsh collapse. If the modeled salinity values change gradually enough for an initially fresh land type to switch to a more salt-tolerant land type, a greater portion of the land will be able to be sustained through a short period of high salinities, reducing the number of abrupt losses through time (e.g., Figure 77) for a more consistent rate of change driven by sea level rise and subsidence rates (e.g., Figure 76).

In many of the ecoregions under the high scenario, it appears that the amount of land remaining at year 50 asymptotically approaches some non-zero number; these limits do not appear in all ecoregions, nor do they generally appear in the low and medium scenarios.

While there are many areas of land loss across the entire model domain, there are some specific areas where the ICM predicts land gain during 50 years of no action being taken. Areas within the model domain that are most evidently gaining land during the low scenario are: the Wax Lake Outlet and Atchafalaya deltas, the West Bay region of the Bird's Foot Delta, the Fort St. Phillip crevasse diversion on the east bank of the Mississippi River, the east bank of the Bird's Foot Delta in the vicinity of Quarantine, and portions of the Gulf Coast Intracoastal Waterway in the vicinity of Franklin. Less evident in the included figures are areas of land gain in the waterways immediately downstream of the Caernarvon diversion outfall. Similar gain is also occurring downstream of the Davis Pond diversion.

The areas of land gain are, intuitively, more evident at year 50 of the low and medium scenarios than at year 50 of the high scenario. At the end of the high scenario, the only areas indicating gain are in the three main active deltas: Wax Lake Outlet, Atchafalaya, and the West Bay portion of the Bird's Foot Delta (Figure 87-Figure 92).

In general terms, the land gain areas do not change much through time nor across scenario. The extent of land gain increases between years 25 and 50, and decreases from low to high scenarios (Figure 75 through Figure 86), but the locations that show this land gain do not change. That is, if land has been gained by year 50 at a location, the land gain was evident by year 25. Contrary to this, there are regions that experience loss *only* in the later years of the simulation when ESLR has risen dramatically and many areas that were not susceptible to collapse in year 25 are collapsed by year 50. This trend also holds when comparing across scenario; more land is susceptible to collapse under the high scenario; however, some regions (e.g., Wax Lake Outlet, Davis Pond, etc.), experience land gain regardless of scenario.

Coast wide over the 50-year FWOA (G001) there is a net change in land area within the model domain of -4,610 km<sup>2</sup>, -7,320 km<sup>2</sup> and -10,990 km for the low, medium, and high scenarios, respectively (Figure 87-Figure 92).

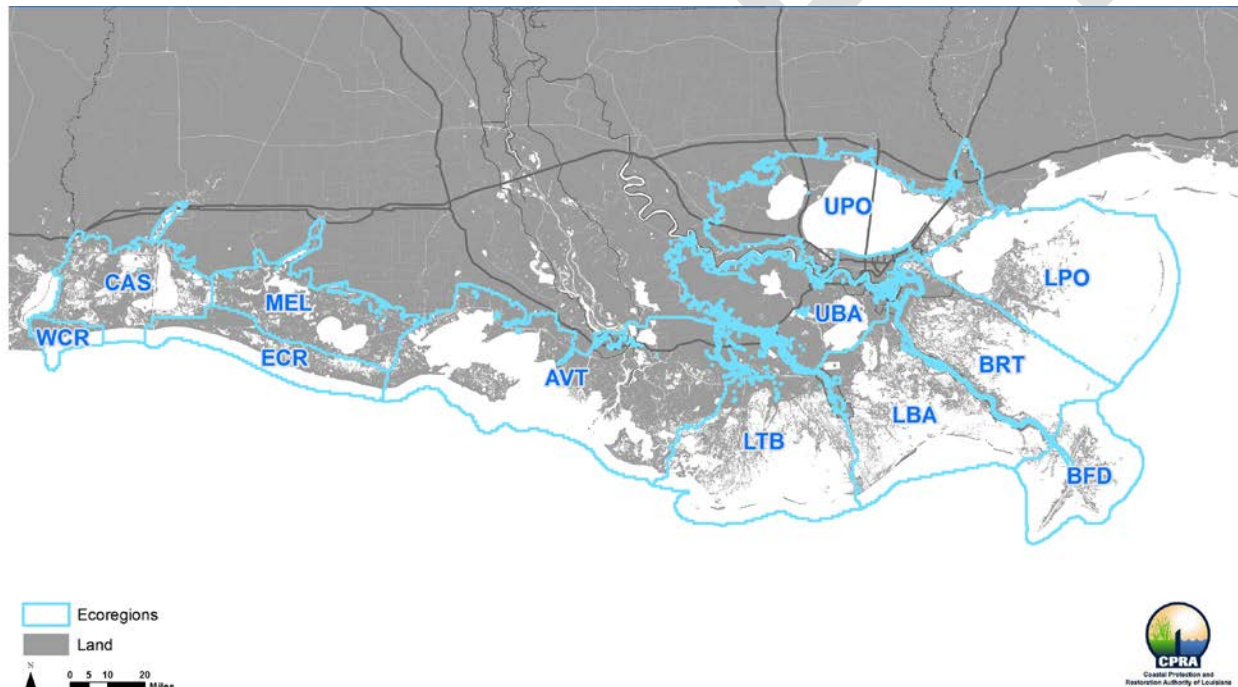


Figure 74: 2017 Coastal Master Plan Ecoregions.

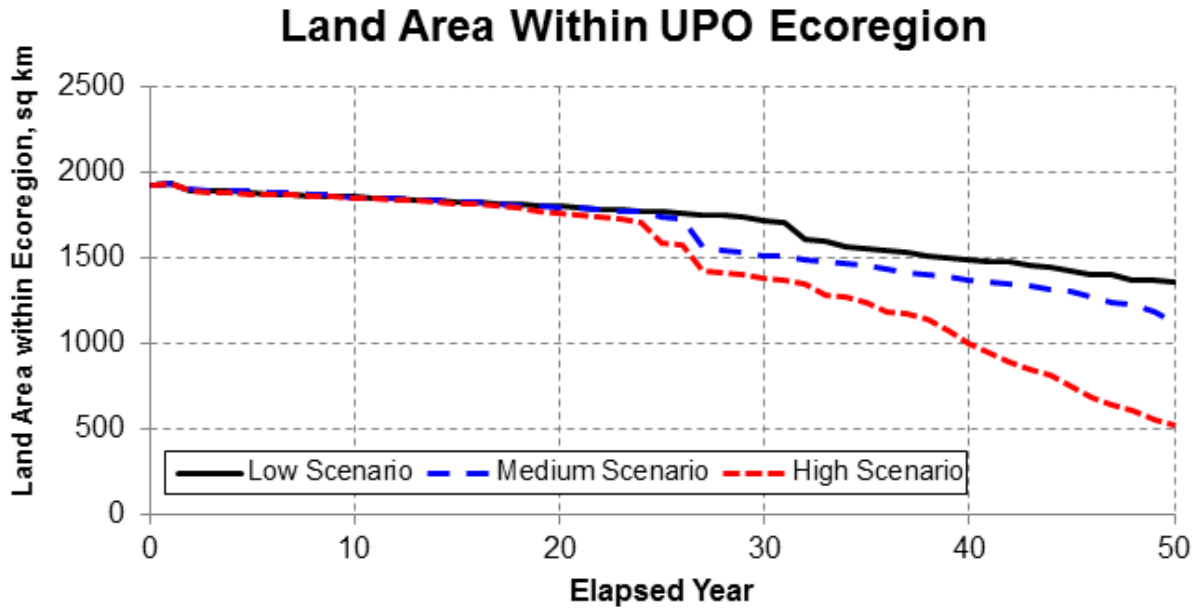


Figure 75: Land Area through Time within the Upper Pontchartrain Ecoregion.

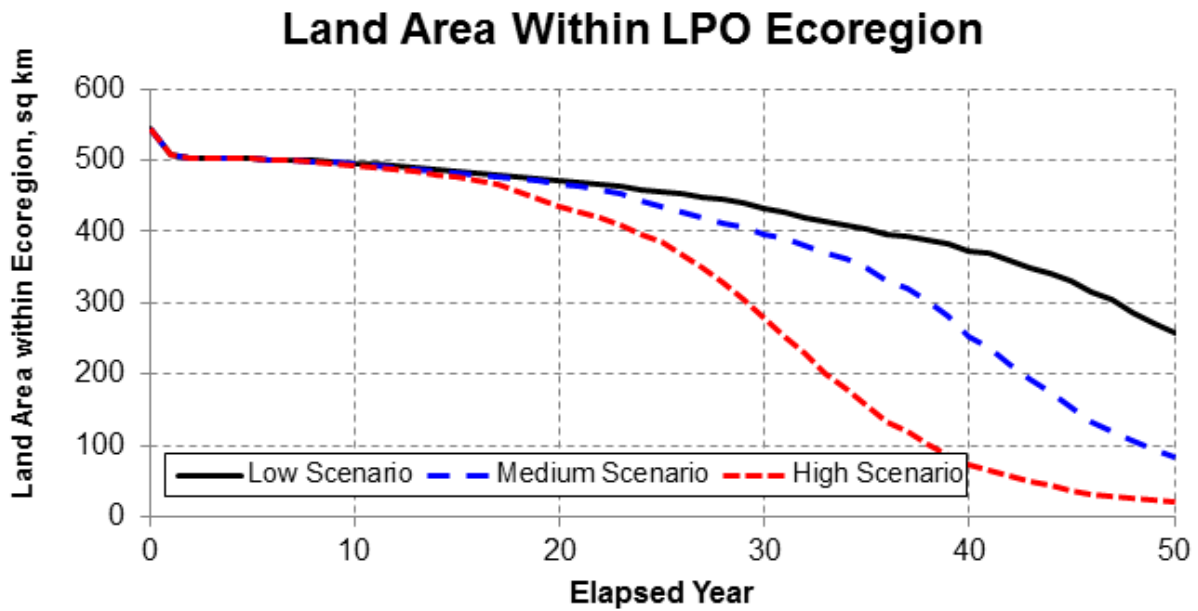


Figure 76: Land Area through Time within the Lower Pontchartrain Ecoregion.

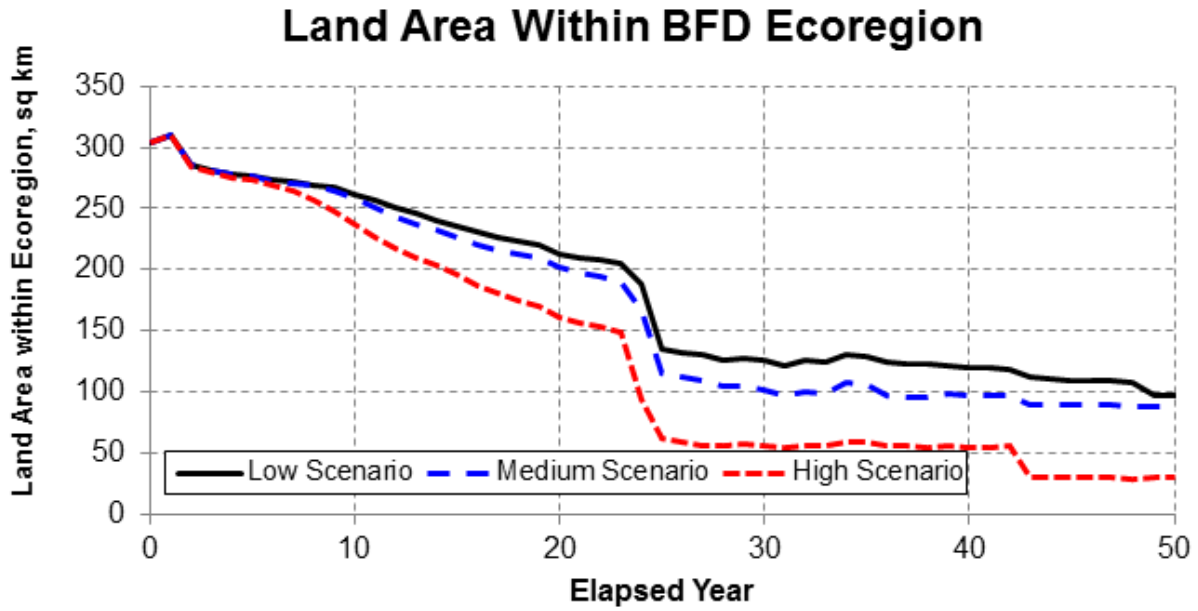


Figure 77: Land Area through Time within the Bird's Foot Delta Ecoregion.

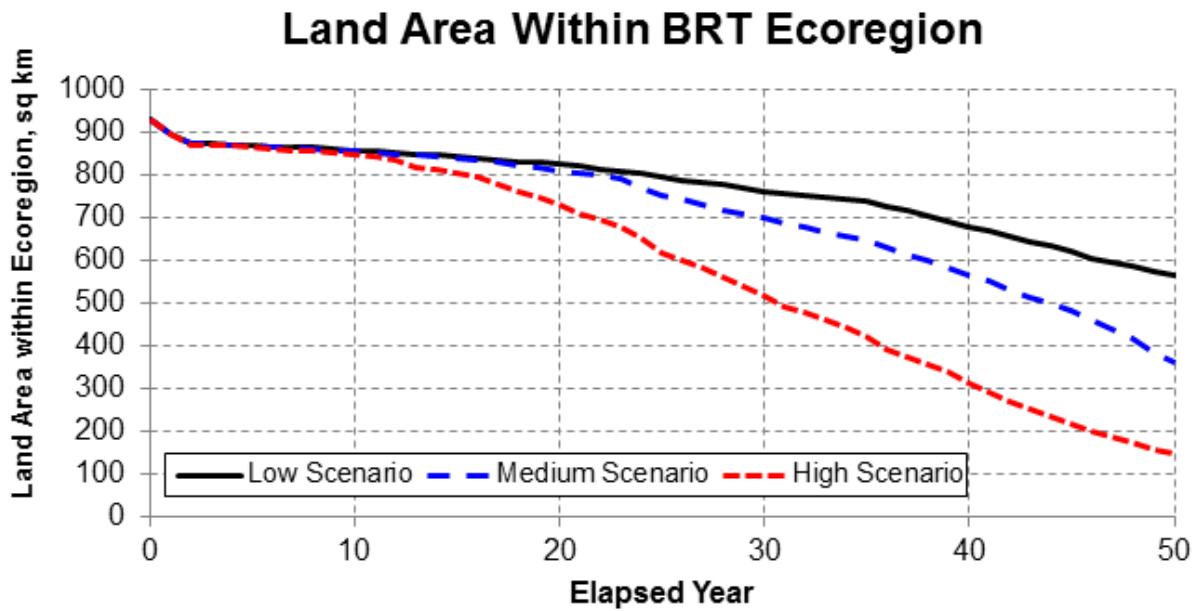


Figure 78: Land Area through Time within the Breton Ecoregion.

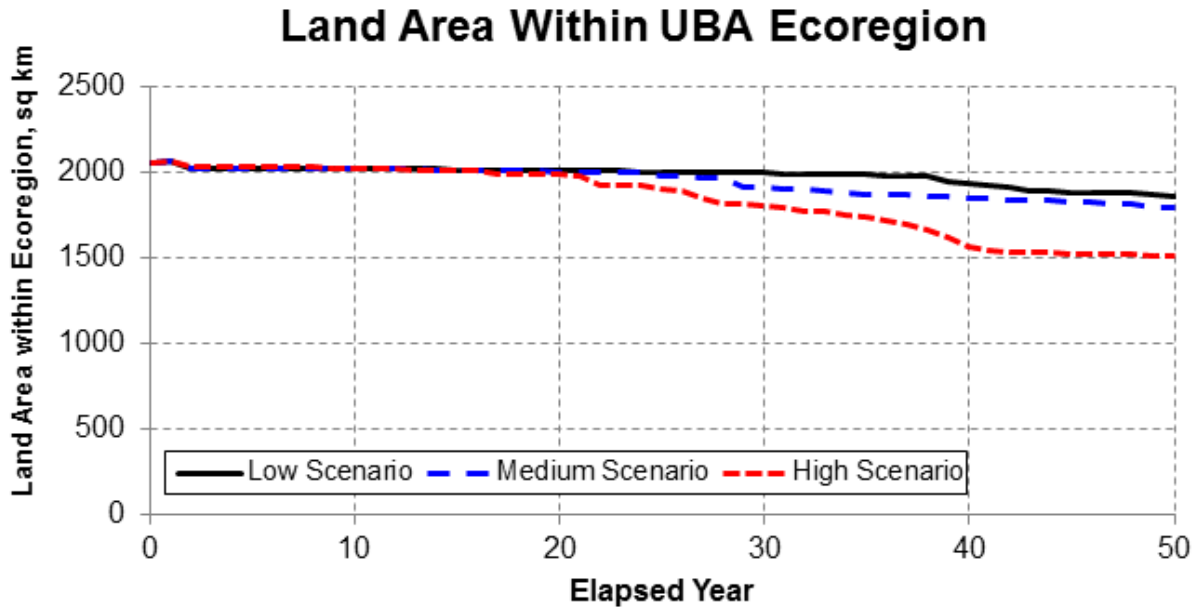


Figure 79: Land Area through Time within the Upper Barataria Ecoregion.

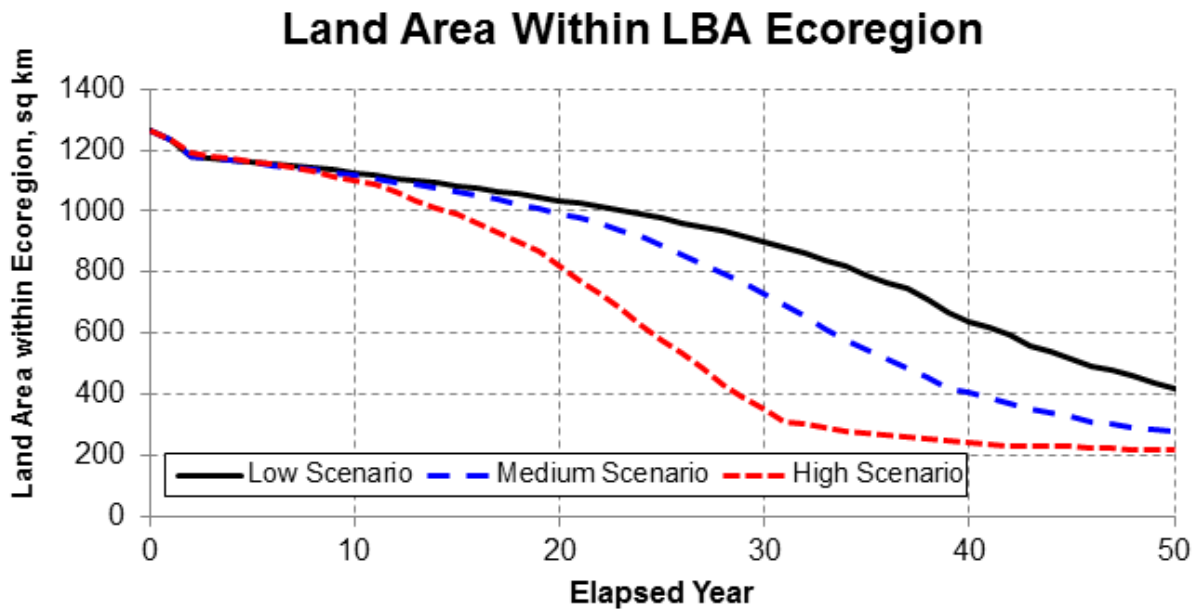


Figure 80: Land Area through Time within the Lower Barataria Ecoregion.

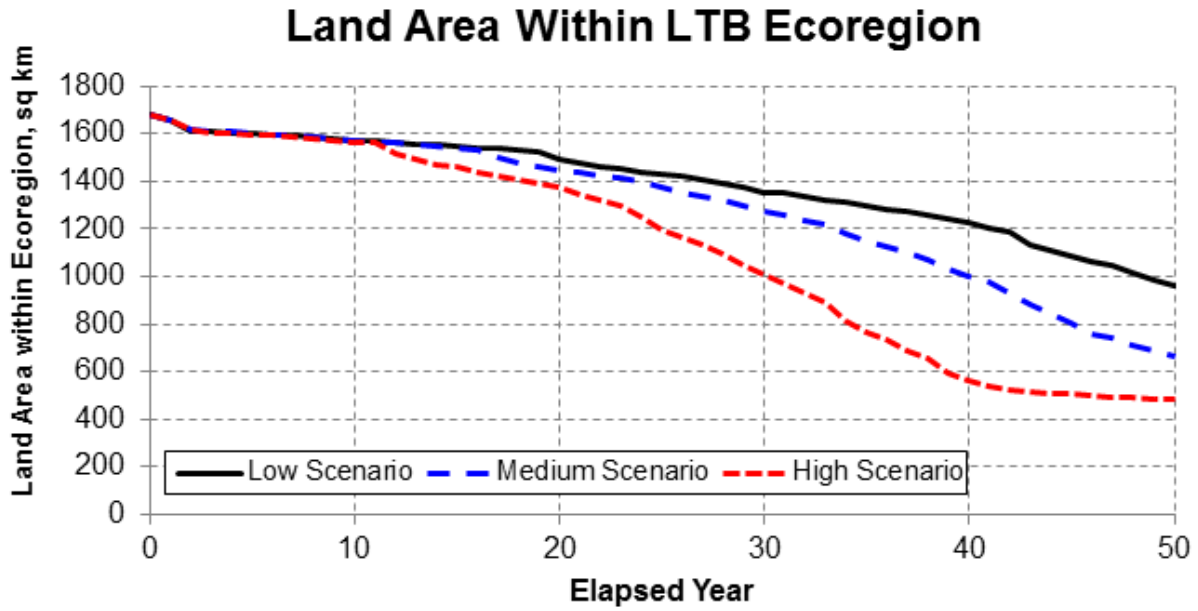


Figure 81: Land Area through Time within the Lower Terrebonne Ecoregion.

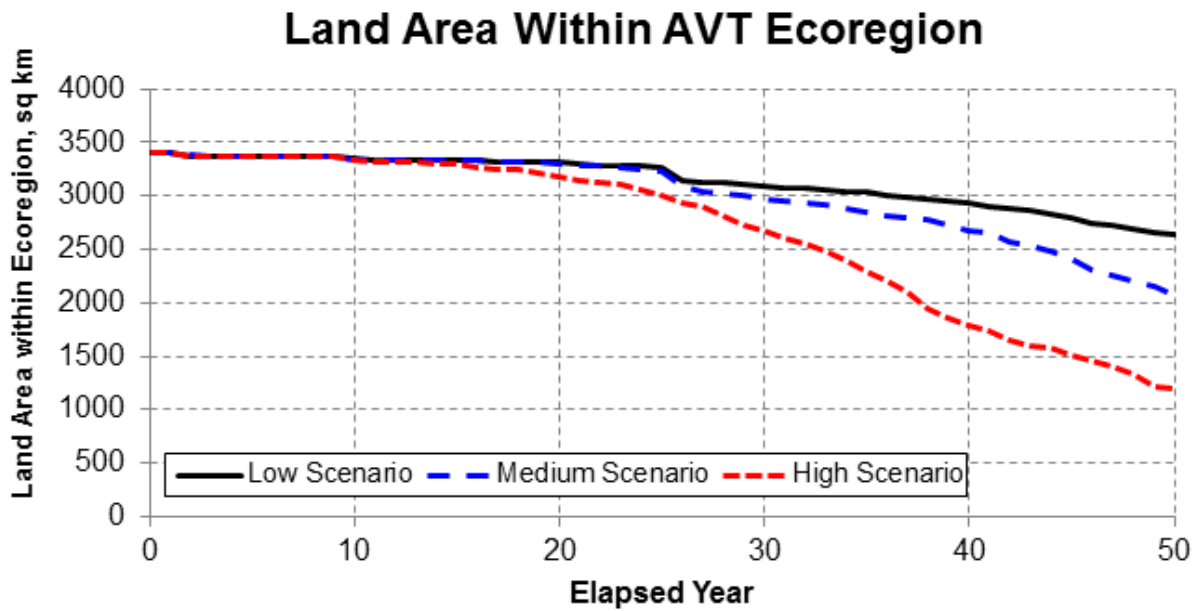


Figure 82: Land Area through Time within the Atchafalaya/Vermilion/Teche Ecoregion.

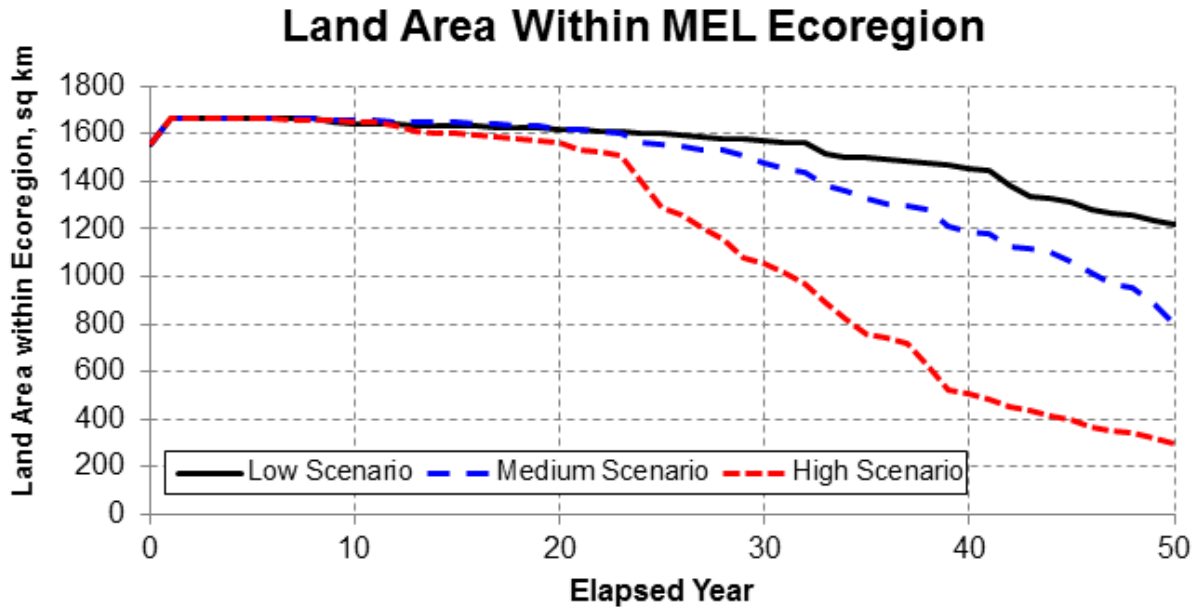


Figure 83: Land Area through Time within the Mermenteau/Lakes Ecoregion.

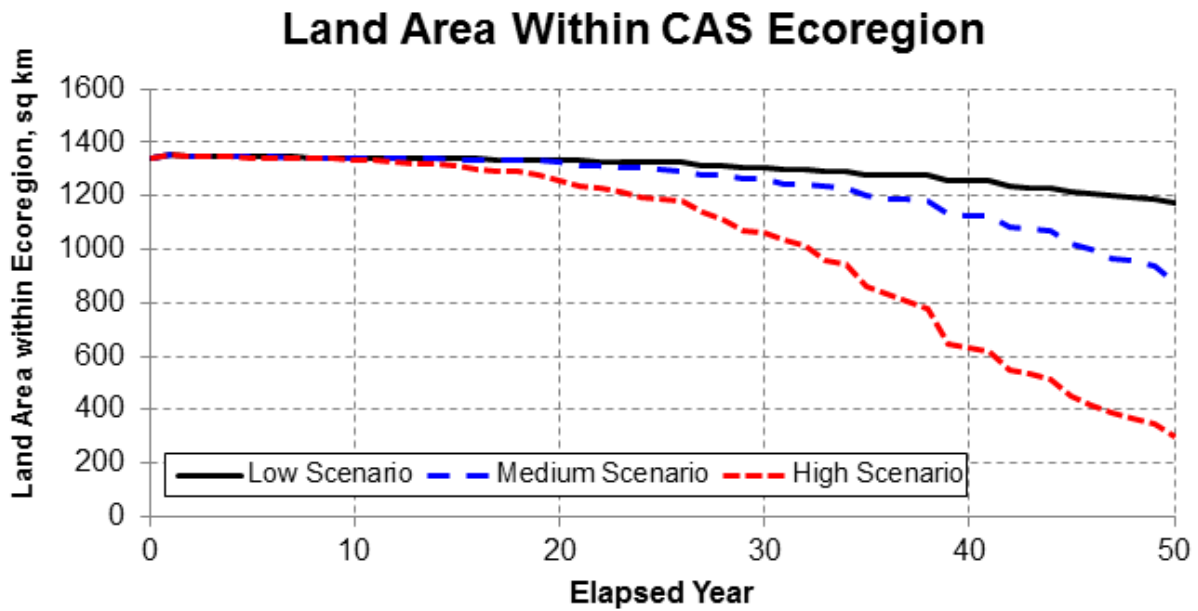


Figure 84: Land Area through Time within the Calcasieu/Sabine Ecoregion.

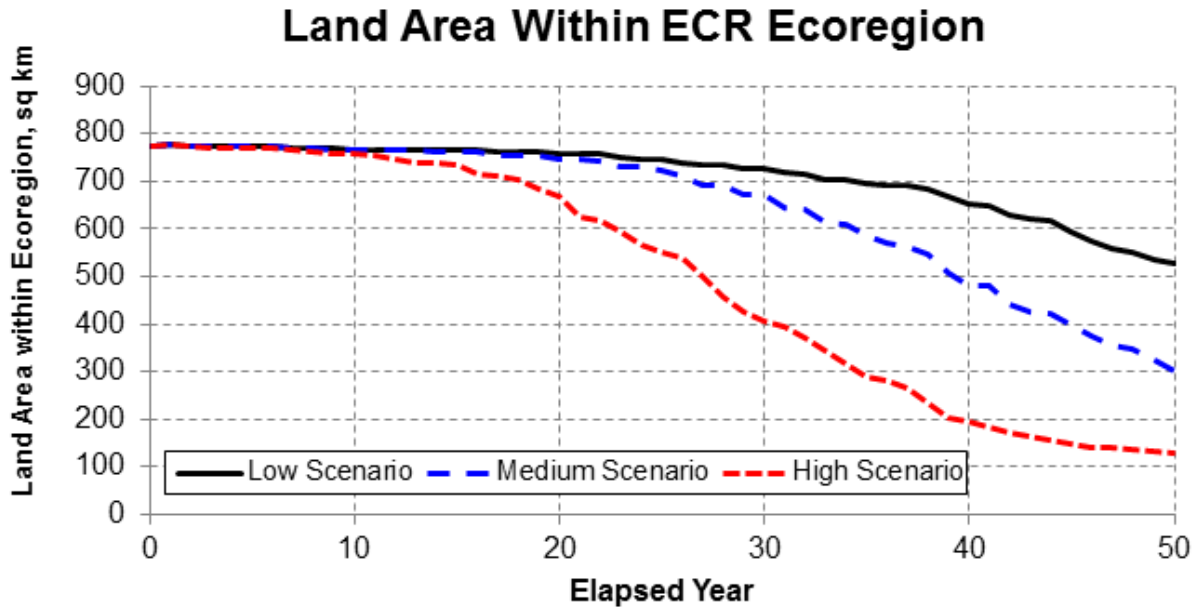


Figure 85: Land Area through Time within the Eastern Chenier Ridge Ecoregion.

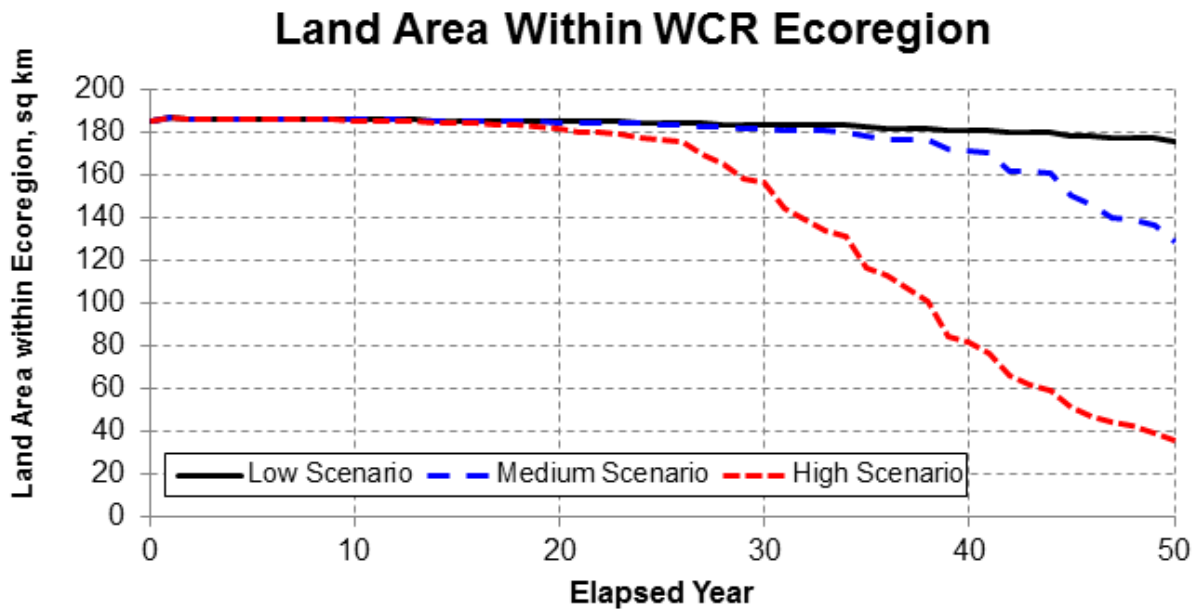


Figure 86: Land Area through Time within the Western Chenier Ridge Ecoregion.

**Table 4: Mechanisms within ICM Driving Land Gain and Marsh Collapse.**

Land Type	Collapse/Gain threshold
Fresh Forested Wetlands	Land will convert to water if it is at, or below, the annual mean water level for the year and the maximum two-week mean salinity during the year is above 7 ppt.
Fresh Marsh	Land will convert to water if it is at, or below, the annual mean water level for the year and the maximum two-week mean salinity during the year is above 5.5 ppt.
Intermediate Marsh	Land will convert to water if the annual mean water depth over the marsh for two consecutive years is greater than 0.358 m.
Brackish Marsh	Land will convert to water if the annual mean water depth over the marsh for two consecutive years is greater than 0.256 m.
Saline Marsh	Land will convert to water if the annual mean water depth over the marsh for two consecutive years is greater than 0.235 m.
Water	Water will be converted to land if the mean water level for two consecutive years is at least 0.2 m lower than the bed elevation of the water area.

DRAFT

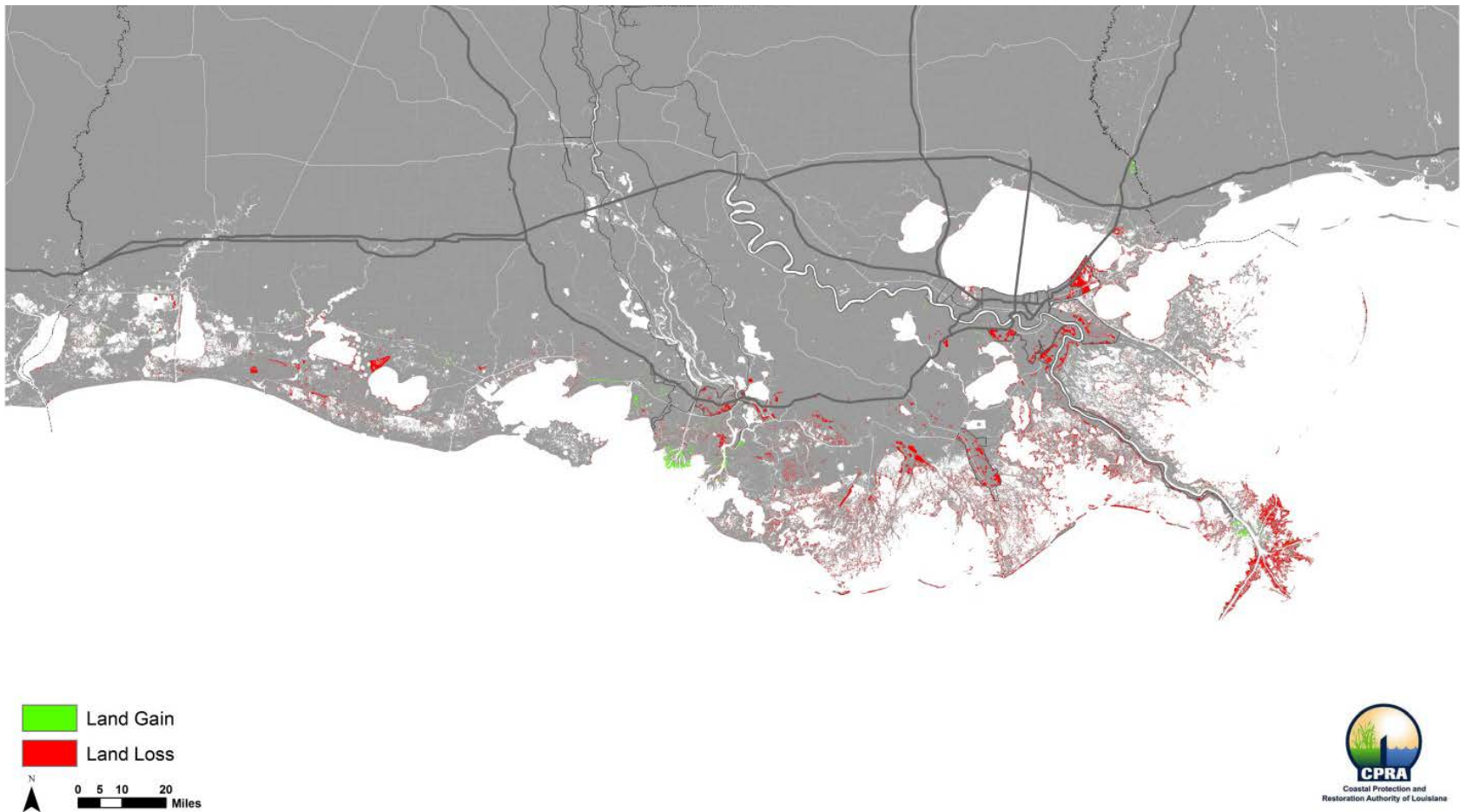


Figure 87: Land Change from Initial Conditions after 25 Years of Low Scenario – FWOA. Net Land Change (Land Gain-Land Loss) at Year 25 is -1,170 km<sup>2</sup> for the Low Scenario.

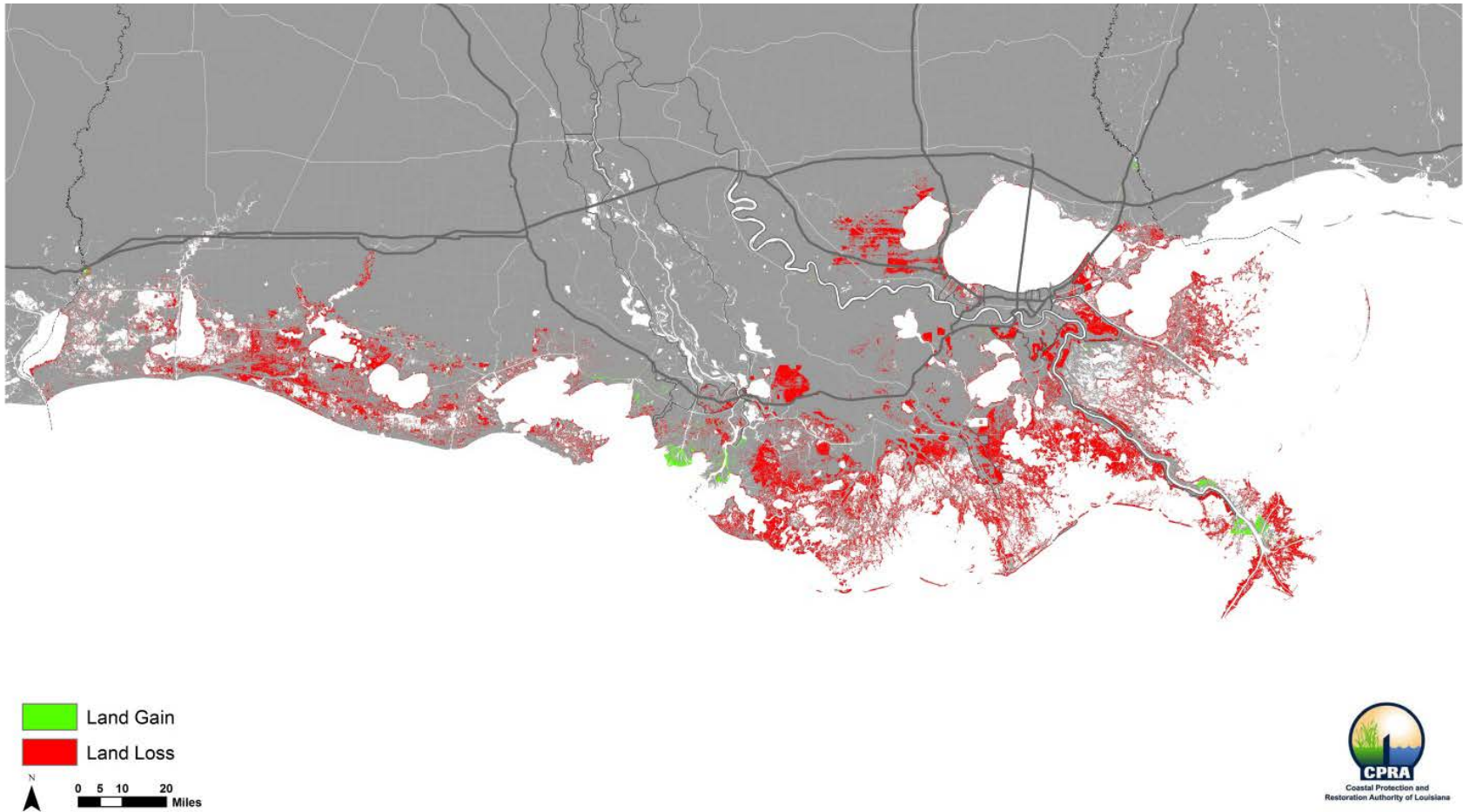


Figure 88: Land Change from Initial Conditions after 50 Years of Low Scenario – FWOA. Net Land Change (Land Gain-Land Loss) at Year 50 is -4,610 km<sup>2</sup> for the Low Scenario.

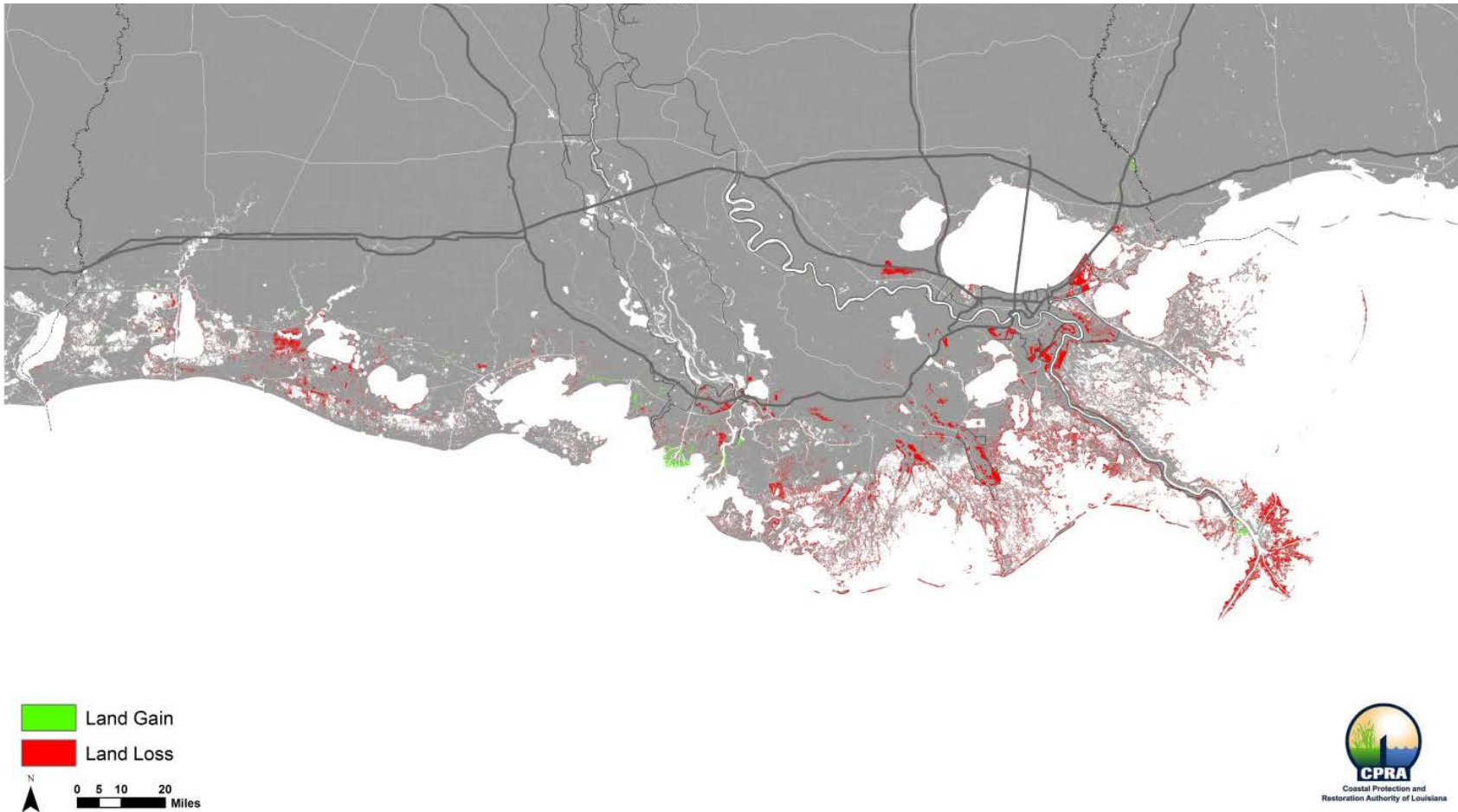


Figure 89: Land Change from Initial Conditions after 25 Years of Medium Scenario – FWOA. Net Land Change (Land Gain-Land Loss) at Year 25 is -1,590 km<sup>2</sup> for the Medium Scenario.

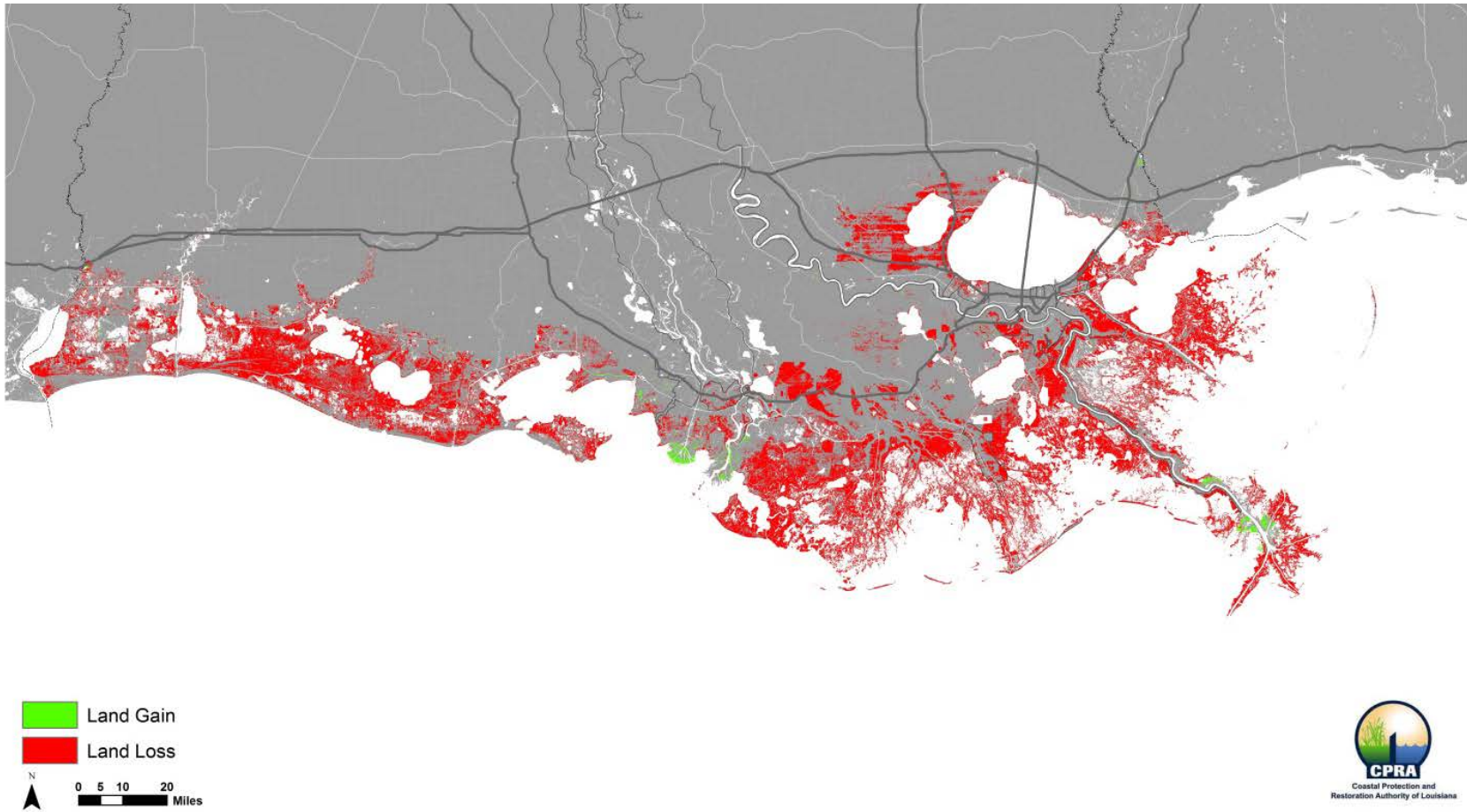


Figure 90: Land Change from Initial Conditions after 50 years of Medium scenario – FWOA. Net Land Change (Land Gain-Land Loss) at Year 50 is -7,320 km<sup>2</sup> for the Medium Scenario.

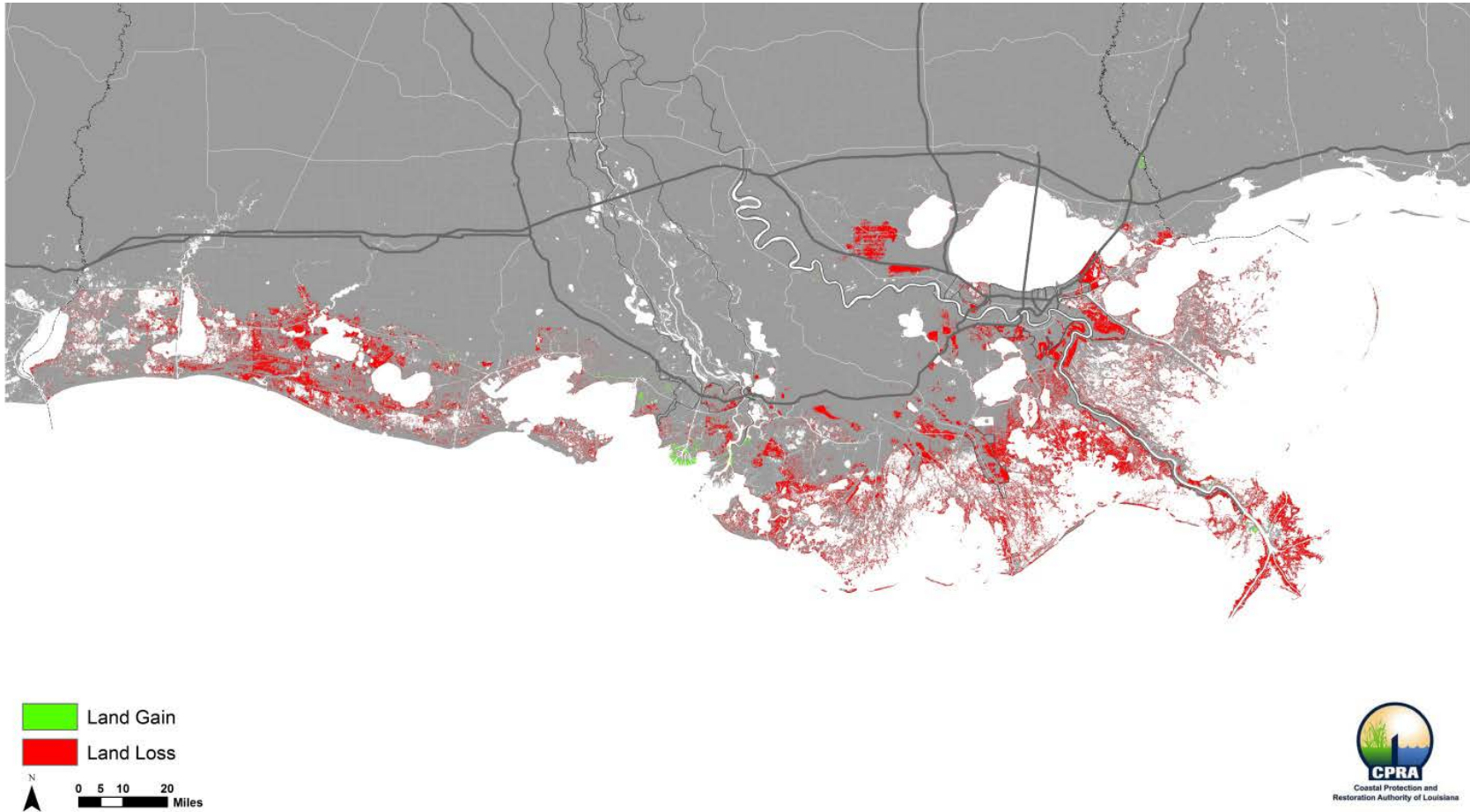


Figure 91: Land Change from Initial Conditions after 25 Years of High Scenario – FWOA. Net Land Change (Land Gain-Land Loss) at Year 25 is -3,340 km<sup>2</sup> for the High Scenario.

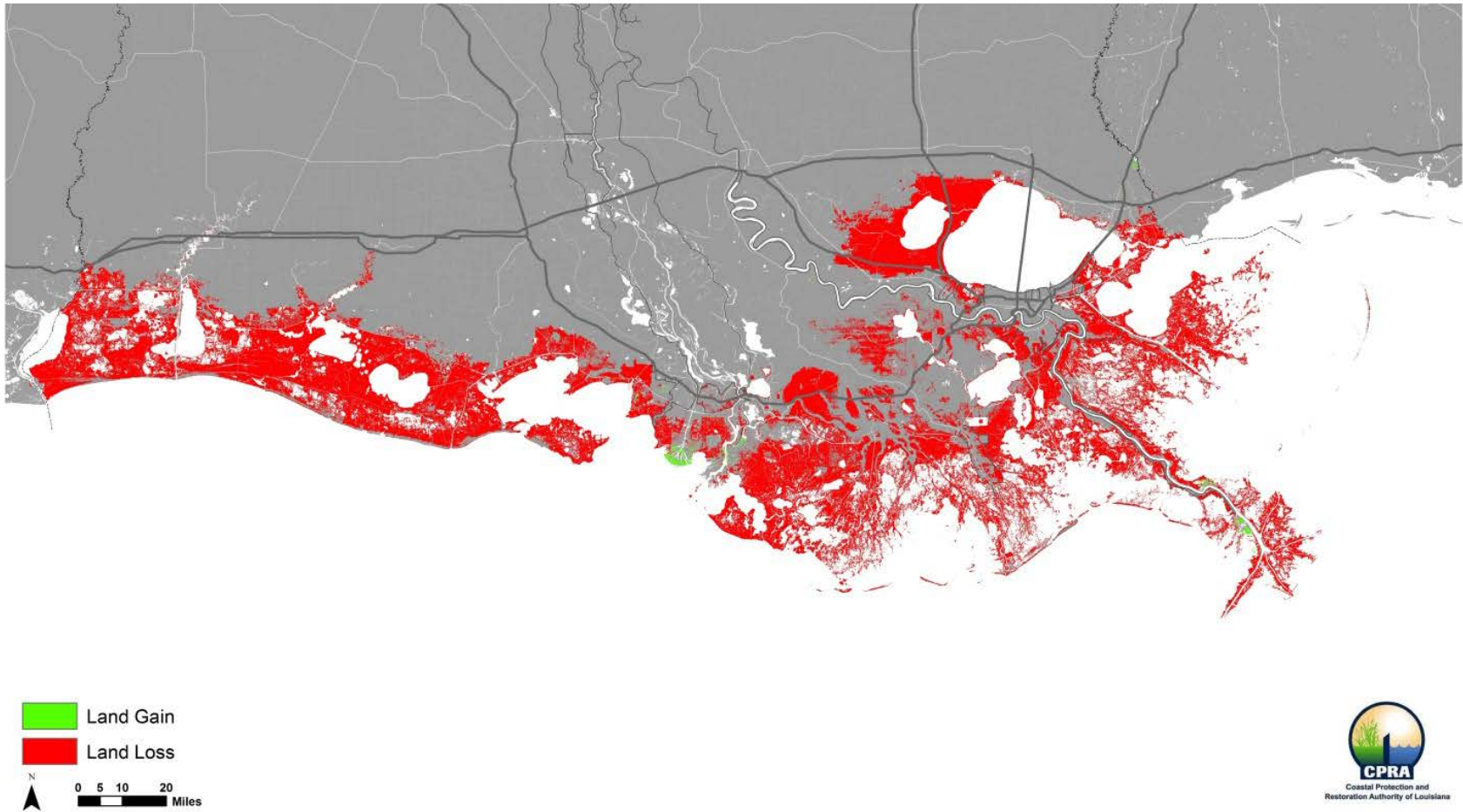


Figure 92: Land Change from Initial Conditions after 50 Years of High Scenario – FWOA. Net Land Change (Land Gain-Land Loss) at Year 50 is -10,990 km<sup>2</sup> for the High Scenario.

### 3.4 Vegetation

In this section, coast wide vegetation changes over 50 years under the three different future scenarios are discussed. For this analysis, individual species in the vegetation subroutine of the ICM (Louisiana Vegetation Model version 2 (LaVegMod v2)) were grouped into six habitats as summarized in Table 5. These habitats are not the same as those described by Chabreck (1972). Chabreck (1972) described habitats based on relative proportions of the different dominant species, while this approach used a simplified scheme of assigning each of the modeled species to only one habitat.

During the first 20 years, the forecasted changes under all three scenarios are very similar (Figure 93 - Figure 98). However, some general spatial patterns were noted. In the first two decades, fresh marsh expands primarily through the conversion of forested wetlands in the eastern coast. Saline marsh expands and replaces brackish marsh, which is most pronounced in the western coast, but this is a coast wide phenomenon.

Under the low scenario, trends observed in the first two decades continue for another two decades (Figure 93 and Figure 94). Under the medium scenario, trends change around year 25, with all habitat types declining coast wide and bare ground increasing (Figure 96). Change in the eastern coast is similar to that observed coast wide (Figure 96). In the central coast, declines are slower than coast wide under the medium scenario. This is most likely due to the input of freshwater and sediments to this region from the Atchafalaya River. Along the western coast, fresh, intermediate, and brackish marshes that are not converted to saline marshes are lost to open water (Figure 95 and Figure 96). Under the high scenario, the model forecasts a precipitous decline in all habitats starting around year 20 and continuing to year 50 (Figure 98) as land is converted to open water and saline habitats migrate inland (Figure 97). The model also shows an increase in bare ground at the same time. The gradual increase in bare ground under the medium and high scenarios is primarily driven by the eastern coast (Figure 97 and Figure 98). It reflects the very rapid salinity intrusion forecasted in these scenarios into Upper Barataria Basin. It seems that the brackish marsh species are able to rapidly migrate inland (Figure 95 and Figure 97), but the saline marsh species are not. This lack of movement of the saline marsh species is most likely due to their lower establishment along the fresher end of the salinity gradient (brackish species establish at a very low likelihood at 0.4 ppt average annual salinity, while saline species start establishment at 4 ppt). This allows brackish marsh species to be present at small percentages at low salinity and rapidly expand when salinity increases, whereas saline species can only expand when salinity consistently increases. In the western coast, both marsh types migrate inland, but bare ground forms along the Gulf shoreline (Figure 97 and Figure 98). Since all species have the same dispersal probability, this is not likely the limiting factor keeping species from colonizing these bare areas. More likely, the future conditions in these areas are outside of the current niche of the species in the model. In the real world, it is likely that these areas would be colonized by other species that are not in the model (e.g., *Batis maritima*). These species are not currently common dominants in Louisiana, but are common dominants in the more saline estuaries in Texas (Mitchell et al., 2014). Under the high scenario, the largest areas of remaining marsh at the end of the 50-year forecast are in the influence area of the Atchafalaya River and at the mouth of the Pearl River (Figure 98). This demonstrates the importance of freshwater input in maintaining existing marshes, especially in the face of significantly increased relative sea level.

**Table 5: List of Vegetation Species Included in Each Habitat Type.**

Habitat	Species
Forested Wetland	<i>Nyssa aquatica</i> L., <i>Quercus laurifolia</i> Michx., <i>Quercus lyrata</i> Walter, <i>Quercus nigra</i> L., <i>Quercus texana</i> Buckley, <i>Quercus virginiana</i> Mill., <i>Salix nigra</i> Marshall, <i>Taxodium distichum</i> (L.) Rich., <i>Ulmus americana</i> L.
Fresh Floating Marsh	<i>Eleocharis baldwinii</i> (Torr.) Chapm., <i>Hydrocotyle umbellata</i> L. <i>Panicum hemitomom</i> Schult.
Fresh Attached Marsh	<i>Cladium mariscus</i> (L.) Pohl, <i>Eleocharis baldwinii</i> (Torr.) Chapm. <i>Hydrocotyle umbellata</i> L., <i>Morella cerifera</i> (L.) Small, <i>Panicum hemitomom</i> Schult., <i>Sagittaria latifolia</i> Willd., <i>Schoenoplectus californicus</i> (C.A. Mey.) Palla, <i>Typha domingensis</i> Pers., <i>Zizaniopsis miliacea</i> (Michx.) Döll & Asch.
Intermediate Marsh	<i>Sagittaria lancifolia</i> L., <i>Phragmites australis</i> (Cav.) Trin. ex Steud., <i>Iva frutescens</i> L., <i>Baccharis halimifolia</i> L.
Brackish Marsh	<i>Paspalum vaginatum</i> Sw., <i>Spartina patens</i> (Aiton) Muhl.
Saline Marsh	<i>Avicennia germinans</i> (L.) L., <i>Distichlis spicata</i> (L.) Greene, <i>Juncus roemerianus</i> Scheele, <i>Spartina alterniflora</i> Loisel.

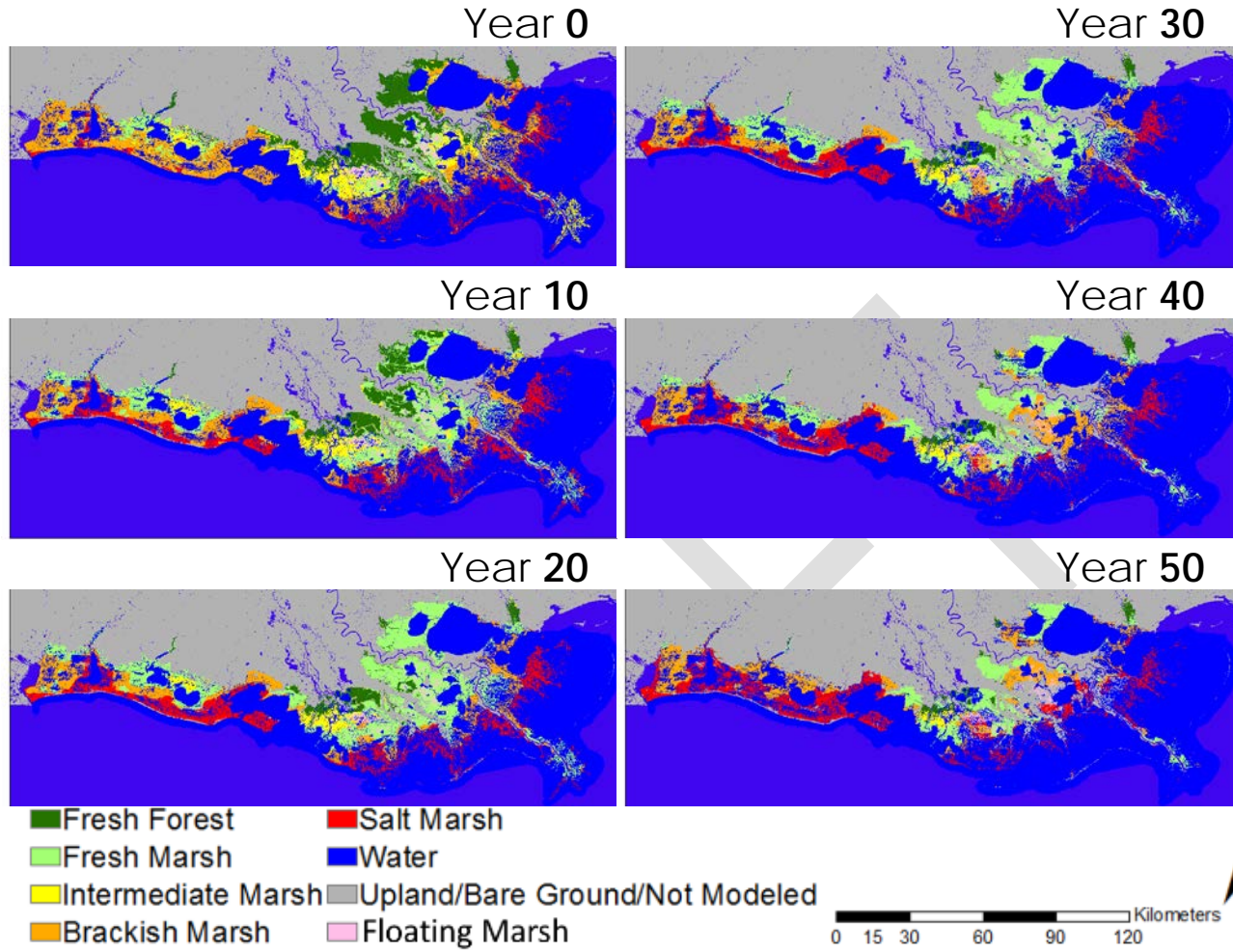


Figure 93: Coast Wide Change in Habitats Over the 50 Year Forecast Using the Low Scenario.

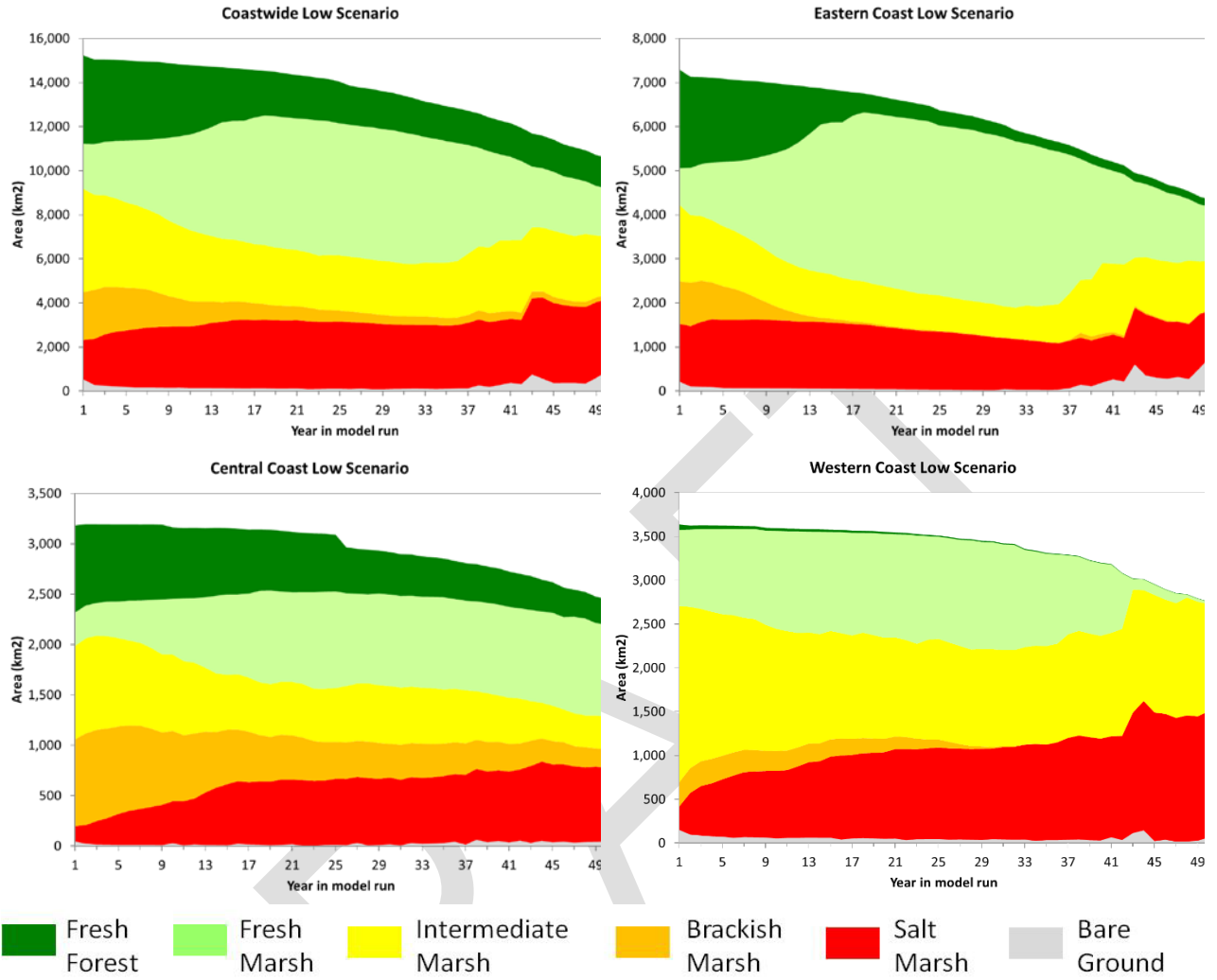


Figure 94: Change in Habitats Forecasted Using the Low Scenario: Coast Wide and Three Regions of the Coast.

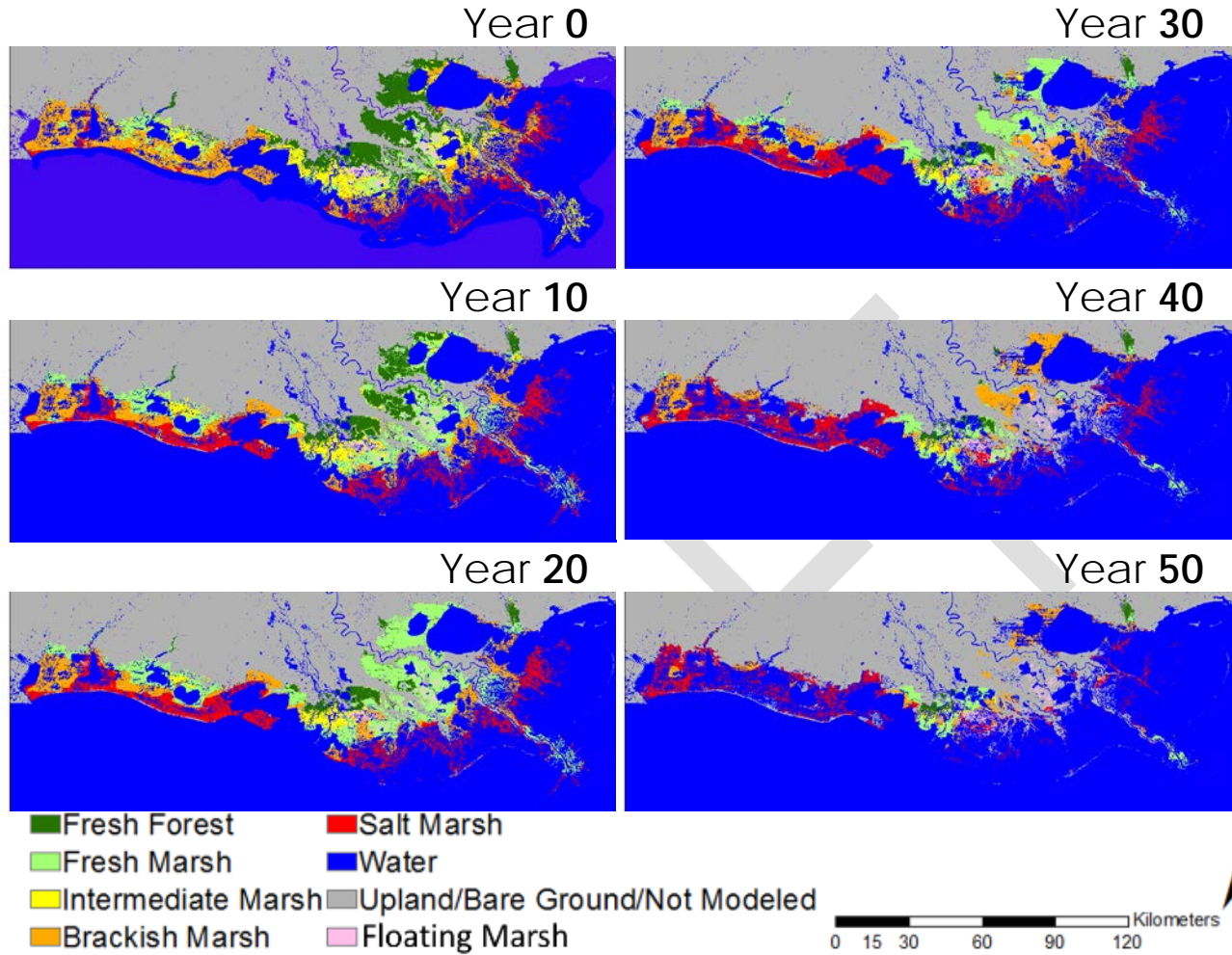


Figure 95: Coast Wide Change in Habitats Over the 50 Year Forecast Using the Medium Scenario.

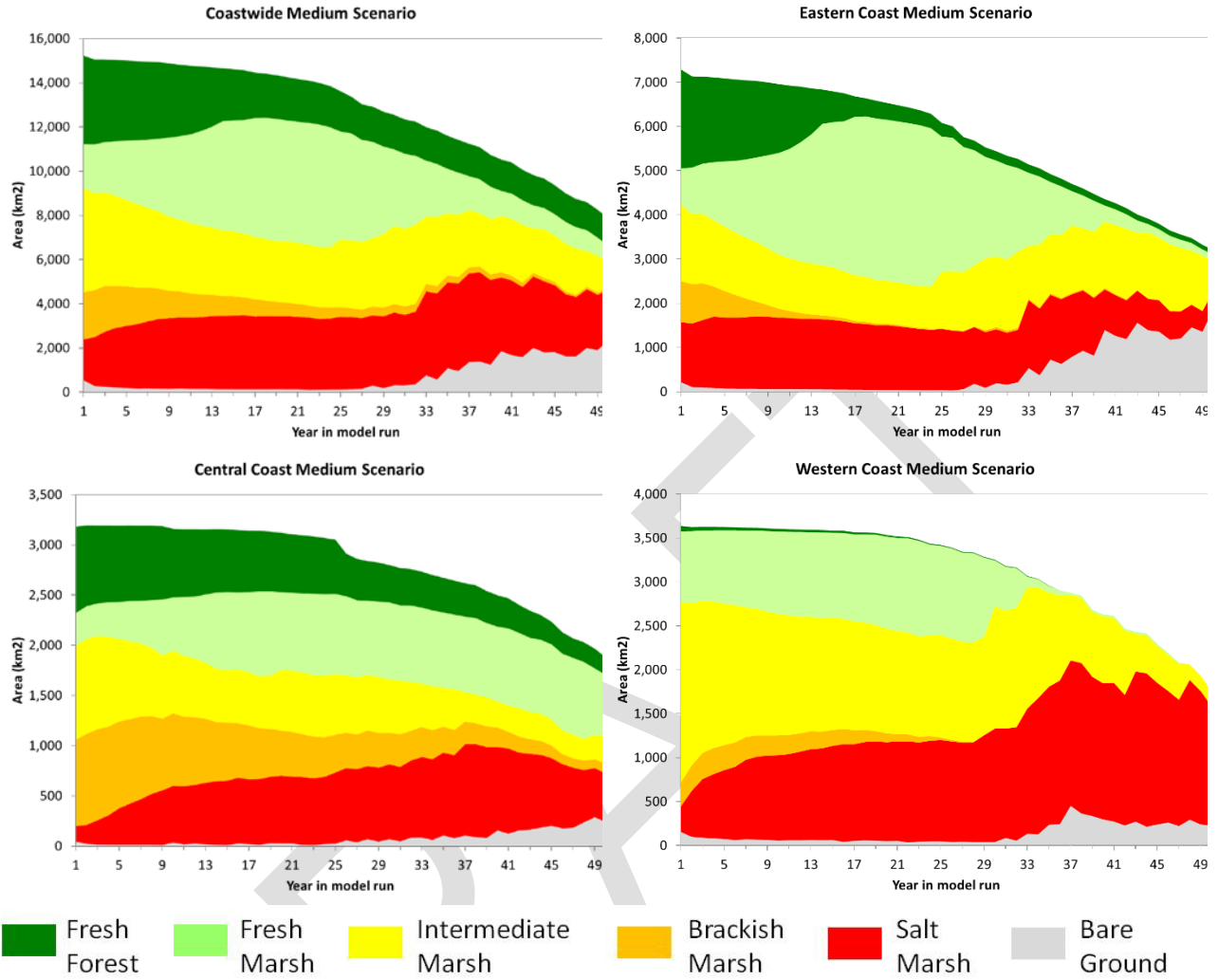


Figure 96: Change in Habitats Forecasted Using the Medium Scenario: Coast Wide and Three Regions of the Coast.

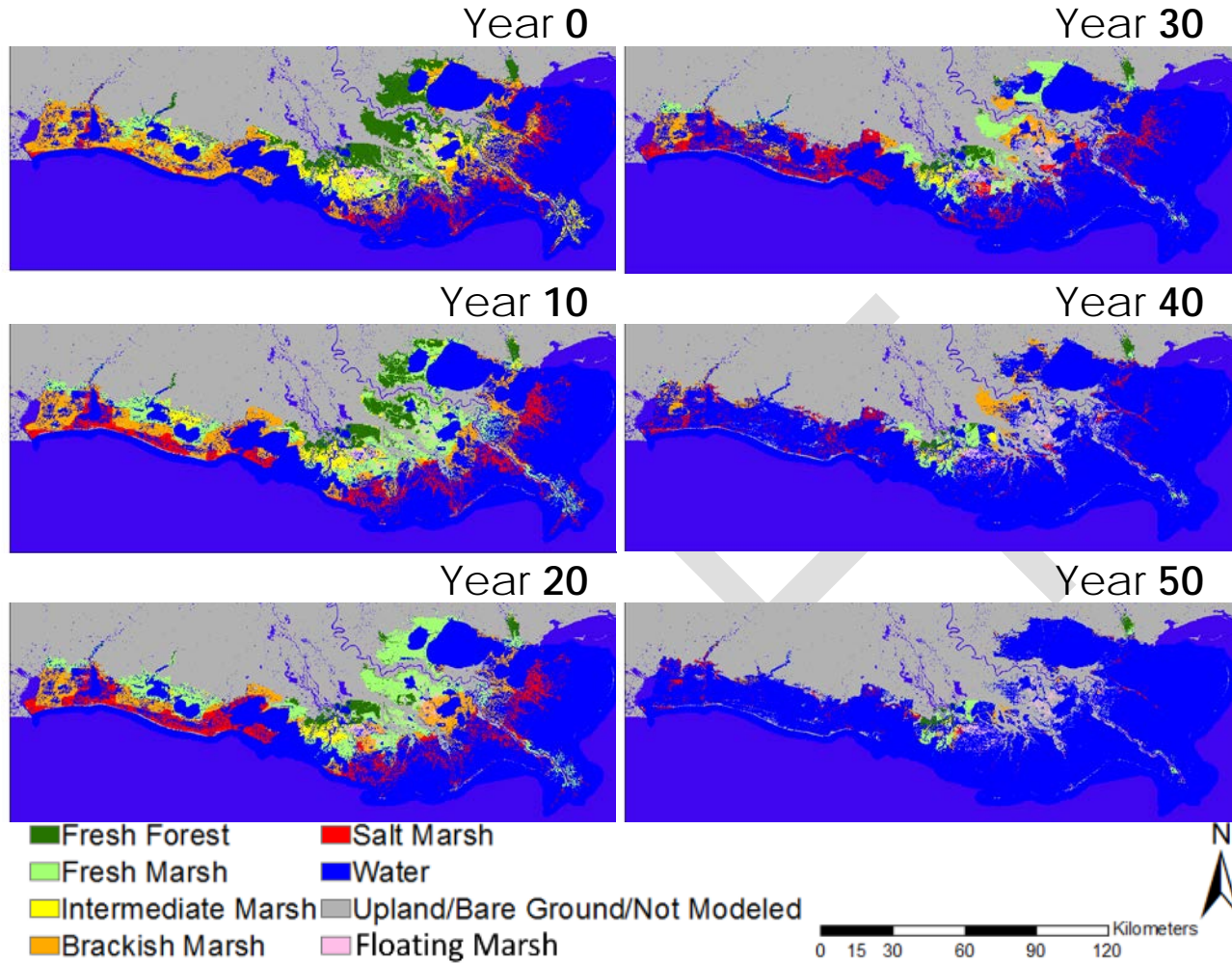


Figure 97: Coast Wide Change in Habitats Over the 50-Year Forecast Using the High Scenario.

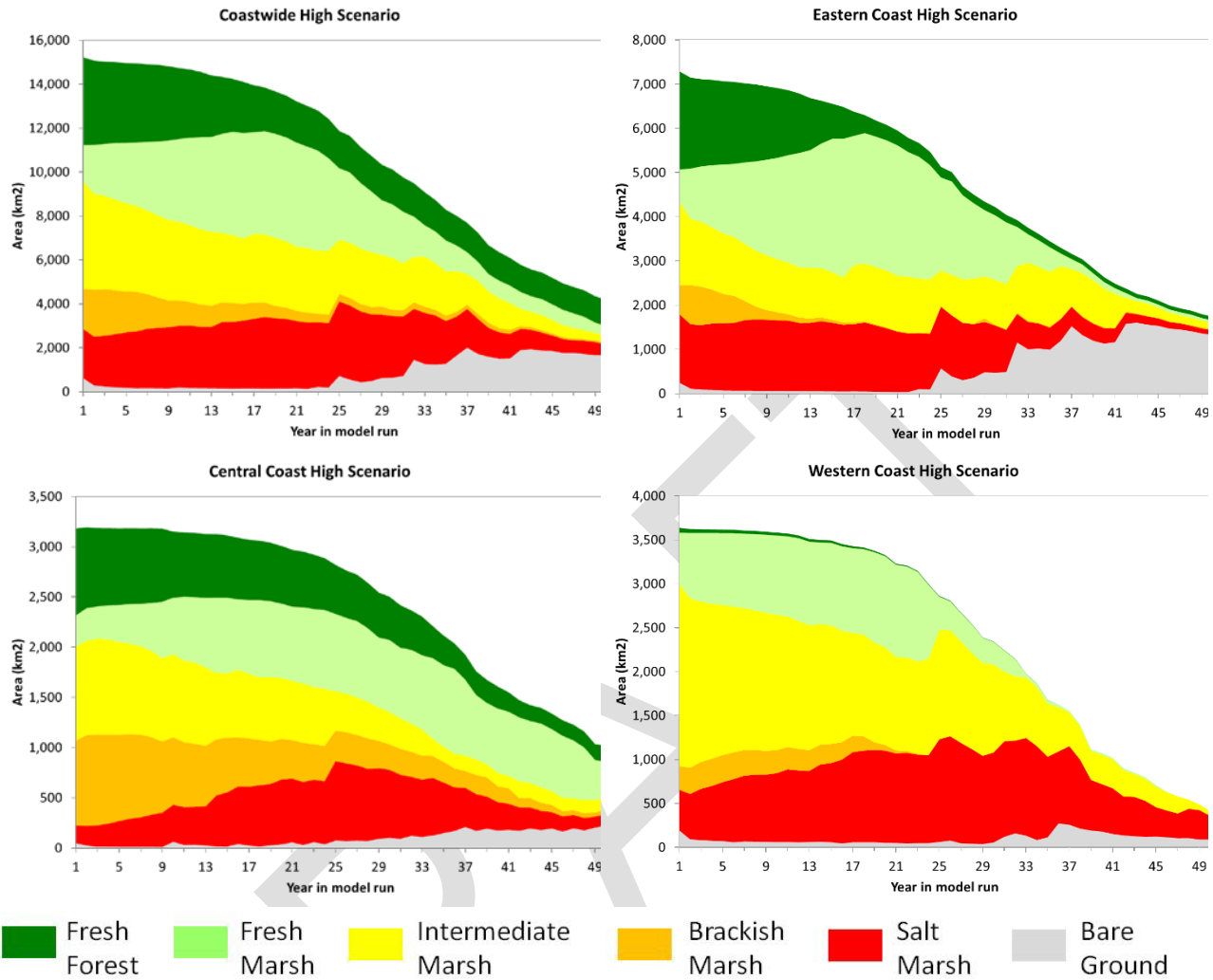
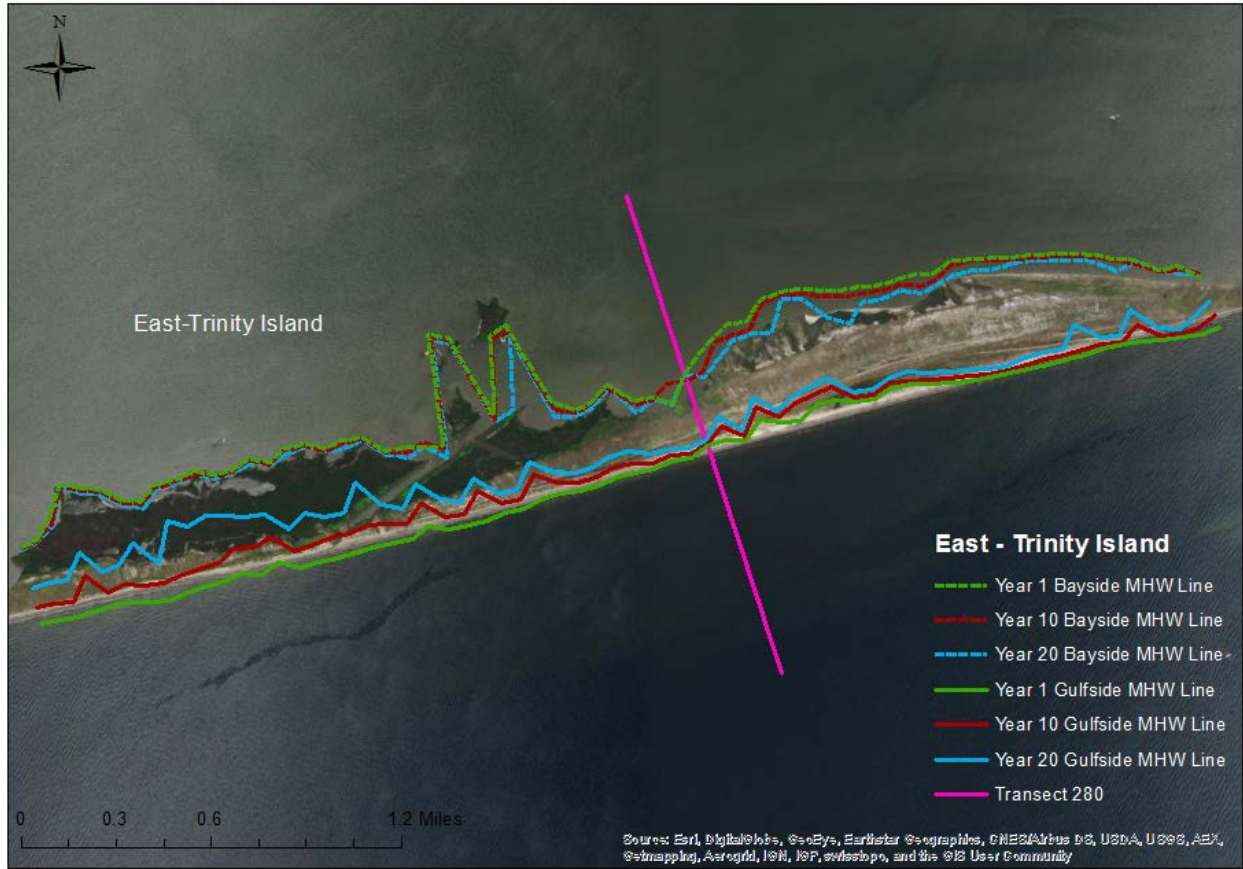


Figure 98: Change in Habitats Forecasted Using the High Scenario: Coast Wide and Three Regions of the Coast.

### 3.5 Barrier Islands

#### 3.5.1 Annual Processes and Forcing Functions

The natural processes and forcing functions for long-shore sediment transport, silt loss, bayside erosion, and relative sea level rise were modeled on an annual basis (see Attachment C3-4 - BIMODE). These processes and functions resulted in barrier shoreline changes and island elevation adjustments. The overall shoreline change trend was net erosion as the barrier shorelines eroded and migrated landward over time. Figure 99 depicts a plan view of shoreline change on decadal time steps through year 20 for East-Trinity Island in the Isles Dernieres. Incremental landward retreat of the Gulf-side shoreline and the bayside shoreline erosion is observed. These erosional shoreline changes result in the narrowing of island width and corresponding land area reduction over time. In the absence of significant storms, Gulf-side changes are attributed primarily to long-shore transport.



**Figure 99: Plan View of East-Trinity Island Shoreline Changes through Year 20.**

Figure 100 depicts a representative cross section for East-Trinity Island at the corresponding decadal time steps through year 20. The shoreface erosion and silt loss on the Gulf-side, erosion of the bayside shoreline, and vertical lowering of the profile to account for the effects of relative sea level rise are observed as the corresponding profile adjustments were instituted in the model. Storm #107 modeled in year 2 passed within 40 km of the island which caused significant erosion of the island (Attachment C3-3 – Storms in the ICM Boundary Conditions).

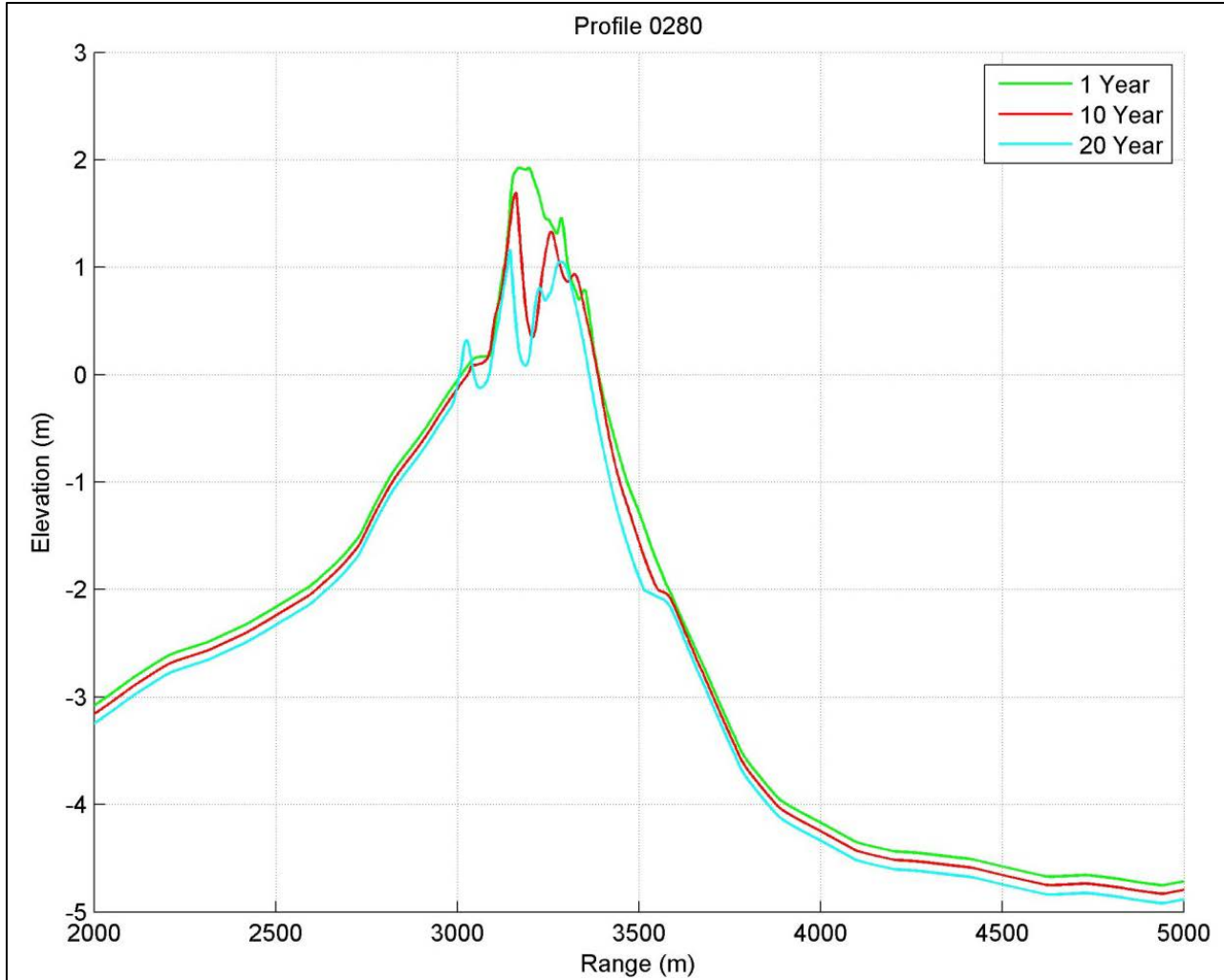


Figure 100: Representative Cross Sectional Comparison of East-Trinity Island through Year 20.

Other observations from viewing the Keyhole Markup Language (KMZ) shoreline files in Google Earth on decadal time steps included localized shoreline advance as the islands elongated and spit formation from sediment movement alongshore. This was observed on the west end of Grand Terre between years 10 and 30 as depicted in Figure 101.



Figure 101: Plan View of Grand Terre Gulf-Side and Bayside Shorelines through Year 30.

### 3.5.2 Episodic Processes and Forcing Functions

The episodic processes and forcing functions for cross-shore sediment transport and breaching were modeled during years when storms impacted the barrier shorelines (Attachment C3-4 – BIMODE). Erosive effects of the storms included erosion of the Gulf-side shoreface, beach berm, dune, and marsh platform resulting in land loss. Accretionary effects of the storms included overwash resulting in land area gains. Figure 102 depicts a representative comparison of pre-storm and post-storm profiles for East-Trinity Island in the Isles Dernieres region. Storm #569 was modeled in year 16 (Attachment C3-3 – Storms in the ICM Boundary Conditions) and passed within approximately 10 km of East-Trinity Island. Shoreface erosion and corresponding overwash are observed on the beach berm. Significant land loss of the back-barrier platform and minor overwash onto the submerged profile in the back bay are also observed.

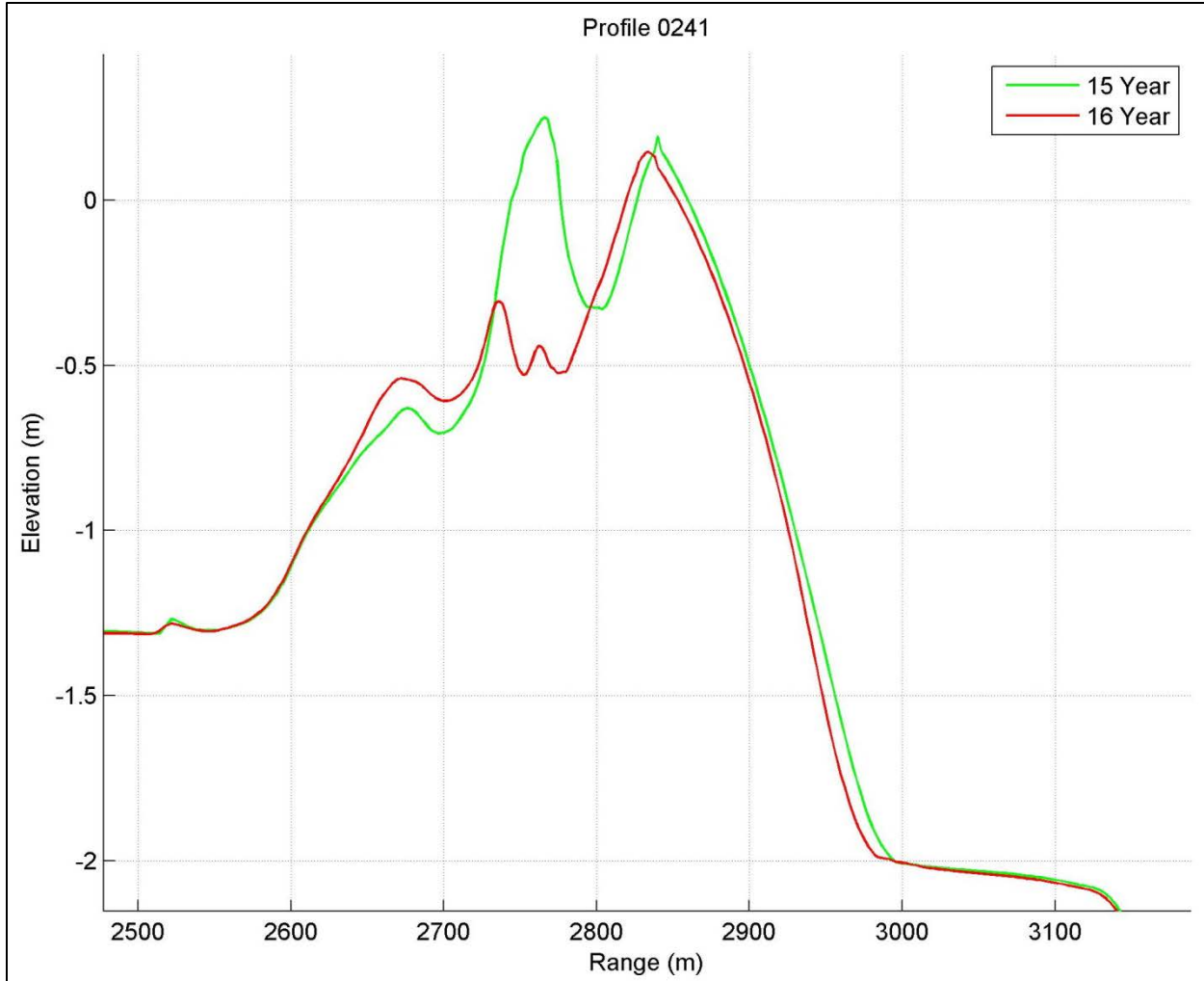


Figure 102: Representative Cross Sectional Comparison of East-Trinity Island through Year 20.

Figure 103 and Figure 104 depict a plan view of pre-storm and post-storm shorelines and pre-storm and post-storm profiles, respectively, for the Chaland Headland which is one of the Barataria Barrier shorelines. Storm #143 was modeled in year 35 (Attachment C3-3 – Storms in the ICM Boundary Conditions) and passed within 80 km of Chaland Headland. Storm impacts resulted in island breaching as evidenced by comparing the pre- and post-storm conditions.



Figure 103: Plan View of Pre and Post-Storm Shorelines for Chaland Headland at Years 34-35.

DRAFT

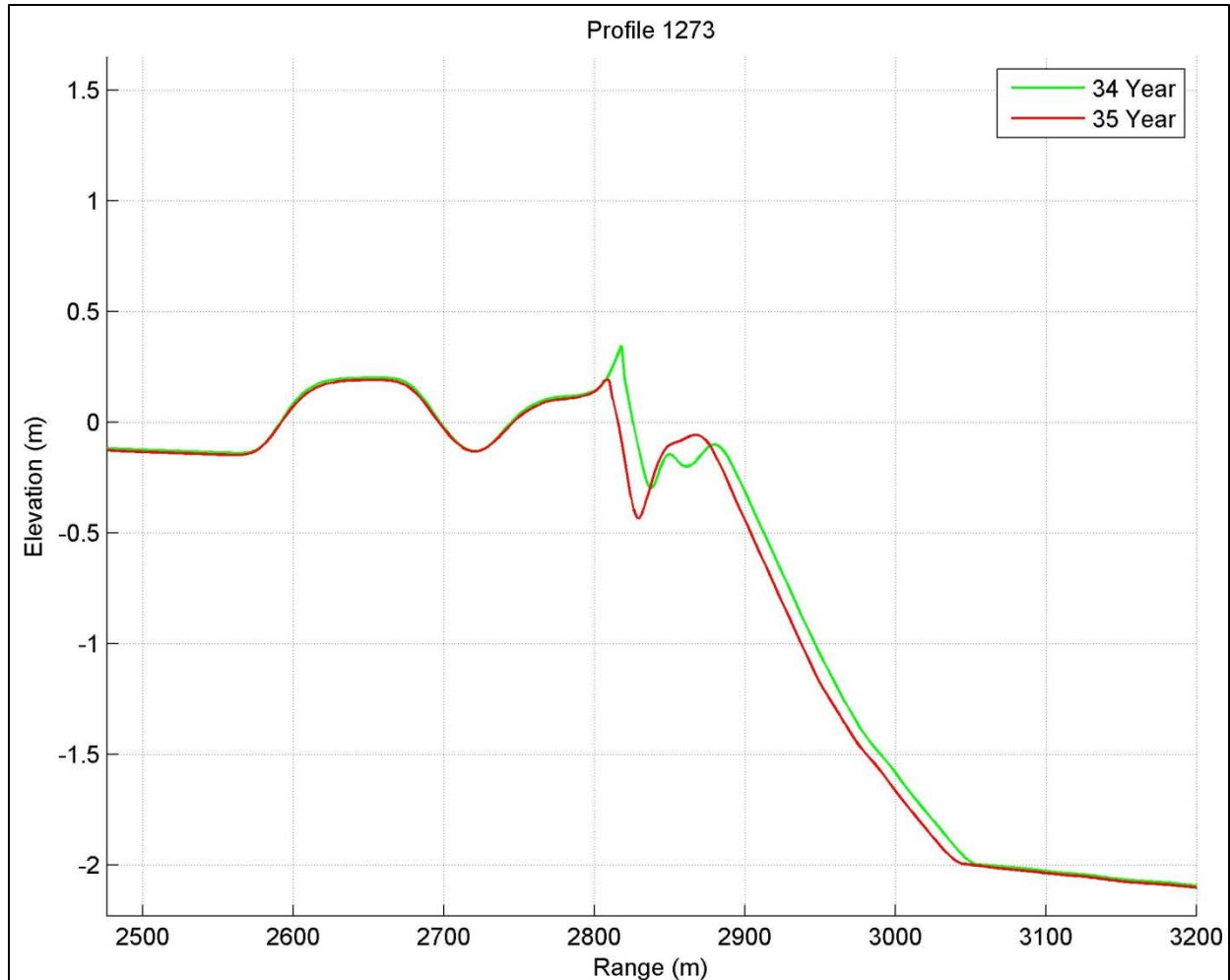


Figure 104: Pre and Post-Storm Cross Sectional Comparison for Chaland Headland at Years 34-35.

### 3.5.3 Regional Results

Presented in Attachment C3-4 – BIMODE are plan views of Gulf-side and bayside shorelines at years 1, 10, 30, and 50 and representative cross sections at years 1, 25, and 50. Figure 105 depicts an example of the shoreline changes over 50 years for East-Trinity Island for the low scenario. Figure 106 depicts an example of the profile changes over 50 years for Caminada Headland for all three scenarios: low, medium, and high. The overall regional trends for the 50-year period include significant land loss over time, island migration due to overwash from storm induced cross-shore transport, island breaching in the wake of a major storm, and island disappearance. The primary difference among the scenarios is the increased vertical lowering of the profiles which translates to increased land loss to account for the increased subsidence and sea level change.

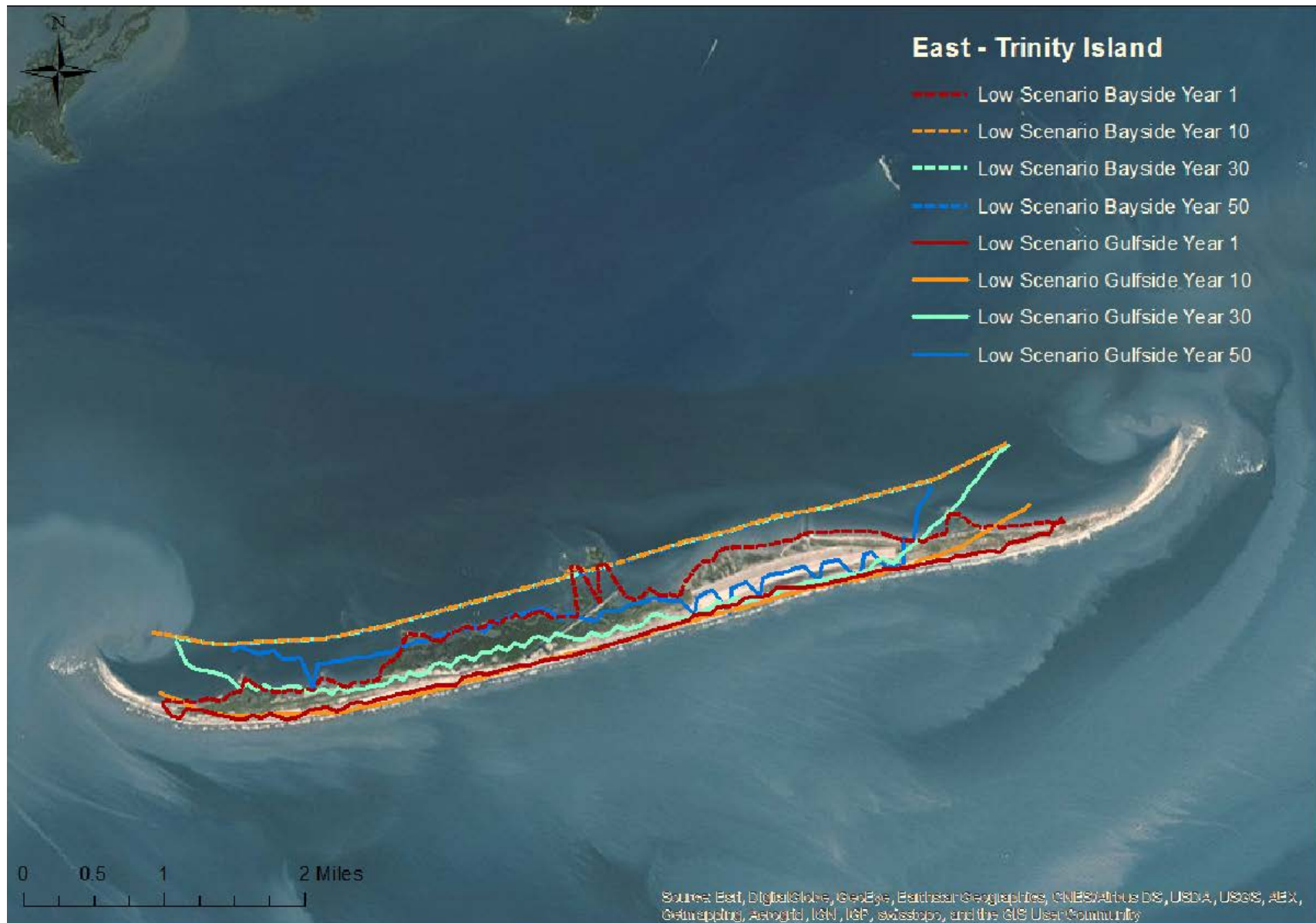


Figure 105: Plan View of East-Trinity Island Gulf-Side and Bayside Shorelines through Year 50 for Low Scenario.

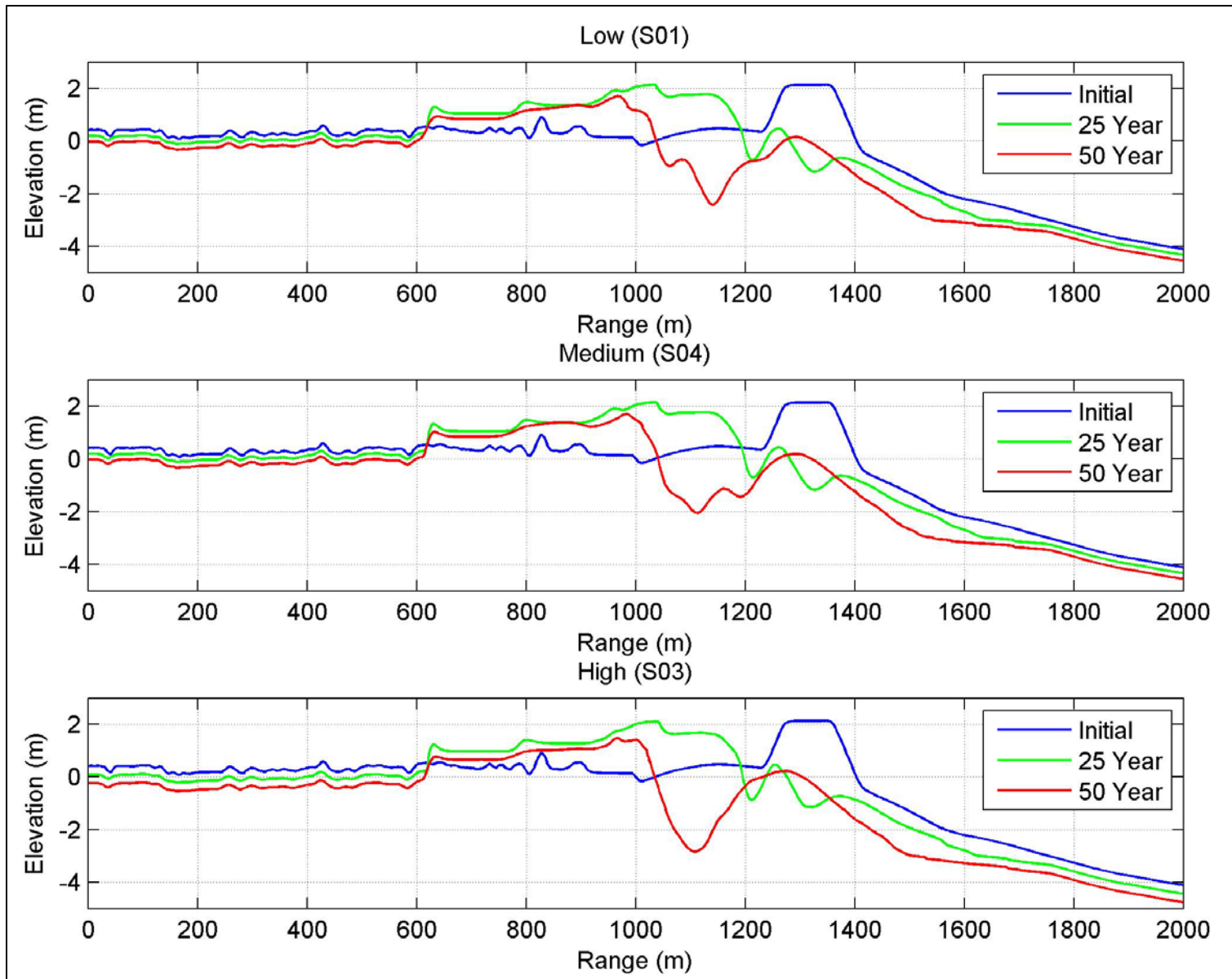


Figure 106: Cross Sections of Caminada Headland through Year 50 for Low, Medium, and High Scenarios.

### 3.5.4 Land Area Analysis

The changes in profiles were used to calculate the change in land area over time for 5-year periods for each scenario for the barrier shorelines using the same algorithm as is used in the morphology subroutine. Figure 107 through Figure 112 present the land area changes over time for different sections of the barrier shorelines. As predicted, higher land loss rates are observed for the medium and high scenarios attributable to accelerated sea level rise and more subsidence. Table 6 through Table 8 present the land area changes over time by region and by scenario, including initial and final land areas, percentage of land loss, and predicted year of disappearance if applicable.

Breton Island and the Chandeleur Islands are predicted to disappear within the 50-year period of analysis. The other four sections are predicted to have some land area remaining. The Caminada barrier shorelines experienced the highest percent land loss while the Barataria Barrier shorelines experienced the lowest percent land loss.

DRAFT

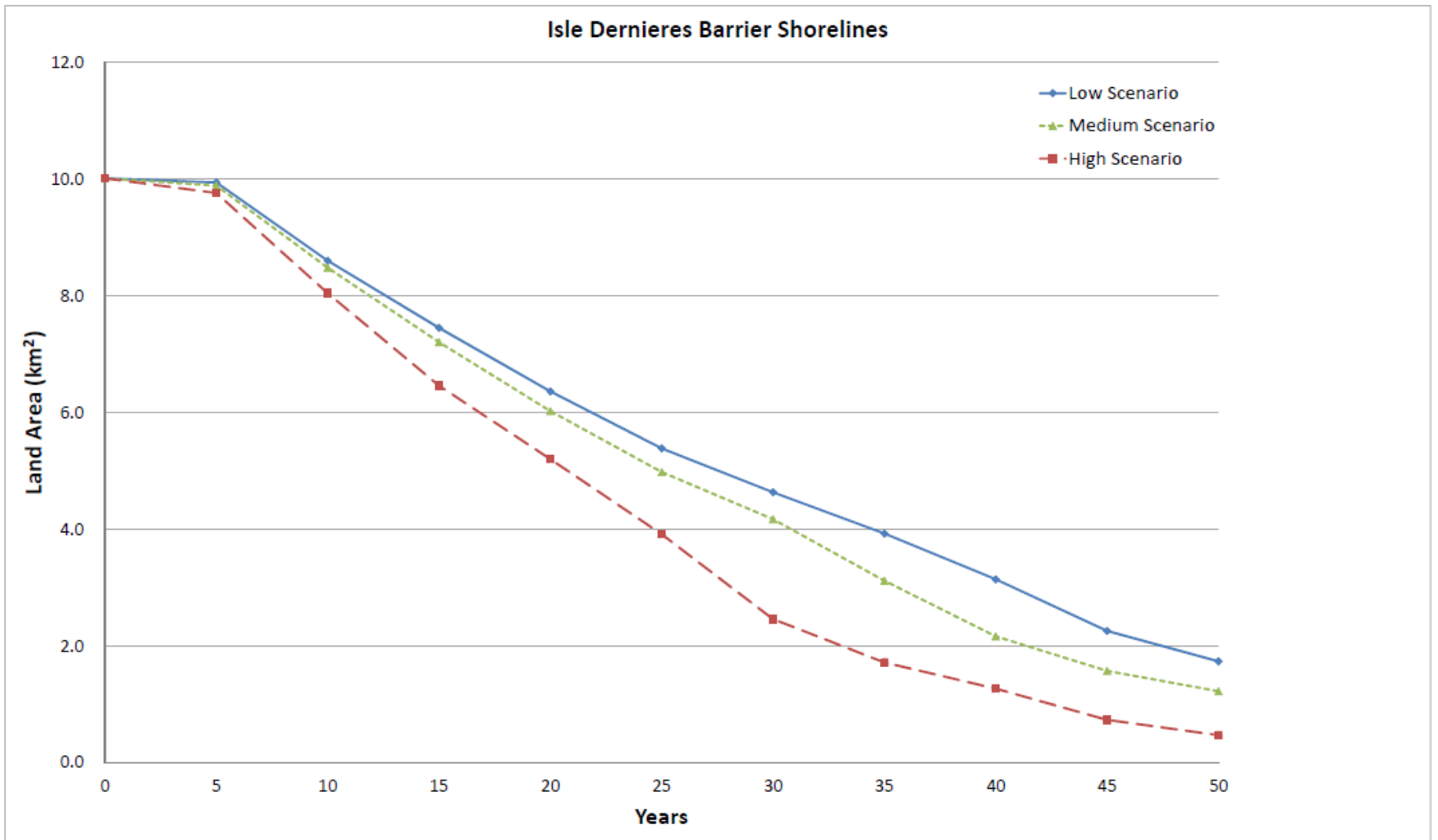


Figure 107: Land Area Changes Over Time for Isle Dernieres Barrier Shorelines.

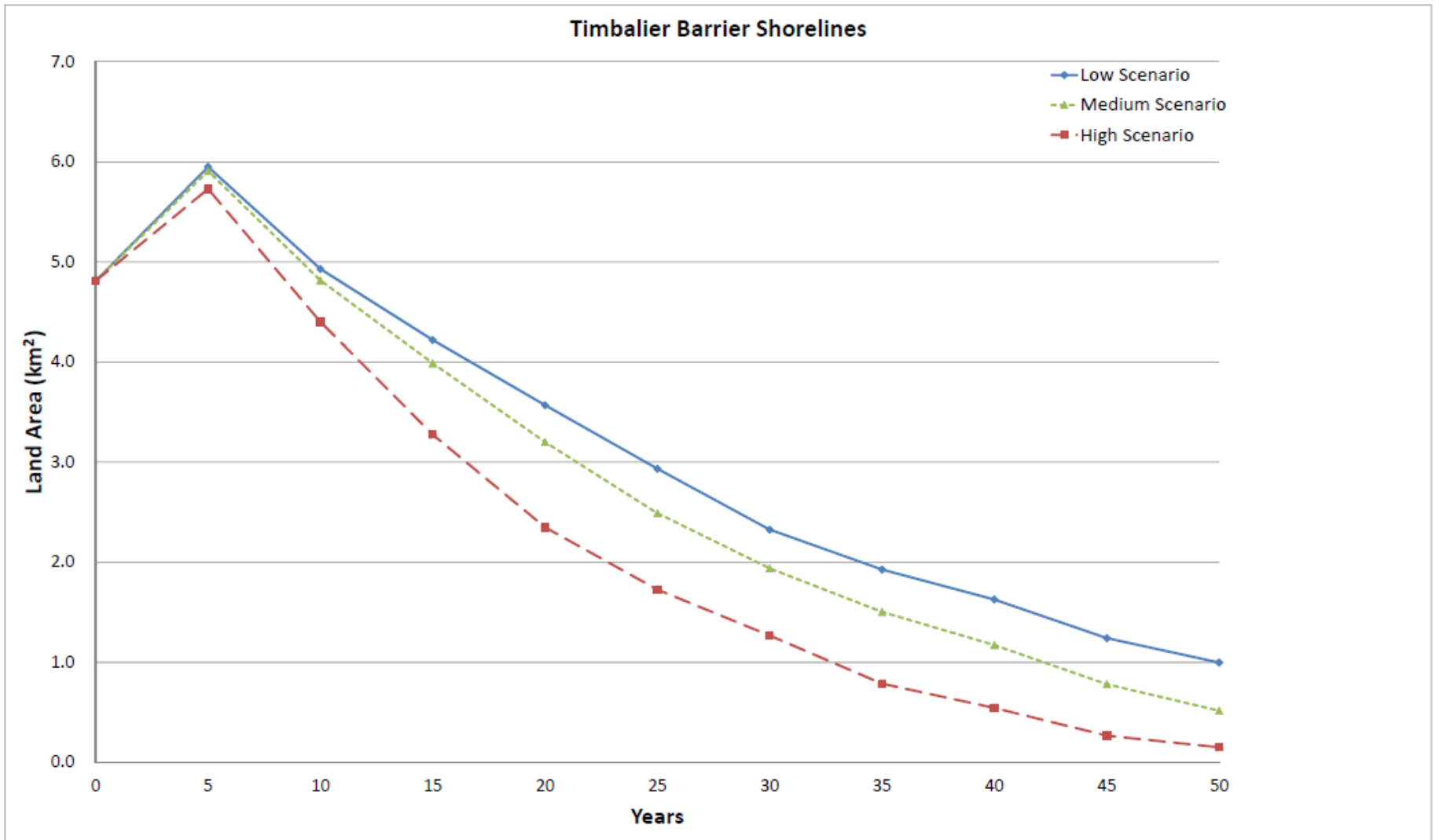


Figure 108: Land Area Changes Over Time for Timbalier Barrier Shorelines.

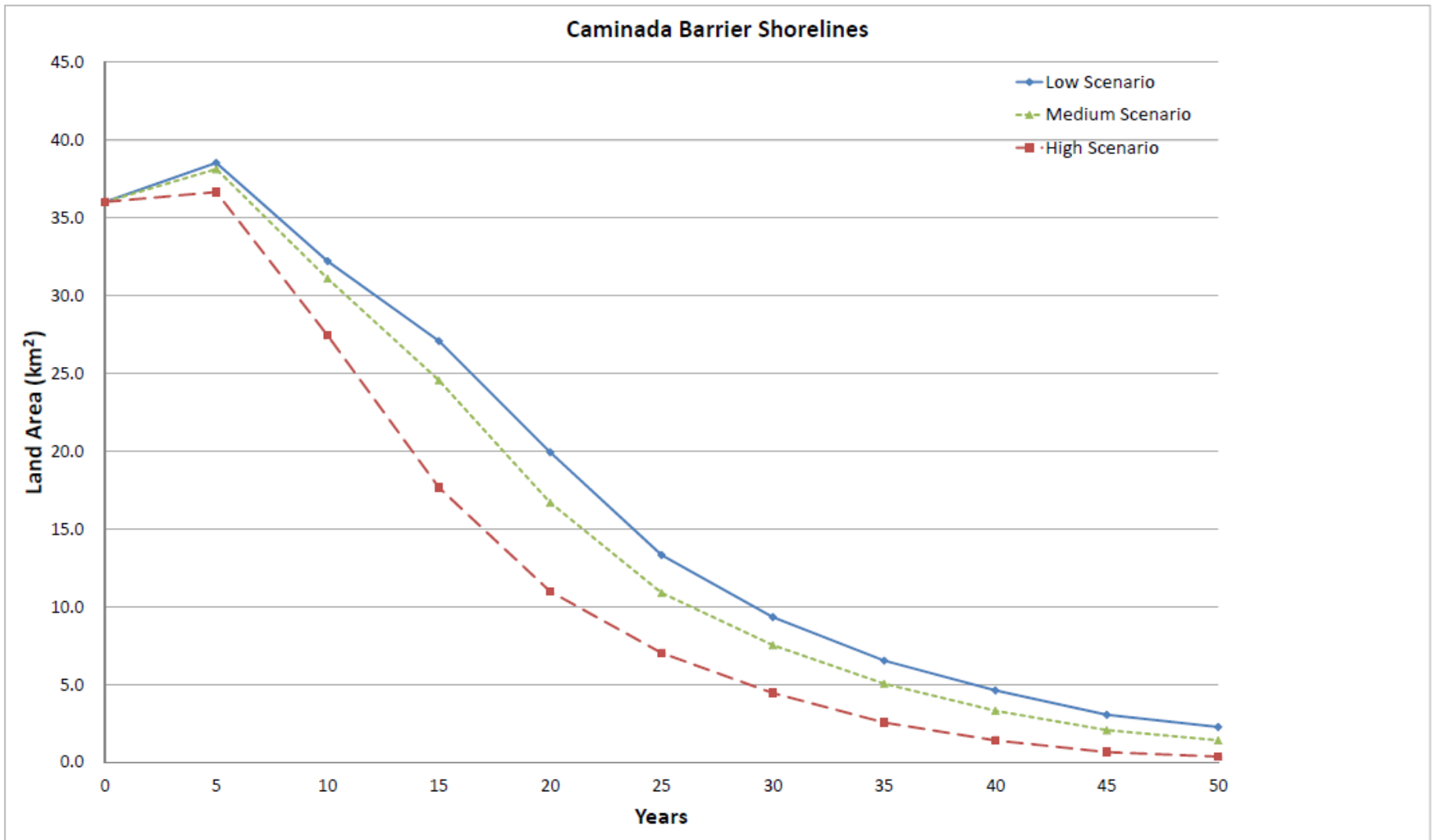


Figure 109: Land Area Changes Over Time for Caminada Barrier Shorelines.

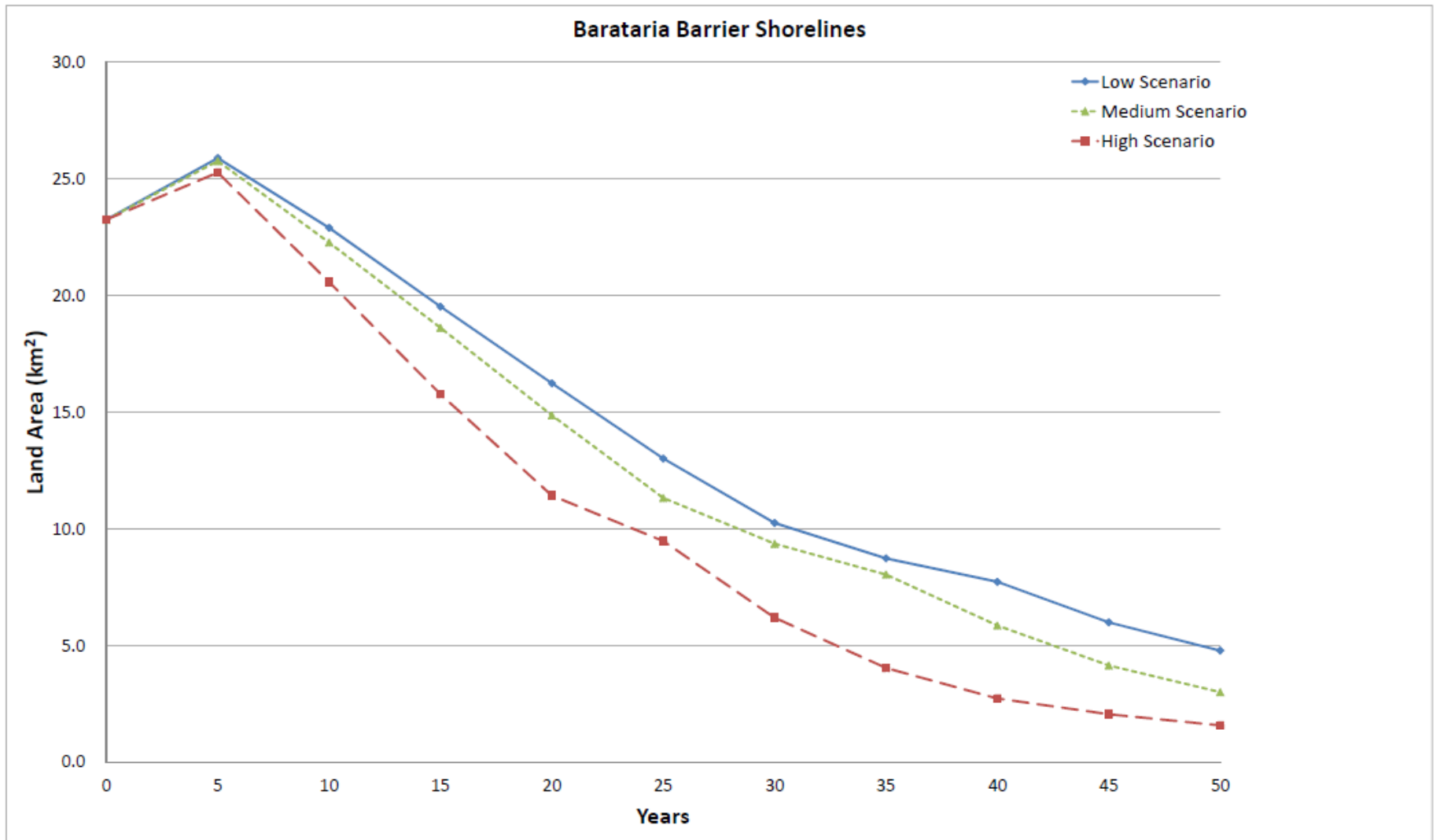


Figure 110: Land Area Changes Over Time for Barataria Barrier Shorelines.

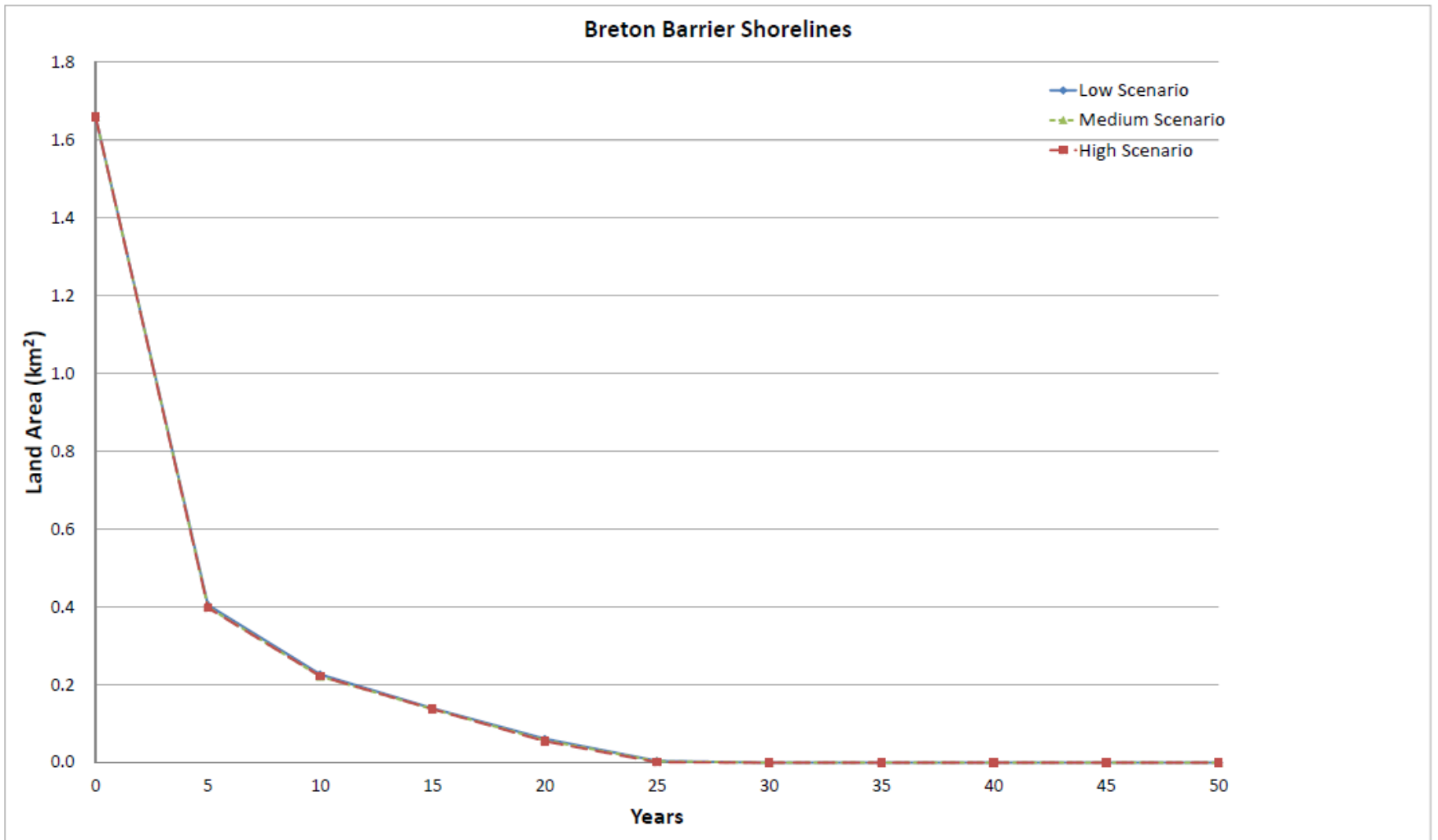


Figure 111: Land Area Changes Over Time for Breton Barrier Shorelines.

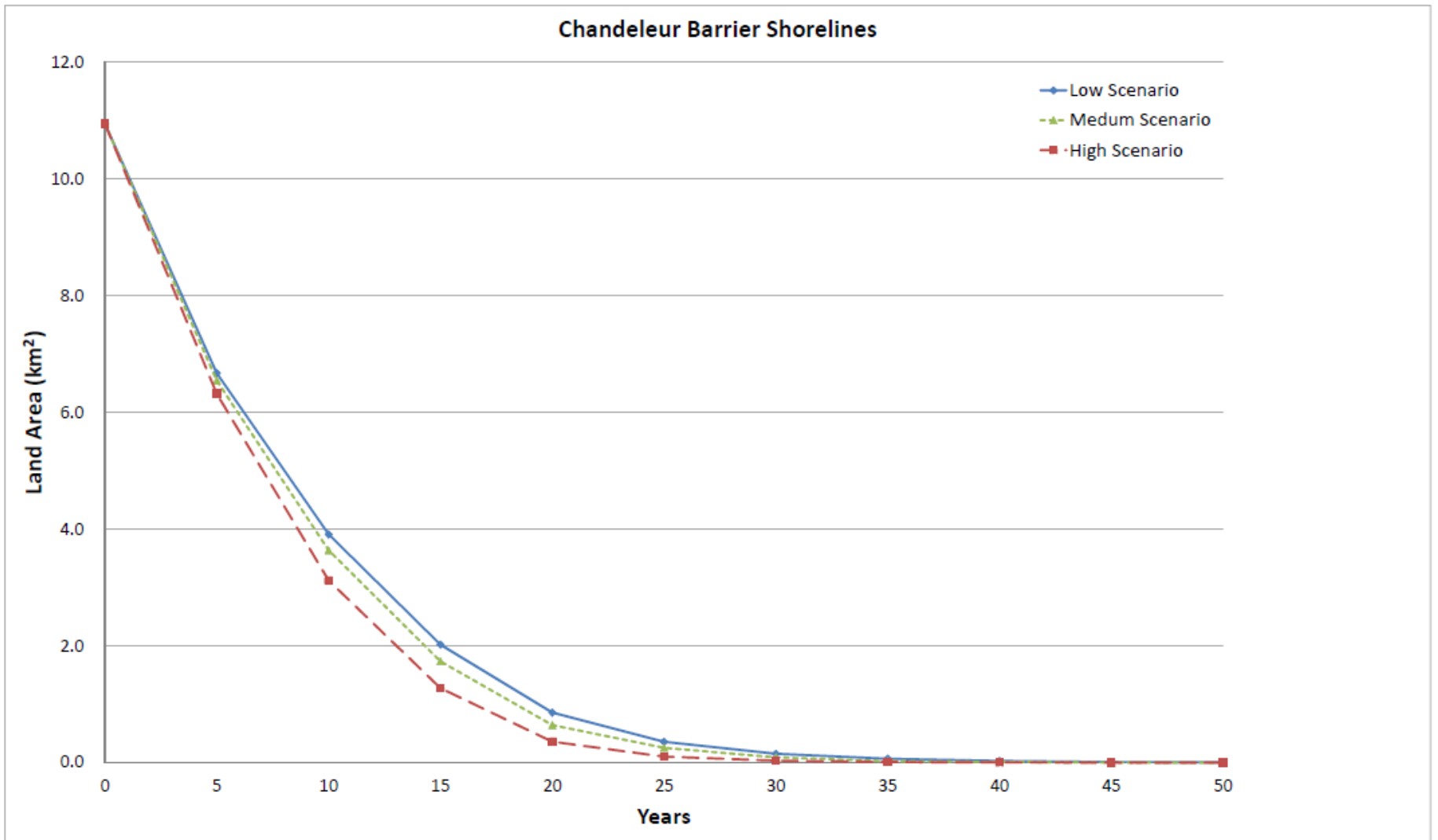


Figure 112: Land Area Changes Over Time for Chandeleur Barrier Shorelines.

**Table 6: Land Area Changes for Low Scenario.**

Region	Land area (initial) (km <sup>2</sup> )	Land area (final) (km <sup>2</sup> )	Percent land loss	Estimated year of disappearance
Isle Dernieres	10.0	1.7	83%	-
Timbalier	4.8	1.0	79%	-
Caminada	36.0	2.3	94%	-
Barataria	23.3	4.8	79%	-
Breton	1.7	0.0	100%	30
Chandeleur	10.9	0.0	100%	40

**Table 7: Land Area Changes for Medium Scenario.**

Region	Land area (initial) (km <sup>2</sup> )	Land area (final) (km <sup>2</sup> )	Percent land loss	Estimated year of disappearance
Isle Dernieres	10.0	1.2	88%	-
Timbalier	4.8	0.5	89%	-
Caminada	36.0	1.4	96%	-
Barataria	23.3	3.0	87%	-
Breton	1.7	0.0	100%	25
Chandeleur	10.9	0.0	100%	35

**Table 8: Land Area Changes for High Scenario.**

Region	Land area (initial) (km <sup>2</sup> )	Land area (final) (km <sup>2</sup> )	Percent land loss	Estimated year of disappearance
Isle Dernieres	10.0	0.5	95%	-
Timbalier	4.8	0.2	97%	-
Caminada	36.0	0.4	99%	-
Barataria	23.3	1.6	93%	-
Breton	1.7	0.0	100%	25
Chandeleur	10.9	0.0	100%	30

## 3.6 Habitat Suitability Indices (HSIs)

The 2017 Coastal Master Plan utilized HSIs to evaluate changes in habitat quality for 14 fish, shellfish, and wildlife species with several of the fish and shellfish species having separate HSI models for the juvenile and adult life stages. The results of the three FWOA scenarios (low, medium, and high) are discussed here for six species: eastern oyster, small juvenile brown shrimp, adult spotted seatrout, largemouth bass, green-winged teal, and American alligator. These species were selected because they are recreationally- or commercially-important, and because they represent a range of different estuarine communities and trophic levels.

### 3.6.1 Eastern Oyster

The variables in the oyster HSI model include several temporal measures of salinity and the percentage of water bottom in an ICM cell that is covered with hard substrate (i.e., "cultch", which did not change in FWOA simulations). According to the model, the most suitable oyster habitat consists of areas with a high percentage of cultch coverage and salinities between approximately 10 and 20 ppt (Attachment C3-12 – Oyster HSI Model).

Although there was some inter-annual variability related to differences in riverine discharge (and thus salinity), the suitability of habitat for oysters generally increased over time in each of the FWOA scenarios, particularly over the last half of the simulation period (Figure 113 - Figure 115). This is consistent with the increasing rate of sea level rise in the scenarios, which forced higher-salinity waters farther up into the estuarine basins. Consequently, interior areas of known or assumed cultch became more suitable habitat for oysters. In contrast, some areas close to the Gulf became less suitable for oysters because salinities were too high during the latter years of the simulations. This was most notable in areas that are currently saline, such as Lower Terrebonne and Lower Barataria basins, and in the high FWOA scenario (Figure 115).

### 3.6.2 Small Juvenile Brown Shrimp

This HSI model represents young-of-the-year brown shrimp that have recently settled to their inshore nursery habitats. Accordingly, the model variables include average salinity and water temperature between April and June (when this life stage is most common in the estuaries), as well as the percentage of the ICM cell that is covered by emergent marsh vegetation (Attachment C3-13 – Brown Shrimp HSI Model). The model indicates that the most suitable habitats are fragmented marshes with average salinities between approximately 10 and 20 ppt.

The low and medium FWOA scenarios showed that habitat suitability for small juvenile brown shrimp increased over time in most areas of the coast (Figure 116 and Figure 117). This increase was most apparent in interior areas during the last half of the simulation period, because the greater salinity intrusion during this time converted low-salinity interior marshes, swamps, and open waters into more suitable habitat for brown shrimp. However, there were some areas of the coast, such as Lower Terrebonne and Lower Barataria basins, where habitat suitability decreased during the latter part of the simulation. This was mostly due to high rates of wetland loss in these areas, though high salinities were also a factor. The net result in these basins was a shift in habitat distribution over time from the lower to the upper estuary.

The negative effects of wetland loss were greater and more widespread in the high FWOA scenario, so that by the end of simulation habitat suitability was decreasing in most areas and

especially in the Deltaic Plain (Figure 118). Consequently, the amount of suitable habitat at year 50 was lower in the high FWOA scenario than in the low and medium FWOA scenarios.

### 3.6.3 Adult Spotted Seatrout

The adult spotted seatrout HSI model includes average salinity and water temperature over the entire year, as well as marsh coverage (Attachment C3-16 – Spotted Seatrout HSI Model). The most suitable habitats are fragmented marshes with salinities >10 ppt and temperatures >20° C. The greater suitability of higher salinities and temperatures indicates that the model is more appropriate for evaluating the adult's summer spawning habitats rather than their overwintering habitats in the estuaries.

The results of FWOA simulations of adult spotted seatrout habitat suitability were similar to those of the small juvenile brown shrimp. Habitat suitability increased over time across the coast, particularly in interior areas (e.g., Upper Barataria Basin, Mermentau Basin, and around Lake Maurepas) as salinity intrusion made these areas more suitable for adult seatrout (Figure 119 - Figure 121). Unlike small juvenile brown shrimp, however, habitat suitability for adult seatrout was relatively unaffected by high rates of wetland loss toward the end of the simulations. This is because adult spotted seatrout are much less dependent on marsh coverage than the brown shrimp, and the model accordingly assigns relatively high habitat suitability to open water areas (Attachment C3-16). There was little difference in these patterns among the FWOA scenarios, except that the increase in habitat suitability due to salinity intrusion was greater with each successive scenario (Figure 119 - Figure 121).

### 3.6.4 Largemouth Bass

The largemouth bass HSI model includes average salinity and water temperature between March and November (the months of highest abundance in the estuaries), as well as marsh coverage (Attachment C3-18 – Largemouth Bass HSI Model). The most suitable habitats for bass are fragmented marshes with salinities <2 ppt.

Habitat suitability for largemouth bass generally decreased over time in each of the FWOA scenarios with the greatest decreases, again, occurring during the last half of the simulation period (Figure 122 - Figure 124). Decreased suitability was due to salinity intrusion, which made interior low-salinity marsh habitats less suitable for bass. Wetland loss was also a major reason for decreased suitability because, in contrast with the other fish and shellfish species modeled, cells that were primarily open water were given almost no habitat value for bass (Attachment C3-18). Areas of increased suitability were observed near the Atchafalaya River and Lake Maurepas due to the fragmentation of formerly solid fresh marshes and the conversion of swamps into suitable marsh habitats. This was most apparent in the low and medium FWOA scenarios (Figure 122 and Figure 123). In the high FWOA scenario, very little suitable habitat remained by the end of the simulation, with most found around the Atchafalaya River (Figure 124).

### 3.6.5 Green-Winged Teal

The variables in the green-winged teal HSI model include habitat type, the percentage of the ICM cell that is open water, and the average water depth of the cell between September and March (when this species occurs in coastal Louisiana)(Attachment C3-7 – Green-winged Teal HSI Model). The model indicates that the most suitable habitats for teal are shallow waters within fragmented fresh, intermediate, and brackish marshes.

The results of the FWOA simulations showed that habitat suitability for green-winged teal generally tracked patterns of wetland loss across the coast. In the low and medium FWOA scenarios, habitat suitability increased over time across much of the coast primarily because wetland loss increased the amount of fragmented marsh/shallow water habitat (Figure 125 and Figure 126). The conversion of swamps into suitable marsh habitats also contributed to the increase in suitability. However, in areas with high rates of wetland loss, such as the Bird's Foot Delta and Lower Barataria Basin, habitat suitability declined sharply over the latter years of the simulations, as these areas converted to mostly open water and the open water became deeper and more saline with sea level rise. This trend of increased habitat suitability over the first half of the simulation followed by a sharp decline was prevalent in the high FWOA scenario (Figure 127). In this scenario, very little highly-suitable teal habitat remained by the end of the simulation period.

### 3.6.6 American Alligator

The variables in the alligator HSI model include: the percentage of the ICM cell that is open water, the amount of wetland edge in a cell, habitat type, average water depth relative to the marsh surface over the year, and average annual salinity (Attachment C3-10 – Alligator HSI Model). According to the model, the most suitable habitats for alligators are fragmented fresh and intermediate marshes associated with moderate water depths.

Alligator habitat suitability generally decreased over time in each of the FWOA scenarios, with much of the decrease occurring during the last half of the simulations (Figure 128 -Figure 130). Decreased suitability was observed in most areas of the coast as a result of salinity intrusion and increased water levels associated with sea level rise. However, there were some areas, such as around Lake Maurepas, where habitat suitability increased due to the conversion of swamps into more suitable fresh marsh. This was most obvious in the low and medium scenarios (Figures Figure 128 and Figure 129). In the high scenario simulation, increased salinities and extensive wetland loss combined to greatly reduce alligator habitat suitability across most of the coast, except around the Atchafalaya River (Figure 130).

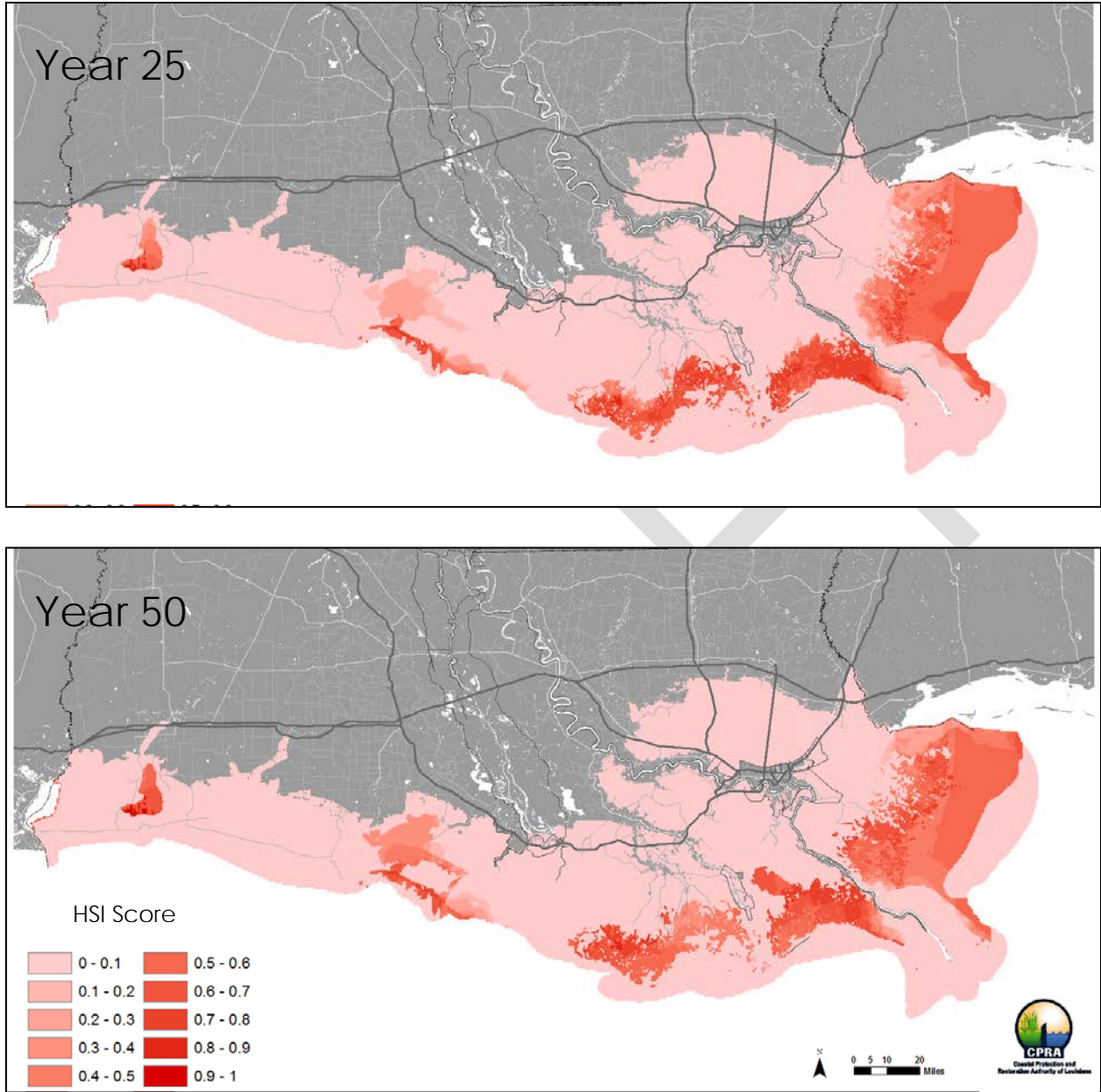


Figure 113: Coast Wide Habitat Suitability for Eastern Oyster at Years 25 and 50 of the Low FWOA Scenario. Dark Red Indicates Areas of Highest Suitability.

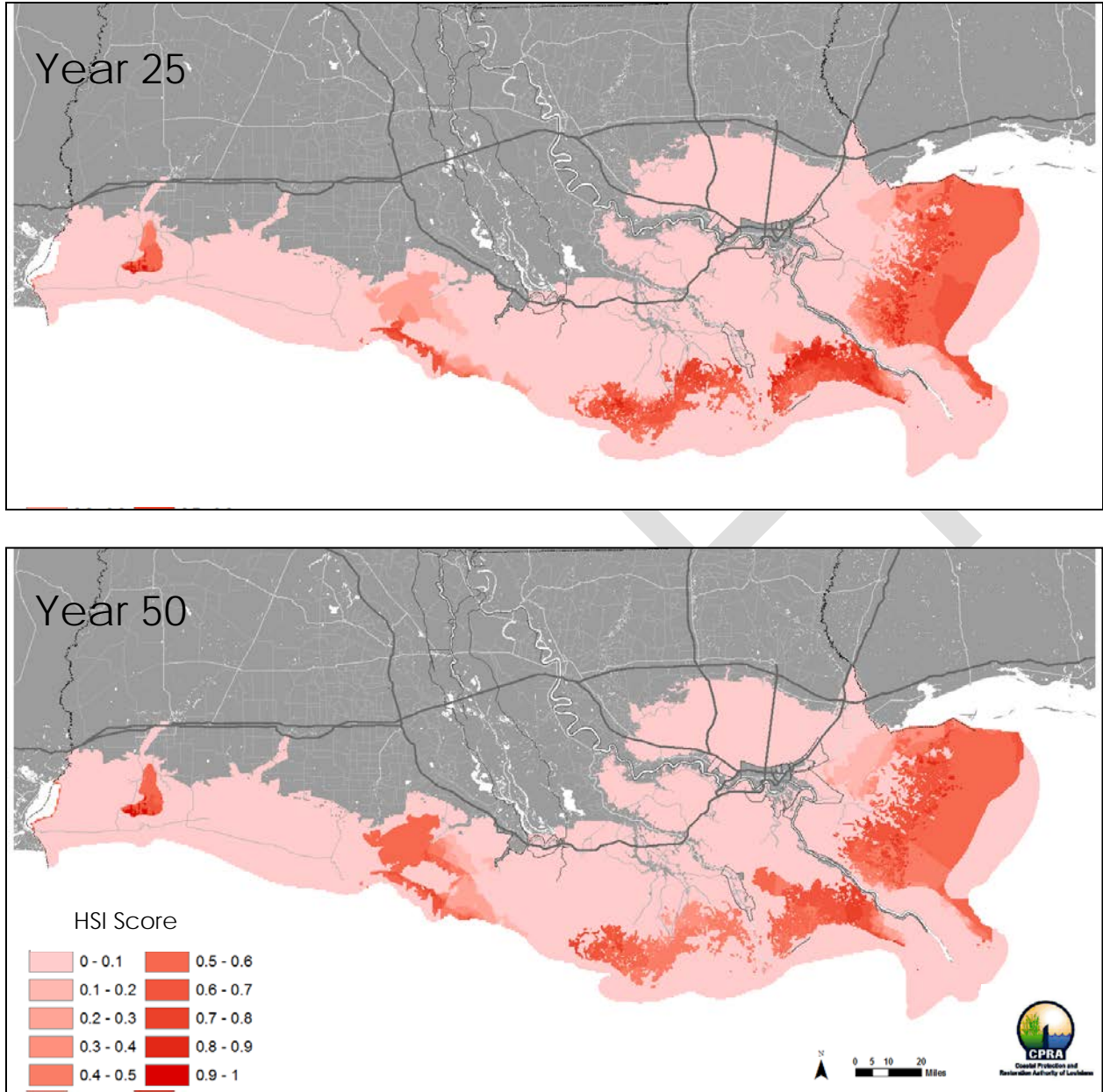


Figure 114: Coast Wide Habitat Suitability for Eastern Oyster at Years 25 and 50 of the Medium FWOA Scenario. Dark Red Indicates Areas of Highest Suitability.

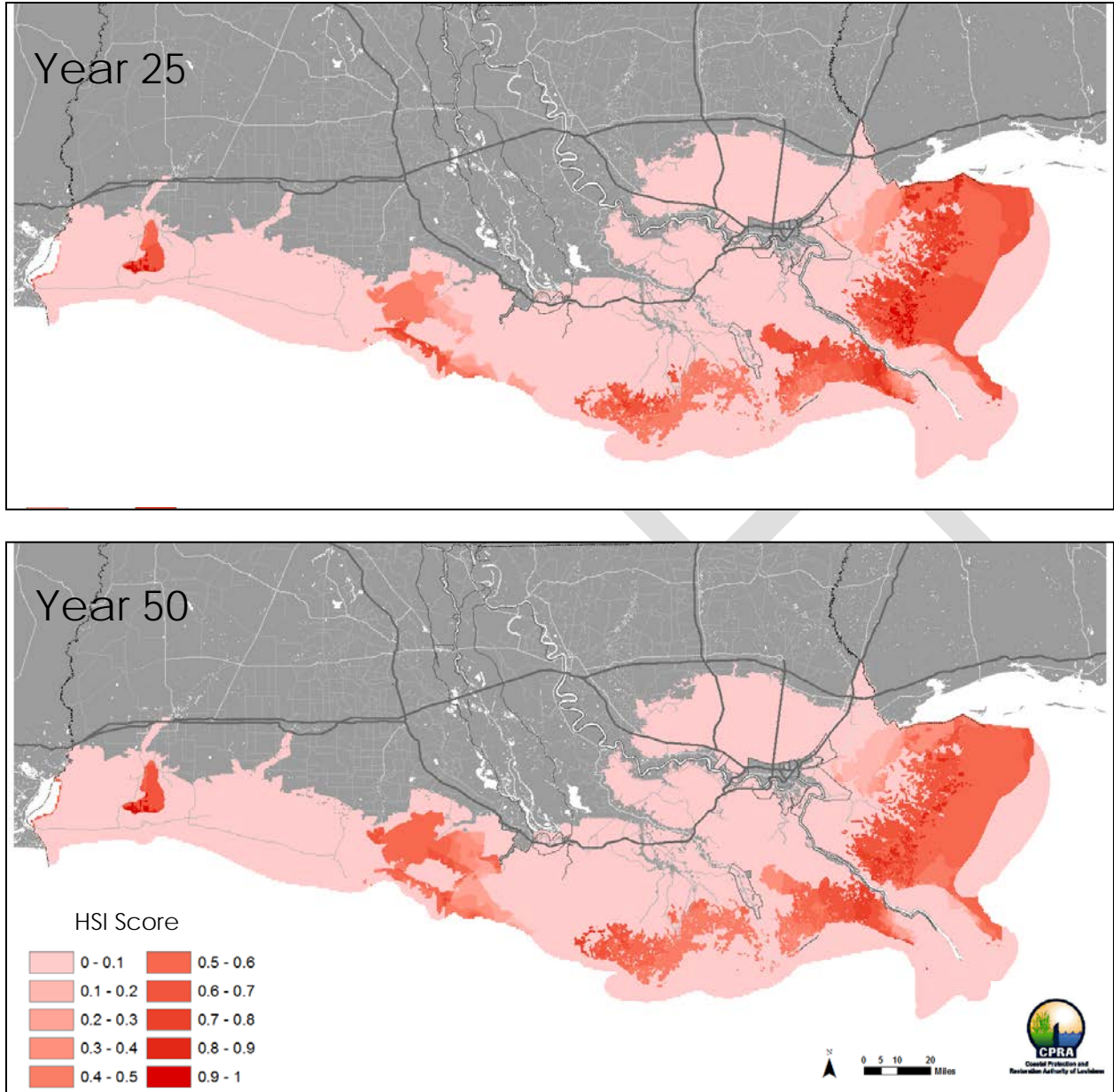


Figure 115: Coast Wide Habitat Suitability for Eastern Oyster at Years 25 and 50 of the High FWOA Scenario. Dark Red Indicates Areas of Highest Suitability.

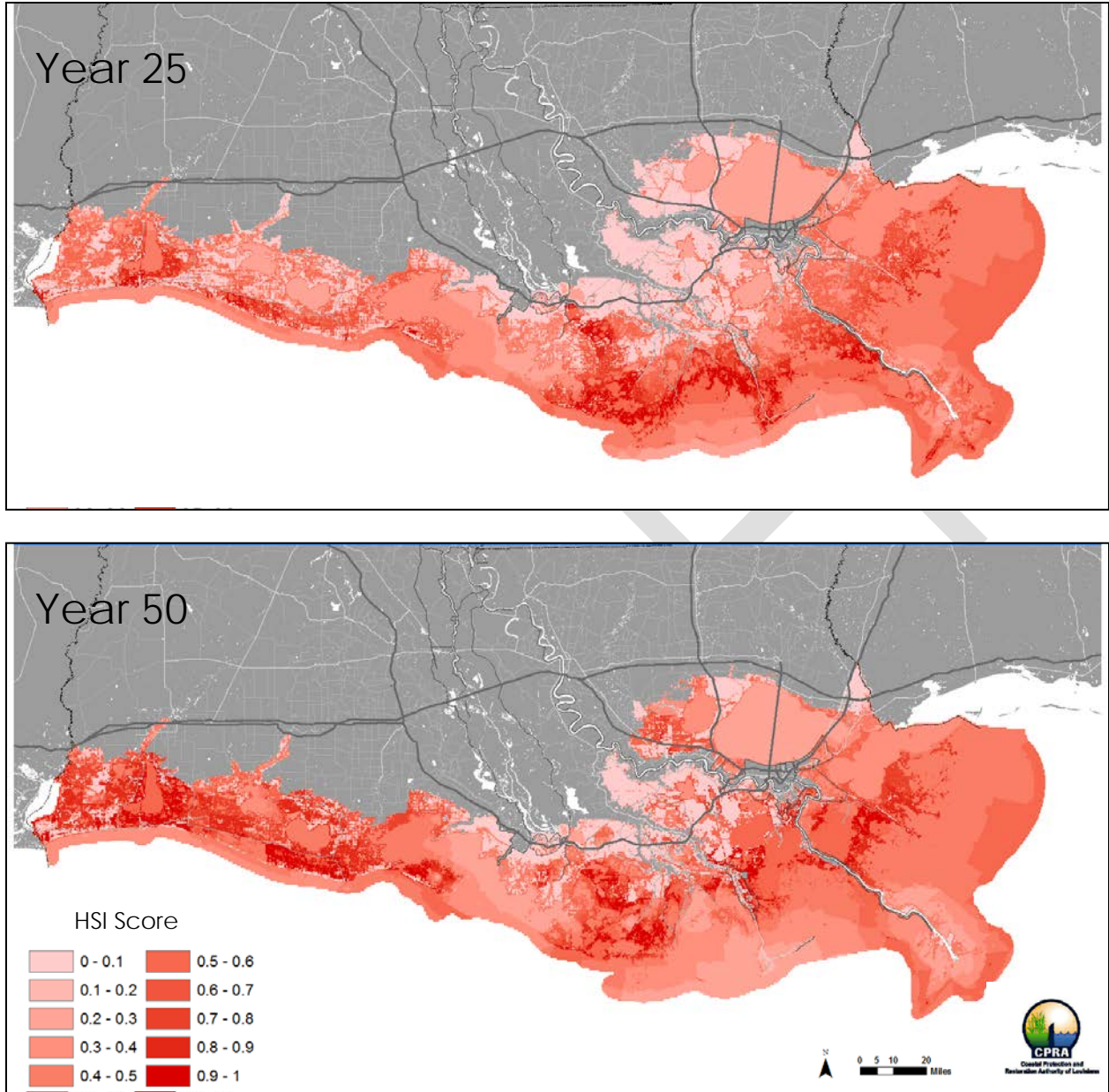


Figure 116: Coast Wide Habitat Suitability for Small Juvenile Brown Shrimp at Years 25 and 50 of the Low FWOA Scenario. Dark Red Indicates Areas of Highest Suitability.

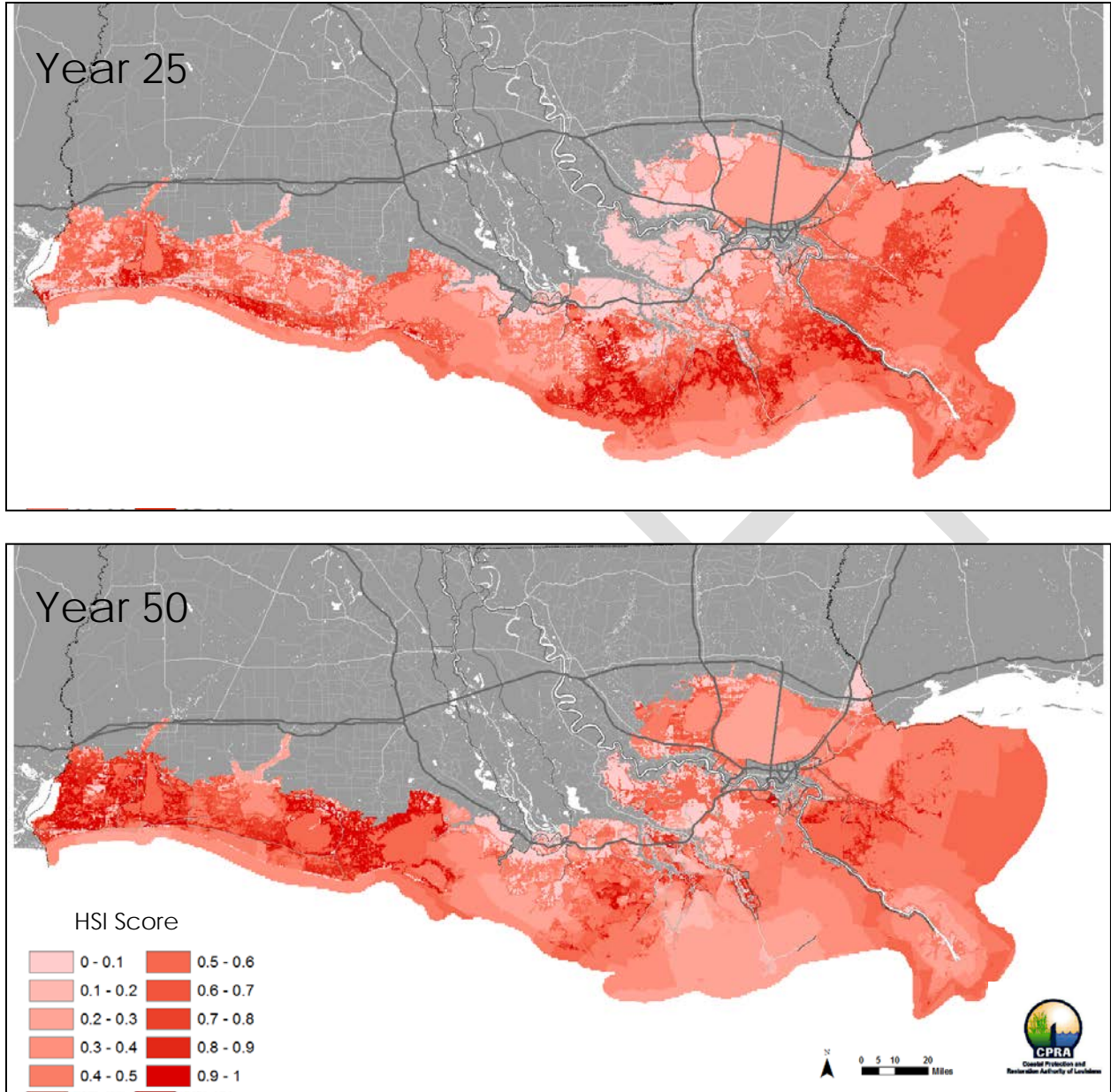


Figure 117: Coast Wide Habitat Suitability for Small Juvenile Brown Shrimp at Years 25 and 50 of the Medium FWOA Scenario. Dark Red Indicates Areas of Highest Suitability.

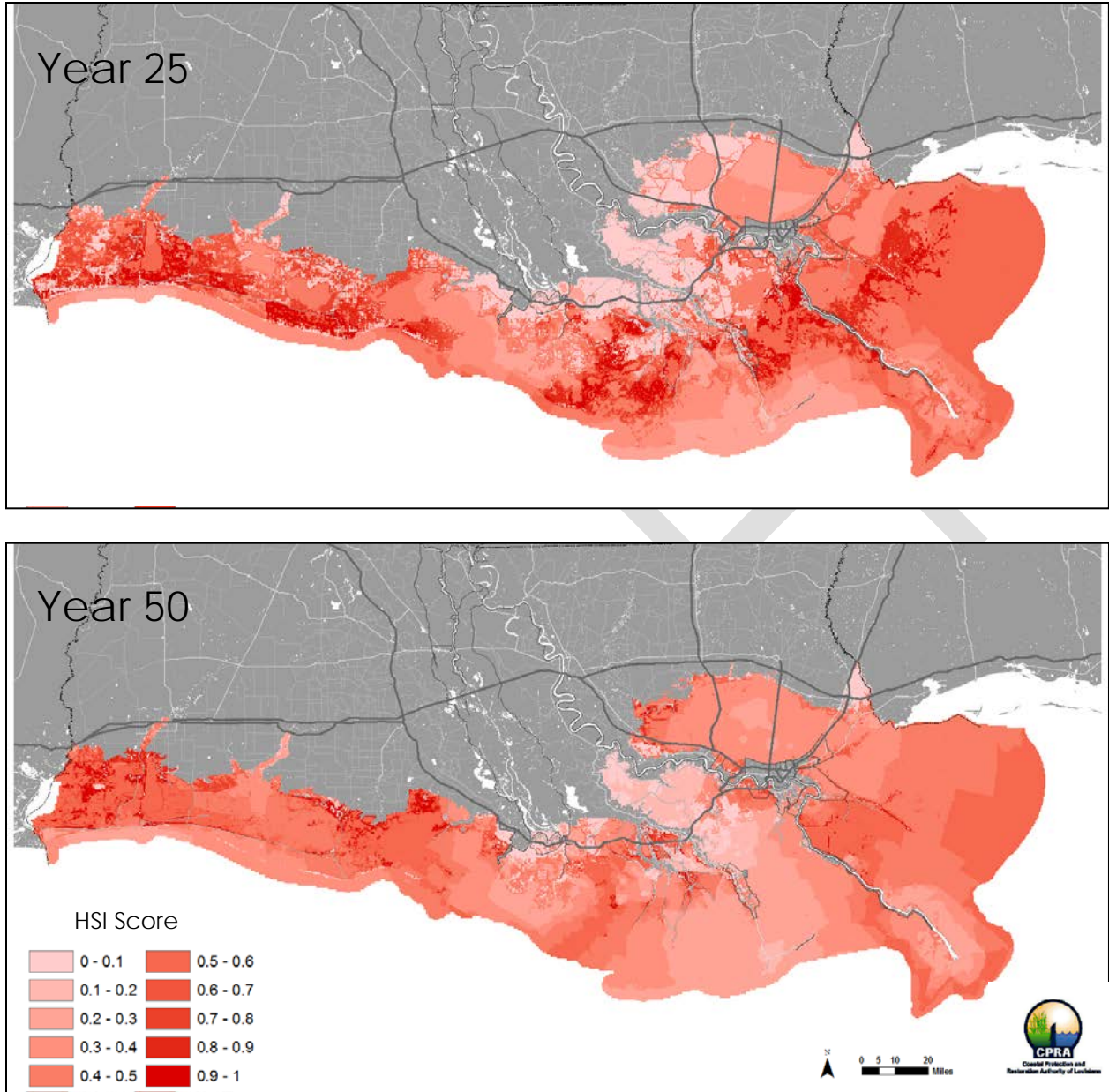


Figure 118: Coast Wide Habitat Suitability for Small Juvenile Brown Shrimp at Years 25 and 50 of the High FWOA Scenario. Dark Red Indicates Areas of Highest Suitability.

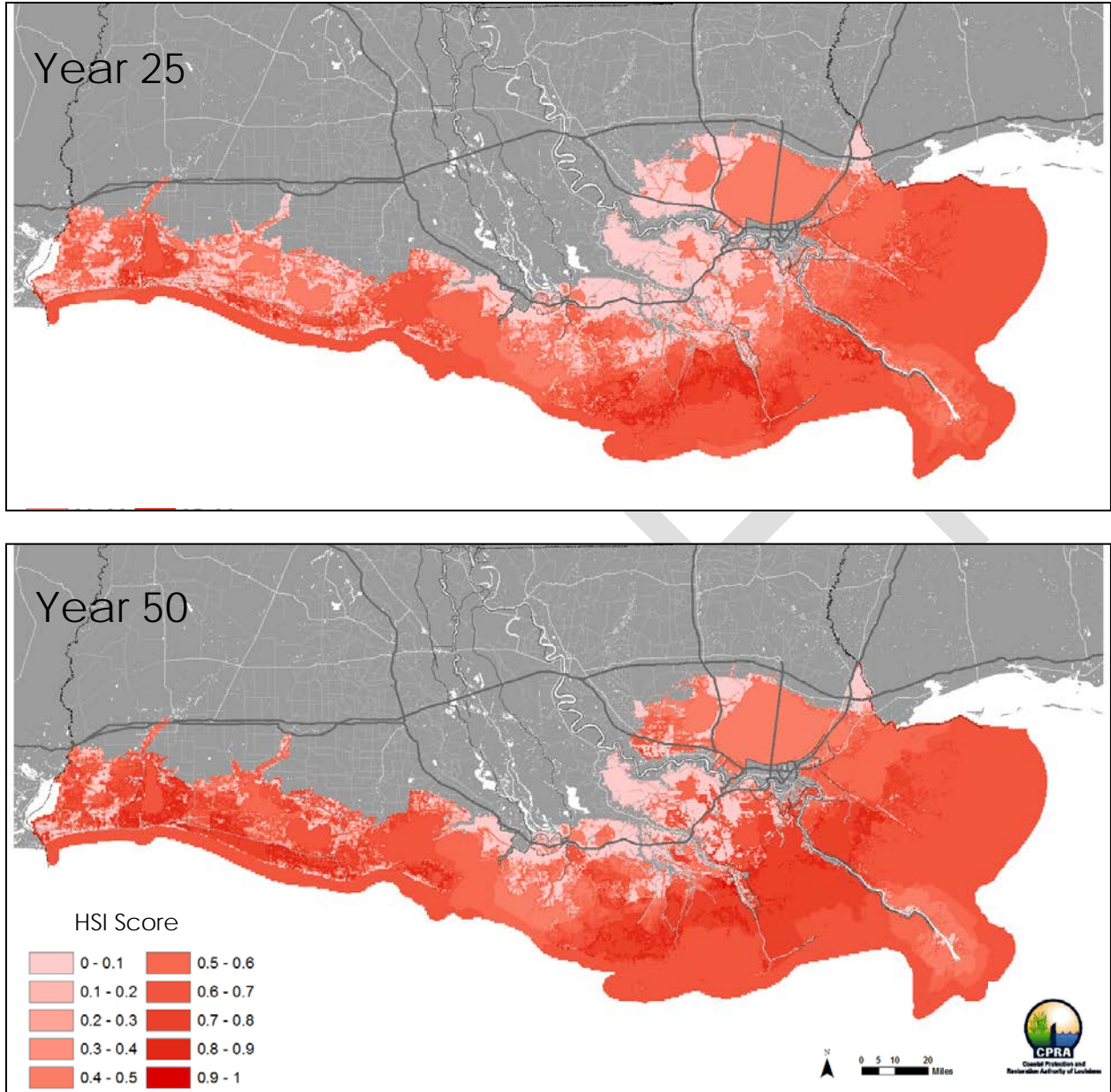


Figure 119: Coast Wide Habitat Suitability for Adult Spotted Seatrout at Years 25 and 50 of the Low FWOA Scenario. Dark Red Indicates Areas of Highest Suitability.

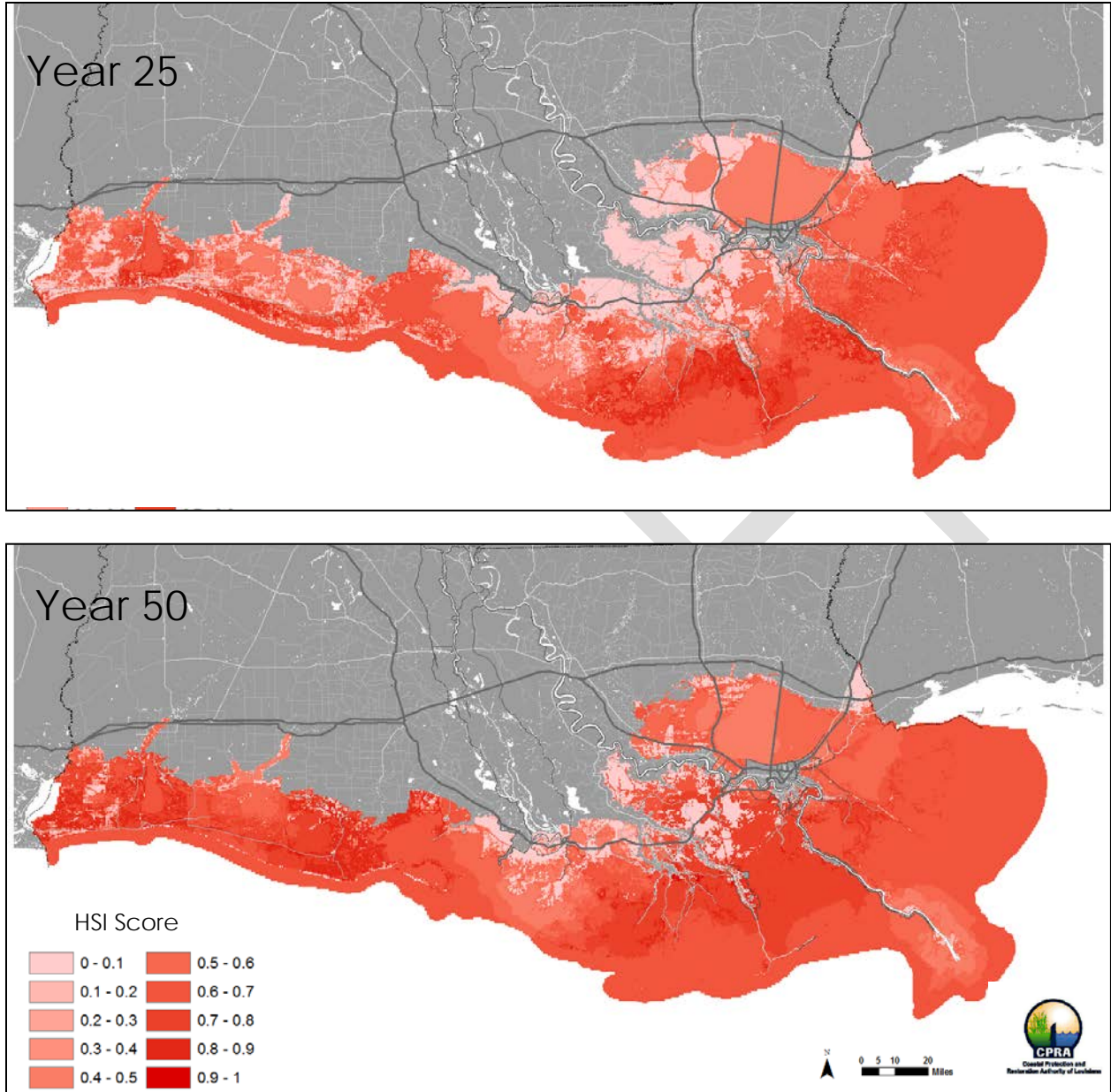


Figure 120: Coast Wide Habitat Suitability for Adult Spotted Seatrout at Years 25 and 50 of the Medium FWOA Scenario. Dark Red Indicates Areas of Highest Suitability.

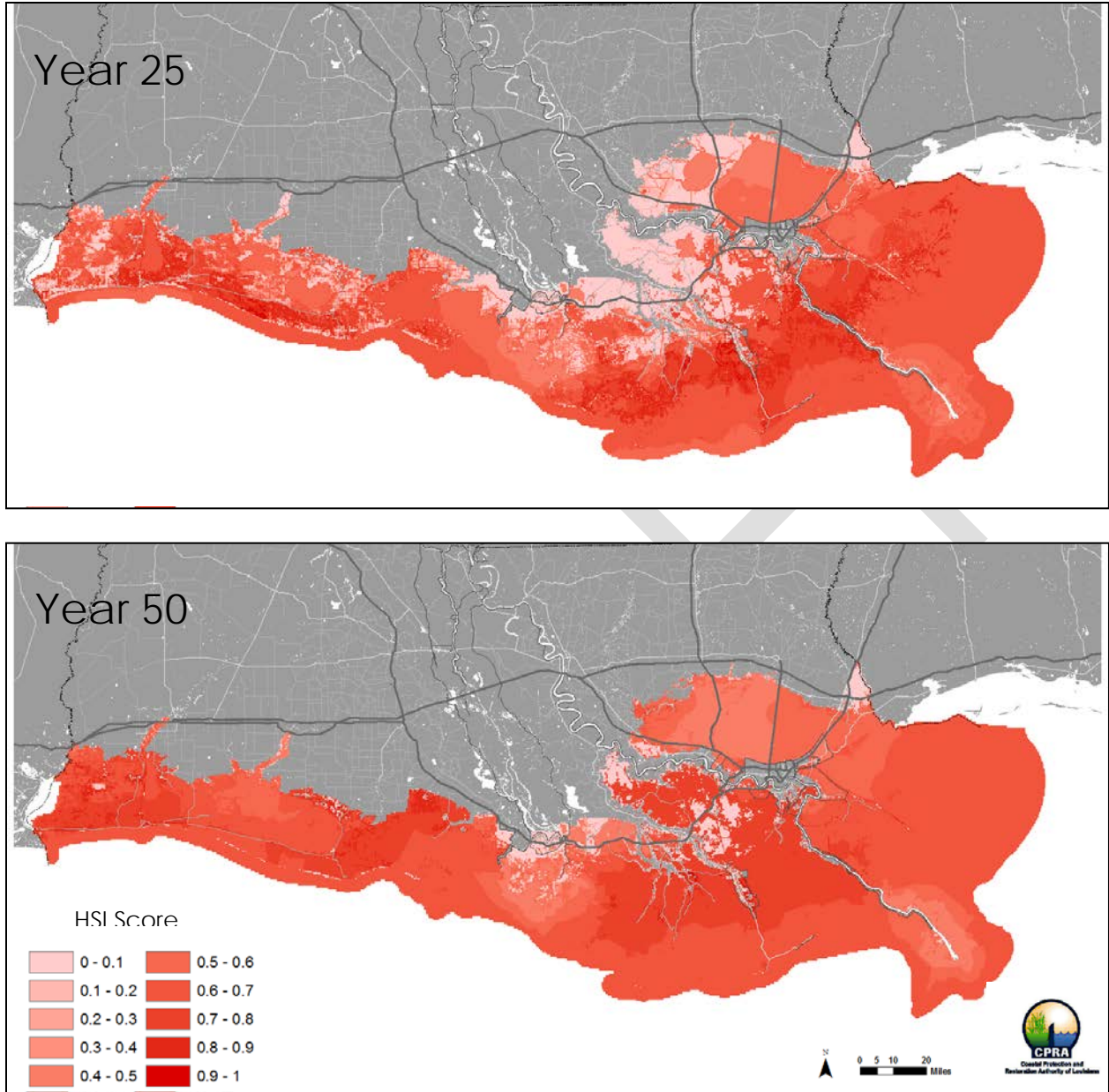


Figure 121: Coast Wide Habitat Suitability for Adult Spotted Seatrout at Years 25 and 50 of the High FWOA Scenario. Dark Red Indicates Areas of Highest Suitability.

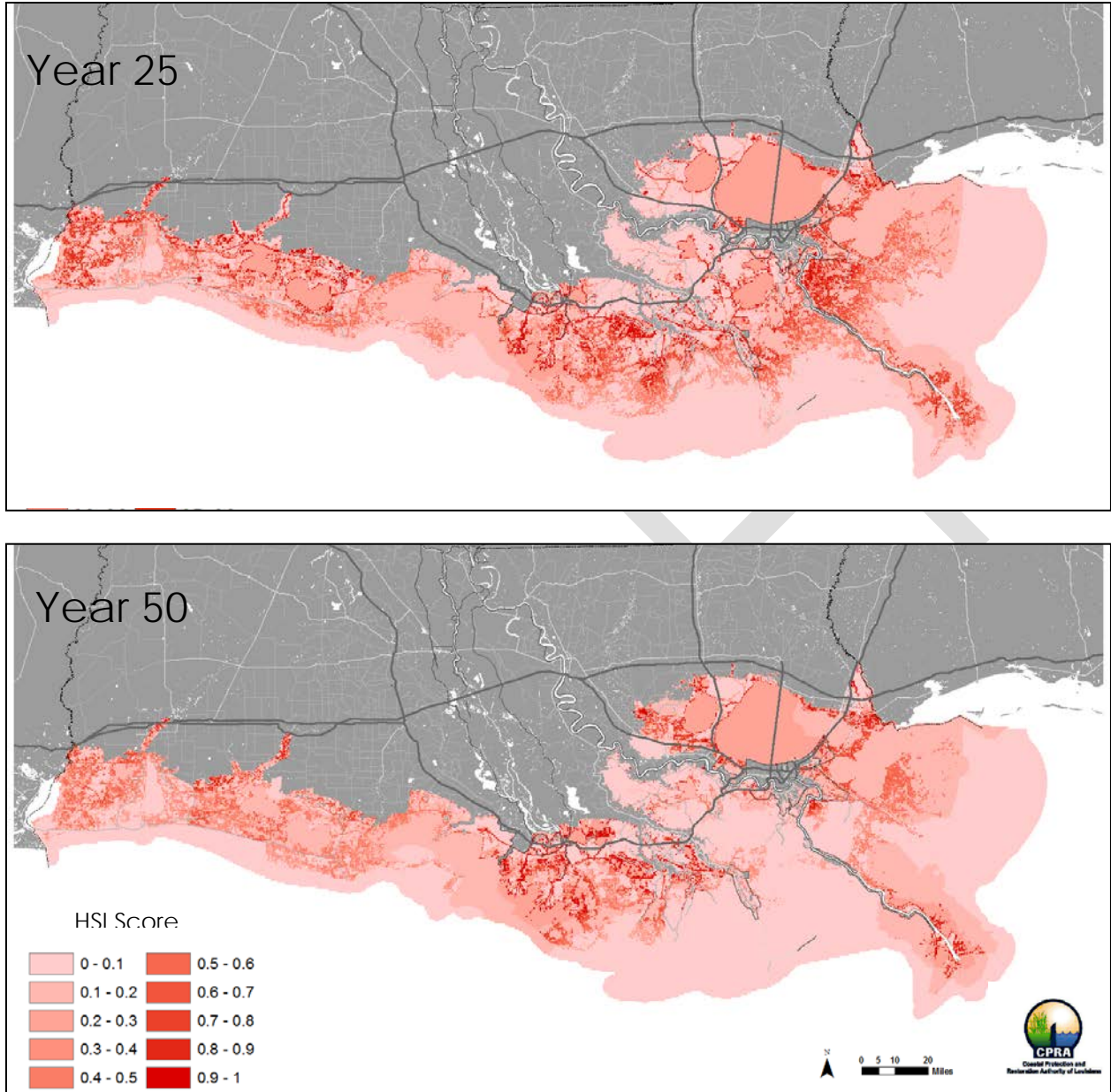


Figure 122: Coast Wide Habitat Suitability for Largemouth Bass at Years 25 and 50 of the Low FWOA Scenario. Dark Red Indicates Areas of Highest Suitability.

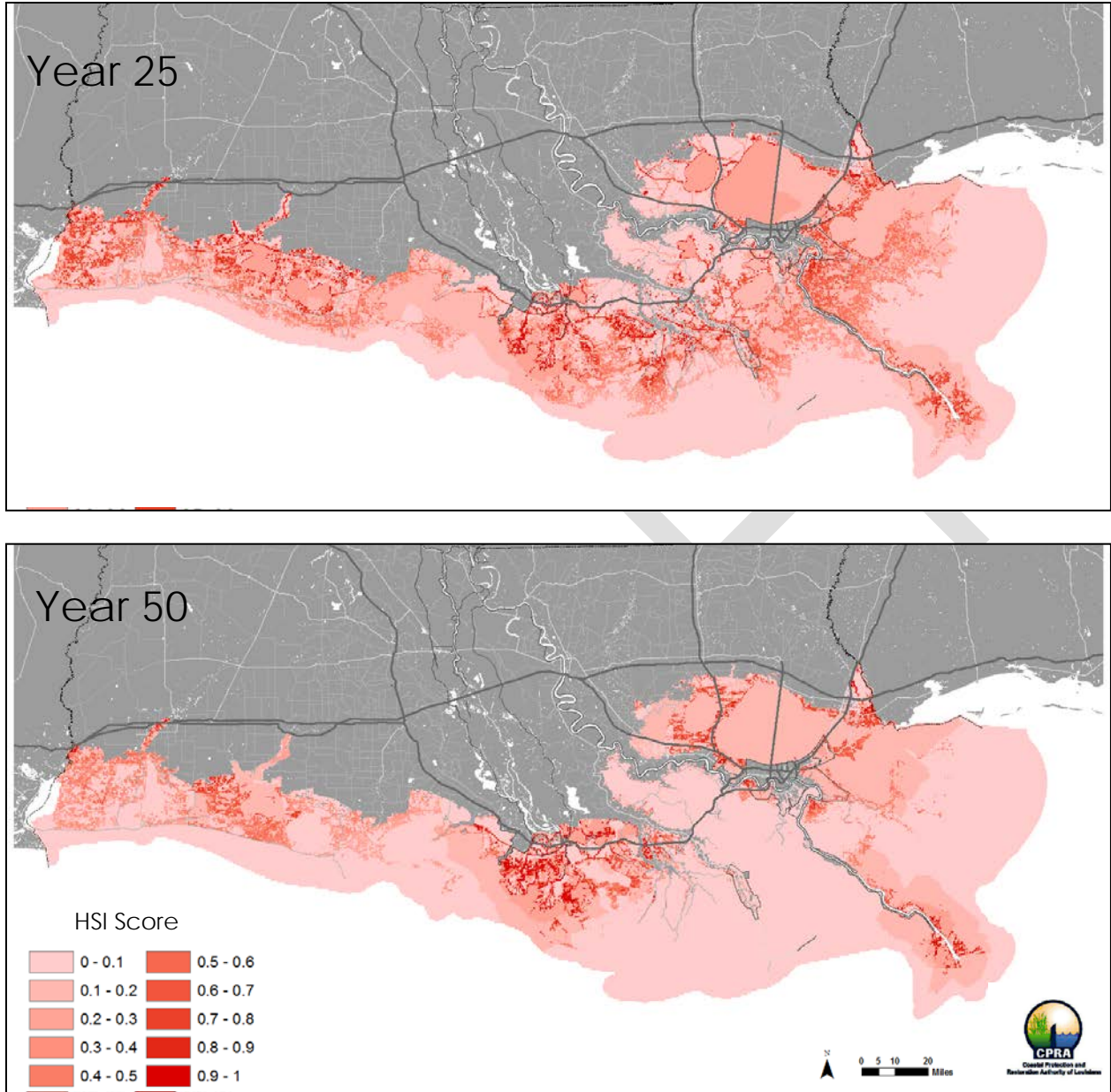


Figure 123: Coast Wide Habitat Suitability for Largemouth Bass at Years 25 and 50 of the Medium FWOA Scenario. Dark Red Indicates Areas of Highest Suitability.

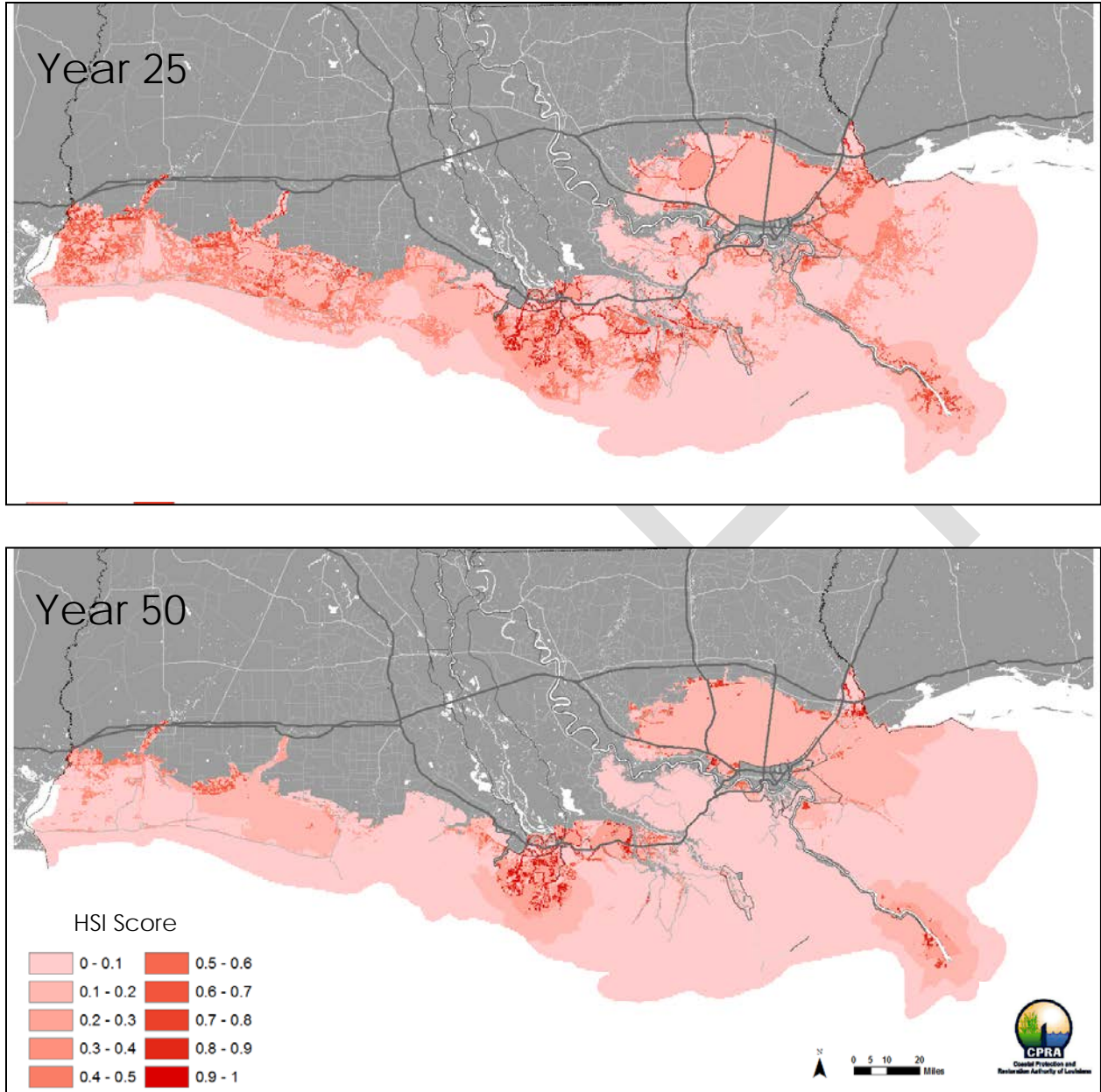


Figure 124: Coast Wide Habitat Suitability for Largemouth Bass at Years 25 and 50 of the High FWOA Scenario. Dark Red Indicates Areas of Highest Suitability.

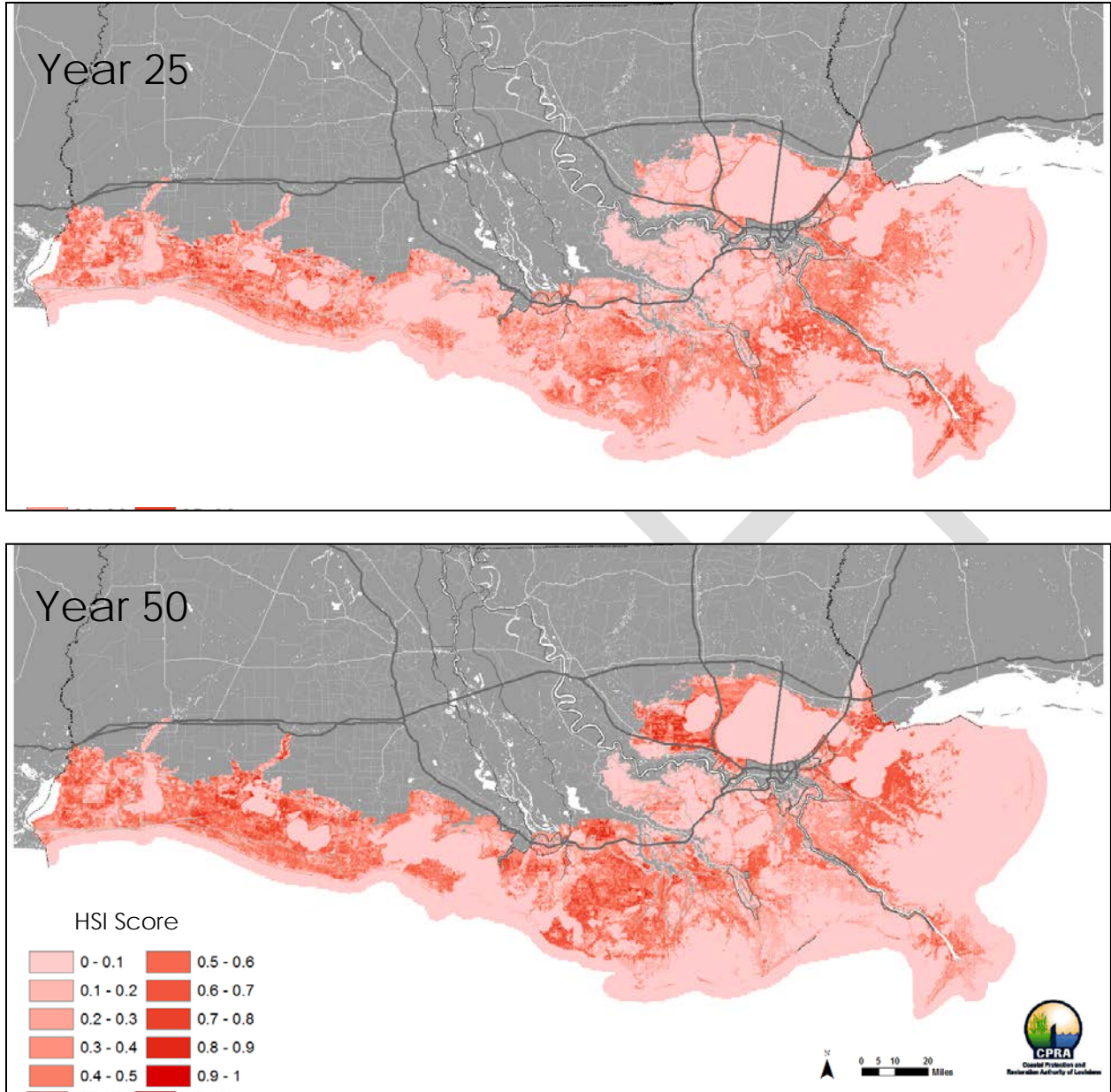


Figure 125: Coast Wide Habitat Suitability for Green-Winged Teal at Years 25 and 50 of the Low FWOA Scenario. Dark Red Indicates Areas of Highest Suitability.

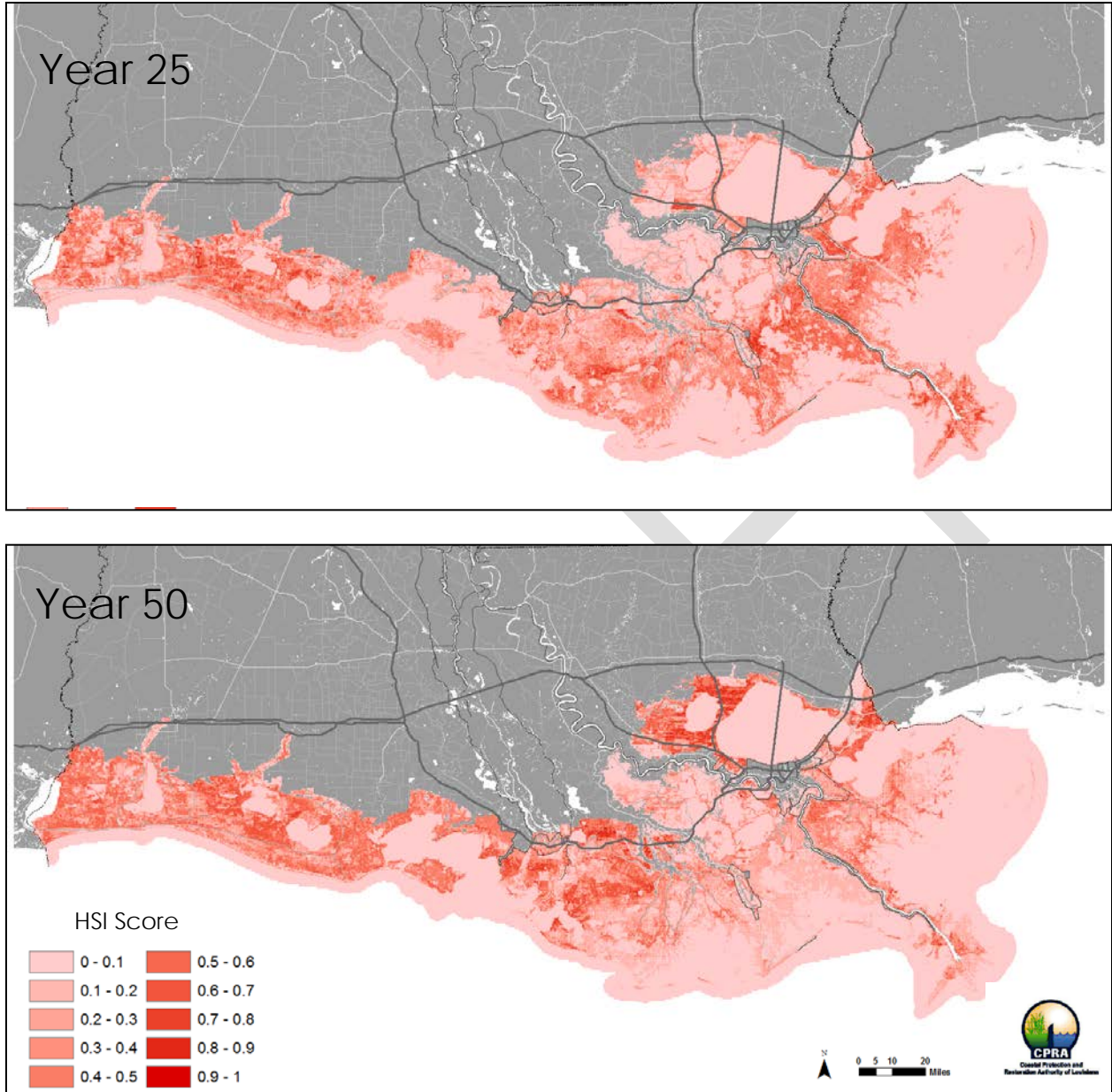


Figure 126: Coast Wide Habitat Suitability for Green-Winged Teal at Years 25 and 50 of the Medium FWOA Scenario. Dark Red Indicates Areas of Highest Suitability.

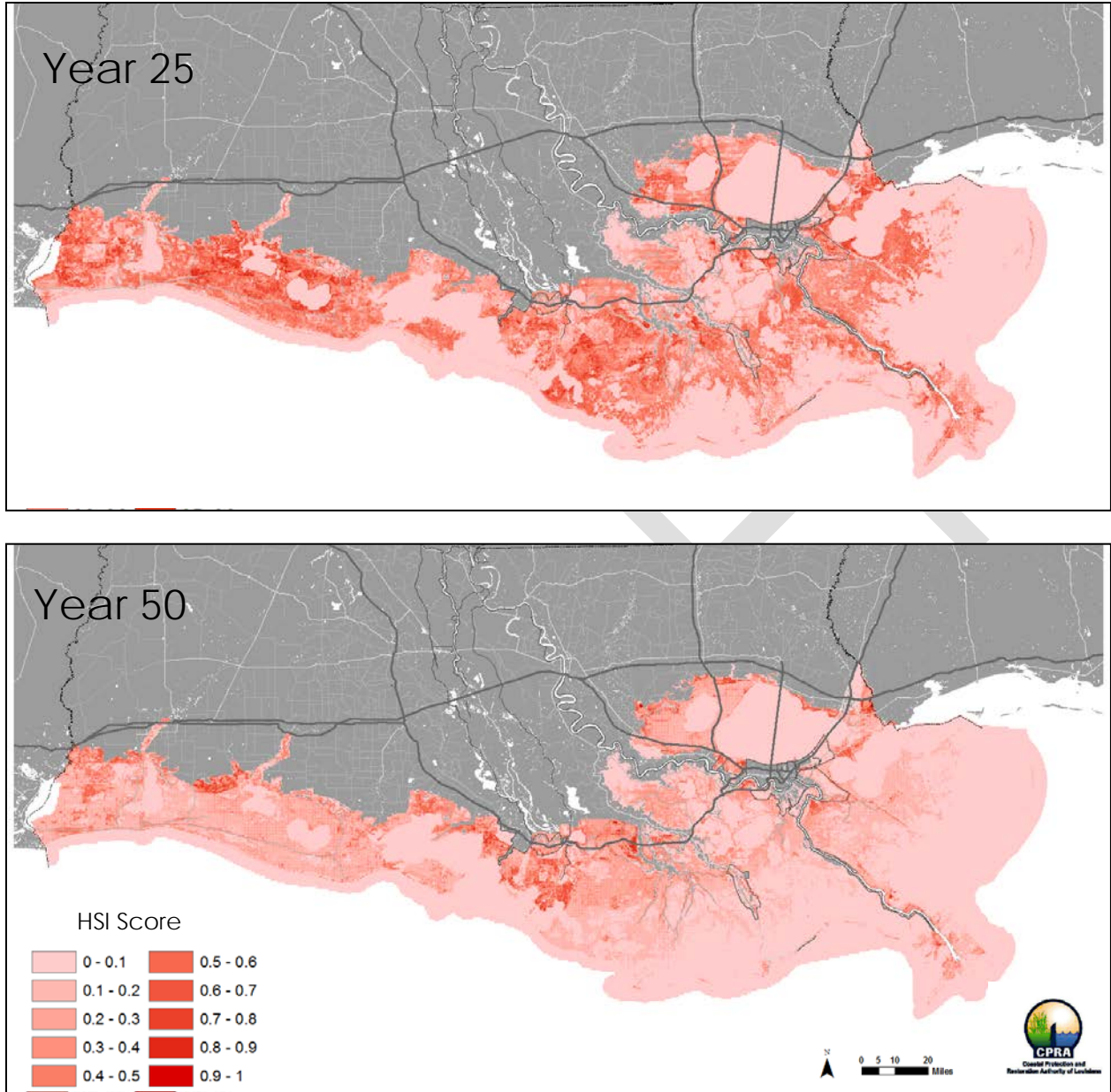


Figure 127: Coast Wide Habitat Suitability for Green-Winged Teal at Years 25 and 50 of the High FWOA Scenario. Dark Red Indicates Areas of Highest Suitability.

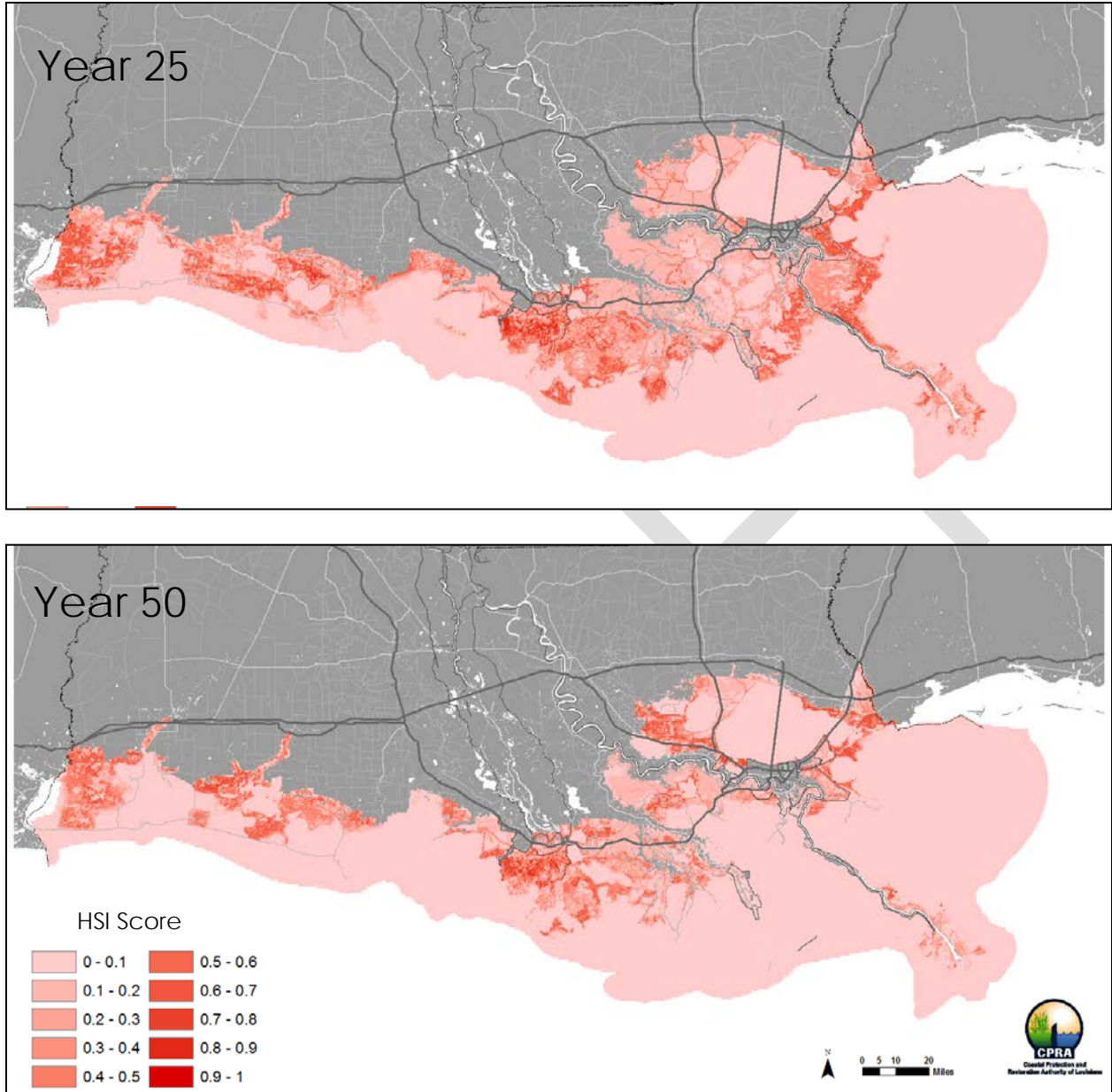


Figure 128: Coast Wide Habitat Suitability for American Alligator at Years 25 and 50 of the Low FWOA Scenario. Dark Red Indicates Areas of Highest Suitability.

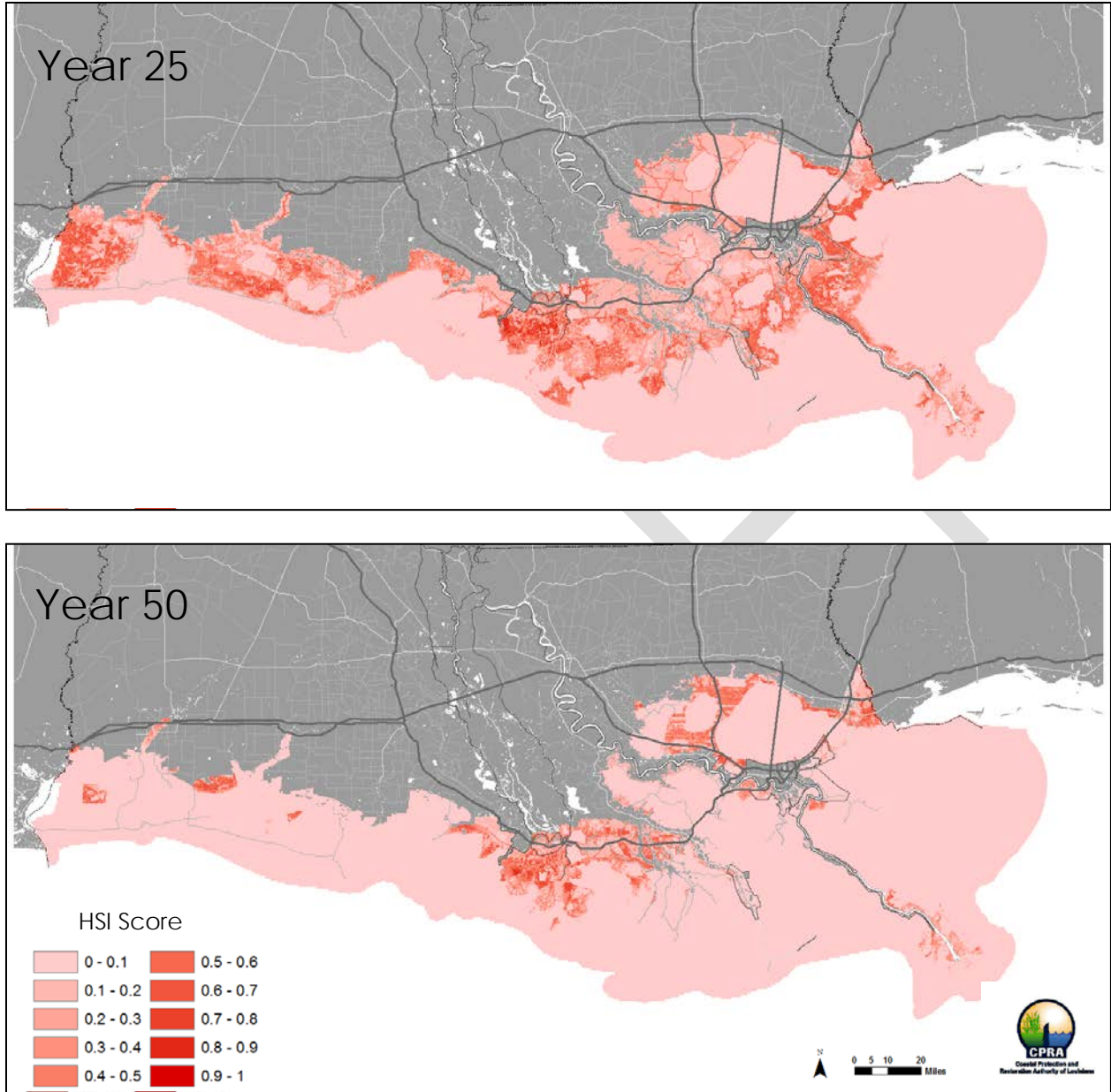


Figure 129: Coast Wide Habitat Suitability for American Alligator at Years 25 and 50 of the Medium FWOA Scenario. Dark Red Indicates Areas of Highest Suitability.

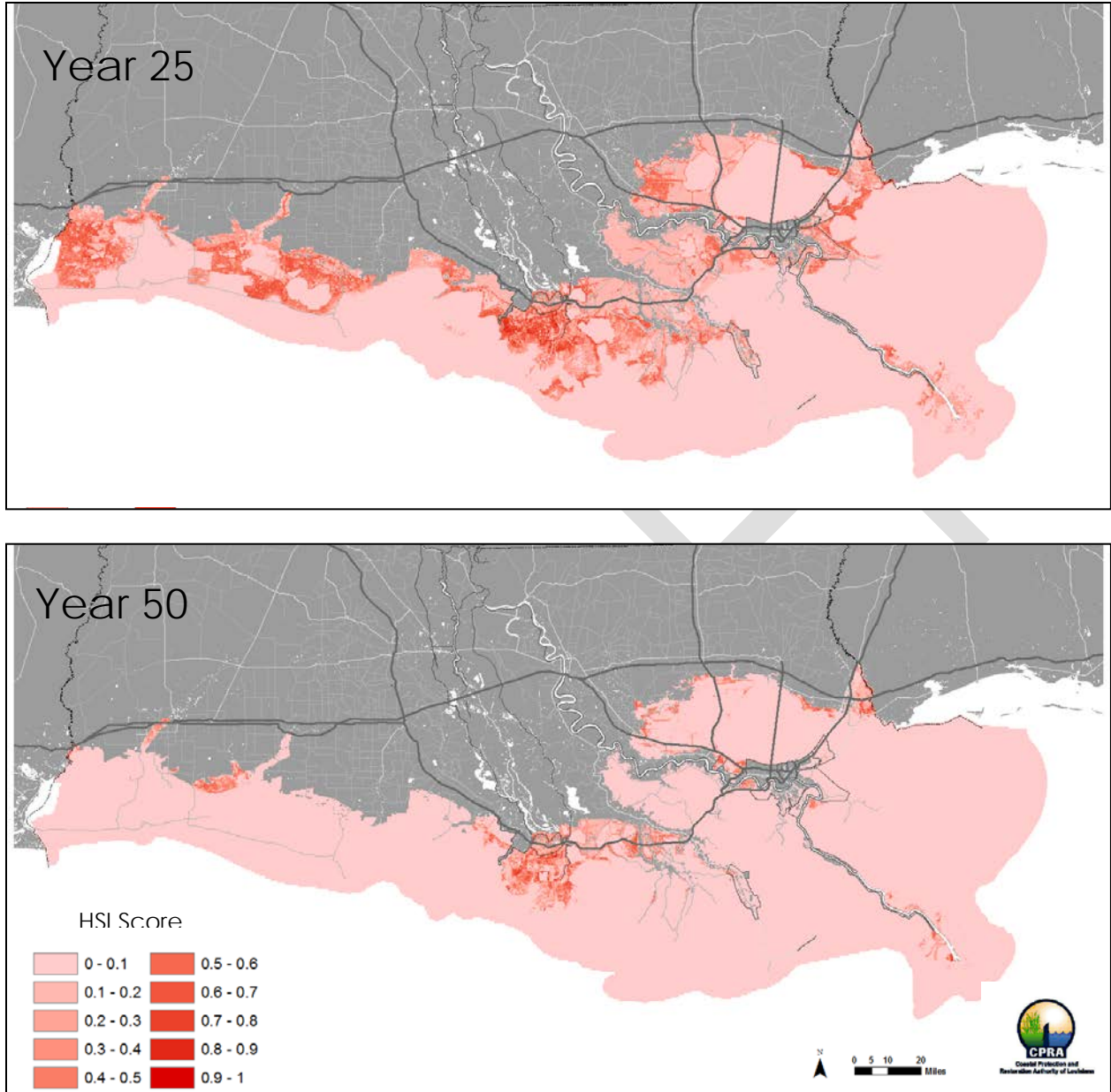


Figure 130: Coast Wide Habitat Suitability for American Alligator at Years 25 and 50 of the High FWOA Scenario. Dark Red Indicates Areas of Highest Suitability.

### 3.7 Ecopath with Ecosim Fish and Shellfish Model

The Fish and Shellfish model has been used to simulate biomass changes of 55 groups over 50 years of FWOA under the low, medium, and high scenarios. In addition to predator-prey interactions and fishing, species in the model respond to environmental factors, including salinity, Total Kjeldahl Nitrogen (TKN) as a measure of primary productivity potential, percent wetland cover, and percent cultch. The results of four species are shown here: the adults of spotted seatrout (*Cynoscion nebulosus*), and eastern oyster (*Crassostrea virginica*), and the juveniles of brown shrimp (*Farfantepenaeus aztecus*), and largemouth bass (*Micropterus salmoides*). The

distribution of biomass for the month of April is shown for each species and scenario. It is important to note that the predictions of absolute biomass shown in these figures are uncertain; therefore, the output is best used to assess relative changes in biomass over time and space. A distribution trend that can be seen in all outputs is a concentration around the Mississippi River Delta. The reason for this is the high concentration of TKN in that area (Figure 131) as compared to other coastal areas. High concentrations of TKN result in a strong bottom-up effect in the food web model, increasing biomass of fish and shellfish. The absence of biomass of high salinity species right at the Bird's Foot Delta (where TKN is highest) is a result of the low salinity there (Figure 134).

Under the low scenario, spotted seatrout and brown shrimp (Figure 132 and Figure 133) are estimated to expand their range more inland over time. The salinity increase in those areas is the most important driver for this change (Figure 134). This salinity effect is a general trend where species with higher salinity tolerances increase their spatial distribution inland. An increase in oysters is seen as well in the low scenario, though its range expansion is limited by a lack of cultch in inland areas (Figure 135). Species that have low salinity tolerance show the opposite effect, as exemplified with largemouth bass (Figure 136). Biomass of largemouth bass decreases in year 50 as compared to year 25.

The medium scenario results in similar patterns as the low scenario, with an expansion of the distribution of higher salinity species into the upper estuaries in year 50. However, in the medium scenario, the effects of saltwater intrusion manifest earlier, resulting in some inland expansion of saltwater species in year 25, which can be seen in the distribution pattern of spotted seatrout (Figure 137). This is a result of salinities increasing sooner and reaching higher levels in the medium and high scenarios. In addition, in year 50 of the medium scenario, another effect becomes apparent; a small reduction in biomass where wetland loss occurs. This can be seen in the juvenile stages of estuarine-dependent species in areas that experience high wetland loss, such as brown shrimp in Barataria Bay (Figure 138). Estimates for eastern oyster and largemouth bass for the medium scenario are similar to the low scenario, with an increase in oyster biomass in year 50 as compared to year 25 (Figure 139), and a decrease in largemouth bass biomass (Figure 140).

Under the high scenario, the saltwater intrusion has taken place earlier in the simulation. As a result, the inland expansion of species with high salinity tolerance occurs earlier (by year 25), as can be seen for spotted seatrout (Figure 141). Spotted seatrout even undergoes a loss of biomass in year 50, which can be partially explained by salinity increases that exceed the tolerance range of spotted seatrout. An additional effect that drives the loss of biomass, mostly occurring in the Barataria Bay, is wetland loss. This wetland effect is clearly visible in year 50 for adult spotted seatrout and juvenile brown shrimp as compared to year 25 (Figure 141 and Figure 142). In the case of adult spotted seatrout, this is an indirect effect of wetland loss on spotted seatrout juveniles. The distribution of juvenile brown shrimp indicates there are still some increases in the upper estuaries as they turn more saline, but overall there is a loss of biomass as a result of wetland loss. The extent of potential wetland loss that is affecting estuarine-dependent species is shown in Figure 143, which is a comparison of year 25 in the low scenario (minimal wetland loss) and year 50 of the high scenario. The eastern oyster shows some minor inland expansion in year 50 of the high scenario in the PB and near the Atchafalaya River outfall (Figure 144). This is a result of salinity increases. Largemouth bass shows a decrease over time in the high scenario, as it did in the low and medium scenarios (Figure 145).

Comparing year 50 of all three scenarios (low, medium, and high), it becomes clear that the combined complex effects of the projected sea level rise, subsidence, precipitation, and evapotranspiration have an effect on the biomass estimates. For brown shrimp, all three

scenarios show an inland expansion of the biomass distribution due to saltwater intrusion, but with higher rates of sea level rise and subsidence, the negative effect of wetland loss on brown shrimp biomass become more apparent (Figure 133, Figure 138, and Figure 142). Since this is after 50 years of simulation, this is not only affecting juveniles; the lower recruitment is reducing adult biomass as well, which can be seen for adult spotted seatrout (Figure 132, Figure 137, and Figure 141). This is most apparent in the Barataria Bay, which has a high rate of wetland loss, and is in addition to direct effects of increased salinity, exceeding the tolerance range of spotted seatrout. The high scenario does not have a negative effect on eastern oysters when compared to the low and medium scenarios (Figure 135, Figure 139, and Figure 144). However, this may be due to the fact that parasitism and disease (which both increase in higher salinities) are not included as direct effects, and that the increase in water depth itself is not included as an effect in the current simulations. An increase in water depth could place oysters below the photic zone, which decreases their food (phytoplankton) availability. Largemouth bass displays biomass concentrations in areas of low salinity, which are inland areas and areas with high freshwater discharge, such as at the outfall of the Caernarvon freshwater diversion and the Bird's Foot Delta (Figure 136, Figure 140, and Figure 145). These biomass concentrations become more restricted in the high scenario. It should be noted that none of the scenarios result in a crash of the fish and shellfish stocks.

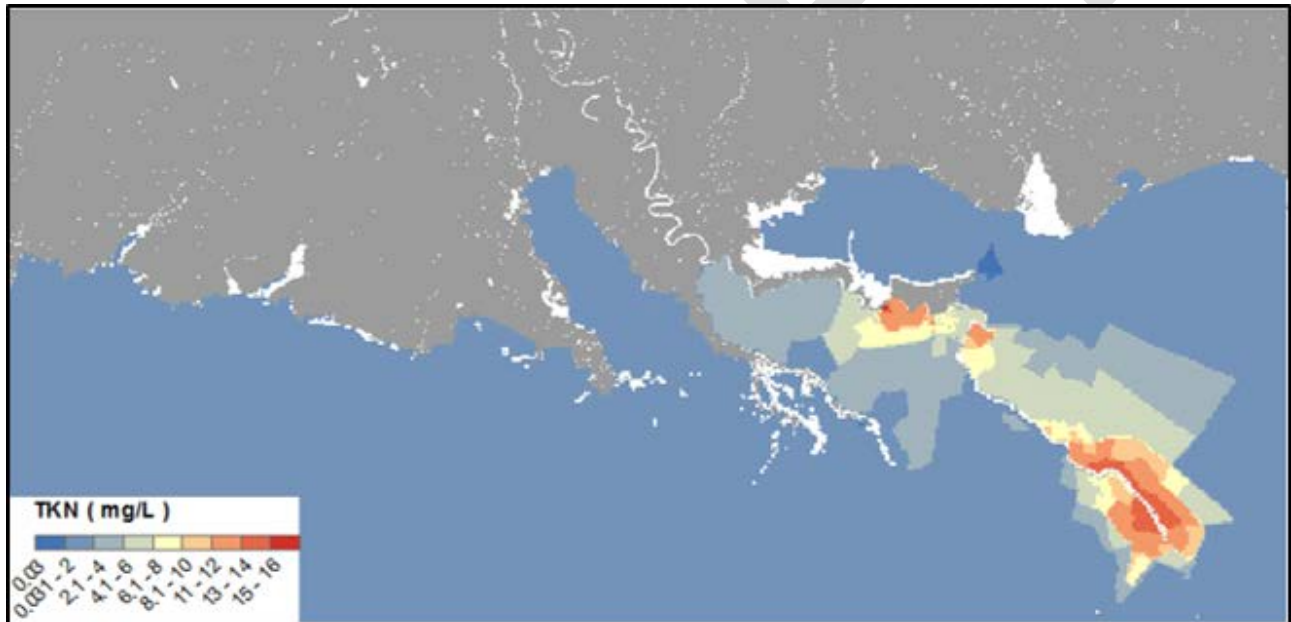


Figure 131: Distribution of TKN: Year 25 of the Low Scenario.

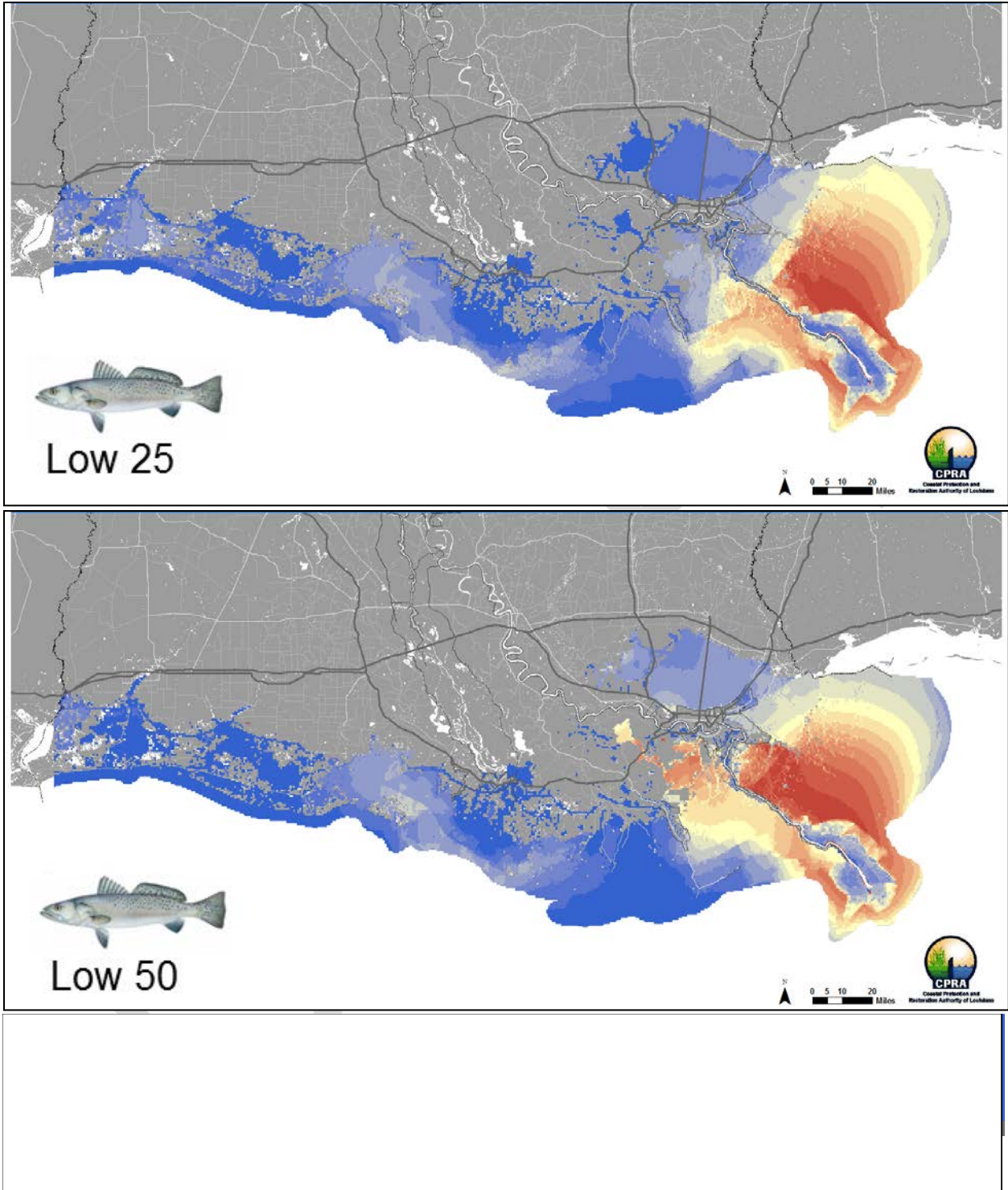


Figure 132: Biomass Distribution of Adult Spotted Seatrout in Year 25 (top) and Year 50 (Bottom) of the Low Scenario.

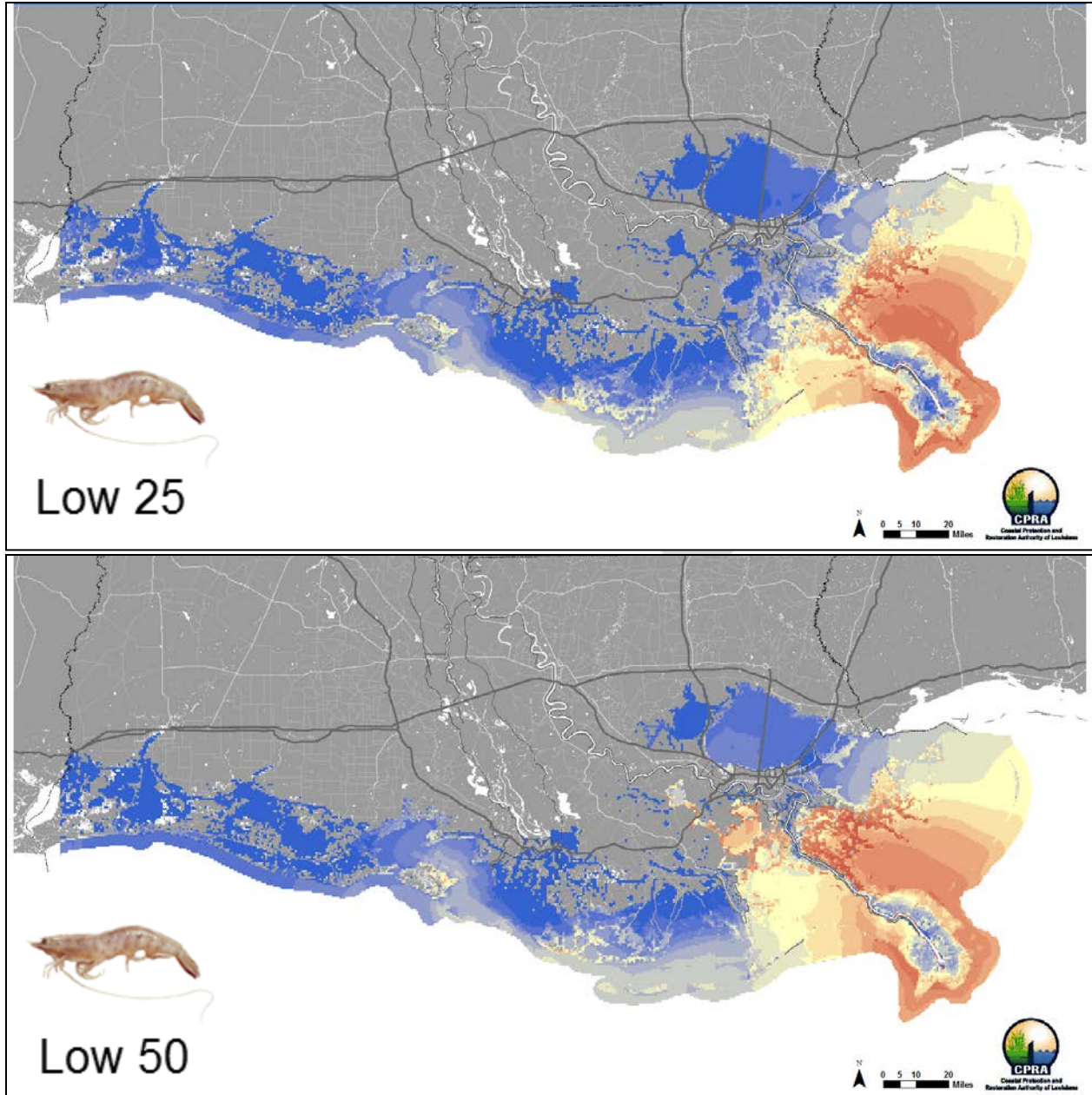


Figure 133: Biomass Distribution of Juvenile Brown Shrimp in Year 25 (top) and Year 50 (Bottom) of the Low Scenario.

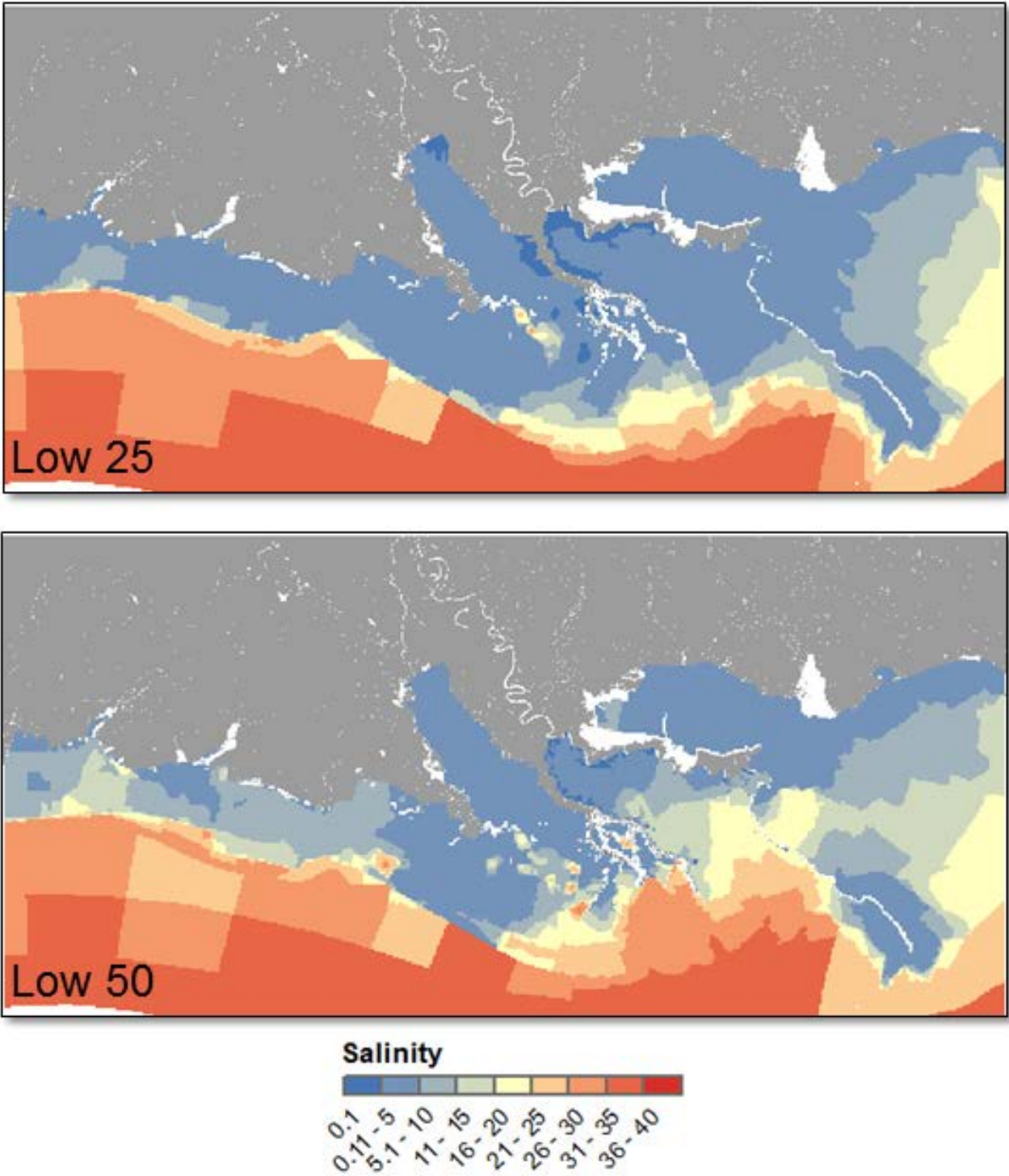


Figure 134: Mean Monthly Salinity in April of Year 25 and Year 50 in the Low Scenario Compared.

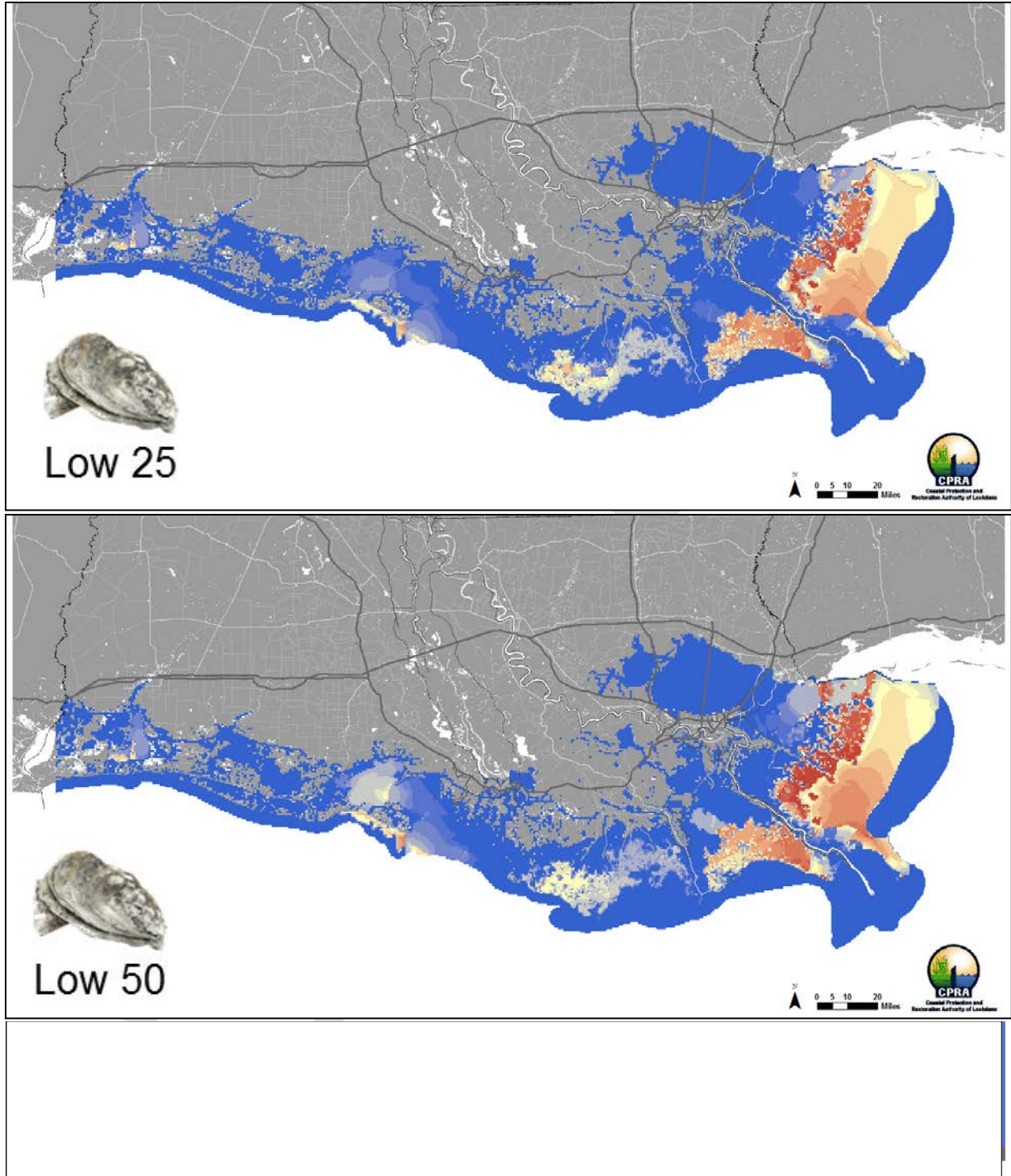


Figure 135: Biomass Distribution of Eastern Oyster (Sack) in Year 25 (Top) and Year 50 (Bottom) of the Low Scenario.

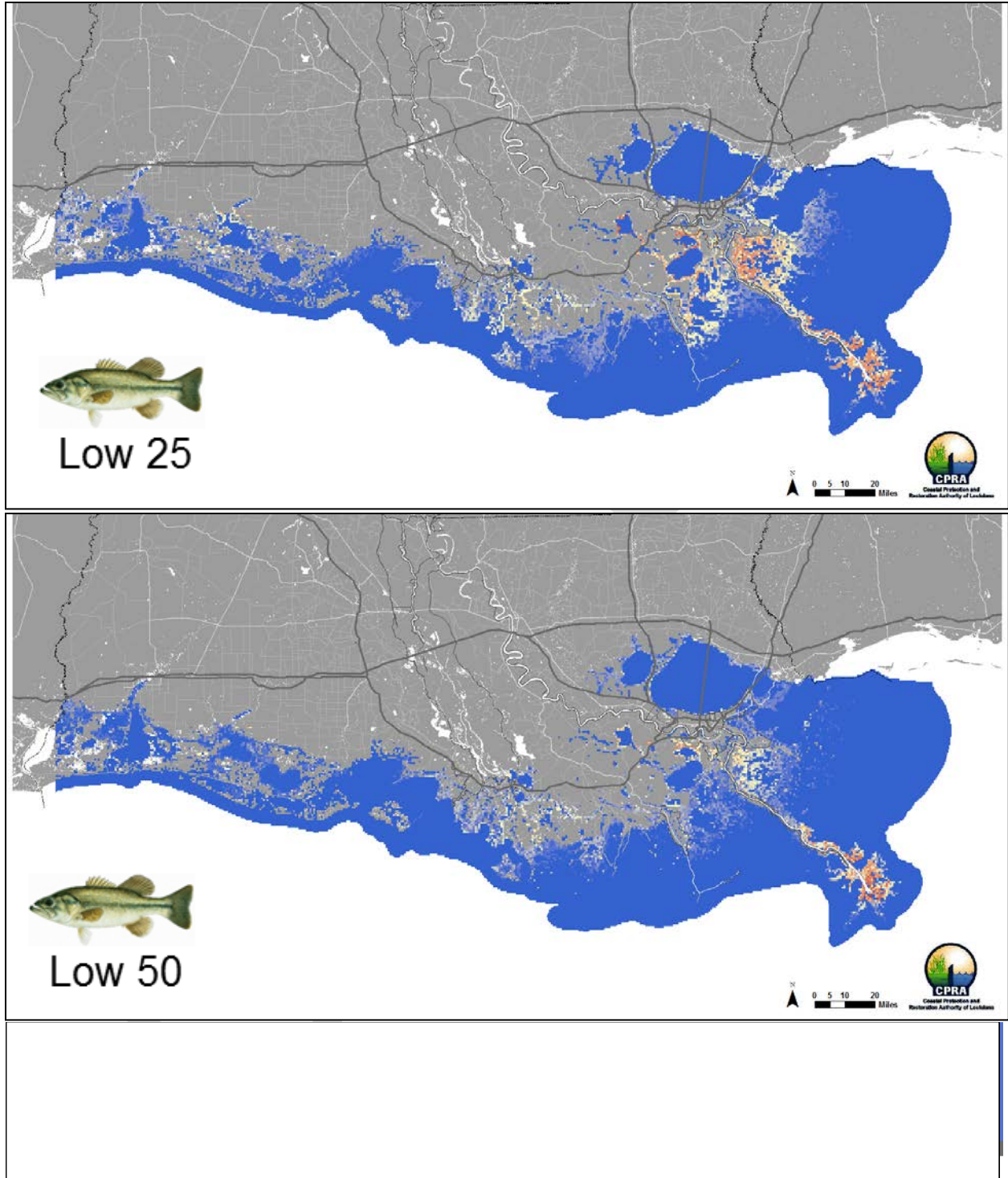


Figure 136: Biomass Distribution of Juvenile Largemouth Bass in Year 25 (Top) and Year 50 (Bottom) of the Low Scenario.

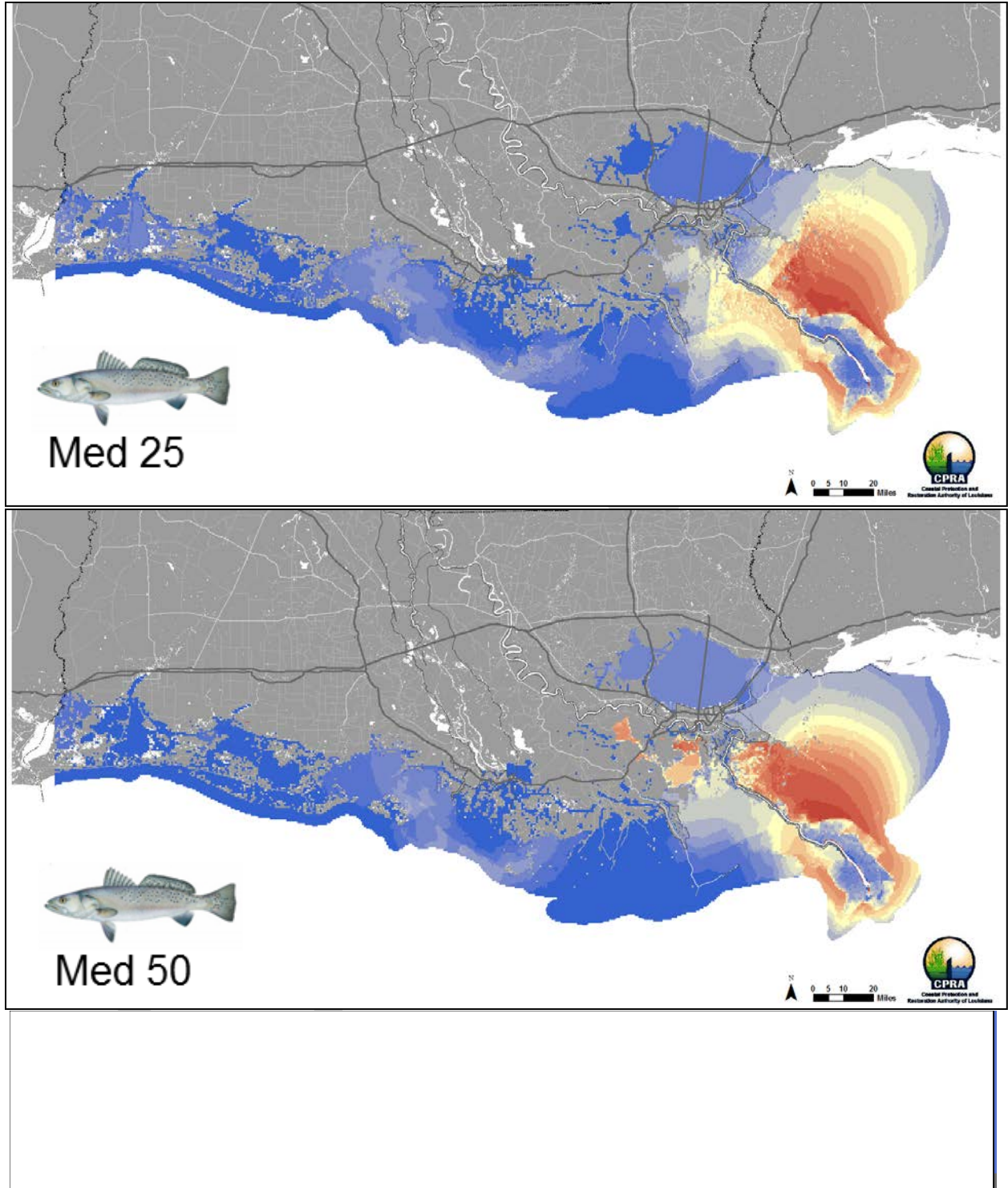


Figure 137: Biomass Distribution of Adult Spotted Seatrout in Year 25 (Top) and Year 50 (Bottom) of the Medium Scenario.

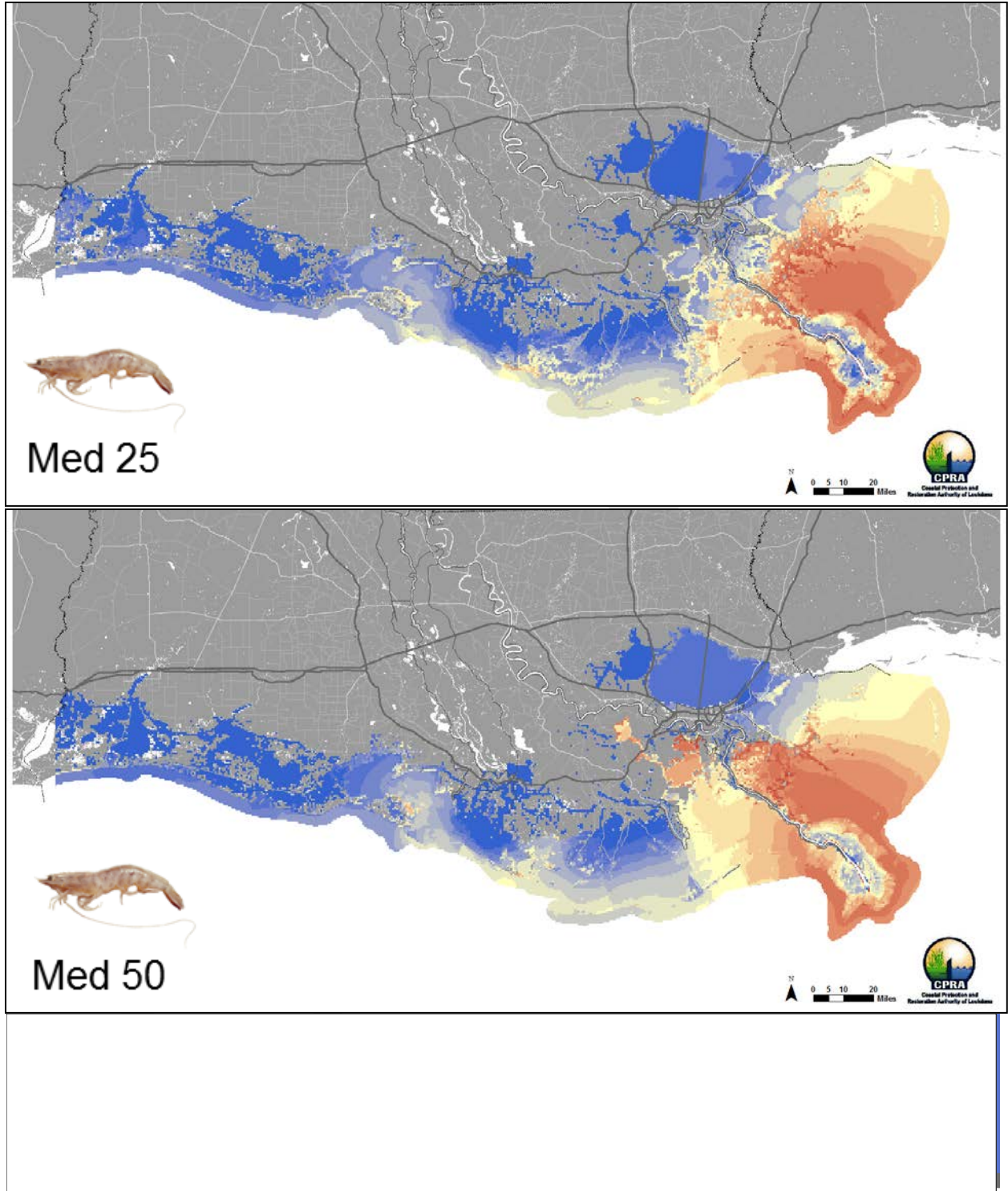


Figure 138: Biomass Distribution of Juvenile Brown Shrimp in Year 25 (Top) and Year 50 (Bottom) of the Medium Scenario.

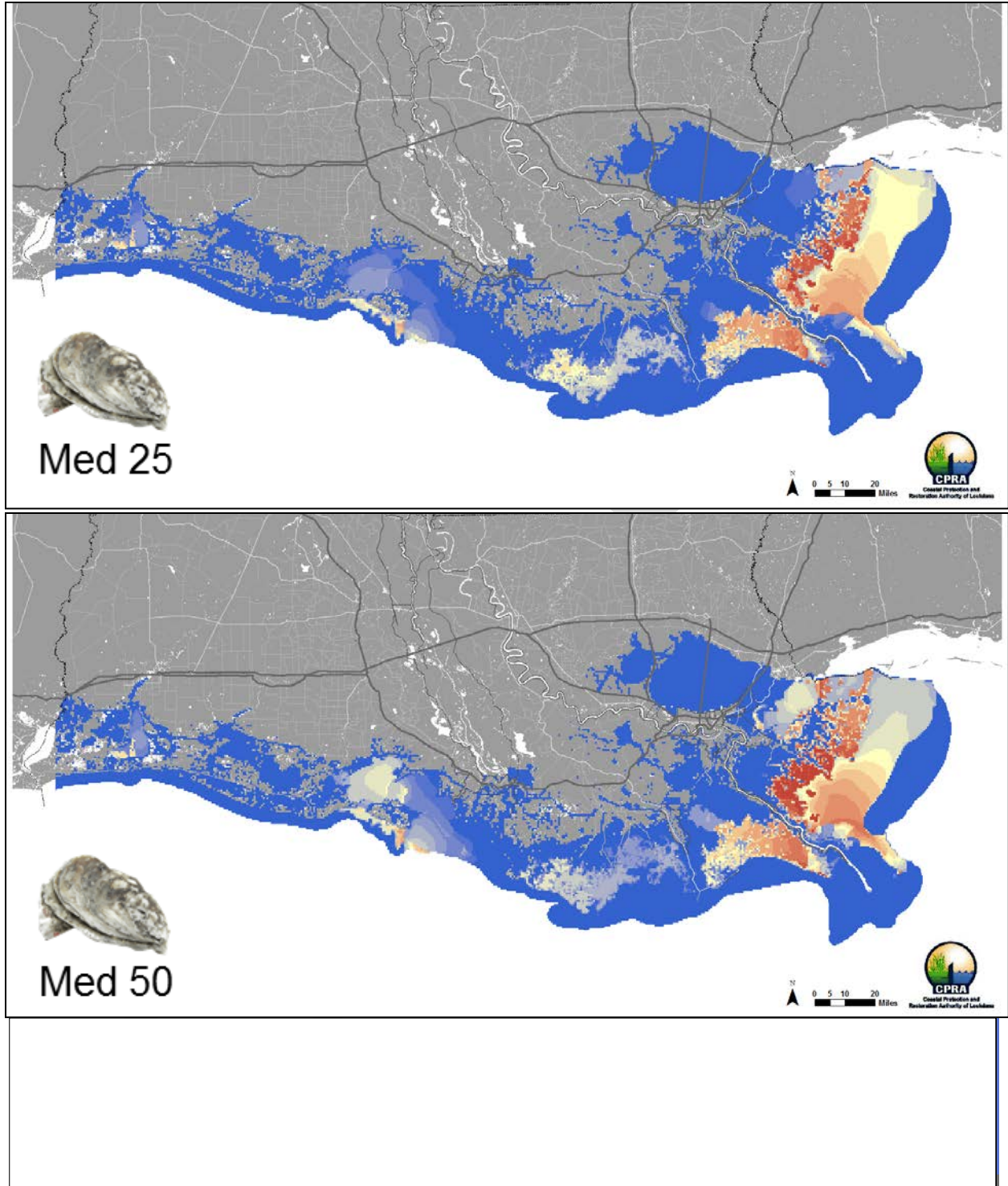


Figure 139: Biomass Distribution of Eastern Oyster (Sack) in Year 25 (Top) and Year 50 (Bottom) of the Medium Scenario.

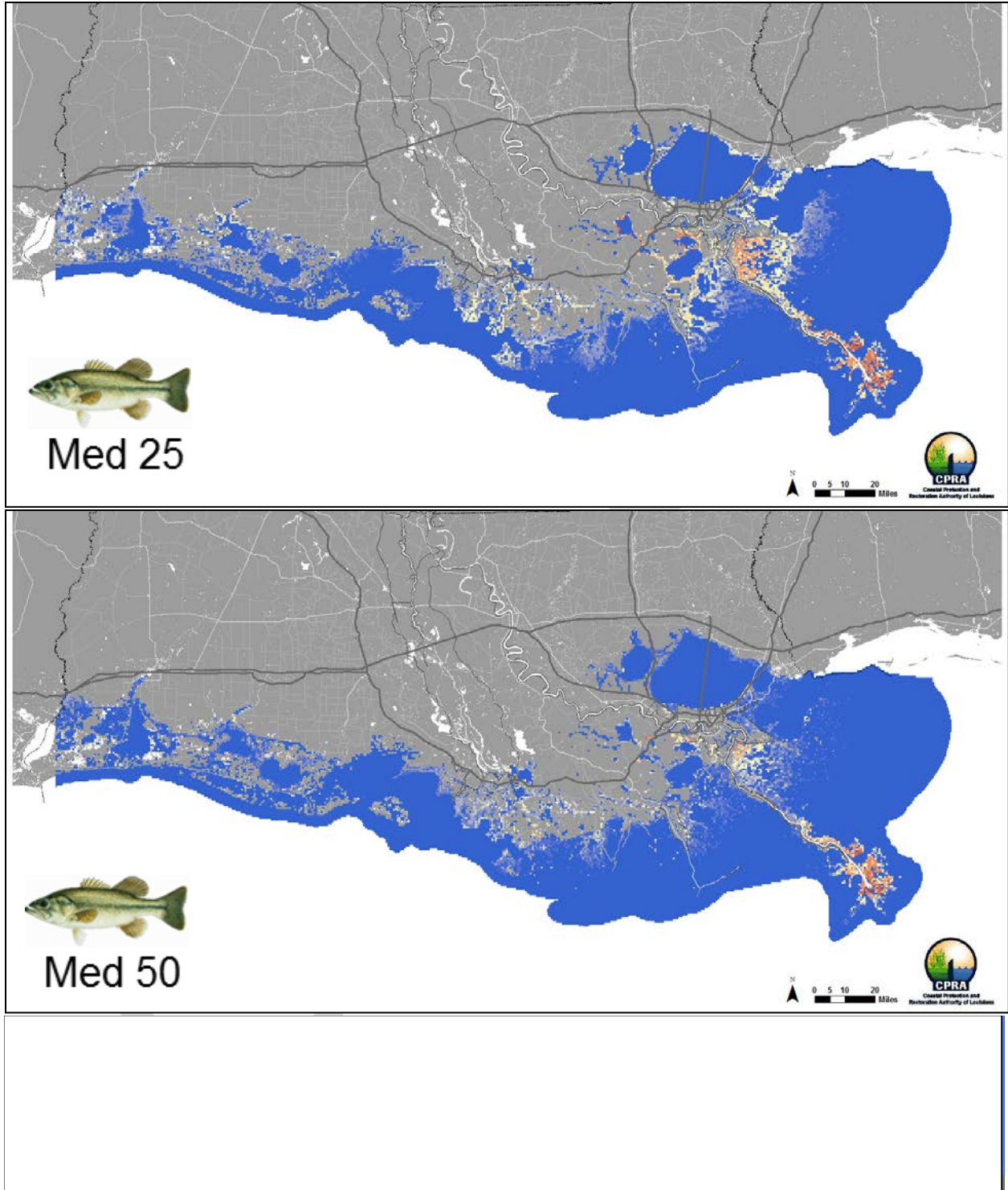


Figure 140: Biomass Distribution of Juvenile Largemouth Bass in Year 25 (Top) and Year 50 (Bottom) of the Medium Scenario.

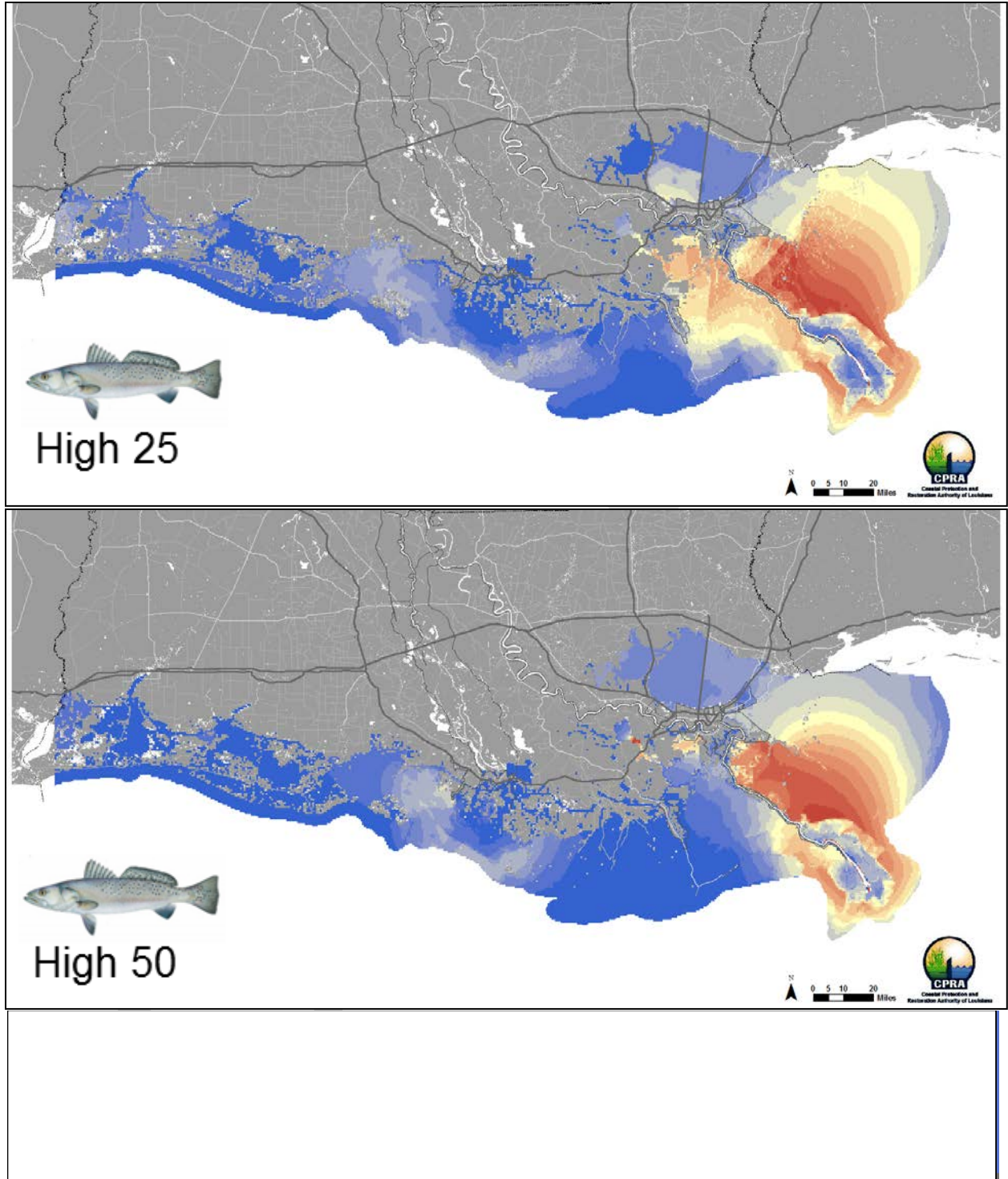


Figure 141: Biomass Distribution of Adult Spotted Seatrout in Year 25 (Top) and Year 50 (Bottom) of the High Scenario.

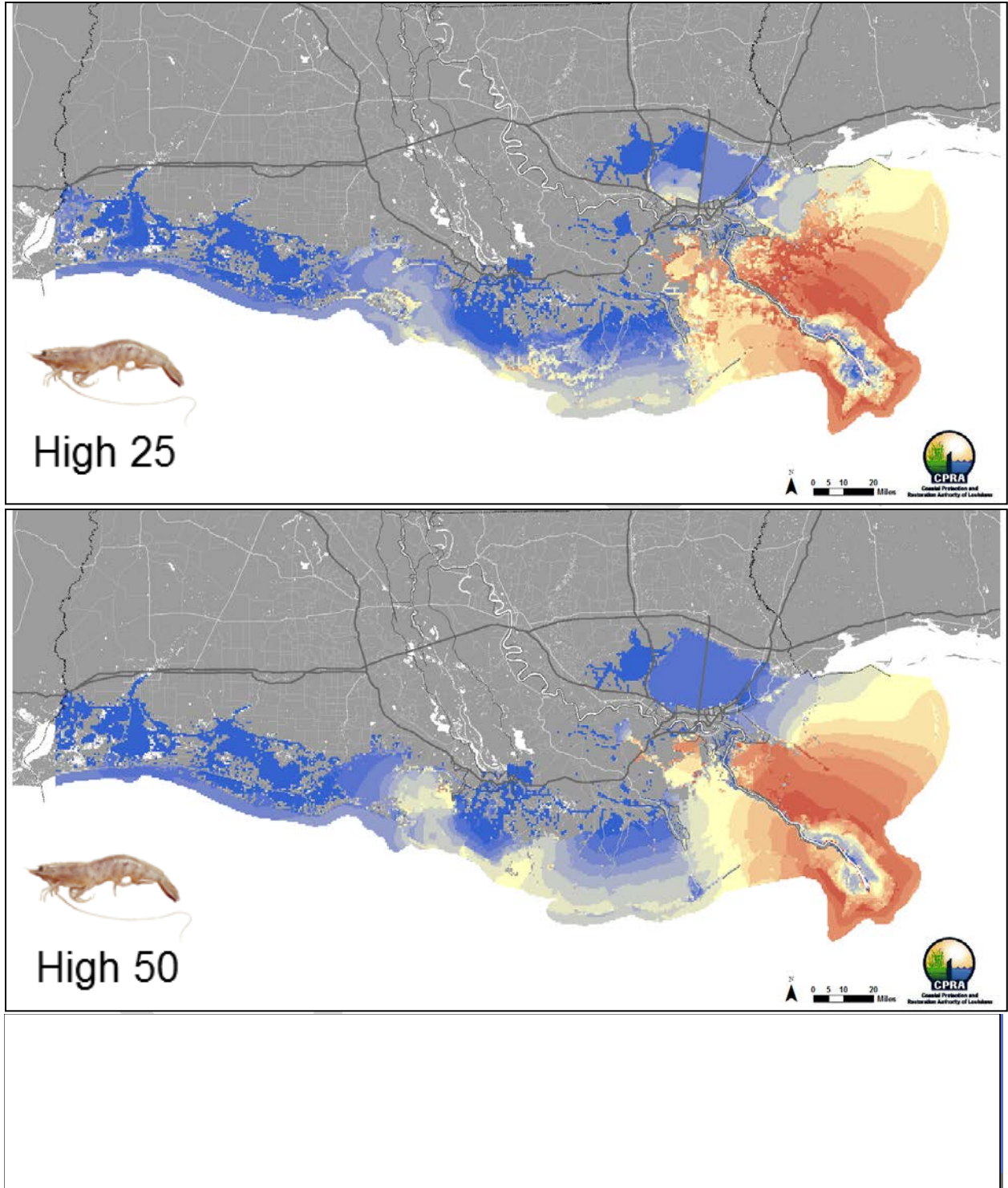


Figure 142: Biomass Distribution of Juvenile Brown Shrimp in Year 25 (Top) and Year 50 (Bottom) of the High Scenario.

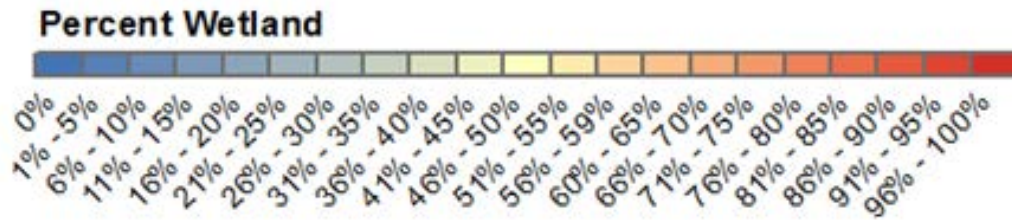
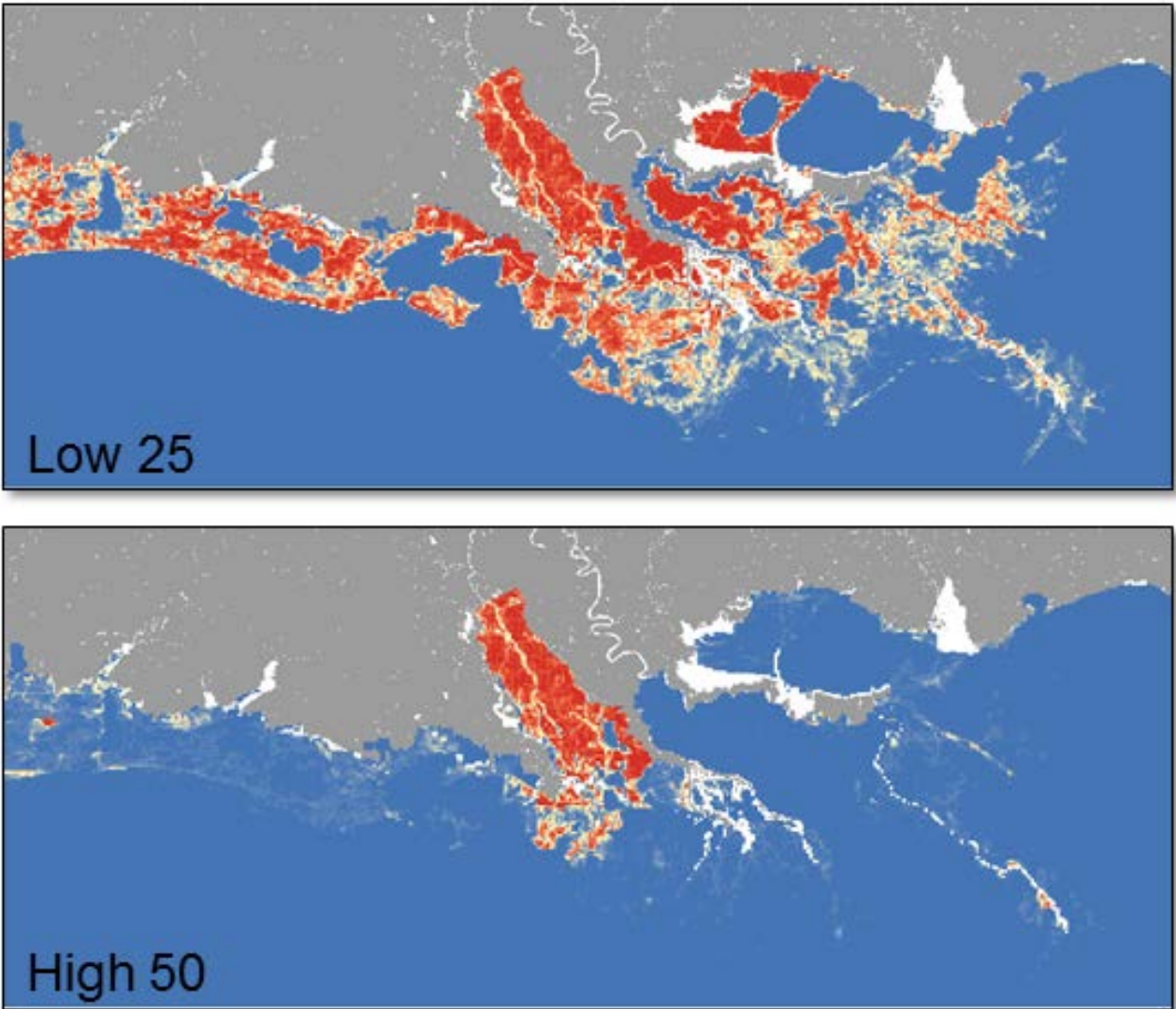


Figure 143: Percent Wetland in Year 25 of the Low Scenario (Top) and Year 50 of the High Scenario (Bottom), Showing the Differences in Projected Wetland Loss Depending on Time and Scenario.

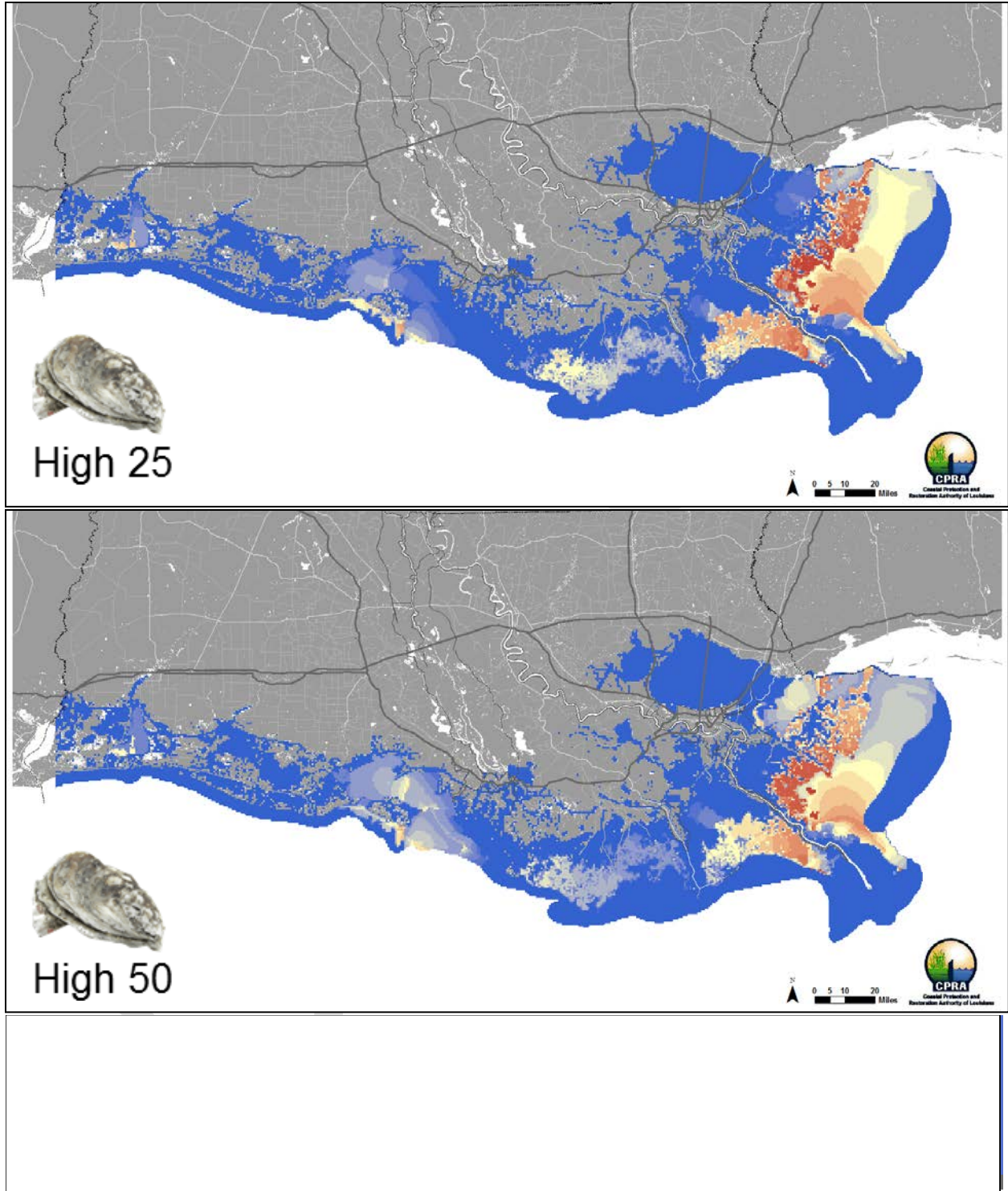


Figure 144: Biomass Distribution of Eastern Oyster (Sack) in Year 25 (Top) and Year 50 (Bottom) of the High Scenario.

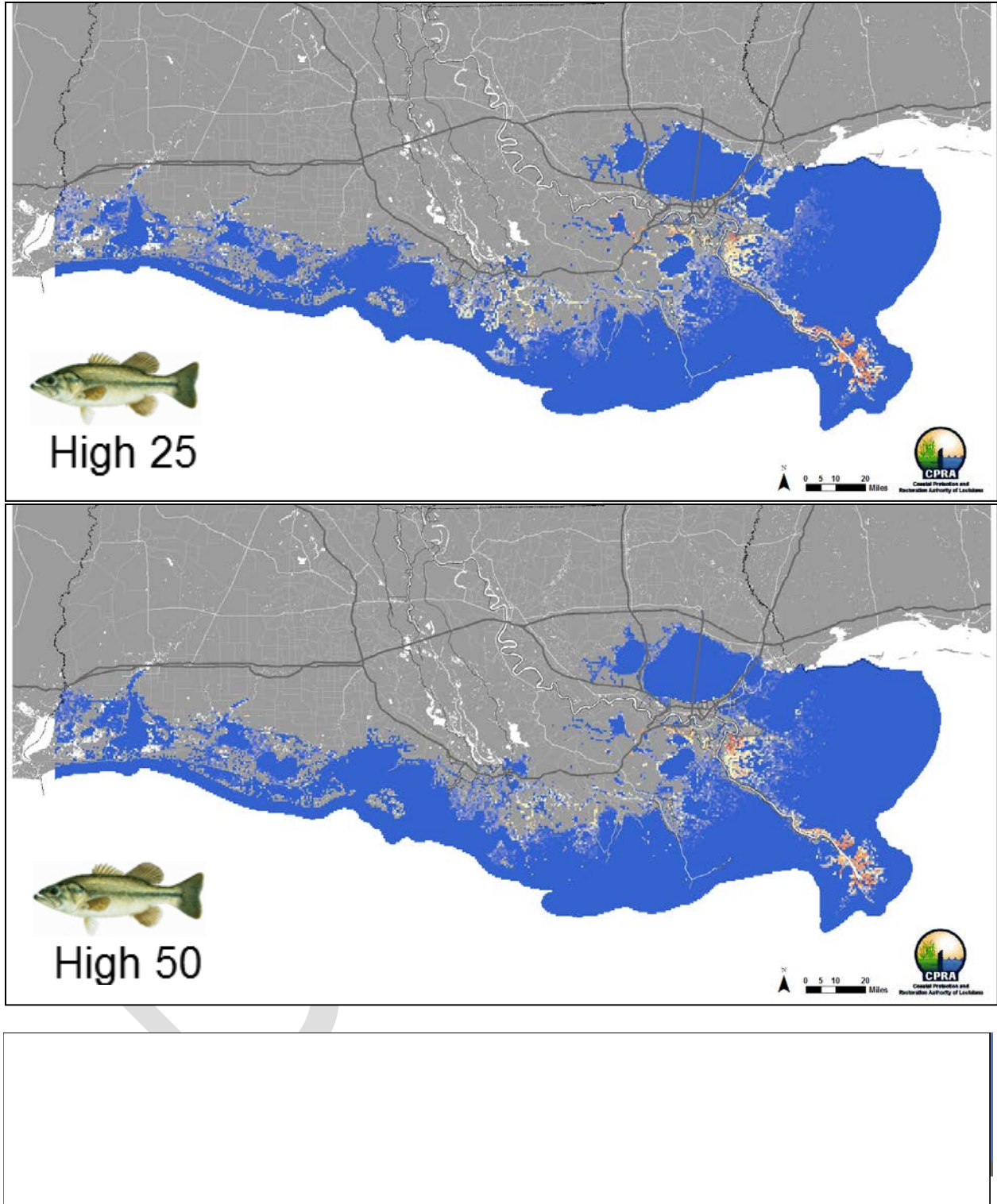


Figure 145: Biomass Distribution of Juvenile Largemouth Bass in Year 25 (Top) and Year 50 (Bottom) of the High Scenario.

### 3.8 Storm Surge and Waves

FWOA simulations using ADCIRC/SWAN were conducted by altering the initial conditions model configuration in the following ways:

- The initial water level was updated to account for sea level rise;
- Topographic and bathymetric values were updated to account for the change in elevations described by the ICM for a given year and scenario combination;
- Frictional characteristics were updated to account for the change in vegetation types described by the ICM for a given year and scenario combination; and
- Levees and raised features (e.g., roadways and coastal ridges) were updated to reflect design elevation upgrades and subsidence where applicable. See Appendix A – Project Definitions for further information regarding development of the levee elevation dataset.

The following sections detail the consequence of these changes in surge and wave results as well as how the results vary over time. The two-dimensional difference plots shown are compared to the initial conditions model results in order to maintain a constant point of reference. Simulations were conducted to represent conditions at year 10, year 25 and year 50.

#### 3.8.1 Low Scenario

Compared to other scenarios, the low scenario shows the least change in surge elevation during a storm simulation at each of the time levels. This is largely due to sea level rise generally playing a greater role in creating higher surge elevations than other model changes such as topographic elevations and changes to frictional characteristics to reflect future landscape conditions. Table 9 shows the sea level rise increment and associated initial water level (meters, NAVD88 2009.55) used during the low scenario for the surge and waves model.

**Table 9: Initial Water Levels and Sea Level Rise Values for the Low Scenario.**

Low scenario		
Year	Sea level rise (meters)	Initial water level (meters, NAVD88 2009.55)
10	0.06	0.37
25	0.18	0.49
50	0.43	0.74

Figure 146 through 151 illustrate differences in the maximum surge elevations and wave heights for Storm 014 for the three simulation years (10, 25, and 50). The contour palette used on Figures 146 through 151 was selected to categorize differences between FWOA and initial conditions simulations. White areas represent absolute changes of less than 0.25 meters. Warm colors represent FWOA maximum surge elevations that are higher than those simulated for initial conditions by more than 0.25 meters. Similarly, cool colors represent FWOA maximum surge elevations that are lower than those simulated for initial conditions by more than 0.25 meters. Areas that appear as brown were flooded in FWOA and were not flooded during the initial

conditions simulations. Areas that appear as gray are areas that were not flooded in FWOA and were flooded in the initial conditions simulation.

DRAFT

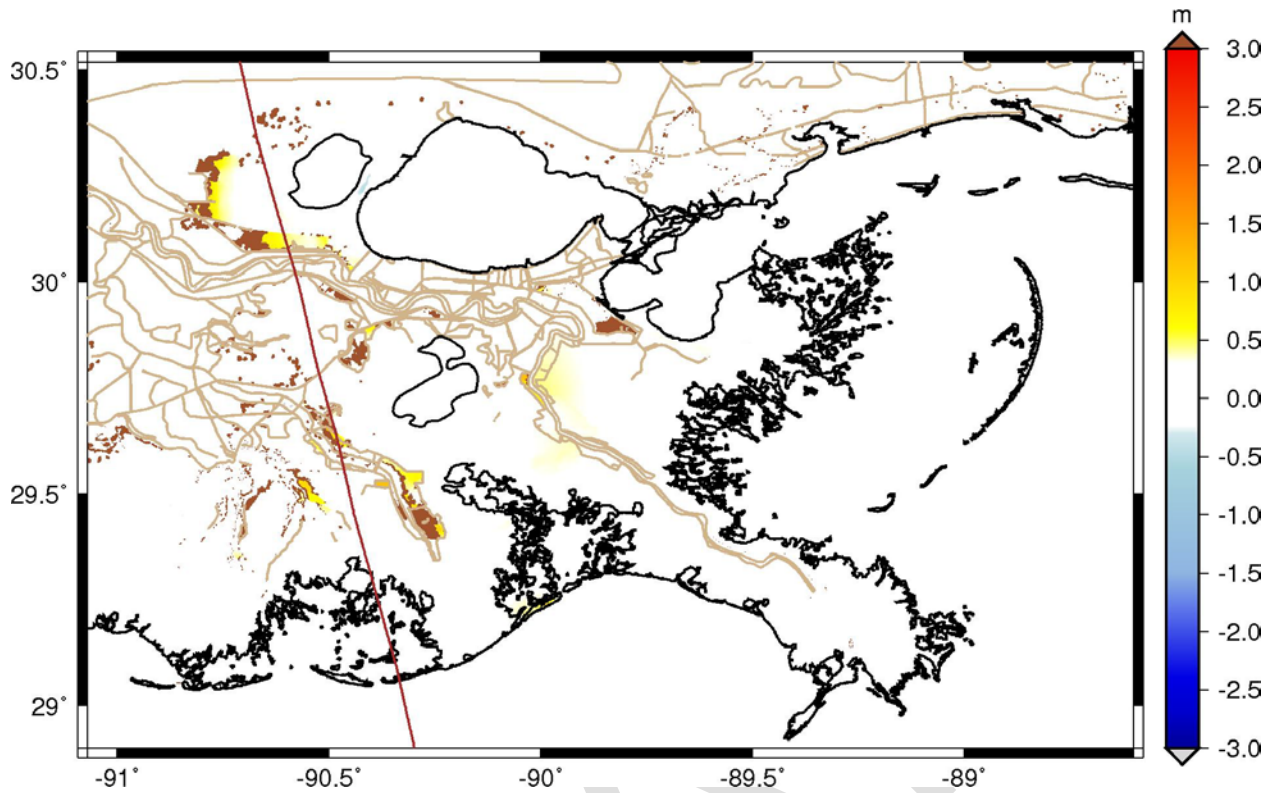


Figure 146: Differences Between Maximum Surge Elevations (meters) in Southeastern Louisiana for FWOA and Initial Conditions for Storm 014 in Year 10 of the Low Scenario.

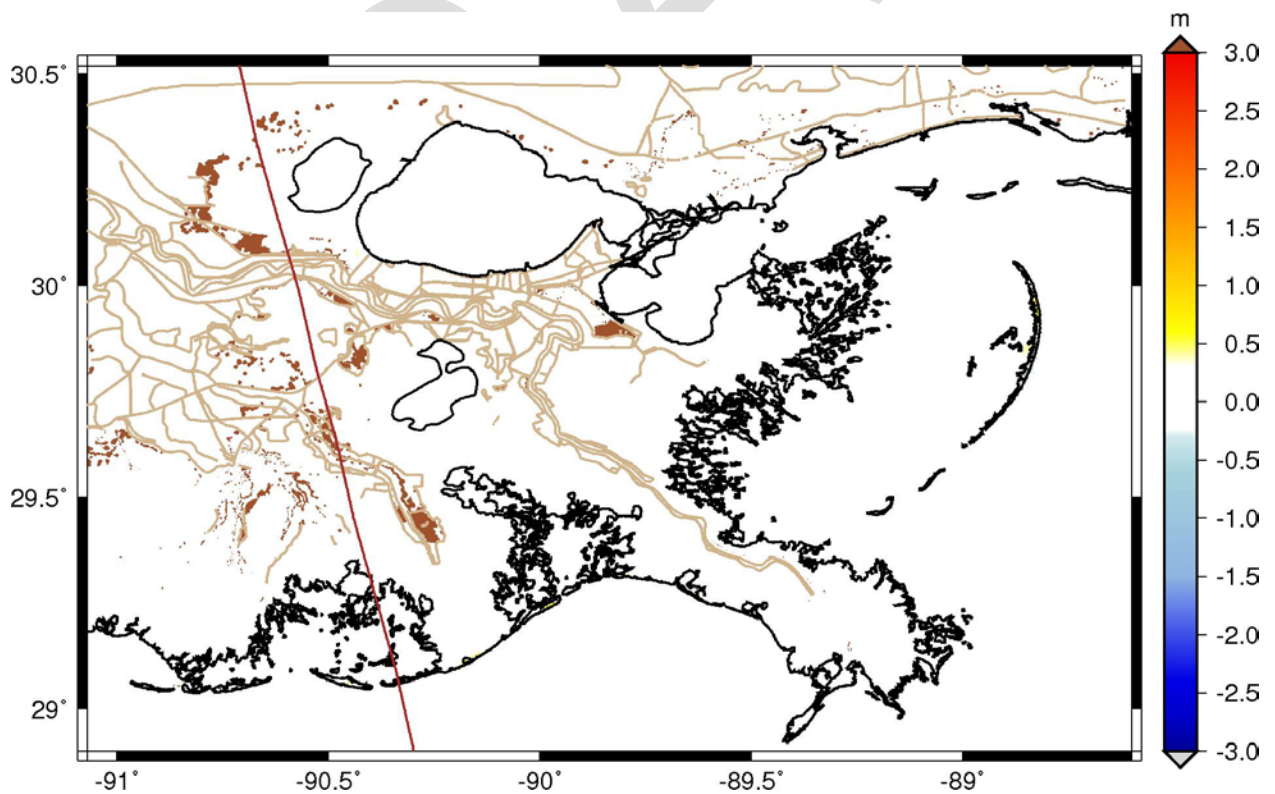


Figure 147: Differences Between Maximum Wave Height (meters) in Southeastern Louisiana for FWOA and Initial Conditions for Storm 014 in Year 10 of the Low Scenario.

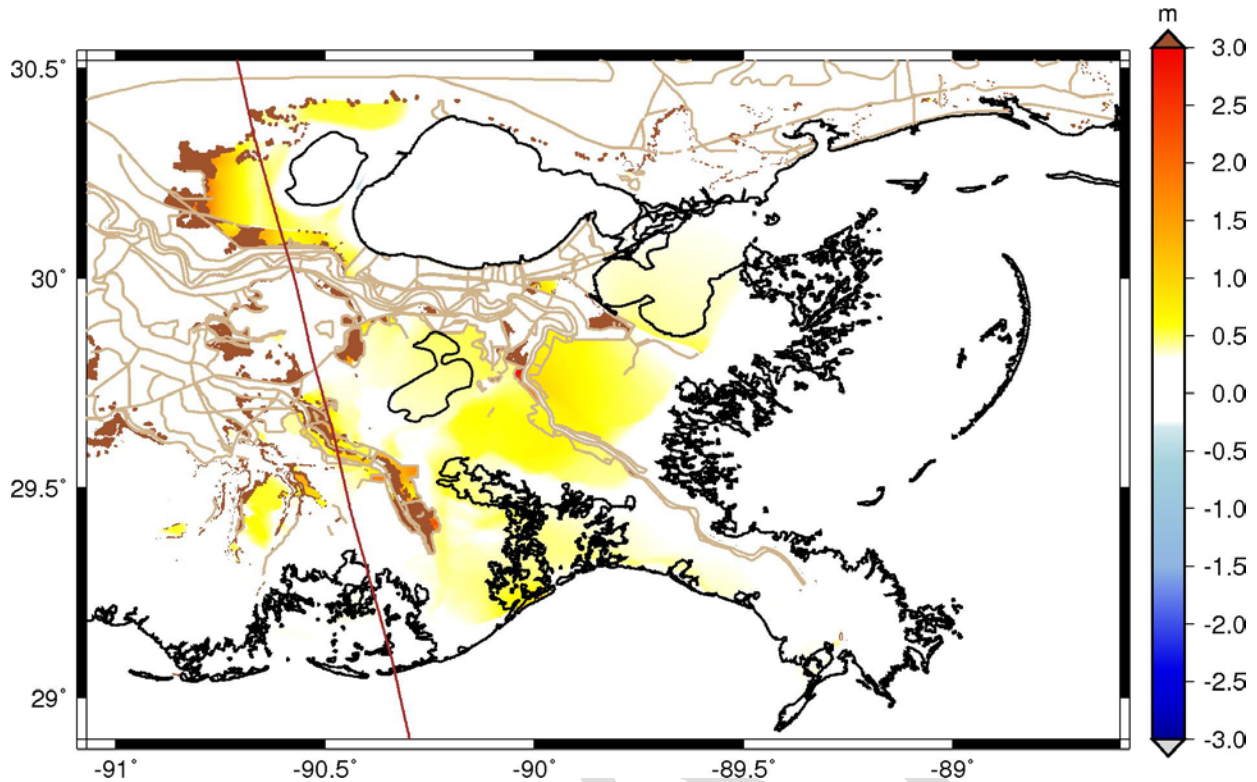


Figure 148: Differences Between Maximum Surge Elevations (meters) in Southeastern Louisiana for FWOA and Initial Conditions for Storm 014 in Year 25 of the Low Scenario.

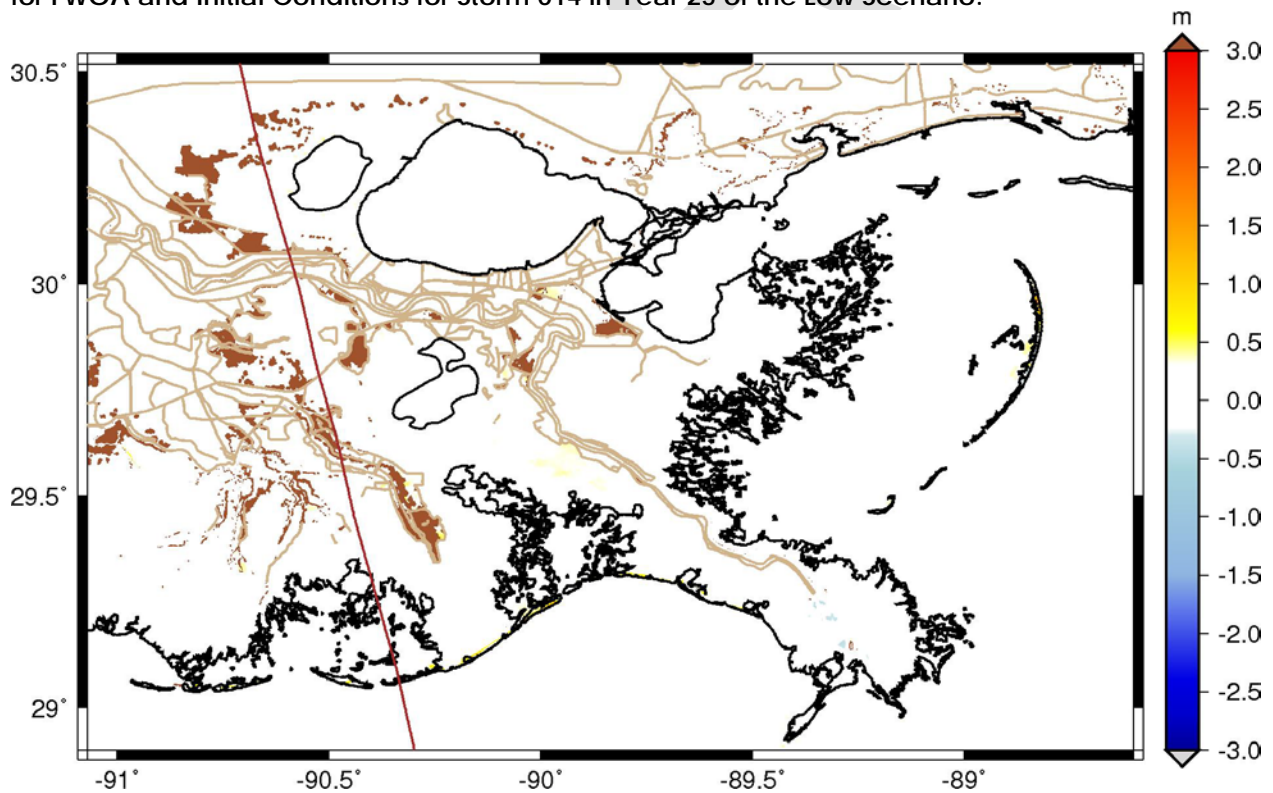


Figure 149: Differences Between Maximum Wave Height (meters) in Southeastern Louisiana for FWOA and Initial Conditions for Storm 014 in Year 25 of the Low Scenario.

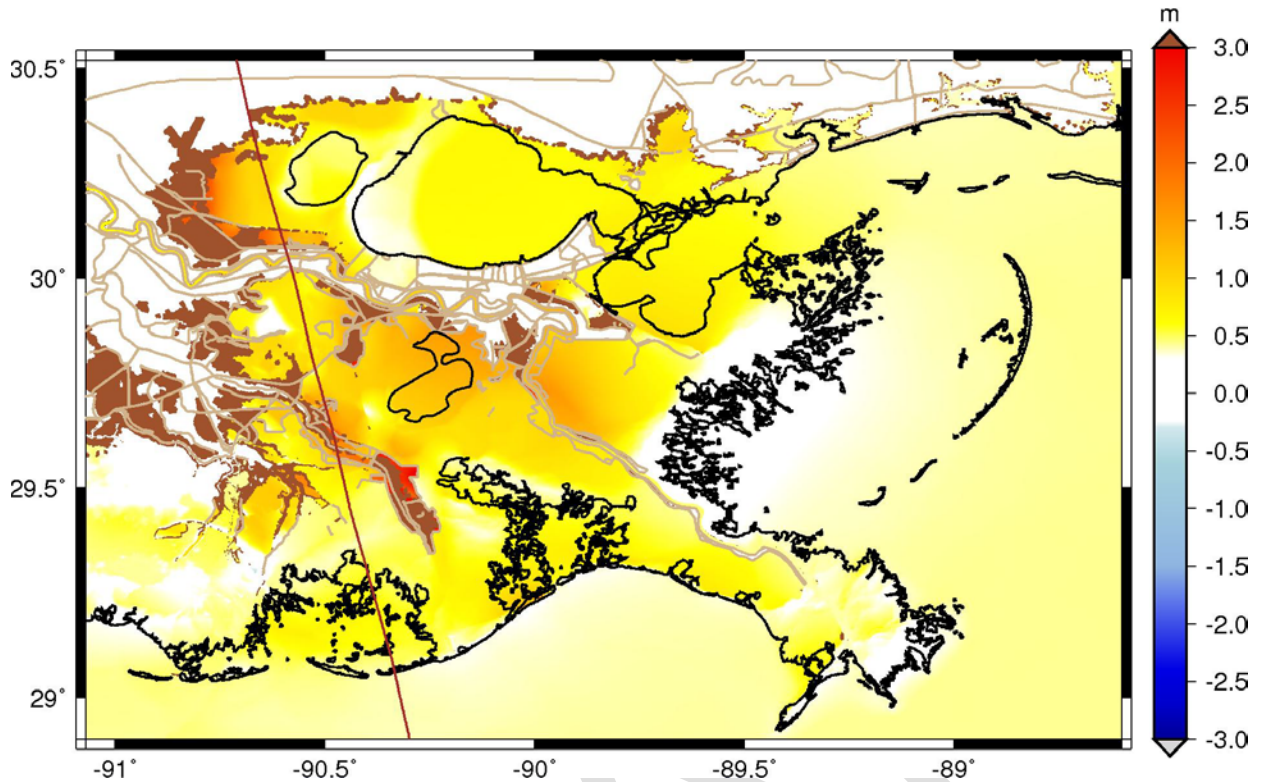


Figure 150: Differences Between Maximum Surge Elevations (meters) in Southeastern Louisiana for FWOA and Initial Conditions for Storm 014 in Year 50 of the Low Scenario.

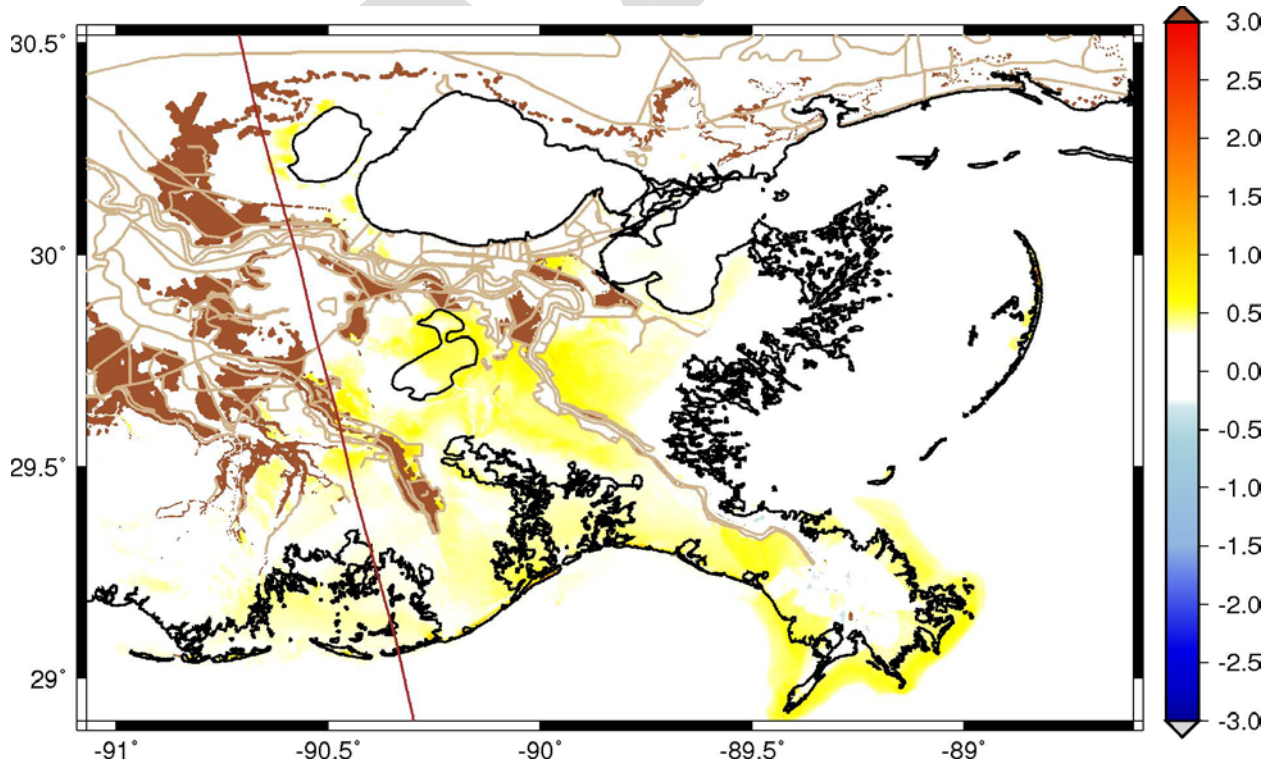


Figure 151: Differences Between Maximum Wave Height (meters) in Southeastern Louisiana for FWOA and Initial Conditions for Storm 014 in Year 50 of the Low Scenario.

In year 10, the off-shore areas are generally white in color due to the relatively small increase in sea level. As this scenario progresses to later years, the off-shore area generally remains a consistent contour for each storm yet increases relative to earlier years. The increase in elevation off-shore largely reflects the sea level rise increment itself. Areas with an increase in maximum surge elevation equivalent to the imposed sea level rise increment demonstrate a linear sea level rise response.

In contrast to off-shore areas, there are inland regions that do not show a change in maximum surge elevation that is consistent with the sea level rise increment. These areas are described as having a nonlinear response. Nonlinear responses are most easily seen inland and in later years. These changes occur due to changes in bottom friction, wind roughness length, and sea level rise, though sea level rise is generally the largest contributor to these changes. In addition to the nonlinear changes in surge elevation, it should also be noted that in later years, especially year 50, there are significant areas that are newly inundated, particularly across the Chenier Plain and west of Lake Pontchartrain. Inundation limits do not significantly change for Storm 014 during year 10. Year 25 sees more drastic changes across the Chenier Plain but only mild changes in Barataria Basin. Year 50 sees the most significant changes in inundation across the coast.

Figures 152 and 153 show surge elevation time series at two locations—Lake Borgne and Barataria Bay—for Storm 014. The Lake Borgne time series plot shows an increase in surge elevation slightly higher than the sea level rise increments, while the Barataria Bay time series plot shows a change in surge elevation slightly lower than the sea level rise increments.

Areas subject to depth-limited wave breaking generally resulted in greater wave heights in response to additional water depth. The areas that demonstrate changes in maximum wave height patterns are similar to those areas with notable changes in maximum surge elevation.

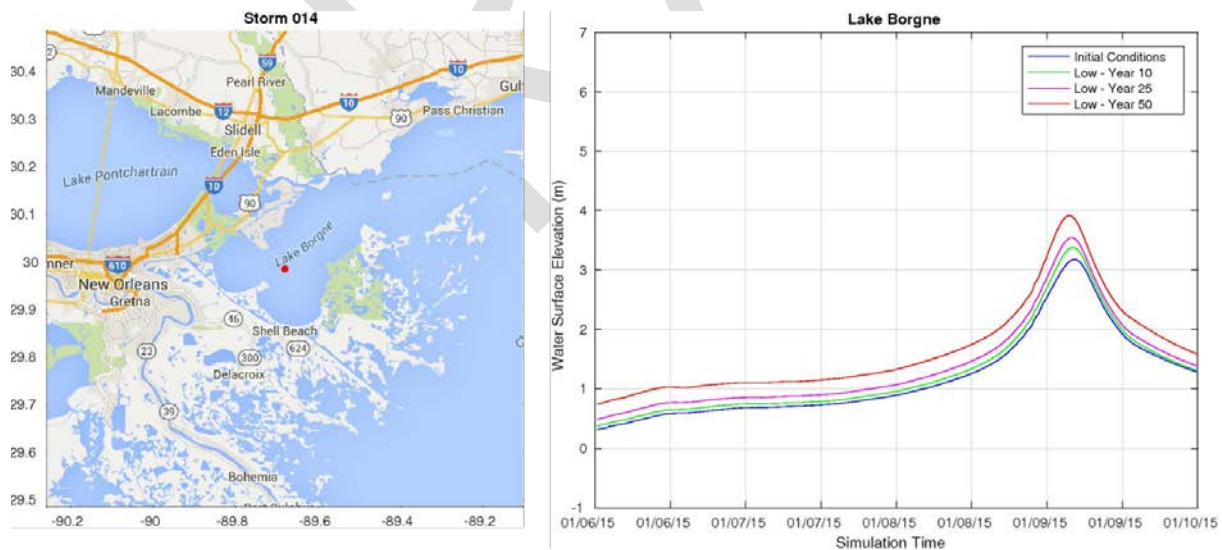


Figure 152: Surge Elevation (meters, NAVD88 2009.55) Time Series for Storm 014 in Lake Borgne for the Low Scenario.

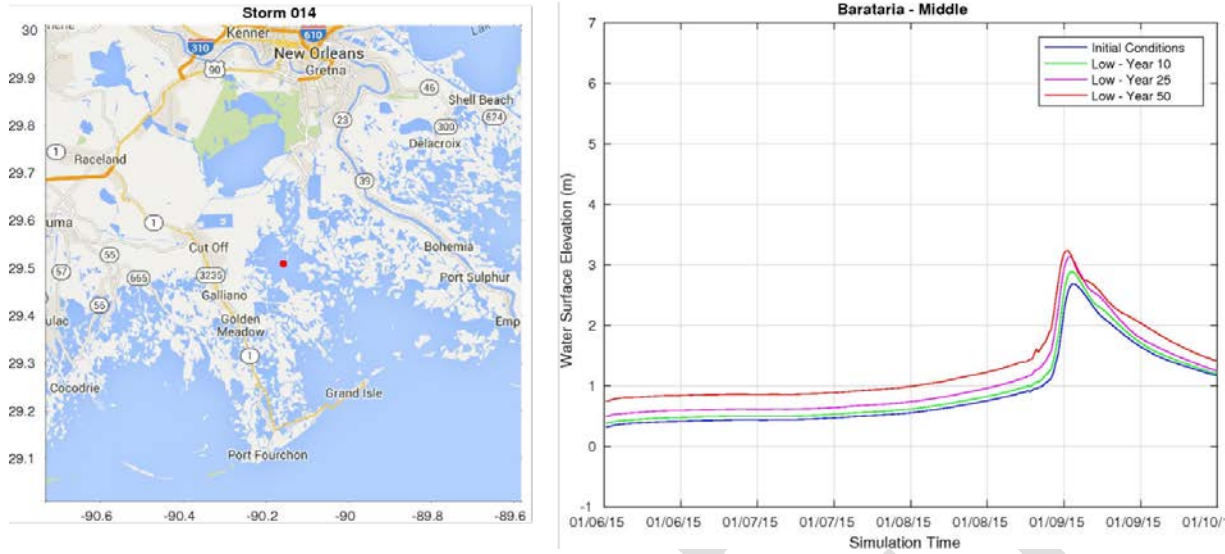


Figure 153: Surge Elevation (meters, NAVD88 2009.55) Time Series for Storm 014 in the Barataria Bay for the Low Scenario.

### 3.8.2 Medium Scenario

Like the low scenario, sea level rise, and changes in the landscape notably impact surge elevations throughout the model domain. Table 10 shows sea level rise values and model initial water levels used for each of the simulation years.

Table 10: Initial Water Levels and Sea Level Rise Values for the Medium Scenario.

Medium scenario		
Year	Sea level rise (meters)	Initial water level (meters, NAVD88 2009.55)
10	0.11	0.40
25	0.25	0.56
50	0.63	0.94

Figures 154 through 159 show the changes in maximum surge elevations and maximum wave heights with respect to the initial conditions simulations, and Figure 160 and Figure 161 show the time series of surge elevation. As expected, when compared to the low scenario and initial conditions model results, larger absolute changes occur off-shore and inland due to the higher sea level rise rate and more significant landscape changes associated with this scenario. Due to higher sea level rise conditions, the areas subject to nonlinear increases in surge elevation are more expansive than the low scenario.

Inundation limits for the medium scenario are not significantly different than initial conditions in Year 10. However, year 25 conditions result in additional inundation, including behind lines of flood protection near Gonzales, Louisiana and across the Chenier Plain. Year 50 results in the most drastic change in inundation areas as expected.

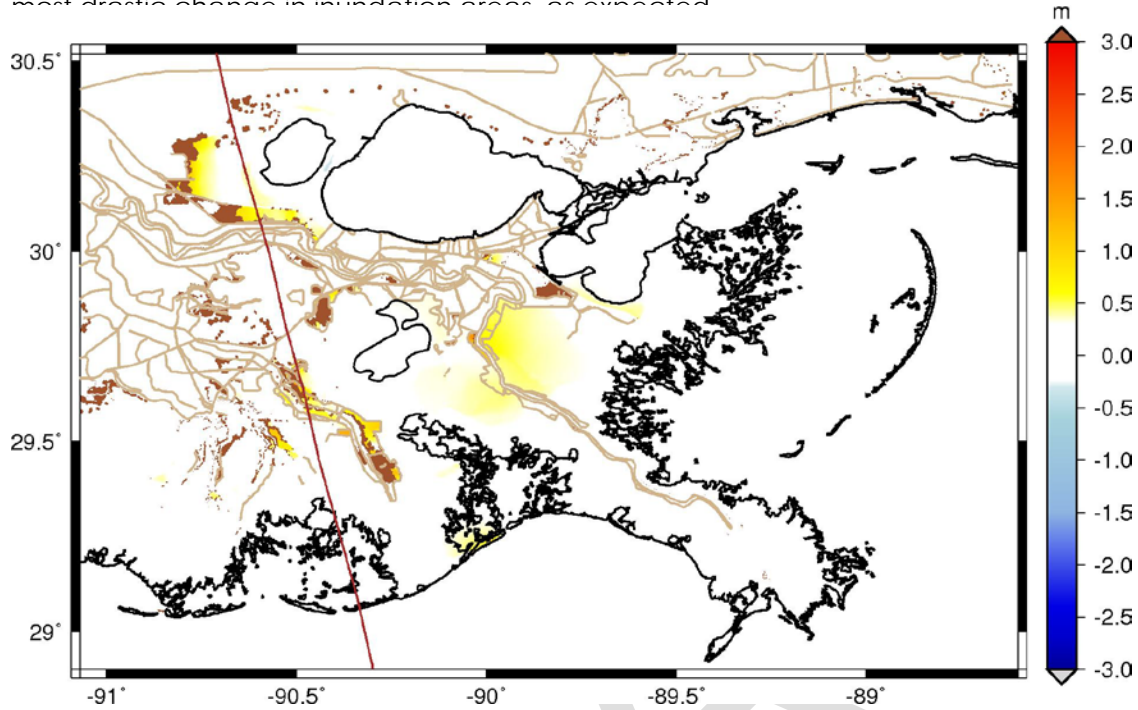


Figure 154: Differences Between Maximum Surge Elevations (meters) in Southeastern Louisiana for FWOA and Initial Conditions for Storm 014 in Year 10 of the Medium Scenario.

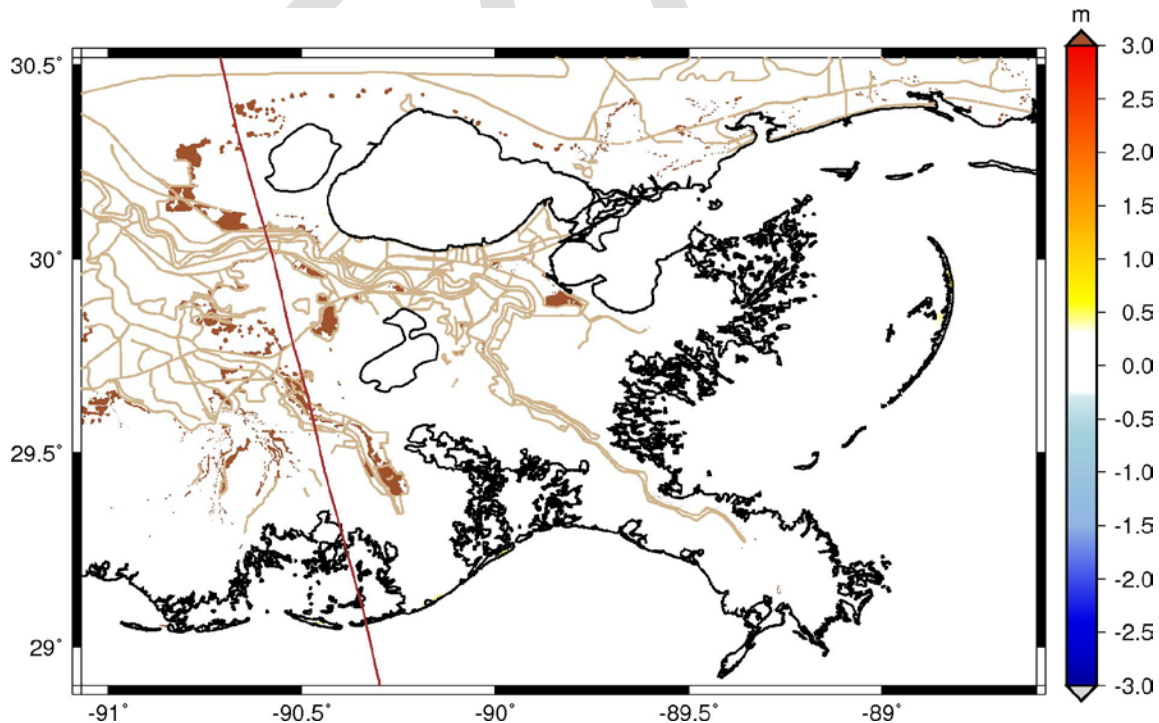


Figure 155: Differences Between Maximum Wave Height (meters) in Southeastern Louisiana for FWOA and Initial Conditions for Storm 014 in Year 10 of the Medium Scenario.

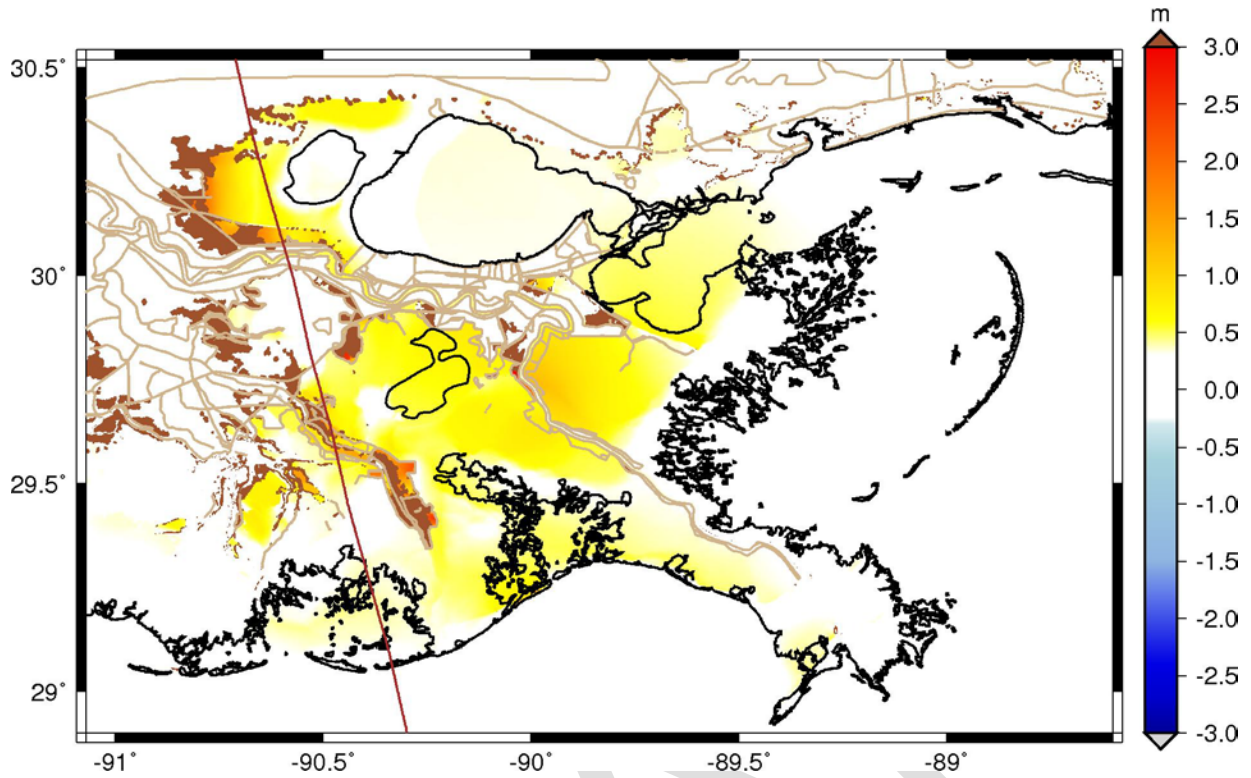


Figure 156: Differences Between Maximum Surge Elevations (meters) in Southeastern Louisiana for FWOA and Initial Conditions for Storm 014 in Year 25 of the Medium Scenario.

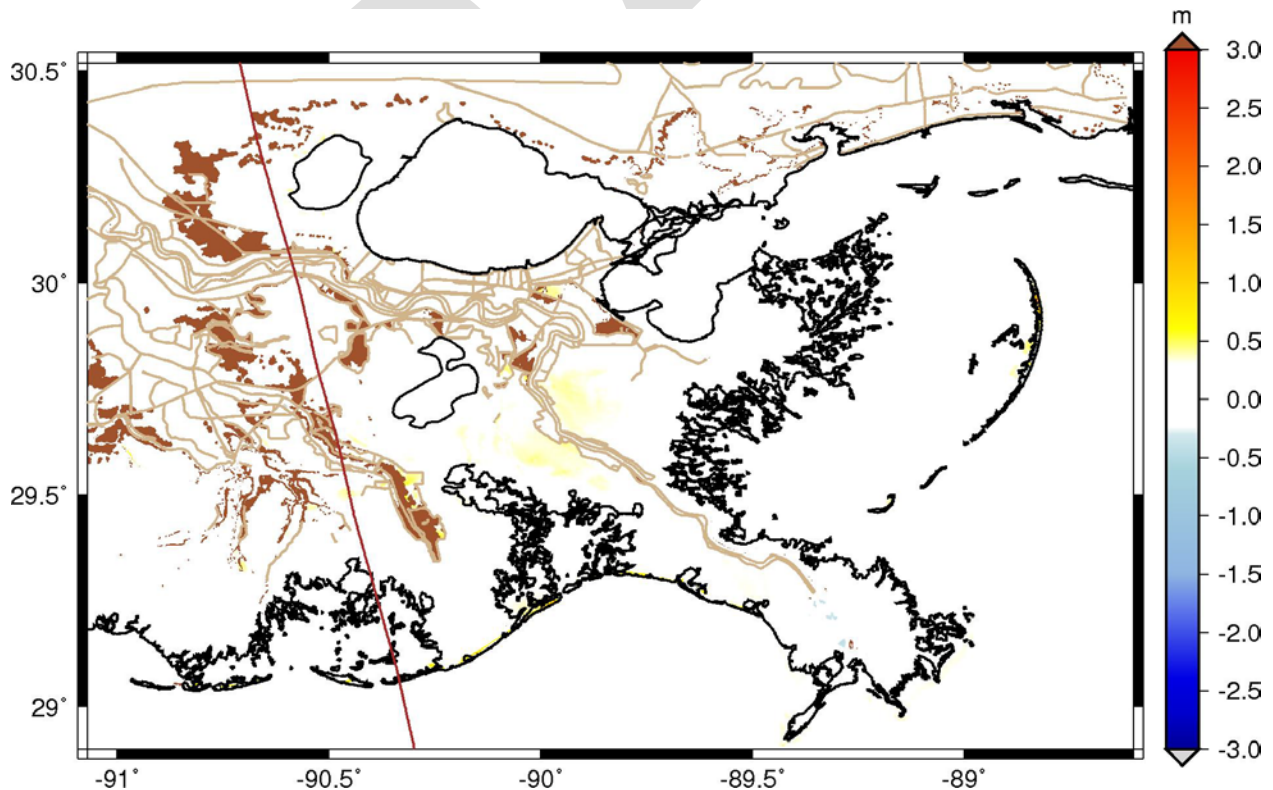


Figure 157: Differences Between Maximum Wave Height (meters) in Southeastern Louisiana for FWOA and Initial Conditions for Storm 014 in Year 25 of the Medium Scenario.

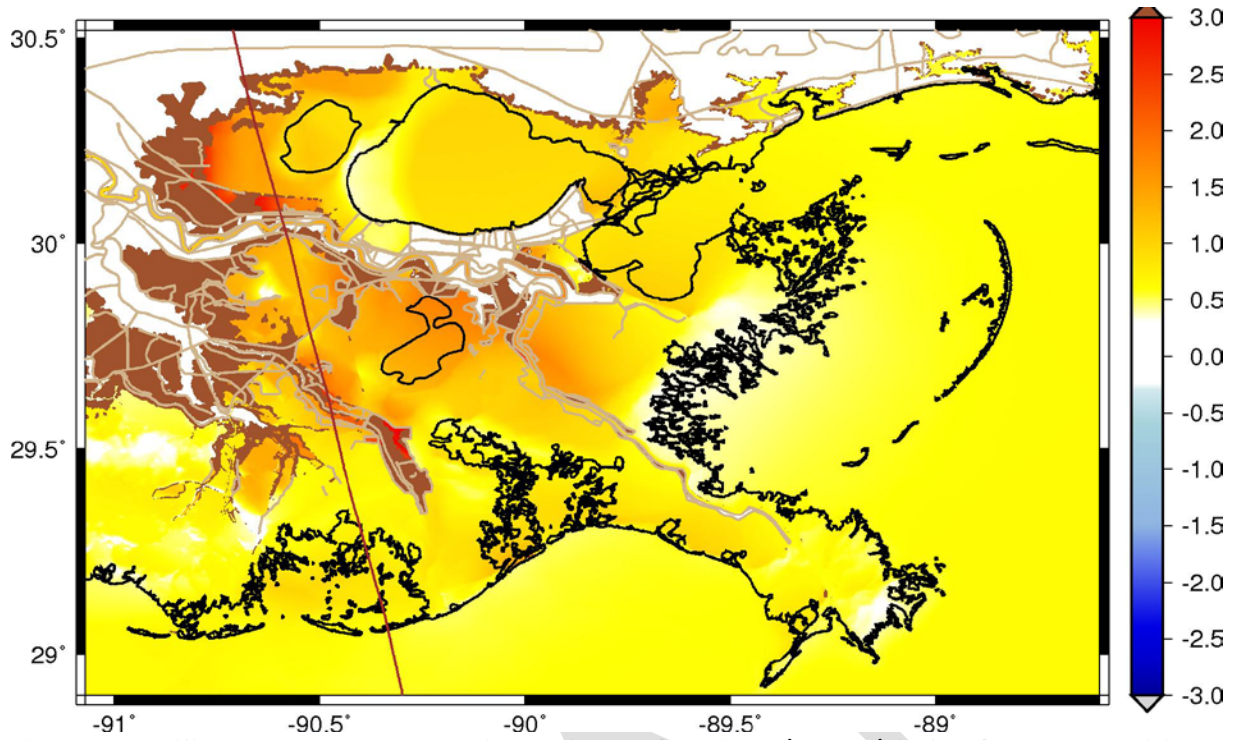


Figure 158: Differences Between Maximum Surge Elevations (meters) in Southeastern Louisiana for FWOA and Initial Conditions for Storm 014 in Year 50 of the Medium Scenario.

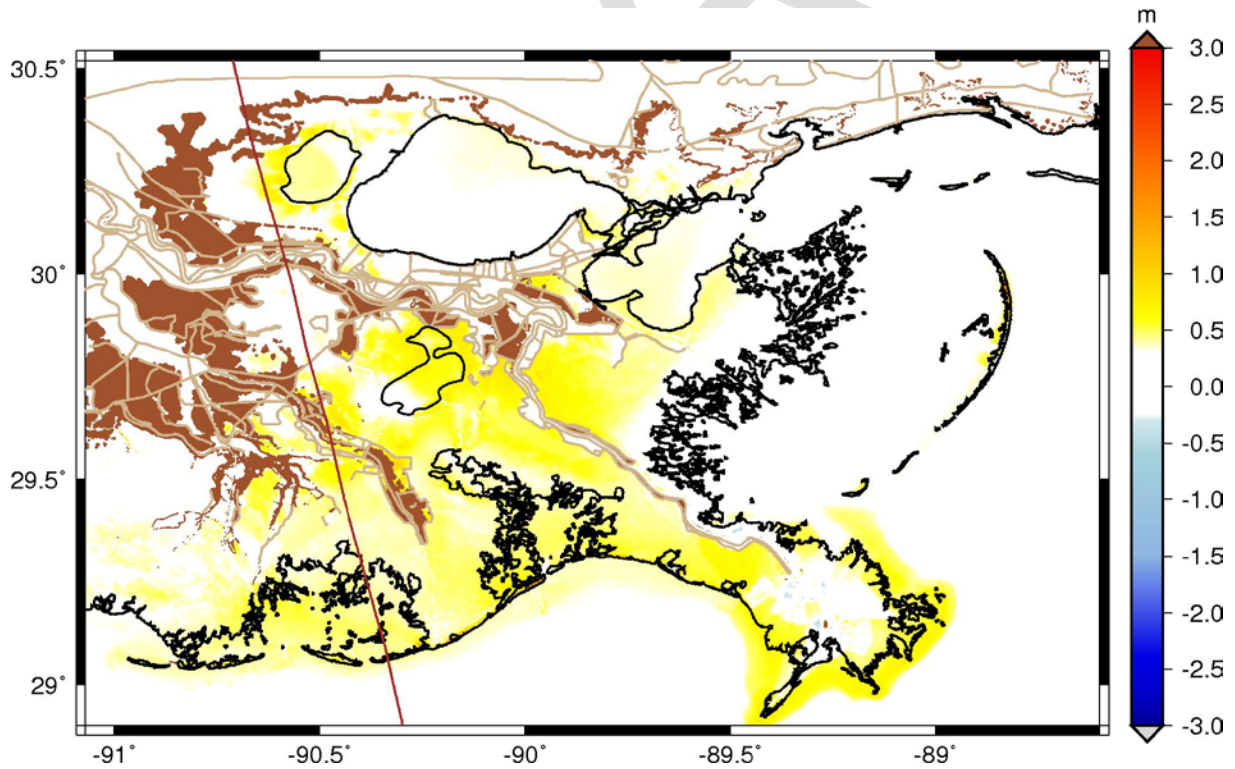


Figure 159: Differences Between Maximum Wave Height (meters) in Southeastern Louisiana for FWOA and Initial Conditions for Storm 014 in Year 50 of the Medium Scenario.

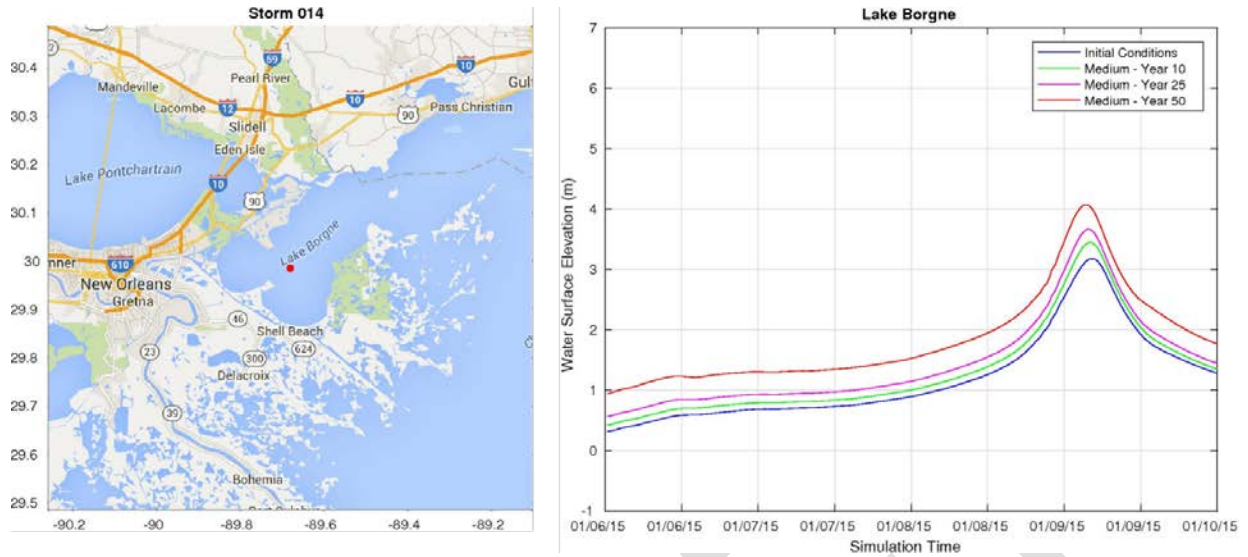


Figure 160: Surge Elevation (meters, NAVD88 2009.55) Time Series for Storm 014 in Lake Borgne for the Medium Scenario.

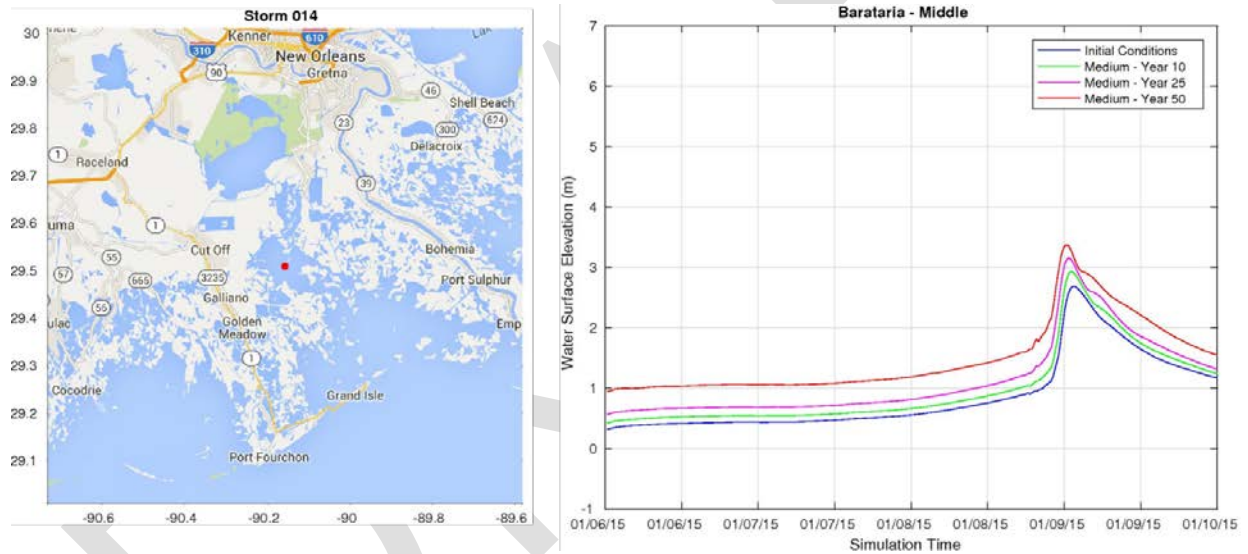


Figure 161: Surge Elevation (meters, NAVD88 2009.55) Time Series for Storm 014 in Barataria Bay for the Medium Scenario.

### 3.8.3 High Scenario

The high scenario shows the greatest increase in surge elevations due to the combination of the highest sea level rise rate, largest regional subsidence, and fewest remaining wetlands and other vegetated communities as defined by the ICM. Table 11 shows sea level rise values and model initial water levels used for each of the simulation years. Figures 162 through 167 show the changes in maximum surge elevations and wave heights with respect to the initial conditions simulations, and Figures 168 and 169 show the time series of surge elevations for Storm 014.

**Table 11: Initial Water Levels and Sea Level Rise Values for the High Scenario.**

High scenario		
Year	Sea level rise (meters)	Initial water level (meters, NAVD88 2009.55)
10	0.11	0.42
25	0.32	0.64
50	0.83	1.14

Inundation extents during year 10 are most significantly different from initial conditions in the Chenier Plain because of the low-lying, relatively flat topography. Areas of nonlinear surge elevation change are most prevalent in this scenario, and the extents of these nonlinear changes cover the greatest area.

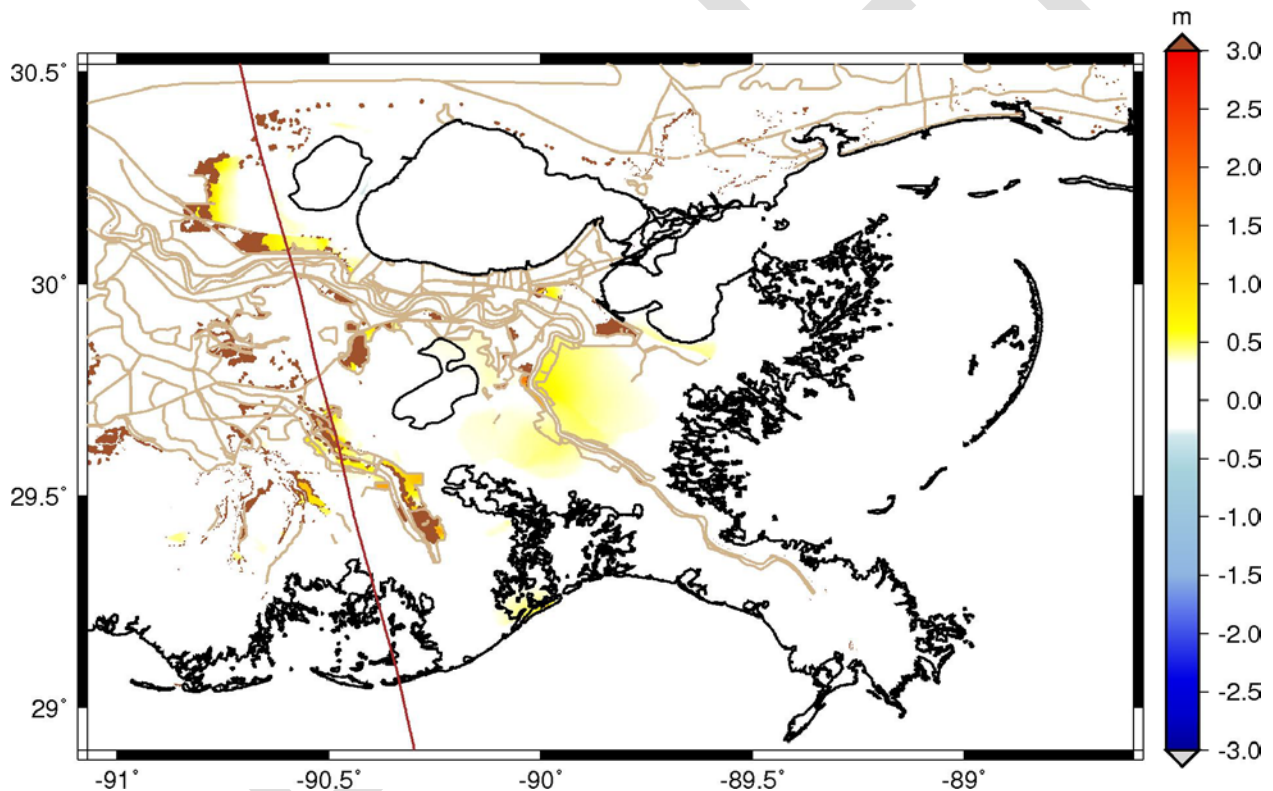


**Figure 162: Differences Between Maximum Surge Elevations (meters) in Southeastern Louisiana for FWOA and Initial Conditions for Storm 014 in Year 10 of the High Scenario.**

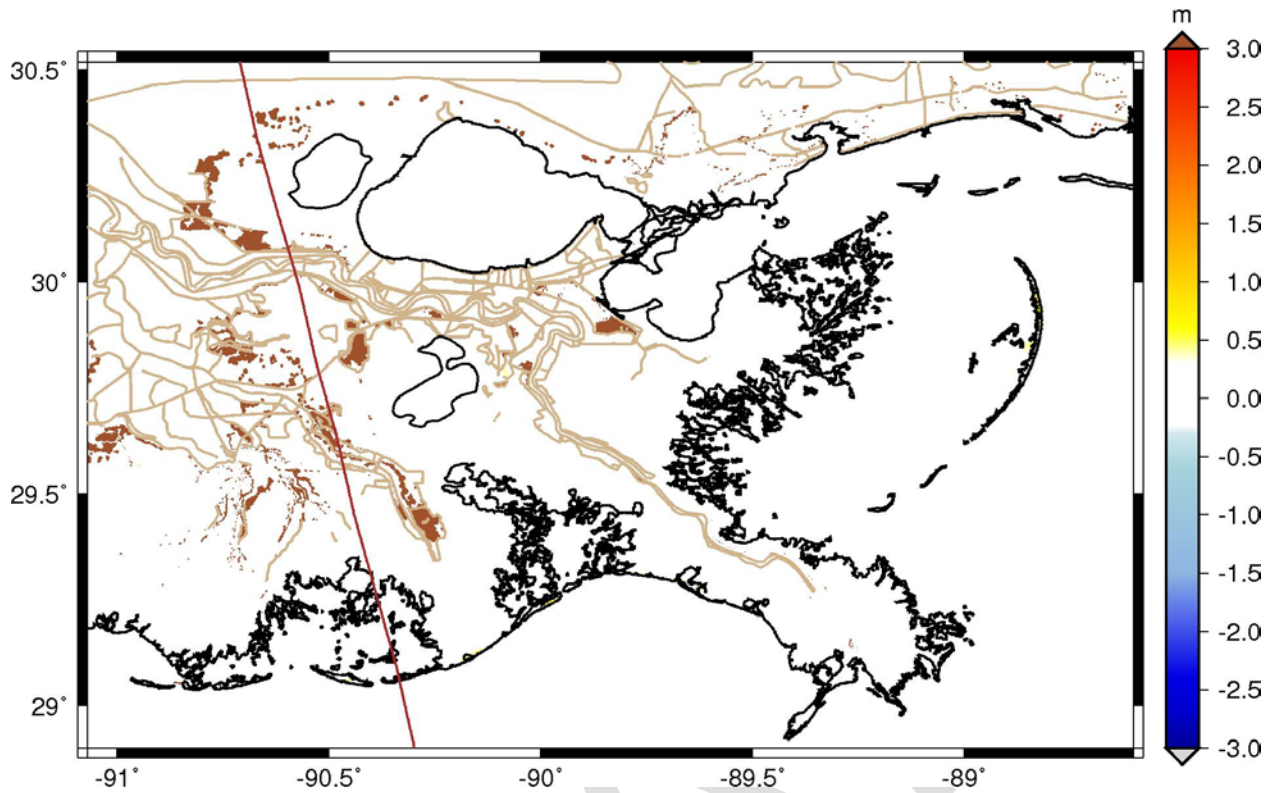


Figure 163: Differences Between Maximum Wave Height (meters) in Southeastern Louisiana for FWOA and Initial Conditions for Storm 014 in Year 10 of the High Scenario.

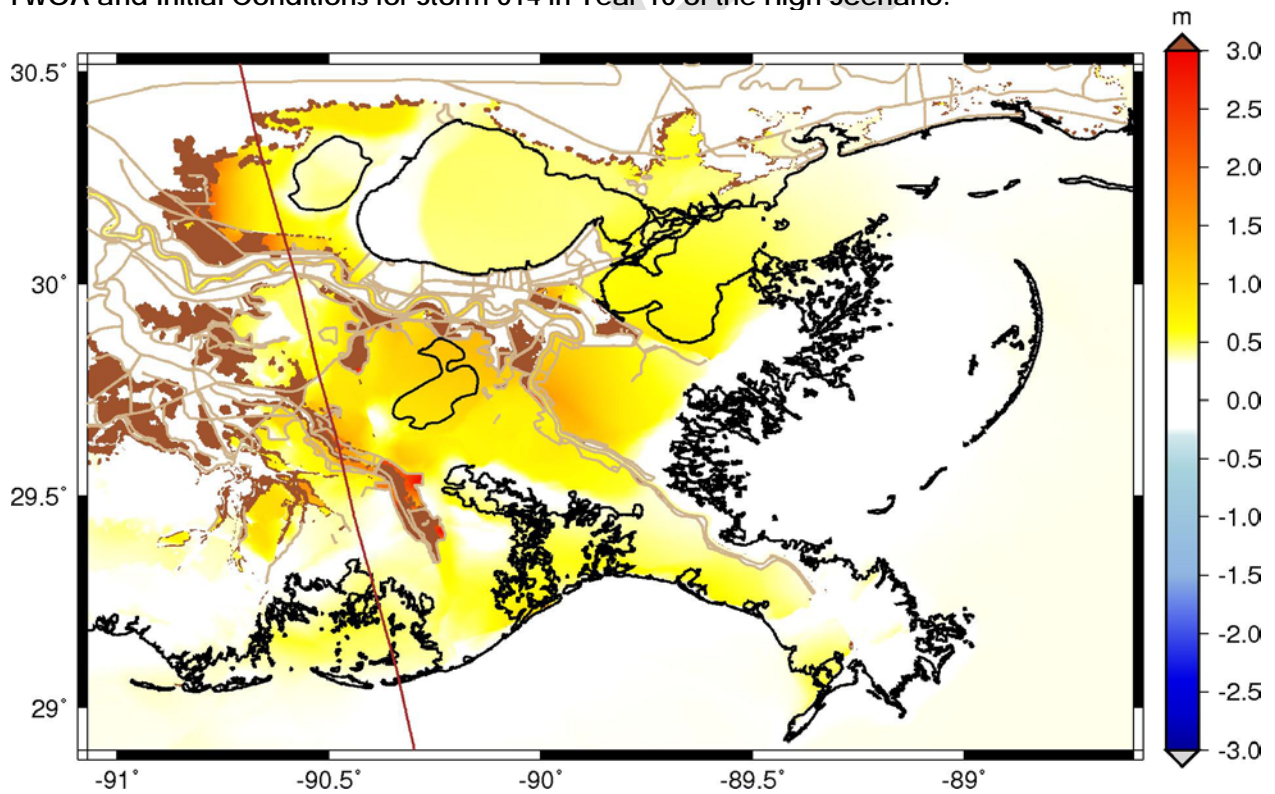


Figure 164: Differences Between Maximum Surge Elevations (meters) in Southeastern Louisiana for FWOA and Initial Conditions for Storm 014 in Year 25 of the High Scenario.

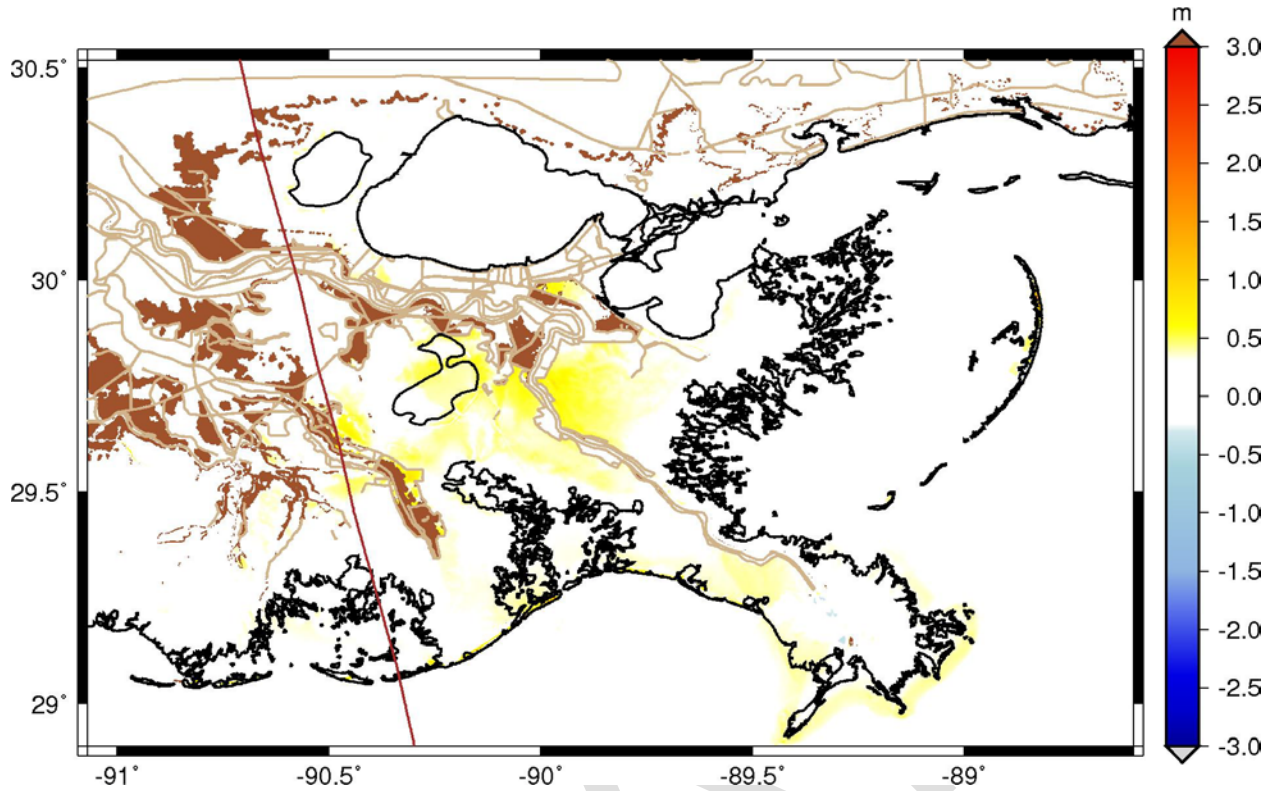


Figure 165: Differences Between Maximum Wave Height (meters) in Southeastern Louisiana for FWOA and Initial Conditions for Storm 014 in Year 25 of the High Scenario.

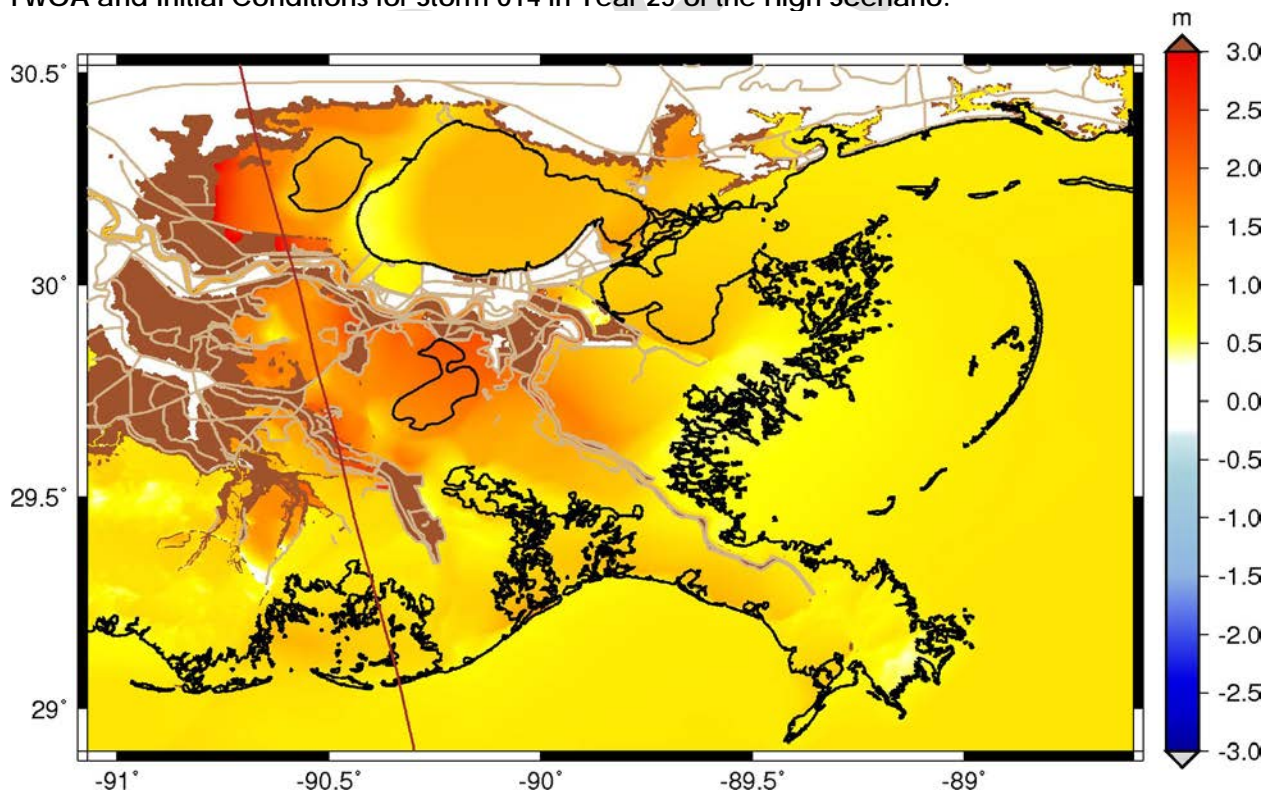


Figure 166: Differences Between Maximum Surge Elevations (meters) in Southeastern Louisiana for FWOA and Initial Conditions for Storm 014 in Year 50 of the High Scenario.

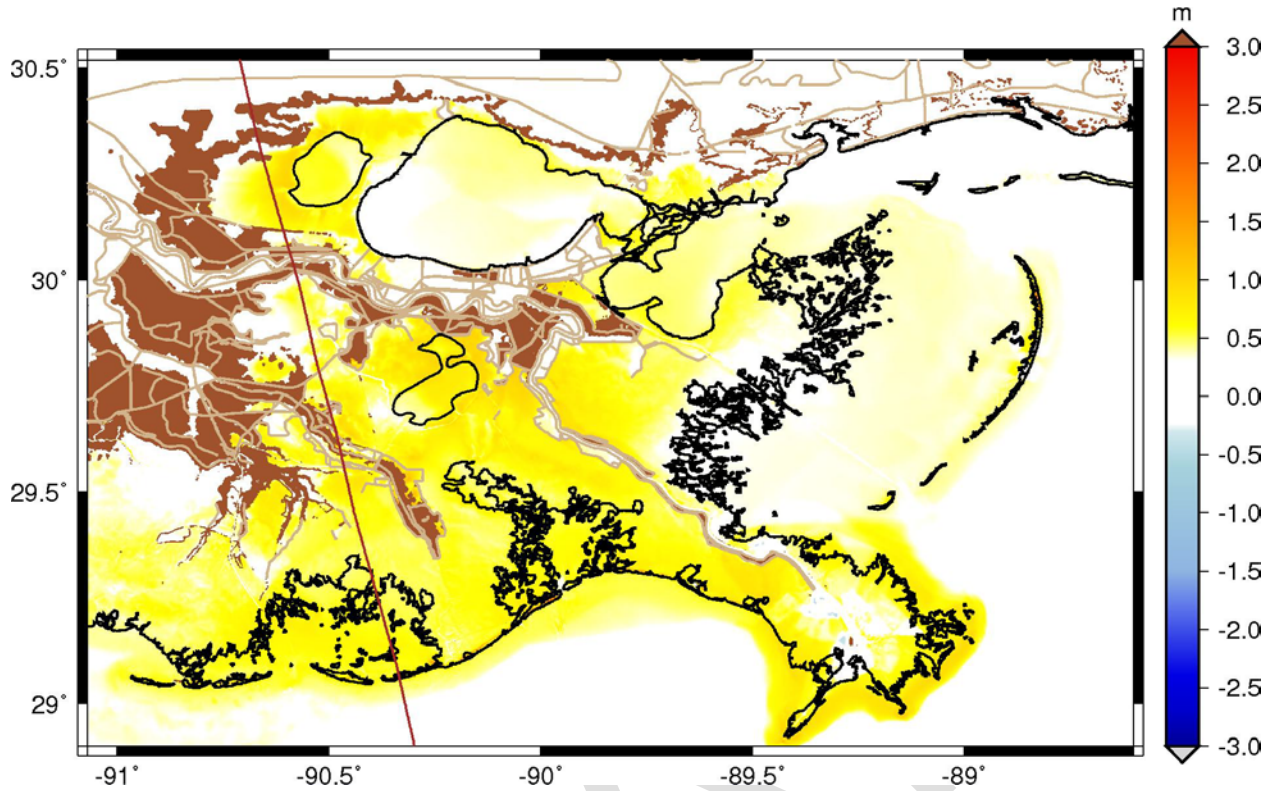


Figure 167: Differences Between Maximum Surge Elevations (meters) in Southwestern Louisiana for FWOA and Initial Conditions for Storm 014 in Year 50 of the High Scenario.

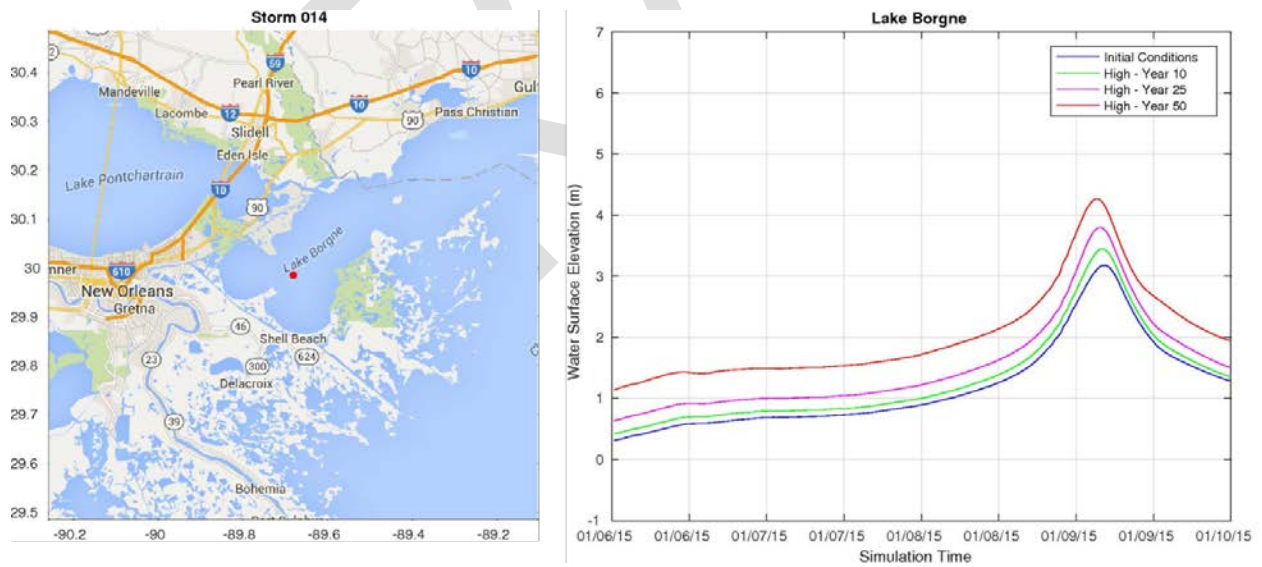


Figure 168: Surge Elevation (meters, NAVD88 2009.55) Time Series for Storm 014 in Lake Borgne for the High Scenario.

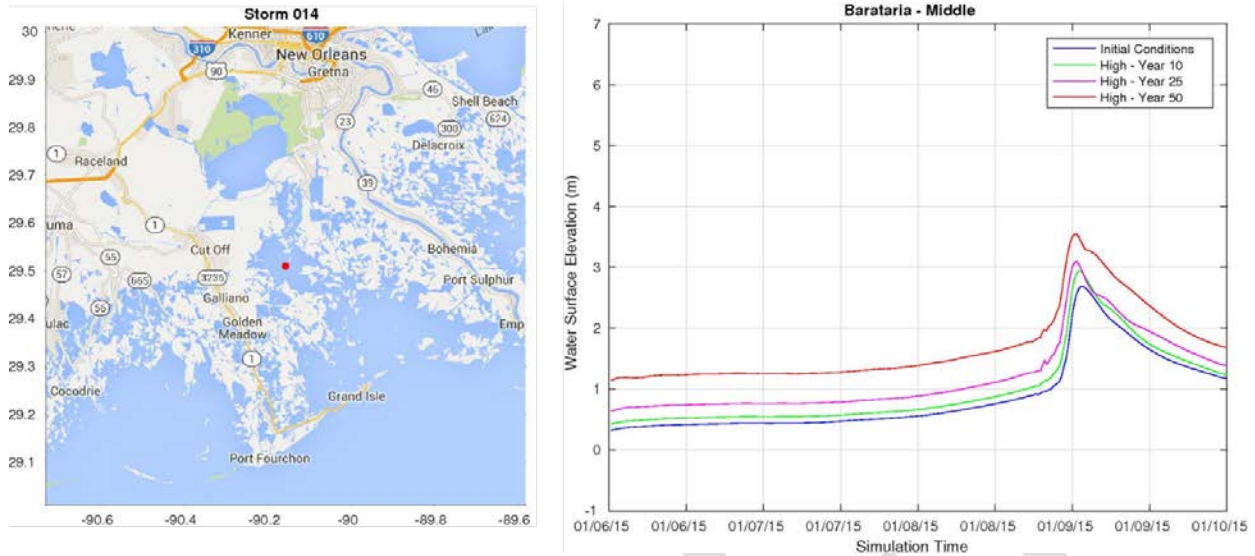


Figure 169: Surge Elevation (meters, NAVD88 2009.55) Time Series for Storm 014 in Barataria Bay for the High Scenario.

### 3.8.4 Cross-Scenario Comparisons

Figures 170 through 172 show how surge increases during each scenario within the Chenier Plain. Surge elevations are consistently greater than the sea level rise increment in areas inland from the coast for all scenarios and years. The increased surge elevations are due to the combination of sea level rise, subsidence of coastal features, and decreased friction across the Chenier Plain.

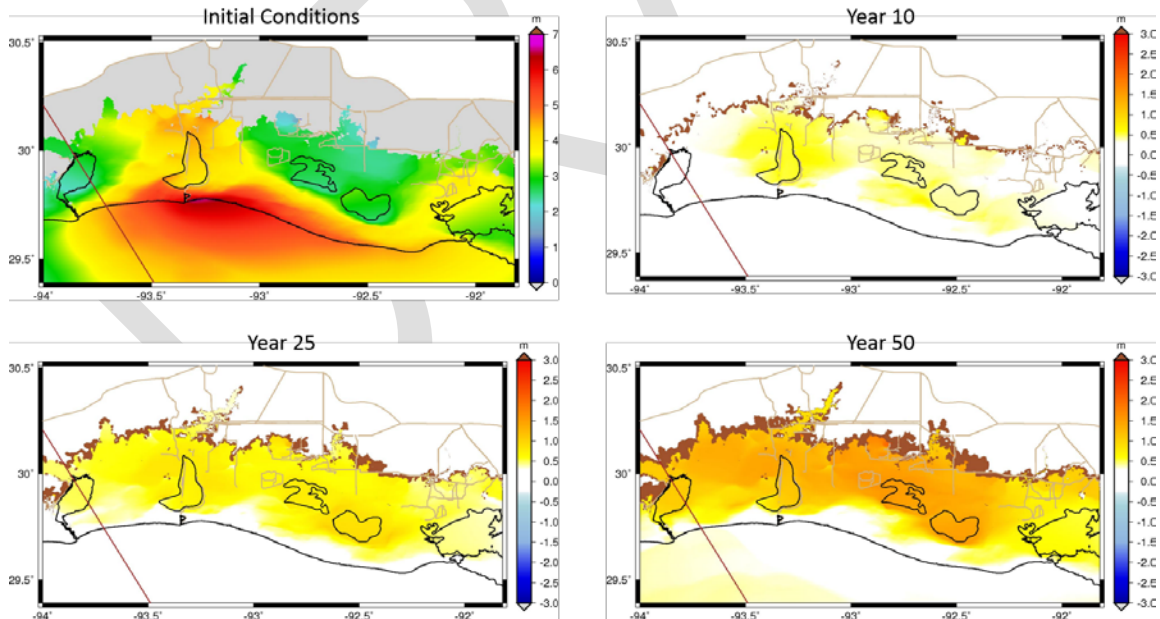


Figure 170: Differences Between Maximum Surge Elevations (meters) in Southwestern Louisiana for FWOA and Initial Conditions for Storm 218 of the Low Scenario.

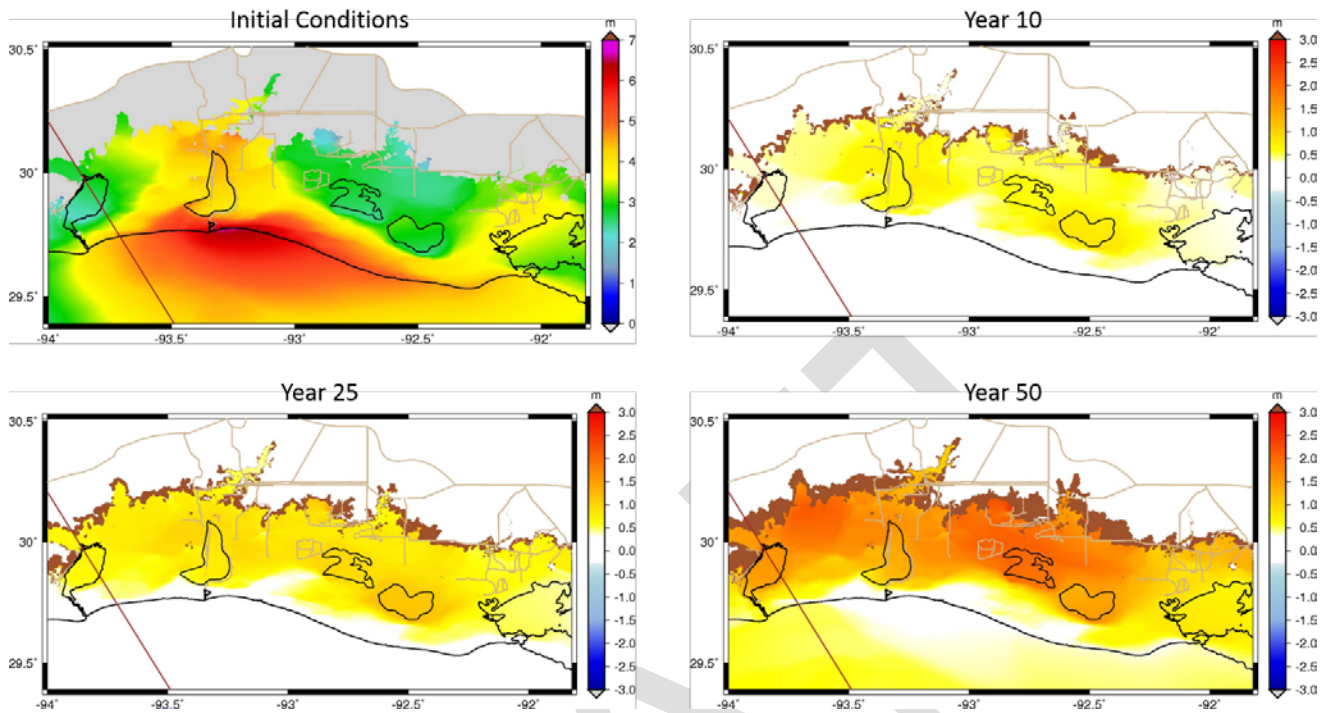


Figure 171: Differences Between Maximum Surge Elevations (meters) in Southwestern Louisiana for FWOA and Initial Conditions for Storm 218 of the Medium Scenario.

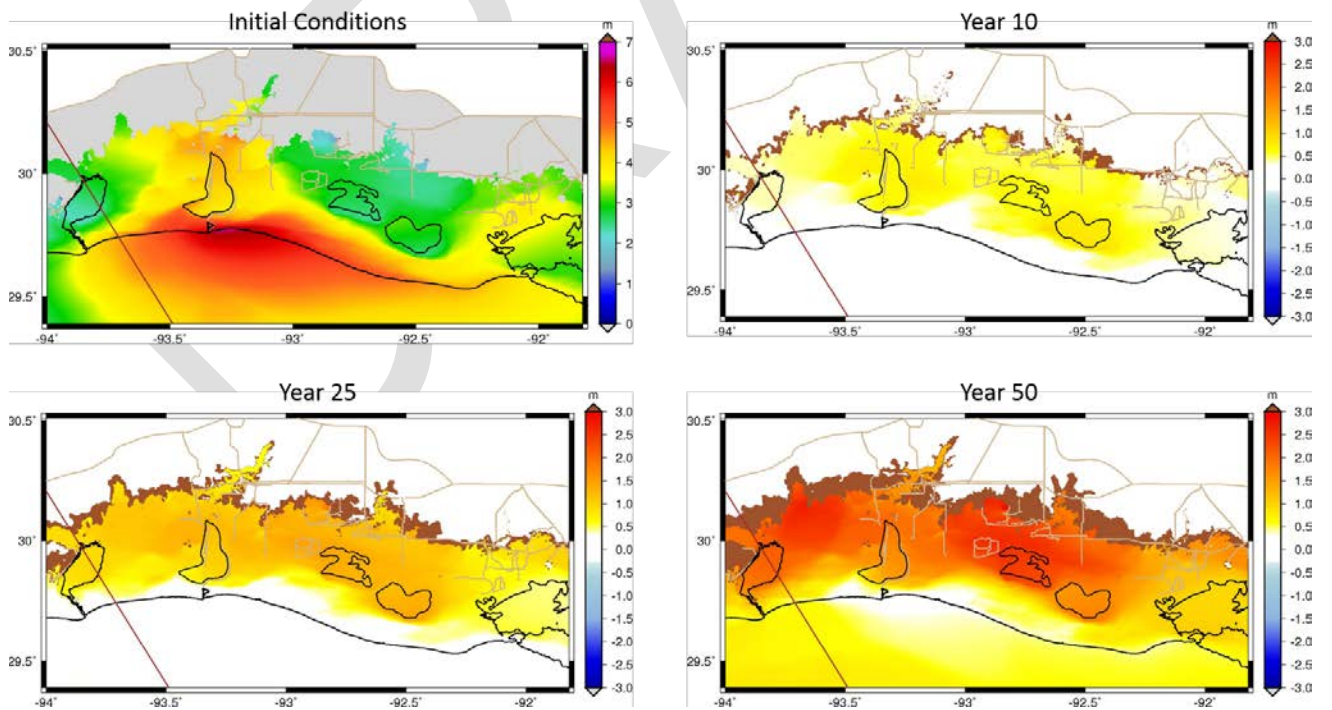


Figure 172: Differences Between Maximum Surge Elevations (meters) in Southwestern Louisiana for FWOA and Initial Conditions for Storm 218 of the High Scenario.

The outcomes of each scenario are most easily visualized at the year 50 interval given the largest relative sea level rise values and greatest landscape and vegetation change. Inspection of figures in the previous sections highlights notable changes to coastal flood hazards across coastal Louisiana. Some areas like the Chenier Plain, north of Barataria and Terrebonne Bays, and west of Lake Maurepas show consistently significant changes under future scenarios. The changes for each area for a given year and scenario vary due to the location along the coast, adjacent flood protection features or other raised features (e.g., highways), and changes in the landscape defined by the ICM.

To highlight the process for evaluating changes across scenarios, the region west of Lake Maurepas near Gonzales, Louisiana, has been selected. This area consistently demonstrates changes in inundation area and surge elevation through all scenarios. Figure 173 shows how the time series of surge elevation differs during year 50 for each scenario within Lake Maurepas, and Figure 174 shows the change in maximum surge elevation for the same simulations. Upon examination, there are two contributing factors. First, is the local topography and raised features. Interstate 55, between Lake Pontchartrain and Lake Maurepas, lies adjacent to Highway Old US 51 and a railroad. While Interstate 55 is elevated, Old US 51 and the railroad are not. This Old US 51 and the railroad are assumed to subside nearly 0.15 meters over the course of 50 years due to regional subsidence. This subsidence, combined with sea level rise, allows more storm surge to cross between Lake Pontchartrain and Lake Maurepas. This is illustrated in Figure 174 as lower magnitude differences on the western shore of Lake Pontchartrain leading to Lake Maurepas, as water can easily cross between the lakes where previously it built up against Old US 51.

Second, a significant frictional change is expected in future conditions as forested areas are degraded over time. Similar to the change due to Old US 51, Figure 174 shows lower magnitude differences on the western shore of Lake Maurepas, where previously frictional resistance caused surge to build up. Figures 175 and 176 show how the model frictional inputs change for future conditions compared to the initial conditions. First, Manning's roughness decreases, reducing bottom friction which had previously slowed the storm surge. Additionally, directional roughness lengths are also decreased, resulting in higher wind speeds interacting with the water column in future years. Figure 176 shows nearly a 40% reduction in directional roughness lengths in the direction of Gonzales, which equates to a 40% increase in the wind speed applied to the water column due to the decrease in shielding provided by the forested area. These landscape changes combine for a significant impact on surge elevations that is larger than the sea level rise increment, particularly when the hurricane winds blow from east to west.

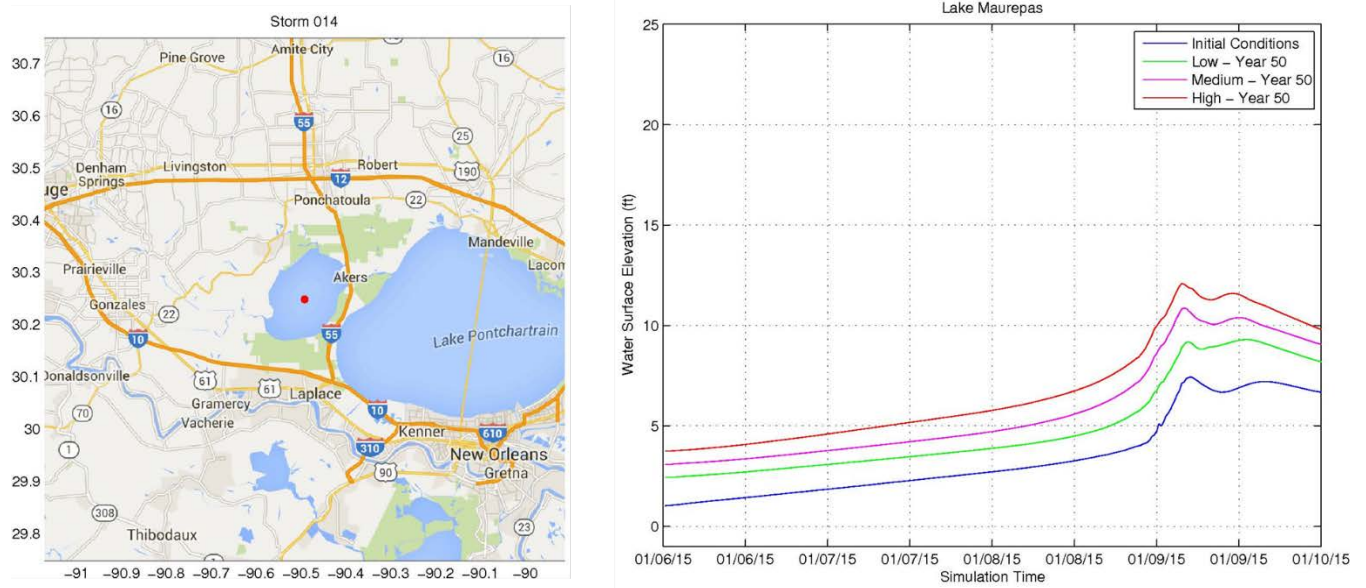


Figure 173: Surge Elevation (meters, NAVD88 2009.55) Time Series for Storm 014 near Lake Maurepas during Year 50 for All Scenarios.

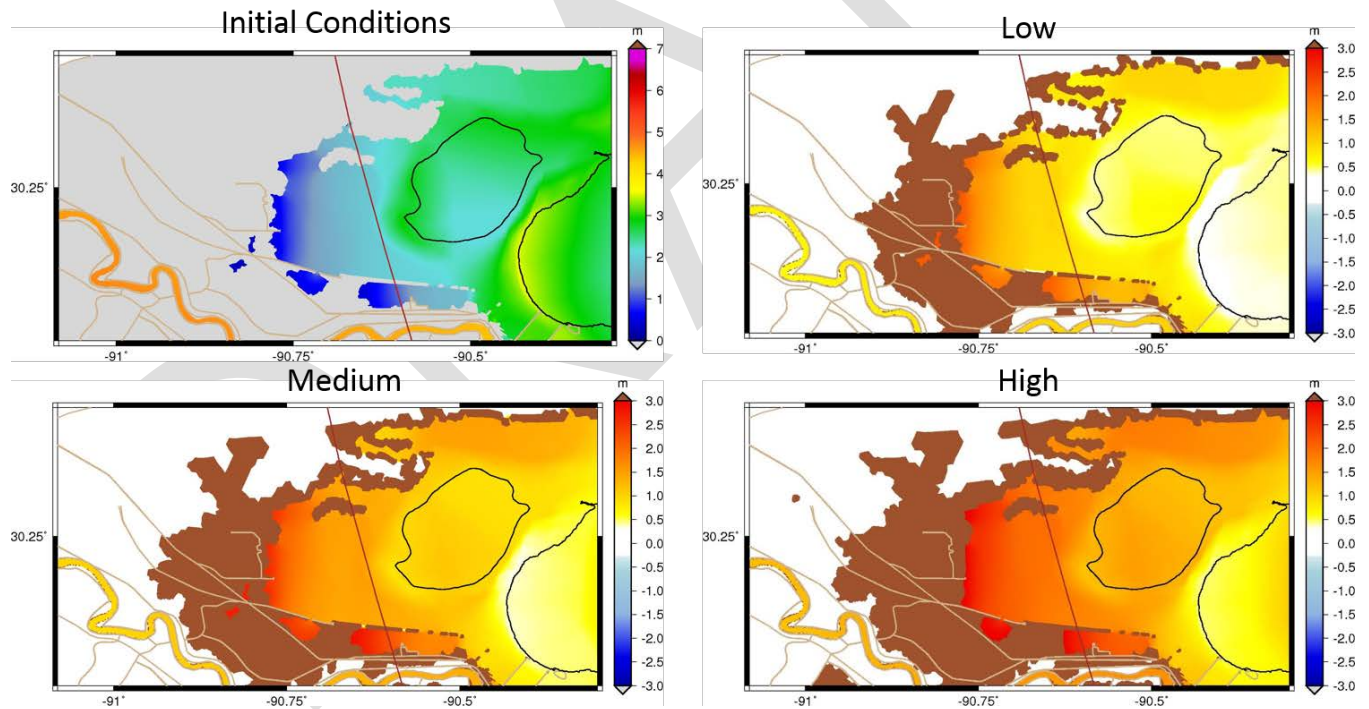
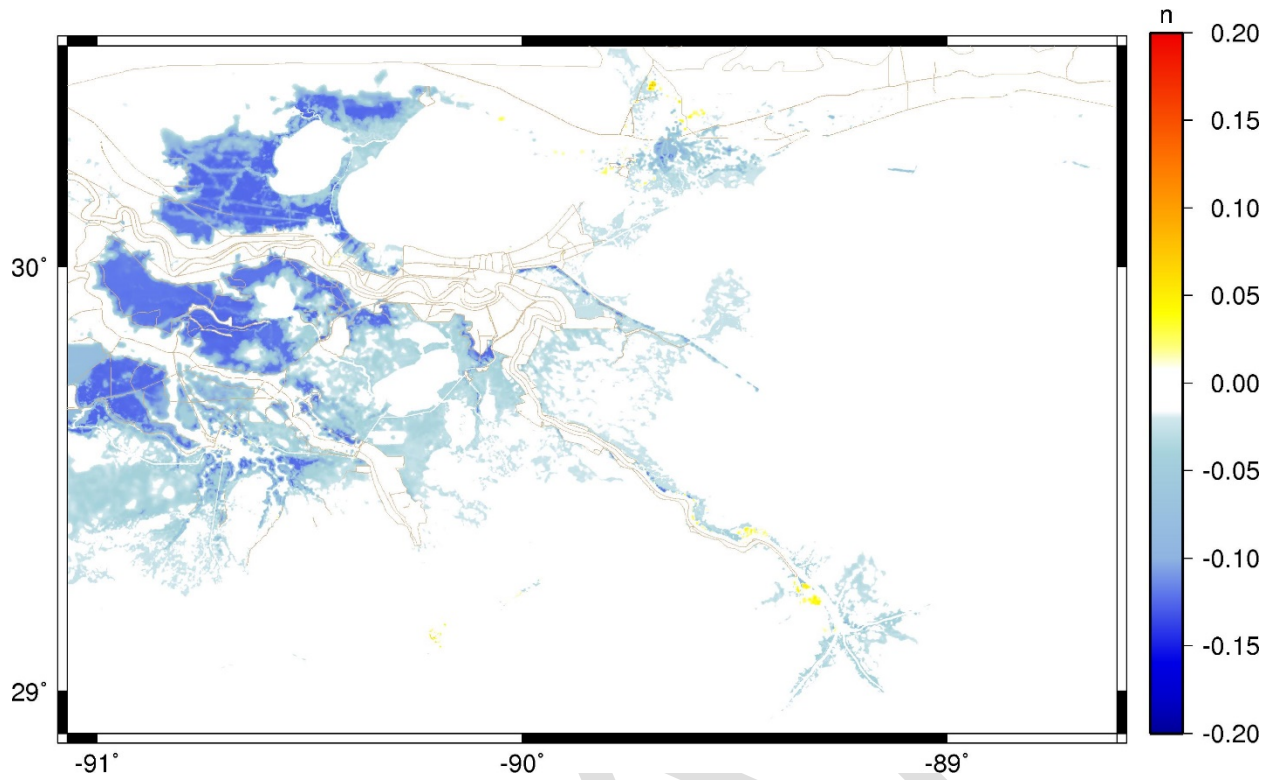
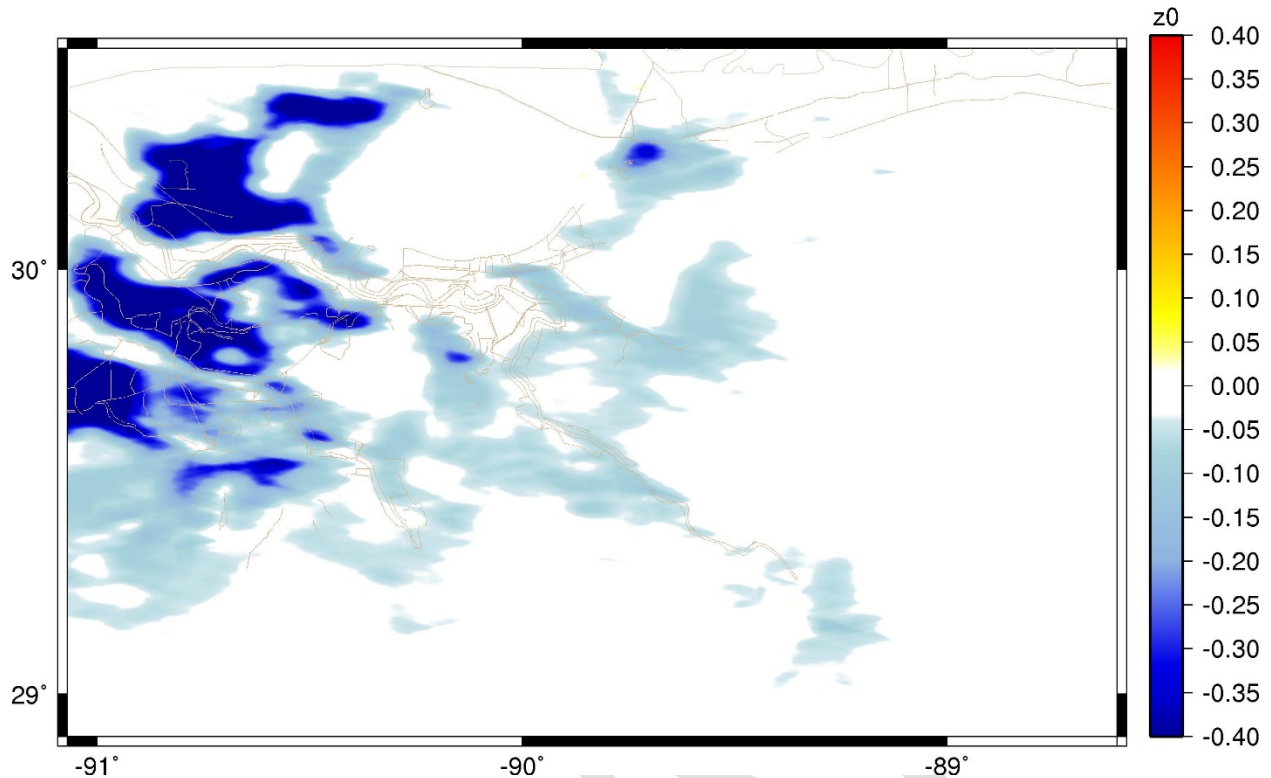


Figure 174: Differences Between Maximum Surge Elevations (meters) near Lake Maurepas for FWOA and Initial Conditions for Storm 014 during Year 50 for All Scenarios.



**Figure 175: Change in Manning's  $n$  Roughness between the Initial Conditions and the High Scenario in Year 50.** Cool colors indicate a decrease in Manning's  $n$  in the high scenario year 50, while warm colors indicate an increase in Manning's  $n$ .

DRAFT



**Figure 176: Change in Directional Roughness Length for an East to West Wind between the Initial Conditions and the High Scenario Year 50.** Cool colors indicate a decrease in directional roughness length in the high scenario year 50, while warm colors indicate an increase in directional roughness length.

### 3.9 Flood Depths and Damage

The CLARA model was applied to estimate flood depths and damage under FWOA. Statistical estimates for FWOA presented here are based on a 60-storm sample consistent with the set of storms used to evaluate individual hurricane protection projects (Attachment C3-25, Sec. 6.5). FWOA flood depth and damage results were separately estimated for the same three fragility scenarios described in Section 2.2. In addition, simulations were conducted for the low, medium, and high environmental scenarios used commonly in all systems models in the 2017 Coastal Master Plan analysis (Appendix C – Chapter 2). Key inputs to the CLARA model that vary by environmental scenario include sea level rise, localized subsidence, overall storm frequency, and average storm intensity.

The CLARA model analysis also considers different assumptions about population and asset growth across the Louisiana coast over the 50-year study period, summarized in three population growth scenarios. Scenarios were developed by first separating CLARA model grid points in the coastal region into low, medium, and high growth areas (or “bins”) based on an index of population density, 100-year flood depths faced in FWOA, and future land loss rate. The approach assumes that lower population density or higher flood and land loss risk would correlate to lower growth rates. These bins are reassigned dynamically and updated throughout the simulation, so that areas facing greater risks from land loss or flooding tend to shift to lower growth bins in future years.

Using this approach, three scenarios were developed building from current population counts and varying two parameters: 1) an assumed coast wide growth rate, and 2) a parameter specifying the plausible difference in the growth rates between low, medium, and high growth bins as compared to medium growth areas. Parameter values were selected and tuned based on historical U.S. Census data. The FWOA population growth scenarios evaluated include:

1. **No growth:** 0.00% per year growth rate, 1.0 % separation between bins;
2. **Concentrated growth:** 0.67% per year growth rate, 1.5% separation between bins; and
3. **Historic growth:** 0.67% per year growth rate, 1.0% separation between bins.

For further information on population growth scenario development, please see Attachment C3-25, Sec. 9.

FWOA scenario results were developed for the combination of three environmental, three fragility, and three population growth scenarios described above, for a total of 27 separate scenarios. These were also evaluated in three future time periods – year 10, year 25, and year 50 – yielding a total of 81 scenario/year combinations (cases). Selected results from this experimental design are described in the remainder of this section.

Flood depth results at the 100-year AEP interval at years 10, 25, and 50 are shown in Figure 177 and Figure 178 for the low and high environmental scenarios, respectively (IPET fragility scenario). In addition, Figure 179 shows the change in flood depths from initial conditions to the future year for all three environmental scenarios. In general, flood depths and 100-year flood extent in the low scenario increase steadily through the simulation period, with smaller increases noted in years 10 and 25, typically less than 1 m, and an expanded flood extent and notably higher flood depths (1-2 m in many locations) by year 50. The high scenario begins with similar results in year 10, by contrast, but shows more dramatic increases over time. In year 50, 100-year flood depth increases are estimated at two or more meters higher than initial conditions for nearly all areas of the coast, including portions of the northern boundary not currently inundated at the 100-year interval.

Enclosed protected system fragility scenario assumptions most notably affect the Greater New Orleans Hurricane and Storm Damage Risk Reduction System (HSDRRS) on the east and west banks of the Mississippi River. The 2017 Coastal Master Plan analysis assumes that the HSDRRS system will be maintained and upgraded regularly over time, counteracting the effects of subsidence on the effective heights of protection structures and largely maintaining the system's 100-year target for flood risk reduction. Nevertheless, 500-year flood depths in HSDRRS are shown to increase from the No Fragility to the IPET and MTTG fragility scenarios, especially in the high environmental scenario (Figure 180). When comparing 500-year flooding results for year 10, 25, and 50 across the three fragility scenarios, substantial flood depths and flood extents are noted within HSDRRS in year 25 and 50 when including plausible assumptions about levee fragility.

Coast wide FWOA damage (EAD) is shown in Figure 181 and Figure 182. Figure 181 shows coast wide EAD over time for each of the environmental and population growth scenarios, using the IPET fragility scenario. Figure 182, by contrast, holds the population growth scenario constant at "Historic Growth" and shows results for all environmental and fragility scenarios in years 10, 25, and 50. The error bars included in Figure 182 show the estimated 95% confidence interval for the damage estimates (see Attachment C3-25, Sec. 6.6).

Coast wide EAD results are similar across all scenarios in year 10, ranging from approximately \$3-4 billion per year. In year 25, little variation is noted across the population growth scenarios (Figure 181), but the environmental scenario results begin to diverge. All FWOA scenarios show

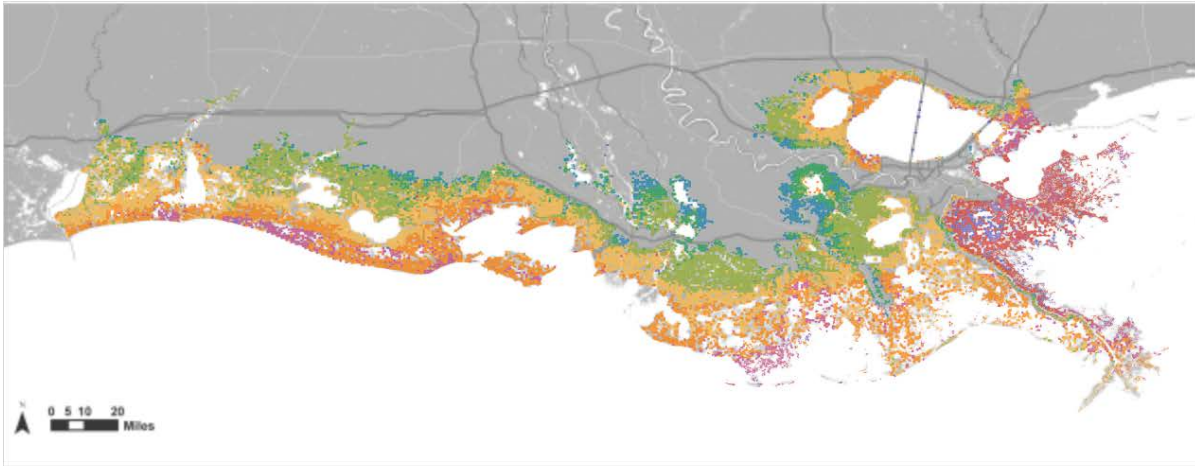
damage increasing, but greater damage increases are noted in the medium (\$5.1-\$5.6 billion) and high (\$6.9-\$7.9 billion) environmental scenarios in year 25 when compared with the low scenario, for instance (Figure 182).

EAD results diverge substantially across scenarios by year 50 of the simulation, ranging from less than \$5 billion (low environmental scenario, no fragility, no growth; not shown) to \$22 billion (high environmental scenario, MTTG fragility, historic growth). Damage totals also vary notably across the population growth scenarios, especially in the medium and high environmental scenarios.

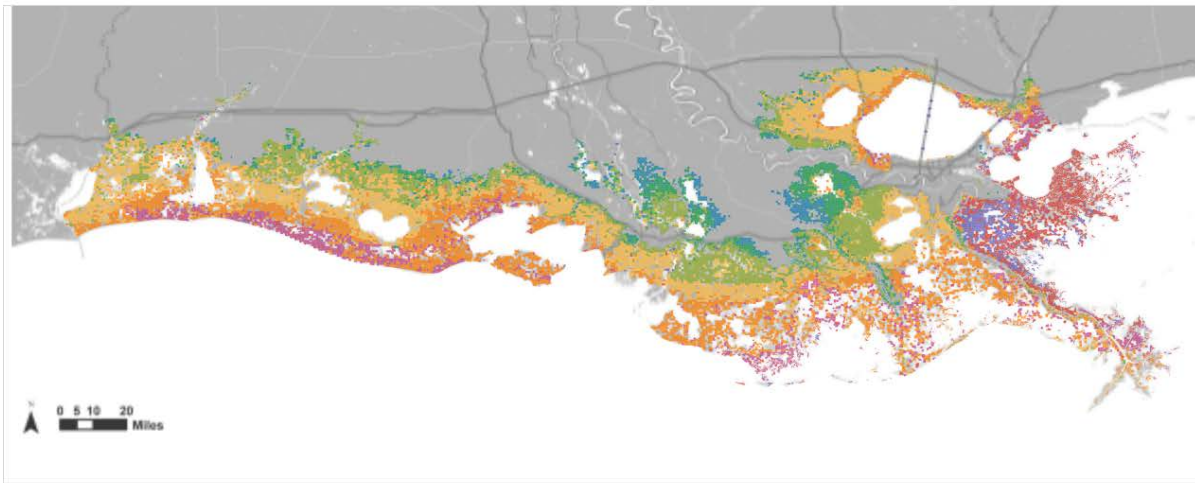
Spatial patterns of EAD across environmental scenario and year are shown in Figure 183. In the low scenario (top row), EAD increases occur largely in developed areas previously noted as high damage in the initial conditions estimate, also including east bank portions of Greater New Orleans. In the high scenario (bottom row), damage increase is more widespread, and a substantial fraction of risk regions show EAD totals greater than \$100 million by year 50. In addition, in this scenario and year the Houma, Raceland, Hahnville/Luling, Laplace, Greater New Orleans-East Bank, and Slidell/St. Tammany Parish regions all show EAD totals in excess of \$1 billion per year.

DRAFT

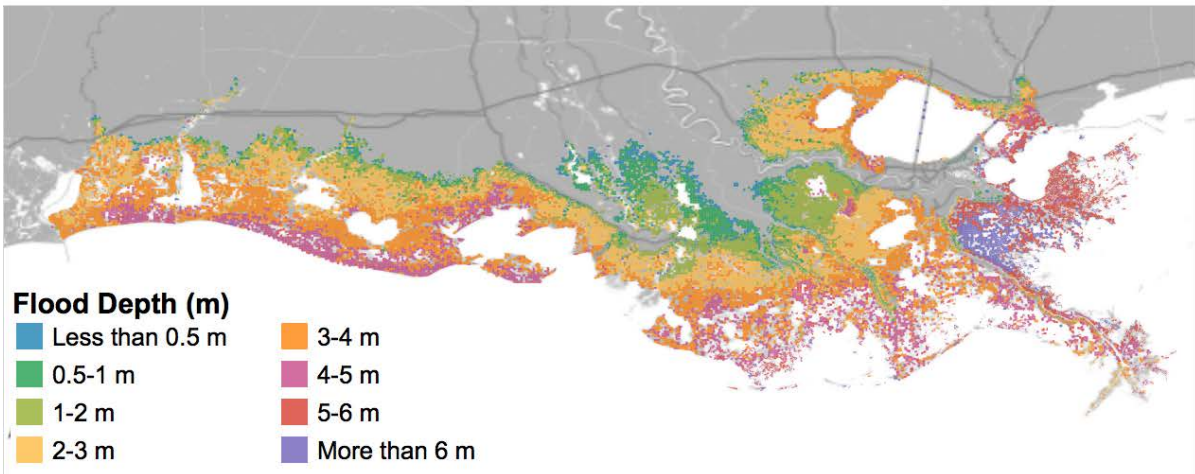
**Year 10**



**Year 25**



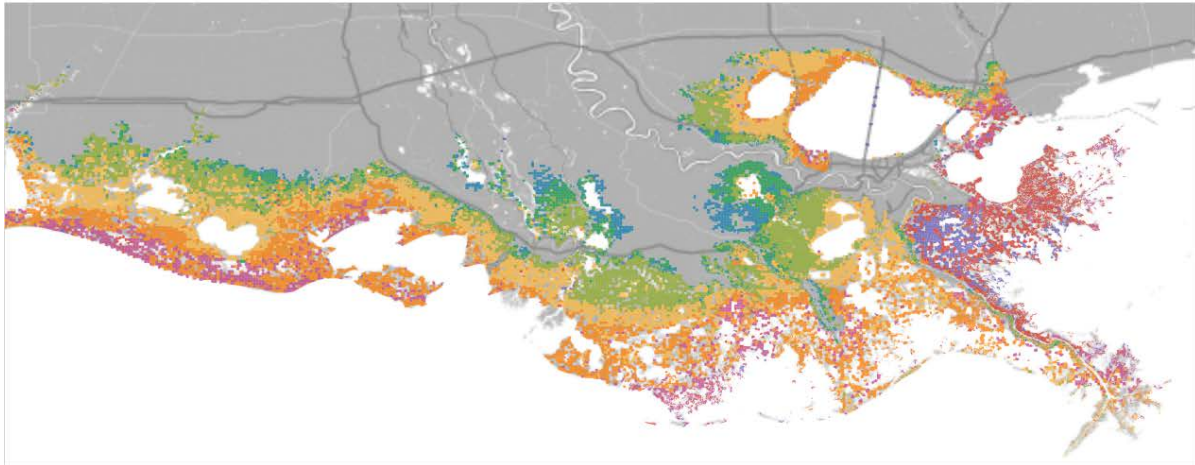
**Year 50**



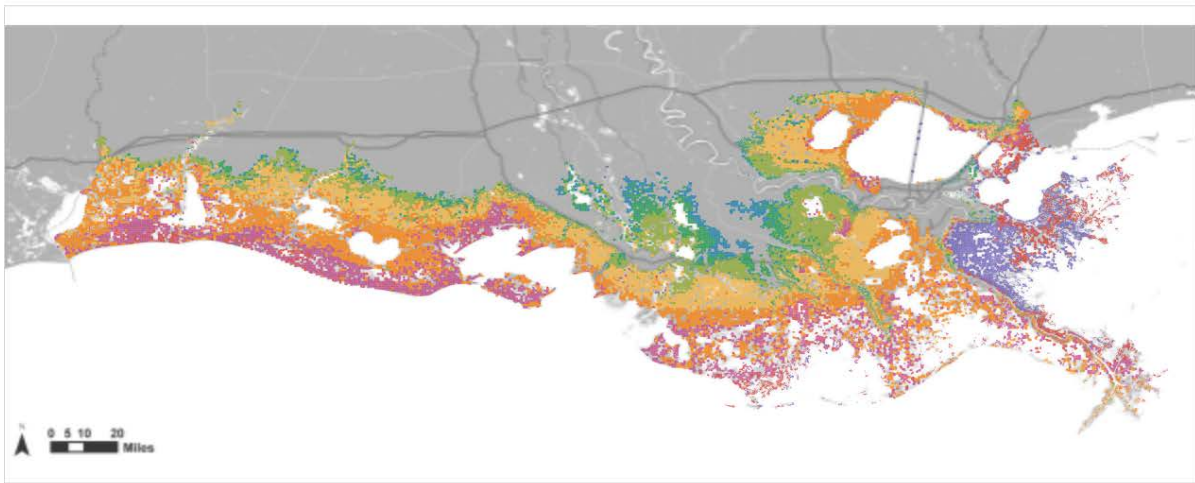
Note: 50th percentile 100-year flood depths of at least 0.2 m shown.

Figure 177: FWOA Low Scenario 100-Year Coast Wide Flood Depths – IPET Fragility Scenario.

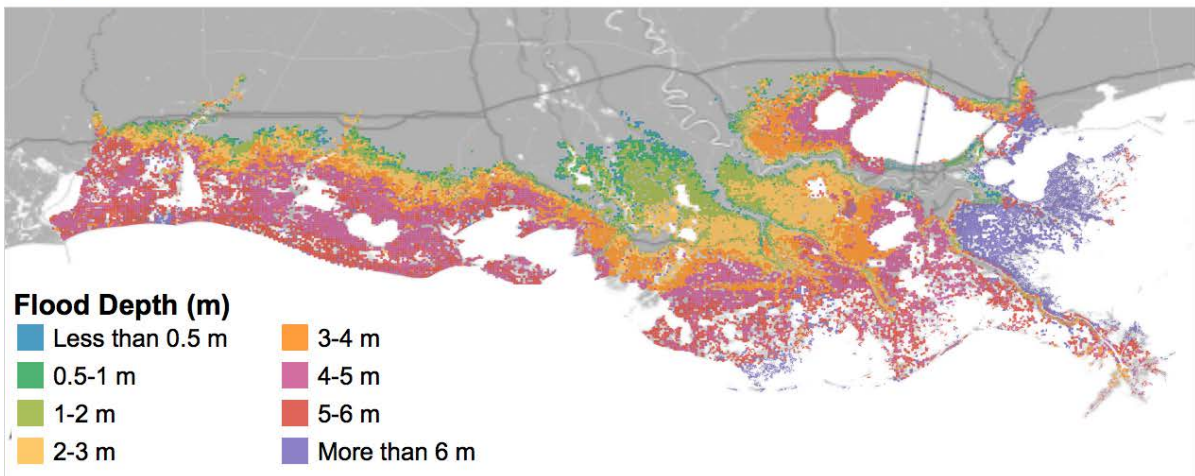
**Year 10**



**Year 25**

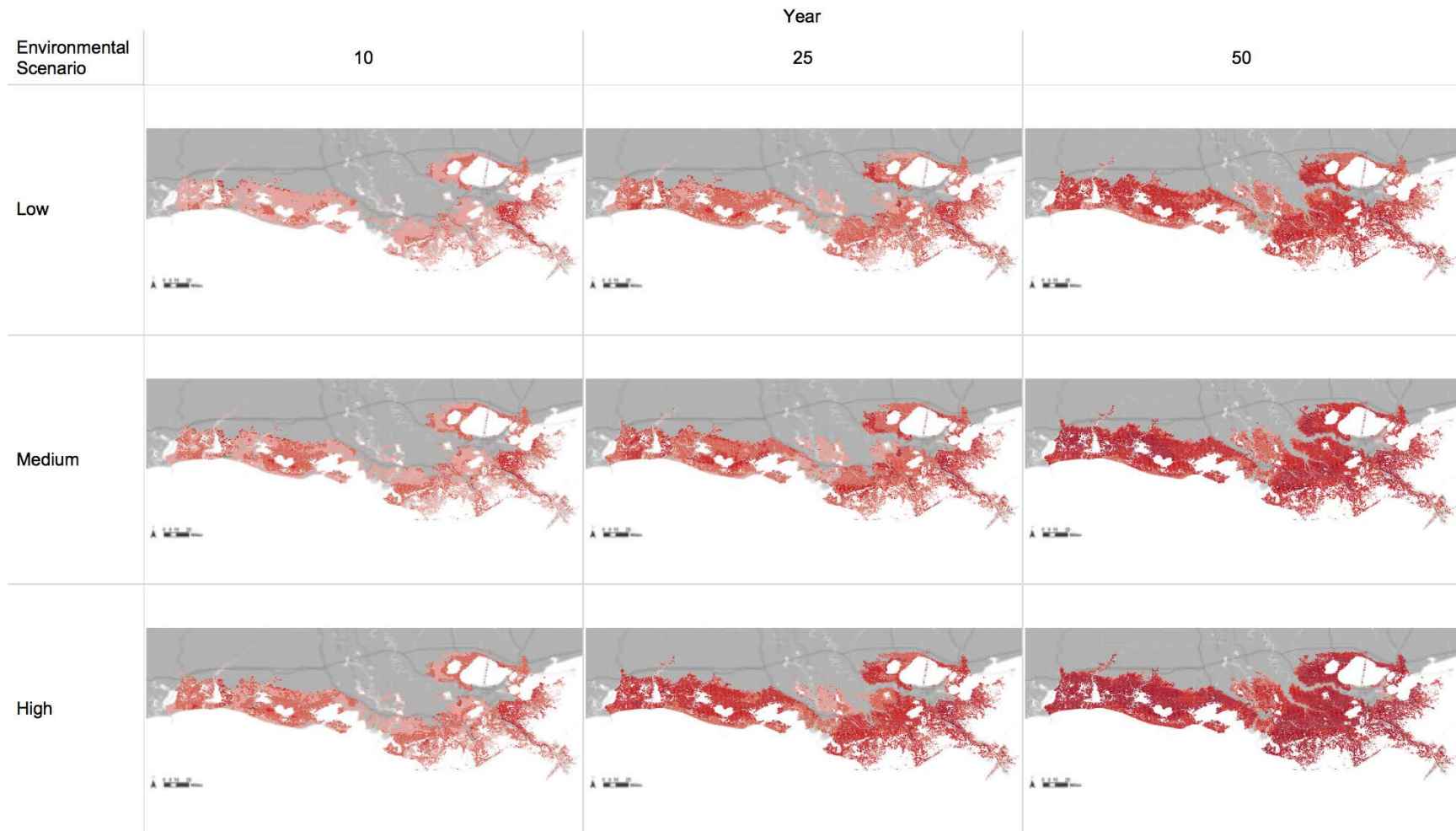


**Year 50**



Note: 50th percentile 100-year flood depths of at least 0.2 m shown.

Figure 178: FWOA High Scenario 100-Year Coast Wide Flood Depths – IPET Fragility Scenario.



Note: Change in 50th percentile 100-year flood depths from Initial Conditions to future year. Only grid points with an increase of at least 0.2 m are shown.

**Change in Flood Depth (m)**



Figure 179: Change in 100-Year Coast Wide Flood Depths by Environmental Scenario and Year – IPET Fragility Scenario.

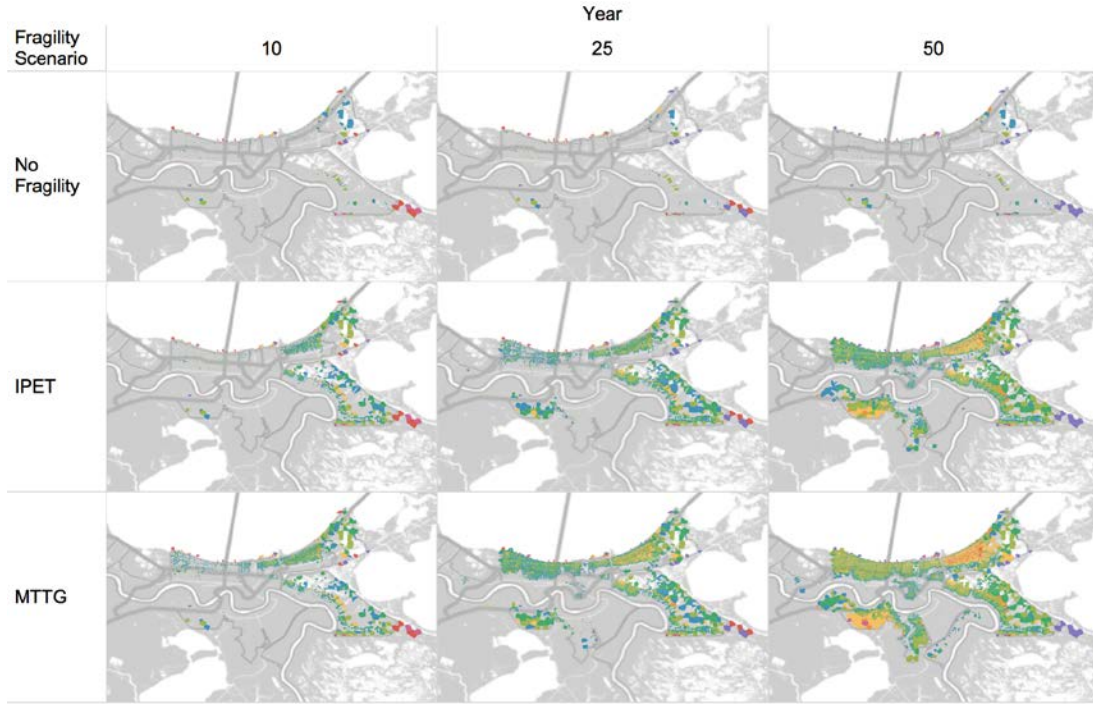
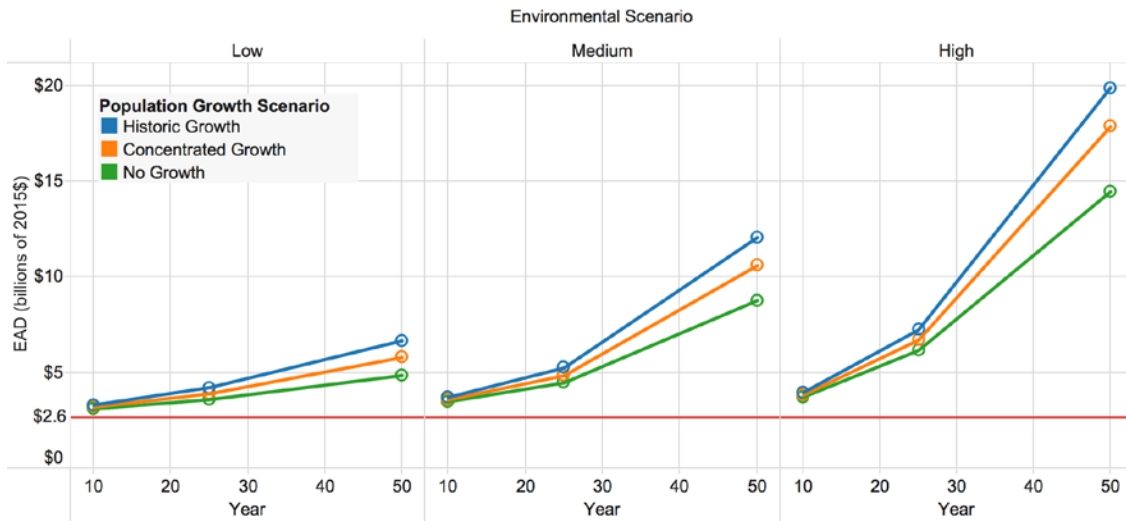
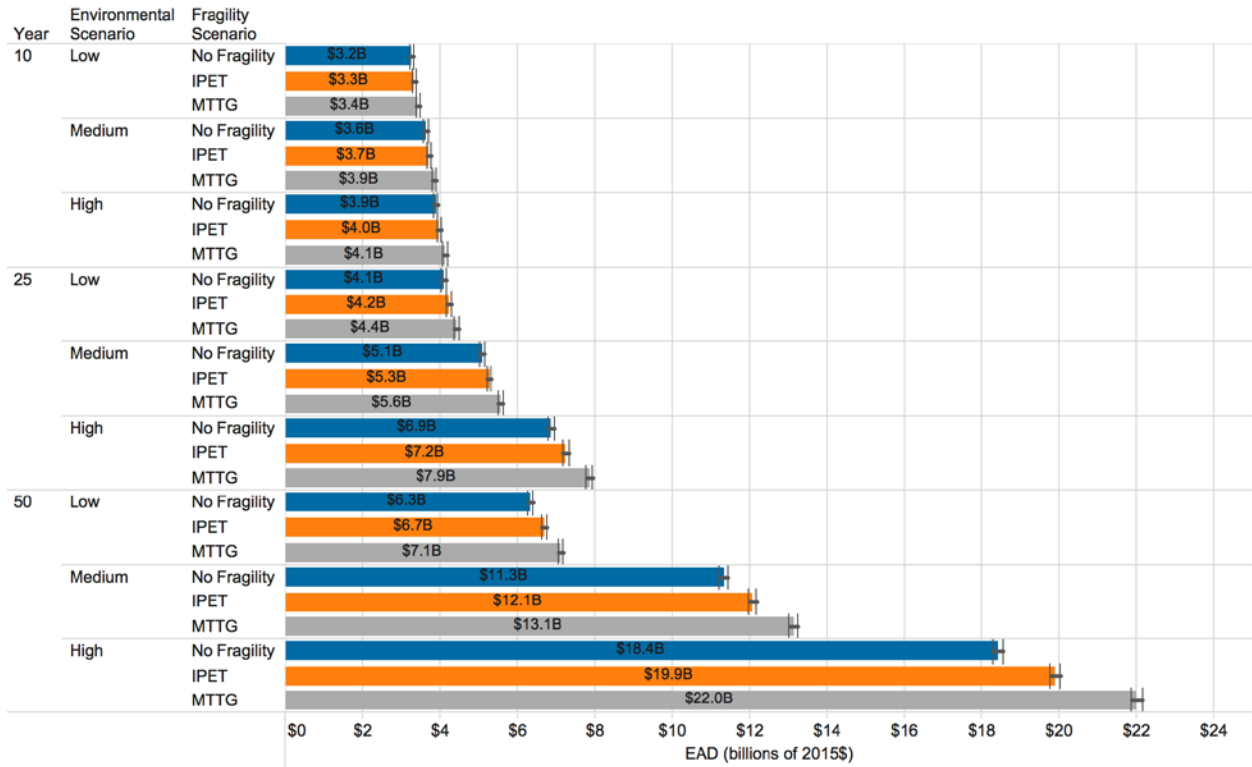


Figure 180: FWOA 500-Year Flood Depths, High Scenario - Greater New Orleans.



Note: Mean values; IPET fragility scenario shown. Red line shows Initial Conditions EAD for comparison.

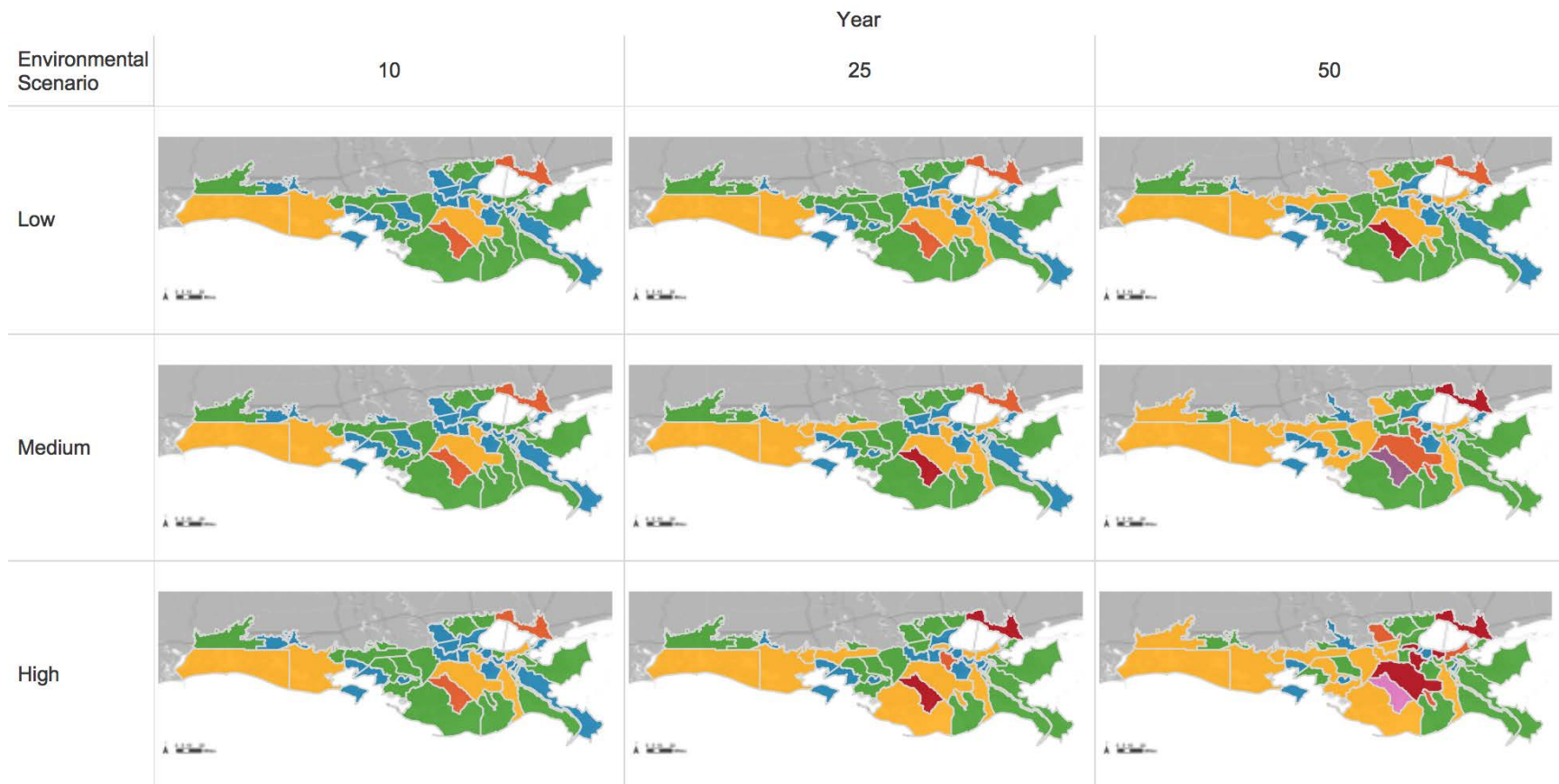
Figure 181: FWOA Coast Wide EAD Over Time by Environmental and Population Growth Scenario.



Note: Barplot shows mean values under the Historic Growth population growth scenario. The lines show 95 percent confidence intervals around the mean.

Figure 182: FWOA Coast Wide EAD Bar plot Summary by Year, Environmental, and Fragility Scenario.

DRAFT



Note: Results shown for the IPET fragility scenario and "Historical Growth" population scenario.

**EAD (2015\$)**

■ < \$10M    
 ■ \$10M - \$100M    
 ■ \$100M - \$500M    
 ■ \$500M - \$1B    
 ■ \$1B - \$2B    
 ■ \$2B - \$4B    
 ■ > \$4B

Figure 183: FWOA Coast Wide EAD Map by Year and Environmental Scenario.

## 4.0 Project Outputs and Interpretations

The project-level analysis was completed to assess the restoration-specific effects of restoration projects and the protection-specific effects of risk reduction projects. The projects highlighted here have been selected to represent examples of the different types of restoration, structural and nonstructural risk reduction projects considered in the 2017 Coastal Master Plan. Project effects, even for the same type of project, will vary from one part of the coast to another and are dependent on local conditions. Thus, these descriptions should be considered illustrative of the nature of the effects that these types of projects could have over time. Each example project is considered individually and compared to FWOA conditions in the project area. Other effects (e.g., effects of restoration projects on risk reduction) are discussed in general terms in the Project Interactions section.

A set of metrics was also developed to reflect expected project outcomes not specifically addressed by outputs from existing models. The metrics utilize outputs from the ICM and CLARA models at varying temporal frequencies and spatial scales to assess the following: Sustainability of Land, Support for Navigation, Traditional Fishing Communities, Support for Oil and Gas Activities and Communities, Support for Agricultural Communities, Use of Natural Processes, Flood Protection of Strategic Assets, Flood Protection of Historic Properties, and a Social Vulnerability Index. Example project-level and alternative-level analyses and outputs are provided in Attachment C4-11.

### 4.1 Mid-Breton Sound Diversion (001.DI.23)<sup>2</sup>

The goal of the Mid-Breton Sound Diversion (001.DI.23) project is to restore wetlands by seasonally diverting a maximum of approximately 1,200 cms from the Mississippi River in the vicinity of Woodlawn, Louisiana into the adjacent wetlands of Breton Sound.<sup>3</sup> The diverted sediments, nutrients, and freshwater are expected to build new wetlands and sustain and enhance the productivity of wetland vegetation. The diversion is implemented in year 7 of the ICM simulation.

#### 4.1.1 Landscape

In the high scenario, the impact of the project is slightly negative by year 10 with small increases in land loss primarily within the Breton Sound ecoregion (loss in eastern coast = -13.3 km<sup>2</sup>; loss in Breton Sound Basin = -9.7 km<sup>2</sup>) (Figure 184). Land loss in the Breton Sound ecoregion consists of small areas lost throughout the basin with the highest concentration of loss near the diversion structure (Figure 185). This initial loss seen with the project compared to FWOA is primarily due to increases in mean annual water level, which is >10 cm throughout most marshes in the Breton Sound ecoregion (Figure 186). At year 10, there is also a significant freshening of this ecoregion relative to the FWOA ranging from 0 to 5 ppt reduction in mean annual salinity (Figure 187). Even

---

<sup>2</sup> Decadal animations of the 50-year simulation outputs can be found in Attachment C4-2 - Mid-Breton Sound Diversion (001.DI.23), including stage, salinity, land, vegetation, HSLs, and EwE.

<sup>3</sup> It is modeled at 991 cms when Mississippi River flow equals 28,317 cms. There is no operation when river flow is below 5,663 cfs. There is a variable flow rate calculated using a linear function for river flow between 5,663 cfs and 28,317 cms and for river flow above 28,317 cms.

with these changes, the vegetation generally stays the same with only minor changes from saline and intermediate marsh converting to brackish and fresh marsh, respectively (Figure 188).

With the project in place, land loss occurs between years 11-15 and land gain occurs between years 16-20, but overall there is a small gain (+45.6 km<sup>2</sup>) in the Breton Sound ecoregion by year 20 (Figure 184). It is interesting to note that overall land gain is smaller when considering the entire eastern coast. This is primarily due to accelerated land loss in the Bird's Foot Delta, due to less water (and thus sediment) being discharged into the Delta as it is removed from the system by the Mid-Breton Sound Diversion.

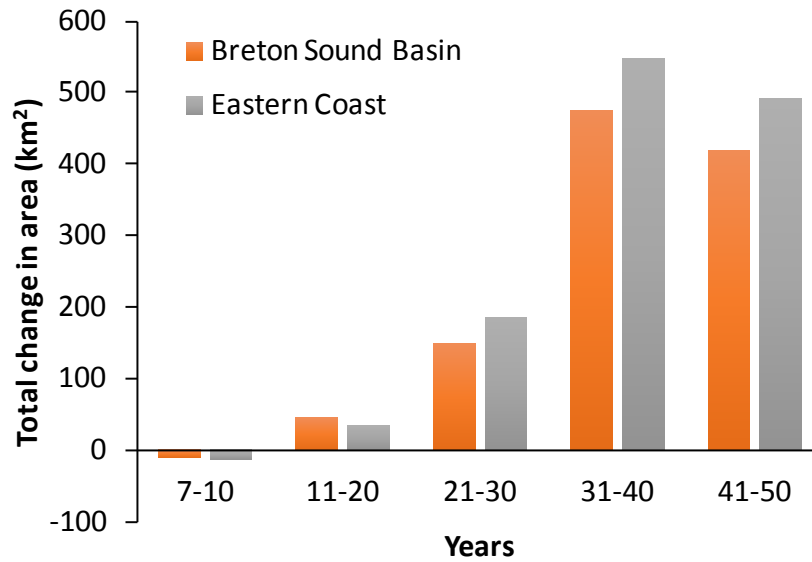


Figure 184: Change in Land Area within the Breton Sound Ecoregion and in the Eastern Coast in Response to the Mid-Breton Sound Diversion (relative to FWOA, high scenario).

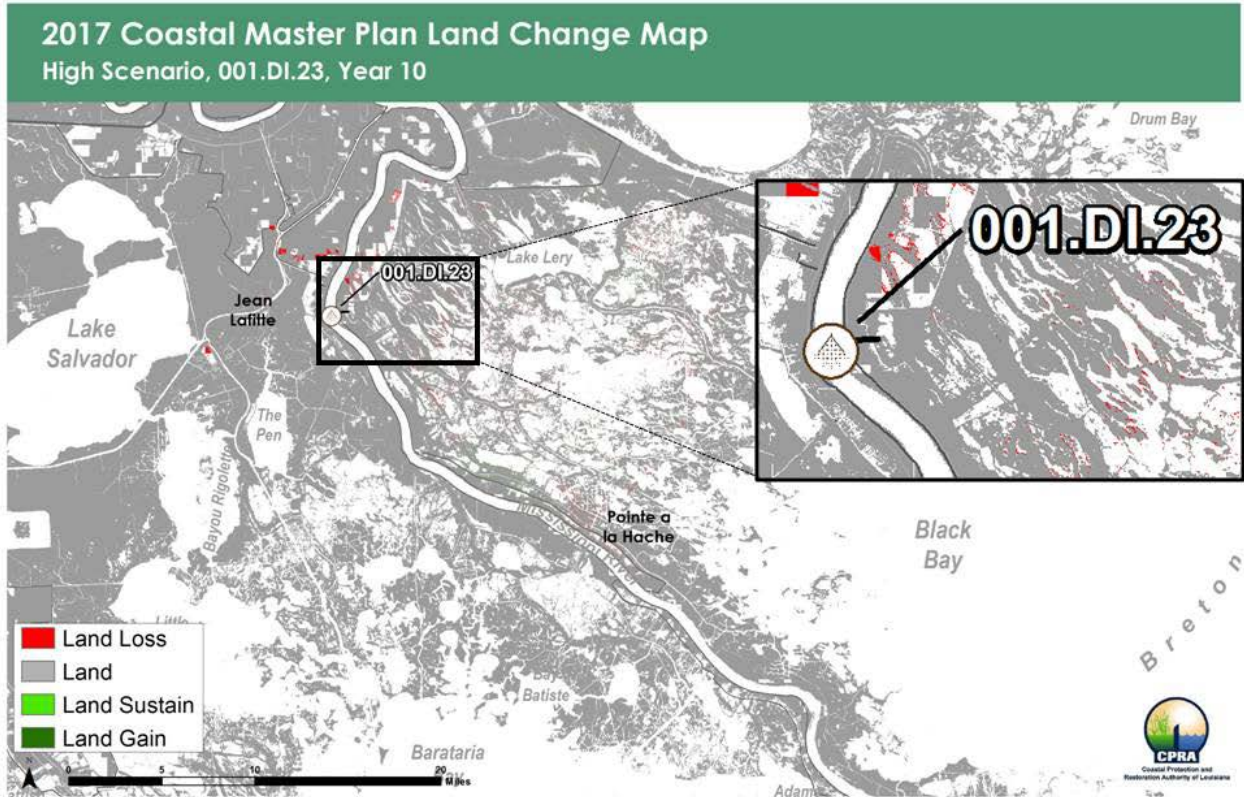


Figure 185: Land Change from the Mid-Breton Sound Diversion Relative to FWOA (year 10; high scenario).

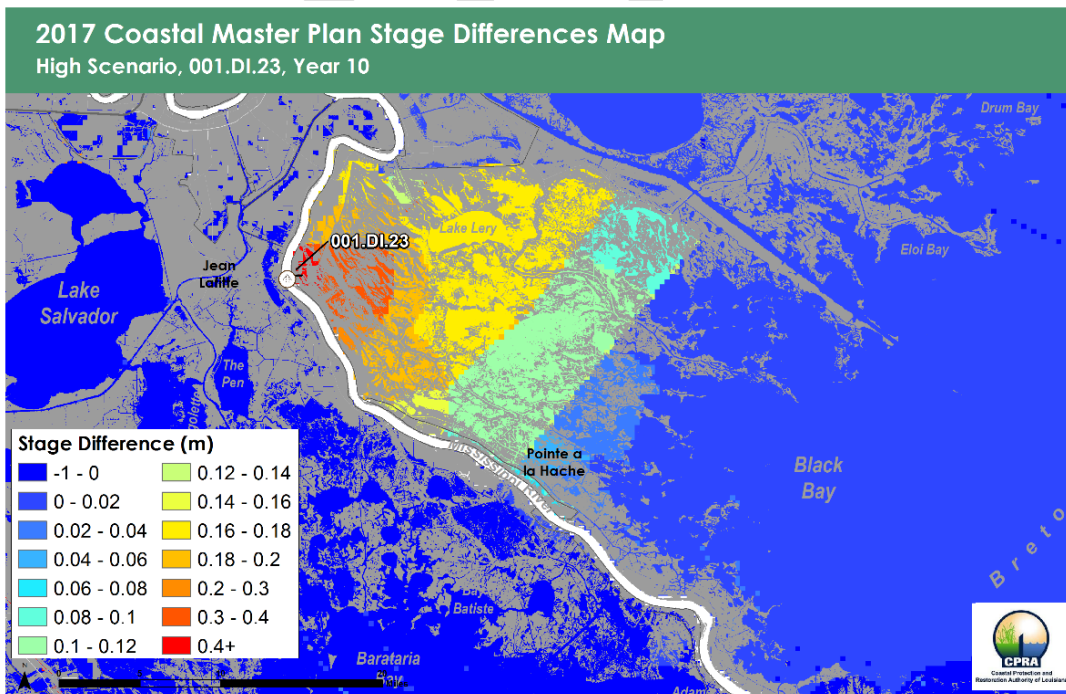


Figure 186: Change in Mean Annual Water Level Resulting from the Mid-Breton Sound Diversion Relative to FWOA (year 10; high scenario).

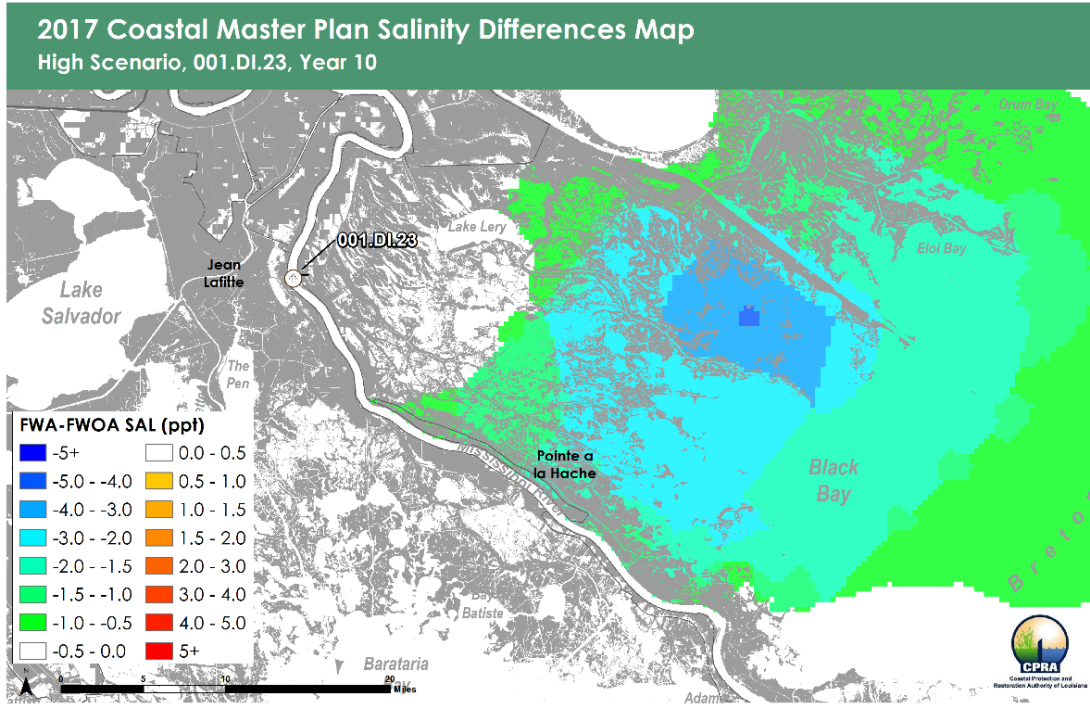


Figure 187: Change in Mean Annual Salinity Resulting from the Mid-Breton Sound Diversion Relative to FWOA (year 10; high scenario).

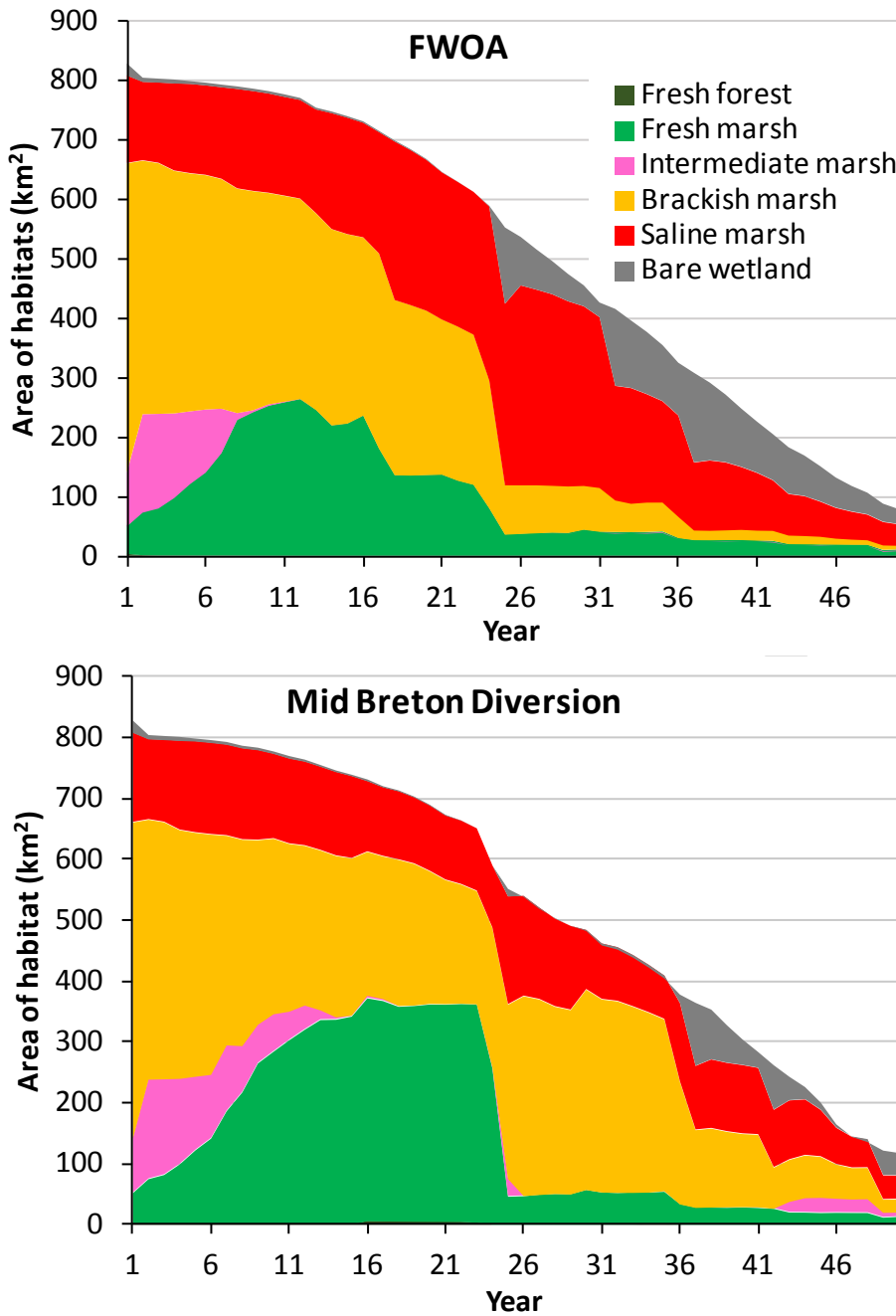


Figure 188: Change in Wetland Habitat Over Time within the Breton Sound Ecoregion under FWOA and with Mid-Breton Sound Diversion (high scenario).

With the diversion in place, there is overall land gain (Breton Sound ecoregion = +14.9 km<sup>2</sup>; entire eastern coast = +18.5 km<sup>2</sup>) compared to FWOA at year 30 (Figure 184). This appears primarily as land that is sustained, as there are only small areas of land gain in the immediate outfall area of the diversion; however, the diversion leads to local land loss in the ecoregion (Figure 189). Land loss occurs in areas where mean annual water levels are raised more than 12 cm (Figure 170), while land is sustained in areas where water levels are raised less than 12 cm and where average annual salinity is reduced by 5 ppt (Figure 191).

The wetland areas at year 30 are somewhat fresher with the diversion than without the diversion (+ 93 km<sup>2</sup> yr<sup>-1</sup> fresh marsh; + 121 km<sup>2</sup> yr<sup>-1</sup> intermediate marsh; - 164 km<sup>2</sup> yr<sup>-1</sup> brackish marsh; and - 40 km<sup>2</sup> yr<sup>-1</sup> bare ground) (Figure 188). However, both in FWOA and with the diversion, a major change occurs in this ecoregion in year 24 (Figure 188). This change is due to a combination of land loss and increased sea level that allows for more overland flow (and thus saline water to move further inland). In FWOA, this changes most of the Breton Sound ecoregion from brackish to saline marsh, while with the diversion, a change from fresh marsh to brackish marsh is more prevalent (Figure 188). Bare ground is primarily a result of conditions becoming so extreme that they fall outside of the current range of species in the model. It is likely that other species accustomed to higher saline conditions would establish in these places, but these are currently not included in the ICM or are too distant for the model's dispersal mechanism to allow colonization.

As relative sea level rises, land loss accelerates rapidly in the Breton Sound ecoregion in FWOA, but the presence of the diversion is able to prevent some of this loss (Figure 184). In year 40, similar to the previous decade, land loss is accelerated in the central basin due to increased water levels, and only small land gains occur in the immediate outfall area. During this period the land gain is primarily in intermediate marsh (+ 182 km<sup>2</sup> yr<sup>-1</sup>), while habitat loss is primarily in saline marsh (- 66 km<sup>2</sup> yr<sup>-1</sup>) (Figure 188).

By year 50, fewer areas are sustained and a drop in the overall land gain from the diversion occurs (Figure 184). At the end of 50 years, the diversion sustains existing land and creates new land with sediment input near the diversion, but land loss in this ecoregion continues even with the diversion in place (Figure 192). However, overall there is a substantial effect of more land (+ 48 km<sup>2</sup>) at end of 50 years with the project than without it (Figure 184).

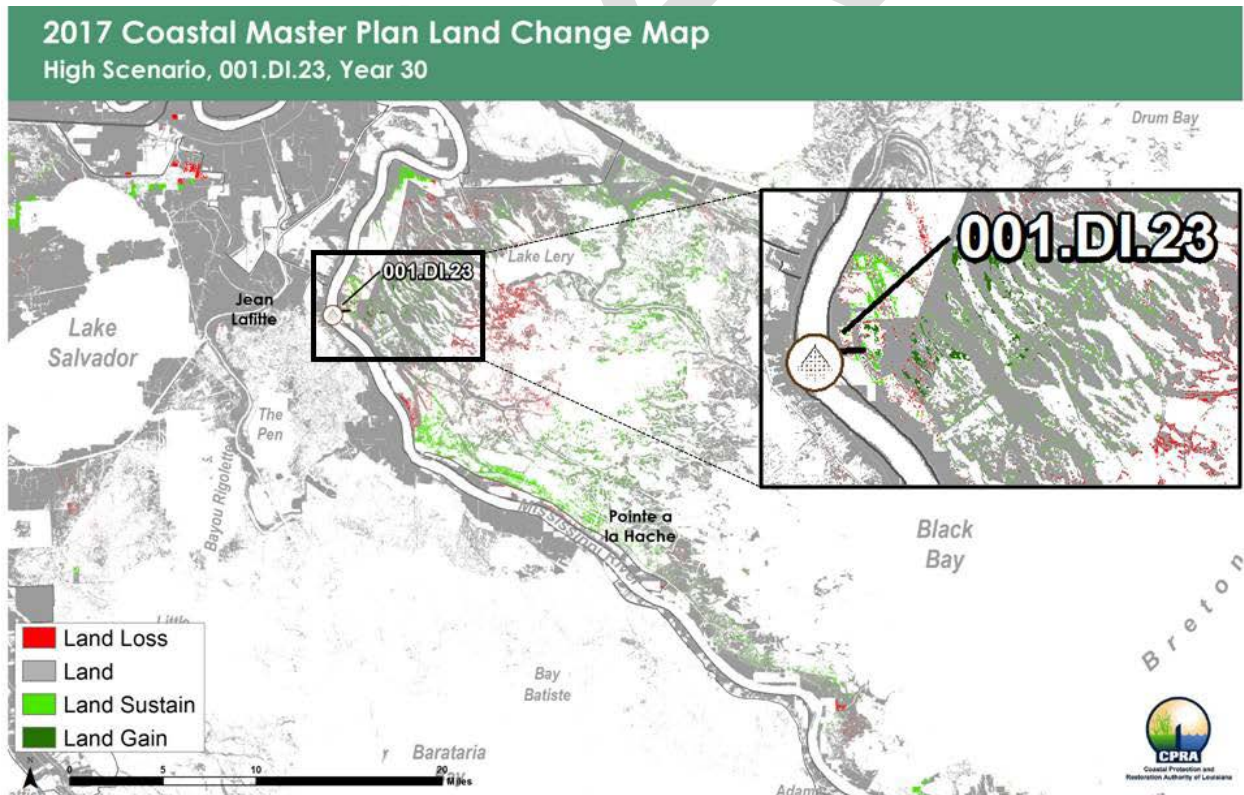


Figure 189: Land Change from the Mid-Breton Sound Diversion Relative to FWOA (year 30; high scenario). Inset focusses on immediate outfall area of the diversion.

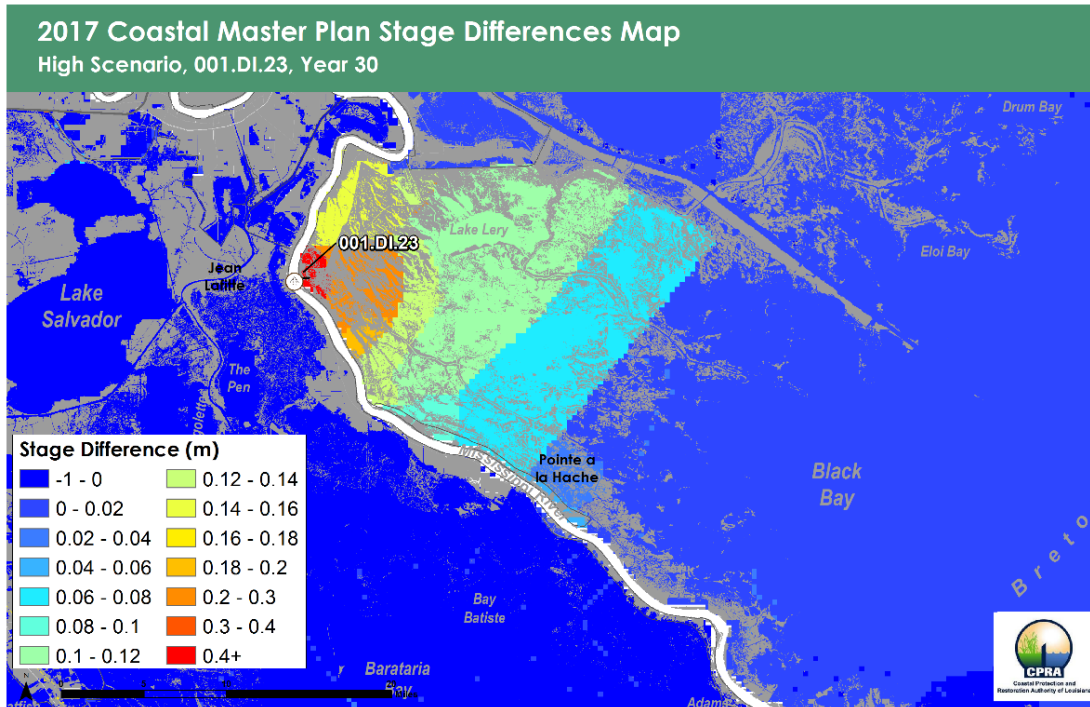


Figure 190: Change in Mean Annual Water Level from the Mid-Breton Sound Diversion Relative to FWOA (year 30; high scenario).

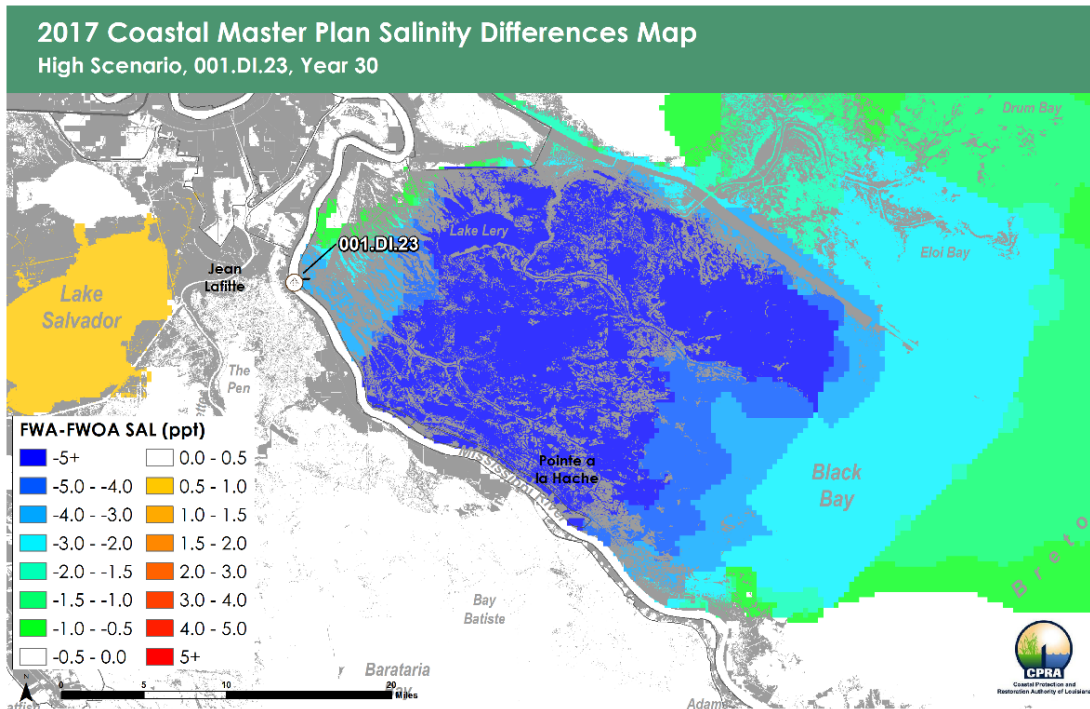


Figure 191: Change in Mean Annual Salinity from the Mid-Breton Sound Diversion Relative to FWOA (year 30; high scenario).

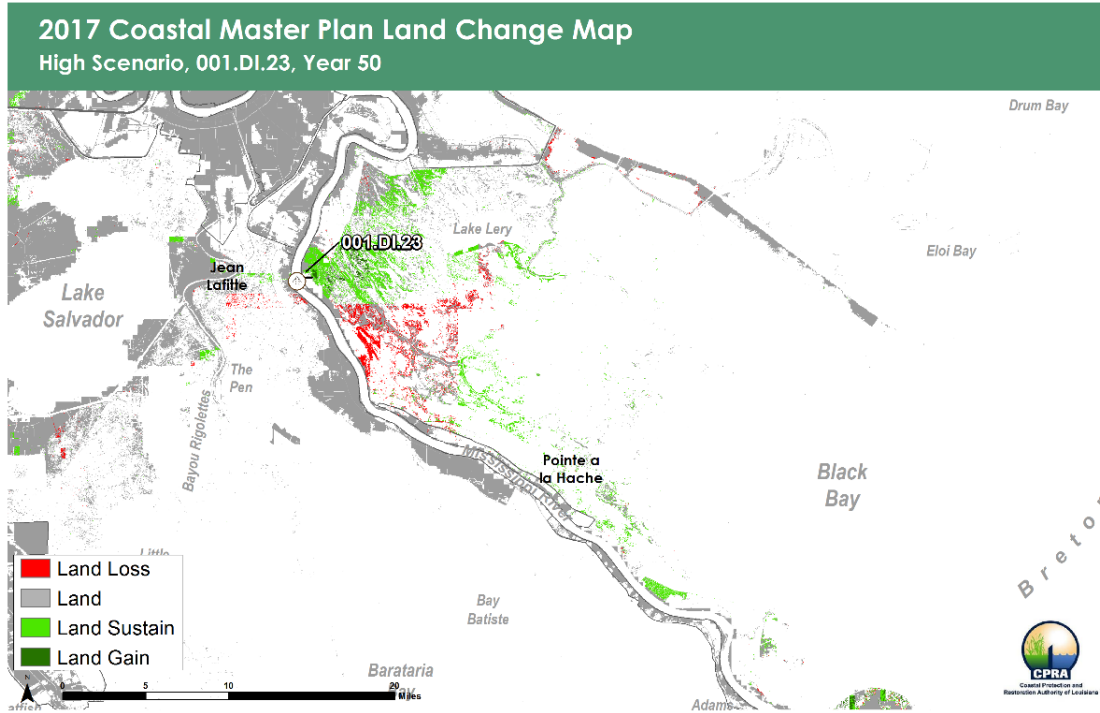


Figure 192: Land Change from the Mid-Breton Sound Diversion Relative to FWOA (year 50; high scenario).

Under the medium scenario, the diversion changes the habitat to fresher wetlands (Figure 193), and land loss is much slower when compared to the high scenario (Figure 184 and Figure 194). Under this scenario, land loss is greater than land sustained plus land gained in the first 20 years. By year 30, land loss due to the diversion is offset by land gained and land sustained. Only by years 40 through 50 of the simulation does the presence of the diversion provide a positive impact (Figure 194). However, at the end of 50 years, there is substantially more land with the project (+79 km<sup>2</sup>) than without it.

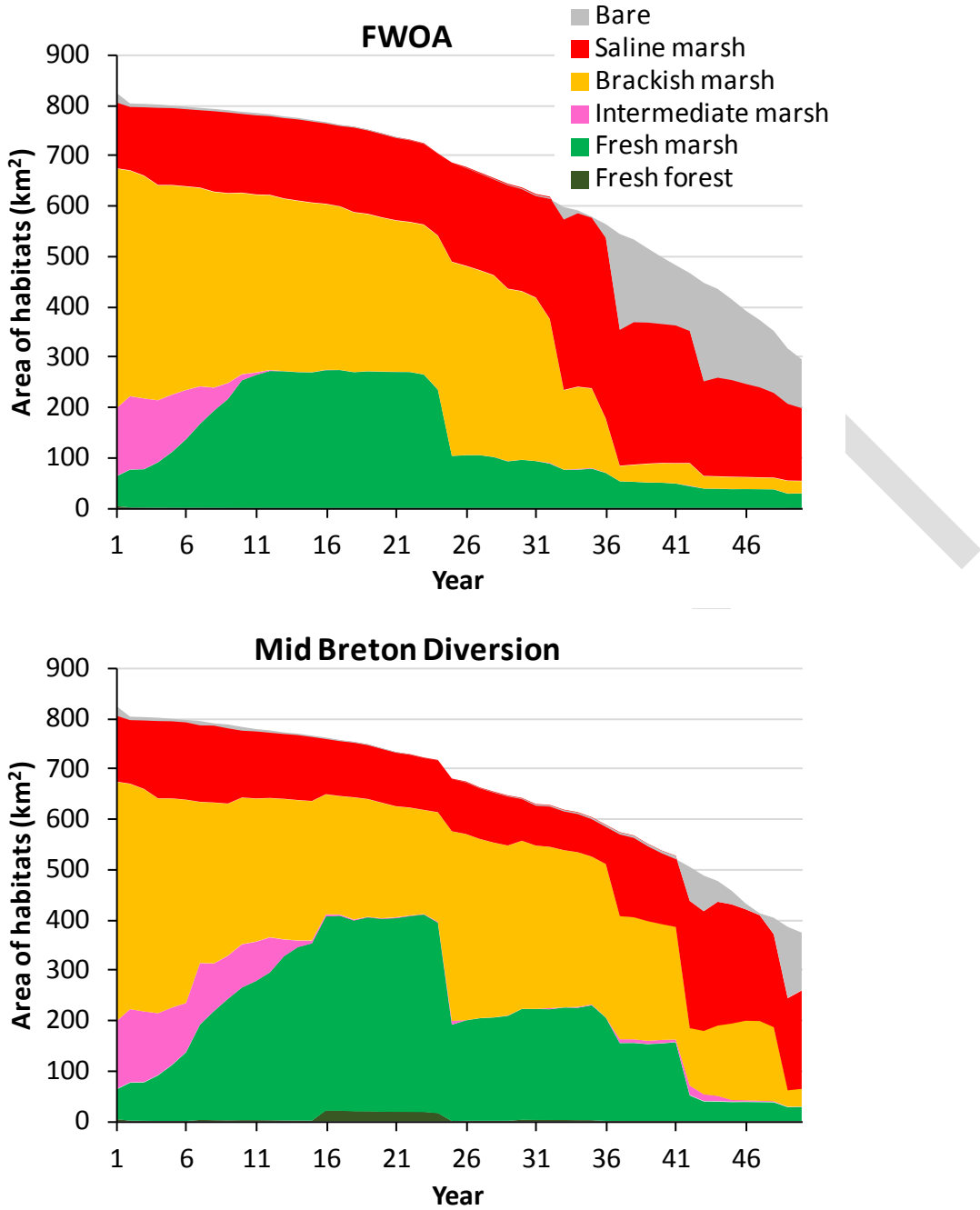


Figure 193: Change in Wetland Habitat over Time within the Breton Sound Basin under FWOA and with the Mid-Breton Sound Diversion (medium scenario).

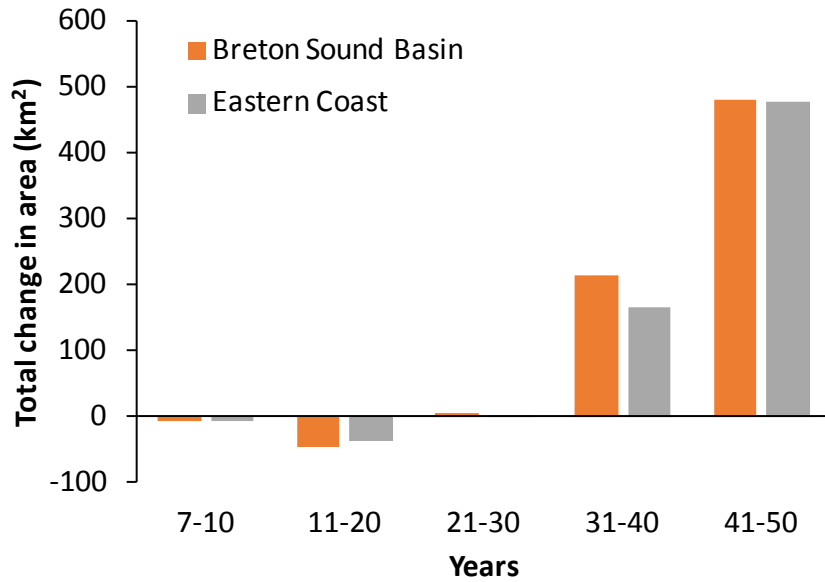


Figure 194: Change in Land Area within the Breton Sound Ecoregion and in the Eastern Coast in Response to the Mid-Breton Sound Diversion (relative to FWOA; medium scenario).

## 4.2 Fish, Shellfish, and Wildlife

Salinity reduction resulting from the diversion discharge decreases habitat suitability for small juvenile brown shrimp, adult spotted seatrout, and oysters. The decrease in suitability for brown shrimp and spotted seatrout typically ranged from -0.1 to -0.4 HSI relative to FWOA (Figure 195). Larger decreases in suitability are observed for oysters (often >0.5 decrease in HSI during the latter part of the simulation) due to this species' greater salinity limitations (Attachment C3-13).

Brown shrimp, spotted seatrout, and oysters all show the same general spatial-temporal pattern of change in habitat suitability relative to FWOA. During the early part of the simulation, the decrease in suitability is moderate and limited to the lower basin where the diversion discharge had the most effect on salinities (Figure 187 and Figure 195). During the latter part of the simulation, however, the difference in salinities between the project simulation and the increasingly saline FWOA is such that larger decreases in habitat suitability are observed throughout the basin for these species (e.g., brown shrimp, year 50; Figure 195). Interannual variability in river flows, and thus diversion discharge, contribute to the observed patterns. The years with high river flow rates, such as year 30 of the simulation, result in larger decreases in suitability; whereas, years with lower river flow rates result in less change in suitability. The increased habitat suitability for brown shrimp observed near the diversion outfall (Figure 195) is related to areas of bare ground in the FWOA (which receives a HSI score of 0.0) that are maintained as suitable vegetated wetland habitat in the diversion simulation.

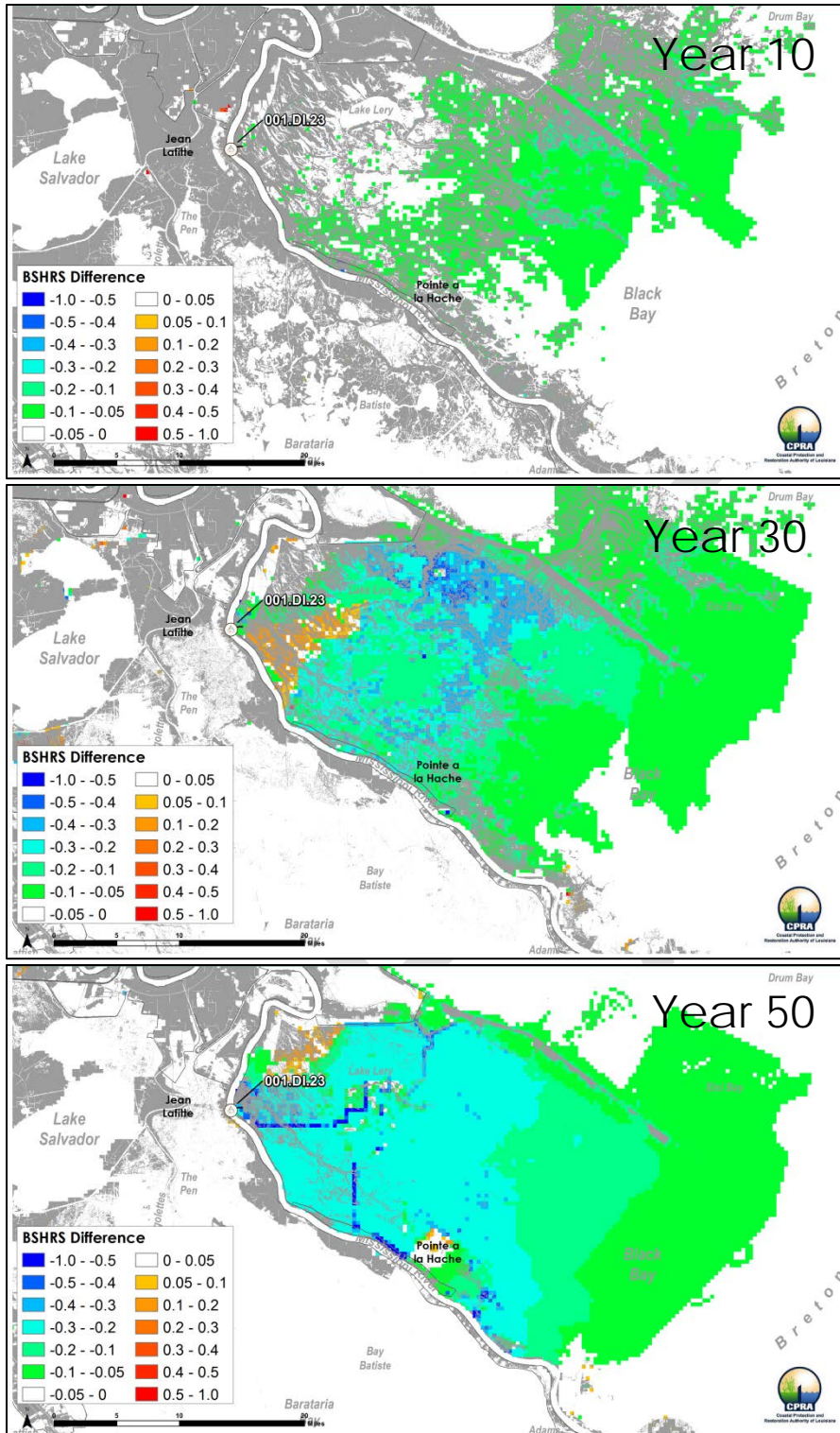


Figure 195: Difference in Small Juvenile Brown Shrimp Habitat Suitability for the Mid-Breton Diversion Relative to FWOA (years 10, 30, and 50; high scenario). Warmer colors indicate an increase in suitability and cooler colors indicate a decrease in suitability with the diversion.

The Mid-Breton Sound Diversion generally increases habitat suitability for largemouth bass, green-winged teal, and American alligator. Increased suitability is due to salinity reduction and the maintenance and expansion of more favorable marsh types for the species (i.e., fresh and intermediate marshes). There are, however, some areas of decreased suitability relative to FWOA observed for alligator and teal during the early part of the simulation (e.g., alligator at year 10; Figure 196). This is due to the elevated water levels from the diversion discharge (Figure 186), which increases water depths in low-elevation marshes and makes them less suitable for the shallow-water oriented alligator and teal (Attachments C3-7 and C3-10). Increased water levels are less evident in the latter part of the simulation, and thus have less of an effect on the HSIs.

The EwE food web model simulations of the Mid-Breton Sound Diversion show similar results to the HSI models. Biomass of largemouth bass generally increases relative to FWOA, whereas, the biomass of juvenile brown shrimp, adult spotted seatrout, and sack oyster generally decreases, particularly during the latter part of the simulation (Figure 197 and Figure 198). For the most part, these differences are due to the salinity reduction from the diversion discharge, which increases or decreases prey consumption depending on the species. However, other environmental factors play a role in the biomass patterns. For example, primary productivity is limited near the diversion outfall and this subsequently results in reduced food availability, which in turn causes the decrease in largemouth bass biomass observed in the area (Figure 197).

DRAFT

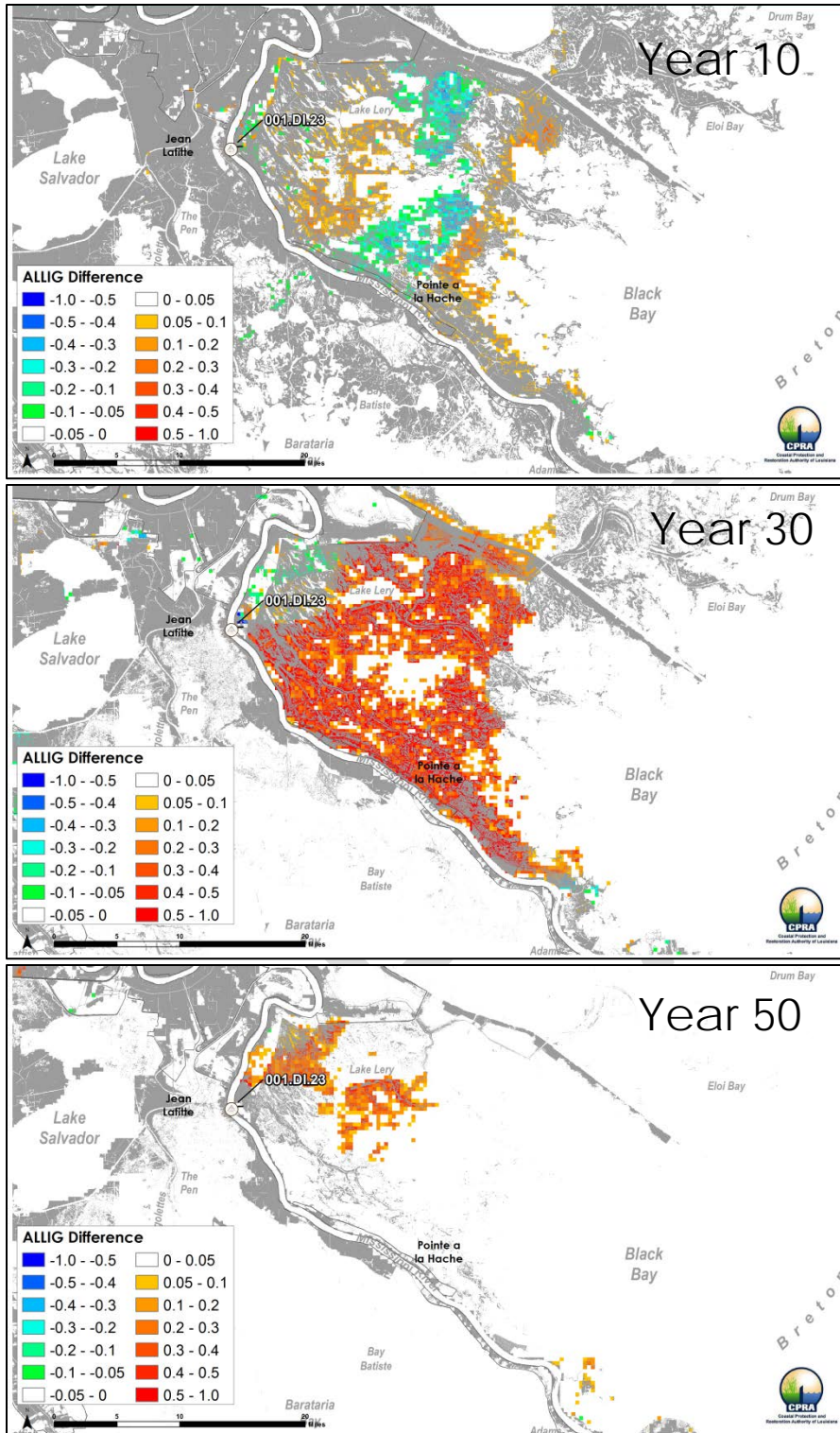


Figure 196: Difference in American Alligator Habitat Suitability for the Mid-Breton Diversion Relative to FWOA (years 10, 30, and 50; high scenario). Warmer colors indicate an increase in suitability and cooler colors indicate a decrease in suitability with the diversion.

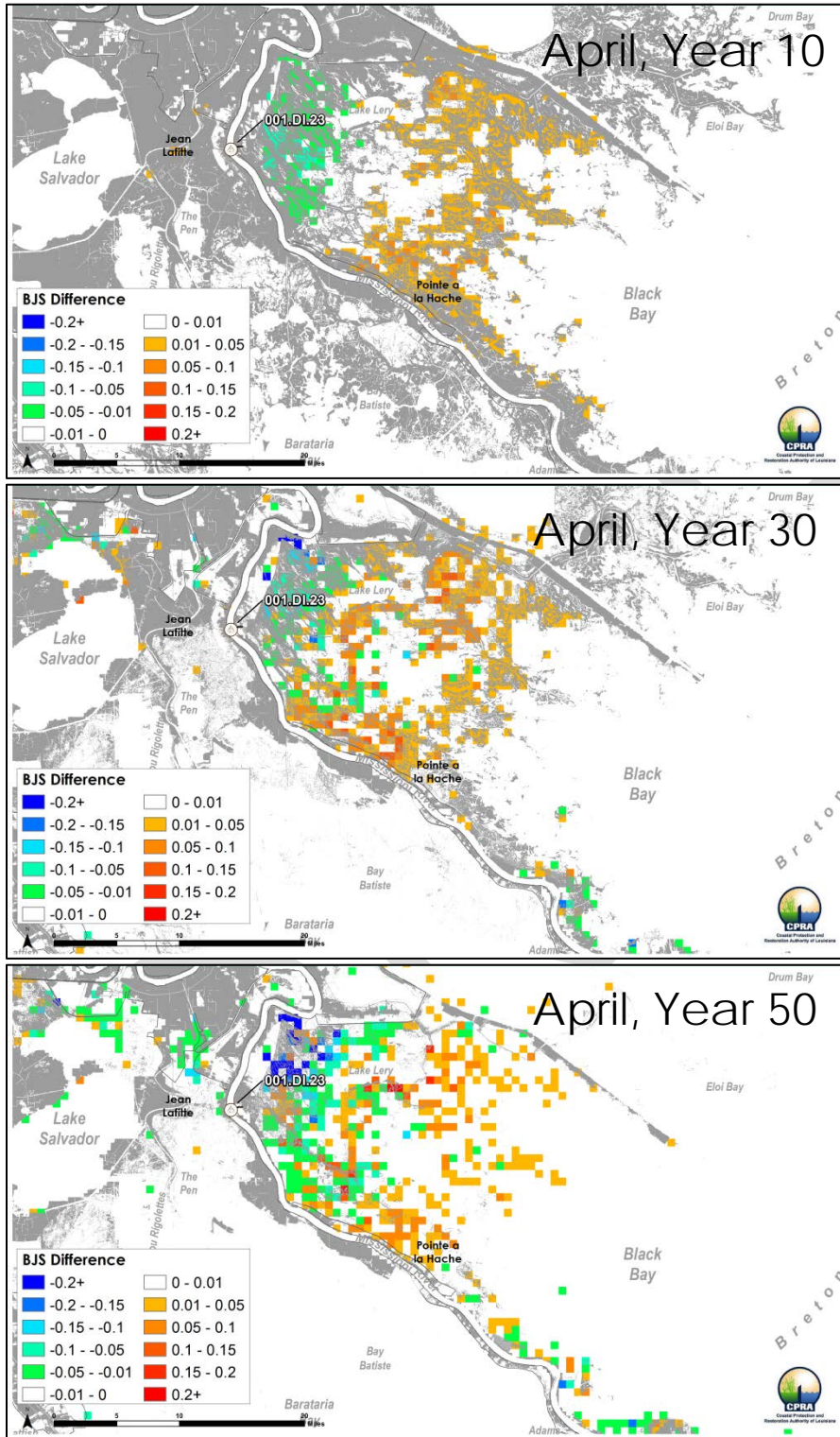


Figure 197: Difference in Juvenile Largemouth Bass Biomass for the Mid-Breton Diversion Relative to FWOA (years 10, 30, and 50; high scenario). Warmer colors indicate an increase in suitability and cooler colors indicate a decrease in suitability with the diversion.

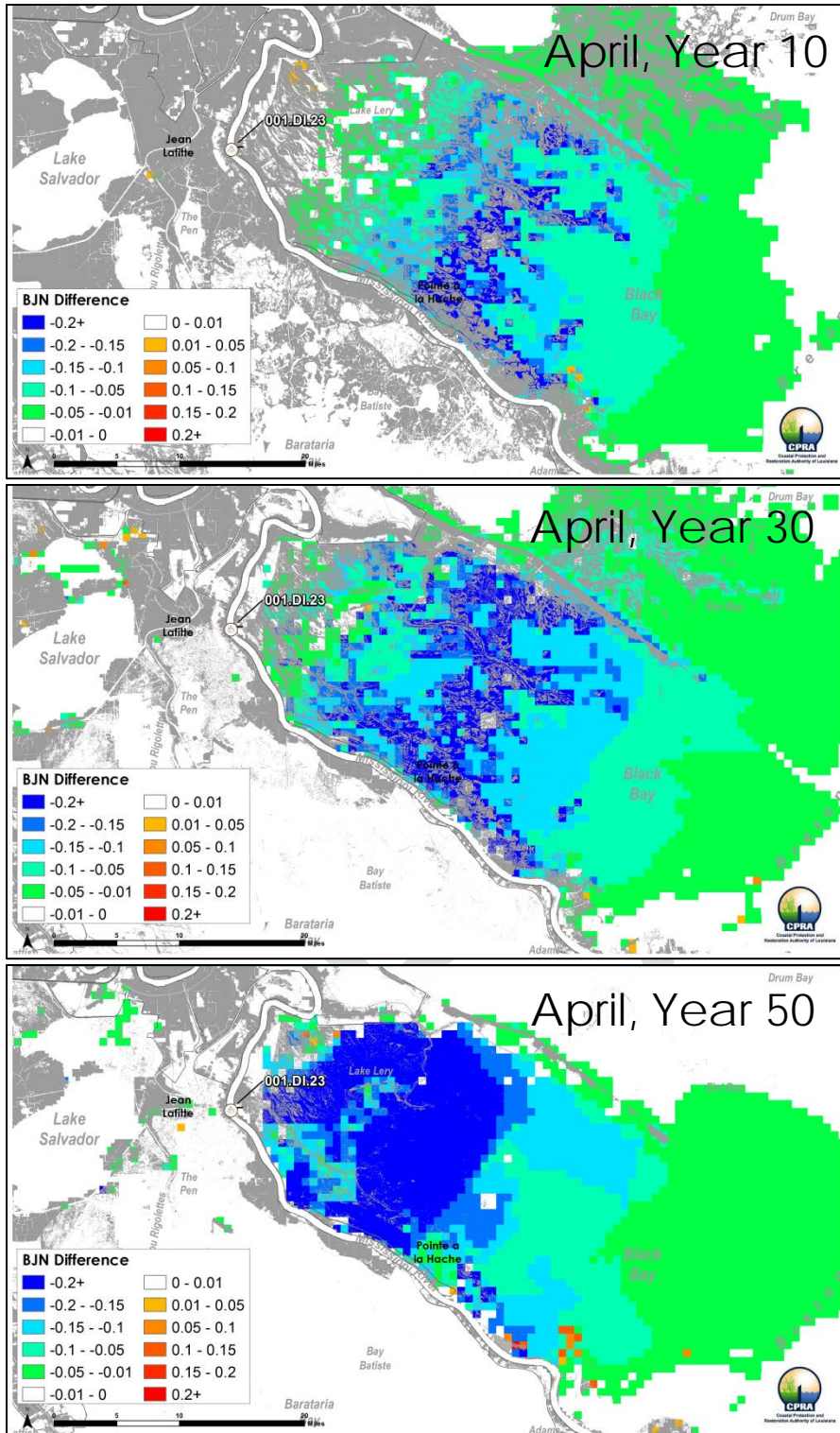


Figure 198: Difference in Juvenile Brown Shrimp Biomass for the Mid-Breton Diversion Relative to FWOA (years 10, 30, and 50; high scenario). Warmer colors indicate an increase in suitability and cooler colors indicate a decrease in suitability with the diversion.

### 4.3 South Terrebonne Marsh Creation project (03a.MC.100)<sup>4</sup>

The South Terrebonne Marsh Creation (03a.MC.100) project is located in central Terrebonne Parish southwest of Dulac, Louisiana. The goal of this project is to re-create marsh and create new wetland habitat by depositing dredged sediment in a 92 km<sup>2</sup> area between Bayou du Large and the Houma Navigation Canal. For modeling purposes, the entire marsh creation project was implemented in year 19 of the ICM simulation. It was initially built to an elevation of 0.61 m (NAVD88).

#### 4.3.1 Landscape

In the high scenario, the effects in year 20 (one year after project implementation) are evident, with land gain (areas that are water in the initial condition and are filled by dredged sediment) throughout the southern portion of the project area (Figure 199). Some areas are also sustained meaning that they were marsh in the initial condition and were lost by the time the project was implemented at which time they were filled with dredged material. Northern portions of the project area show open water even after project implementation indicating the depth criterion for marsh creation (0.76 m) was exceeded.

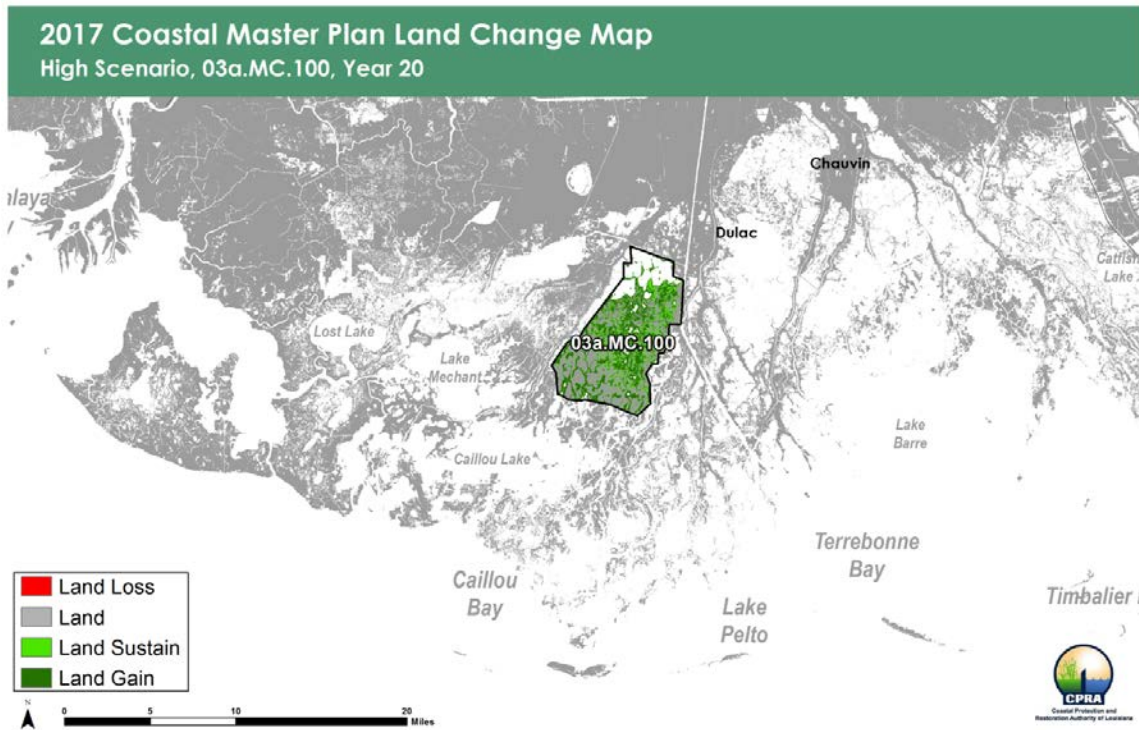


Figure 199: Land Change from the South Terrebonne Marsh Creation Relative to FWOA (year 20; high scenario).

<sup>4</sup> Decadal animations of the 50-year simulation outputs can be found in Attachment C4-3 - South Terrebonne Marsh Creation (03a.MC.100), including land and HSI.

By year 30, the land sustaining effects of the project become more prevalent (Figure 200). This effect is likely due to the increased elevation resulting from project implementation, causing marshes to persist that otherwise would be lost to open water. There is also an area of exacerbated land loss north of the project area (northwest of Dulac, LA). This occurs due to an increase in stage in this area caused by a change in flow patterns from the presence of the project. There are also far-field effects evident in year 30 (south of Turtle Bayou) which are likely due to salinity inconsistencies in the ICM Version 1 code.<sup>5</sup> Salinity instabilities in the Avoca Island Cutoff region of the model, as well as a model compartment in Central Terrebonne in Version 1, may have been dampened due to the changed flow patterns in this Central Terrebonne region, resulting in these far field differences. Figure 201 shows the difference in salinity with the project compared to FWOA for the hydro compartment just north of the project area.

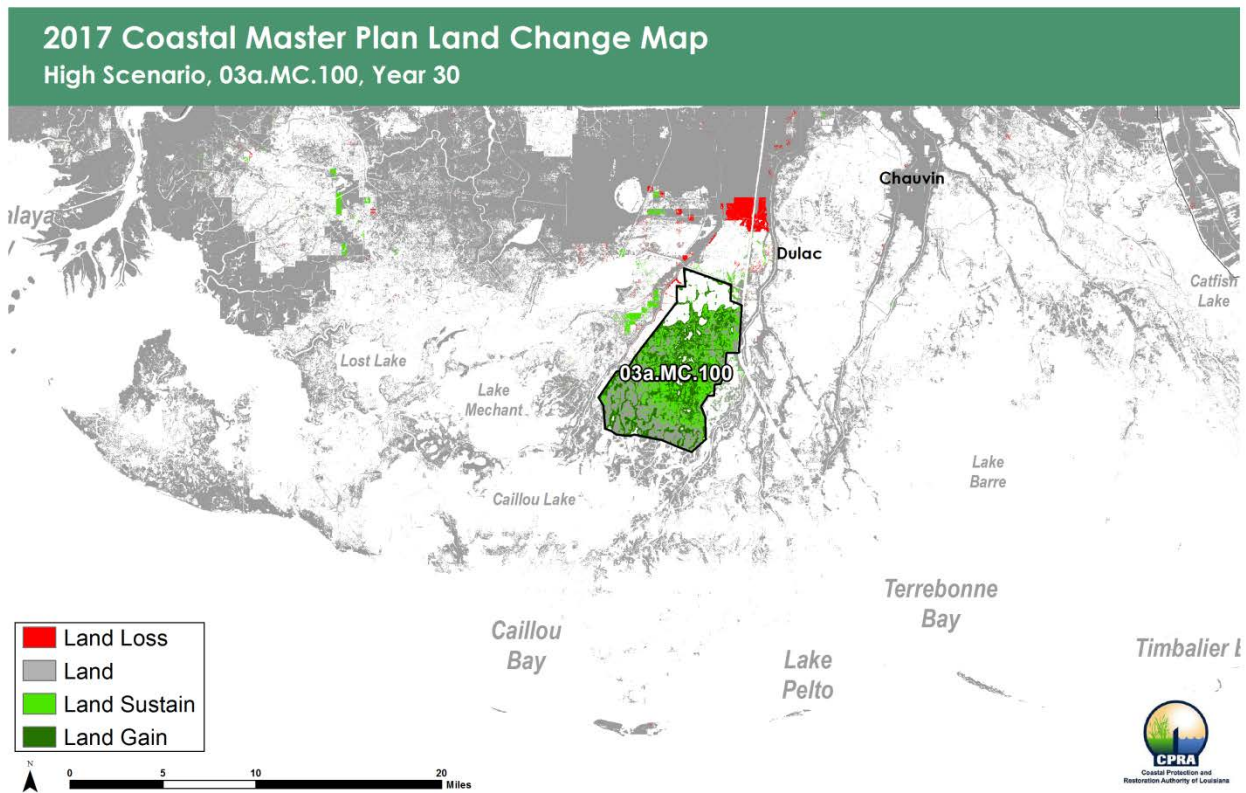
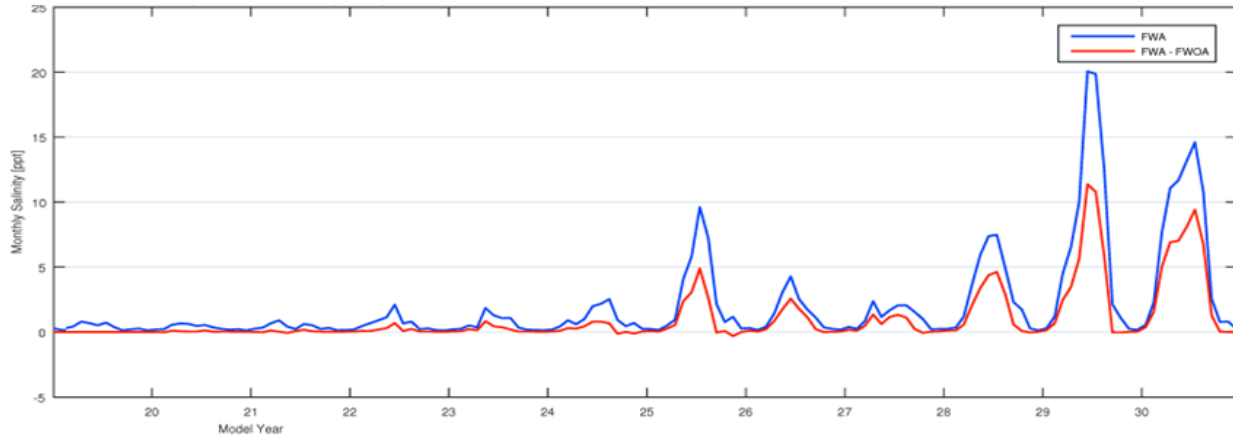


Figure 200: Land Change from the South Terrebonne Marsh Creation Relative to FWOA (year 30; high scenario).

<sup>5</sup> For information on the ICM Version 3 salinity/calibration adjustments, refer to Attachment C3-23 ICM Calibration, Validation, and Performance Assessment.



**Figure 201: Monthly Salinity (ppt) for the ICM Hydrology Compartment North of the South Terrebonne Marsh Creation Area between Years 19 and 30 of the Simulation.** The blue line indicates salinity with the project, and the red line is the difference between the project and FWOA.

By year 50, much of the initial benefit in the form of land gained or sustained is lost (Figure 202). The area is projected to mostly convert to open water under both FWOA and FWA conditions. Also by year 50, some of the far-field effects such as the hastened land loss northwest of Dulac are no longer evident, suggesting the area will experience loss eventually regardless of project implementation.

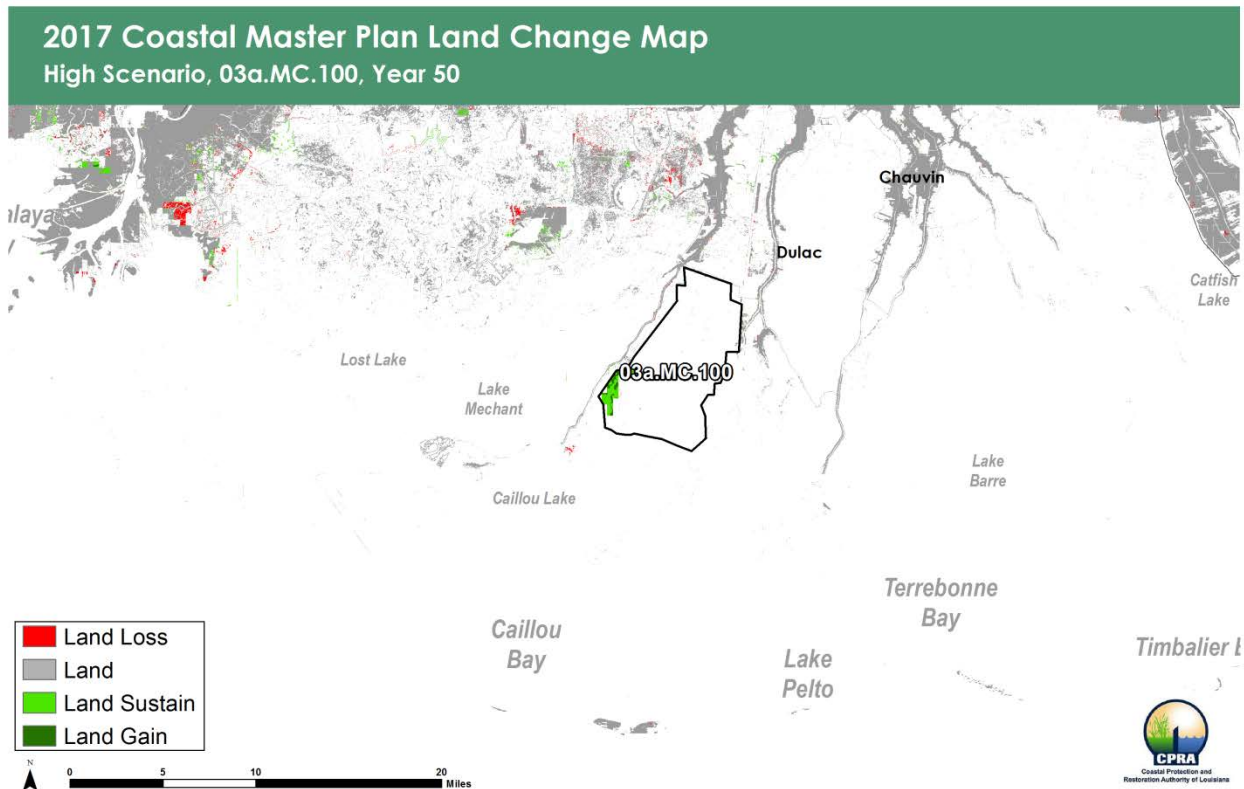


**Figure 202: Land Change from the South Terrebonne Marsh Creation Relative to FWOA (year 50; high scenario).**

Considering the overall project life, there is a substantial benefit to net land area as compared to FWOA; however, the duration of these benefits is limited. Model output indicates accretion is insufficient to maintain marsh elevations over time. The limited availability of mineral sediments needed to support prolonged accretion in this region (less than 150 g/m<sup>2</sup> are deposited on the constructed marsh surface during any given model year) contributes to an elevation deficit relative to relative sea level rise (RSLR). This deficit leads to loss of elevation relative to water level which leads to prolonged depth and duration of marsh inundation, eventually triggering the marsh collapse threshold and the conversion of that marsh to open water.

The land area benefits, which are maintained through the end of the 50-year simulation, are all areas containing the vegetation type "bare ground/upland." Bare ground occurs when the change in environmental conditions is too rapid for the model's vegetation dispersal mechanism (i.e., there is no vegetation that can tolerate the conditions within the dispersal distance). In Version 1 of the ICM, bare ground areas were not subject to a collapse criterion. These areas would likely convert to another vegetation type and then be lost in subsequent years if the modeling period were extended.

The effects due to the project in the low and medium scenarios are far more persistent, with the majority of the land gained or sustained persisting through the end of the modeling period. A land sustaining effect is more evident in the medium scenario indicating these areas would have been lost due to RSLR if not for the additional elevation due to project implementation.

#### **4.3.2 Fish, Shellfish, and Wildlife**

In general, the South Terrebonne Marsh Creation project transforms fragmented marsh into an area of relatively solid marsh. This change in landscape configuration results in a decrease in habitat suitability for small juvenile brown shrimp, adult spotted seatrout, largemouth bass, green-winged teal, and American alligator, all of which primarily utilize fragmented marsh habitats with a high degree of marsh edge. There are, however, some areas of fragmented marsh that are maintained in the northern part of the project area, which results in localized increases in habitat suitability for most of these species when compared to FWOA (e.g., small juvenile brown shrimp and largemouth bass; Figures 5 and 6).

As previously mentioned, this project also appears to modify the local hydrology, as evidenced by higher salinities within and around the project area as compared to FWOA (Figure 201). Consequently, the existing low-salinity areas north of the project area become less suitable for largemouth bass and alligator and more suitable for brown shrimp and spotted seatrout (Figure 203 and Figure 204). At the same time, the saline areas south and east of the project area become less suitable for eastern oyster and brown shrimp (Figure 203), both of which are more common at salinities between approximately 10 and 20 ppt (Attachments C3-12 and C3-13, respectively).

By the end of the 50-year simulation, the widespread saltwater intrusion and wetland loss associated with the high scenario eliminates the project's effects, resulting in essentially no difference between the project and FWOA with regard to habitat suitability (Figure 203 and Figure 204). Very little highly suitable habitat remains in the project area in the high scenario for the majority of the species.

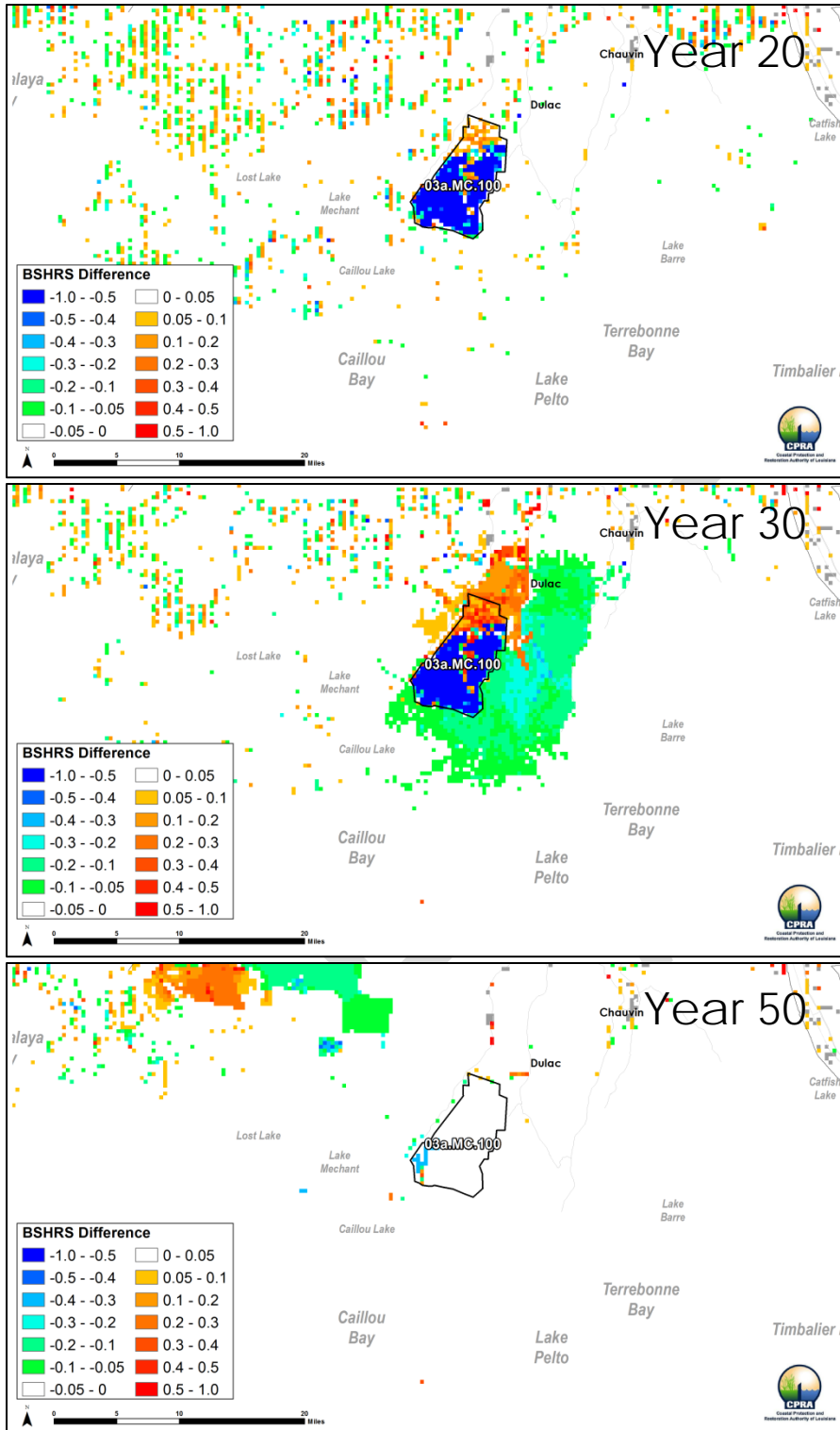


Figure 203: Difference in Small Juvenile Brown Shrimp Habitat Suitability Associated with the South Terrebonne Marsh Creation Relative to FWOA (years 20, 30, and 50; high scenario). Warmer colors indicate an increase in suitability and cooler colors indicate a decrease in suitability with the project. Land areas are removed to better show the changes in suitability.

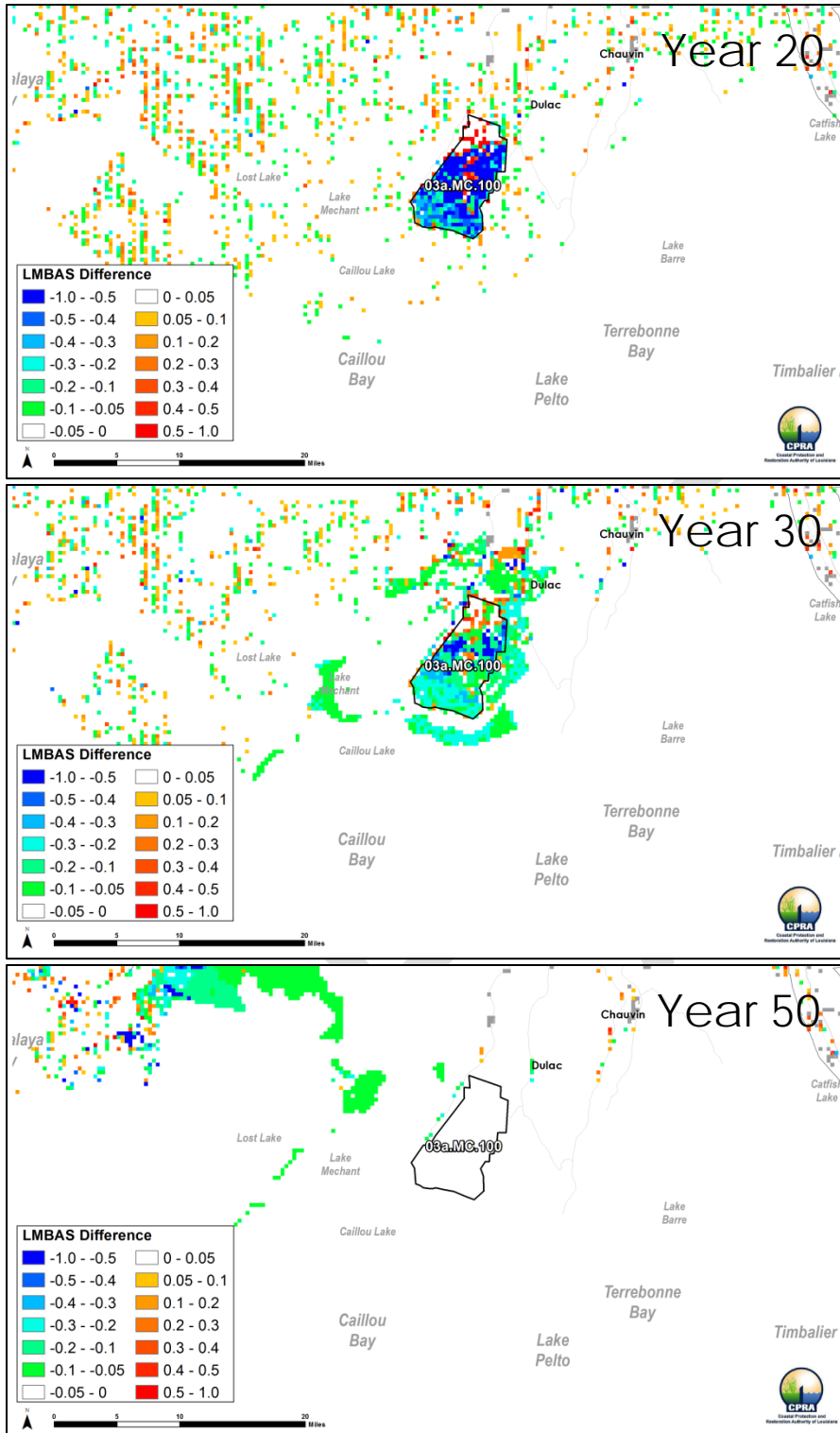


Figure 204: Difference in Largemouth Bass Habitat Suitability Associated with the South Terrebonne Marsh Creation Relative to FWOA (years 20, 30, and 50; high scenario). Warmer colors indicate an increase in suitability and cooler colors indicate a decrease in suitability with the project. Land areas are removed to better show the changes in suitability.

## 4.4 Calcasieu Ship Channel Salinity Control Measures (004.HR.06)<sup>6</sup>

The goal of the Calcasieu Ship Channel Salinity Control Measures (004.HR.06) project is to reduce saltwater intrusion into Calcasieu Lake and surrounding wetlands, thus helping to sustain the wetlands and the ecosystem benefits they provide. The project consists of an array of earthen berms and water control structures that will be built along the length of the Calcasieu Ship Channel in Calcasieu Lake and at key waterways leading into interior marshes, such as Alkali Ditch and Kelso Bayou. The project is implemented in year 4 of the ICM simulation.

### 4.4.1 Landscape

In the high scenario, this project has a strong impact, reducing mean annual salinity in the southern section of Lake Calcasieu by  $\geq 5$  ppt in year 10 (Figure 205). In addition, mean annual salinity is lowered by at least 0.5 ppt from the Sabine freshwater impoundment in the west to areas 8 km east of Highway 27 and as far north as Lake Charles (Figure 205). However, these changes in hydrology have no effect on land change in the region in year 10 (Figure 206). The salinity changes do affect the vegetation, and there is  $67 \text{ km}^2 \text{ yr}^{-1}$  more fresh marsh and  $3 \text{ km}^2 \text{ yr}^{-1}$  more forested wetland in the Calcasieu/Sabine ecoregion with the project than in FWOA, while brackish ( $- 40 \text{ km}^2 \text{ yr}^{-1}$ ) and saline marsh ( $- 30 \text{ km}^2 \text{ yr}^{-1}$ ) extent both decline in year 10 (Figure 207).

At year 20, there is a positive effect on land change in the Calcasieu/Sabine ecoregion (Figure 208), which is due to wetland areas sustained along the Gulf Intracoastal Waterway. The project also induces some land loss in the area just north of Lower Mud Lake, where fresh marsh occurs among Chenier ridges with the project thus more vulnerable to salinity intrusion (see year 20 land change map in Attachment C4-4). In FWOA, this area is brackish and less sensitive to salinity increases. At year 20, the project induces land loss in the Mermentau Lakes, which is primarily due to a small increase ( $< 2 \text{ cm}$ ) in mean annual water level. Therefore, the overall effect of the project on land along the western coast is negative at this point in the simulation (Figure 208).

---

<sup>6</sup> Decadal animations of the 50-year simulation outputs can be found in Attachment C4-4 - Calcasieu Ship Channel Salinity Control Measures (004.HR.06), including stage, salinity, land, vegetation, HSLs, and EwE.

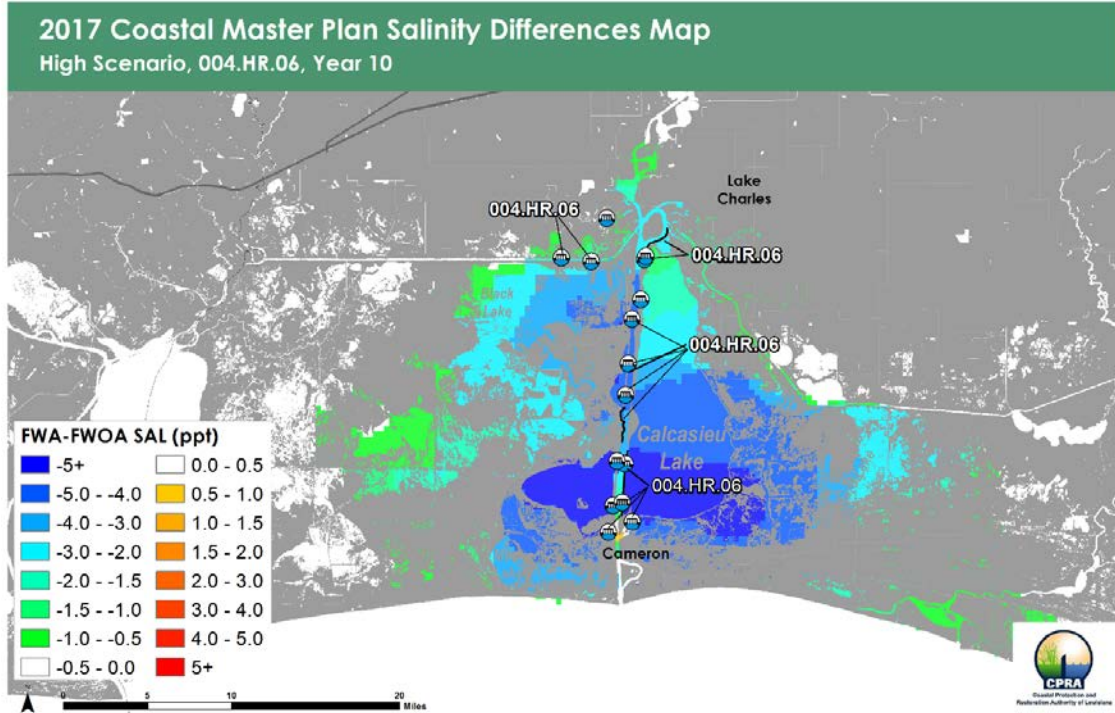


Figure 205: Change in Salinity from the Calcasieu Ship Channel Salinity Control Measures Project Relative to FWOA (year 10; high scenario).



Figure 206: Land Change from the Calcasieu Ship Channel Salinity Control Measures Project Relative to FWOA (year 10; high scenario).

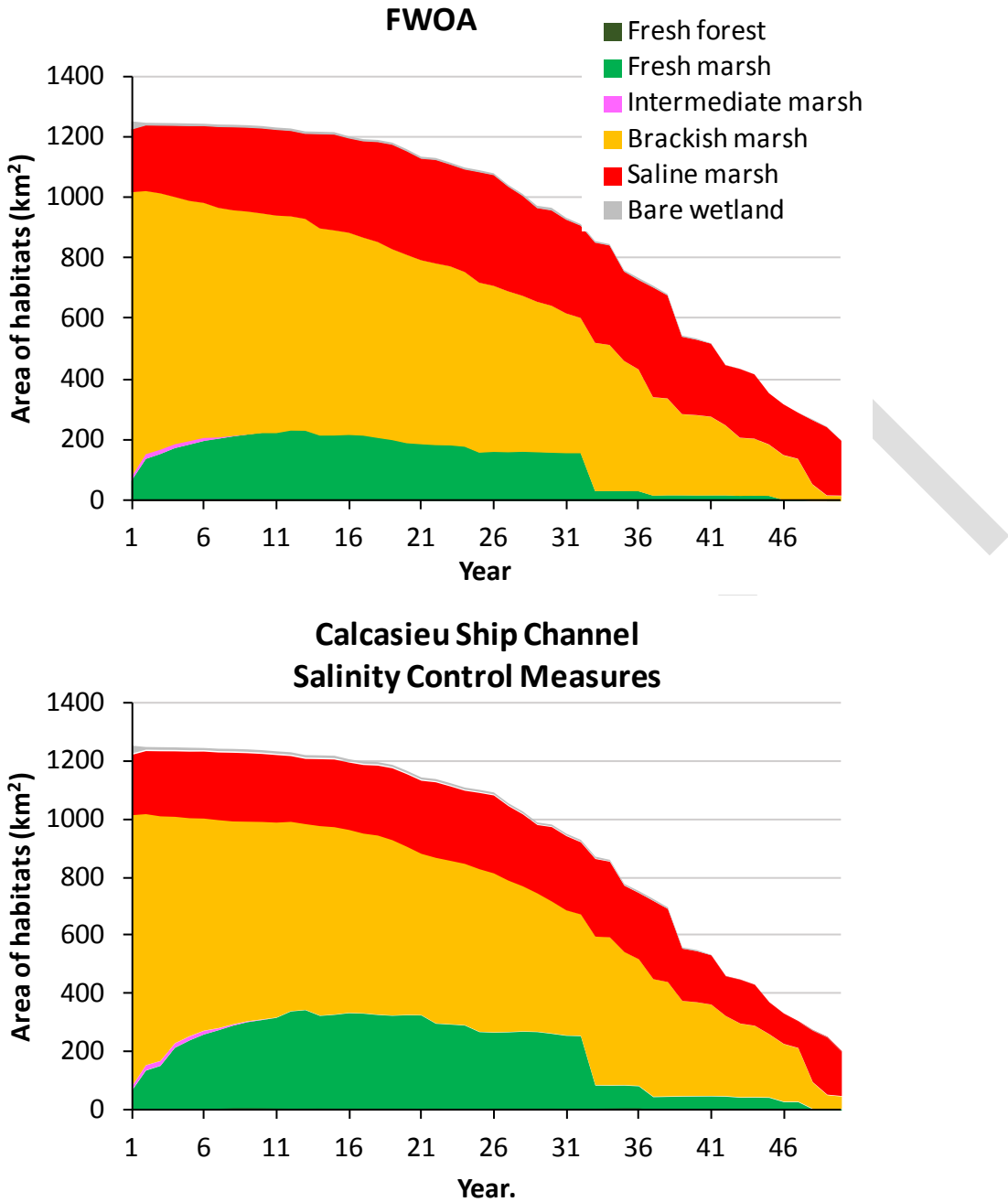
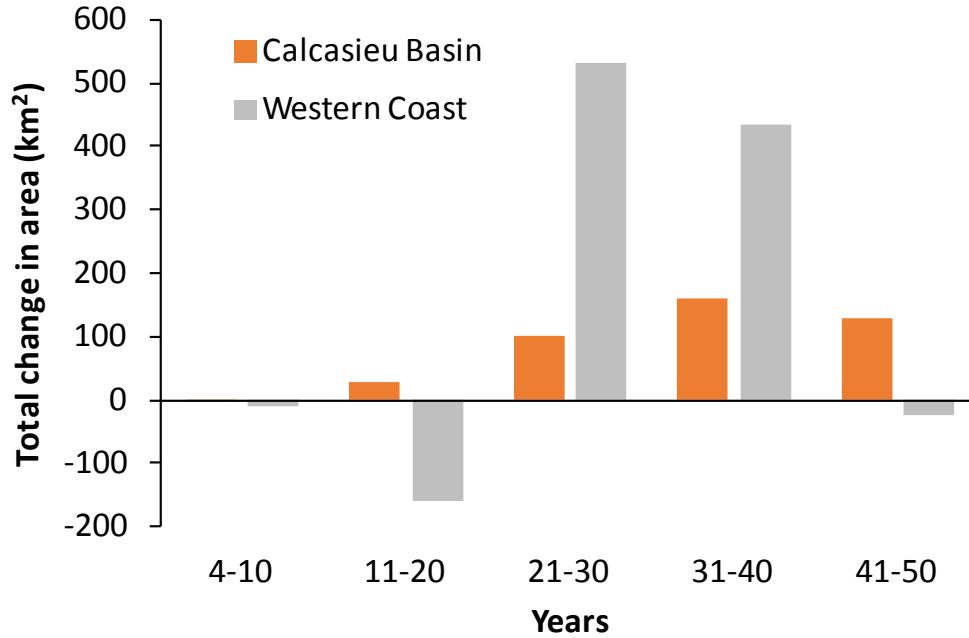


Figure 207: Change in Wetland Habitat over Time within the Calcasieu/Sabine Ecoregion in FWOA and with the Calcasieu Ship Channel Salinity Control Measures Project (high scenario).



**Figure 208: Change in Land Area within the Calcasieu/Sabine Ecoregion and in the Western Coast in Response to the Calcasieu Ship Channel Salinity Control Measures Project (relative to FWOA; high scenario).**

At year 30, the project has positive effects on land change both in Calcasieu/Sabine ecoregion and the western coast (Figure 208). In the Calcasieu/Sabine ecoregion, sustained land is scattered throughout, but in the Mermentau Lakes ecoregion more land is sustained than lost (Figure 209). Most of the land loss due to the project occurs in year 24 of the simulation. A large swath of marsh is maintained as fresh marsh with the project through year 23. In year 24, increased sea level rise combined with land loss in the region allows for more overland flow and thus more saline water to penetrate deeper into the coast, and these fresh marsh areas are lost. In FWOA, the marsh in this region is already brackish and therefore less susceptible to the salinity increase associated with the increased overland flow. The areas sustained include fresh water marshes north of the Gulf Intracoastal Waterway, where salinity is changed less than 0.5 ppt and where water levels are lowered by less than 2 cm (Figure 210 and Figure 211). The marshes sustained in the Calcasieu/Sabine ecoregion primarily occur in areas of high (>4 ppt) reduction in salinity, adjacent to Black Lake and Sweet Lake.



Figure 209: Land Change from the Calcasieu Ship Channel Salinity Control Measures Project Relative to FWOA (year 30; high scenario).

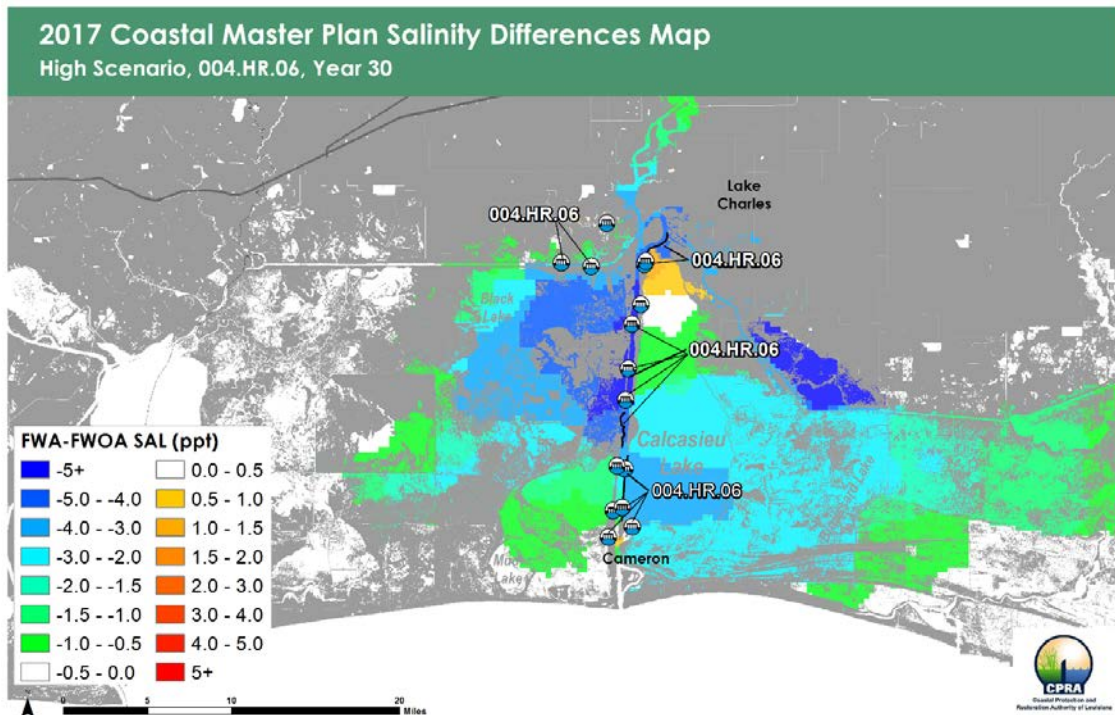


Figure 210: Change in Salinity Resulting from the Calcasieu Ship Channel Salinity Control Measures Project Relative to FWOA (year 30; high scenario).

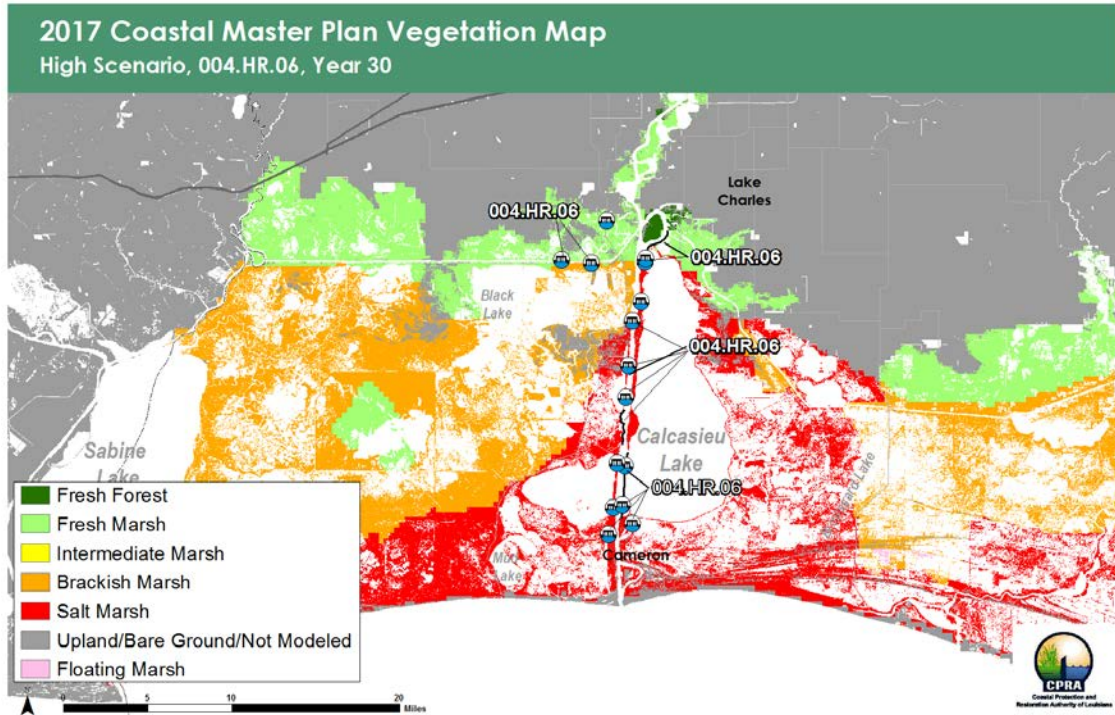
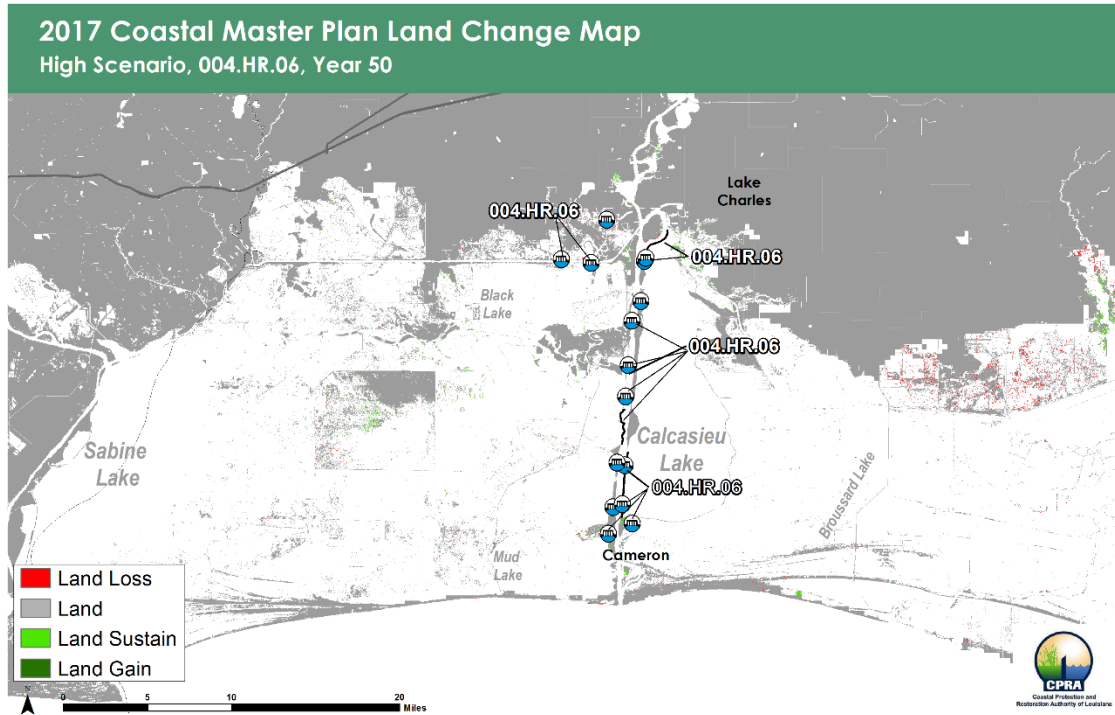


Figure 211: Wetland Habitat Distribution Associated with the Calcasieu Ship Channel Salinity Control Measures Project (year 30; high scenario).

Under the high scenario, drastic land loss occurs throughout the Calcasieu/Sabine ecoregion by years 40 and 50 (Figure 207 and Figure 208), and similar rates of loss also occur in the Mermentau Lakes and Eastern Chenier ridge ecoregions. The presence of the Calcasieu Ship Channel Salinity Control Measures project allows some wetland areas to be sustained longer than in FWOA, which results in the land gain associated with the project in years 40 and 50. However, by year 50, most of the wetlands in the area have converted to open water either with or without the project (Figure 212).



**Figure 212: Land Change from the Calcasieu Ship Channel Salinity Control Measures Project Relative to FWOA (year 50; high scenario).**

Under the medium scenario, habitat change the Calcasieu/Sabine ecoregion is much lower than under the high scenario (Figure 207 and Figure 213). Under the medium scenario, the project has a positive impact on land change throughout the western coast especially in the last 30 years of the model run (Figure 214). In the Calcasieu/Sabine ecoregion, when comparing average annual land gain relative to FWOA under the two scenarios, the project has a greater average amount of land gained over the 50-year simulation under the high scenario ( $41.5 \text{ km}^2 \text{ yr}^{-1}$ ) compared to the medium scenario ( $34.9 \text{ km}^2 \text{ yr}^{-1}$ ).

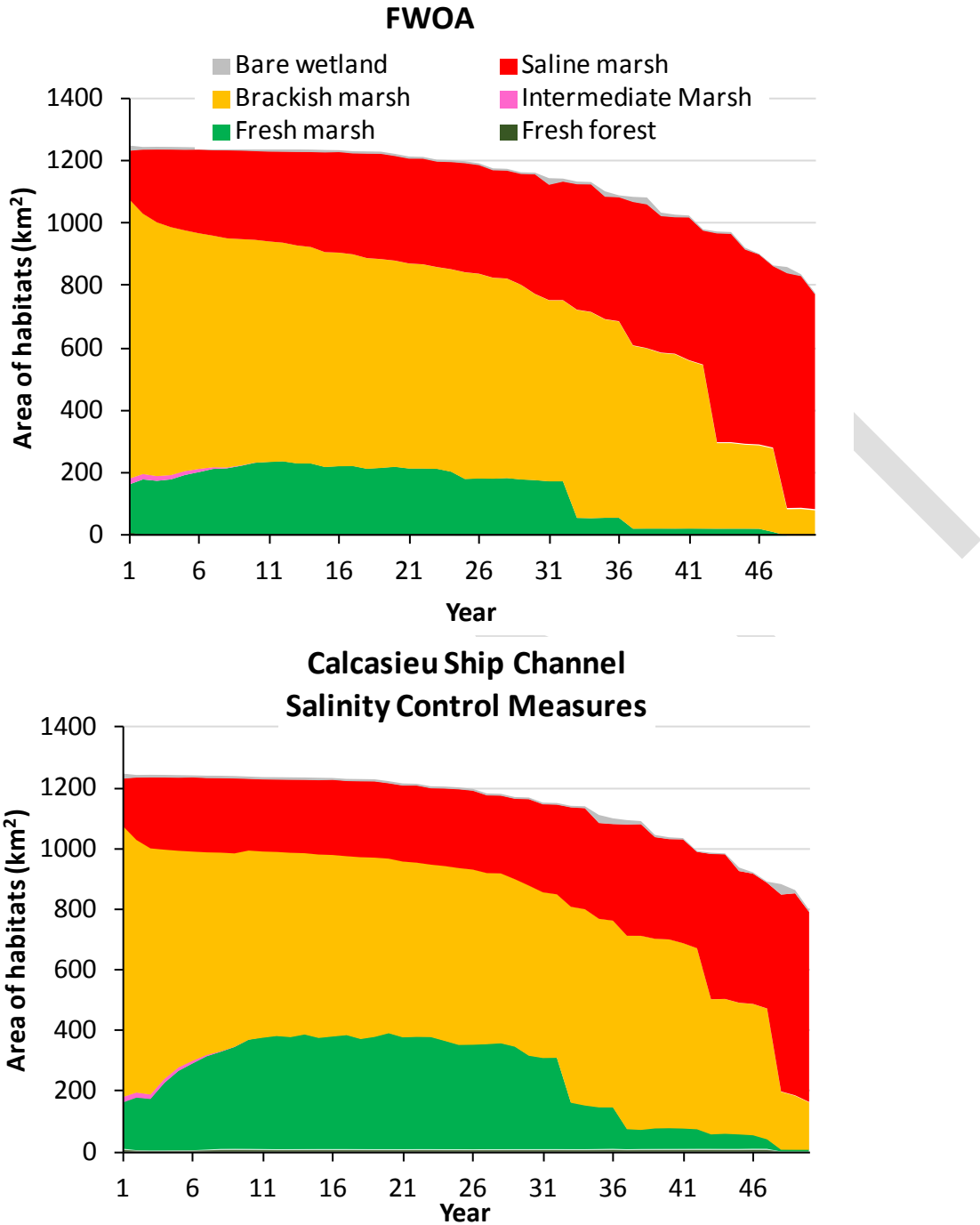


Figure 213: Change in Wetland Habitat over Time within the Calcasieu/Sabine Ecoregion in FWOA and with the Calcasieu Ship Channel Salinity Control Measures Project (medium scenario).

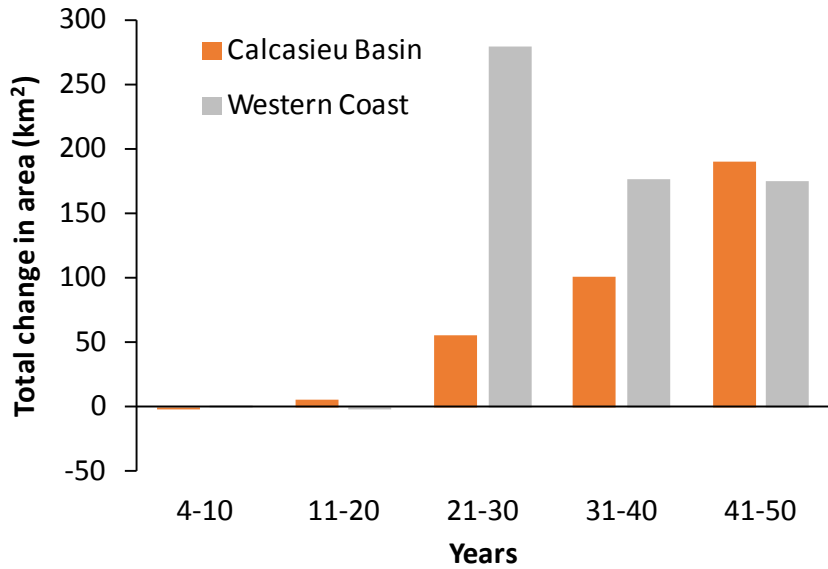


Figure 214: Change in Land Area within the Calcasieu/Sabine Ecoregion and in the Western Coast in Response to the Calcasieu Ship Channel Salinity Control Measures Project (relative to FWOA; medium scenario).

Under the medium scenario, water level changes are similar to the high scenario in amplitude and extent, but the area where salinity is dropped by >2 ppt is larger in extent under the medium scenario compared to the high scenario (Figure 215). Despite the impact of the project, most of the remaining wetland area in the Calcasieu/Sabine ecoregion is saline marsh under either scenario at year 50 (Figure 207 and Figure 213). Only a slight increase in brackish marsh at year 50 occurs due to the Calcasieu Ship Channel Salinity Control Measures project.

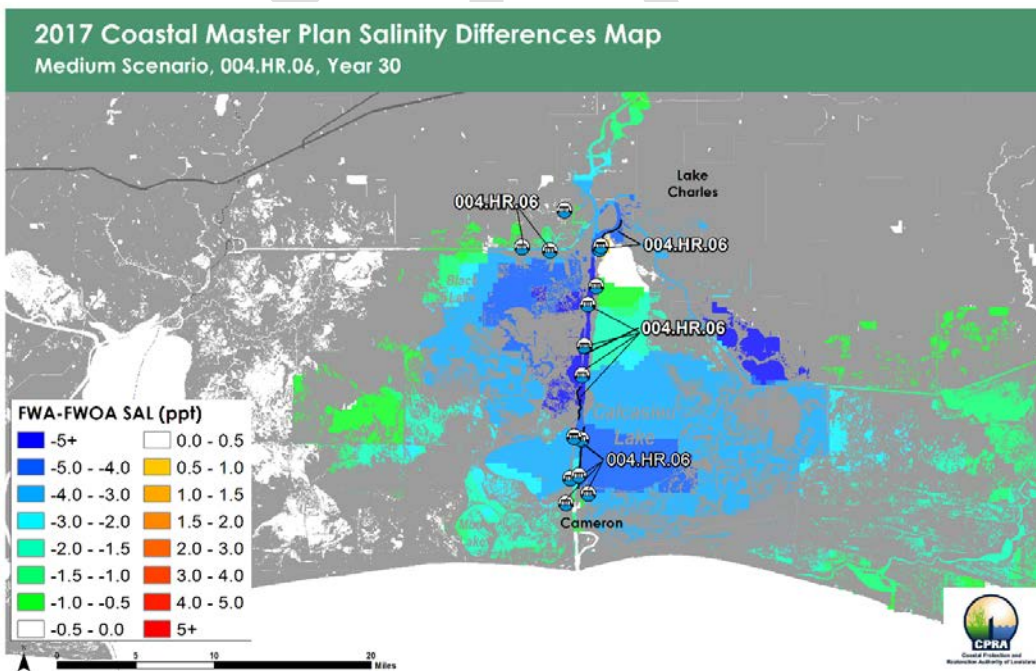


Figure 215: Change in Salinity from the Calcasieu Ship Channel Salinity Control Measures Project Relative to FWOA (year 30; medium scenario).

#### 4.4.2 Fish, Shellfish, and Wildlife

The salinity reduction associated with the Calcasieu Ship Channel Salinity Control Measures project generally decreases habitat suitability relative to FWOA for small juvenile brown shrimp, adult spotted seatrout, and oysters throughout much of the project influence area. The decrease in habitat suitability for brown shrimp and spotted seatrout is relatively small (mostly <0.2 decrease in HSI relative to FWOA) due to these species' broader salinity tolerances (Attachments C3-13 and C3-16). Larger decreases in suitability are observed for oysters, particularly in the southern part of Calcasieu Lake, where salinity reduction is greatest and the majority of cultch substrate is located (Figure 216). In the northern part of Calcasieu Lake, the minimal amount of cultch assumed for this area increases in suitability relative to FWOA (Figure 216). This is because the project also reduces the negative effect that seasonal, low-salinity flooding events have on oyster habitat in northern Calcasieu Lake (Attachment C3-12).

In contrast, the salinity reduction increases habitat suitability relative to FWOA for largemouth bass, green-winged teal, and American alligator. Consistent with these species' habitat utilization patterns, the interior fragmented marshes generally show the greatest increases in suitability (e.g., largemouth bass; Figure 217). Alligator, however, primarily utilize areas with a high proportion of wetland and do not utilize habitat classified as salt marsh (Attachment C3-10); therefore, increases in alligator habitat suitability are less extensive than for bass and teal.

The high rate of RSLR associated with the high scenario overwhelms the project's effects on salinity and thus habitat suitability during the latter part of the 50-year simulation. Consequently, there is little difference in species' habitat suitability between the project and FWOA at year 50 (e.g., oyster and largemouth bass; Figure 216 and Figure 217). However, the project does maintain lower salinities in the northern part of the project area near the Calcasieu River, resulting in areas of high habitat suitability for largemouth bass and alligator (Figure 217).

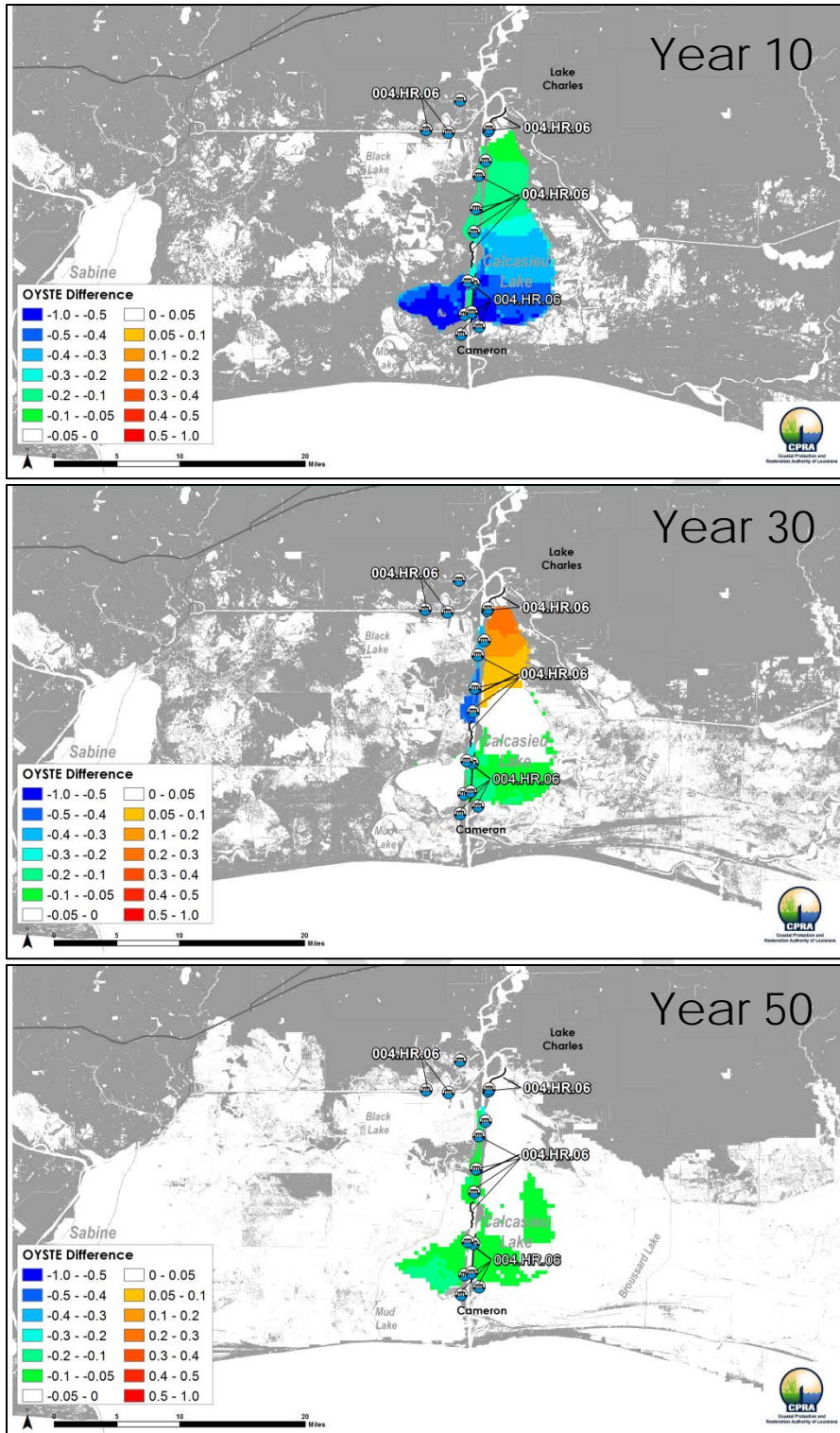


Figure 216: Difference in Eastern Oyster Habitat Suitability Associated with the Calcasieu Ship Channel Salinity Control Measures Project Relative to FWOA (years 20, 30, and 50; high scenario). Warmer colors indicate an increase in suitability and cooler colors indicate a decrease in suitability with the project.

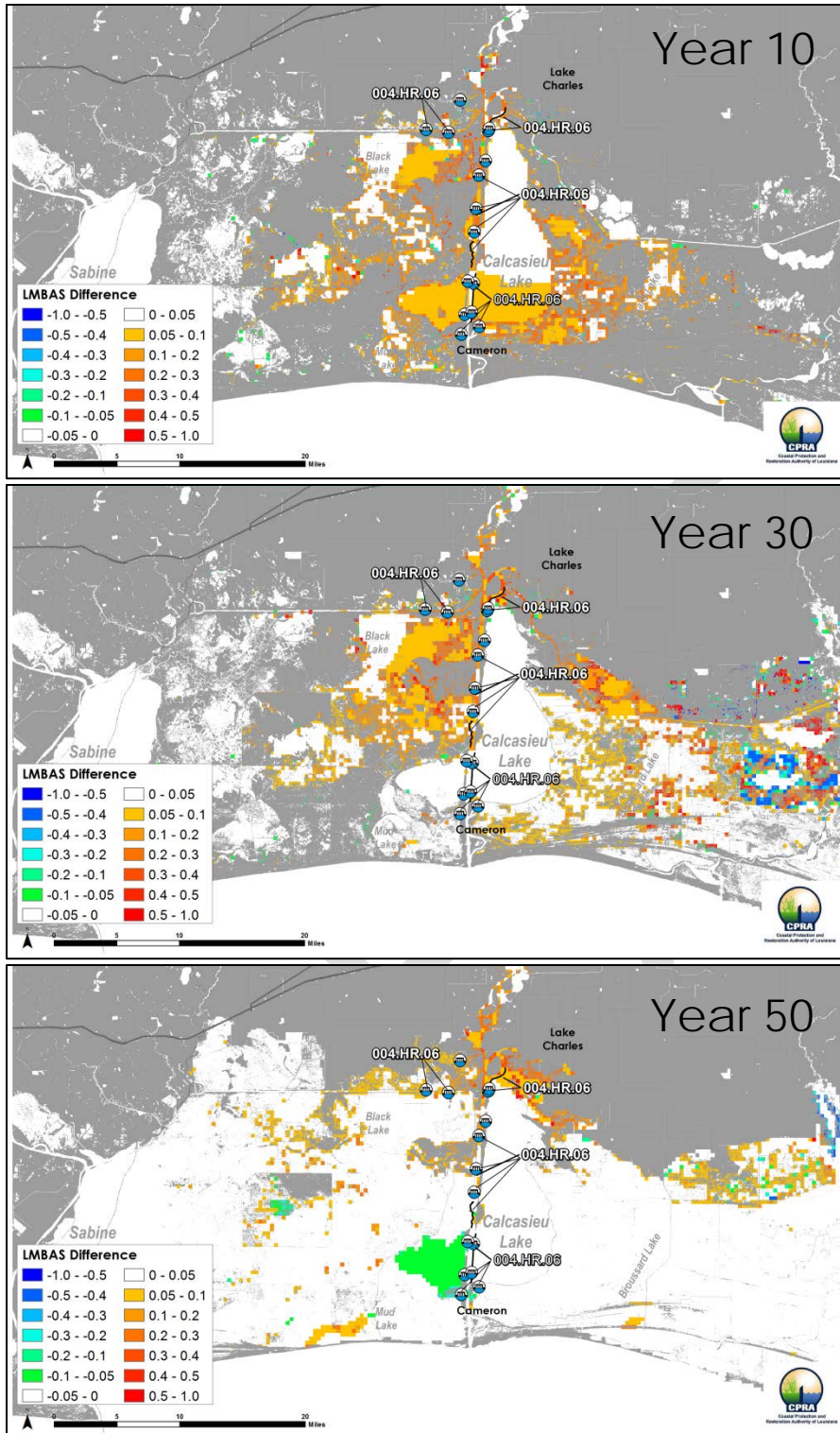


Figure 217: Difference in Largemouth Bass Habitat Suitability Associated with the Calcasieu Ship Channel Salinity Control Measures Project Relative to FWOA (years 20, 30, and 50; high scenario). Warmer colors indicate an increase in suitability and cooler colors indicate a decrease in suitability with the project.

## 4.5 Lake Hermitage Shoreline Protection (002.SP.100)<sup>7</sup>

The Lake Hermitage Shoreline Protection (002.SP.100) project (implemented in year 5) is located in Plaquemines Parish, Louisiana around Lake Hermitage. The project includes shoreline protection using rock breakwaters of approximately 2,343 m around the southern shore of Lake Hermitage to preserve shoreline integrity and reduce wetland degradation from wave erosion.

In the high scenario, the effects in year 10 are the most extreme effects over the 50-year simulation, even though the change is minimal (Figure 218). There is a very small area of sustained land (as compared to FWOA) in a small pond south of Lake Hermitage near the shoreline protection project. Just south of that small area of sustained land, there is an equally sized area of land loss.

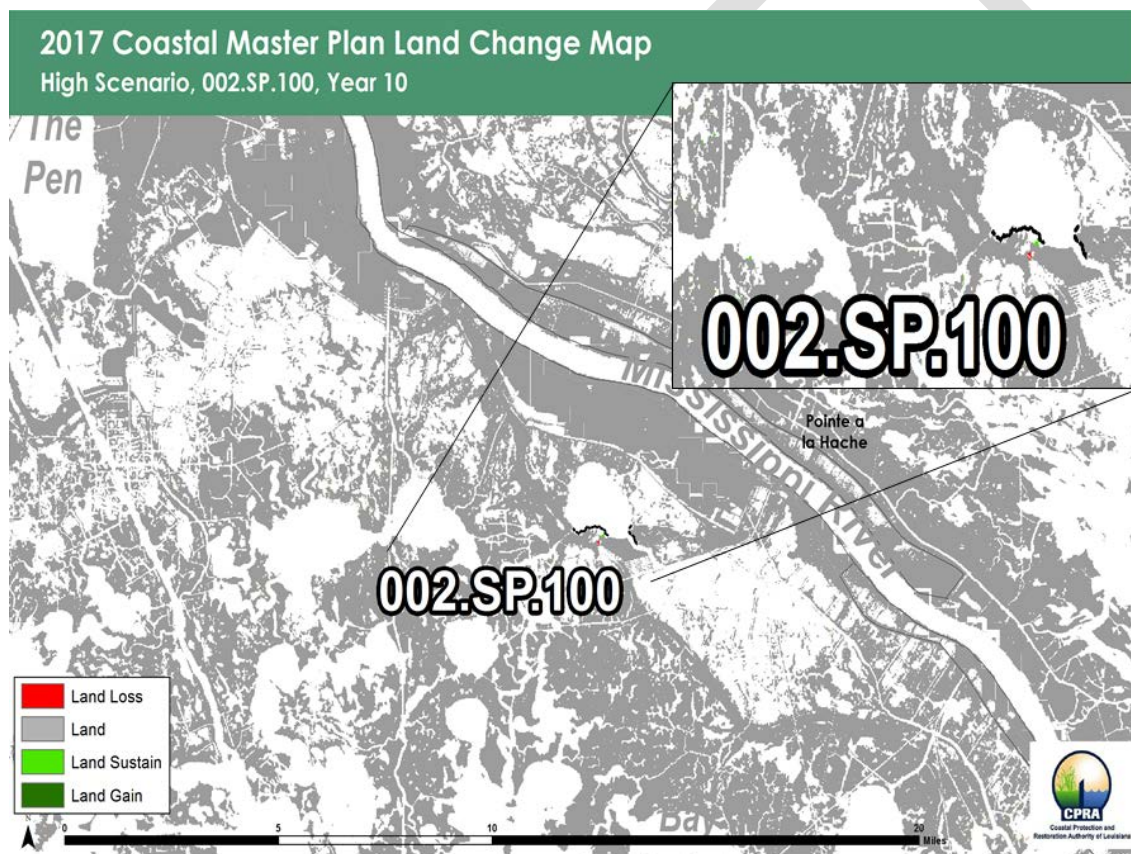


Figure 218: Land Change from Lake Hermitage Shoreline Protection Relative to FWOA (year 10; high scenario). The project is represented by the black line on the southern shore of Lake Hermitage.

<sup>7</sup> Decadal animations of the 50-year simulation outputs can be found in Attachment C4-5 - Lake Hermitage Shoreline Protection (002.SP.100), including land.

The small area of land loss south of Lake Hermitage is not present in the results for the low scenario. In year 20, there are less scattered, minor areas of land loss in the low scenario versus the high scenario. In years 30 through 50 for the low scenario, there is no project-induced land change, as was also observed in the high scenario. With the exception of the results at year 20, there is no noticeable difference in project effect between the low and medium scenario. In year 20, there is more scattered land loss in the medium scenario than in the low scenario in the area west of the project site. Otherwise, the project effects are very similar between the low and medium scenario. The low scenario is the only simulation in which the project has land adjacent to it in year 50, and thus it represents the only conditions simulated under which the project seems to have any effect.

The overall lack of project effects observed is likely in part due to the spatial resolution of the model.

#### **4.6 Grand Lake Bank Stabilization (004.BS.01)<sup>8</sup>**

The Grand Lake Bank Stabilization (004.BS.01) project (implemented in year 8) is located in Cameron Parish, Louisiana, around Grand Lake and Mallard Bay. The project includes bank stabilization through earthen fill placement, high performance turf reinforcement mat, and vegetative plantings of approximately 91,048 m of perimeter shoreline at Grand Lake to preserve shoreline integrity and reduce wetland degradation from wave erosion.

In the high scenario, the project effects in year 10 (two years after project implementation) are minimal, with minor land sustained (as compared to FWOA) in two small ponds along the western edge of Grand Lake and along the southeast/east edge of Grand Lake (where the project was placed). In year 20, there is more area along the eastern edge of the lake in which land was sustained (Figure 219).

---

<sup>8</sup> Decadal animations of the 50-year simulation outputs can be found in Attachment C4-6 - Grand Lank Bank Stabilization (004.BS.01), including land.

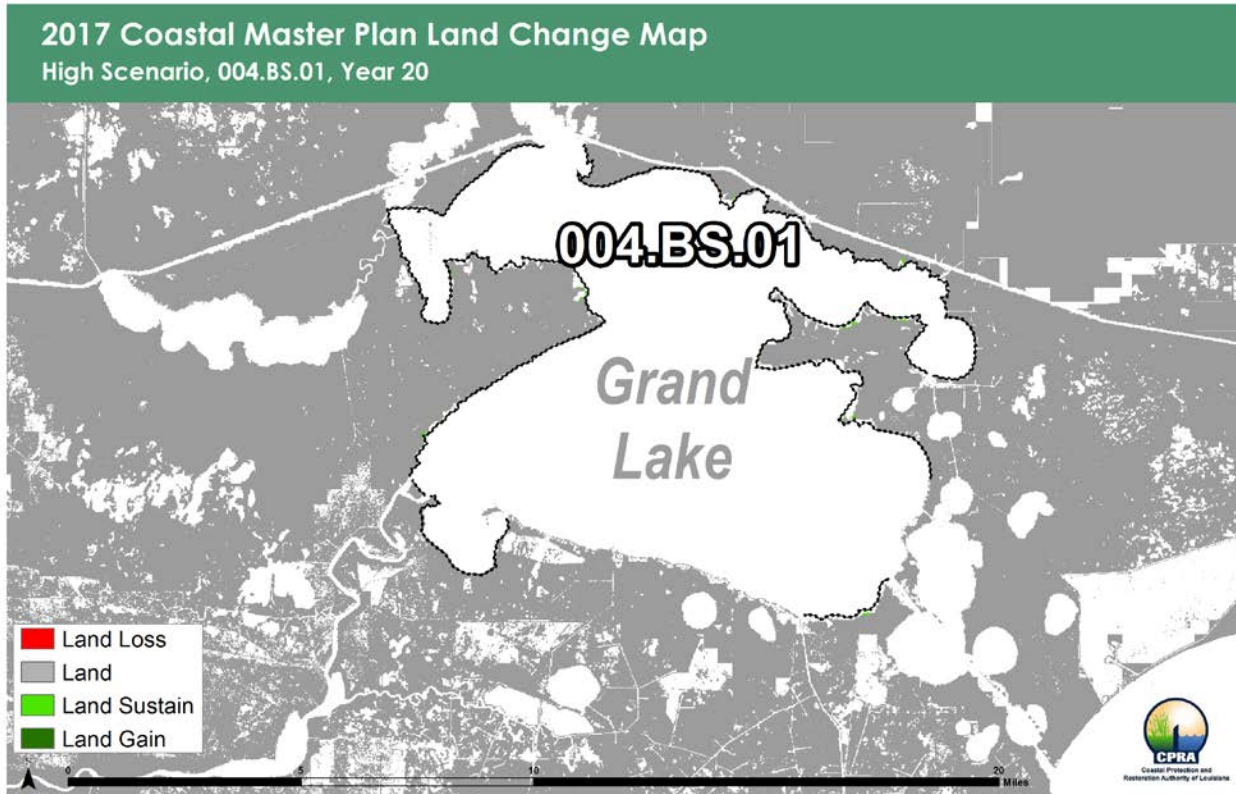


**Figure 219: Land Change from Grand Lake Bank Stabilization Relative to FWOA (year 20; high scenario).** The project is represented by the black line along the perimeter of Grand Lake.

In year 30, the land surrounding the lake has undergone major losses due to marsh collapse rather than the edge erosion the project is designed to limit. The project seems to have lost what little positive effect it previously had on the region due to the surrounding land loss. Small areas of sustained land can be seen in two locations on the west side of Grand Lake. The land difference observed north of Grand Lake, due to slightly altered hydrology, falls within the model uncertainty, and thus is not considered a major project effect.

In year 40, the banks of Grand Lake are barely detectable among the surrounding deteriorated land (Figure 220). No areas of sustained land or land gain due to the project are visible; however, small areas of land loss are seen in the region north of Mallard Bay.

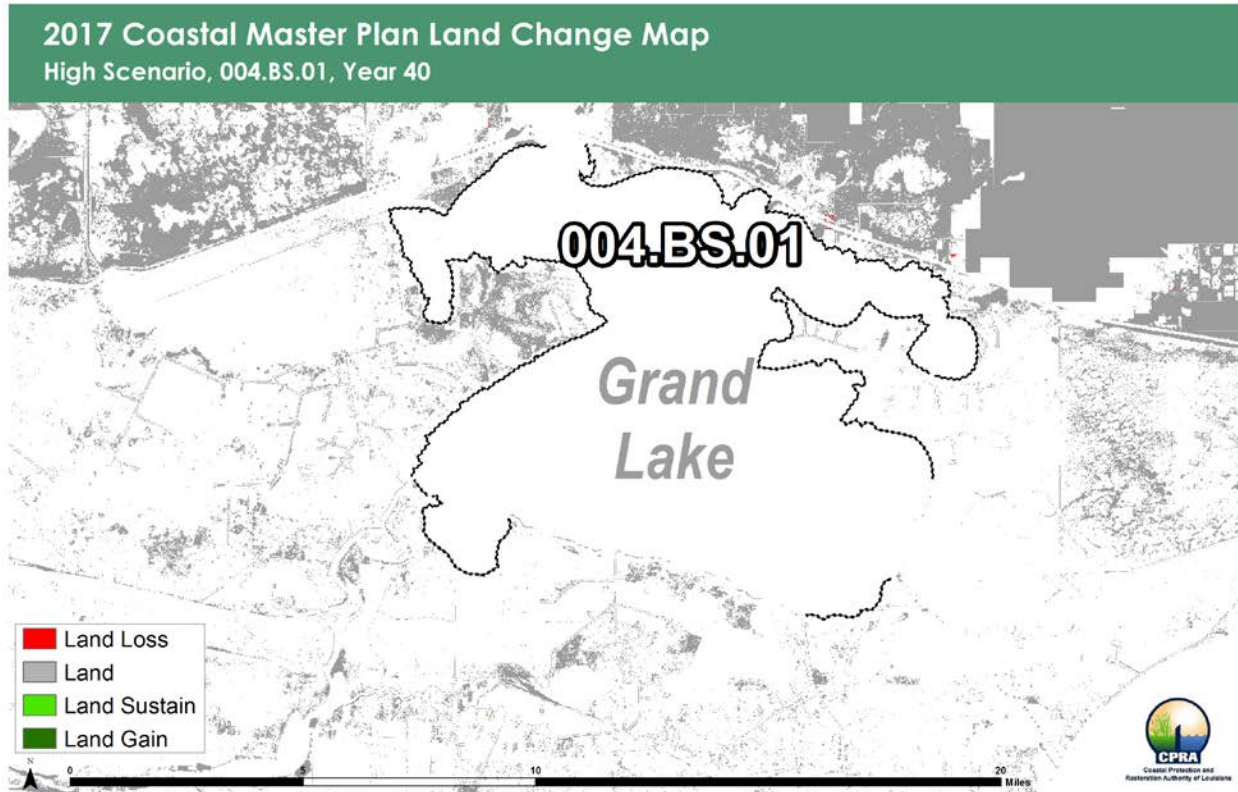


**Figure 220: Land Change from Grand Lake Bank Stabilization Relative to FWOA (year 40; high scenario).** The project is represented by the black line along the perimeter of Grand Lake.

Similar results are seen in year 50 in the high scenario. By this time in the simulation, the land south of the Gulf Intracoastal Waterway is lost in both FWOA and with the project in place, with only a few residual land fragments remaining. A small area of land loss due to the project is observed north of Mallard Bay.

There is little to no change in effects due to the project in the low scenario versus the high scenario in years 10 and 20. In years 30 through 50, the land loss north of Mallard Bay seen in the high scenario is not visible in the low scenario, which verifies that this land loss is associated with marsh collapse (as opposed to marsh edge erosion). In the low scenario, land sustained in years 30 through 50 is still evident. The medium scenario shows effects similar to the low scenario; however, some very small areas of land difference north of Mallard Bay are seen in years 40 and 50. The results indicate that the project performs as intended (by protecting the land in the immediate vicinity of the stabilization project) prior to major land loss in the surrounding area due to marsh collapse processes. The greater the rate of ESLR prescribed within each scenario, the more quickly the project loses its protective capabilities.

The overall lack of project effects observed is likely in part due to the spatial resolution of the model.

## 4.7 Bayou Decade Ridge Restoration (03a.RC.01)<sup>9</sup>

The Bayou Decade Ridge Restoration (03a.RC.01) project (implemented in year 5) is located in Terrebonne Parish, Louisiana from Lake Decade to Lost Lake. The project includes the restoration of approximately 12,986 m of historic ridge along Bayou Decade to provide coastal upland habitat, restore natural hydrology, and provide wave attenuation.

In the high scenario, the effects in year 10 are minimal, with minor land loss (as compared to FWOA) south of the project between the project site and Lake Mechant. In year 20, there is minor land loss in the same area, but more exaggerated losses north of the project near Lost Lake, Lake Penchant, and Lake Decade (Figure 221). This is likely due to altered hydrologic connections in the model. In year 30, the ridge is surrounded by deteriorated and fragmented land. Spatially variable regions of land loss and sustained land under project implementation compared to FWOA are seen approximately 8 km northeast and 8 km northwest of the project. No clear or substantive pattern of land change is evident. In year 40, the project is entirely surrounded by water due to continued land loss (Figure 222), though some fringe marsh is present between the project and off-shore. The area around Lake Mechant and Bayou Dularge shows the greatest amount of sustained land during the simulation. There is also an area of land loss closer to Lake Mechant (again, likely due to altered hydrologic connections in the model). In year 50, additional land is lost north of the project, and the land sustained near Bayou Dularge continues from year 40.

---

<sup>9</sup> Decadal animations of the 50-year simulation outputs can be found in Attachment C4-7 - Bayou Decade Ridge Restoration (03a.RC.01), including land.

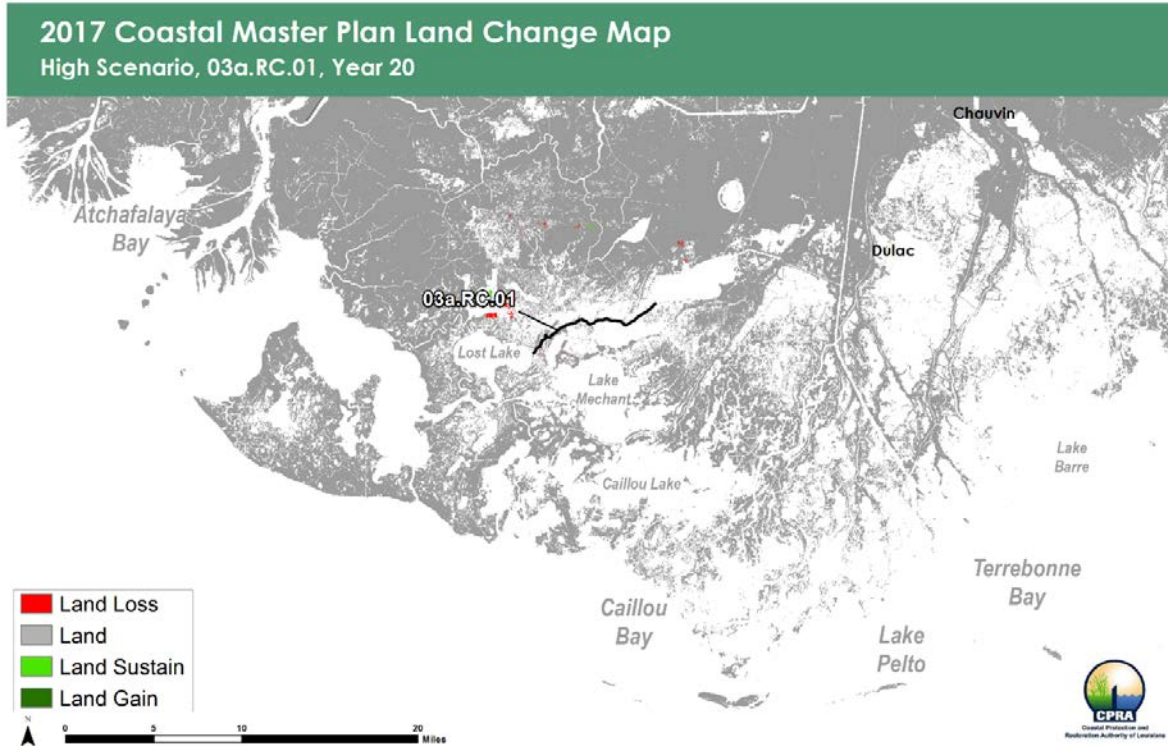
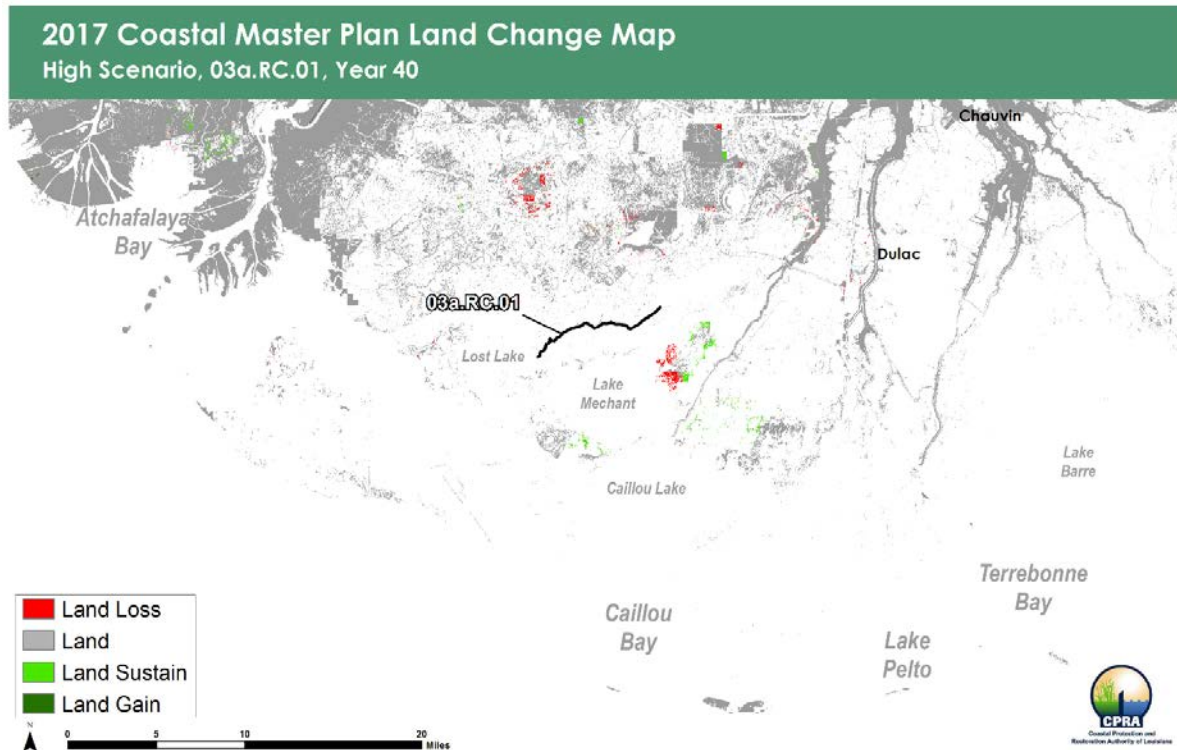


Figure 221: Land Change from Bayou Decade Ridge Restoration Relative to FWOA (year 20; high scenario).

DRAFT



**Figure 222: Land change from Bayou Decade Ridge Restoration relative to FWOA (year 40; high scenario).**

Overall, during the 50-year simulation, there is no substantive, consistent, or spatial pattern of sustained, gained, or lost land except for an apparent trend of sustained land in the area around Bayou Dularge. The region shows a general shift from saline marsh to bare ground between years 30 and 40 in the high scenario and a complete loss of land with both project implementation and FWOA by year 50. The sustained land areas in year 50 all contain the vegetation type "bare ground/upland." In Version 1 of the ICM, bare ground areas were not subject to a collapse criterion. This meant that the hydrologic conditions were not suitable to nearby vegetation species that could disperse into the area, and the loss of vegetated cover occurred prior to any collapse mechanism being triggered within the morphology subroutine. Therefore, while it appears that some land may be sustained at year 50, it is likely unsuitable for any modeled vegetation species to establish there. These areas of persistent bare ground were handled differently in Version 3 of the ICM; a collapse mechanism was put in place to account for these areas. For more information regarding these adjustments made to Version 3 of the ICM code, refer to Attachment C3-22.

There are some far-field land changes that are likely due to differences in salinity calculations. While some of the difference is potentially due to hydraulic flow constrictions post-project, it is likely also a function of salinity calculation instability in later years when hydraulic flow paths are substantially different than those present on the landscape during the model calibration/validation period. For more details on these instabilities (which were resolved in Version 3 of the ICM), please refer to Attachment C3-23.

The effects due to the project in the low scenario are minimal, with the majority of the land change being spatially variable. The area of primary change in the high scenario (northeast of Lake Mechant) shows no change in the low scenario for project implementation compared to FWOA. This implies that the conditions in the high scenario are more conducive to larger project

effects. Results in the low and the medium scenarios are similar, but the medium scenario does show a slightly greater occurrence of land sustained throughout the 50 years. Land loss similar to that seen in the high scenario, but at a smaller scale, can be seen in the area northeast of Lake Mechant in the medium scenario.

The overall lack of project effects observed is likely in part due to the spatial resolution of the model.

#### **4.8 Barataria Pass to Sandy Point Barrier Island Restoration (002.BH.04)<sup>10</sup>**

The restoration of the barrier islands between Barataria Pass and Sandy Point is intended to provide beach, dune, and back barrier marsh habitat and to provide storm surge and wave attenuation for the Barataria Basin. It is implemented in year 7 of the ICM simulation.

The barrier island model (BIMODE subroutine - Attachment C3-4) simulates the effects of long-shore sediment transport, silt loss, bayside erosion, and RSLR on an annual basis. The results of the simulations for implementing this project are compared to those for FWOA; all analyses discussed herein are for the high scenario and focus on the Chaland Headland portion of the project. While these processes and functions result in similar barrier shoreline erosion and landward migration trends, the restored barrier islands experience less shoreline erosion and migration. The primary reasons are two-fold. First, a restored island subjected to the same wave field experiences less shoreline erosion than an unrestored island due to the raised beach berm elevation which increases the effective profile height (Attachment C3-4). Second, the BIMODE assumes that the sediment utilized for restoration is coarser than the existing island's native beach; thus, the percent silt loss is reduced for a restored island reducing net erosion (Attachment C3-4).

Figure 223 depicts a plan view of shoreline change on decadal time steps through year 20 for the eastern segment of the Chaland Headland. The island was restored in year 7 as part of the Barataria Pass to Sandy Point Barrier Island Restoration (002.BH.04) project, which is shown by the movement of the bayside shoreline between year 1 and year 10. Incremental landward retreat of the gulf side shoreline and erosion of the bayside shoreline occurs with corresponding island width and land area reductions over time. The trends are similar to those under FWOA although at lower rates as discussed below.

---

<sup>10</sup> Decadal animations of the 50-year simulation outputs can be found in Attachment C4-8 - Barataria Pass to Sandy Point Barrier Island Restoration (002.BH.04), including land and pelican HSI.

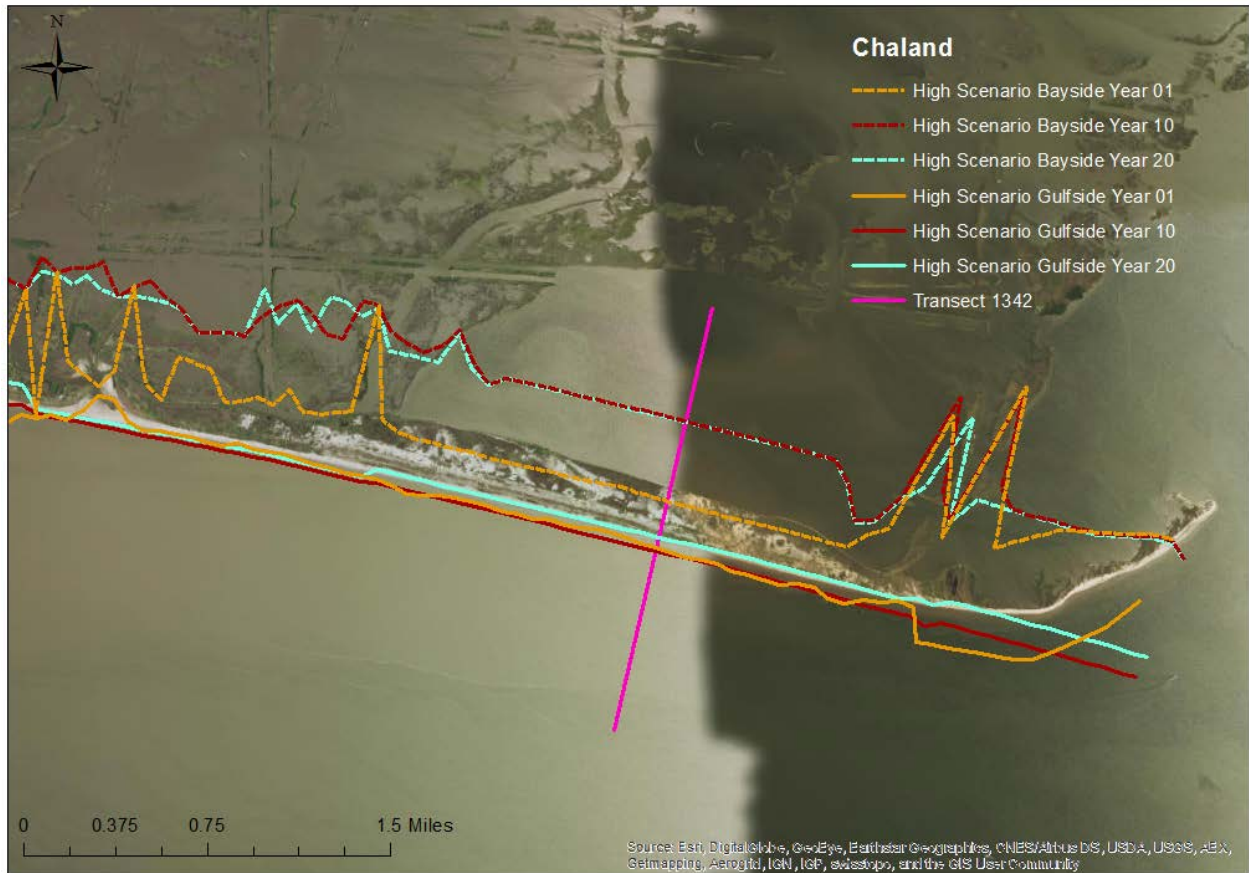


**Figure 223: Plan View of Chaland Headland Shoreline Changes through Year 20 with Project Implementation.**

Figure 224 depicts a representative cross section for the Chaland Headland for FWOA and with the project in place through year 20, corresponding to the plan view depiction (Figure 223). The shoreface erosion and silt loss on the gulf side, erosion of the bayside shoreline, and vertical lowering of the profile to account for the effects of RSLR is shown in both FWOA and with the project. The unrestored island experienced greater erosion, loss of berm elevation, and profile change than the restored island. For example, at Profile 1342, between year 10 and year 20, the erosion rates measured at the 0.8 m contour were -9.6 m/yr and -8.6 m/yr, and the mean berm elevation change was -0.5 m and -0.4 m, for FWOA and with the project, respectively.

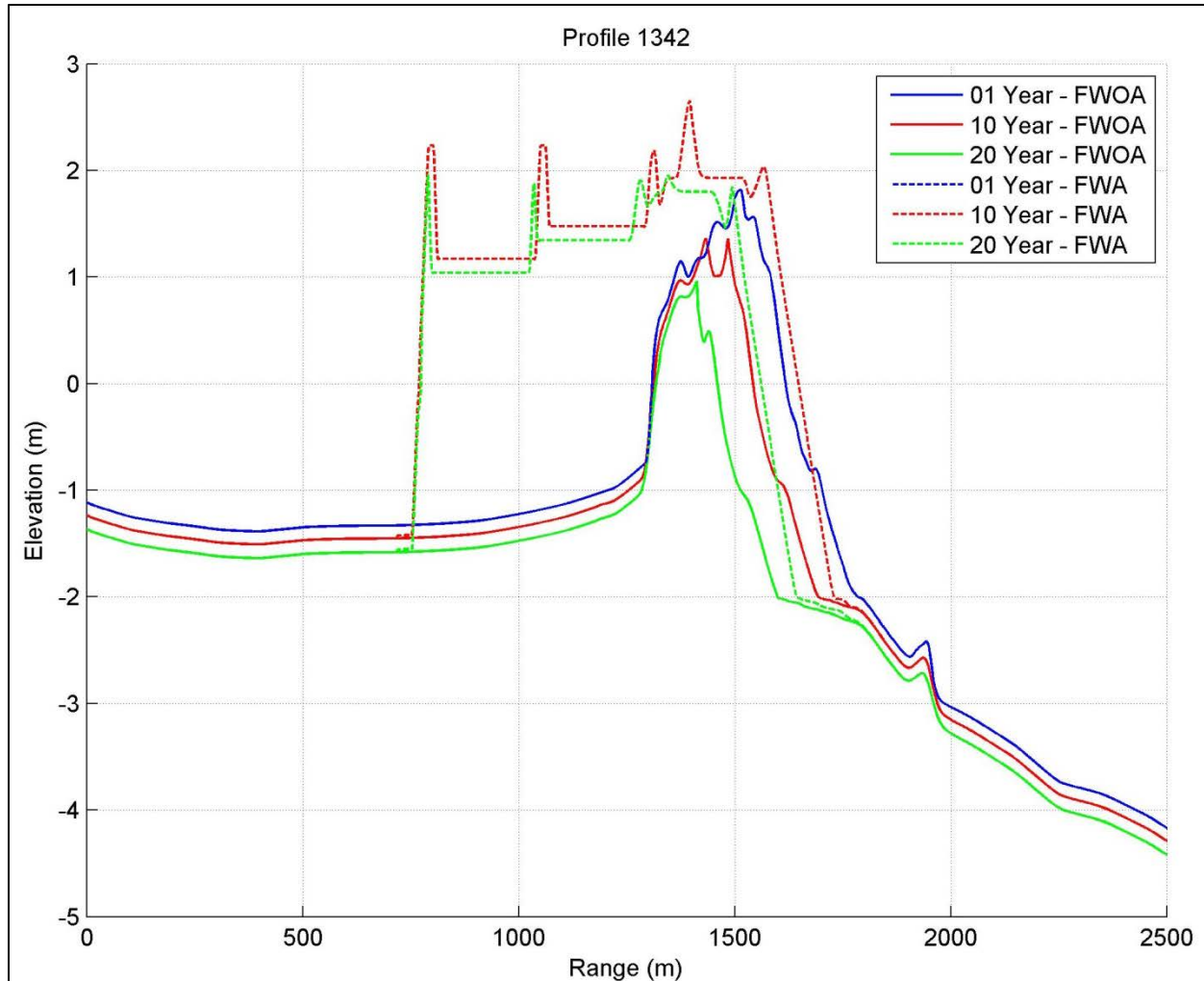


**Figure 224: Representative Cross Sectional Comparison of Eastern Chaland Headland through Year 20 for FWOA and with the Project (FWA); Year 1 FWOA and with the Project are the Same Profile.**

Cross-shore sediment transport and breaching were modeled during years when storms impacted the barrier shorelines. While the restored islands experience erosion of the gulf side shoreface, beach berm, dune, and marsh platform resulting in land loss, overwash is reduced because of higher restored beach and dune elevations compared to FWOA. Figure 225 and Figure 226 depict a plan view of pre-storm and post-storm shorelines and pre-storm and post-storm profiles, respectively, for the Chaland Headland which was restored in year 7 as part of the Barataria Pass to Sandy Point Barrier Island Restoration project. Storm 143 was modeled in year 35 and passed within 80 km of Chaland Headland. Overwash occurs as shown between the range of 600 m and 650 m in FWOA by higher berm elevations in year 35, equal to  $1.0 \text{ m}^3/\text{m}$  compared to year 34; while, minimal overwash is observed with the project in place between the range of 400 m and 450 m, equal to  $0.3 \text{ m}^3/\text{m}$ .



Figure 225: Plan View of Pre- and Post-Storm Shorelines for Chaland Headland at Years 34-35 with Project Implementation.

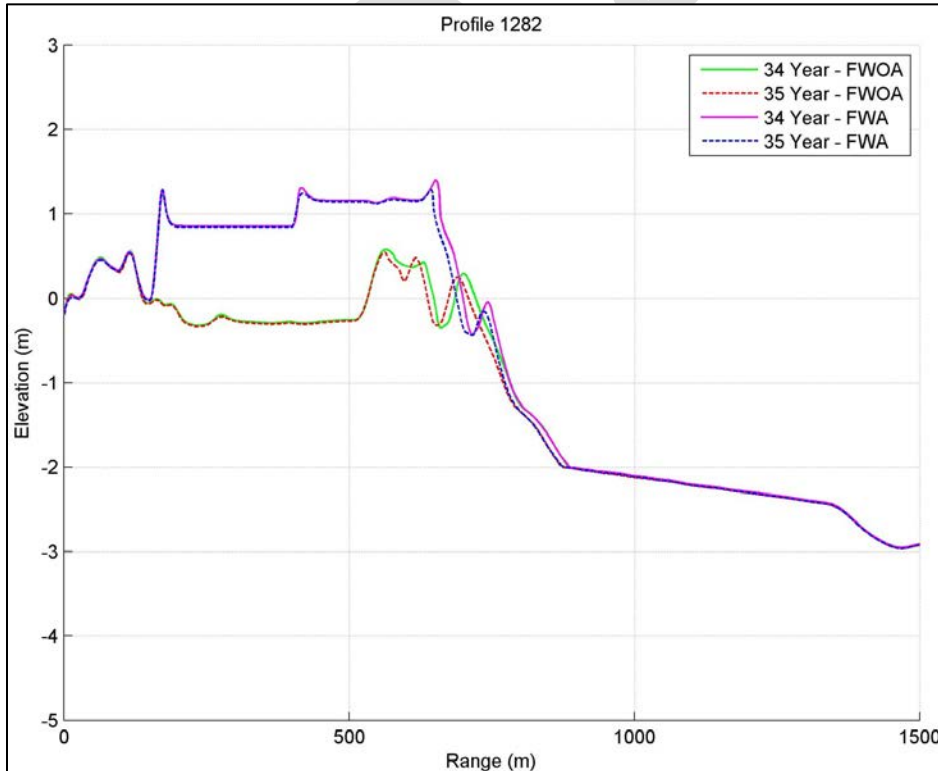


Figure 226: Pre- and Post-Storm Cross Sectional Comparison for Chaland Headland at Years 34-35 for FWOA and with the Project (FWA).

Significant reductions in breaching are observed on the restored islands within the 50-year period. Figure 227 and Figure 228 depict a plan view and a corresponding representative cross section for the central segment of the Chaland Headland for FWOA and with the project in place through year 20. While breaching occurs on the unrestored island in FWOA, which is shown by the gap in both the gulf side and bayside shorelines in year 20 in the plan view, the restored island did not breach. The individual islands within the project area experience 18 breaches under FWOA versus no breaches with the project in place, within the 50-year simulation.

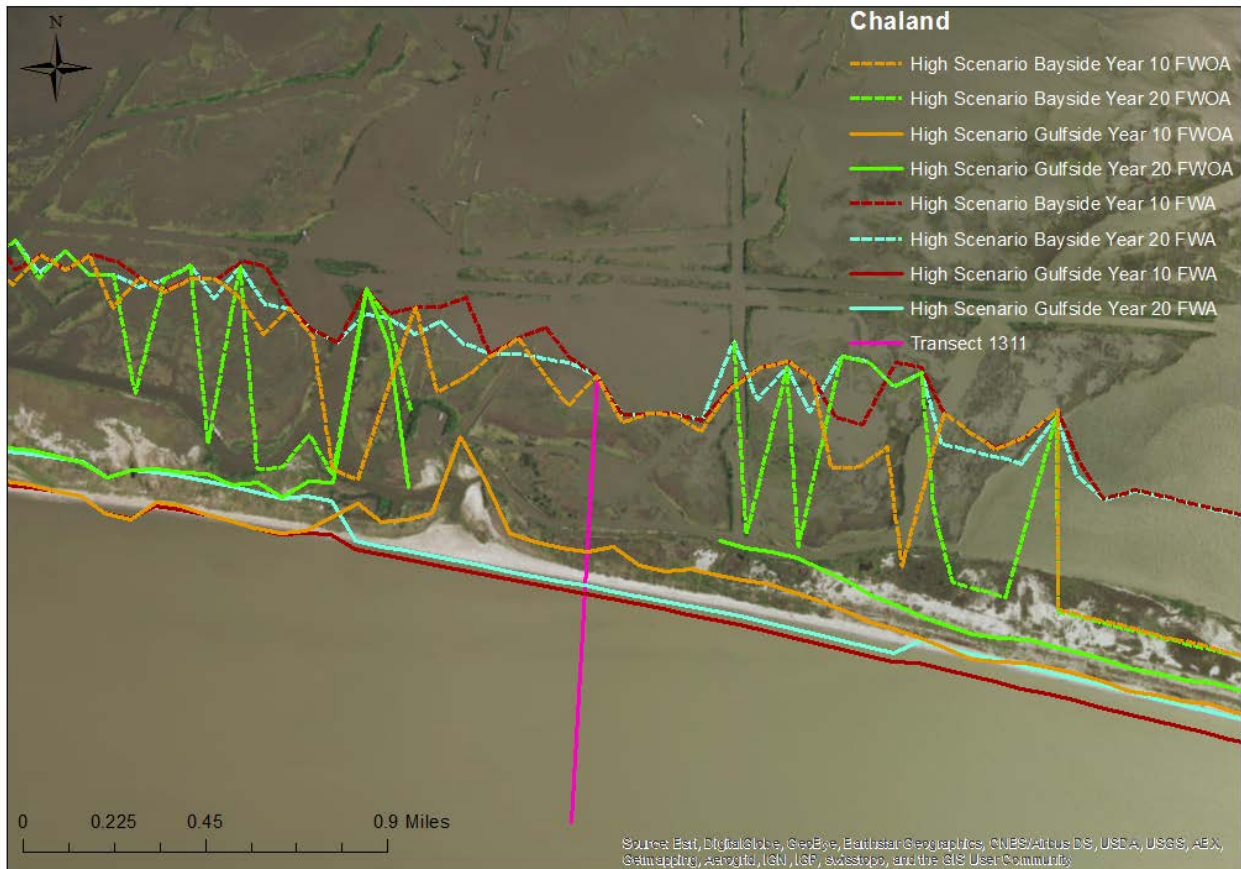
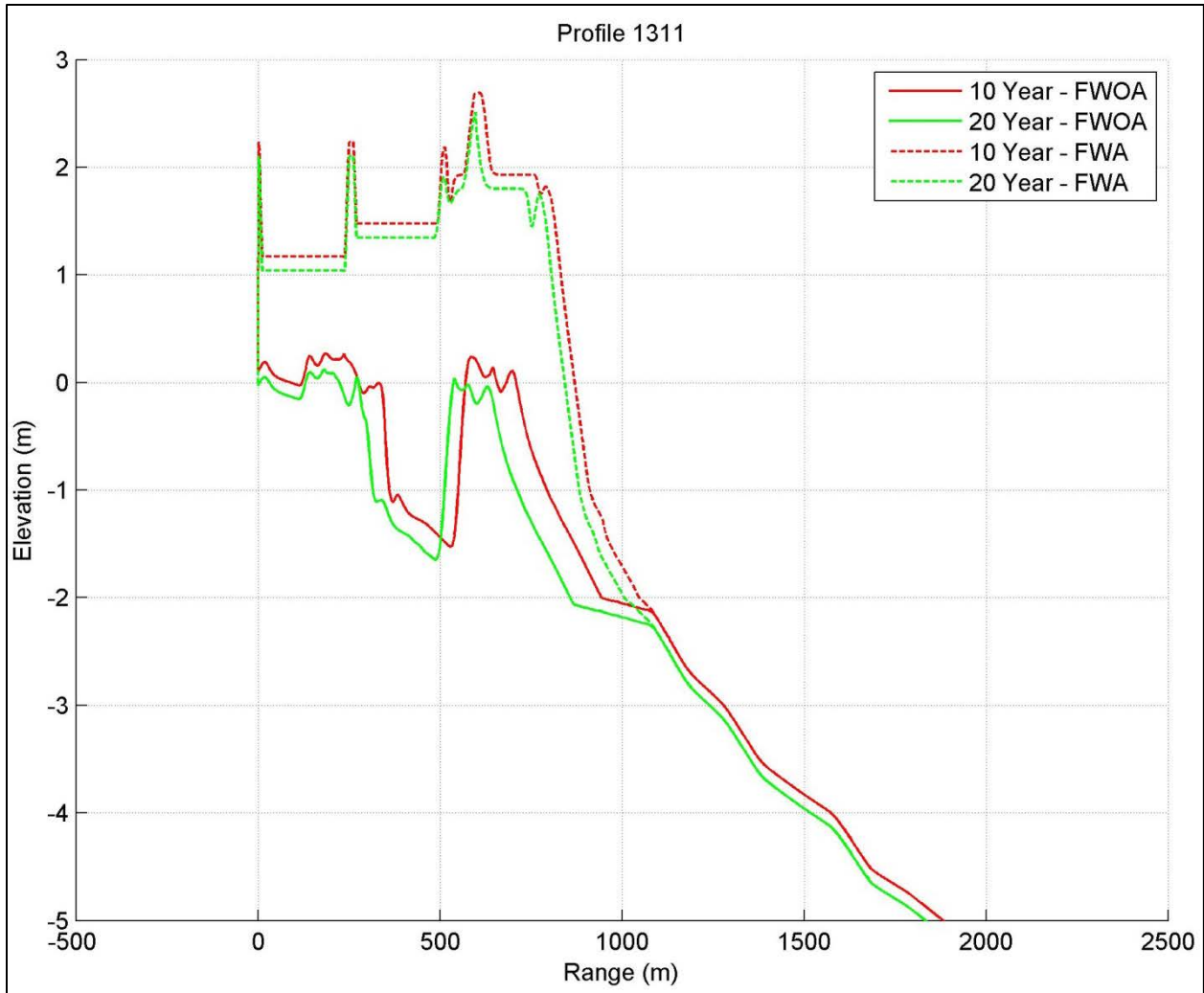


Figure 227: Plan View of Central Chaland Headland Shoreline Changes through Year 20 for FWOA and with the Project (FWA).



**Figure 228: Representative Cross Sectional Comparison of Central Chaland Headland through Year 20 for FWOA and with the Project (FWA).**

Land area changes were computed in 5-year increments over the 50-year period with the project in place. The FWOA land area changes (Chapter 4 – FWOA Section) were subtracted from the with-project land area changes to compute the barrier island restoration “effect,” that is, the land area benefits attributed to the restoration project, over the 50-year period. Figure 229 presents the land area project benefits over time for the islands restored with the Barataria Pass to Sandy Point Barrier Island Restoration project. The average benefits over the 50-year period for comparison equaled over 14 km<sup>2</sup>.

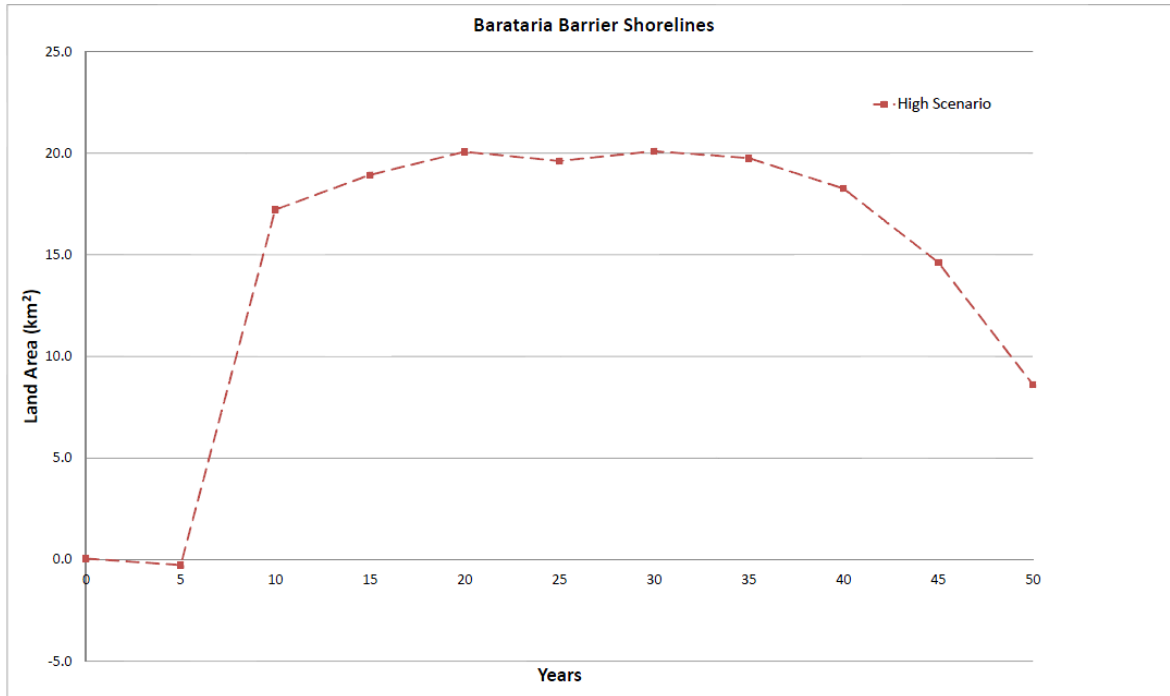


Figure 229: Net Change in Land Area over Time for the Barataria Pass to Sandy Point Barrier Island Restoration Project.

## 4.9 Biloxi Marsh Oyster Reef (001.OR.01a)<sup>11</sup>

The Biloxi Marsh Oyster Reef (001.OR.01a) project is located in St. Bernard Parish, Louisiana, north of Drum Bay in the Biloxi Marsh. The project includes the creation of approximately 34,231 m of oyster barrier reef along the eastern shore of the Biloxi Marsh. In addition to protecting nearby shorelines from wave-driven erosion, the goal of the project is to augment local oyster habitat by introducing suitable hard substrate upon which new oyster colonies may develop. This project is implemented in year 7 of the ICM simulation.

### 4.9.1 Landscape

In all scenarios (low, medium, and high), there is no observed change in land due to the project in any year (Figure 230 and Figure 231). The effects of ongoing land loss processes are clearly visible over time, but as determined by a comparison against FWOA, there is no change due to the project. This result is reasonable since oyster reef projects are implemented off-shore and are represented in the model solely as a reduction in marsh edge erosion rates. The oyster reef project reduces edge erosion rates for marsh areas that are completely exposed to sea level rise. Other shoreline protection projects tend to show some minor impact in earlier years if the adjacent land area remains and is protected from wave erosion by the project.

<sup>11</sup> Decadal animations of the 50-year simulation outputs can be found in Attachment C4-9 - Biloxi Marsh Oyster Reef (001.OR.01a), including land and oyster HSI.

However, the oyster reef projects are implemented in an environment that is more similar to the later decades of the shoreline protection projects, where inundation-driven land loss results in no net project impact, with respect to land area.

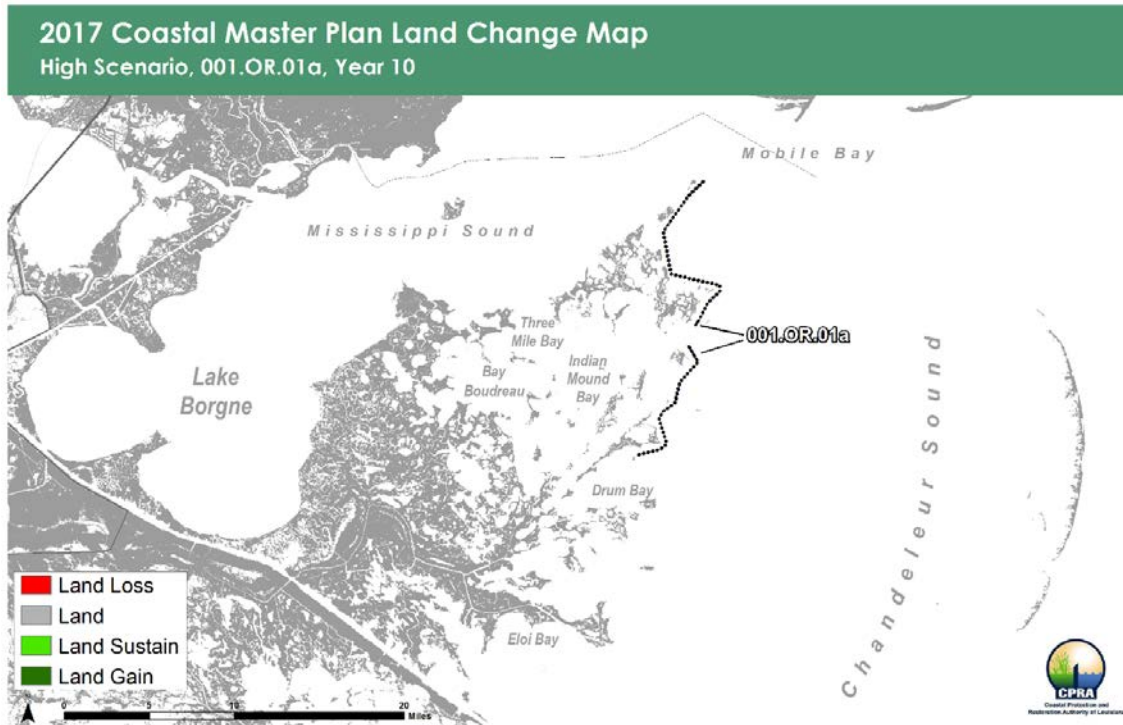


Figure 230: Land Change from Biloxi Marsh Oyster Reef Relative to FWOA (year 10; high scenario).

DRAFT

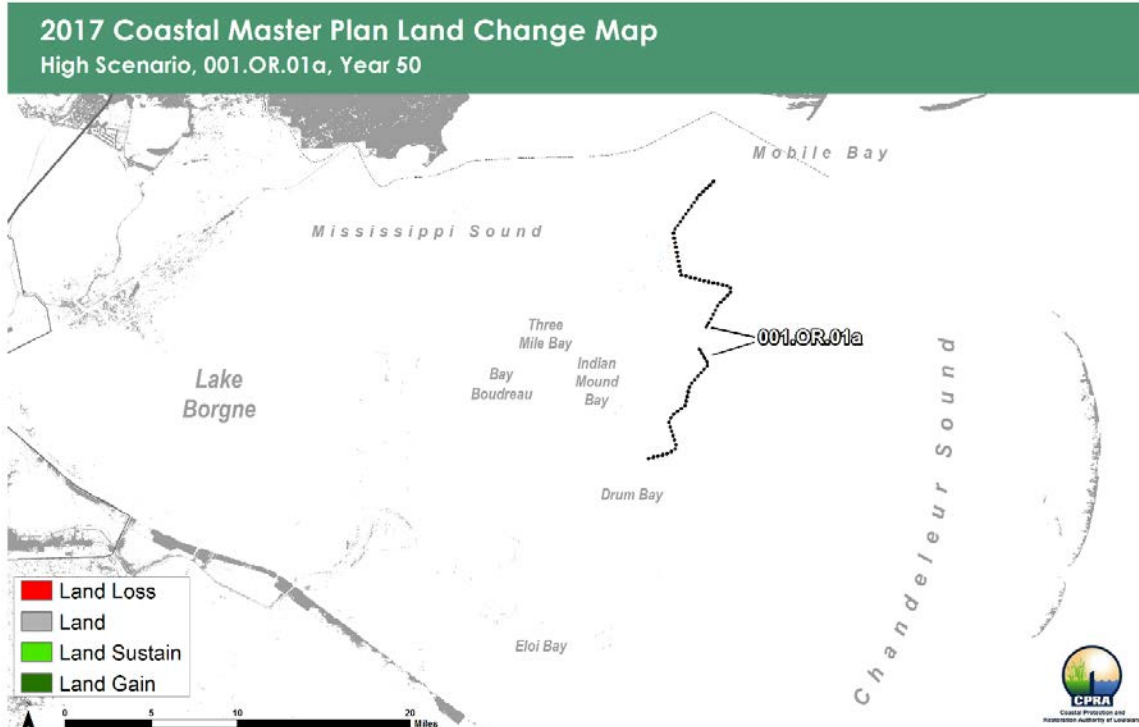


Figure 231: Land Change from Biloxi Marsh Oyster Reef Relative to FWOA (year 50; high scenario).

#### 4.9.2 Oyster Habitat Suitability

The hard substrate provided by the Biloxi Marsh Oyster Reef project results in an increase in oyster habitat suitability relative to FWOA, but primarily during the latter half of the 50-year simulation (Figure 232). During the first half of the model run, there are frequent low-salinity flooding events that greatly reduce the suitability of the project for oyster (Attachment C3-12), particularly in year 10 of the simulation (Figure 232). These events do not occur during the latter half of the simulation because sea level rise generally increases salinities, and as a result, conditions are more suitable for oysters.

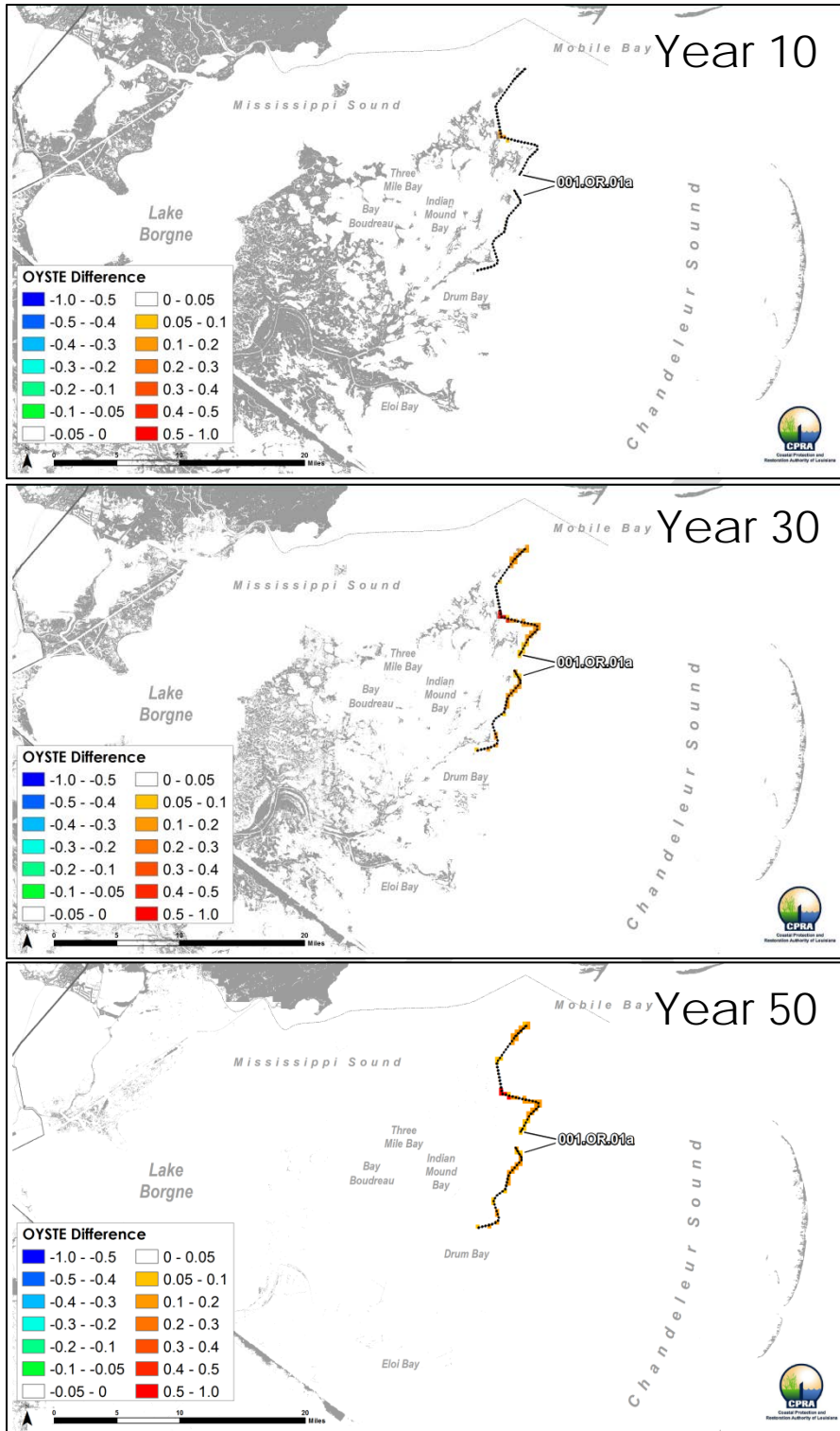
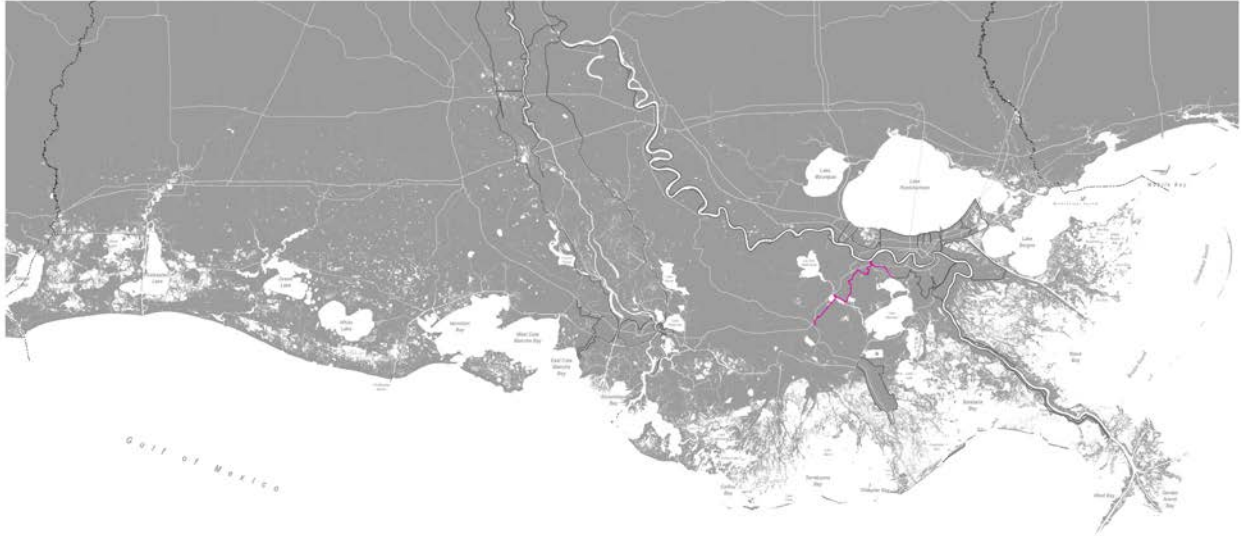


Figure 232: Difference in Eastern Oyster Habitat Suitability Associated with the Biloxi Marsh Oyster Reef Relative to FWOA (years 20, 30, and 50; high scenario). Warmer colors indicate an increase in suitability and cooler colors indicate a decrease in suitability with the project.

## 4.10 Upper Barataria Risk Reduction (002.HP.06)

The Upper Barataria Risk Reduction project alignment (002.HP.06) is shown on Figure 233. For the purposes of modeling efficiency, this project and the Lake Pontchartrain Barrier project alignment (001.HP.08) are simulated simultaneously. The two projects do not alter water surface elevation or waves in the same areas.



**Figure 233: Upper Barataria Risk Reduction Alignment, as Indicated by the Pink Line.**

Figure 234 and Figure 235 show the changes in maximum water surface elevation resulting from project implementation for two hurricanes of different strengths under the high scenario for the year 50 FWOA landscape. Figure 234 shows a moderately sized storm, Storm 012, generating storm surge in the area. The project provides benefits to the Upper Barataria region as well as areas along the West Bank of the Mississippi River. Like Figure 234, Figure 235 shows water surface elevation reduction in the upper reaches of the Barataria Basin but for a much larger storm, Storm 018. Storm surge builds against both the Upper Barataria Risk Reduction project and the HSDRRS levee system, eventually increasing water levels on the interior of HSDRRS. It should be noted that the West Bank area is flooded both with and without the Upper Barataria Risk Reduction project for Storm 018; however, with the project in place, water levels are increased by approximately 0.5 m.

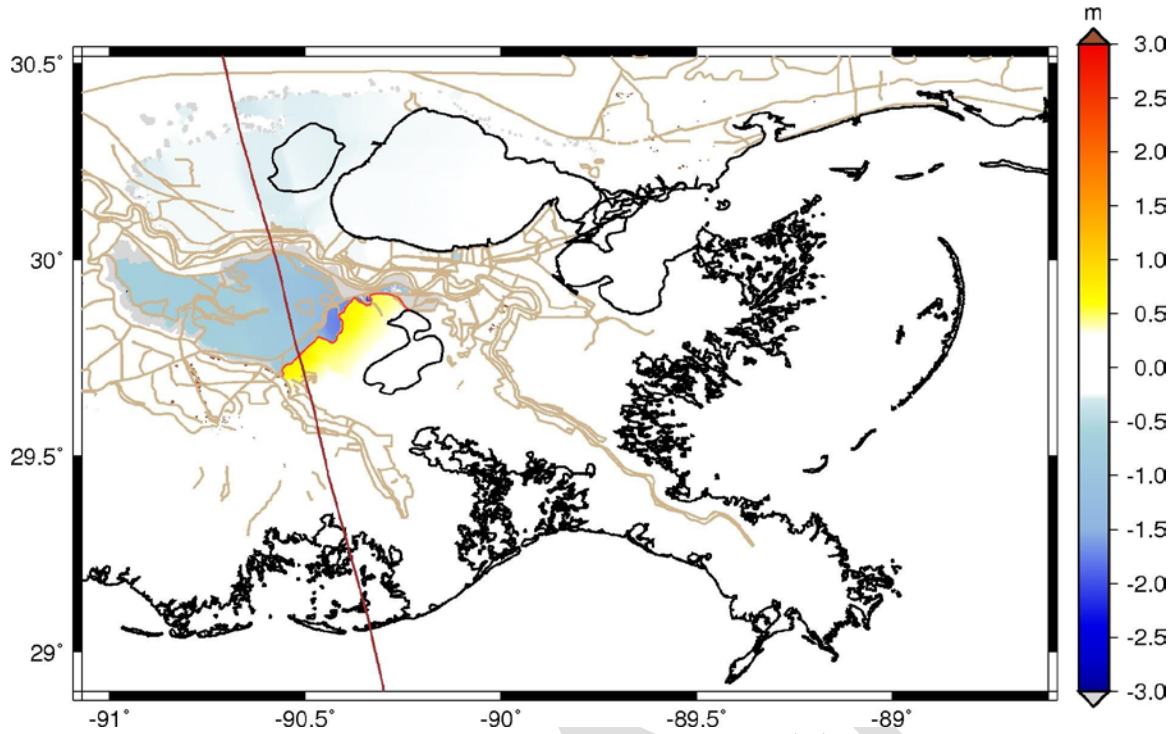


Figure 234: Differences in Maximum Water Surface Elevation (m) due to Implementation of the Upper Barataria Risk Reduction Project (year 50; high scenario) during Storm 012. Positive values denote an increase with the project in place. The project alignment is shown in red and the storm track is shown in brown.

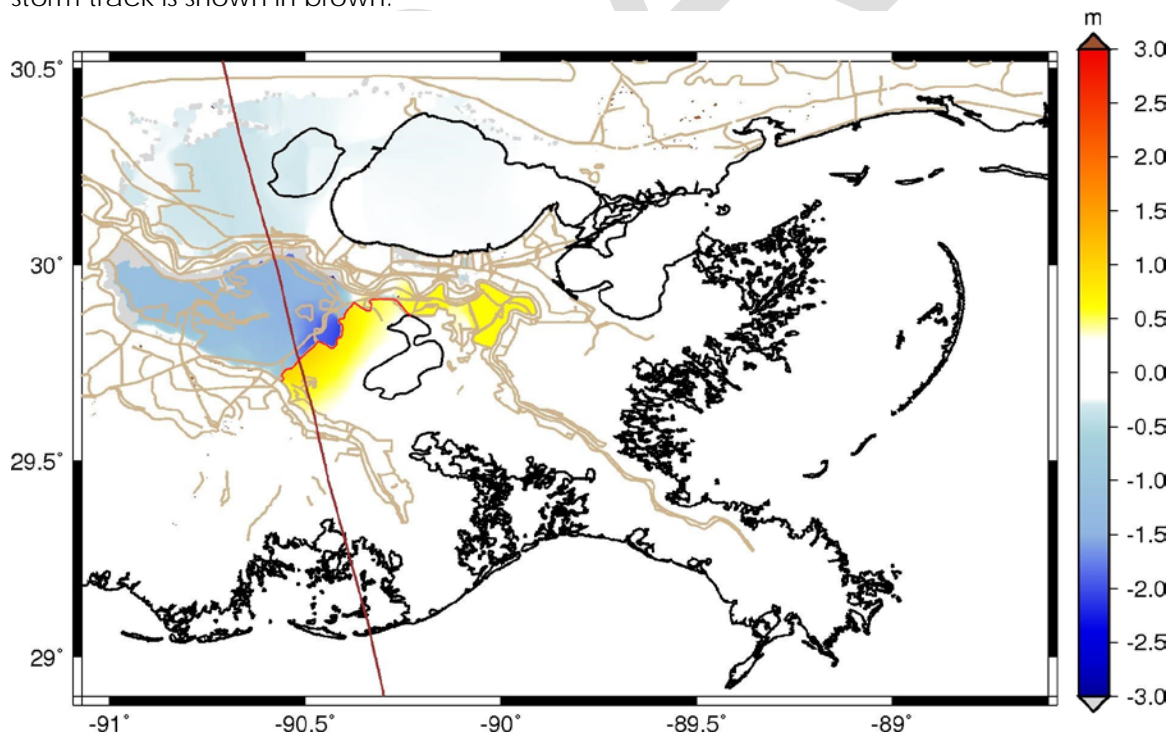


Figure 235: Differences in Maximum Water Surface Elevation (m) due to Implementation of the Upper Barataria Risk Reduction Project (year 50; high scenario) during Storm 018. Positive values denote an increase with the project in place. The project alignment is shown in red and the storm track is shown in brown.

Figure 236 shows the impact of the Upper Barataria Risk Reduction project on 100-year flood depths in year 50 of the high scenario as compared to FWOA. The figure shows the CLARA model median estimates using the IPET fragility curve in enclosed areas, which encounter some induced flooding (in red) on the West Bank HSDRRS system. General reductions (in green) of 1-2 m are evident at the 100-year return period throughout the Upper Barataria basin behind the project alignment when compared to FWOA. The largest reductions, approximately 2.5 m, are in the Des Allemands area; reductions are generally smaller in communities along the ridges on the outer boundaries of the green region from the figure, such as Thibodaux and Raceland on the southern ridge and Vacherie in the north on the west bank of the Mississippi River.

The magnitude and geographic distribution of flood depth reductions are very similar at the 50- and 500-year return periods, except in the northwest corner of the basin where 50-year flood depths are less than a meter (not shown). In the low and medium scenarios, 100-year flood depths in Des Allemands are reduced by 3-4 m. In other parts of the basin that are protected by the alignment, reductions are generally smaller than in the high scenario, less than 1 m in the low scenario and less than 1.5 m in the medium scenario. In the high scenario, project effects in Des Allemands are greater in year 25 (reductions of 3-4 m), but the geographic extent of both flood depth reductions and increases is considerably smaller.

The project also induces increased flooding at the 100-year return period in the high scenario over a large region in front of the levee alignment, extending all the way to Lafitte to the east and Larose to the south. The large majority of the induced flooding is in unpopulated wildlife management areas near Lake Salvador, but one important exception is the potential for induced flooding on the West Bank of HSDRRS.

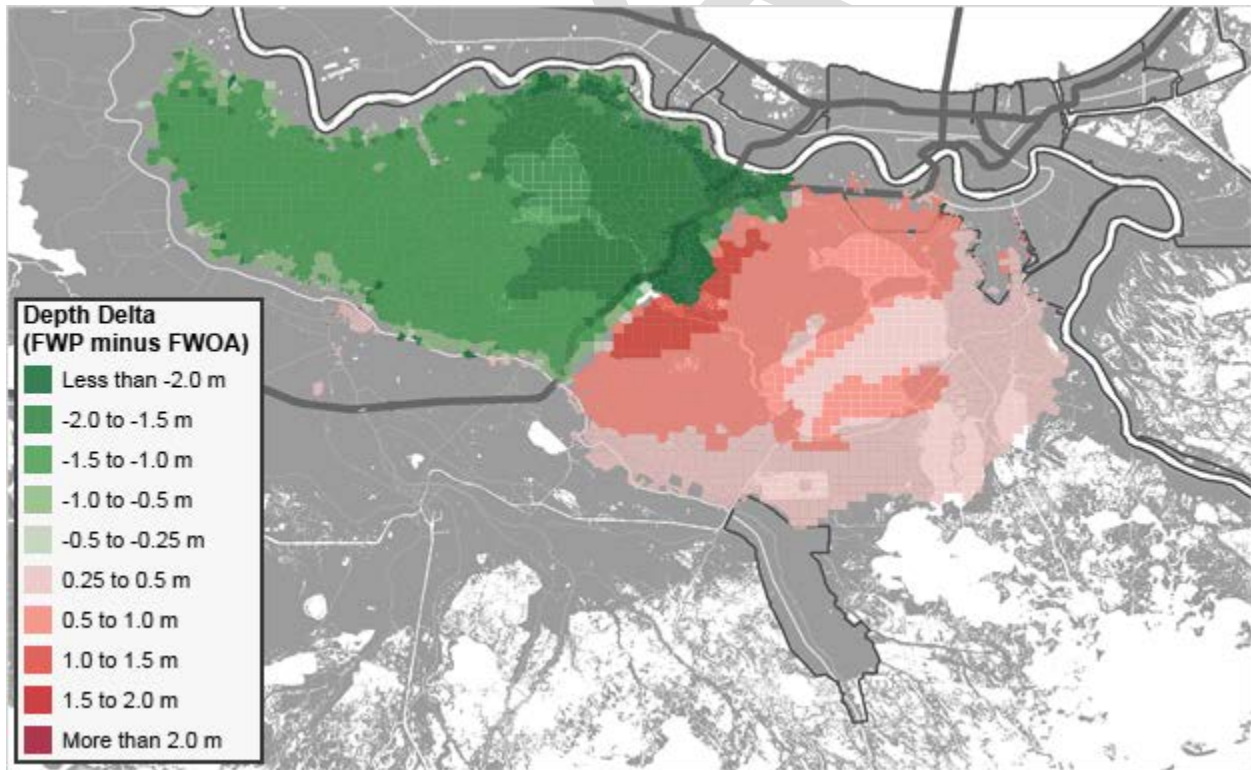


Figure 236: Difference in Median 100-Year Flood Depths due to Implementation of the Upper Barataria Risk Reduction Project (FWP) compared to FWOA (year 50; high scenario). IPET fragility scenario shown in enclosed areas.

The EAD in year 50 of the high scenario is reduced by an estimate of \$618 million in the impacted area shown in Figure 237, with the Upper Barataria Risk Reduction project in place (under the IPET fragility assumption and historic growth population scenario) as compared to FWOA. Benefits accrue primarily to the St. Charles Parish region that includes Des Allemands, where flood depth reductions are also the greatest. The rest of the communities along the ridges also benefit from the project, with the exception of some induced damage in Thibodaux (as also shown with the small pink shaded region just south of the ridge in Figure 236). In this scenario, induced damage is \$237 million on the West Bank of HSDRRS in Jefferson Parish (JEF.04R risk region), followed by \$52 million within the Larose to Golden Meadow protection system (LAF.02R). The full set of EAD impacts is presented by risk region in Figure 237.

In year 25, corresponding to the smaller extent of flood depth impacts, net EAD benefit in this scenario is \$507 million, with a reduction of \$503 million in the St. Charles region. Induced damage in the Larose to Golden Meadow region is \$31 million. Impacts in all other regions are small and not statistically significant.

In the medium scenario, net benefits are \$646 million in year 50, greater than the high scenario. This is due to an absence of induced damage in HSDRRS. In year 25, the benefits are \$335 million due to lower baseline FWOA damage.

### EAD Reduction Benefits by Region

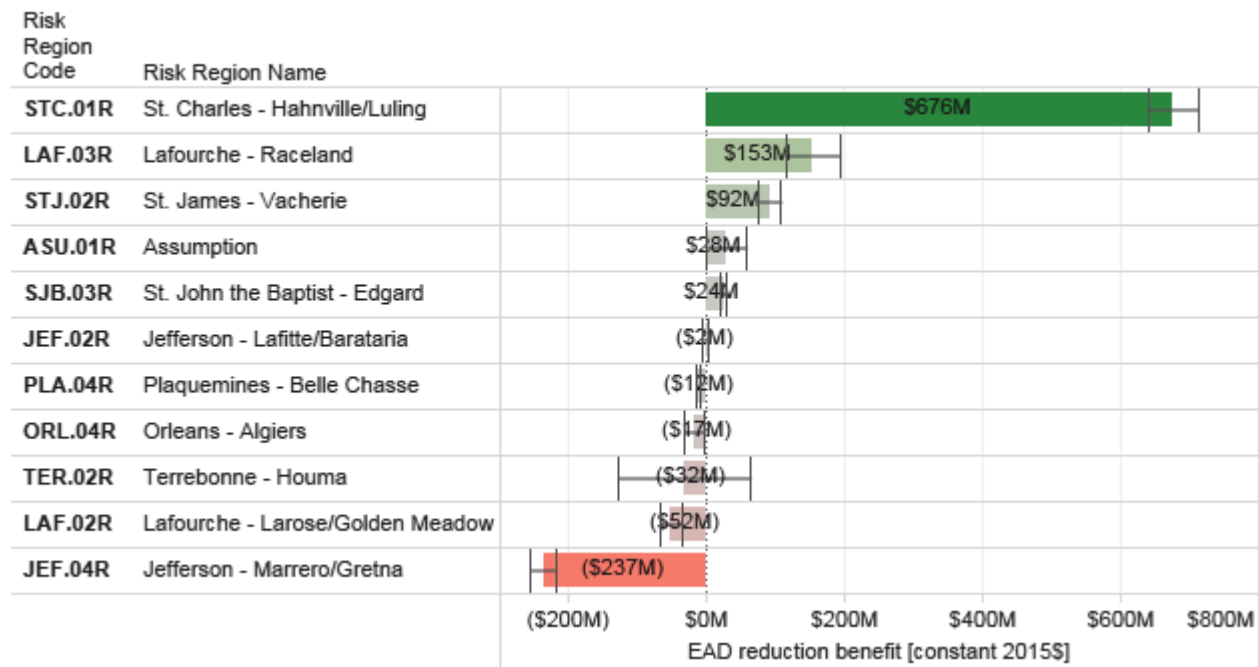
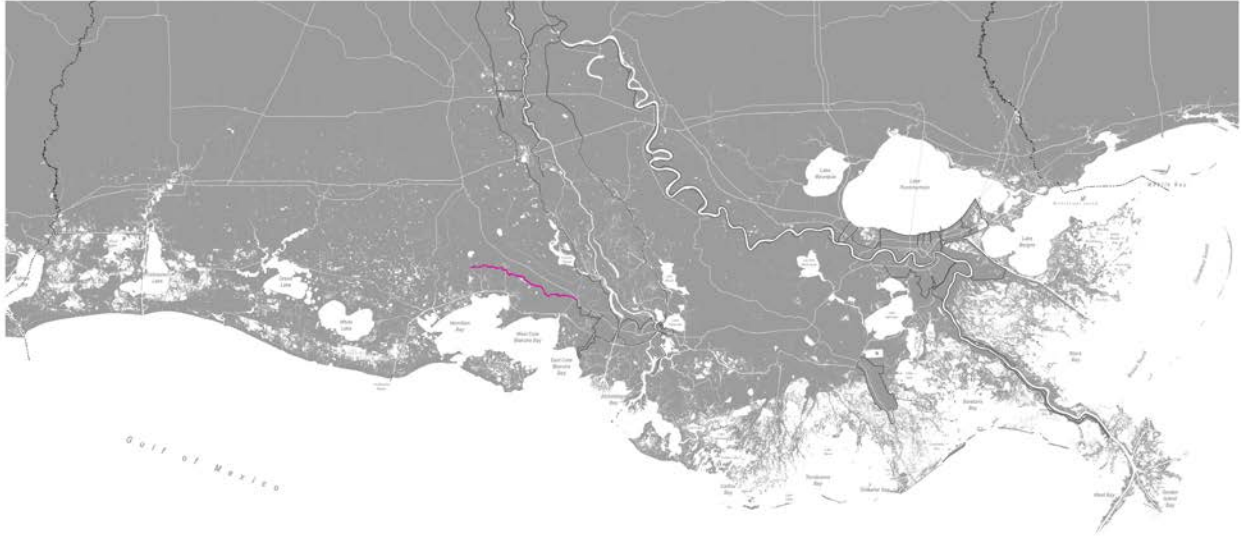


Figure 237: Change in EAD from Implementation of the Upper Barataria Risk Reduction Project (year 50; high scenario; historical growth; IPET fragility scenarios). Colored bar and labels show mean change in EAD; lines show an estimate of the 95% confidence interval.

## 4.11 Iberia/St. Mary Upland Levee (03b.HP.14)

The Iberia/St. Mary Upland Levee alignment (03b.HP.14) is shown on Figure 238. For the purposes of modeling efficiency, this project and the Morgan City Back Levee (03a.HP.20) are simulated simultaneously. The two projects do not alter water surface elevation or waves in the same areas.



**Figure 238: Iberia/St. Mary Upland Levee Alignment, as Indicated by the Pink Line.**

Figure 239 and Figure 240b show the changes in maximum water surface elevation that occur when implementing the project for two storms of different strengths and tracks west of the project. The simulations are for the year 50 FWOA landscape for the high scenario. Storm 223 (Figure 239) makes landfall near Lake Calcasieu, while Storm 232 (Figure 240) makes landfall closer to the project and near White Lake. For storms that make landfall east of and far to the west of the project, such as Storm 223, the project is generally able to provide significant storm surge reduction to all areas behind the levee; storm surge runaround is limited for these storm tracks. However, many storms that make landfall nearer to the project, including Storm 232, lead to storm surge runaround at the western extents of the project. The areas behind the project alignment that experience storm surge runaround are illustrated within the red circles in Figure 240a and b. The western reach of the project experiences a reduction of approximately 0.5 m; however, water surface elevations are still nearly 3.5 m due to the significant flooding caused by runaround.

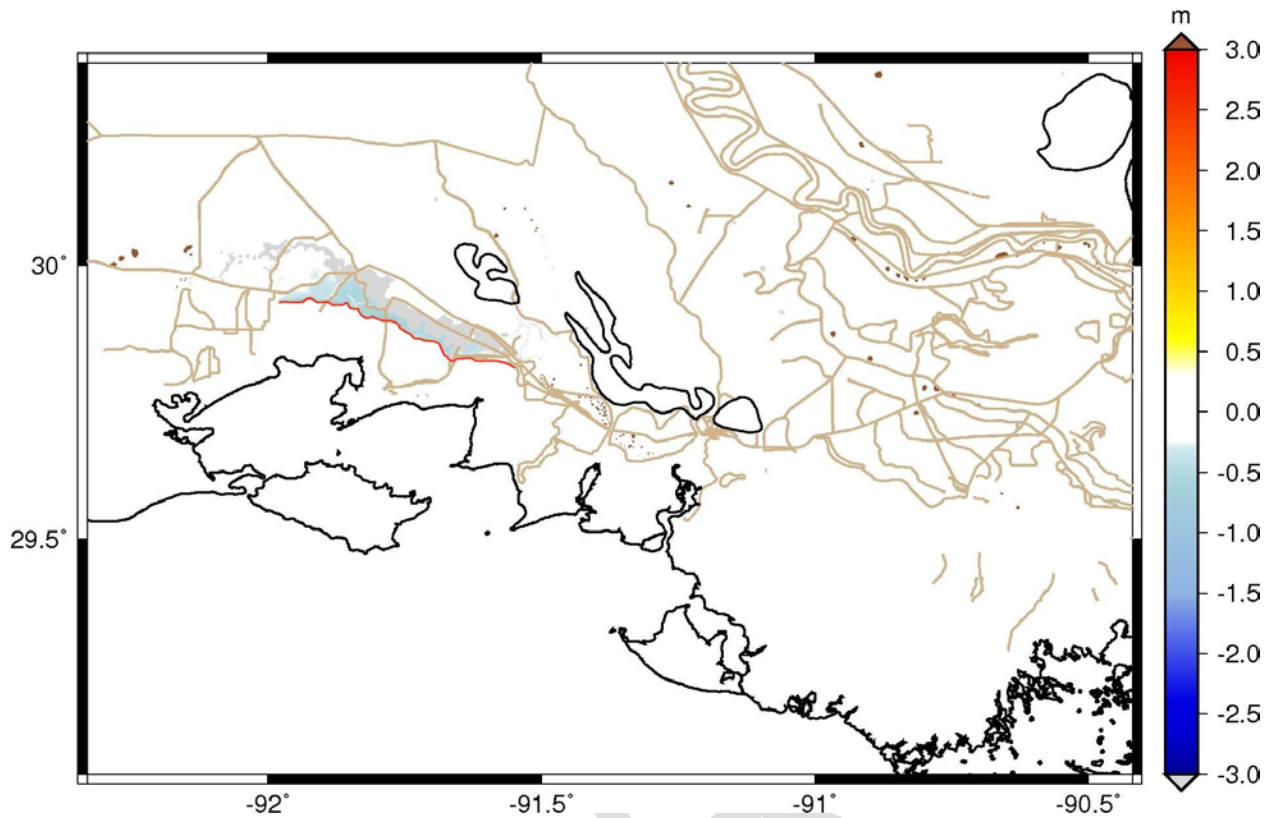


Figure 239: Differences in Maximum Water Surface Elevation (m) due to Implementation of Iberia/St. Mary Upland Levee Alignment (year 50; high scenario) during Storm 223. Positive values denote an increase with the project in place.

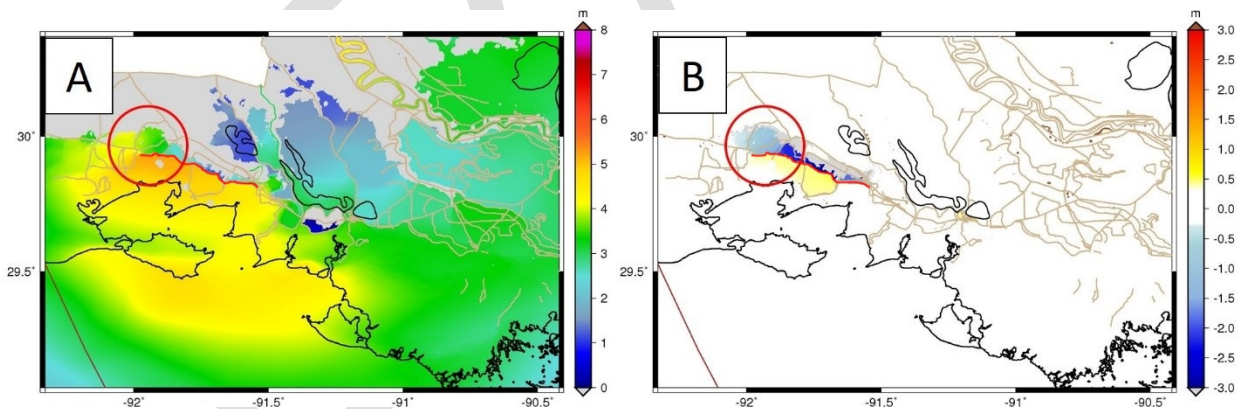
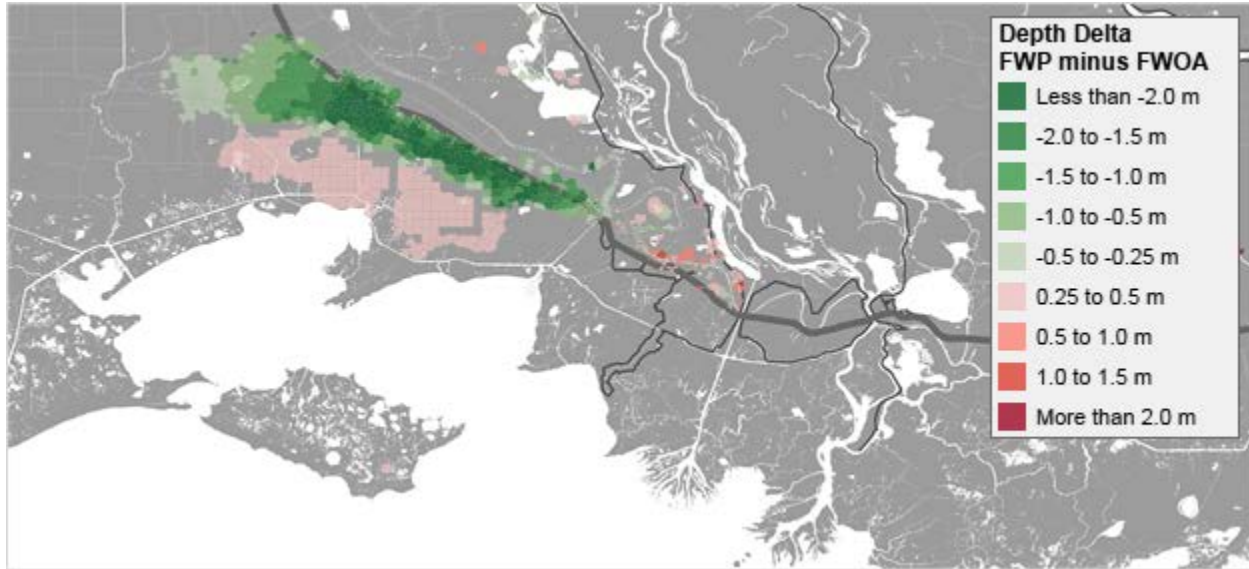


Figure 240: (A) Maximum Water Surface Elevation (m, NAVD88) and (B) Differences in Maximum Water Surface Elevation (m) due to Implementation of Iberia/St. Mary Upland Levee Alignment (year 50; high scenario) during Storm 232. Positive values denote an increase with the project in place. Red circle denotes area where storm surge runaround has occurred. The project alignment is shown in red and the storm track is shown in brown.

Figure 241 illustrates the difference in median 100-year flood depths associated with implementation of the Iberia/St. Mary Upland Levee Alignment in year 50 of the high scenario. Flood depth reductions extend all the way from the project's western terminus in Delcambre to Baldwin in the east, where the alignment would tie in to the Franklin and Vicinity levee system. The 100-year flood depths are reduced by 2-3.5 m in some areas between the alignment and

Highway 90. Despite the evidence of surge runaround produced by specific storms, when examining the statistical results, reductions of 0.5 m or less extend slightly beyond the western end of the alignment. In a small number of grid points near New Iberia and Baldwin, reductions also extend north beyond Highway 90.



**Figure 241: Difference in Median 100-Year Flood Depths from the Iberia/St. Mary Upland Levee Alignment Project (FWP) Compared to FWOA (year 50; high scenario).**

The induced flood depths in front of the alignment are typically less than 0.5 m at the 100-year return period, although a small number of points east of the project and north of the highway see larger increases. Virtually no additional flooding is induced at the 50-year return period (not shown). The differences in 500-year flood depths with the project are very similar to the 100-year differences.

Reductions in the 100-year flood depths are similar in magnitude and extent in the medium scenario. In the low scenario, reductions are generally about 0.5 m smaller in magnitude, disappearing at some higher-elevation areas near Highway 90. Impacts in year 25 of the high scenario are similar to those in year 50 of the low scenario; the lower FWOA flood depths and extent of flooding place a limit on the reduction that can occur.

The EAD in year 50 of the high scenario is reduced by a mean estimate of \$250 million with the Iberia/St. Mary Upland Levee Alignment project in place (IPET fragility assumption, historic growth population scenario) as compared to FWOA. Benefits of \$211 million accrue to the Iberia Parish region south of Highway 90, where flood depth reductions are also the greatest. A smaller EAD reduction of \$40 million is seen in St. Mary Parish for assets along Highway 90 from Jeanerette to Franklin. Impacts on Vermilion Parish, to the west of the project alignment, are not statistically significant. The full set of EAD impacts is presented by risk region in Figure 242.

In year 25 of the high scenario, corresponding to the smaller extent of flood depth impacts, net benefit is \$134 million, with \$116 million of that impact located in Iberia Parish. Induced damage in year 25 is negligible. In the medium scenario, net benefit is \$155 million in year 50, again with the large majority of benefit (\$142 million) in Iberia Parish. In Year 25, net benefit is \$103 million, due primarily to a lower level of baseline risk in FWOA.

**EAD Reduction Benefits by Region**

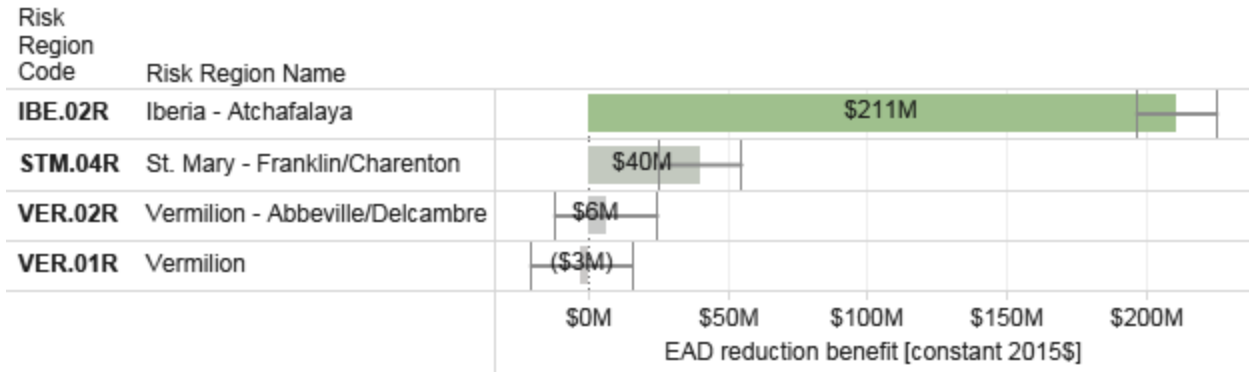
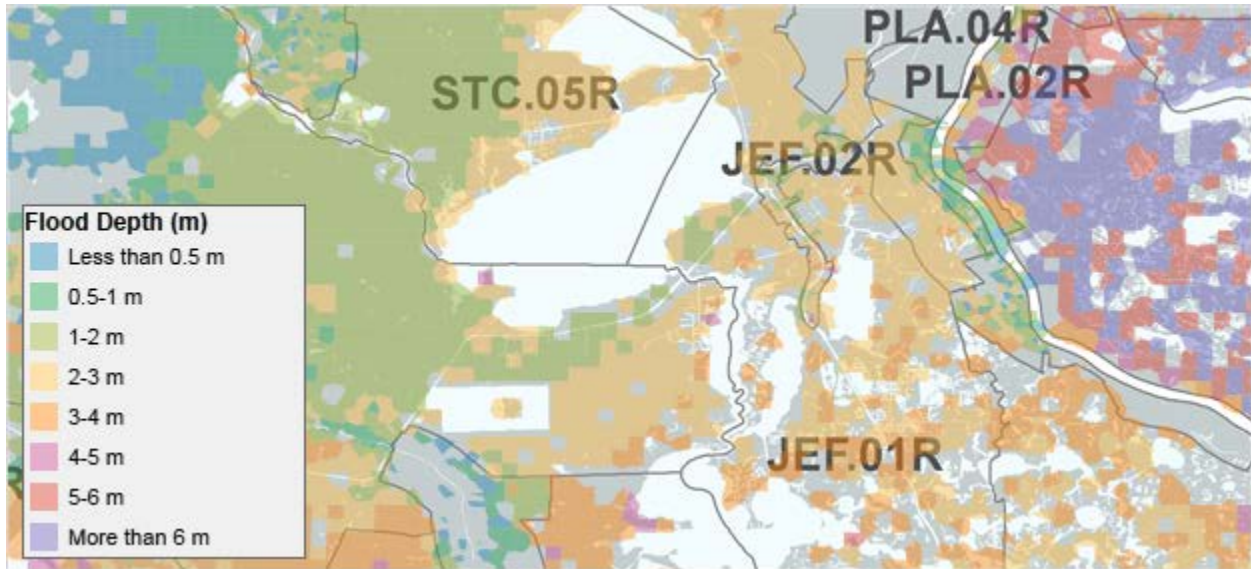


Figure 242: Change in EAD from the Iberia/St. Mary Upland Levee Alignment Project (year 50; high scenario; historical growth; IPET fragility scenarios). Colored bar and labels show mean change in EAD; lines show an estimate of the 95% confidence interval.

**4.12 Nonstructural Risk Reduction Project (Jefferson Parish – Lafitte/Barataria; JEF.02N)**

JEF.02R is a small risk region consisting of the area within the proposed Lafitte Ring Levee risk reduction project (002.HP.07). Approximately 2,046 structures in the region are eligible for nonstructural risk reduction in the JEF.02N project. Forty-two percent of households are low to moderate income, and 765 of the structures are in locations that have experienced repetitive loss or severe repetitive loss in the past.

The flood depth standard for nonstructural risk reduction in the region is based on median 100-year flood depths in year 10 of the high scenario, which range from 1.5 to 4 m and are shown in Figure 243. Under initial conditions, the 100-year values are generally 1.2-2 m; by year 50 this value is over 4.5 m in some points, so flood depths are projected to increase significantly over time.



**Figure 243: Median 100-Year Flood Depths in the Vicinity of the Jefferson Parish - Lafitte/Barataria Region (year 10; high scenario).**

The CLARA model's mean estimate of current EAD in the region is \$91 million. With the nonstructural risk reduction project JEF.02N implemented, EAD is reduced by a mean of \$24 million in year 10 compared to FWOA, \$27 million in year 25, and \$16 million in year 50 of the high scenario (historic growth scenario). Risk reduction is achieved primarily through residential elevation, with 1,237 structures elevated, compared to only nine flood-proofed structures and two structure acquisitions. This represents mitigation of 61% of the total structures eligible for nonstructural risk reduction. Total costs are estimated at \$201 million with a 5-year duration to complete construction. While benefits were modeled only in year 10, year 25, and year 50, they would accrue in all subsequent years after implementation of the project.

#### **4.13 Nonstructural Risk Reduction Project (Lower Terrebonne; TER.01N)**

TER.01R represents the region of Terrebonne Parish south of the proposed Morganza to the Gulf structural protection alignment (03a.HP.103). Given that the Morganza to the Gulf system alignment is intended to reduce risk for population centers within Terrebonne and other adjacent parishes, the number of nonstructural-eligible structures in Lower Terrebonne south of the alignment, 796, is small. Sixty-one percent of the households in the region are low to moderate income, and 455 of the structures are in locations that have experienced repetitive loss or severe repetitive loss in the past.

The flood depth standard for nonstructural protection in the region is based on median 100-year flood depths in year 10 of the high scenario. Exposed assets are primarily in unincorporated communities such as Theriot and Cocodrie, where year 10, 100-year depths range from 2.5-5 m as shown in Figure 244. Under initial conditions, the 100-year values are generally 2.5-4.5 m; by year 50 this value is over 5 m in some points, a statistically significant increase over time.

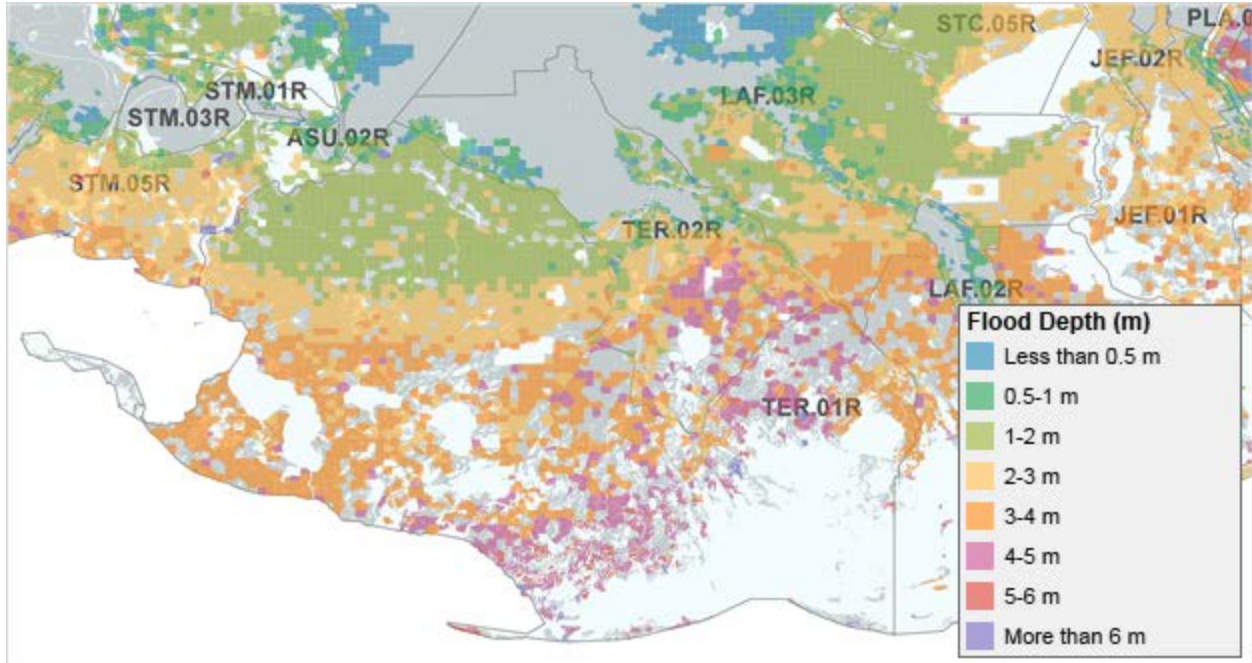


Figure 244: Median 100-Year Flood Depths in the Vicinity of the Lower Terrebonne Region (year 10; high scenario).

The CLARA model's mean estimate of initial condition EAD in the region is \$88 million. With the nonstructural risk reduction measures in place, EAD is reduced by a mean of \$8 million in year 10 compared to FWOA, \$9 million in year 25, and \$9 million in year 50 of the high scenario, under historic growth assumptions. Risk reduction is achieved through a mixture of acquisitions and elevations, with 262 structures elevated, 121 acquisitions, and only two flood-proofed structures. This represents mitigation of 48% of the total structures eligible for nonstructural risk reduction. Total costs are estimated at \$87 million, and the project has assumed construction duration of three years. While benefits were modeled only in year 10, year 25, and year 50, they would accrue in all subsequent years after implementation of the project.

#### 4.14 Nonstructural Risk Reduction Project (Vermilion – Abbeville/Delcambre; VER.02N)

VER.02R represents the upland portion of Vermilion Parish ranging from Delcambre on the eastern boundary of the parish west to Abbeville, north of the proposed Abbeville and Vicinity structural risk reduction project (004.HP.15). Approximately 2,438 structures in the region are eligible for nonstructural risk reduction. Forty percent of households are low to moderate income, and 965 of the structures are in locations that have experienced repetitive loss or severe repetitive loss in the past.

The flood depth standard for nonstructural protection in the region is based on median 100-year flood depths in year 10 of the high scenario, which range from no flooding to 3 m and are shown in Figure 245. In initial conditions, the 100-year flood depths range from no flooding to 2.5 m; by year 50 the 100-year flood depths range up to 4.2 m in some points, so flood risks are projected

to increase significantly over time. The CLARA model's mean estimate of current EAD in the region is \$45 million.

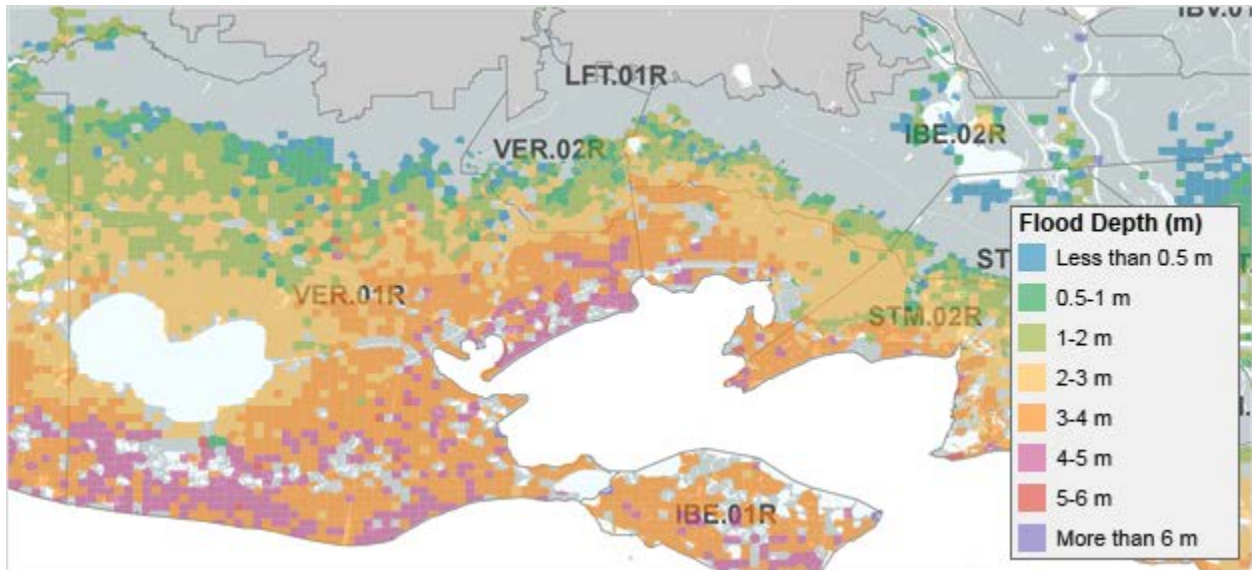


**Figure 245: Median 100-Year Flood Depths in the Vicinity of the Vermilion – Abbeville/Delcambre Region (year 10; high scenario).**

With the nonstructural risk reduction measures in place, the EAD is reduced by a mean of \$24 million in year 10 compared to FWOA, \$38 million in year 25, and \$46 million in year 50 of the high scenario, under historic growth assumptions. A total of 710 structures receive nonstructural risk mitigation over the assumed four-year implementation period, for a total cost of \$156 million. The risk reduction is achieved through a mixture of elevation and flood-proofing, with 635 residences elevated and 60 commercial properties flood proofed. Only 14 properties are acquired; this represents mitigation of 29% of the total structures eligible for nonstructural risk reduction. While benefits were modeled only in year 10, year 25, and year 50, they accrue in all subsequent years after implementation of the project.

## 5.0 References

- Chabreck, R.H. (1972). Vegetation, water and soil characteristics of the Louisiana coastal region. Bulletin/Agricultural Experiment Station, Louisiana State University, p. 664.
- Coastal Protection and Restoration Authority of Louisiana (CPRA). (2015). 2017 Coastal Master Plan Appendix C3-25.1. Coastal Protection and Restoration Authority of Louisiana, Baton Rouge, LA. p. 99.
- Department of Housing and Urban Development (HUD) (2015). FY 2014 Low to Moderate Income Summary Data (LMISD). June 9, 2016. <https://www.hudexchange.info/manage-a-program/acs-low-mod-summary-data-national>
- Fischbach, J.R., Johnson, D.R., Kuhn, K., Pollard, M., Stelzner, C., Costello, R., Molina, E., Sanchez, R., Syme, J., Roberts, H., & Cobell, Z. (2016). 2017 Coastal Master Plan Modeling: Attachment C3-25 – Storm Surge and Risk Assessment. Version 2. (pp. 1-226). Baton Rouge, Louisiana: Coastal Protection and Restoration Authority.
- Fischbach, J.R., Johnson, D.R., Ortiz, D.S., Bryant, B.P., Hoover, M., & Ostwald, J. (2012). Coastal Louisiana Risk Assessment Model: Technical Description and 2012 Coastal Master Plan Analysis Results. Santa Monica: RAND Corporation, TR-1259-CPRA.
- Groves, D.G., Panis, T., & Sanchez, R. (2016). Louisiana's Comprehensive Master Plan for a Sustainable Coast, Appendix D: Planning Tool Methodology. Baton Rouge, Louisiana: Coastal Protection and Restoration Authority of Louisiana.
- Interagency Performance Evaluation Taskforce (IPET). (2009). Performance Evaluation of the New Orleans and Southeast Louisiana Hurricane Protection System, Vol. VIII: Engineering and Operational Risk and Reliability Analysis: U.S. Army Corps of Engineers.
- McMann, B., Schulze, M., Sprague, H., & Tschirky, P. (2016) 2017 Coastal Master Plan: Appendix A: Project Definitions. Version I. (103 pp). Baton Rouge, Louisiana: Coastal Protection and Restoration Authority.
- Mitchell, M.K., Ballard, B.M., Visser, J.M., Brasher, M.G. & Redeker, E.J. (2014). Delineation of Coastal Marsh Types along the Central Texas Coast. *Wetlands*, 34(4): 653-660.
- Moffatt & Nichol. (2016). Rating curves during combined operations: evaluation of 03a.DI.05 Atchafalaya River Diversion and 03b.DI.04 Increase Atchafalaya Flow projects. Prepared for The Water Institute of the Gulf and the Coastal Protection and Restoration Authority of Louisiana. May 23, 2016.
- United States Army Corp of Engineers (USACE). (2008a). Flood Insurance Study: Southeastern Parishes, Louisiana. Intermediate Submission 2: Off-shore Water Levels and Waves. Vicksburg, Mississippi: USACE, p. 152.
- United States Army Corp of Engineers (USACE). (2008b). Flood Insurance Study: Southwestern Parishes, Louisiana. Intermediate Submission 2. Vicksburg, Mississippi: USACE, p. 697.

United States Army Corps of Engineers (USACE). (2012). Hurricane and Storm Damage Risk Reduction System Design Guidelines. USACE New Orleans District Engineering Division, New Orleans, LA. p. 606.

United States Army Corps of Engineers (USACE). (2013). Final Post Authorization Change Report: Morganza to the Gulf of Mexico, Louisiana (pp. 122). New Orleans, LA: U.S. Army Corps of Engineers, Louisiana Coastal Protection and Restoration Authority Board, and Terrebonne Levee and Conservation District.

DRAFT